The Institute for Solid State Physics
The University of Tokyo

Activity Report 2017

© 2018 The Institute for Solid State Physics, The University of Tokyo

ISSP

Activity Report 2017

Contents

	Pages
Preface	1
Research Highlights	2 - 29
Joint Research Highlights	30 - 47
Progress of Facilities	48 - 55
Conferences and Workshops	56 - 61
Subjects of Joint Research	62 - 157
Publications	158 - 196

Preface

We would like to offer the readers the scientific activity report of the Institute for Solid State Physics (ISSP) for the Japanese FY 2017.

ISSP was established in 1957 as a joint-use/research institute attached to the University of Tokyo. In every era, we aim to lead the frontier of "condensed matter and materials sciences" and contribute to science and technology from the view of basic research. We have promoted activities focused on research, education, and joint-use/joint-research.

The first part of the reports "Research Highlights / Joint Research Highlights" exhibits experimental and theoretical achievements in condensed matter and materials sciences. In 2017, the number of granted joint-research proposals is 1,391 and the total number of participants is 8,191.

The second part includes the reports on progress of facilities in 2017 as follows. (1) In International MegaGauss Science Laboratory, the pulse magnet has achieved 985 (T) as the world strongest as an in-door record by destructive methods. (2) The Supercomputer Center (SCC) has started "Project for advancement of software usability in materials science" for enhancing the usability of the ISSP supercomputer system. In Center of Computational Materials Science, the website "MateriApps" for information on application software in computational science has been constructed to support community members as the major contractor of K- and Post-K Computer Projects. (3) In Neutron Science Laboratory, the technical progress of High Resolution Chopper (HRC) spectrometer has been proceeded under high pressure and low temperature environment in cooperation with KEK. (4) In Laser and Synchrotron Research (LASOR) center, the powerful technique by spin- and angle-resolved photoelectron spectroscopy (SARPES) has clarified the spin-dependent electronic states in topological materials. In Synchrotron Radiation Laboratory, operand spectroscopy is available by using lasers at Harima branch.

In the following parts, six reports of international conferences and workshops, subjects of joint research, and list of publications have been presented.

In order to develop the international scientific network as scientific hub based upon the successful experience of JSPS Program for Advancing Strategic International Networks to Accelerate the Circulation of Talented Researchers for "Leading Research Network Topological Phenomena in Novel Quantum Matter" (TopoNet) (2014-2016), new programs, the short time (~3 months) international collaboration, international visiting researchers, and graduate students study abroad, as well as foreign visiting professor and international workshop programs, have started in 2017.

All these facts confirm that ISSP continues to develop successfully and dynamically as the global center of excellence of condensed matter and materials sciences. We appreciate continuous support and cooperation of communities for our activities.

June, 2018

Hatsumi MORI
Director
Institute for Solid State Physics,
The University of Tokyo

Anisotropic Proton Conductivity Arising from Hydrogen-Bond Patterns in Anhydrous Organic Single Crystals

Mori Group

Proton conduction is a fundamentally important phenomenon not only in living systems but also in solid materials, such as fuel cells. Especially, the development of high proton conducting materials and the elucidation of the conducting mechanism are one of pivotal issues in this research field. Recently, organic acid-base salts have attracted increasing attention as a promising candidate of anhydrous proton conductors, which can be utilized as electrolyte of fuel cell above 100 ºC. In this study, we have successfully disclosed the relationship between proton conductivity and hydrogen-bond (H-bond) interactions in such kinds of organic salts, composed of dicarboxylic acid and imidazole [1].

We have grown high-quality single crystals of imidazolium succinate (Im-Suc) or glutarate (Im-Glu) by evaporation method in dehydrated methanol and dehydrated acetonitrile with a typical size of 0.5 × 0.7 × 1.0 mm^3 (Im-Suc). As shown in Fig. 1, the crystal is composed of two-dimensional (2D) sheet structures, in which the imidazolium cations (Im) and succinate anions (Suc) are connected with hydrogen bonds (H-bonds) [2]. Two N–H moieties of the Im molecule are connected to carbonyl oxygen atoms of the Suc molecule with d_{NO} of 2.72 Å (red dashed lines) and 2.87 Å (brown dashed lines) and also form short contacts with the adjacent oxygen atoms of the Suc molecule with d_{NO} ~ 3.05, 3.15 Å (blue dashed lines), like bifurcated H-bonds. In addition, a C-H···O short contact (gray dashed lines, d_{CO} ~ 3.08 Å) is observed between the Im and Suc molecules. Furthermore, there is an O-H···O H-bond between the Suc molecules (green dashed lines, d_{OO} ~ 2.49 Å). On the other hand, although the shortest C···C distance (3.39 Å) between the networks is less than the sum of van der Waals radii (3.40 Å), no effective H-bonds are found between these 2D networks (Fig. 1). The shortest N···O distances between the networks are 3.50 and 3.56 Å which are much longer than the sum of van der Waals (vdW) radii of N and O atoms (3.07 Å).

The relationship between the crystal shape and crystallographic axes was determined by X-ray diffraction measurements, where the [1 0 0] and [1 4 –9] directions are within the 2D network and the [0 1 1] is perpendicular to the 2D network (Fig. 1). Therefore, by measuring and comparing the proton conductivity in these three directions, we have revealed the effects of the H-bonding interactions and molecular arrangement on the proton conduction. By the measurement of ac proton conductivity, the complex impedance planes (Cole-Cole plots) gave almost perfect semicircle profiles at each temperature, which means that a single Debye-type relaxation occurs in our single-crystal measurements and thus the obtained conductivity is the intrinsic proton conductivity without contributions from the grain boundaries. Then, we compare the proton conducting properties in these three directions (Fig. 1). First, the proton conductivity σ in the directions parallel to the H-bonding network ($\sigma_{[1\ 0\ 0]}$ and $\sigma_{[1\ 4\ -9]}$) and that in the direction perpendicular to the network ($\sigma_{[0\ 1\ 1]}$) are compared. At around 115 °C, the former two directions ($\sigma_{[1\ 0\ 0]}$ = 4.94 × 10^{-7} S cm^{-1} and $\sigma_{[1\ 4\ -9]}$ = 1.27 × 10^{-7} S cm^{-1}) provide almost two orders higher conductivity than the latter one ($\sigma_{[1\ 0\ 0]}$ = 3.55 × 10^{-9} S cm^{-1}). This large difference is maintained in the present temperature range, indicating that the proton conduction occurs more readily in the H-bonding network than in its perpendicular direction.

Next, σ in the two directions parallel to the H-bonding network ($\sigma_{[1\ 0\ 0]}$ and $\sigma_{[1\ 4\ -9]}$) are compared. At 115 °C, the [1 0 0] direction has about four times higher σ (4.94 × 10^{-7} S cm^{-1}) than the [1 4 –9] direction (1.27 × 10^{-7} S cm^{-1}) and this trend is unchanged in this temperature region. The difference of σ between these two directions (about four times) is much smaller than that between the parallel and perpendicular directions (two orders) shown above. However, this small difference is significant in connection with anisotropy of the proton conduction in the 2D H-bonding network, especially in terms of the intermolecular interactions and molecular arrangement.

Moreover. in order to gain further insight into this relationship between the difference in ΔpK_a and the difference in the proton conductivity, we compare the present results with those of the analogues. The 1:1 co-crystals of benzimidazole, an imidazole derivative with pK_{aH} = 5.49, and dicarboxylic acid are a similar type of H-bonded proton

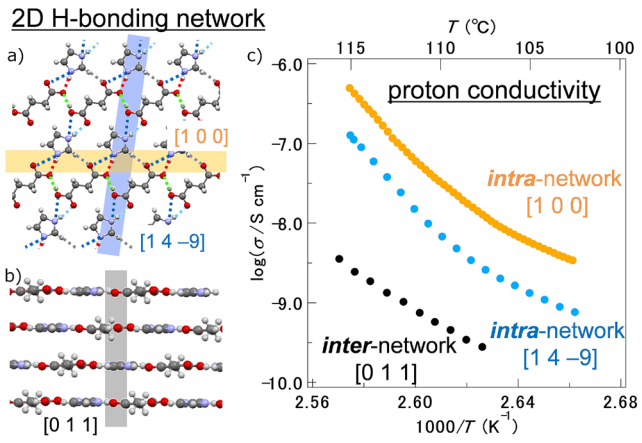

Fig. 1. a) Intra- and b) inter-2D-hydrogen (H)-bonded network [2], and c) anisotropic proton conduction along the [1 0 0], [1 4 –9], and [0 1 1] directions, respectively [1] for an anhydrous proton conductor, imidazolium succinate (Im-Suc). The proton conductivity in intra-network is by two-orders higher than that in inter-network. Moreover, the anisotropic proton conduction in intra-network demonstrates the importance of H-bonded molecular arrangement.

conductors, showing σ = ~10^{-5} S cm^{-1} in the glutaric acid (pK_{a1} = 4.34) salt and ~10^{-4} S cm^{-1} in the sebacic acid (pK_{a1} = 4.72) salt in the compressed pellet state at around 77 °C. This result indicates that the latter salt with a smaller ΔpK_a of 0.77 (= 5.49 – 4.72) shows a higher proton conductivity than the former salt with a ΔpK_a of 1.15 (= 5.49 – 4.34). This trend is similar to that in the present imidazole systems, suggesting that the proton conductivity significantly increases with decreasing ΔpK_a. However, the degree of the conductivity increase seems to be somewhat different in the benzimidazole and imidazole systems. Namely, the proton conductivity of the former system is increased one order of magnitude by the ΔpK_a difference of 0.38 (= 1.15 – 0.77), whereas that of the latter is increased 2–3 orders of magnitude by the ΔpK_a difference of 0.15 (= 2.76 – 2.61) as described before. Thus, simply stated, the proton conductivity of the present imidazole system is more sensitive to the pK_a change than that of the benzimidazole system. This difference of the pK_a effect on the proton conductivity probably originates from the difference in the molecular structure of imidazole and benzimidazole. Although these two systems have a similar overall crystal structure, the molecular structure difference would modulate the details, such as the intermolecular distances, H-bonding manners, and molecular arrangements, which result in the above-described difference in the pK_a effect.

In conclusion, we have revealed the "intrinsic" proton conductivity without grain boundary contributions in acid-base type anhydrous organic single co-crystals, imidazolium succinate (Im-Suc) and imidazolium glutarate (Im-Glu), with a 2D H-bonding network. The obtained conductivities are 1~5 × 10^{-7} S cm^{-1} (Im-Suc) and 2 × 10^{-6} S cm^{-1} (Im-Glu) within the 2D H-bonding network, which are much higher than those in the perpendicular direction to the 2D network [4 × 10^{-9} S cm^{-1} (Im-Suc) and 6 × 10^{-8} S cm^{-1} (Im-Glu)]. These results demonstrate that the H-bonds significantly promote proton conduction in this kind of anhydrous materials. Furthermore, we have shown that this proton conduction is 1) more significant in the H-bonds between the acid and base molecules than in those between the acid and its conjugate base and is 2) enhanced by decreasing the difference of pK_a between the H-bonded acid and base molecules. In addition, the present results offer the possibility that the molecular motions of imidazole play a crucial role in the proton conduction not only in the 2D H-bond network but also between the networks. The details about the inter-network proton conduction and also the non-Arrhenius-type profile of proton conductivity in the H-bond network are currently under investigation in terms of the molecular dynamics by using solid-state NMR and IR spectroscopies, high-temperature X-ray analysis, and theoretical calculations.

References

[1] Y. Sunairi, A. Ueda, J. Yoshida, K. Suzuki, and H. Mori, J. Phys. Chem. C, in press.

[2] J. C. MacDonald, P. C. Dorrestein, and M. M. Pilley, Cryst. Growth Des. **1**, 29 (2001).

Authors

Y. Sunairi, A. Ueda, J. Yoshida, K. Suzuki, and H. Mori

Search for Topological States in an Organic Dirac Semimetal

Osada Group

A layered organic conductor, α-(BEDT-TTF)$_2$I$_3$, has been known as a two-dimensional (2D) gapless Dirac fermion system, namely, Dirac semimetal, with a pair of spin-degenerated Dirac cones. Generally, the Dirac semimetal is a starting point to obtain various topological insulating phases. In graphene, for example, Haldane showed that the Chern insulator (quantum anomalous Hall insulator) appears by attaching the alternating flux pattern breaking time reversal symmetry (TRS) [1]. On the other hand, Kane and Mele showed that the Z_2 topological insulator (quantum spin Hall insulator) appears by introducing the spin-orbit interaction (SOI) [2]. We have experimentally and theoretically explored the topological phases starting from the organic Dirac semimetal.

At ambient pressure, α-(BEDT-TTF)$_2$I$_3$ undergoes a metal-insulator transition into an insulating phase due to the charge order (CO) at T_c=135K. This CO phase is suppressed by applying pressure, and it perfectly vanishes at about P_c~1.25GPa, as illustrated schematically in the inset of Fig. 1(a). Figure 1(a) shows the temperature dependence of in-plane resistance measured at several pressures. In the weak CO state around P_c, the resistance shows increase due to CO below T_c~50K, but the insulator-like increase turns to metal-like decrease at lower temperatures as shown by the red dashed circle. In addition, in the Dirac semimetal state above P_c, the resistance exhibits the insulator-like increase at low temperatures below 10K as indicated by the blue dashed circle. These behaviors have never been explained.

As their mechanisms, we propose the emergence of topological states in this organic system. First, we discuss the possible Chern insulator state in the weak CO state [3]. In the vicinity of CO transition, the NMR measurement by Kanoda's group clarified that not only the charge density but also spin density are modulated breaking TRS, as indicated by the clouds in Fig. 2(a). We assume a pattern of site potential and staggered magnetic flux on the α-(BEDT-TTF)$_2$I$_3$ lattice so as to reproduce the observed potential and magnetic modulations (Fig. 2(a)). We shows that the system becomes a Chern insulator, where gaps open at two Dirac points, under large enough magnetic modulation, and one chiral edge state appears in the gap along each crystal edge (Fig. 2(a)). This is an organic analogue of the Haldane model. The conduction through these edge states explains

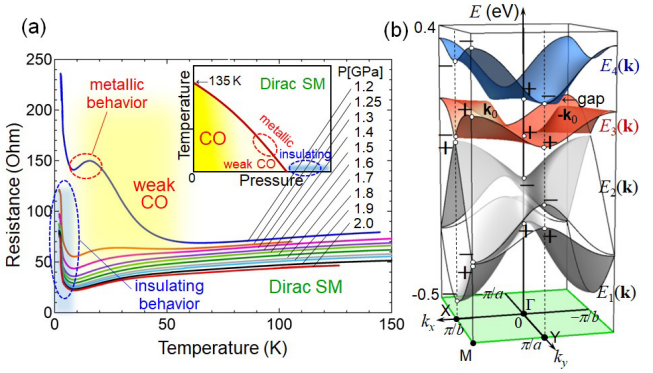

Fig. 1. (a) Temperature dependence of resistance in α-(BEDT-TTF)$_2$I$_3$ at several pressures. (b) Band dispersion of α-(BEDT-TTF)$_2$I$_3$. The symbols, "+" and "−", indicate parity at the time reversal invariant wave numbers.

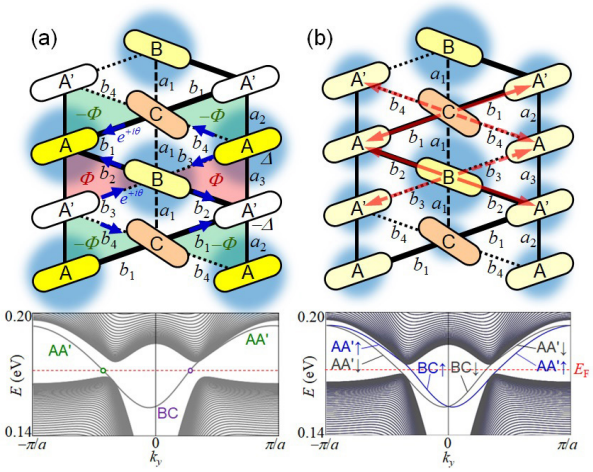

Fig. 2. (a) Flux configuration in the organic Haldane model. The lower panel shows the chiral edge state in the energy spectrum of the nanoribbon. (b) Inter-chain hopping with SOI in the organic Kane-Mele model. The lower panel shows the helical edge state in the energy spectrum of the nanoribbon.

the anomalous metallic behavior of resistance observed in the weak CO state.

Next, we discuss that the Z_2 topological insulator state with small gaps emerges in the Dirac semimetal state under finite SOI [4]. Using first principles calculations, Valenti *et al*. discussed that SOI in BEDT-TTF compounds could reach 1~2 meV, and finite SOI opens small gaps at Dirac points causing insulating behavior at low temperatures (Fig. 1(b)). We assume a pattern of inter-chain hopping accompanied by SOI on α-(BEDT-TTF)$_2$I$_3$ lattice reflecting the charge disproportionation indicated by the clouds in Fig. 2(b). We demonstrate that gaps open at Dirac points causing resistance increase, and one helical edge state, which is characteristic to the topological insulator, appears in the gap along each crystal edge. This is an organic analogues of the Kane-Mele model. In addition, we generally discuss that a topological insulator appears under finite SOI as long as SOI does not cause any band inversion, based on the Fu-Kane parity product theory (Fig. 1(b)) [5]

References

[1] F. D. M. Haldane, Phys. Rev. Lett. **61**, 2015 (1988).
[2] C. L. Kane and E. J. Mele, Phys. Rev. Lett. **95**, 226801 (2005).
[3] T. Osada, J. Phys. Soc. Jpn. **86**, 123702 (2017).
[4] T. Osada, arXiv: 1804.09420.
[5] L. Fu and C. L. Kane, Phys. Rev. B **76**, 045302 (2007).

Authors

T. Osada, A. Mori, K. Yoshimura, M. Sato, T. Taen, and K. Uchida

Thermal Hall Effect of Phonons

Yamashita and Nakatsuji Groups

Hall measurements are fundamental probes for studying the physical properties of metals. Recently, Hall measurements in insulators, which are observed as *thermal* Hall effects (THEs), are being recognized as a new probe to study the elementary excitations in insulators. Since there is no charged heat carries in insulators, a THE in an insulator is not originated from the Lorentz force, but from intrinsic (e.g. Berry phase effect) or extrinsic (e.g. skew scatterings) mechanisms as the anomalous Hall effect. In fact, a THE of magnons has been observed in ferromagnetic insulators below the Curie temperature [1], which has been understood in terms of the Berry phase effect [2, 3]. A THE of paramagnetic spins has also been reported in the spin-liquid phase of a kagomé antiferromagnet [4].

In spite of these recent studies of spin THEs, a phononic THE has remained elusive. A phonon THE was actually reported at 2005 in $Tb_3Ga_5O_{12}$ (TbGG) [5] prior to the observations of the spin THEs [1, 4]. However, the measurement of the phonon THE in TbGG was done only at ~5 K, disabling to find the temperature dependence of the thermal Hall conductivity (κ_{xy}). To find the theoretical model describing the phonon THE, it is indispensable to measure κ_{xy} in a wide temperature range and to compare the temperature dependence with the theoretical predictions. Furthermore, because TbGG is paramagnetic at ~5 K, it is impossible to exclude a spin THE.

To this end, we performed thermal Hall measurements in the spin-liquid candidate $Ba_3CuSb_2O_9$ (BCSO) [6]. BCSO is a perovskite-type insulator, in which the spins of Cu^{2+} ions form a honeycomb structure. NMR measurements show that a spin gap opens below ~50 K, enabling us to detect a phono THE without a spin THE.

Our main result is to find a distinct thermal Hall signal in a wide temperature range of 2-60 K, revealing that the phonon THE in BCSO shows $|\kappa_{xy}| \propto T^2$. As shown in Fig. 1, κ_{xy} is negative in the entire temperature range measured, shows a peak around 50 K, and decreases at lower temperatures. A log-log plot of $|\kappa_{xy}|$ (inset of Fig. 1) shows that $|\kappa_{xy}| \propto T^2$ at low temperature. We conclude that the THE comes from phonons because a spin THE is supposed to show an activated temperature dependence owing to the spin gap formed below 50 K.

What is the mechanism of the phonon THE in BCSO? In TbGG, phonon scatterings by excess Tb^{3+} ions have been pointed out as a possible mechanism of the phonon THE [8]. In BCSO, we also find the longitudinal thermal conductivity is strongly suppressed by a random structure of Cu^{2+}-Sb^{5+} dumbbells. Therefore, this strong scattering effects on phonons in BCSO can be related to the phonon THE as that in TbGG. However, the T^2 dependence of κ_{xy} has not been successfully reproduced by theories, which may be owing to the difference in scattering effects on phonons by the $4f$ Tb^{3+} ions with a large quadrupole moment and those by the $3d$ Cu^{2+} ions. We believe that our finding of $|\kappa_{xy}| \propto T^2$ leads to further theoretical and experimental studies to clarify the mechanism of phonon THEs in insulators.

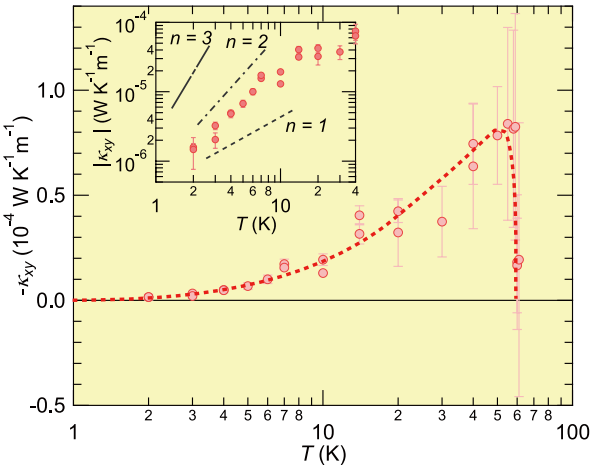

Fig. 1. The temperature dependence of thermal Hall conductivity (κ_{xy}). The dashed line is a guide for the eyes. The inset shows $|\kappa_{xy}|$ in log-log scale. The solid lines show slopes for $|\kappa_{xy}| \propto T^n$ (n = 1, 2, 3).

References
[1] Y. Onose *et al.*, Science **329**, 297 (2010).
[2] H. Katsura, N. Nagaosa, and P. A. Lee, Phys. Rev. Lett. **104**, 066403 (2010).
[3] R. Matsumoto, R. Shindou, and S. Murakami, Phys. Rev. B **89**, 054420 (2014).
[4] D. Watanabe *et al.*, Proc. Natl. Acad. Sci. USA **113**, 8653 (2016).
[5] C. Strohm, G. L. J. A. Rikken, and P. Wyder, Phys. Rev. Lett. **95**, 155901 (2005).
[6] S. Nakatsuji *et al.*, Science **336**, 559 (2012).
[7] K. Sugii, M. Shimozawa, D. Watanabe, Y. Suzuki, M. Halim, M. Kimata, Y. Matsumoto, S. Nakatsuji, and M. Yamashita, Phys. Rev. Lett. **118**, 145902 (2017).
[8] M. Mori *et al.*, Phys. Rev. Lett. **113**, 265901 (2014).

Authors
K. Sugii, M. Shimozawa, D. Watanabe, Y. Suzuki, M. Halim, M. Kimata, Y. Matsumoto, S. Nakatsuji, and M. Yamashita

Quantum-Disordered State of Magnetic and Electric Dipoles in a Hydrogen-Bonded Organic Mott System

Yamashita and Mori Groups

Strongly enhanced quantum fluctuations often lead to a rich variety of quantum-disordered states. A representative case is liquid helium, where zero-point vibrations of the helium atoms prevent its solidification at low temperatures. A similar behavior is found for the internal degrees of freedom in electrons. Among the most prominent is a quantum spin liquid (QSL), in which highly correlated localized spins fluctuate even at absolute zero. Recently, a coupling of spins with other degrees of freedom has been proposed as an innovative approach to generate even more fascinating QSLs, but such an idea is limited to the internal degrees of freedom in electrons.

The hydrogen-bonded organic Mott insulator κ-H_3(Cat-EDT-TTF)$_2$ (hereafter abbreviated as H-Cat) [1-3] synthesized by Mori group in ISSP shows considerable promise as a new type of QSLs, where H_2Cat-EDT-TTF is catechol-fused ethylenedithiotetrathiafulvalene. This compound has been reported to exhibit a two-dimensional (2D) QSL state; however, in contrast to other 2D organic QSL materials, the 2D π-electron layers of H-Cat are connected by hydrogen bonds, not separated by non-magnetic insulating layers. From the previous theoretical works [4,5], zero-point motion associated with this hydrogen atoms (termed "proton fluctuations") is believed to be strongly enhanced, leading to the realization of a QSL state through strong coupling between the hydrogen bonds and the π-electrons. However, it has not been established whether such strong quantum proton fluctuations are indeed present in H-Cat, and if so, how the quantum fluctuations affect the QSL state.

Here we demonstrate, by using a combination of dielectric permittivity and thermal conductivity measurements, that the quantum proton fluctuations in H-Cat provide a quantum-disordered state of magnetic and electric dipoles through the coupling between π-electrons and hydrogen atoms [6]. First of all, we focus on proton dynamics in H-Cat. As shown in Fig. 1, the dielectric constant ε_r (T) of H-Cat steeply increases with decreasing temperature and then saturates below 2 K. The temperature dependence of ε_r (T) for H-Cat is a typical dielectric behavior in quantum paraelectric (QPE) materials such as $SrTiO_3$, in which long-range electric order is suppressed by strong quantum fluctuations. From the fitting result by Barrett formula describing the QPE state, we have found the presence of an antiferroelectric (AFE) interaction in H-Cat, which is consistent with the AFE configuration resulting from a hydrogen-bond order in the deuterated analog of H-Cat, κ-D_3(Cat-EDT-TTF)$_2$ (denoted as D-Cat) [3]. Thus, the observed quantum paraelectricity in H-Cat clearly shows the presence of strong quantum fluctuations that suppress the hydrogen-bond order as observed in D-Cat, that is, the persistence of enhanced proton fluctuations down to low temperatures.

We next examine how the proton dynamics in the QPE state affects the nature of the QSL state in H-Cat. For this purpose, in Figure 1, we plot the temperature dependence of the thermal conductivity divided by temperature κ/T (this work) and the magnetic susceptibility χ [2] for H-Cat, together with the above-mentioned ε_r. Below 2 K, the thermal conductivity increases upon entering the QPE state, where ε_r saturates. The characteristic temperature coincides with the temperature at which the susceptibility becomes constant; this occurs when the spin correlation develops in the QSL state. The coincidence of the QPE and QSL states is surprising and strongly suggests that the development of the quantum proton fluctuations triggers the emergence of the QSL. We now theoretically analyze the effects of proton dynamics on the QSL state. According to our model that captures the essence of H-Cat system [7], low-energy proton fluctuations (~1 meV) modulate the amplitude of the electron transfers and the energy levels of the molecular orbitals. These effects may induce a dynamical modulation of exchange coupling energy J as well as a reduction of the on-site Coulomb repulsion U due to the bi-polaron effect. As a result, the magnetic long-range order would be suppressed by proton dynamics of H-Cat, inducing a QSL.

In conclusion, we have successfully discovered a quantum-disordered state of magnetic and electric dipoles in a hydrogen-bonded organic Mott system, H-Cat. Importantly, this system has 2D π-electron layers connected by hydrogen bonds, in contrast to the other organic QSL candidates with those separated by anion layers. This structural feature of H-Cat enables us to discover a new mechanism to stabilize the QSL state, where the electron and proton degrees of freedom are strongly coupled. Utilizing such a strong coupling between multiple degrees of freedom will advance our explorations of quantum phenomena such as orbital–spin liquids and electric–dipole liquids.

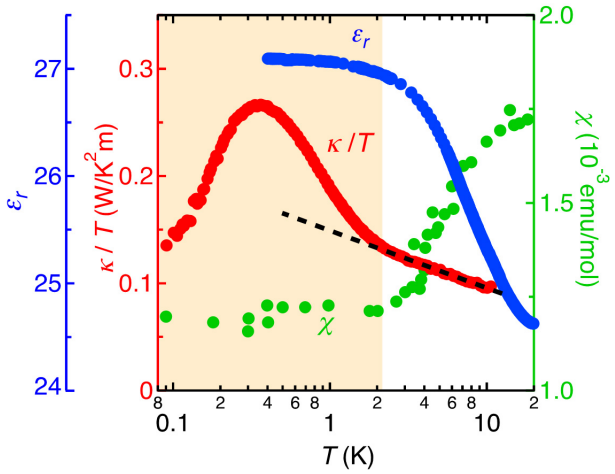

Fig. 1. A combination of the temperature dependences of the dielectric constant ε_r (blue, left axis), the thermal conductivity divided by temperature κ/T (red, left axis) and the magnetic susceptibility χ (green, right axis) for H-Cat. The values of χ are taken from ref. 2. The dashed line is an eye guide. The shaded region represents the QPE and QSL phases.

References
[1] T. Isono *et al.*, Nat. Commun. **4**, 1344 (2013).
[2] T. Isono *et al.*, Phys. Rev. Lett. **112**, 177201 (2014).
[3] A. Ueda *et al.*, J. Am. Chem. Soc. **136**, 12184 (2014).
[4] T. Tsumuraya, H. Seo, R. Kato and T. Miyazaki, Phys. Rev. B **92**, 035102 (2015).
[5] K. Yamamoto *et al.*, Phys. Chem. Chem. Phys. **18**, 29673(2016).
[6] M. Shimozawa *et al.*, Nat. Commun. **8**, 1821 (2017).
[7] M. Naka and S. Ishihara, arXiv:1801.04661.

Authors
M. Shimozawa, K. Hashimoto[a], A. Ueda, Y. Suzuki, K. Sugii, S. Yamada, Y. Imai, R. Kobayashi[a], K. Itoh[a], S. Iguchi[a], M. Naka[b], S. Ishihara[b], H. Mori, T. Sasaki[a], and M. Yamashita
[a]Institute for Materials Research, Tohoku University
[b]Tohoku University

Disguised Antiferromagnetic Order in a Two-Dimensional Quasicrystal

Tsunetsugu Group

Quasicrystals are the alloys with a lattice structure that is not consistent with translation symmetry but its Fourier pattern $S(\boldsymbol{k})$ comprises a set of delta-function peaks like those in crystals. In most of quasicrystals, however, the structure factor has a rotation symmetry that is prohibited in crystals and also self-similarity $S(\lambda^{-n}\boldsymbol{k}) \sim \Lambda^{-n} S(\boldsymbol{k})$. It is expected that this unique lattice structure has a crucial effect on magnetic order driven by strong electron correlation, and we have explored this issue in the simplest quasicrystal, the Penrose lattice in two dimensions. The Penrose lattice has the five-fold rotation symmetry, characterized by the geometrical factor known as the golden ratio $\tau = 2\cos(\pi/5) = (\sqrt{5}+1)/2$

To study an antiferromagnetic order in the Penrose lattice, we have employed the half-filled Hubbard model with sites on the vertices of rhombus units. When the Coulomb repulsion is switched off ($U = 0$), this model has a thermodynamically degenerate single-electron states called *confined states*; each of them is strictly confined in a finite region of the lattice [1]. Since their energy locates at the center of spectrum $E = 0$, they contribute to the formation of magnetic moments, upon switching on U.

Magnetic moments have nonvanishing amplitudes at most of sites, even in the limit of $U \to +0$; the site average of moment size is $81/2\text{–}25\ \tau \sim 0.05$. We know that they should exhibit an antiferromagnetic long-range order at zero temperature, because the Penrose lattice is bipartite despite the lack of translation symmetry. A big surprise is that this antiferromagnetic order is disguised and the moments exhibit a very complicated fractal-like spatial pattern. The magnetic order is cluster antiferro; moments are polarized in the same direction in each cluster, and neighboring clusters polarize in the opposite directions [2]. The clusters have sizes ranging from 31 sites to infinity, and their densities follow a power-law scaling with their size. This is an intricate consequence of quasiperiodic lattice structure. With increasing U, the magnetizations of minority spin continuously evolve, and the magnetic order approaches a conventional Néel type with staggered magnetization. This crossover depends on local environment of each site, and it is also dominated by the quasiperiodic structure.

This study is performed by collaboration with Akihito Koga at Tokyo Institute of Technology.

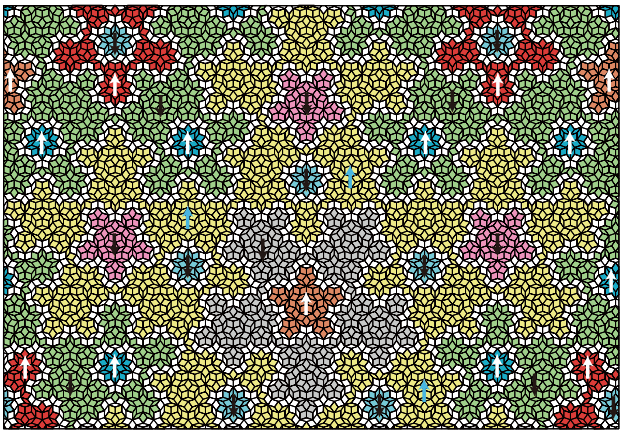

Fig. 1. Disguised antiferromagnetic order in the Penrose lattice. In each cluster, only one-sublattice sites have nonvanishing magnetic moments at U=+0, and they polarize in the same direction marked by arrow, whereas the moment size is zero everywhere in the other sublattice.

References
[1] M. Arai, T. Tokihiro, T. Fujiwara, and M. Kohmoto, Phys. Rev. B **38**, 1621 (1988).
[2] A. Koga and H. Tsunetsugu, Phys. Rev. B **96**, 214402 (2017).

Author
H. Tsunetsugu

Interaction Effect on Adiabatic Charge Pumping via a Single-Level Quantum Dot

Kato Group

Charge transport from one reservoir to another reservoir induced by periodic operation on devices is called "charge pumping". Recent development of device fabrication and measurement technique has enabled us to realize charge pumping in nanoscale devices such as quantum dots (QDs). In particular, quasi-static pumping under slow parameter driving, i.e., "adiabatic" pumping is an important phenomenon because pumping charge depends only on a trajectory in the parameter space. Application of adiabatic pumping to, e.g., current standard and single electron injection has been discussed in a number of theoretical and experimental works [1].

For adiabatic pumping, we need to take a period of driving as larger than characteristic time scales of the system. Therefore, coherent transport in quantum dots strongly coupled with electronic leads, which have a short relaxation time, is suitable to fast adiabatic pumping. However, theoretical framework for charge pumping in QDs strongly mixed with leads has not been studied so far. In our previous paper [2], we calculated pumping charge within the first-

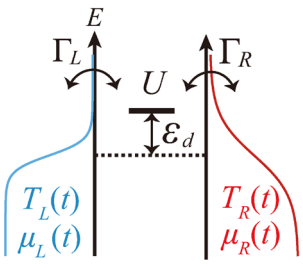

Fig. 1. Schematics of our model for adiabatic charge pumping due to driving of reservoir parameters (temperatures and electrochemical potentials). Here, ε_d and U are an energy level and a Coulomb interaction in a quantum dot, respectively. The dot-reservoir couplings are denoted by Γ_L and Γ_R.

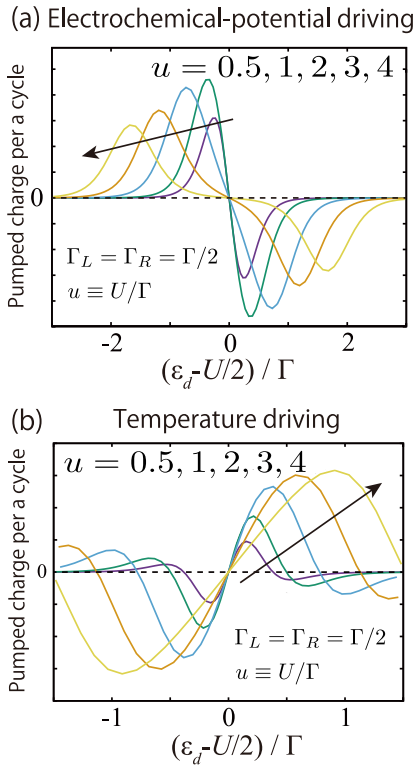

Fig. 2. Pumped charge per one cycle obtained by the renormalized perturbation theory for (a) the electrochemical-potential driving case and (b) the temperature-driving case.

order perturbation theory with respect to Coulomb interaction. In the present study [3], we aimed to construct general formalism, which can treat arbitrary strength of Coulomb interaction beyond our previous work.

We considered adiabatic charge pumping via a single-level QD system induced by reservoir parameter driving in the coherent transport region (see Fig. 1). We formulated pumped charge for arbitrary Coulomb interaction by nonequilibrium Green's function method. To handle the time-dependent reservoir temperatures, we introduced a thermomechanical field, which describes temperature modulation via an energy rescaling of the reservoirs. We also employed the adiabatic approximation to obtain pumped charge under adiabatic operation.

We derived a general formula for the pumped charge in terms of the Berry connection. It is expressed by the two-particle Green's function of electrons in the QD. Our formalism covers the low-temperature strongly-correlated region, which cannot be treated in the previous theoretical methods. Based on our general formulism, we calculated the pumped charge by employing the renormalized perturbation theory (see Fig. 2). We showed that for both the electrochemical-potential-driven and the temperature-driven case, the pumping strength has a maximum and a minimum as a function of the QD energy level, and the position of the maximum (minimum) moves away from the particle-hole symmetric point as the Coulomb interaction increases. For the electrochemical-potential-driven case, the maximum value of the pumping strength is once enhanced, and then suppressed as the Coulomb interaction increases (see Fig. 2 (a)). On the other hand, for the temperature-driven case, the maximum value continues to increases as the Coulomb interaction increases (see Fig. 2 (b)). This difference was explained from the renormalized parameters consistently.

Our formalism states that adiabatic charge pumping can be evaluated by the two-particle Green's function of the electrons in the QD, which is in principle calculated by numerical methods. It is an important future problem to compute the pumped charge without any approximation in the strong Coulomb interaction region. From the viewpoint of non-equilibrium thermodynamics, it is also a challenge to generalize the present formalism to heat pumping and work exchange and to discuss quantum effects on efficiency of small engines.

References
[1] J. P. Pekola *et al.*, Rev. Mod. Phys. **85**, 1421 (2013).
[2] M. Hasegawa and T. Kato, J. Phys. Soc. Jpn. **86**, 024710 (2017).
[3] M. Hasegawa and T. Kato, J. Phys. Soc. Jpn. **87**, 044709 (2018).

Authors
M. Hasegawa and T. Kato

Crossover between Kondo States in Carbon Nanotube Quantum Dot Observed by an Ultrasensitive Noise Measurement

Kato Group

We have realized the SU(2) and SU(4) Kondo many-body states in a carbon nanotube quantum dot made by the cutting-edge nanofabrication technology, and finely controlled a crossover phenomenon between the two Kondo states by applying magnetic fields. Our very accurate current noise measurement successfully elucidated that the local moment structure within the quantum dot can be adjusted to increase the quantum fluctuation of the Kondo state [1].

The Kondo effect is a typical quantum many-body phenomenon, where electrons gather around the moment of a localized electron and form a new state (Kondo state) together and quantum fluctuation of the angular moment of the electrons plays the essential role in formation of the Kondo state. The electrons confined in the carbon nanotube quantum dot hold not only spin but also additional degrees of freedom, namely, the direction of electron motion (see Fig. 1), which brings a variety to the Kondo state. However, it is not easy to distinguish the SU(2) and SU(4) Kondo states by power laws emerging in observed current as function of temperatures or applied bias-voltages, because both of the Kondo states are governed by the local Fermi liquid. The key idea of our work is to observe and analyze current noise. The Fano factor given by the ratio of the nonlinear current noise and the nonlinear current repre-

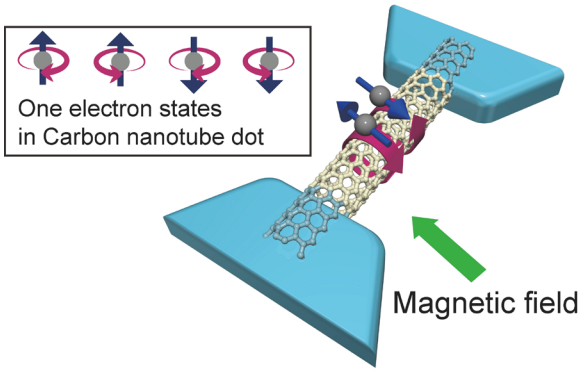

Fig. 1. Two aluminum electrodes (cyan) are attached to a carbon nanotube quantum dot (yellow). Electric current and its noise through them are investigated. Electrons confined in the carbon nanotube dot hold not only the spin degree freedom but also a degree of freedom due to the direction of electron motion (red arrows wrapped around the nanotube), which can bring a rich variety of the Kondo state.

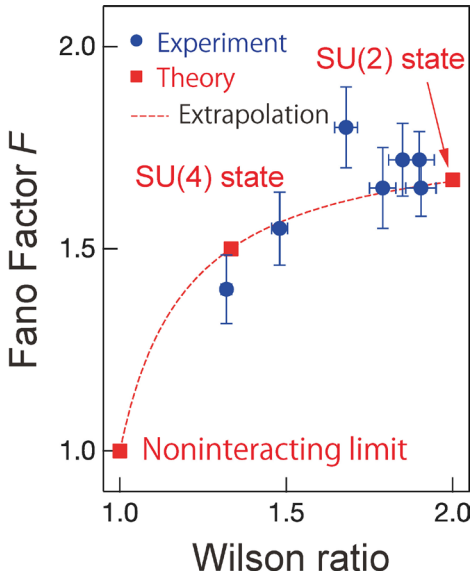

Fig. 2. Fano factor as a function of the Wilson ratio.

sents a strength of the local-Fermi-liquid interaction, which indicates a strength of quantum fluctuation of the Kondo ground state. The Fano factor also shows an intrinsic value corresponding to the local moment which causes the Kondo state.

Figure 2 shows the observed Fano factor F as a function of the Wilson ratio R. In our experiment, the Wilson ratio is controlled by applied magnetic field. The values of the Wilson ratio corresponding to experimentally applied magnetic field are estimated by numerical renormalization calculation [2]. The Wilson ratio are varied from $R = 4/3$ at the zero magnetic field, where the SU(4) Kondo state is realized, to $R = 2$, the large magnetic field limit where the SU(2) Kondo state is realized. In Fig. 2, the Fano factor varies from $F = 1.4 \pm 0.1$ at the zero field to $F = 1.7 \pm 0.1$ at a large field. These observations well agree with $F = 3/2$ and 5/3 theoretically predicted for the SU(2) and SU(4) Kondo states, respectively [3, 4].

In this research, we have experimentally demonstrated that the strength of quantum fluctuation depends on the type of Kondo states. Both the Kondo effect and quantum fluctuation are central issues in physics. Our result brings a deeper understanding of quantum many-body phenomena, and opens a new way to control quantum fluctuation and to explore new function of materials.

Refernces

[1] M. Ferrier, T. Arakawa, T. Hata, R. Fujiwara, R. Delagrange, R. Deblock, Y. Teratani, R. Sakano, A. Oguri, and K. Kobayashi, Phys. Rev. Lett. **118**, 196803 (2017).
[2] Y. Teratani, R. Sakano, R. Fujiwara, T. Hata, T. Arakawa, M. Ferrier, K. Kobayashi, and A. Oguri, J. Phys. Soc. Jpn. **85**, 094718 (2016).
[3] R. Sakano, T. Fujii, and A. Oguri, Phys. Rev. B **83**, 075440 (2011).
[4] R. Sakano, A. Oguri, T. Kato, and S. Tarucha, Phys. Rev. B **83**, 241301(R) (2011).

Authors

R. Sakano, M. Ferrier[a], T. Arakawa[b], T. Hata[c], K. Kobayashi[b], Y. Teratani[d], and A. Oguri[d]
[a]Université de Paris-Sud
[b]Osaka University
[c]Tokyo Institute of Technology
[d]Osaka City University

In-Plane Spin Filtering in a Resonant Diode with Double Quantum Well

Katsumoto Group

A quantum resonant diode is a device that filters the electron momentum perpendicular to the quantum well. Combined with the energy conservation, this restricts the electrons which can tunnel through the device into a circle on the Fermi surface in the source. The momentum selection may lead to spin selection due to spin-momentum locking via strong spin-orbit interaction (SOI). This can be achieved, for example, in a series connection of two quantum wells with opposite sign Rashba SOI coupling constants to each other [1]. However this device does not have practical meaning because Rashba-type SOI does not have in-plane anisotropy and without in-plane selection of momentum, the device does not work as a spin-filter. Now, if Dresselhaus-type SOI co-exists, the in-plane symmetry of the system lowers and the device can have bi-directional spin-filtering effect.

Here we have realized such a device of double quantum well with n-p-n type doping, which provides opposite sign Rashba SOI for the two quantum wells. The materials are zinc-blende InGaAs quantum wells and AlInAs barriers lattice matched to a (001) InP substrate. Hence the system has a Dresselhaus SOI lacking the inversion symmetry. On top of the resonant diode layers, an iron single crystal with body-centered cubic (bcc) lattice structure is deposited.

The left panel of Fig. 1 shows the differential resistance as a function of bias voltage in negative bias range. Negative resistances appear at two resonant energies as double dips reflecting the double well avoided crossing. Around the origin of the I-V characteristics, no trace of Fe magnetization appears in the in-plane field magnetoresistance. Just above E_1 resonance, hysteretic magnetoresistance (MR) shown in the right panel of Fig. 1 appears. The lineshape resembles to that of so called anisotropic magnetoresistance (AMR) suggesting that the lineshape itself has the same origin, that is the magnetic domain formation in the Fe layer. However, the amplitude in the resistance is far above the AMR in Fe.

The left panel of Fig. 2 shows the MR for the field down sweep in color plot versus the plane of field strength and directional angle from $[\bar{1}10]$. As shown in the polar plot at the right, the anisotropy apparently reflects the symmetry of the Dresselhaus SOI while the coercive force as observed in the width of MR, reflects the four-fold bcc symmetry of the Fe layer. All the observations indicate the resonant double

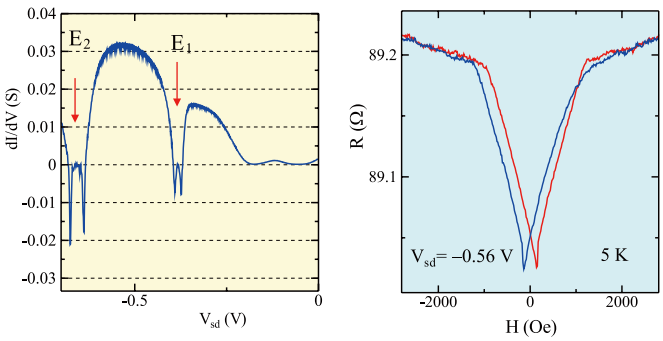

Fig. 1. Left: Differential resistance of an InGaAs double quantum well resonant diode as a function of source-drain negative bias voltage. E_1 and E_2 correspond to the resonant energy levels. Right: Hysteretic in-plane magnetoresistance appeared above the resonant level E_1. The field direction is along $[\bar{1}10]$. Blue and red lines correspond to down and up field sweeps respectively.

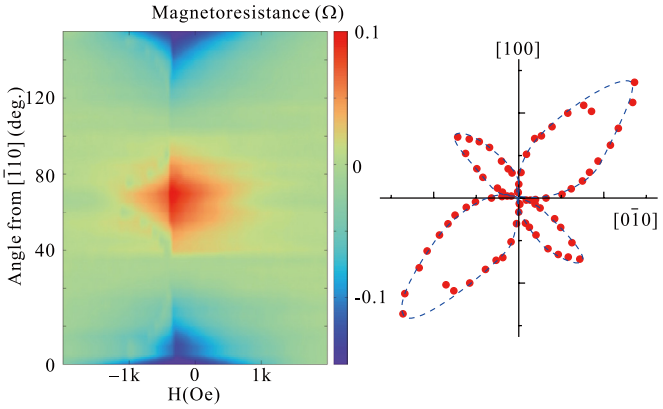

Fig. 2. Left: Color level plot of the magnetoresistance as a function of field strength and angle from [110]. The sign is reversed around [100] (45°) and [010] (90°). Right: Polar plot of magnetoresistance amplitude for the in-plane field direction.

well diode is working as an in-plane spin filter caused by the combined effect of Rashba and Dresselhaus SOIs.

Reference
[1] T. Koga, J. Nitta, H. Takayanagi, and S. Datta, Phys. Rev. Lett. **88**, 126601 (2002).

Authors
T. Nakamura, Y. Hashimoto, and S. Katsumoto

Clear Variation of Spin Splitting by Changing Electron Distribution at Non-magnetic Metal/Bi_2O_3 Interfaces

Otani Group

Edelstein effect, the spin-to-charge current interconversion at interfaces [1], has attracted much attention. An efficient interconversion at Cu/Bismuth oxide (Bi_2O_3) interface has been discovered [2, 3], which is attributed to a large Rashba splitting in the electronic state at the metal/oxide interface (see Fig. 1 (1)). However, the guiding principle of designing the metal/oxide interface with large Rashba splitting for the efficient conversion is missing. In this study, we report strong non-magnetic (NM) material dependence of spin splitting at NM/Bi_2O_3 interface and discuss the origin of the NM dependence with first-principles calculations.

We employed spin pumping technique to inject spin current into the NM/Bi_2O_3 (NM = Al, Cu, Ag, Au) interface. The injected spin current is converted to charge current by the inverse Edelstein effect (spin-to-charge conversion at the interface, see Fig. 1 (b)). We evaluated the conversion coefficient and the Rashba parameter α_R which determines the splitting in momentum between spin-up and spin-down electrons. The evaluated α_R are −0.055, −0.25, +0.15

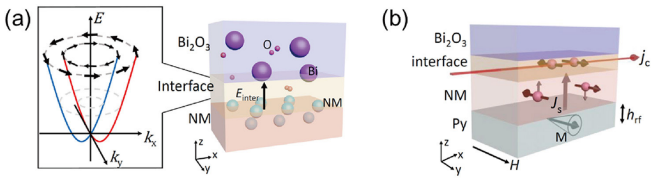

Fig. 1. (a) Rashba spin splitting at NM/Bi_2O_3 interface. (b) Schematic of spin-to-charge conversion at the NM/Bi_2O_3 interface. A spin current is injected from the Py layer into the NM/Bi_2O_3 interface, and then converted to the charge current via the inverse Edelstein effect.

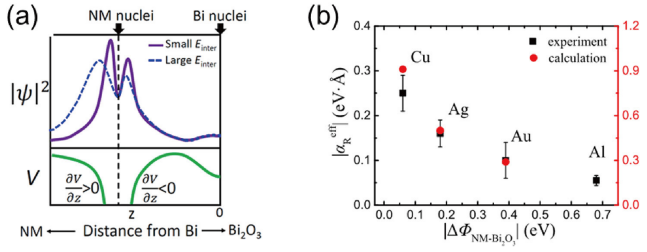

Fig. 2. (a) An asymmetry distribution of $|\Psi|^2$ generated by interfacial electric field. Purple line and blue line show the $|\Psi|^2$ under smaller and larger electric field, respectively. Green line show electrostatic potential V. (b) Absolute value of α_R estimated by the experiment and the calculation in different NM/Bi_2O_3 interfaces as a function of $|\Delta\Phi_{NM\text{-}Bi2O3}|$.

and −0.09 eV·Å for NM = Al, Cu, Ag and Au, respectively.

The Rashba parameter α_R can be described as,

$$\alpha_R = \frac{2}{c^2}\int \frac{\partial V}{\partial z}|\Psi|^2\, dz, \qquad (1)$$

where c, $\partial V/\partial z$ and $|\Psi|^2$ are the speed of light, potential gradient and electron density distribution, respectively. Schematic illustration of V and $|\Psi|^2$ at NM/Bi_2O_3 interfaces based on our ab-initio calculation is shown in Fig. 2 (a). $|\Psi|^2$ can be modulated by the out-of-plane electric field E_{inter} at the interface. Note that E_{inter} originates from work function difference $\Delta\Phi_{NM\text{-}Bi2O3}$ between NM and Bi_2O_3. The asymmetry feature of $|\Psi|^2$ which depends on E_{inter} and $\Delta\Phi_{NM\text{-}Bi2O3}$ should be important for the magnitude and the sign of α_R.

Figure. 2(b) shows $|\alpha_R|$ estimated by experiment and calculation in different NM/Bi_2O_3 as function of $|\Delta\Phi_{NM\text{-}Bi2O3}|$. $|\alpha_R|$ decreases as $|\Delta\Phi_{NM\text{-}Bi2O3}|$ increases and the trend of calculated $|\alpha_R|$ is in good agreement with the experiment. This trend can be explained as follows (see Fig. 2 (a)). $|\Psi|^2$ is strongly localized near NM nuclei when E_{inter} is small, while $|\Psi|^2$ could be shifted from nuclei and delocalized when E_{inter} is large. The steepest $\partial V/\partial z$ is located near NM nuclei. Thus, larger E_{inter} (larger $|\Delta\Phi_{NM\text{-}Bi2O3}|$) gives smaller integral in Eq. (1). The opposite sign of α_R between Ag/Bi_2O_3 and other interfaces may be explained by different sign of $\Delta\Phi_{NM\text{-}Bi2O3}$ at Ag/Bi_2O_3 from others. Assuming that Ag/Bi_2O_3 and Cu/Bi_2O_3 interfaces have similar hybridization state, the opposite direction of E_{inter} may shift the $|\Psi|^2$ to different side of NM or Bi_2O_3 and cause the sign change of the integral.

We found that the asymmetry feature of $|\Psi|^2$ which can be modulated by $\Delta\Phi_{NM\text{-}Bi2O3}$ results in strong NM dependence on α_R. Our study suggests that control of interfacial electron distribution by changing the difference in work function across the interface may be an effective way to tune the magnitude and sign of Rashba splitting and the spin-to-charge current interconversion at interface.

References
[1] J. C. R. Sánchez *et al.,* Nat. Commun. **4**, 2944 (2013).
[2] S. Karube, K. Kondou, and Y. C. Otani, Appl. Phys. Express **9**, 033001(2016).
[3] J. Kim, Y. T. Chen, S. Karube, S. Takahashi, K. Kondou, G. Tatara, and Y. Otani, Phys. Rev. B **96**, 140409(R) (2017).

Authors
H. Isshiki and Y. Otani

Modulation of Electron-Phonon Coupling in One-Dimensionally Nanorippled Graphene

Komori Group

Electron-phonon coupling plays various roles in solids such as inducing phase transitions and electron energy relaxation. In graphene, it is actually one of the dominant sources of the energy relaxation, and can be locally detected by tunneling spectroscopy with scanning tunneling microscopy as an increase of the tunneling current at the absolute value of the sample-bias voltage corresponding to the phonon energy through an inelastic tunneling (IET) process [1]. We have studied local electron-phonon coupling of a one-dimensionally (1D) nanorippled graphene (3.4 nm period) [2] .

The sample was prepared on a vicinal SiC(0001) substrate by thermal decomposition in an Ar atmosphere. Local atomic and electronic structures of the graphene were characterized using scanning tunneling microscopy/spectroscopy (STM/STS), and the phonon signals were locally detected by IET spectroscopy.

Figure 1 shows STM images of the surface, which consists of terraces and macrofacets of 27° off from the (0001) surface. The macrofacet surface is covered by continuous graphene with 1D periodic undulation. The 1D super periodicity of the graphene is evidenced by satellite band signals in the angle-resolved photoemission spectroscopy (ARPES) images of the graphene Dirac band from the macrofacet shown in Fig. 2(a). ARPES signals from the second-layer graphene were clearly observed using 40.8 eV photons as in Fig. 2 (b). Thus, the interface between surface graphene and the SiC substrate consists of alternate nanoribbons of graphene and the carbon buffer layer.

In the STS measurement, we observed IET signals due to phonons in the vertical direction of the graphene plane. The signal intensity periodically oscillates in the 1D undulation direction of graphene with the same periodicity. This means that the intensity of the inelastic scattering due to the electron-phonon interaction oscillates in the tilting direction of the macrofacet. Since the STM image of the graphene surface looks uniform, we conclude that the IET intensity oscillation is attributed to the subsurface interface layer. The tunneling electrons are easy to move from the surface graphene to the second layer graphene nanoribbon, but not

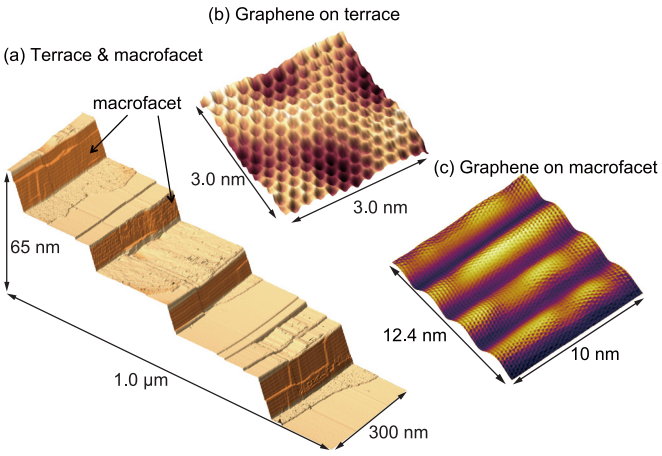

Fig. 1. STM images of graphene grown on a vicinal SiC(0001) substrate. (a) Wide image indicating terrace and macrofacet structure of the substrate. 1D undulation can be seen on the macrofacets (b) Graphene honeycomb lattice on the terrace. (c) 1D periodically-undulated graphene on the macrofacet.

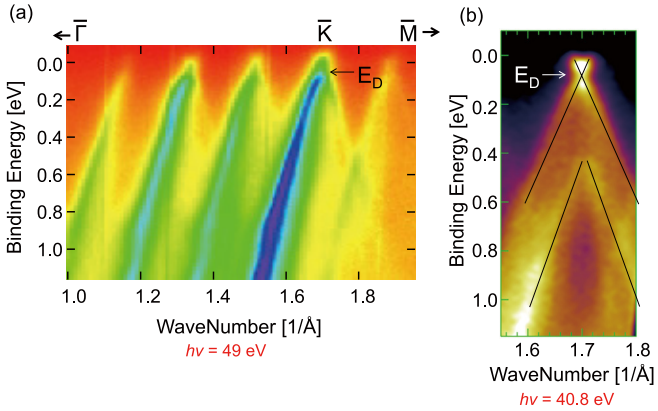

Fig. 2. ARPES spectra using 49 eV (a) and 40.8 eV (b) photons. Four replica bands are seen as well as the true graphene Dirac band in (a). The separation of the bands is consistent with the period of the 1D undulated graphene. Using 40.8 eV photons, the signal from the subsurface graphene nanoribbons was detected in (b).

to in the buffer layer because of the long interlayer distance. Due to this difference, the probability that tunnel electrons interact with the phonon system is larger on the buffer layer.

References

[1] C.-H. Kim *et al.*, Nature Phys. **4**, 213 (2008).
[2] K. Ienaga *et al.*, Nano. Lett. **17**, 3527 (2017).

Authors

K. Ienaga, T. Miyamachi, K. Yaji, K. Fukuma[a], A. Visikovsliy[a], S. Tanaka[a], and F. Komori

[a]Kyushu University

Orbital Ordering Visualized by Scanning Tunneling Microscopy

Hasegawa Group

Orbital-related physics attracts growing interest in condensed matter research and there have been reported topics ranging from orbital orders and colossal magnetoresistance to various non-trivial new phenomena, such as superconductivity mediated by orbital fluctuations, orbital Kondo effect, and ordering of multipole moments. However, orbital sensitive probes have so far proved quite limited and there has been no direct access to the real-space form of the orbitals. On the other hand, recent progress of scanning tunneling microscopy (STM) enables the orbital-selective tunneling depending on the tip-sample distance (TSD). Here, we utilize the orbital sensitivity of STM to investigate the surface of the well-known heavy fermion superconductor $CeCoIn_5$ and successfully unveil a surface-assisted cobalt *d*-orbital order with the support of first principles calculations [1]. Our finding suggests that the surface-assisted orbital ordering could be ubiquitous in transition metal oxides, heavy fermion superconductors, and other materials but has been overlooked.

Our target material $CeCoIn_5$ is naturally born at the quantum critical point having the unconventional d-wave superconducting phase below the critical temperature T_C = 2.3 K. The compound has a tetragonal structure composed of three different layers, cerium (Ce)-indium (In), In, and cobalt (Co) layers, stacked in the order of CeIn-In-Co-In-CeIn along the c axis as shown in the left panel of Fig. 1. The second highest critical temperature among heavy fermion superconductors and the availability of high-quality single

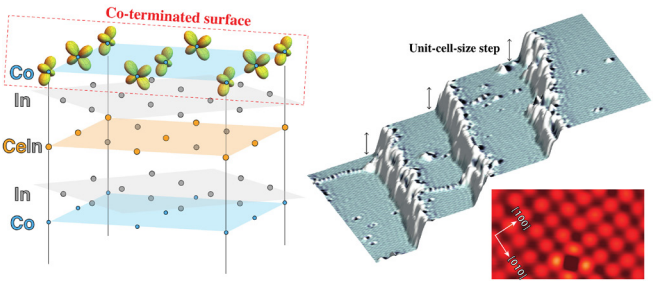

Fig. 1. (left panel) Schematic of the tetragonal crystal structure of $CeCoIn_5$ with d_{xz}-d_{yz} orbital order at the topmost cobalt plane. (right-top panel) Overview of a typical cleaved surface in this study. Narrow terraces are separated by a step of the unit cell along c axis. The topographic images are colorized with their derivatives to emphasize the atomically resolved lattice structures. (right-bottom panel) Typical atomically resolved STM image taken on the surface.

crystals make this compound the most investigated heavy fermion superconductor.

We cleaved this compound in ultra-high-vacuum condition and measured with low-temperature STM. The right-top panel of Fig. 1 is a typical overview image of the Co-terminated surface of $CeCoIn_5$. Atomically-flat terraces are separated with steps whose height are the unit-cell size along the c axis. In the normal tunneling conditions; when the tip is far away from the surface, spherical-shaped cobalt atoms are visualized on the square lattice as shown in the right-bottom panel of Fig. 1. This atomic shape is coming from states derived from the Co 4*s* orbital, which has the longer decay into the vacuum than the 3*d* orbitals. By decreasing TSD extremely to be sensitive to 3*d* orbitals, we witness drastic changes of the Co atomic shapes as shown in Fig. 2. The Co atomic shape changes from the spherical shape to the elongated dumbbell by decreasing TSD. The elongated directions are the [100] or the [010] directions, which alternate between the adjacent atomic sites. This observation is well reproduced with first principles calculations (the right side of the right panel) and interpreted as the surface-assisted d_{xz}-d_{yz} orbital ordered state.

This surface-assisted orbital order has been overlooked by surface insensitive measurement techniques and even by STM. Since we have experience in STM measurements with very small tip-sample distances [2], which is the first experiment successfully achieving point contact imaging with even smaller tip-sample distances than the present work, we were able to uncover this new phenomenon, achieving the first direct visualization of orbital order in real space. The surface-assisted orbital order is a new concept, but it is not exclusive for heavy fermion compounds. This kind of orbital order should show up in many other compounds containing orbital degrees of freedom in bulk. Therefore, our finding has

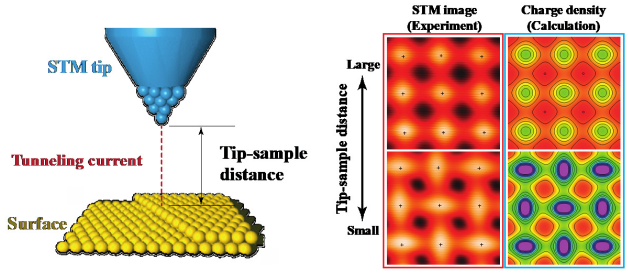

Fig. 2. STM images of Co-terminated surface with large and small tip-sample distances with corresponding calculated density-of-state mappings based on first principles calculations. The experimental observations are well reproduced with the calculations demonstrating the emergence of d_{xz}-d_{yz} orbital order on the surface.

major relevance not only in heavy fermion physics but also in the broad range of condensed matter physics and material science. Although we have yet to clarify this, there could very well be links between this orbital order and the bulk properties of the compounds. Applying this technique to the other compounds that have been investigated heavily but still poorly understood, such as URu_2Si_2, we might find a new avenue to explore unsolved mysteries.

References

[1] H. Kim, Y. Yoshida, C-.C. Lee, T.-R. Chang, H.-T. Jeng, H. Lin, Y. Haga, Z. Fisk, and Y. Hasegawa, Science Advances **3**, eaao0362 (2017).
[2] H. Kim and Y. Hasegawa, Phys. Rev. Lett. **114**, 206801 (2015).

Authors
H. Kim, Y. Yoshida, C.-C. Lee[a], T.-R. Chang[b], H.-T. Jeng[c, d], H. Lin[a], Y. Haga[e], Z. Fisk[e, f], and Y. Hasegawa
[a]National University of Singapore
[b]National Cheng Kung University
[c]National Tsing Hua University
[d]Institute of Physics, Academia Sinica
[e]Japan Atomic Energy Agency
[f]University of California, Irvine

Hole Trapping in $SrTiO_3$

Lippmaa Group

Well-known perovskite titanates such as $SrTiO_3$ and $BaTiO_3$ generally exhibit *n*-type semiconductor behavior due to the prevalence of oxygen vacancies that can form under common synthesis conditions. Each oxygen vacancy donates two electrons and in $SrTiO_3$, for example, a metallic state appears at a relatively low carrier density of about 10^{17} cm^{-3}. Besides oxygen vacancies, cation vacancies may also form in titanates. In particular, formation of *A*-site cation (Sr, Ba) vacancies is energetically favorable and leads to effective acceptor doping. It is known experimentally that the Fermi level in intrinsic $SrTiO_3$ is close to the conduction band bottom, i.e., the material is effectively an *n*-type wide-gap semiconductor, which means that compensation by acceptor-type cation vacancies is not observed and the cation defect densities must be much lower than 10^{17} cm^{-3}, which can be ignored in conventional transport analysis.

The situation is very different when optoelectronic applications are considered, where photogenerated carrier mobility, trapping, and lifetime are important parameters. The presence of cation defects needs to be considered because the presence of acceptor states close to the top of the valence band can influence hole trapping and thus the recombination rate of photogenerated non-equilibrium carriers. Unfortunately, typical optical absorption or photoelectron emission spectroscopic techniques cannot detect such low-density vacancy states. We have therefore developed a technique based on measuring the infrared quenching effect on photocurrent, which is illustrated in Fig. 1. Carriers are generated by ultraviolet light across the band gap and the photocurrent is measured as a function of temperature. The magnitude of the photocurrent is determined by the recombination rate of photocarriers, which depends on whether holes are trapped or delocalized. Hole trapping normally occurs at low temperatures in the presence of acceptor defects, reducing the recombination rate and increasing the photocurrent, as can be seen at around 35 K in Figs. 1(a,b). If a crystal is illuminated with ultraviolet and infrared light at the same time, the holes trapped at so-called sensitizing centers can

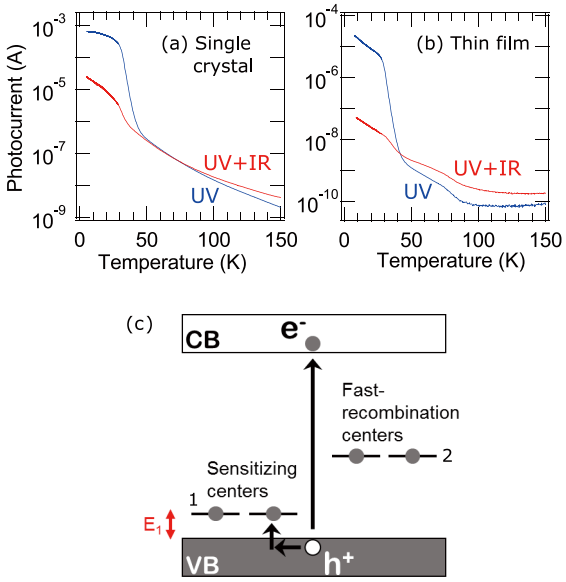

Fig. 1. Photocurrent in $SrTiO_3$ as a function of temperature under ultraviolet (UV) or simultaneous ultraviolet and infrared (UV+IR) excitation for (a) bulk crystal and (b) thin film. Infrared quenching of photocurrent can be seen below 35 K. (c) Energy level diagram illustrating the localization of photogenerated holes. Photocurrent quenching occurs when the trapped holes are released by infrared light illumination.

be detrapped and the photocurrent drops due to the increased recombination rate. The energy level diagram illustrating this mechanism is shown in Fig. 1(c). The delocalization of holes depends on the depth of the acceptor state, E_1, and the temperature. For Sr vacancy defects in $SrTiO_3$, thermal detrapping occurs between 30 K and 90 K, depending on how the crystal was grown. The value of E_1 can be obtained by fitting the photocurrent temperature dependence close to the infrared quenching transition temperature. For the $SrTiO_3$ samples used in this study, E_1 is about 60 meV.

Bulk $SrTiO_3$ crystals are grown by the Verneuil method and always contain Sr vacancies due to the high crystal growth temperature. Thin films are usually grown at much lower temperatures and it is thus not clear if the Sr vacancy density would be similar to bulk crystals or not. As shown in Fig. 1(b), the photocurrent behavior of a thin film grown at 1200°C is indeed similar to the bulk behavior and the infrared quenching effect can be clearly observed. No infrared quenching is observed in films grown at lower temperatures, but the photocurrent is also much lower due to higher density of lattice defects and strong carrier trapping.

The work shows that attempts to improve titanate lattice quality by increasing the crystal growth temperature can be counter-productive in optoelectronic applications due to the spontaneous formation of cation vacancies at higher temperatures. We demonstrate that photocurrent measurement with multiple light sources can be a simple technique for verifying the presence of cation defects that can be difficult or impossible to detect by other spectroscopic techniques [1].

References

[1] N. Osawa, R. Takahashi, and M. Lippmaa, Appl. Phys. Lett. **110**, 263902 (2017).

Authors

N. Osawa, R. Takahashi, and M. Lippmaa

Gas Exposure Effects on Monolayer Pentacene Field-Effect Transistor Studied by Using Non-Invasive Liquid-Metal GaIn Probes

Yoshinobu Group

The interactions of gaseous molecules with organic field effect transistors (OFETs) play a crucial role in the electronic transport property. Chemical interactions including oxidization are a serious issue for degradation of long-term stability of organic devices. Physical adsorption can also modify electronic states of OFETs. Gaseous molecules may diffuse into OFET film through defect sites such as grain boundaries, resulting in a change in the film structure and/or the formation of a gap state.

Recently, we have developed the non-invasive liquid-metal GaIn four-probe measurement method for the FET properties of organic monolayer and thin films [1, 2]. In this Research Highlight, we report that the electrical transport property of monolayer pentacene is highly sensitive to a small amount of exposure to O_2, N_2 and Ar gases using independently-driven four GaIn probes [2]. Liquid metal GaIn probes have been used as non-invasive conductivity electrodes for monolayer OFET films in a vacuum chamber (Fig. 1). We carried out the fabrication of monolayer pentacene and the four-probe measurement without exposure to atmospheric air. Four GaIn probes were used *in situ* to measure conductivity in the channel separately from the overall characteristics including contact resistance at the electrode probes [3].

The experimental results show that O_2 exposure of 1 L (10^{-6} Torr s) reduces mobility to 8% of the original value in the monolayer film, and the reduction is irreversible at room temperature, i.e., mobility does not recover its original value after the evacuation of gaseous molecules (Fig. 2). Since chemically inert gases of N_2 and Ar also reduce the mobility, physisorption of gaseous molecules should be involved in these gas exposure effects. For a 3 ML pentacene film, O_2 exposure also reduces its mobility, but the mobility is saturated at 70% of the original value between 10 L to O_2

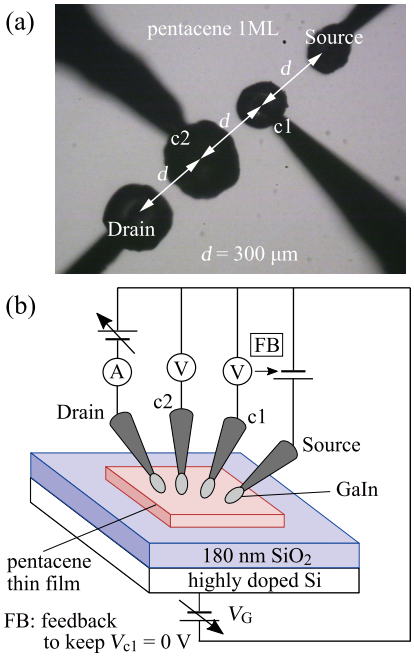

Fig. 1. (a) Optical microscope image of four GaIn probes contacted with 1 ML pentacene. (b) Schematic of the electrical circuits.

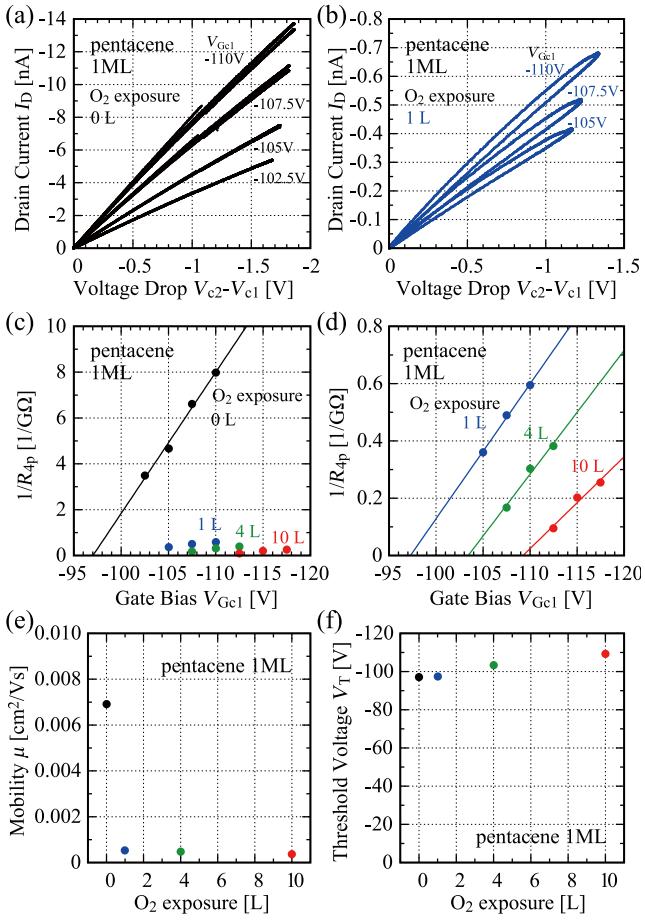

Fig. 2. Four-probe I–V curves (a) before and (b) after O_2 exposure measured with the probe alignment shown in Figure 1(a). (c) and (d) Inverse of four-probe resistance $1/R_{4p}$ as a function of gate to channel bias V_{Gc1}, respectively. (e) Estimated mobility and (f) threshold voltage.

atmosphere. Thus, we assume that physical adsorption of gaseous molecules is important for the initial gas exposure effects, because chemically inert gases of N_2 and Ar also reduced the mobility in monolayer pentacene. Taking these findings together with the results of photoelectron spectroscopy and atomic force microscopy measurements, the reduction in mobility can be attributed to the physisorption of gases at grain boundaries formed by the coalescence of pentacene monolayer islands [2].

References

[1] S. Yoshimoto, K. Takahashi, M. Suzuki, H. Yamada, R. Miyahara, K. Mukai, and J. Yoshinobu, Appl. Phys. Lett. **111**, 073301 (2017).
[2] S. Yoshimoto, R. Miyahara, Y. Yoshikura, J. Tang, K. Mukai, and J. Yoshinobu, Organic Electronics **54**, 34 (2018).
[3] S. Yoshimoto, T. Tsutsui, K. Mukai, and J.Yoshinobu, Rev. Sci. Instrum. **82**, 093902 (2011).

Authors

S. Yoshimoto, R. Miyahara, Y. Yoshikura, J. Tang, K. Mukai, and J.Yoshinobu

Large Magneto-Optical Kerr Effect and Imaging of Magnetic Octupole Domains in the Non-Collinear Antiferromagnetic Metal Mn_3Sn

Nakatsuji Group

When a polarized light beam is incident upon the surface of a magnetic material, the reflected light undergoes a polarization rotation. This magneto-optical Kerr effect (MOKE) has been intensively studied in a variety of ferro- and ferrimagnetic materials because it provides a powerful probe for electronic and magnetic properties as well as for various applications including magneto-optical recording. Recently, there has been a surge of interest in antiferromagnets (AFMs) as prospective spintronic materials for high-density and ultrafast memory devices, owing to their vanishingly small stray field and orders of magnitude faster spin dynamics compared to their ferromagnetic counterparts [1]. In fact, the MOKE has proven useful for the study and application of the antiferromagnetic (AF) state. Although limited to insulators, certain types of AFMs are known to exhibit a large MOKE, as they are weak ferromagnets due to canting of the otherwise collinear spin structure [2]. In the fully compensated collinear AFMs, where the MOKE is usually absent, quadratic magneto-optical effects such as the Voigt effect can be useful to determine the Néel vector [3]. On the other hand, recent theoretical and experimental progress has revealed that systems such as certain spin liquids and non-collinear AFMs can exhibit a large anomalous Hall effect (AHE) in zero applied magnetic field despite a vanishing magnetization [4, 5]. Because the AHE has the same symmetry requirements as the MOKE [6], it is possible that the same class of AFMs may exhibit a Kerr rotation. Thus, the recent experimental discovery of a large AHE in the non-collinear AFM Mn_3Sn [5], which is recently reported to be the first example of a Weyl magnet [7], as well as its

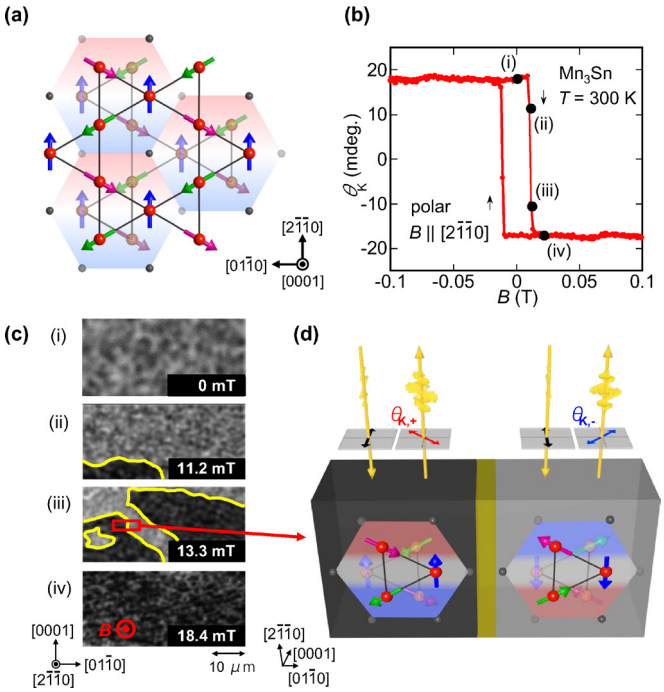

Fig. 1. (a) Cluster magnetic octupole ordering of Mn_3Sn. Large red (small dark grey) and large transparent orange (small transparent grey) spheres represent Mn (Sn) atoms forming kagome planes at $z = 0$ and 1/2, respectively. The Mn magnetic moments (arrows) lie in the (0001) plane and form an inverse triangular spin structure. Different colored arrows represent three sublattices. The spin structure on the kagome bilayers can be considered as ferroic order of cluster magnetic octupoles. (b) Field B dependence of the polar magneto-optical Kerr rotation angle θ_K for the (2$\bar{1}$$\bar{1}$0) plane in $B \parallel [2\bar{1}\bar{1}0]$. (c) Evolution of the antiferromagnetic domains of the (2$\bar{1}$$\bar{1}$0) plane as a function of $B \parallel [2\bar{1}\bar{1}0]$ ($-21\,\mathrm{mT} \le B \le 21\,\mathrm{mT}$). The imaging area is $25\,\mu\mathrm{m} \times 50\,\mu\mathrm{m}$. Grey and black regions correspond to positive and negative values of the MOKE signal. (d) Schematic illustration of two regions with different MOKE image contrasts (grey/black areas) due to opposite signs of the Kerr angles $\theta_{K,-/+}$, corresponding to two types of cluster magnetic octupole domains that have inverse triangular spin structures with opposite spin directions within the (0001) plane. The two regions should be separated by a domain wall (yellow area).

soft response to a magnetic field give promise for a potentially large MOKE character.

Mn_3Sn is a hexagonal antiferromagnet (space group: $P6_3/mmc$), which has the ABAB sequence of the Mn kagome layer along [0001] and exhibits the non-collinear AF spin structure below the Néel temperature of T_N ~ 430 K [4]. This three-sublattice AF state on the kagome bilayers can be viewed as "ferroic ordering of cluster magnetic octupoles" (Fig. 1(a)) [8]. In addition to this dominant order parameter, the moments cant slightly in the plane to produce a small net ferromagnetic (FM) moment of ~0.002 μ_B/Mn within the (0001) plane. Although the subdominant FM order is not responsible for the AHE [4] (and MOKE as we discuss below), it is essential (together with concomitant weak in-plane anisotropy) for magnetic field to control the AF spin structure. This is demonstrated, for example, by the sign reversal of the AHE using a small applied field of B ~ 15 mT within the (0001) plane, corresponding to the in-plane rotation of the Mn moments.

We carried out field-swept measurements of the polar MOKE using the Mn_3Sn $(2\bar{1}\bar{1}0)$ plane with a λ = 660 nm linearly polarized laser at 300 K. Significantly, a large zero-field Kerr rotation angle θ_K ~ 20 mdeg and a clear square hysteresis loop are observed in $B \parallel [2\bar{1}\bar{1}0]$ (Fig. 1(b)), which is comparable to the case for ferromagnetic materials. The coercive field B_C ~ 12 mT is consistent with the hysteresis curve obtained in $\rho_H(B)$, indicating that the magnetic properties at the surface are nominally identical to those in the bulk [4]. Moreover, our polar MOKE spectroscopy and first-principles calculation for the frequency dependence of the Kerr rotation $\theta_K(\omega)$ have clarified that ferroic ordering of magnetic octupoles in the non-collinear Néel state may cause a large MOKE even in its fully compensated AF state. The large MOKE signal without spin magnetization sharply contrasts with the previously known AF insulator cases where weak ferromagnetism has been believed to be essential for the presence of the MOKE. This large MOKE further allows imaging of the magnetic octupole domains and their reversal induced by B. Figure 1(c) presents a series of the polar MOKE images of the Mn_3Sn $(2\bar{1}\bar{1}0)$ plane under $B \parallel [2\bar{1}\bar{1}0]$ ($-$ 21 mT $\leq B \leq$ 21 mT) which obtained at the points (i)-(iv) in Fig. 1(b). Here, grey and black colors correspond to positive and negative values of the polar MOKE signal parallel to the $[2\bar{1}\bar{1}0]$ direction originating from the two types of the cluster magnetic octupole domain in Fig. 1(d). This is the first observation of domain reversal in an AF metal and of magnetic octupole domain reversal by MOKE microscopy [7]. The large MOKE observed in an AF metal should open new avenues for the study of domain dynamics as well as spintronics using AFMs.

References

[1] T. Jungwirth *et al*., Nat. Nanotech. **5**, 231 (2016).
[2] F. J. Kahn *et al*., Phys. Rev. **186**, 891 (1969).
[3] V. Saidl *et al*., Nat. Photon. **11**, 91 (2017).
[4] Y. Machida *et al*., Nature **463**, 210 (2010); H. Chen *et al*., Phys. Rev. Lett. **112**, 017205 (2014); N. Kiyohara, T. Tomita, and S. Nakatsuji, Phys. Rev. Applied **5**, 064009 (2016).
[5] S. Nakatsuji, N. Kiyohara, and T. Higo, Nature **527**, 212 (2015).
[6] W. Feng *et al*., Phys. Rev. B **92**, 144426 (2015).
[7] K. Kuroda and T. Tomita *et al*., Nat.Mater. **16**, 1090 (2017).
[8] T. Higo, H. Man, D. Gopman, L. Wu, T. Koretsune, O. van 't Erve, Y. Kabanov, D. Rees, Y. Li, M.-T. Suzuki, S. Patankar, M. Ikhlas, C. L. Chien, R. Arita, R. Shull, J. Orenstein, and S. Nakatsuji, Nat. Photon. **12**, 73 (2018).

Authors

T. Higo, H. Man, D. Gopman[a], L. Wu[b], T. Koretsune[c,d], O. van 't Erve[e], Y. Kabanov[a], D. Rees[b], Y. Li[f], M.-T. Suzuki[c,d], S. Patankar[b], M. Ikhlas, C. L. Chien[f], R. Arita[c,g], R. Shull[a], J. Orenstein[b], and S. Nakatsuji

[a]National Institute of Standards and Technology
[b]University of California, Berkeley
[c]RIKEN-CEMS
[d]Tohoku University
[e]U.S. Naval Research Laboratory
[f]Johns Hopkins University
[g]The University of Tokyo

Strongly Correlated Zero-Gap Semiconductor $Pr_2Ir_2O_7$

Nakatsuji Group

In the field of the solid state physics, materials exhibiting novel physical properties are vigorously explored. Zero-gap semiconductors are one fascinating group of materials where topological functionalities lead to high carrier mobility and the quantum Hall effect. It is known that electrons behave as if they are massless in materials such as graphene because of the linear band dispersion near the point where the valence and the conduction bands come in contact with each other. For graphene, new phenomena were discovered one after another and it became the subject of the Nobel Prize in Physics in 2010. So far, the physics of zero-gap semiconductors have only been studied in materials where the interaction between electrons is weak.

An example of a zero-gap structure is a Luttinger semimetal with quadratic band touching whose band dispersion is parabolic near the band touching point as illustrated in Fig. 1. It was predicted more than 40 years ago that materials in a Luttinger semimetal state would show novel electronic states because of the strong electronic correlations that are unobtainable in conventional metals. However, in materials known so far, such as α–Sn and HgTe, it has been difficult to identify experimentally the effects of electronic correlations because the effective mass of electrons is small and hence the electronic correlations are weak.

To clarify the effect of the strong electronic correlations, we focused on $Pr_2Ir_2O_7$ [1]. It is already known that $Pr_2Ir_2O_7$ is a Luttinger semimetal with quadratic band touching and that the effective mass of electrons is about 6 times larger than the mass of the free electron in vacuum [2]. We therefore carried out a terahertz spectroscopy study on the $Pr_2Ir_2O_7$ thin films and observed a very large dielectric constant of about 180 at a temperature of 5 K as shown in Fig. 2 [3]. This value is several tens of times larger than

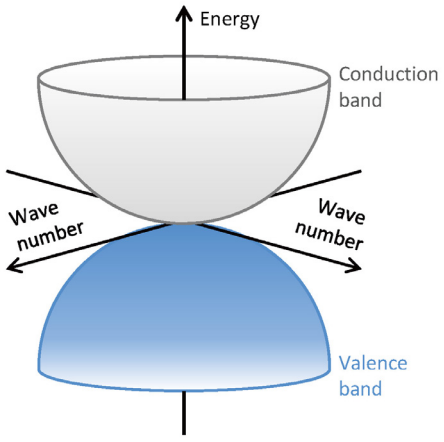

Fig. 1. Band structure of a Luttinger semimetal, which is a zero-gap semiconductor. The valence band, which is filled with electrons (blue spheres) and the empty conduction band both have a three-dimensional parabolic shape, and are in contact with each other at a single point close to the Fermi level.

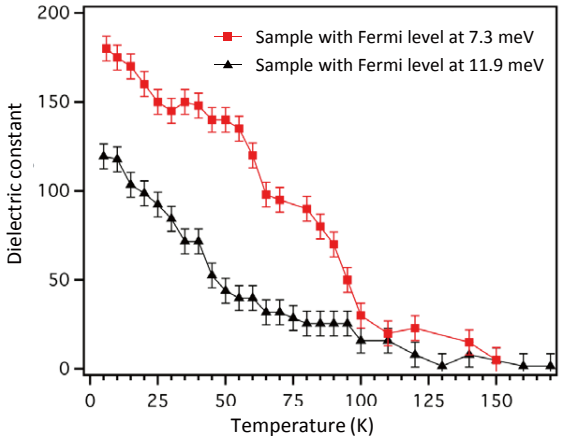

Fig. 2. Temperature dependence of the dielectric constant. The low-temperature value is several tens of times larger than that of known zero-gap semiconductors (e.g. α–Sn and HgTe). The dielectric constant becomes larger when the Fermi level approaches the band touching point.

that of zero-gap semiconductors (e.g. α–Sn and HgTe) known so far. Additionally, in a Luttinger semimetal state, the dielectric constant is a measure of the scale of electronic correlations. By using this fact, when the magnitude of the electronic correlations is estimated from the dielectric constant, the scale of electronic correlations is about 2 orders of magnitude larger than the kinetic energy.

We have thus demonstrated that electronic correlations are indeed very strong in a Luttinger semimetal with quadratic band touching. In the future, it is expected that further understanding of the role of electronic correlations in determining the physical properties of zero-gap semiconductors will lead to the creation of novel metallic states and new functional materials.

References

[1] T. Ohtsuki, Z. Tian, A. Endo, M. Halim, S. Katsumoto, Y. Kohama, K. Kindo, S. Nakatsuji, and M. Lippmaa, arXiv:1711.07813 (2017).
[2] T. Kondo, M. Nakayama, R. Chen, J. J. Ishikawa, E.-G. Moon, T. Yamamoto, Y. Ota, W. Malaeb, H. Kanai, Y. Nakashima, Y. Ishida, R. Yoshida, H. Yamamoto, M. Matsunami, S. Kimura, N. Inami, K. Ono, H. Kumigashira, S. Nakatsuji, L. Balents, and S. Shin, Nat. Commun. **6**, 10042 (2015).
[3] B. Cheng, T. Ohtsuki, D. Chaudhuri, S. Nakatsuji, M. Lippmaa, and N. P. Armitage, Nat. Commun. **8**, 2097 (2017).

Authors
T. Ohtsuki, B. Cheng[a], D. Chaudhuri[a], S. Nakatsuji, M. Lippmaa, and N. P. Armitage[a]
[a]Johns Hopkins University

Large Anomalous Nernst Effect at Room Temperature in a Chiral Antiferromagnet

Nakatsuji Group

The anomalous Nernst effect (ANE) is the thermoelectric counterpart to the anomalous Hall effect (AHE), that is, when one applies thermal gradient to a ferromagnetic conductor, spontaneous voltage drop will appear perpendicular to both the applied heat current and the direction of the magnetization. In earlier studies, these two phenomena have been considered to be proportional to the magnetization. However, modern theory of transport properties based on Berry phase has opened up the possibilities of observing anomalous transport effects in materials with zero net magnetization, such as in antiferromagnets (AFM) [1].

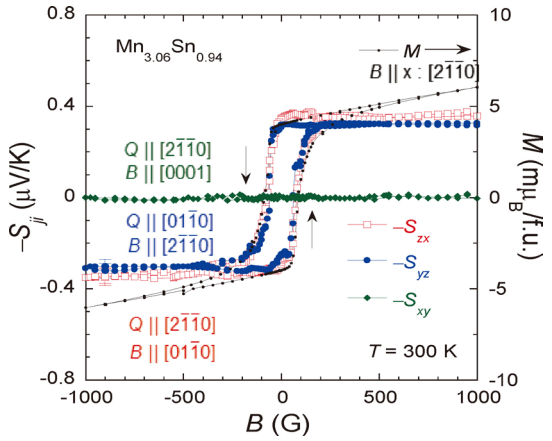

Fig. 1. Anisotropic magnetic field dependence of the Nernst signal S_{ji} ($i, j = x$: [2$\bar{1}\bar{1}$0], y: [01$\bar{1}$0], z: [0001]) in Mn_3Sn.

Mn_3Sn is a metallic AFM crystallizing in the hexagonal structure, with Mn atoms forming a kagome lattice in the *ab* plane that is stacked along the *c*-axis. Below the Neel temperature of 430 K, Mn spins undergo a transition from a paramagnetic state to a non-collinear, inverse triangular spin structure [2]. The orthorhombic symmetry of this magnetic orders permits an exceedingly tiny in-plane spontaneous magnetization ~ $2m\mu_B$/Mn to appear, the direction of which can be controlled by a small magnetic field of ~ 200 Oe. Experimentally, Mn_3Sn exhibits large anomalous Hall conductivity in this non-collinear phase, the first case for AFM [3]. In this study, we measured magneto-thermoelectric transport of two off-stoichiometric Mn_3Sn single crystals with slightly different compositions, $Mn_{3+x}Sn_{1-x}$ (x = 0.06 and x = 0.09). We found that for $Mn_{3.06}Sn_{0.94}$, the anomalous Nernst coefficient S_{zx} is 0.35 μV/K at room temperature (Fig. 1) and reaches 0.6 μV/K at 200 K [4], comparable to the maximum value measured for ferromagnetic metal [5]. This Nernst coefficient is around 100 times larger than what we would naively expect based on the size of its magnetization (Fig. 2).

The anomalous Nernst coefficient S_{zx} is governed by the transverse thermoelectric conductivity α_{zx}, which is related to the Hall conductivity σ_{zx} through the Mott relation. From this relation, we can infer that ANE can be enhanced when the Berry curvature takes a large value in the vicinity of E_F. First-principles calculations suggest the existence of Weyl nodes around $E \approx E_F + 60$ meV at which the Hall conductivity peaks. Moreover, the Mn off-stoichiometry is predicted to provide electron carriers that shift E_F towards the location of the Weyl nodes, which may account for the difference in the magnitude and temperature dependence of the σ_{zx} and α_{zx}

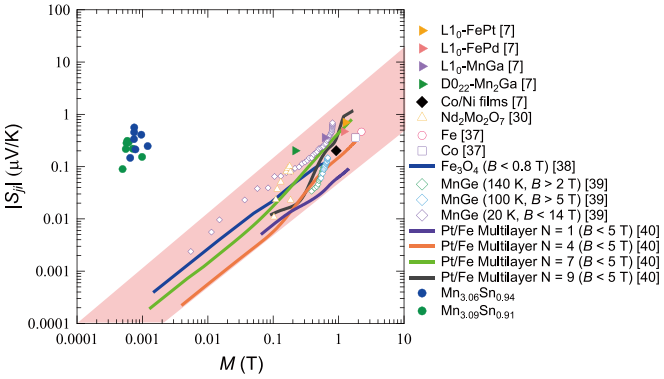

Fig. 2. Magnetization dependence of the spontaneous Nernst signal $|S_{ji}|$ for various ferromagnets and Mn_3Sn. References for each listed materials can be found in [4].

between the two measured single crystals.

From a practical standpoint, the anomalous Nernst effect may become useful as the orthogonal orientation between the voltage output and the input heat current allows the construction of thermoelectric module much simpler than the usual pillar-like design utilizing the Seebeck effect. In spite of the small magnitude of the ANE observed in this material, our study may provide a guide for the search of materials more suitable for future thermoelectric power generation.

References

[1] M.-T. Suzuki, T. Koretsune, M. Ochi, and R. Arita, Phys. Rev. B. **95** (2017).
[2] T. Nagamiya, and Y. Yamaguchi, Solid State Commu. **42** (1982).
[3] S. Nakatsuji, N. Kiyohara, and T. Higo, Nature **527** (2015).
[4] M. Ikhlas, T. Tomita, T. Koretsune, M.-T. Suzuki, D. Nishio-Hamane, R. Arita, Y. Otani, and S. Nakatsuji, Nat. Phys. **13** (2017).
[5] K. Hasegawa, M. Mizuguchi, Y. Sakuraba, T. Kamada, T. Kojima, T. Kubota, S. Mizukami, T. Miyazaki, and K. Takanashi, Appl. Phys. Lett. **106** (2015).

Authors

M. Ikhlas, T. Tomita, T. Koretsune[a], M.-T. Suzuki[a], D. Nishio-Hamane, R. Arita[a], Y. Otani, S. Nakatsuji
[a]RIKEN-CEMS

Effects of Pressure and Magnetic Field on Superconductivity in $ZrTe_3$: Local Pair-Induced Superconductivity

Uwatoko Group

Up to now, the coexistence and competition between charge density waves (CDWs) and superconductivity (SC) have attracted much attention in transition-metal di- and trichalcogenides. Among these compounds, $ZrTe_3$ shows the highly anisotropic SC transition, where the resistance along the a axis, R_a, is reduced at 4 K but those along the b axis, R_b, and c' axis, $R_{c'}$ are reduced at 2 K. This unusual behavior can be explained by two scenarios, conventional superconducting fluctuation and SC induced by locally bound electron pairs (local pairs). In the former, the reduction in R_a is attributed to a fluctuation in the bulk SC enhanced by the low dimensionality. In the latter, the transitions of R_a and $R_{b,c'}$ correspond to filamentary (highly one dimensional: 1D) and bulk (3D) SC, which originate from the formation of local pairs, namely bi-polarons, and Cooper pairs induced by the transfer of the local pairs, respectively. However, at this moment, it remains unclear which interpretation is acceptable.

In this work [1], to understand SC in more detail, we discuss the influence of pressure and the magnetic field on the SC, as determined via R_a and R_b measurements. In the measurements, the samples with different current configurations were mounted on the same sample holder and piston-cylinder-type cell, and the data were simultaneously taken.

Figures 1 (a) and (b) show the R_a and R_b at various pressures in the low temperature region, respectively. For P = 0 GPa, the R_a drops to zero at 2.2 K, while the R_b decreases to zero at 1.4 K. The highly anisotropic SC transitions are reflected by 1D and bulk nature of the SC. A P-T phase diagram can be constructed from the data, as shown in Fig. 1(c). Strikingly, the Tc of the bulk SC also decreases in the same manner as that of the 1D SC. This means that the origin of the bulk SC can be related to that of the 1D SC.

To investigate the connection between 1D and bulk SC

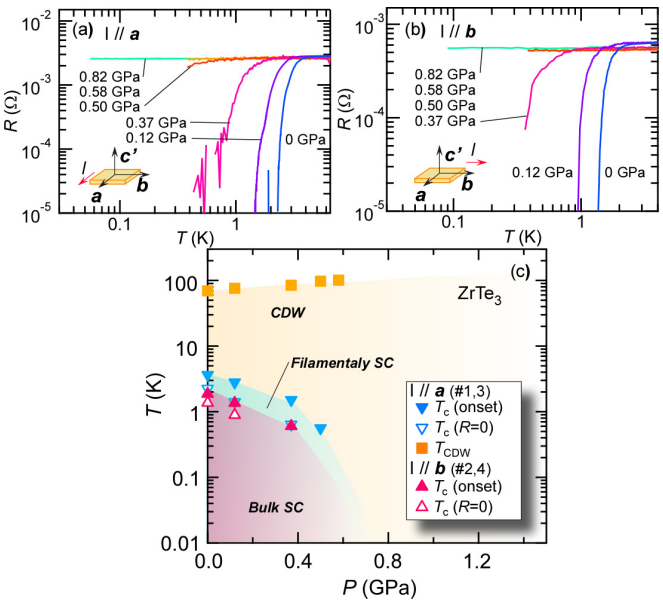

Fig. 1. (a),(b): Temperature dependence of the R_a and R_b at various pressures. (c): P-T phase diagram of $ZrTe_3$. The blue and red triangles are T_c obtained from the R_a and R_b measurements, respectively.

further, we show that the pressure dependence of H_{c2} of the 1D SC is similar to that of the bulk SC. These similarities indicate that the origin of the bulk SC can be related to that of the 1D SC. Moreover, in analysis of the excess conductivity, our results are in good agreement with the 1D Aslamazov-Larkin model rather than the 3D model, for both the I configurations, suggesting that the conventional fluctuation theory is not appropriate for our data. These findings favor the local-pair-induced SC scenario rather than conventional SC. According to the local-pair induction scenario, 1D SC is attributed to the formation of local pairs owing to a peculiar electronic structure after the CDW transition. The formation of the ordinary Cooper pairs in the bulk SC is induced by the transfer of the local pairs in addition to the 1D SC. This mixing of two kinds of SC, that is, the unconventional mechanism of the bulk SC increases the complexity of the fluctuation phenomena, which may explain the unusual excess conductivity. Moreover, this picture is consistent with the previous studies, such as anomalous behavior of the specific heat [2].

References

[1] S. Tsuchiya, K. Matsubayashi, K. Yamaya, S. Takayanagi, S. Tanda, and Y Uwatoko, New J. Phys. **19**, 063004 (2017).
[2] K. Yamaya, S. Takayanagi, and S. Tanda, Phys. Rev. B **85**, 184513 (2012).

Authors

S. Tsuchiya[a], K. Matsubayashi[b], K. Yamaya[a], S. Takayanagi[a], S. Tanda[a,c] and Y. Uwatoko
[a]Hokkaido University
[b]The University of Electro-Communications
[c]Center of Education and Research for Topological Science and Technology, Hokkaido University

High-T_c Superconductivity in FeSe at High Pressure: Dominant Hole Carriers and Enhanced Spin Fluctuations

Uwatoko Group

The Fermi surface (FS) topology and its interplay with magnetism have been considered key ingredients in under-

standing the mechanism of the iron-based high-T_c superconductors. For the FeAs-based superconductors, the FS typically consists of hole and electron pockets near the Brillouin zone center and corners, respectively. As such, an interband scattering between the hole and electron pockets has been proposed as an important mechanism for electron pairing in the iron-based superconductors, leading to an $s_{\pm}$ pairing state favored by the antiferromagnetic fluctuations. This picture, however, is challenged by the observed distinct FS topology in the FeSe-derived high-T_c (> 30 K) superconductors, including $A_xFe_{2-y}Se_2$ (A = K, Cs, Rb, Tl), (Li,Fe)OHFeSe, and monolayer FeSe film, in which only the electron pockets are observed near the Fermi level. Therefore, the distinct FS topology between FeAs- and FeSe-based materials has challenged current theories on a unified understanding of the mechanism of iron-based superconductors.

In contrast to electron-doping approaches, the application of high pressure does not introduce extra electron carriers, yet can still enhance T_c of bulk FeSe from 8 K to 38 K near 6 GPa. Our recent high-pressure study on FeSe has shown explicitly that the optimal T_c is achieved when the long-range antiferromagnetic order just vanishes, reminiscent of the situations seen frequently in the FeAs-based superconductors [1]. To make this connection, it is important to have information about the evolution of the FS under high pressure—a regime in which ARPES experiments are impractical, and where quantum oscillation measurements are challenging. Alternatively, we measured the Hall effect under hydrostatic pressures up to 8.8 GPa with the cubic anvil cell technique to gain further insights into the electronic structure evolution of FeSe at high pressure.

The main results are summarized in the phase diagram of Fig. 1. Our results demonstrate that the electrical transport properties of FeSe at high pressures with T_c^{max} = 38.3 K are dominated by the hole carriers, which is in contrast with the known FeSe-derived high-T_c superconductors that are usually heavily electron doped. In addition, we observed an enhancement of Hall coefficient R_H near the critical pressure where the optimal T_c is realized with a simultaneous suppression of the long-range magnetic order. This implies a strong reconstruction of the Fermi surface due to antiferromagnetic order, consistent with the ordering pattern driven by inter-

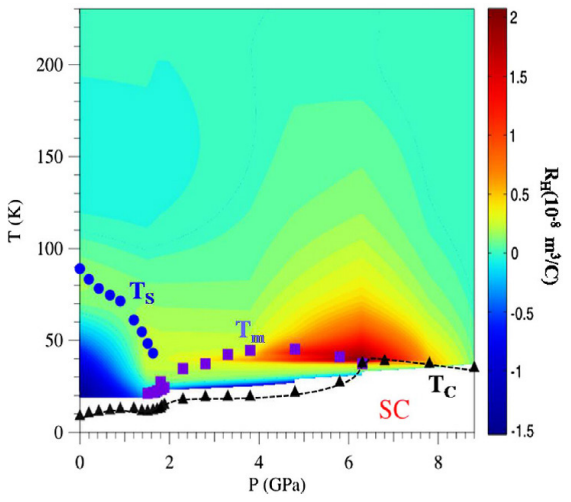

Fig. 1. Phase diagram and Hall coefficient of FeSe. Temperature-pressure phase diagram of FeSe is superimposed by a contour plot of Hall coefficient R_H, which is defined as the field derivative of ρ_{xy}, $R_H \equiv d\rho_{xy}/dH$, at the zero-field limit at each temperature and pressure. The structural (nematic) transition (T_s), pressure-induced magnetic transition (T_m), and superconducting (SC) transition (T_c) have been determined by the resistivity measurements under pressure [1]. The dashed curve is a guide for the eyes.

band scattering. Importantly, their results show a continuous path to high-T_c superconductivity in chalcogenides without electron doping.

Thus, our present work can be considered as a significant step forward in making a unified picture on the current understanding of iron-based high-T_c superconductors, specifically by demonstrating that high Tc in FeSe can be achieved with an electronic structure and other characteristics similar to the FeAs-based high-T_c superconductors.

References

[1] J. P. Sun, K. Matsuura, G. Z. Ye, Y. Mizukami, M. Shimozawa, K. Matsubayashi, M. Yamashita, T. Watashige, S. Kasahara, Y. Matsuda, J.-Q. Yan, B.C. Sales, Y. Uwatoko, J.-G. Cheng, and T. Shibauchi, Nature Commun. **7**, 12146 (2016).

[2] J. P. Sun, G. Z. Ye, P. Shahi, J.-Q. Yan, K. Matsuura, H. Kontani, G. M. Zhang, Q. Zhou, B. C. Sales, T. Shibauchi, Y. Uwatoko, D. J. Singh, and J.-G. Cheng, Phys. Rev. Lett. **118**, 147004 (2017).

Authors

J. P. Sun[a], G. Z. Ye[a,b], P. Shahi[a], J.-Q. Yan[c], K. Matsuura[d], H. Kontani[e], G. M. Zhang[f], Q. Zhou[b], B. C. Sales[c], T. Shibauchi[d], Y. Uwatoko, D. J. Singh[g], and J.-G. Cheng[a]

[a]Institute of Physics, Chinese Academy of Sciences
[b]Yunnan University,
[c]Oak Ridge National Laboratory
[d]The University of Tokyo
[e]Nagoya University
[f]Tsinghua University
[g]University of Missouri

Pressure induced Bulk Superconductivity in a Layered Transition-Metal Dichalcogenide 1*T*-Tantalum Selenium

Uwatoko Group

Charge density wave (CDW) and superconductivity (SC) are two low-energy collective excitations in condensed matter physics. The periodic electron density modulations of CDWs and the anisotropic energy gaps at Fermi surface generates multiple commensal electronic orders, either compete or cooperate. The resultant electronic phase

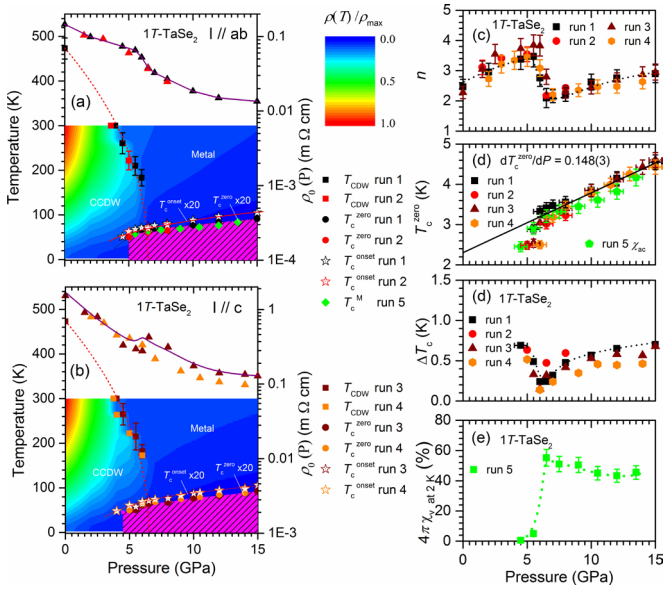

Fig. 1. *T*-*P* diagram and the colors describe the evolution of resistivity; the residual resistivity ρ_0 is estimated by fitting $\rho = \rho_0 + AT^n$ up to 20 K. The dashed red line, the red line, the triangle points represent the trend of T_{CDW}, T_c^{onset}, and ρ_0; the parameters versus pressure: (c) the exponent n, (d) T_c^{zero} and T_c^M, (e) ΔT_c, (f) $4\pi\chi_v$ (2K).

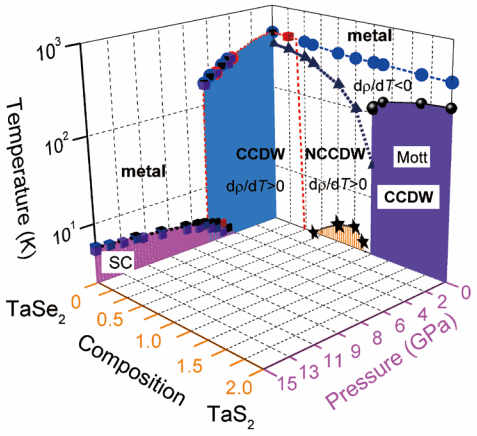

Fig. 2. Phase diagram of 1*T*-$TaSe_2$ in temperature, pressure, and composition. Here, the $d\rho/dT$ is the differential coefficient of resistivity. The red dished line separates the CCDW and NCCDW and the triangle symbols divide the negative and positive $d\rho/dT$.

diagrams have been devoted extensive efforts by controlling external stimulations to reveal the intrinsic physics.

Layered transition-metal dichalcogenides (TMDs) have been studied for nearly 50 years, but the key factors on the interplay of CDW and SC are far from clear. In one case, the superconducting transition temperature assumes a dome-like shape close to the collapsed CDWs; while in other cases, T_c changes insensitively and/or increases monotonously without domes. In former, the superconducting dome resembles that of unconventional SC neighboring quantum critical point. One scenario is proposed that CDW fluctuation glues superconducting pairs since CDW and SC originate from Fermi surface instabilities and electron-phonon coupling. Howbeit, an opposite scenario is argued that CDW is weakly connected to SC (e.g., 1*T*-TaS_2) in 1*T*-TMDs, and the dome-shaped superconducting diagram is far from CDW, which tally with the evidences of conventional single-gapped *s*-wave SC. Additionally, superconducting diagram and the coexisting model of CDW and SC depends on tuning routes even from the same starting point. Some argue that CDW and SC coexist on a macroscopic scale in real space, while others support that the insulating CDW domain walls coexist with superconducting interdomains. It implies that the SCs are distinct in superconducting diagrams generated by different parameters, and the coexisting model of CDW and SC is essential to understand the superconducting mechanism.

1*T*-$TaSe_2$, with a higher commensurate CDWs transition temperature ~ 473 K and a larger unit-cell volume compared to isostructural compounds, has attracted our attention as a starting point to explore SC and reveal the interplay of CDW instability and SC by pressure. In this work, we report a pressure-driven SC in the vicinity of CCDW in TMDs 1*T*-$TaSe_2$ by resistivity and ac susceptibility. The superconducting phase enters at 4.5 GPa and bulk SC emerges along with the collapse of CCDW at a critical pressure P_c ~ 6.5 GPa. Higher than P_c, T_c keeps increasing linearly, without a dome-shaped superconducting diagram in our pressure range. T_c reaches ~ 5.3 K at 15 GPa. The comprehensive analysis shows that electronic correlations of CCDW phase open energy gaps, which prohibits coopers pairing; while the superconducting channels and CCDW domain wall coexist in three-dimensions above P_c. The evolutions of Fermi surface and the softening of phonon models under pressure are proposed to explain the monotone increase of T_c. The findings reveal the interplay of CCDW and SC in 1*T*-$TaSe_2$ by a clean method viz. high-pressure, and shed light on the underlying superconducting mechanism in the relevant systems.

Reference

[1] B. S. Wang, Y. Liu, K. Ishigaki, K. Matsubayashi, J. -G. Cheng, W. J. Lu, Y. P. Sun, and Y. Uwatoko, Phys. Rev. B. (rapid) **95**, 220501(R) (2017)

Authors

B. S. Wang[a], K. Ishigaki, K. Matsubayashi, Y. Liu[a], W. J. Lu[a], Y. P. Sun[a,b], J.-G. Cheng[c], and Y. Uwatoko

[a]Institute of Solid State Physics, CAS

[b]High Magnetic Field Laboratory, CAS

[c]Institute of Physics, CAS

Bilayer Sheet Protrusions and Vesicle Budding Induced by Chemical Reactions

Noguchi Group

In living cells, membrane composition continually changes by lipid metabolism. However, the effects of non-constant membrane composition on shape transformations of cells are not understood so well. We have studied membrane shape transformations under hydrolysis and condensation reactions using dissipative particle dynamics simulation [1]. The hydrolysis and condensation reactions result in the formation and dissociation of amphiphilic molecules, respectively as shown in Fig. 1. Because the dissociated hydrophilic and hydrophobic molecules are typically dissolved in surrounding fluids and embedded in the bilayer, we refer to them as the hydrophilic solute (HS) and embedded oil (EO), respectively.

Asymmetric reactions between the inner and outer leaflets of a vesicle can transport amphiphilic molecules

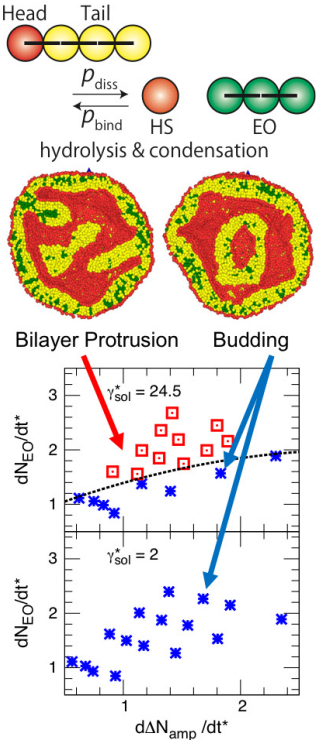

Fig. 1. Top: Schematic picture of hydrolysis and condensation reactions. Middle: Snapshots of bilayer sheet protrusions (BP) and budding of vesicles. Bottom: Dynamic phase diagram of shape transformations for the increase rate of the amphiphilic molecular number difference, $\Delta N_{amp} = N_{amp,\,out} - N_{amp,\,in}$ between the inner and outer leaflets and the EO synthesis rate dN_{EO}/dt at high viscosity (γ^*_{sol} = 24.5) and low viscosity (γ^*_{sol} = 2) of the surrounding fluid at a low reduced volume.

between the leaflets via EO diffusion. We consider high HS density in the inner fluid of the vesicle and investigate how the transport into the inner leaflet changes the membrane shapes. We found that the resulting area difference between the two leaflets induces bilayer sheet protrusion (BP) and budding at low reduced volumes of the vesicles (see the snapshots in Fig. 1), whereas BP only occurs at high reduced volumes. The probabilities of these two types of transformations depend on the shear viscosity of the surrounding fluids compared to the membrane as well as the reaction rates. For high surrounding fluid viscosity, BP formation occurs at high reaction rates, but for low viscosity, budding always occurs before BP formation (see the bottom graphs in Fig. 1). In the budding, the membrane mainly moves normal to the membrane surface, but sliding between two leaflets occurs in BP formation. Thus, the viscosity of the surrounding fluids affects budding more than it does BP formation, while the viscosity in the membrane affects BP formation more. The inhomogeneous spatial distribution of the hydrophobic reaction products forms the nuclei of BP formation, and faster diffusion of the products enhances BP formation. Our results revealed that adjustment of the viscosity is important to control membrane shape transformations.

Reference
[1] K. M. Nakagawa and H. Noguchi, Soft Matter **14**, 1397 (2018).

Authors
K. M. Nakagawa and H. Noguchi

Structure of Critical Gel Clusters Formed by Tetra-Functional Polymers

Shibayama Group

Critical gel clusters are polymer clusters about to become a gel. With a bit more reaction, the critical clusters percolate the system and system changes from fluid "sol" to solid "gel". Polymer gels can be synthesized by various chemical methods: radical polymerization of monomers and crosslinkers, crosslinking the side groups of linear polymer chains by cross-linkers or by irradiation of γ-rays, coupling end-groups of star polymers, etc. Although there are many different reaction schemes to synthesize gels and different network structure are formed depending on the synthesis

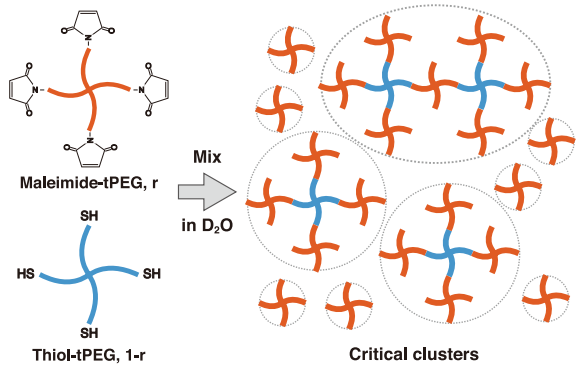

Fig. 1. Schematic for preparation of critical clusters from two different tetra-PEG units carrying mutual reactive end-groups. The excess red polymers cover the surface of the clusters and the reaction automatically stops. With one addition blue units, the clusters will percolate the system. Reprinted with permission from SANS Study on Critical Polymer Clusters of Tetra-Functional Polymers, Xiang Li, Kazu Hirosawa, Takamasa Sakai, Elliot P. Gilbert, and Mitsuhiro Shibayama, Macromolecules 2017 50 (9), 3655-3661. Copyright 2018 American Chemical Society.

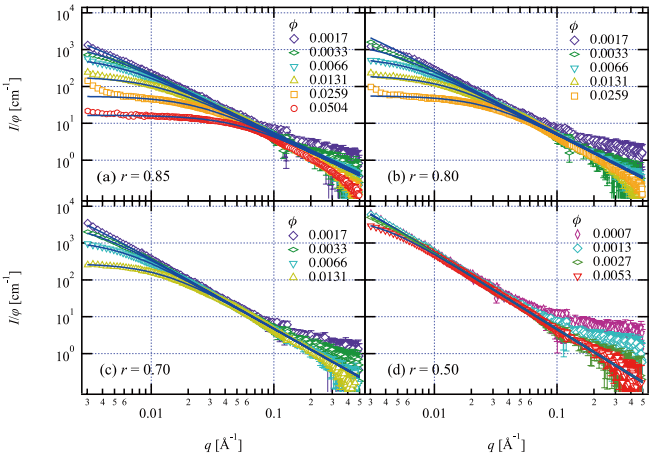

Fig. 2. Scattering profiles of various critical clusters based on the 2D sol-gel phase diagram (a, r=0.85; b, r=0.80; c, r=0.70; d, r=0.5). The profiles of the dilution of each clusters-solution are also shown. The blue curves show the fitting curves of the Bastide-Candau model for scattering profiles of critical clusters solution with finite polymer concentration. Reprinted with permission from SANS Study on Critical Polymer Clusters of Tetra-Functional Polymers, Xiang Li, Kazu Hirosawa, Takamasa Sakai, Elliot P. Gilbert, and Mitsuhiro Shibayama, Macromolecules 2017 50 (9), 3655-3661. Copyright 2018 American Chemical Society.

schemes, a set of universal scaling laws are commonly observed near the gel point, including size-distribution, weight-averaged molecular weight, correlation length.

Although those scaling laws of critical clusters have already been well studied, most of the studies only focused on reaction-conversion-limited clusters (1D phase diagram). The sol-gel phase diagram indeed has three variables: the polymer (or monomer) concentration (φ), the crosslinker density and the reaction conversion. The lack of studies based on the multi-dimension phase diagram is due to poor reproducibility in forming critical clusters, and difficulty in controlling the polymer concentration and crosslinker density.

Recently, we have successfully synthesized a new type of critical clusters by mixing two different types of tetra-armed poly(ethylene glycol) polymers (tetra-PEGs) with mutual reactive end-groups by offstoichiometric molar ratios (r, r = 0.5 denotes equal stoichiometric ratio) (Fig. 1). By changing the polymer concentration and the molar ratio of two tetra-PEGs (= crosslinker density), we can easily draw a 2D-phase diagram of the critical clusters. Here, we report the structure of these critical clusters studied by means of small angle neutron scattering (SANS) [1-2].

Figure 2 shows the normalized scattering intensity (I/φ) for different critical clusters formed based on the 2D-phase diagram. The normalized scattering intensity (I/φ) converged at the q-range of the size of prepolymers ($q > 0.1$Å^{-1}) because all the polymer clusters are formed with the same prepolymers. The slight upper deviation of low concentration sample are due to the low couniting statistics of scattered neutrons. In the q-range of the size larger than a prepolymer ($q < 0.1$Å^{-1}), the SANS profiles are well reproduced by the Bastide-Candau model, which is designed for the scattering of critical gel clusters at finite concentration regime. The fractal dimension (D_s) of swollen critical clusters and the size-distribution exponent (Fisher exponent, τ) were estimated from the fitting parameters. D_s was a unique value (= 2.0 ± 0.1) irrespective of preparation condition while the values of τ increased from 1.90 to 2.25 with deviating r from the stoichiometric ratio (r = 0.5), suggesting that smaller polymer clusters tend to be formed

in off-stoichiometric ratio. This study clearly shows that the fractal structure of the critical clusters is universal irrespective of the synthesized condition, while the size-distribution of critical clusters is a tunable parameter, which was unexpected by the classical percolation theory.

References

[1] X. Li, K. Hirosawa, T. Sakai, E. P. Gilbert, and M. Shibayama, Macromolecules **50**, 3655 (2017).
[2] K. Hayashi, F. Okamoto, S. Hoshi, T. Katashima, D. C. Zujur, X. Li, M. Shibayama, E. P. Gilbert, U.-I. Chung, S. Ohba *et al.*, Nat. Biomed. Eng. **1**, 0044 (2017).

Authors

X. Li and M. Shibayama

Dynamics of Alkylammonium-Based Ionic Liquids with Plastic-crystalline Phases

Yamamuro Group

One of the characteristic and interesting features of ionic liquids (ILs) is nanometer-sized structure (nanostructure). For example, imidazolium-based ILs (ImILs) have nanostructures consisting of the polar-domains with imidazolium rings and anions and the non-polar domains with alkyl-chains of the cations. We have revealed that the nanostructure is essentially the same as that of a liquid-crystalline (LC) phase [1-3, 5] and investigated the dynamics of ImILs by means of quasielastic neutron scattering (QENS) [1, 2, 4, 5]. Recently, Yamada et al. found that some of alkylammonium-based salts, which are another popular ILs, have plastic-crystalline (PC) phases that are the counterparts to the LC phase; i.e., the LC phase has an orientationally-ordered positionally-disordered structure, while the PC phase has an orientationally-disordered positionally-ordered one.

We have measured the DSC, neutron diffraction (ND) and QENS data of methyldiethylisopropyl-ammonium bis (trifluoromethylsulfonyl)imide (abbreviated as N_{1223}·Tf_2N) and the methyl-ethylpropylisopropylammonium salt (N_{1233}·Tf_2N) in a temperature range between 4 and 400 K. The former cation is more spherical and non-chiral while the latter more ellipsoidal and chiral. The DSC and ND works revealed that both of two samples have, in the order of deceasing temperature, liquid (L), PC1, PC2 and crystalline (C) phases; PC1 may be a normal isotropic PC phase and PC2 an anisotropic PC phase where the cations undergo more restricted rotations. The QENS data were collected in a

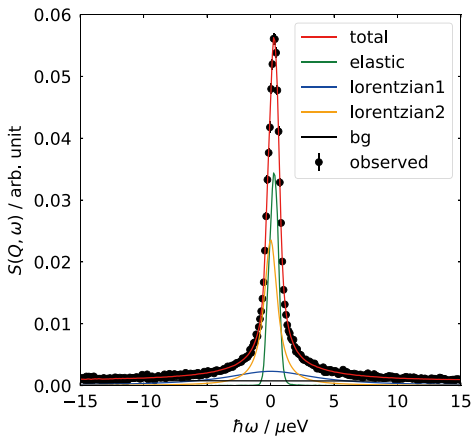

Fig. 1. The experimental QENS spectrum (closed circles) of the PC1 phase of N_{1233}·Tf_2N obtained by HFBS. The result of the fitting, a fitted curve and each component, is also shown in the figure.

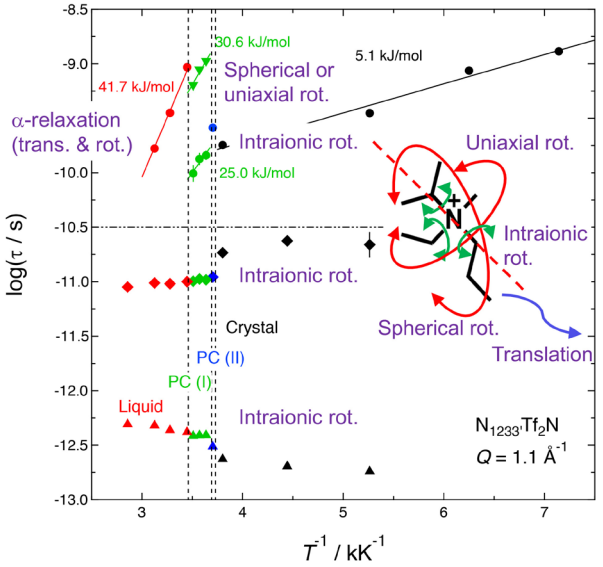

Fig. 2. Arrhenius plot of N_{1233}·Tf_2N and assignment of each relaxation mode. The structure of N_{1233}· cation and possible intraionic and overall motions are schematically shown in the inset.

time range between 0.1 ps and 10 ns by means of HFBS and DCS spectrometers in NIST, USA.

As a representative result, Fig. 1 shows the QENS data for the PC1 phase of N_{1233}·Tf_2N which were obtained at 1.1 $Å^{-1}$ and 280 K by using HFBS. The data for the PC and C phases were fitted to an elastic and two Lorentz functions, while those for the L phase to a KWW function. As shown in Fig. 1, the fittings were satisfactory for all Q and T data of both N_{1223}·Tf_2N and N_{1233}·Tf_2N. Figure 2 shows the Arrhenius plot of N_{1233}·Tf_2N. In a wide time-range covering 4 orders of magnitude, there are basically 4 relaxation modes in the PC phases and 3 modes in L and C phases. Faster two modes are almost continuous over whole temperature. By analyzing the Q-dependence of the relaxation times and elastic incoherent structure factors (EISF), the relaxation modes were assigned as shown in Fig. 2. The faster two (for the L phase) or three (for the PC and C phases) modes are clearly of intraionic rotations. The slowest mode in the PC phases is due to the spherical and/or uniaxial rotation. The slowest mode in the L phase is the α relaxation consisting of coupled overall rotational and translational motions. A similar mode assignment was performed for N_{1223}·Tf_2N. Thus, our QENS work has clarified how the intra- and overall ionic motions are activated through the sequential phase transitions (L-PC1-PC2-C).

References

[1] O. Yamamuro *et al.*, J. Chem. Phys. **135**, 054508 (2011).
[2] M. Kofu *et al.*, J. Phys. Chem. B **117**, 2773 (2013).
[3] F. Nemoto *et al.*, J. Phys. Chem. B **119**, 5028 (2015).
[4] M. Kofu *et al.*, J. Chem. Phys. **143**, 234502 (2015).
[5] F. Nemoto *et al.*, J. Chem. Phys., submitted.

Authors

O. Yamamuro, M. Nirei, M. Kofu[a], M. Matsuki[b], T. Yamada[b], and M. Tyagi[c,d]
[a]J-PARC
[b]Kyushu University
[c]NIST
[d]University of Maryland

Novel Magnetoelectric Phase in Multiferroic $BiFeO_3$

Tokunaga Group

Simultaneous emergence of multiple "ferroic" orders, such as (anti)ferromagnetism, ferroelectricity, and ferroelasticity, brought about fruitful physics caused by non-trivial coupling among various degrees of freedom in condensed matters. Among numerous multiferroic materials, $BiFeO_3$ is perhaps the most extensively studied because of its huge spontaneous electric polarization (P_S) as well as high ferroelectric and antiferromagnetic ordering temperatures. Our recent careful studies of magnetoelectric effects in high-quality crystals of $BiFeO_3$ revealed existence of novel electric polarization (P_T) normal to the P_S that can be controlled by magnetic and electric fields in a non-volatile way [1, 2]. These findings clarified that $BiFeO_3$ will be useful for non-volatile memory devices writable by electric fields, readable simply by measuring their resistance, and stable against external magnetic fields at least up to 4 T.

Emergence of P_T suggests breaking of the three-fold rotational symmetry around P_S. Although this kind of distortion was proposed by earlier experimental studies using a synchrotron x-ray radiation facility [3], relation between magnetic order and lattice distortion has been veiled. We studied magnetostriction of a single crystal of $BiFeO_3$ with using a renewed capacitance dilatometer in pulsed magnetic fields up to 55 T (Fig. 1(a)). The results clearly resolved existence of slight (1/50,000) lattice deformation, which can be controlled by applied magnetic fields in irreversible way indicating ferroelastic nature of this material [4].

In addition to the irreversible behavior below 10 T, we observed non-monotonic change in magnetostriction between 10-15 T that suggests emergence of an intermediate phase between cycloidal and canted-antiferromagnetic phases. This feature of the intermediate phase is also observed in measurements of isothermal magnetization and electric polarization [4]. The intermediate phase grows up with increasing temperature as shown by shaded area in Fig. 1(b). According to a model calculation based on the standard Hamiltonian for this material, conical antiferromagnetic order as illustrated in Fig. 1(c) can be stabilized at a certain parameter space. Field induced transition from the cycloidal to this conical phase is expected to rotate the spin modulation vector from X to Y direction in Fig. 1(c). Our neutron experiment revealed that incommensurate spin modulation along the X-direction in the cycloidal state becomes commensurate in the intermediate phase, which is consistent with our expectation. The magnetoelectric effects in this intermediate phase is considerably larger than those in the other phases. Our findings will open novel possibility in this well-known material.

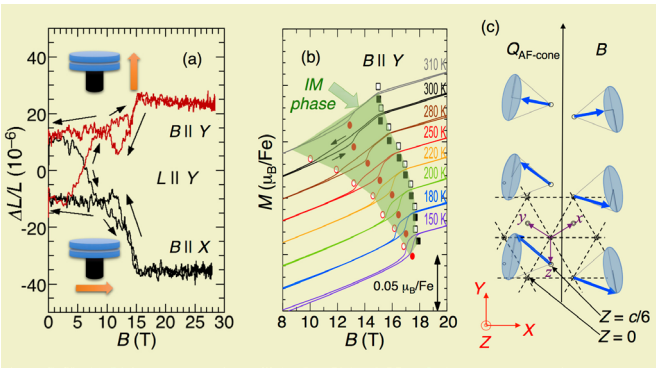

Fig. 1. (a) Magnetostriction of $BiFeO_3$ single crystal at 300 K measured with using the capacitance method. The insets show schematics of the capacitance cell and applied magnetic field. (b) Isothermal magnetization curves at various temperatures between 150 K and 310 K. We observed anomaly in the shaded area and assigned it as the intermediate phase. (c) Proposed spin order in the intermediate phase. This conical antiferromagnetic state can be regarded as a superposition of the cycloidal state in the YZ plane and the canted antiferromagnetic state within the XY plane.

References

[1] M. Tokunaga *et al.*, Nat. Commun. **6**, 5878 (2015).
[2] S. Kawachi *et al.*, Appl. Phys. Lett. **108**, 162903 (2016).
[3] I. Sosnowska *et al.*, J. Phys. Soc. Jpn. **81**, 044604 (2012).
[4] S. Kawachi *et al.*, Phys. Rev. Mater. **1**, 024408 (2017).

Authors
S. Kawachi, A. Miyake, T. Ito[a], M. Matsuda[b], W. Ratcliff II[c], S. Miyahara[d], N. Furukawa[e], and M. Tokunaga
[a]National Institute of Advanced Industrial Science and Technology (AIST)
[b]Oak Ridge National Laboratory (ORNL),
[c]NIST Center for Neutron Research, NIST,
[d]Fukuoka University,
[e]Aoyama Gakuin University

Magnetostriction Measurements up to 190 T

Y. Matsuda and Kobayashi Groups

Magnetic field is a unique parameter that directly acts on the spin, orbital angular momentum and phases of wavefunction of electrons in solids. High magnetic field of 100 T roughly corresponds to 100 K in energy scale. Therefore, it is expected that novel state of matter emerges under high magnetic fields, besides being just a controlling parameter of matter. Researches using non-destructive pulsed magnetic fields has been greatly successful in the last several decades both in magnet technique and measurement techniques. On the other hand, despite the fact that the ultra-high magnetic fields well above 100 T have been available using destructive pulse magnets in ISSP since 1980s, the deepening of condensed matter physics using those destructive pulse magnets is still to come. It is due to the limited space and time of the generated ultrahigh magnetic fields that is making

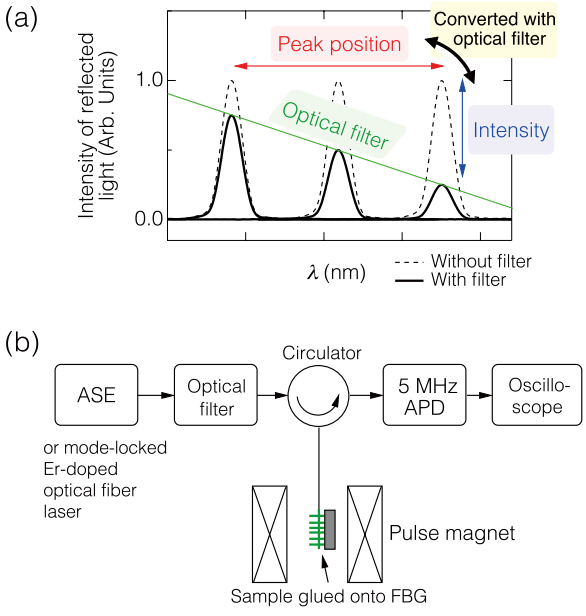

Fig. 1. (a) Schematic drawing of optical filter method for FBG peak detection (b) Schematics of developed FBG and optical filter based magnetostriction measurement system.

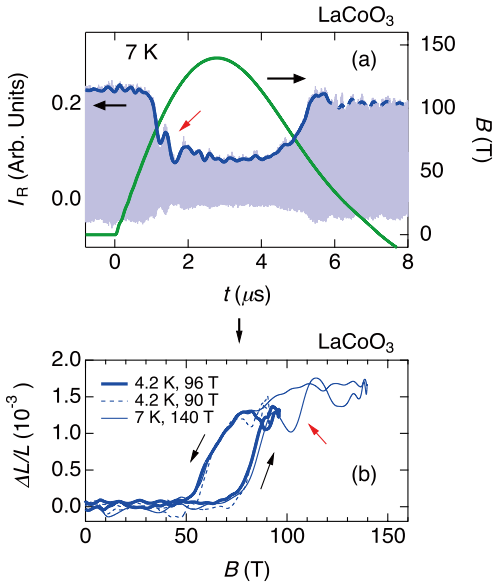

Fig. 2. (a) FBG signal from $LaCoO_3$ at 7 K up to 150 T whose pulse duration is 7 μs. (b) Magnetostriction of $LaCoO_3$ at 7 K up to 150 T obtained from the above data.

various solid state measurements difficult such as resistivity, magnetization and others.

In the present study, we report the achievement of the measurement of magnetostriction which is one of the macroscopic measure that was impossible so far under ultrahigh magnetic fields above 100 T. Developed magnetostriction measurement system relies on fiber Bragg grating (FBG) technique. FBG is an optical fiber with which one is able to detect strain of matter by observing the Bragg wavelength in the reflection. In the present study, we employed the optical filter method where the information of the shift of the Bragg wavelength is converted to the intensity of the reflected light as shown in Fig. 1(a), which can be detected at high speed of 100 MHz. The high-speed of 100 MHz is indispensable for

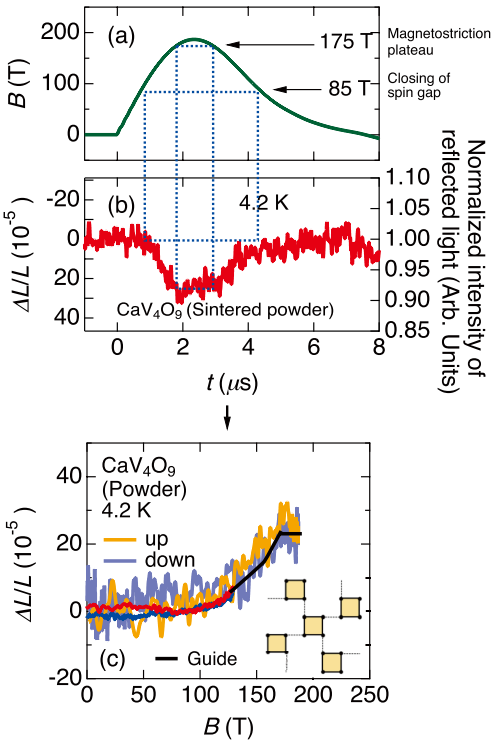

Fig. 3. (a) FBG signal from CaV_4O_9 at 4.2 K up to 190 T (b) Generated pulsed magnetic field using single turn coil whose pulse duration is 7 μs. (c) Magnetostriction of CaV_4O_9 at 4.2 K up to 190 T obtained from the above data, showing the closing of spin gap and entering into a plateau region.

the measurement under ultrahigh magnetic field generated with destructive pulse magnet because the pulse duration is only a few micron seconds. As a light source, a mode-locked Er-doped optical fiber laser is utilized as shown in Fig. 1(b). This enables one to use the modulated measurement which is more robust against noises.

We have confirmed that we are able to measure magnetostriction of $LaCoO_3$ up to 150 T as shown in Figs. 2(a) and 2(b) [1, 2], and CaV_4O_9 up to 190 T with the best resolution of 2.0×10^{-5} as shown in Figs. 3(a), 3(b) abd 3(c). Using the technique with the electromagnetic flux compression technique generating magnetic field of above 500 T is under way. Also, we have applied the developed FBG based strain measurement system to non-destructive pulse magnets, where we have been successful in measuring the magnetostriction of volborthite with the resolution of 1.0×10^{-6} [3]. The FBG based magnetostriction study under ultrahigh magnetic field for the valence fluctuation system, quantum spin system, spin-crossover systems are being carried out.

References

[1] A. Ikeda, T. Nomura, Y. H. Matsuda, S. Tani, Y. Kobayashi, H. Watanabe, K. Sato, Rev. Sci. Instrum. **88**, 083906 (2017).
[2] A. Ikeda, T. Nomura, Y. H. Matsuda, S. Tani, Y. Kobayashi, H. Watanabe, K. Sato, Physica B **536**, 847 (2018).
[3] A. Ikeda and Y. H. Matsuda, arXiv:1803.03404.

Authors

A. Ikeda and Y. H. Matsuda

Discovery of 2D Anisotropic Dirac Cones

I. Matsuda, Sugino, and Komori Groups

As the fifth element in the periodic table, boron atoms form numerous bulk allotropes and provide a rich chemistry and physics. Boron atomic sheets, borophene, also have an enormous number of two-dimensional (2D) polymorphs. Recently, various borophene phases have been synthesized on metal substrates, such as the β_{12} sheet. Theoretical works have revealed numerous novel properties of these borophene phases, such as phonon-mediated superconductivity, but experimental examinations of their electronic structures are far from enough.

In the present research, we report observation of 2D anisotropic Dirac cones, Dirac delta (Δ)-cone, in χ_3 borophene by the first principles calculations and angle-

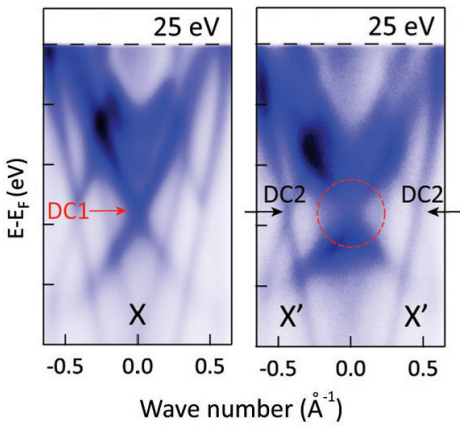

Fig. 1. Photoemission intensity plots measured with 25 eV p polarized photons at the X and X′ points. Red arrows and black arrows indicate positions of the Dirac cones of DC1 and DC2, respectively. Red broken circle show a region where one finds gap-opening for the DC1 band.

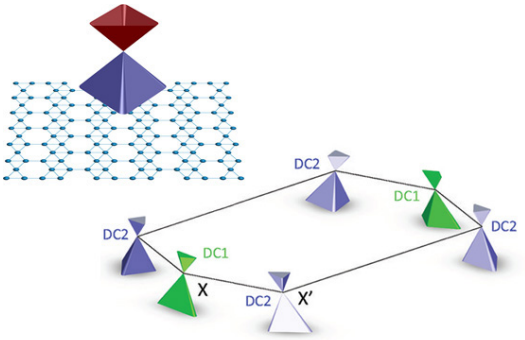

Fig. 2. Schematic drawing of the structure model of χ_3 borophene and the anisotropic Dirac cones, Δ-Dirac ones.

resolved photoemission spectroscopy measurements using synchrotron radiation. The Dirac cones are centered at the X and X′ points of the Brillouin zone, as shown in Fig.1. The calculation reveals that these Dirac cones are mainly derived from the p_z orbitals of boron, with negligible contributions from the silver orbitals of the substrate. This represents that the χ_3 borophene sheet is the quasi-freestanding layer.

The atomic structure and the electronic structure of the Dirac Fermion are summarized in Fig. 2. Our results validate χ_3 borophene as the first 2D material that hosts anisotropic Dirac cones. This may stimulate further research interest and enable the realization of high-performance boron devices.

References
[1] B. Feng, J. Zhang, S. Ito, M. Arita, C. Cheng, L. Chen, K. Wu, F. Komori, O. Sugino, K. Miyamoto, T. Okuda, S. Meng, and I. Matsuda, Adv. Mater. **30**, 1704025 (2018).
[2] B. Feng, O. Sugino, R.-Y. Liu, J. Zhang, R. Yukawa, M. Kawamura, T. Iimori, H. Kim, Y. Hasegawa, H. Li, L. Chen, K. Wu, H. Kumigashira, F. Komori, T.-C. Chiang, S. Meng, and I. Matsuda, Phys. Rev. Lett. **118**, 096401 (2017).

Authors
I. Matsuda, O. Sugino, and F. Komori

Discovery of Two-Dimensional Dirac Nodal Line Fermions in the Monolayer Cu_2Si

I. Matsuda and Sugino Groups

Tremendous research interest has recently focused on topological semimetals which have vanishing densities of states at the Fermi level. In these materials, the valence and conduction bands can touch at either discrete points or extended lines. In the latter case, it forms nodal line semimetals. The band degeneracy points or lines are also protected by symmetries and are thus robust against external perturbations.

Two-dimensional materials have also attracted broad scientific interest because of their exotic properties and possible applications in high-speed nano-devices. Thus, realization of two-dimensional topological semimetals will

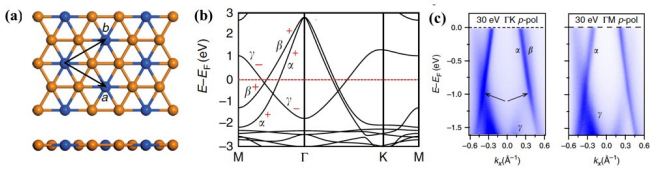

Fig. 1. (a) Atomic structure model of the monolayer Cu_2Si. (b) The calculated band dispersion curves. (c) Result of the photoemission band mapping.

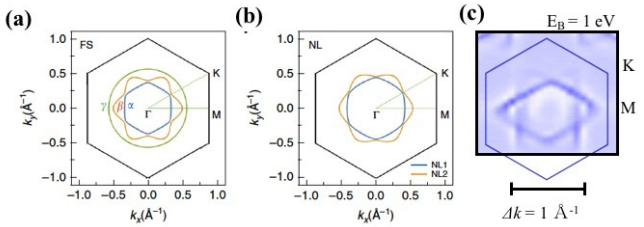

Fig. 2. (a) Fermi surface (FS), (b) nodal line (NL) of the metallic bands, α,β,γ in Fig.1. (c) Result of the photoemission band mapping for NL taken at photon energy of 30 eV and at binding energy (E_B) of 1 eV.

provide new platforms in academic and technological fields. In this work, we study monolayer Cu_2Si, which is composed of a honeycomb Cu lattice and a triangular Si lattice. As shown in Fig.1, all the Si and Cu atoms are coplanar and thus there is the mirror reflection symmetry with respect to the xy plane. This symmetric feature is significant for the existence of two-dimensional nodal lines. A commensurate monolayer Cu_2Si has been synthesized on a Cu (111) surface by the Si deposition. Our comprehensive theoretical calculations show the existence of two Dirac nodal loops centered around the Γ point (Fig. 1). The gapless nodal loops are protected by mirror reflection symmetry. These characteristic band structures were directly observed by angle-resolved photoemission spectroscopy measurements (Figs. 1 and 2). The theoretical and experimental results unambiguously confirm the two concentric Dirac nodal loops in monolayer Cu_2Si (Fig. 2). These results not only extend the concept of Dirac nodal lines from three- to two-dimensional materials, but also provide a new platform to realize novel devices at the nanoscale.

Reference
[1] B. Feng, B. Fu, S. Kasamatsu, S. Ito, P. Cheng, C.-C. Liu, S. K. Mahatha, P. Sheverdyaeva, P. Moras, M. Arita, O. Sugino, T.-C. Chiang, K. Wu, L. Chen, Y. Yao, and I. Matsuda, Nature Comm. **8**, 1007 (2017).

Authors
I. Matsuda and O. Sugino

Determination of Element-Specific Complex Permittivity with Soft X-Ray Segmented Cross Undulator at SPring-8 BL07LSU

I. Matsuda, Akai, Wadati, Harada, and Shin Groups

Permittivity (or conductivity) is a quantity that characterizes a response of a matter by an electric field, such as an electromagnetic wave. It has historically been used to develop varieties of electronic and optical devices that have supported our society today. Determinations and understandings of permittivity of matters have been one of the highest priority tasks of science and technology. Recently, the requirement has reached to the ultraviolet (UV) ~soft X-ray (SX) region due to necessity of developing the extended-UV (EUV) lithography for the advanced technologies or ultra-high-resolution SX experiments for the frontier sciences, for examples.

A permittivity has been often approximated as a (dielectric) constant but it is essentially the tensor quantity that is composed of diagonal and off-diagonal components. The diagonal and the off-diagonal element carries non-magnetic

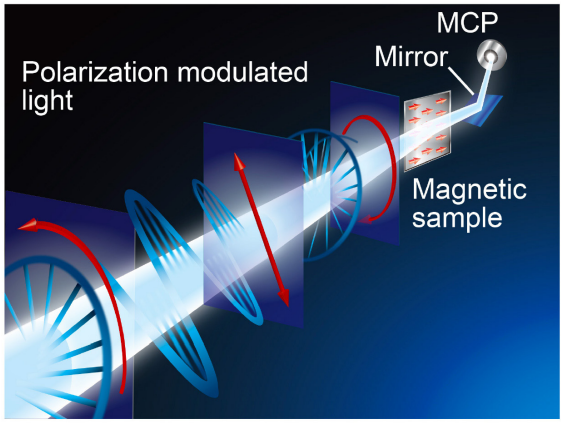

Fig. 1. Image of the polarization modulated light with the L-MOKE set up at SPring-8 BL07LSU.

and magnetic information of a matter, respectively, and it is the latter that has been significant to understand the spin polarization or the magnetization. The individual elements are complex, being composed of the real and imaginary parts. The determination has been widely made by a probing light with the polarization modulation (frequency of p) and the measurement of the sample optical responses at the two frequencies (p, 2p). Such an experiment is easily achieved by transmitting the incident light through crystals that allow electric or mechanic controls of the polarization. Nowadays, one can find varieties of commercial polarization modulators for visible light and hard X-ray but for the EUV SX region. This is mainly because the light absorbance in a matter in this region is so large that it does not allow the transmission and the light can only survive in vacuum due to absorption by air molecules. In addition, the 'abnormal' optical response at the absorption edges of the composing element has also intervened the precise evaluation. Up to now, the determination has been made only with a help of simulations based on the atomic parameters and the indirect experimental data,

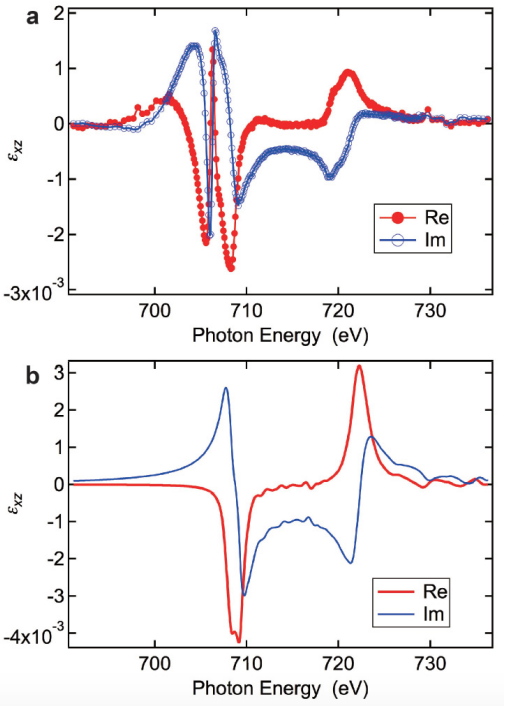

Fig. 2. a. ε_{xz} spectra of the Fe nanofilm at the L-edge obtained by the L-MOKE measurement with the polarization modulated light. Red lled circles and blue open circles represent its real and imaginary parts, respectively. b. ε_{xz} spectra of bulk Fe (bcc) at the L-edge obtained by the first-principles calculation with the KKR formalism. Red and blue lines represent its real and imaginary parts, respectively.

which has often left the large uncertainty in the permittivity values. Thus, the estimation has been made for systems that are simple and not for the complicated or non-uniform ones. To overcome these difficulties, one can use synchrotron radiation, generated by electrons that already exist in vacuum and one can control the polarization by the electron trajectory that is regulated by the external magnetic field.

Here, we developed a novel SX source of the segmented cross undulator that can make the continuous polarization modulation (p) of the light and carried out the magneto-optical measurement (p, 2p) of the buried Fe nanolm at the Fe L-edge absorption edge in SX region (Fig. 1). As shown in Fig. 2, we succeeded in directly determining the complex permittivity and we found that the first-principles calculation with the Korringa-Kohn-Rostoker (KKR) formalism gave the perfectly matching results. It is of note that a spectral dip/peak at 705 eV in experiment is due to the optical response by the film structure that has not been taken into account in the calculation. Our procedure determines the permittivity of a sample in UV~SX region with high precisions, which is significant for the better understanding of the light-matter interaction. It also opens new technical examination method to seek for the best materials for optical elements, for examples, in the EUV lithography technology or in the laser technology of high harmonic generation lasers, high-brilliant synchrotron radiation, and X-ray free electron laser.

References

[1] S. Yamamoto, Y. Senba, T. Tanaka, H. Ohashi, T. Hirono, H. Kimura, M. Fujisawa, J. Miyawaki, A. Harasawa, T. Seike, S. Takahashi, N. Nariyama, T. Matsushita, M. Takeuchi, T. Ohata, Y. Furukawa, K. Takeshita, S. Goto, Y. Harada, S. Shin, H. Kitamura, A. Kakizaki, M. Oshima, and I. Matsuda, J. Syn. Rad. **21**, 352 (2014).
[2] I. Matsuda, A. Kuroda, J. Miyawaki, Y. Kosegawa, S. Yamamoto, T. Seike, T. Bizen, Y. Harada, T. Tanaka, and H. Kitamura, Nucl. Instrum. Methods Phys., Sect. A **767**, 296 (2014).
[3] Y. Kubota, Sh. Yamamoto, T. Someya, Y. Hirata, K. Takubo, M. Araki, M. Fujisawa, K. Yamamoto, Y. Yokoyama, M. Taguchi, S. Yamamoto, M. Tsunoda, H. Wadati, S. Shin, and I. Matsuda, J. Elec. Spec. Rel. Phenom. **220**, 17 (2017).
[4] Y. Kubota, M. Taguchi, Sh. Yamamoto, T. Someya, Y. Hirata, K. Takubo, M. Araki, M. Fujisawa, H. Narita, K. Yamamoto, Y. Yokoyama, S. Yamamoto, M. Tsunoda, H. Wadati, S. Shin, and I. Matsuda, Phys. Rev. B **96**, 134432 (2017).
[5] Y. Kubota, Y. Hirata, J. Miyawaki, S. Yamamoto, H. Akai, R. Hobara, Sh. Yamamoto, K. Yamamoto, T. Someya, K. Takubo, Y. Yokoyama, M. Araki, M. Taguchi, Y. Harada, H. Wadati, M. Tsunoda, R. Kinjo, A. Kagamihata, T. Seike, M. Takeuchi, T. Tanaka, S. Shin, and I. Matsuda, Phys. Rev. B **96**, 214417 (2017).

Authors
Y. Kubota, Y. Hirata, J. Miyawaki, S. Yamamoto, H. Akai, M. Araki, Y. Harada, H. Wadati, S. Shin, and I. Matsuda

Interface Hydrogen Bonds at the HeteroJunction between Proton-Donating and Proton-Accepting Self-Assembled Monolayers

I. Matsuda, Mori, amd Yoshinobu Groups

Hydrogen bondings have been significant in chemical and biological systems. It has been known to fix molecular configurations and it is also flexible for breaking and making bonds between molecules at room temperature. Additionally, a hydrogen bond also effectively assists the proton (H^+) transfer between the donor and the acceptor sites along the bond. The transfer of one whole H^+ ion substantially changes charge distributions between the molecules. Based

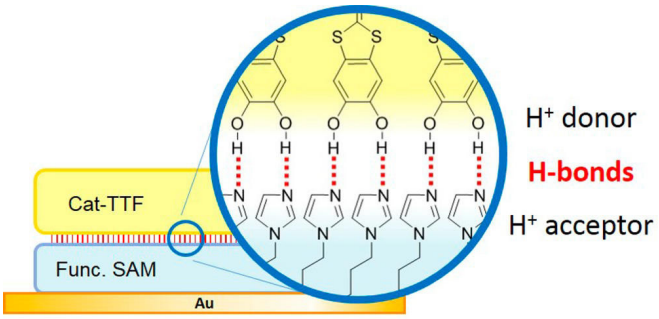

Fig. 1. Schematic drawing of hydrogen bonds at the interface between Cat-TTF and functional SAM (Im-SAM) on Au(111).

on this electron-proton concerting effect, highly conductive pure organic molecular crystals have been realized at the partially deprotonated molecular crystals of catechol-fused ethylenedithiotetrathiafulvalene (H_2Cat-EDT-TTF). These facts motivate us to design a possible control of the film conductivity depending of the proton position between H^+ donor and acceptor layers, which leads to a new concept for driving electronic device. As the first step of this ambitious goal, we created a hydrogen-bonding heterogeneous interface consisting of a bilayer of the H^+-donating and –accepting molecules on a substrate (Fig. 1).

For the H^+-acceptor molecular layer, we adopted an imidazole-terminated alkanethiolate self-assembled monolayer (Im-SAM) prepared on the Au(111) substrate. The imidazole molecule can accept H^+ at the imino N site and stabilize it as an imidazolium cation. At the saturation coverage of alkanethiolate-based SAMs, the molecules are in a closely packed standing-up form and the end group tends toward the open side on the SAM. The molecular orbitals and chemical properties of the functional end groups are hardly perturbed from Au substrates due to the sufficient thickness of the closely packed alkylene chains in the SAMs. Thus, the imino N atom on Im-SAMs is expected to make hydrogen bonds as H^+ acceptor sites with H^+-donating molecules.

For the counterpart, the H^+-donor molecular layer, we focused on the adsorption of the catechol-fused bis(methylthio)tetrathiafulvalene (H_2Cat-BMT-TTF) molecules on the Im-SAM film. The hydroxyl groups at the catechol moiety in H_2Cat-BMT-TTF should act as the H^+-donating group, by analogy to the conductive H_2Cat-EDT-TTF complexes, in which it has been elucidated that the TTF moiety is electron-donating and the hydroxyl groups in the catechol moiety accept the electron by pushing out H^+.

We confirm the formation of a hydrogen-bonding heterogeneous bilayer that consists of the H_2Cat-BMT-TTF layer and the Im-SAM film, systematically elucidated by AFM, X-ray photoelectron spectroscopy, infrared absorption spectroscopy, and density functional theory calculations. Figure 2 shows one of the evidence showing clear infrared spectral signals of the bilayer system. The broad feature at frequency of 2500-3500cm^{-1} indicates strong hydrogen bonds at the heterointerface. These results provide new insight for designing electron-proton functions in adsorption systems.

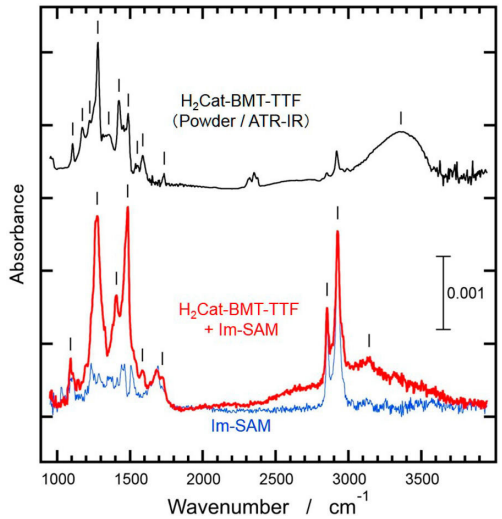

Fig . 2. Infrared (IR) reflection absorption spectra for H_2Cat-BMT-TTF adsorbed on Im-SAM (red) and for Im-SAM (blue), in comparisons with the IR spectrum for the H_2Cat-BMT-TTF powder (black).

Reference

[1] H. S. Kato, S. Yoshimoto, A. Ueda, S. Yamamoto, Y. Kanematsu, M. Tachikawa, H. Mori, J. Yoshinobu, and I. Matsuda, Langmuir **34**, 2189 (2018).

Authors

H. S. Kato, H. Mori, J. Yoshinobu, and I. Matsuda

Observation of Second Harmonic Generation in Soft X-Ray and Study of its Element Selectivity

I. Matsuda, Akai, Wadati, and Shin Groups

Second harmonic generation (SHG) is the well-known nonlinear optical frequency conversion and it has been a significant probe to investigate the electronic properties of matter. In the SHG process, optical fields interact with a medium of broken inversion symmetry, resulting in production of a double field frequency. Recent development of a free electron laser (FEL), the high brilliant laser in the energy range from vacuum ultraviolet to X-ray, allows to explore nonlinear optical effects in these energy ranges. All of the earlier studies on non-linear optics in those energy ranges reported experiments conducted under a transmission geometry in order to acquiring enough signals by meeting phase-matching condition. In the soft X-ray range, the reflection geometry is preferred because the light in the energy range is strongly absorbed by materials. However, in the reflection geometry, the non-linear optical experiments suffer the extremely low signals due to the absence of coherent amplification caused by the phase matching.

Here, we demonstrate observation of SHG from a non-centrosymmetric crystal by employing the resonance effect described below, even under the reflection geometry (Fig. 1). The experiment was carried out by using a soft

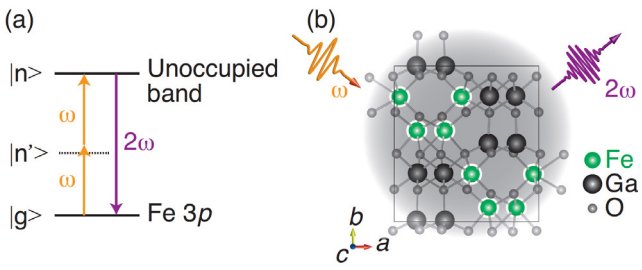

Fig. 1. Second harmonic generation in the $GaFeO_3$ crystal using Fe 3p resonance. (a) Energy diagram of SHG. The notations, g, n', and n represent the ground state, virtual state, and excited state, respectively. (b) Projection view along the c axis of the crystal structure of $GaFeO_3$.

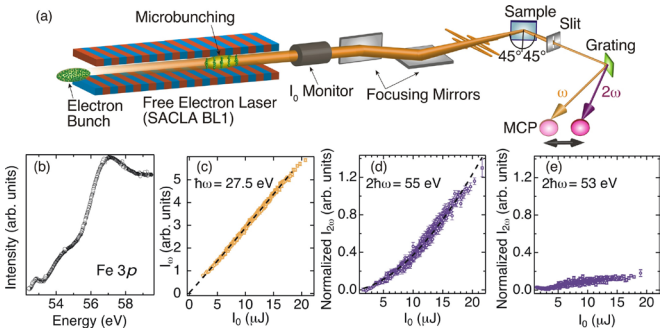

Fig. 2. (a) Schematic diagram of the SXFEL beamline at SACLA and the SHG measurement system. (b) Fe 3*p* absorption spectrum of the $GaFeO_3$ crystal. (c) Intensity plot of the ω component of the reflected SXFEL pulses, I_ω, with respect to the correspondent incident intensity, I_0, at the photon energy $\hbar\omega$ = 27.5 eV. (d) Plot of $I_{2\omega}$ at the photon energy of $2\hbar\omega$ = 55 eV. (e) Plot of $I_{2\omega}$ at the photon energy of $2\hbar\omega$ = 53 eV. The dashed lines shown in (c) and (d) were fitted by a power law.

X-ray FEL (SXFEL) at SACLA in Harima. SHG signals were detected when the photon energy with double frequency 2ω was above the absorption edge of the sample, as shown in Fig. 2. The metal M-edge resonance inherently indicates addition of element specificity to the SHG experiment. Moreover, the reflection measurement geometry indicates that the present method can be used for various samples and experimental conditions. The optical frequency conversion with SXFEL is expected to selectively probe the electronic properties of nonlinear bulk crystals and the interfaces in heterostructures that are composed of multi-element materials.

Reference

[1] Sh. Yamamoto, T. Omi, H. Akai, Y. Kubota, Y. Takahashi, Y. Suzuki, Y. Hirata, K. Yamamoto, R. Yukawa, K Horiba, H. Yumoto, T. Koyama, H. Ohashi, S. Owada, K. Tono, M. Yabashi, E. Shigemasa, S. Yamamoto, M. Kotsugi, H. Wadati, H. Kumigashira, T. Arima, S. Shin, and I. Matsuda, Phys. Rev. Lett. **120**, 223902 (2018).

Authors

Sh. Yamamoto, Y. Hirata, S. Yamamoto, H. Wadati, S. Shin, and I. Matsuda

Dzyaloshinskii-Moriya Interaction in α-Fe_2O_3 Measured by Magnetic Circular Dichroism in Resonant Inelastic Soft X-ray Scattering

Harada Group

Dzyaloshinskii-Moriya interaction (DMI) is an asymmetric exchange interaction induced by a lack of inversion symmetry in materials through spin-orbit coupling. Even though DMI is much weaker than the Heisenberg exchange interaction, DMI plays an essentially important role to determine magnetism and related physical properties in various systems. DMI is expressed by the formula $D_{ij} \cdot S_i \times S_j$, but the direction and magnitude of D_{ij} has been difficult to determine both theoretically and experimentally. Among new approaches explored to measure DMI, selective observation of the electronic structure that is responsible for the DMI is of crucial importance. α-Fe_2O_3 is a prototype material of DMI and shows weak ferromagnetism due to the DMI at room temperature. However, even for α-Fe_2O_3, the electronic structure leading to its weak ferromagnetism has not been experimentally identified. Thus, we measured magnetic circular dichroism (MCD) in resonant inelastic soft x-ray scattering (SX-RIXS) of α-Fe_2O_3 [1]. RIXS-MCD enables us to probe the MCD for each *dd* excitation, which is very sensitive to the symmetry of the *d* orbitals, and is expected to give an insight into the origin of the weak ferromagnetism induced by DMI in α-Fe_2O_3.

The x-ray absorption spectra (XAS) and RIXS experiments of an α-Fe_2O_3 single crystal were conducted at the HORNET end-station at BL07LSU in SPring-8. MCD in XAS and RIXS was measured by using a compact magnetic circuit with permanent Nd-Fe-B magnets [2]. Figure 1(a) compares the experimental and calculated results of XAS of α-Fe_2O_3. Peak splittings (Nos. 1 and 2) attributed to the crystal field effect and a satellite feature at $h\nu \approx 713.25$ eV assigned to a charge-transfer state were clearly observed. No discernible XAS-MCD signal was detected. XAS is well reproduced by *ab initio* charge-transfer multiplet calculation. Figures 1(b) and 1(c) show RIXS-MCD spectra measured by two different experimental configurations. In the configuration of $\boldsymbol{k}_{\rm in} \parallel \langle 11\bar{2}0 \rangle$ (Fig. 1(b)), the magnitude of RIXS-MCD was relatively small at any excitation energies employed compared with that in the configuration of $\boldsymbol{k}_{\rm in} \parallel \langle 1\bar{1}00 \rangle$ (Fig. 1(c)), where the *dd* excitation at 1.8 eV (peak B) showed RIXS-MCD for $h\nu > 713.25$ eV (No. 3, the charge-transfer satellite), while no RIXS-MCD was observed by the excitation of the main absorption peaks (Nos. 1 and 2). Thus, RIXS-MCD showed the crystal orientation and excitation energy dependences. The observed RIXS-MCD is qualitatively well described by the calculations (Fig. 1(d)). RIXS-MCD in peak B′ is almost absent for the excitations around the main peaks of the L_3 edge (Nos. 1′ and 2′), while small but clear RIXS-MCD is found at peak B′ for the excitations above the satellite structure (No. 3′). The more detailed configuration analysis has revealed that the RIXS-MCD derives from spin flip excitations at delocalized e_g orbitals. By the combination of the experiments and calcu-

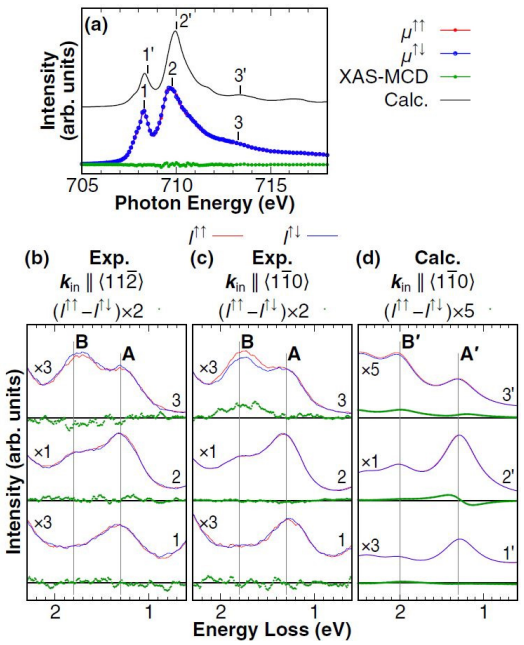

Fig. 1. Experimental and calculated results of Fe L_3-edge XAS- and RIXS-MCD spectra of α-Fe_2O_3. (a) Experimental and calculated Fe L_3-edge XAS spectra. (b) and (c) Experimental RIXS-MCD spectra in the configurations of $\boldsymbol{k}_{\rm in} \parallel \langle 11\bar{2}0 \rangle$ and $\boldsymbol{k}_{\rm in} \parallel \langle 1\bar{1}00 \rangle$. (d) Calculated RIXS-MCD spectra in the configuration of $\boldsymbol{k}_{\rm in} \parallel \langle 1\bar{1}00 \rangle$. The red ($I^{\uparrow\uparrow}$) and blue ($I^{\uparrow\downarrow}$) spectra represent the intensity of the scattered x ray for the spin polarization of the incident x ray parallel and antiparallel to the direction of the sample magnetization, respectively. The numbers in (b,c,d) indicate the excitation energies shown in (a).

lations, RIXS-MCD has unraveled that the origin of DMI in α-Fe_2O_3 is the e_g orbitals, which are strongly hybridized with the 2*p* orbitals of oxygen atoms.

The results demonstrate the important capability of RIXS-MCD to sensitively extract the magnetic information from MCD of each *dd* excitation in the weak-ferromagnet, where the net magnetic moments are so small that XAS-MCD is not applicable. With this advantage, RIXS-MCD is expected to be more widely applied to the weak ferromagnetism and spin spiral induced by DMI. Furthermore, bulk sensitivity and element selectivity of RIXS will also promote the measurement of RIXS-MCD, and thus RIXS-MCD could be a promising technique to obtain the information about the ground-state spin state. Finally, it is worth mentioning that the computational calculations have now become powerful enough to discuss the very small magnitude of RIXS-MCD for the realistic low-symmetry system, and will advance the more precise analysis of the experimental results and give more complete comprehension of physical properties.

References

[1] J. Miyawaki, S. Suga, H. Fujiwara, M. Urasaki, H. Ikeno, H. Niwa, H. Kiuchi, and Y. Harada, Phys. Rev. B **96**, 214420 (2017).
[2] J. Miyawaki, S. Suga, H. Fujiwara, H. Niwa, H. Kiuchi, and Y. Harada, J. Synchrotron Rad. **24**, 449 (2017).

Authors

J. Miyawaki, S. Suga[a], H. Fujiwara[a], M. Urasaki[b], H. Ikeno[b], H. Niwa, H. Kiuchi, and Y Harada
[a]Osaka University
[b]Osaka Prefecture University

Enhancement of the Hydrogen-Bonding Network of Water Confined in a Polyelectrolyte Brush

Harada Group

In the crowded environment of a living cell, several biomolecular polyelectrolytes–especially proteins, nucleic acids, and complex sugars–are compressed together. Water encapsulated between the aforementioned entities is no longer a simple space-filling medium but is believed to exhibit intriguing hydrogen-bonding networks depending on its molecular dimensions and interfacial properties. This unique hydrogen-bonding structure of water in the vicinity of polyelectrolytes should significantly affect the specific structure and functions of biomolecules and their assemblies. Hence, it is imperative to devise a novel method for investigating the local hydrogen-bonding structure of water near polyelectrolytes, which can aid in the understanding of the functions of biological systems. A polyelectrolyte brush, a surface-tethered polymer layer is a proper model interface of polymeric soft materials, such as proteins. A recent study using microscopic infrared (IR) spectroscopy indicated that water molecules are confined in a polyelectrolyte brush with a highly ordered hydrogen-bonding network. The formation of a hydration layer of polyelectrolytes and the resulting hydrogen-bonding network is expected to be crucial to controlling the properties of biomolecules, such as lubrication and antifouling. This study sheds light on the local hydrogen-bonding structure of water confined in a charged polyelectrolyte brush and reveals that the hydrogen-bonding structure of water confined in the polyelectrolyte brush is very similar to ice I_h, even at room temperature [1].

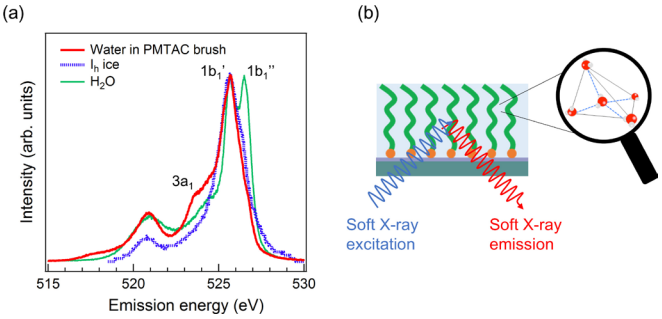

Fig. 1. (a) O 1s soft X-ray emission spectra of water confined in the polyelectrolyte brush, the dry brush measured in vacuum, liquid H_2O, and ice I_h. The excitation energy is 550.3 eV, which is well above the ionization threshold. (b) Schematic of the hydrogen-bonding structure of water confined in the PMTAC brush.

O 1s X-ray emission spectroscopy (XES) experiments of water confined in the polyelectrolyte brush were performed at the SPring-8 synchrotron radiation facility using the BL07LSU HORNET station. Figure 1(a) compares the O 1s XES spectra of the water confined in the poly[2-(methacryloyloxy)- ethyltrimethylammonium chloride] (PMTAC) brush, bulk liquid water, and ice I_h. The XES spectra of the bulk liquid water and ice I_h are shown with the same $1b_1$ peak intensity as that of confined water to compare the spectral shape. The XES spectra of the confined water and ice I_h are very similar; the $1b_1$" peak, which is observed in the spectrum of bulk liquid water, is negligible. The similarity between the two XES spectra is quite surprising as a significant enhancement of hydrogen-bonding is observed even at room temperature in the water confined in the PMTAC brush. Moreover, enhanced spectral intensity is observed around the $3a_1$ region for the confined water as compared to that in ice I_h and bulk liquid water. The $3a_1$ peak, which is attributed to the dipole-forbidden transition ($3a_1 \rightarrow 1a_1$) in tetrahedral symmetry, is not observed for ice I_h and is smeared out in the case of bulk liquid water because of the high sensitivity of the $3a_1$ orbital to the distribution of the hydrogen-bond strength. Therefore, the enhancement of the $3a_1$ peak observed for the confined water can be explained by the fact that the hydrogen bonds are distorted (not straight O–H···O bonds), albeit somewhat ordered, in the PMTAC brush.

Our XES results confirm that these techniques are extremely sensitive to the presence/absence and distortion of hydrogen-bonding. A majority of water molecules in the polyelectrolyte brush are held together by one type of hydrogen-bonding configuration: possibly a slightly distorted but ordered hydrogen-bonding configuration even at room temperature. The distorted picture is only a speculation from the emergence of the $3a_1$ state and the consideration of the possible hydrogen-bond structure in the vicinity of the charged site, which needs further study from both experimental and theoretical aspects. We believe that XES will pave the way for novel, important research fields in the near future.

Reference

[1] K. Yamazoe, Y. Higaki, Y. Inutsuka, J. Miyawaki, Y. –T. Cui, A. Takahara, and Y. Harada, Langmuir **33,** 3954 (2017).

Authors

K. Yamazoe, Y. Higaki[a], Y. Inutsuka[a], J. Miyawaki, Y. –T. Cui, A. Takahara[a], and Y. Harada
[a]Kyusyu University

Capturing Ultrafast Magnetic Dynamics by Time-Resolved Soft X-Ray Magnetic Circular Dichroism

Wadati, I. Matsuda, and Shin Groups

Control of electron, magnetic, and lattice states by optical excitations in magnetically ordered materials has attracted considerable attention due to their potential applications in electronic and magnetic recording media functioning on an ultrafast time scale below nanosecond (ns, 10^{-9} second, GHz range). To capture their non-equilibrium dynamics, ultrafast time-resolved experiments have been carried out using a bunched synchrotron light source, and x-ray free electron lasers [1]. FePt thin films have drawn intense research interest owing to their potential for high density recording applications by using their magnetism. Recently, Lambert *et al*. have showed that circularly polarized laser pulses can induce a small helicity-dependent magnetization in FePtAgC granular film [2]. This finding suggests the possibility of all-optical switching of the magnetism in FePt having very short recording-time windows on the ps time scale.

Here, we present a setting for time-resolved (Tr-) x-ray absorption spectroscopy (XAS) and Tr- x-ray magneto circular dichroism (XMCD) in the partial electron yield (PEY) and total fluorescence yield (TFY) modes to measure non-transmissive as-grown samples at nearly normal incidence [3]. The results of Tr-XMCD experiments for as-grown FePt films with non-transmissive substrates are reported. A photo-induced ultrafast demagnetization at the Fe sites of the FePt thin film are observed within the experimental time resolution of 50 ps for Tr-XMCD at SPring-8.

Figure 1 shows an overview of the experimental setup for Tr-XAS, Tr-XMCD, and Tr- resonant soft x-ray scattering (RSXS) measurements in the soft x-ray region at BL07LSU of SPring-8. Tr-RSXS is performed at the $\theta < 90°$ side of the experimental chamber. The scattering is detected by the micro-channel plate (MCP) or avalanche photodiode (APD) installed on the 2θ motion of the diffractometer. On the other hand, XAS and XMCD in the PEY or TFY modes are measured at the $\theta > 90°$ side of the chamber. Emitted photoelectrons or x-ray fluorescence are caught by another MCP topped on the linear motion. The femtosecond Ti:sapphire laser with a wavelength of 800 nm is introduced into the XAS and RSXS chamber. The laser irradiates samples and photo-induced dynamics of the electronic and structural evolutions are examined by means of a pump-probed technique. The laser pulses with 1 kHz repetition rate are synchronized with selected bunches of the synchrotron and delayed electronically. The signals of the MCP or APD are amplified and gated on the oscilloscope or Boxcar integrator which is triggered by the laser pulses (Fig. 1 (b)).

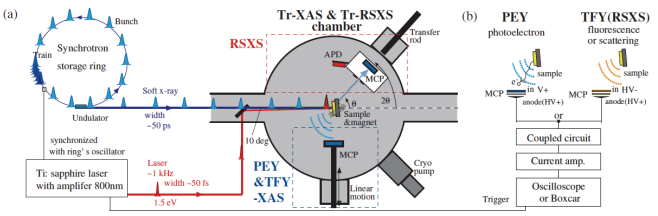

Fig. 1. (a) Overview of the setup for Tr-XAS and Tr-RSXS measurements at BL07LSU of SPring-8. The Ti-sapphire laser with a ~1 kHz repetition rate, which is synchronized with the bunches of the synchrotron, is introduced into the experimental chamber. (b) Electrical circuits for the detectors.

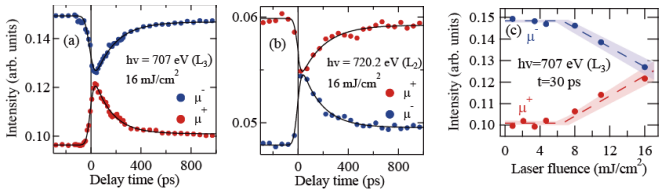

Fig. 2. (a) Time-evolutions of XMCD taken in the PEY mode at(a) L_3 (hν=707.0 eV) and (b) L_2 (hν=720.2 eV) edges for the FePt thin film at room temperature. (c) Laser-fluence dependence of Tr-XMCD intensities (μ+ and μ–) at t=30 ps on the L_3 edge (hν=707.0 eV). The dashed lines denote results of the linear fittings having a threshold.

The time evolutions of the FePt thin film with 16 mJ/cm^2 laser irradiations are given in Fig. 2 (a) at hν=707.0 eV (L_3 edge) and (b) at 720.2 eV (L_2 edge), respectively. As can be seen, almost similar time-evolutions are observed for the Fe $L_{2,3}$ edges. XMCD exhibits a reduction in its intensity by ~90% of the original value ~30 ps after the pump pulse. Then the XMCD exhibits a slow recovery of the magnetization with a time constant of ~150 ps. In addition, the magnetization is not recovered to the original value even at t=1500 ps, which is completed before the next bunch arrives after ~342 ns. Figure 2 (c) gives the Tr-XMCD intensities at t = 30 ps as a function of the laser fluence. Threshold-like behavior is observed at 6.5 mJ/cm^2 for t = 30 ps, which is estimated by the linear fittings for the fluence dependences. These results indicate that the photoinduced effect will not be a simple thermal effect.

The less-distorted PEY method presented in this study will provide an opportunity for applying a sum rule analysis to XMCD spectra in the ultrafast pump-probed spectroscopy for various magnetic materials, which would be very useful to explore the all-optical switching in spintronics devices such as FePt, Co/Pt multi-layers and so forth. On the other hand, the bulk sensitive TFY method will allow us to measure the dynamics of bulk samples showing various quantum phenomena.

References

[1] A. Kirilyuk, A. V. Kimel, and T. Rasing, Rev. Mod. Phys. **82**, 2731 (2010) and reference there in.
[2] C.-H. Lambert, S. Mangin, B. S. D. Ch. S. Varaprasad, Y. K. Takahashi, M. Hehn, M. Cinchetti, G. Malinowski, K. Hono, Y. Fainman, M. Aeschlimann, and E. E. Fullerton, Science **345**, 1337 (2014).
[3] K. Takubo, K. Yamamoto, Y. Hirata, Y. Yokoyama, Y. Kubota, S. Yamamoto, S. Yamamoto, I, Matsuda, S. Shin, T. Seki, K. Takanashi, and H. Wadati, Appl. Phys. Lett. **110**, 162401 (2017).

Authors
K. Takubo, K. Yamamoto, Y. Hirata, Y. Yokoyama, Y. Kubota, S. Yamamoto, S. Yamamoto, I. Matsuda, S. Shin, T. Seki[a], K. Takanashi[a], and H. Wadati
[a]Institute for Materials Research, Tohoku University

Anomalous Change in the de Haas-van Alphen Oscillations of $CeCoIn_5$ at Ultralow Temperatures

H. Shishido, Y. Yanase, and M. Yamashita

A very strange quantum behavior is found in a strongly-correlated superconductor at unprecedented ultralow temperatures [1]. The heavy-fermion compound $CeCoIn_5$ is the celebrated, one of the most-studied *d*-wave superconductor [2]. Its unconventional superconductivity has been thought to be arisen by quantum fluctuations near the magnetically ordered state. However, in spite of many efforts, the ordered state has yet to be discovered.

By using our home-made nuclear-demagnetization cryostat at ISSP, we performed the de Haas-van Alphen (dHvA) measurements of $CeCoIn_5$ down to 2 mK. In a normal metal, a dHvA amplitude increases with a lowering temperature in accordance with the Lifshitz-Kosevich (LK) formula. However, in $CeCoIn_5$, we unexpectedly find that the dHvA amplitudes deviate from the LK formula and show an anomalous decrease with a shift of the dHvA frequencies below a transition temperature T_n (Fig. 1). This anomalous change suggests that the long-presumed ordered state is finally discovered at ultralow temperatures unreachable for conventional cryostats.

The revised H–T phase diagram of $CeCoIn_5$ (Fig. 2(a)) reveals that the field-induced AFM phase is located at the boundary of the unconventional superconductivity. Given that the field-induced phase is observed at very low temperature, the H–T phase diagram of $CeCoIn_5$ at ambient pressure may be considered to be a cross section at the vicinity of the AFM QCP in the H–T–x phase diagram (Fig. 2(b)) obtained by the pressure dependence of the H–T phase diagram of $CeRhIn_5$ [3]. Thus, our study shows that $CeCoIn_5$ is a prominent superconductor where the interplay of unconventional superconductivity, magnetic order, and non-Fermi liquid behaviors near the QCP can be studied without the ambiguity caused by the application of pressure or chemical doping.

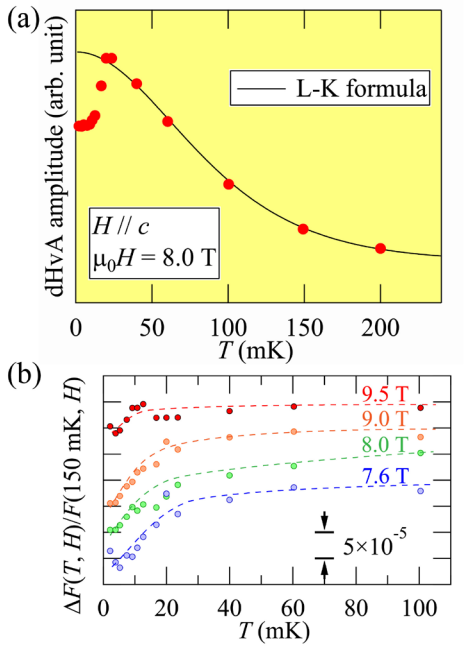

Fig. 1. (a) The temperature dependence of the dHvA amplitude of α_3 branch of $CeCoIn_5$. The solid line shows the fit of the data from the standard Lifshitz-Kosevich formula. (b) The temperature dependence of the normalized shift of the dHvA frequency $\Delta F(T, H) / F(150\ \mathrm{mK}, H)$ of α_3 branch. The data are shifted for clarity. The dashed lines are guides for the eye.

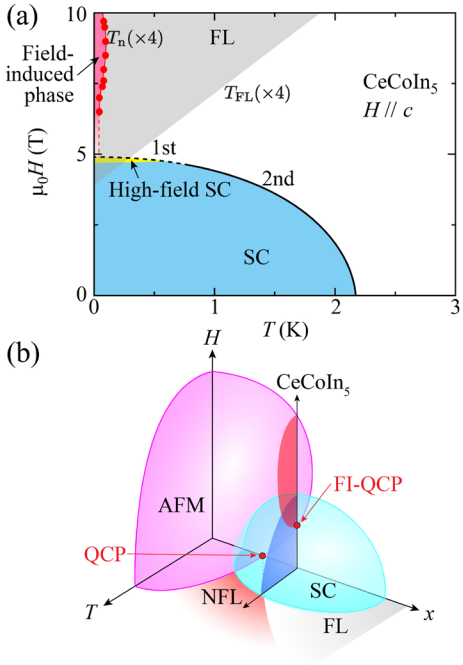

Fig. 2. (a) The H-T phase diagram of $CeCoIn_5$. Field-induced phase found by our measurements (pink), the Fermi liquid (FL) region (gray), the superconducting (SC) phase (blue), and the high-field SC phase (yellow) are shown. Both T_n (the red circles) and T_{FL} are multiplied by 4 for clarity. (b) A schematic H–T–x phase diagram near the AFM QCP, where x denotes pressure or chemical substitution. The cross section corresponds to the H–T phase diagram of $CeCoIn_5$, in which a presumed field-induced QCP (FI QCP) is also shown at the intersection with the AFM boundary.

We also find that the transition temperature T_n depends on field only weakly for 7–10 T even though the Zeeman energy at 10 T is about 3 orders of magnitude larger than k_BT_n. This field dependence implies that AFM order is enhanced by suppressing the critical spin fluctuations in the vicinity of the AFM QCP in high fields, which gives rise to the weak field dependence of T_n, as supported by the FLEX calculation [4].

Future studies for the detailed structure of the newly-found state would reveal the origin of the unconventional superconductivity in the proximity of a magnetically ordered state. As demonstrated by this study, we believe that the development of the ultralow-temperature measurements

has extensive potential to shed a new light on unexplored phenomena.

References
[1] H. Shishido *et al.*, Phys. Rev. Lett. **120**, 177201 (2018).
[2] K. Izawa *et al.*, Phys. Rev. Lett. **87**, 057002 (2001).
[3] J. L. Sarrao and J. D. Thompson, J. Phys. Soc. Jpn. **76**, 051013 (2007).
[4] Y. Yanase, J. Phys. Soc. Jpn. **77**, 063705 (2008).

Authors
H. Shishido[a,b], S. Yamada, K. Sugii, M. Shimozawa, Y. Yanase[c], and M. Yamashita
[a]Osaka Prefecture University
[b]Institute for Nanofabrication Research, Osaka Prefecture University
[c]Kyoto University

Spin Current Noise of the Spin Seebeck Effect and Spin Pumping

M. Matsuo and T. Kato

In the research field of mesoscopic physics, current noise measurement is an important tool to obtain useful information on electronic transport such as determination of the effective charge, evaluation of electron entanglement, and even spin accumulation. In the research field of spintronics, the pure spin current induced by, e.g., spin pumping and spin Seebeck effect (see the upper two schematic pictures in Fig. 1), is a central research subject. Recently, the noise of this pure spin current has measured by using the inverse spin Hall effect [1]. Although the noise of the pure spin current is expected to have useful information, its theoretical study has, however, been overlooked for a long time, and has just started recently in a few papers [2].

In our study [3], we considered a normal metal(NM)/ ferromagnetic insulator(FI) bilayer system, which is an important platform of spintronics. We considered a general model Hamiltonian with both spin-conserving and non-spin-conserving processes, and formulated the spin current and the spin-current noise within the framework of Keldysh Green's function [4]. Using the second-order perturbation with respect to the NM-FI interface coupling, we derived expressions of them in terms of the propagators of electrons and magnons. The lower panel of Fig. 1 shows temperature dependence of the spin-current noise using parameters for a yttrium-iron-garnet-(YIG-)platinum interface. As indicated from the figure, temperature dependences of the spin-current noise contain useful information, which can distinguish the mechanism of the spin-current generation.

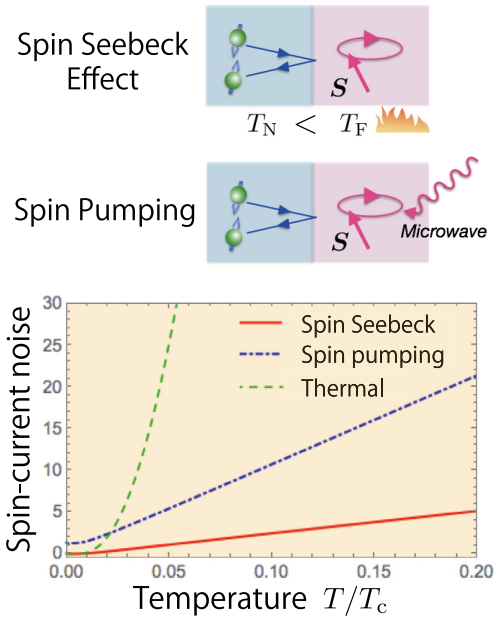

Fig. 1. Upper two pictures: Schematics of spin-current generation by spin Seebeck effect and spin pumping. Lower panel: Temperature dependence of spin-current noise. The temperature is normalized with the Curie temperature of the ferromagnetic insulator. Temperature dependence of thermal spin-current noise is also shown.

We also demonstrated that simultaneous measurement of the spin current and the non-equilibrium spin-current noise provides important information on spin transport. The Fano factor, which is the ratio between the spin-current noise and the spin current, was shown to be constant at low temperatures for both spin Seebeck effect and spin pumping. This low-temperature Fano factor includes information of effective spin in spin transport, which is $\hbar$ if the spin conserving process is dominant. As the weight of the spin non-conserving process increases, the effective spin increases by mixture of the two types of spin transport process. In actual experiments of spin pumping, the spin current can be generated also by spin Seebeck effect due to sample heating by microwave irradiation. Discrimination of spin pumping signal from heating effect has been a problem for long time. We proposed a method to estimate an increase of the sample temperature by combining the spin current and the spin-current noise. Finally, we discussed a spin Hall angle, which indicates an efficiency of the inverse spin Hall effect: conversion of spin current into charge current in metals. In a special situation, we can know the Fano factor a priori. For example, the Fano factor is $\hbar$ at low temperatures if the spin non-conserving process can be neglected. For such a situation, we can use it as a standard for the spin current and the spin current noise. By comparing this Fano factor with actual measurement of charge current and current noises in the inverse spin Hall effect, we can obtain the spin Hall angle at the interface.

We hope that the present calculation serves as a bridge between two well-established research areas, mesoscopic physics and spintronic physics. This collaborated research started from close discussion with M. Matsuo who was a visiting professor of ISSP in academic year 2016.

References
[1] A. Kamra *et al.*, Phys. Rev. B, **90**, 214419 (2014).
[2] A. Kamra and W. Belzig, Phys. Rev. Lett. **116**, 146601 (2016); S. Takei and M. Mohseni, Phys. Rev. B **97**, 014427 (2018).
[3] M. Matsuo, Y. Ohnuma, T. Kato, and S. Maekawa, Phys. Rev. Lett. **120**, 037201 (2018).
[4] Y. Ohnuma, M. Matsuo, and S. Maekawa, Phys. Rev. B **96**, 134412 (2017).

Authors
M. Matsuo[a,b], Y. Ohnuma[b], T. Kato, and S. Maekawa[b]
[a]Advanced Institute for Materials Research, Tohoku University
[b]Advanced Science Research Center, Japan Atomic Energy Agency

Spin-Orbit Interaction in Nanoparticle-Decorated Graphene

J. Haruyama and S. Katsumoto

Introduction of spin-orbit interactions (SOIs) into two-dimensional (2D) honeycomb lattices is predicted to create 2D topological phases [1]. Graphene is a representative 2D honeycomb lattice, whereas it lacks SOIs due to the

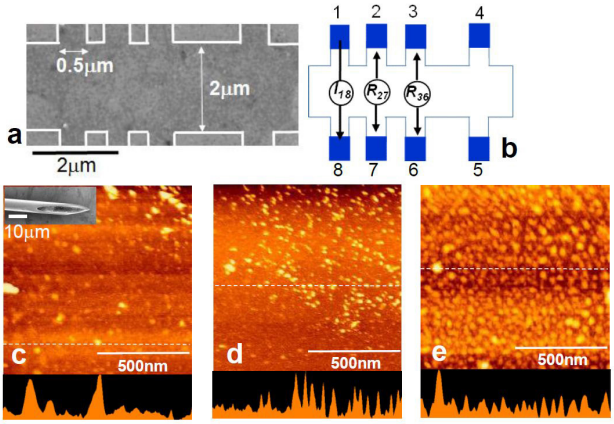

Fig. 1. (a)(b) Scanning electron micrograph and schematic top views of graphene formed into a multiple Hall bar pattern used for non-local resistance (R_{NL}) measurements. (c -e) Atomic force microscope images of the Bi_2Te_3 nanoparticle decorated on graphene using a nano needle method (inset of (c)) with three different-densities (D) ; (c) – (e) for D ~ 4/(100 nm)^2 (coverage ~ 3%), D ~ 10/(100 nm)^2 (coverage ~ 8%), and D ~ 23/(100 nm)^2 (coverage ~ 20%), respectively. Lower panels show the height along white broken lines in the upper panels.

lightness of carbon atom and the complete flatness of the lattice. Though many trials to introduce SOIs into graphene with various perturbations have been reported so far, the number of sound experiments has remained small [2]. A way to introduce SOI is to distribute nanoparticle with heavy mass atoms onto graphene. Here we precisely control small-amount of nanoparticles (platinum (Pt) or bismuth telluride (Bi_2Te_3)) randomly distributed on graphene and observe the appearance of SOI-induced (inverse) spin Hall effect (SHE).

Pt or Bi_2Te_3 nanoparticles with diameters of 3 ~ 5 nm are dispersed on monolayer graphene grown by chemical vapor deposition and formed into a multiple Hall bar (Figs. 1(a), 1(b); area for $w = 2 \times L_{sa} = 5(\mu m)^2$). High quality of the monolayer graphene has been confirmed by Raman spectra and X-ray Photoelectron Spectroscopy. The electron concentration in the graphene can be controlled with the back-gate voltage. For this experiment, we develop a specific tool, that is, a nano-needle to carry out clean and noninvasive decoration of graphene surface with nanoparticles. Dropping a small fleck of acetone, into which the nanoparticles are dispersed with ultrasound, we can precisely control the nanoparticle density (D) on the graphene surface. Examples of thus dispersed random nanoparticles are shown in Fig. 1 (c-e) for D ~ 4, 10 and 23/(100 nm^2), respectively. After the decoration, samples are annealed at 400 ºC for 10 minutes under high vacuum to advance chemical bonding between the nanoparticles and the carbons.

Figures 1 (b) also shows the terminal configuration for the non-local resistance measurement. The external current is applied along 1-8, which causes the spin current along the Hall bar via the SHE. The spin current next produces voltages between 2 and 7, 3 and 6 through the inverse SHE. Figure 2 shows the temperature variation of thus measured non-local resistance R_{27} as a function of in-plane external magnetic field, which causes the precession of electron spins and hence diminish the non-local resistance. This can be viewed as, in a sense, a Hanle measurement. The behavior of R_{27} shown in Fig. 2 clearly indicates the introduction of considerably strong SOI into graphene. The estimated spin separation by the SOI is as large as 50 meV, which is the largest among so far reported. The value is supported by scanning tunneling microscopy spectra.

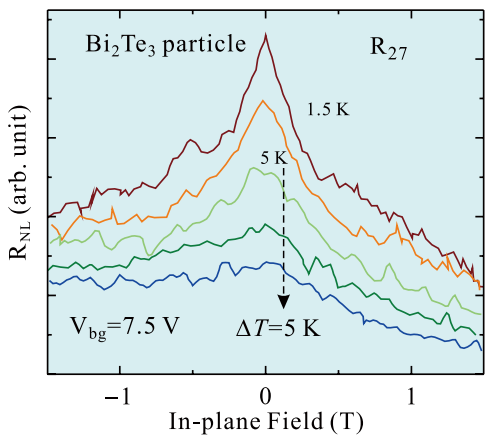

Fig. 2. Temperature variation of non-local resistance R_{27} as a function of in-plane external magnetic field.

References

[1] C. L. Kane and E. J. Mele, Phys. Rev. Lett. **95**, 226801 (2005).
[2] J. Balakrishnan, G. K. W. Koon, M. Jaiswal, A. C. Neto, and B. Özyilmaz, Nat. Phys. **9**, 284 (2013).

Authors

T. Namba[a], K. Tamura[a], K. Hatsuda[a], C. Ohata[a], T. Nakamura, S. Katsumoto, and J. Haruyama[a]
[a]Aoyama Gakuin University

STM Study of In-Gap Surface States on Single-Phase SmB_6 (001)

S. Suga, F. Iga, and F. Komori

Strong electron correlation in the Kondo insulator samarium hexaboride (SmB_6, Fig. 1(a)) has attracted great attention over decades. The hybridization of localized 4*f* states with itinerant 5*d* states triggers a gap opening at Fermi energy E_F, and induces a metal-insulator transition with decreasing temperature [1]. Recently, it was proposed that the observed saturation in the electrical resistivity at

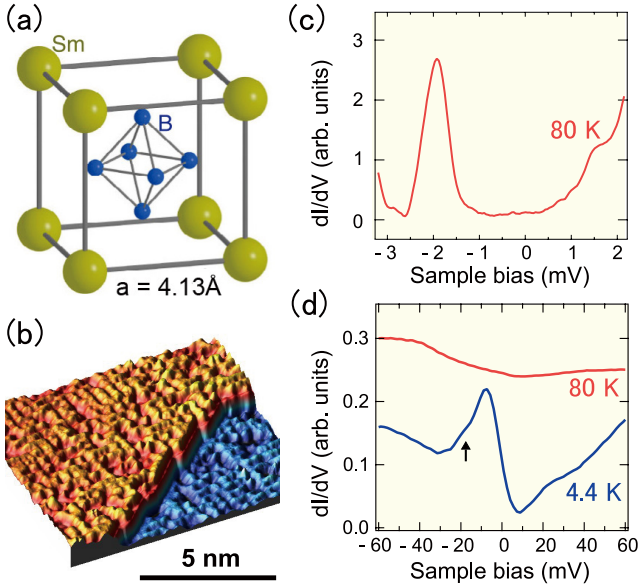

Fig. 1. (a) Schematic structure model of single-crystal SmB_6. (b) Atomically-resolved STM image of the SmB_6(001) surface prepared by the cycles of Ar^+ sputtering and 1030 ºC annealing. (c) Spatially-averaged *dI/dV* spectrum over a wide range of sample bias from -3.2 V to 2.2 V at 80 K. The peak at -2 V indicates Sm termination of the prepared SmB_6(001) surface. (d) Temperature dependence of the spatially-averaged *dI/dV* spectra on the SmB_6(001) surface in the hybridization gap area at 80 K and 4.4 K. The arrow indicates the fine shoulder structure located at -15 meV possibly derived from localized bulk f-states.

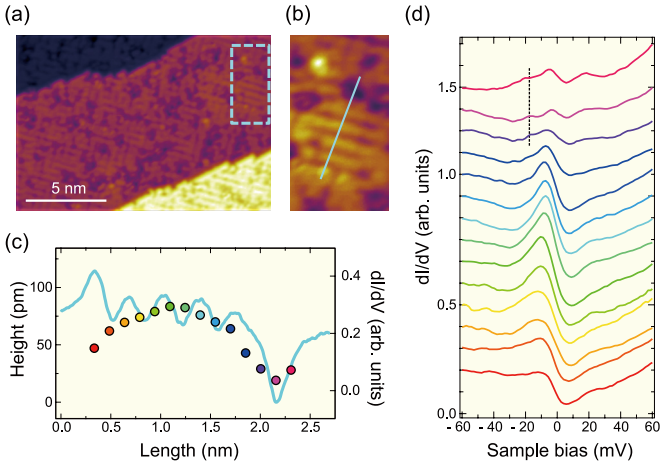

Fig. 2. (a) Atomically-resolved STM image of the $SmB_6(001)$ surface. (b) Magnified STM image of the $SmB_6(001)$ surface surrounded by blue dotted lines in (a). (c) (Left axis) STM height profile along the blue line in (b). Two types of defects, a small protrusion and a dip, are visible at ~ 0.3 (left) and at 2.2 (right) nm, respectively. (Right axis) differential conductivity *dI/dV* along the blue line in (b). At each position, the magnitude of the *dI/dV* of the peak structure located at -8 meV in (d) is plotted. (d) Series of 14 *dI/dV* spectra recorded along the blue line in (b). The colors indicate the recorded positions of the *dI/dV* spectra marked as dots with the same colors in (c), i.e, the spectra from bottom to top in (d) corresponds to the dots from left to right in (c). The dotted line indicates the energy position of a fine structure in the in-gap state.

low temperature is attributed to a topological surface state inside the hybridization gap. Experimentally, however, spatially-resolved surface characterizations by scanning tunneling microscopy (STM) have revealed that several types of surface structures randomly coexist on the cleaved $SmB_6(001)$ surfaces. This makes it difficult to investigate the intrinsic surface electronic properties by spatially-averaged methods. As an alternative to the crystal cleavage, a cyclic Ar^+ ion sputtering and annealing was recently performed to prepare a single-phase $SmB_6(001)$ surface reproducibly [2]. Nevertheless, the atomically-resolved structure characterization of the surface is still necessary for detailed discussion of its in-gap surface state.

Using STM, we have investigated structural and electronic properties of a clean $SmB_6(001)$ surface prepared by the sputtering and annealing method [3]. Our atomically-resolved observations shown in Fig. 1 (b) reveals that a non-reconstructed $p(1 \times 1)$ lattice with point defects is successfully and homogeneously formed over the entire surface using an optimal annealing temperature. In the tunneling (*dI/dV*) spectra on this surface, we found a peak in the density of states at – 2 eV below E_F (Fig. 1(c)), which indicates the B 2*p* dangling bonds on a Sm-terminated surface. The hybridization gap with an in-gap state located around – 8 meV below E_F develops in the tunneling spectra with decreasing temperature as shown in Fig. 1(d). In Fig. 2, we show spatial dependence of the in-gap state near E_F at 4.4 K. The state is sensitive to the structural variation on the surface; it is significantly suppressed near the point defect on the ordered region, but survives on the whole surface irrespective of defects. The existence of a robust surface state, which can be an evidence of a topologically-protected surface state, is confirmed inside the Kondo hybridization gap in this system.

References
[1] P. Coleman, Handbook of Magnetism and Advanced Magnetic Materials, **1**, 95 (Wiley, 2007).
[2] M. Ellguth, C. Tusche , F. Iga, and S. Suga, Philos. Mag. **96**, 3284, (2016).
[3] T. Miyamachi *et al.*, Sci. Rep. **7** 12837, (2017).

Authors
T. Miyamachi, S. Suga[a,b], M. Ellguth[c], C. Tusche[b,d], C. M. Schneider[b,d], F. Iga[e], and F. Komori
[a]Institute of Scientific and Industrial Research, Osaka University
[b]Peter Grünberg Institut, Forschungszentrum Jülich
[c]Institut für Physik, Johannes-Gutenberg-University
[d]Fakultät für Physik, Universität Duisburg-Essen
[e]Ibaraki University

Atomic Contacts Easily Broken by Bias Voltage under Tensile Stress

S. Kurokawa, Y. Hasegawa, and A. Sakai

A single-atom contact (SAC) of a metal is the smallest contact where a single atom makes a link between a pair of electrodes. One notable characteristic of SACs is found in their conductance, which is described as $(\Sigma_n \tau_n)G_0$. Here τ_n is the transmission probability of the n-*th* conduction channel and $G_0 = 2e^2/h$ is the quantum conductance. Among various metals, SACs of noble metals (Au, Ag, and Cu) are of particular physical and practical importance, because they have only a single conduction channel with $\tau_1 \sim 1$, making the conductance ~G_0; a material-independent constant. These unique characteristic makes them useful in logic circuits, and some atomic devices employing SACs as functional elements have already been developed.

For the device applications, SACs have to be stable under operating bias voltages. Conventionally, the stability of SACs is discussed in terms of their lifetime τ, which is given by the following thermal-activation-type-formula: $\tau = \tau_0 e^{W/kT}$; $W = W_0 - \alpha V - \beta F$ (α, $\beta > 0$), where τ_0 is a pre-exponential factor, V and F represent the bias and the tensile force applied to an SAC, respectively, and W_0 is the activation barrier at $V = F = 0$. The term αV represents the reduction of the barrier by the bias voltage. Similarly, the term βF determines the ultimate tensile strength to break the SAC.

In the equation, both V and F additively contribute to reduce the activation barrier and shorten the lifetime, which means that the bias stability depends on the amount of F. To date, the bias stability has been experimentally studied for some metal SACs that had been, in most cases, prepared by mechanical breaking, which is usually subjected to

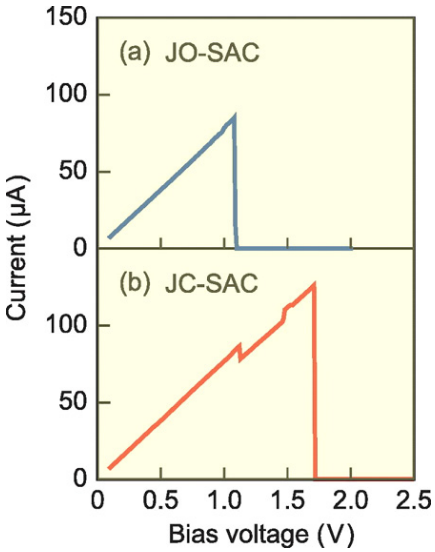

Fig. 1. Examples of I–V curves observed at Au SACs produced (a) by junction opening (JO) and (b) by junction closing (JC). The junction current increases linearly up to the high-bias breakdown.

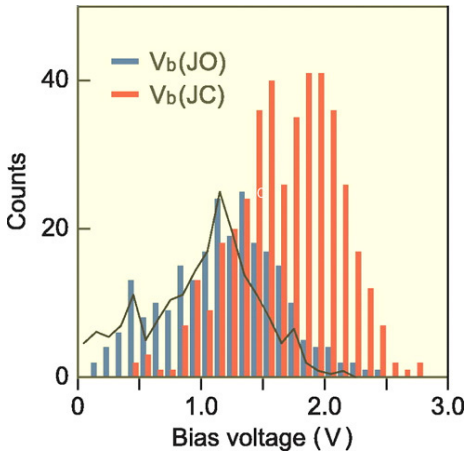

Fig. 2. The distribution of the junction breaking voltages of Au SACs. The blue and red histograms represent the distributions for JO- and JC-SACs, respectively. The solid line indicates the V_b data for JO-SACs collected by Smit *et al*. [3] The distribution of JC (red) is obviously shifted to the high bias side compared to that of JO (blue). The observed high-bias shift of V_b for JC indicates high stability of JC-SACs against the bias voltage applied across the junction.

built-in tensile stress. In this work [1], we investigated the break voltages of Au and Pb SACs created by junction closing (JC), instead of breaking, and compared the results with those produced by junction opening (JO) or breaking. Because JC essentially involves no junction stretching, the JC-SACs should contain lower tensile forces than JO-SACs and are thus expected to show higher break voltages.

Our break-voltage measurements were made on Au contacts produced by mechanically controllable break junction (MCBJ) method at 4 K. We also performed similar break-voltage experiments on Pb SACs using a cryogenic ultrahigh-vacuum STM at 1.7 K and fabricated Pb SACs by touching a Pb-coated tungsten tip to a clean Pb surface [2].

Figures 1(a) and 1(b) show examples of the I–V curves observed for JO- and JC-SACs, respectively. In both I–V curves, the junction current increases with the voltage and suddenly drops to zero at the point of break junction. From the breaking point we determined the break voltage V_b. Figure 2 summarizes the results of our V_b measurements on Au SACs. In the figure, the two histograms colored in blue and red represent the distributions of V_b for JO- and JC-SACs, respectively. Both histograms cover a wide voltage range, but the distribution of JC (red) is obviously shifted to the high bias side compared to that of JO (blue). The observed high-bias shift of V_b for JC confirms our assumption that JC-SACs show higher break voltages than JO-SACs.

We also measured the break voltages of Pb SACs. The V_b distribution of JC moves to the high bias side relative to that of JO. Thus, as for Au, the JC-SACs of Pb tend to break at higher biases than the JO-SACs. The observed high-bias shift of JC indicates that JC is a viable method for improving the bias stability of SACs.

From our results we also estimated the magnitude of the force reduction in our Au JC-SACs. According to the equation mentioned above, a variation in the tensile force ΔF is related to the variation in the break voltage ΔV_b as $\Delta F = -(\alpha/\beta)\Delta V_b$. Our ΔV_b for Au SACs is 0:52 V. Substituting the value of α and β adapted from Ref. 3, we obtain the force reduction ΔF = 0:15 nN. Smit et al. [3] estimated F in JO is 0.95 nN; thus, we find F in JC is 0.80 nN. This indicates that the JC reduced the tensile force as expected, but the force was still positive and remained tensile.

The tensile force in JC might appear counter-intuitive because a JC-SAC is formed by the touching of two electrodes. We consider that it is due to the short-range attractive force. At the close distances the apex atom moves towards the counter electrode by the attractive force exerted on the atom. As a result, the bonds between the contact atom and the electrode atoms are slightly stretched and exert a tensile force on the contact atom. This explains why we obtained tensile force for our Au JC-SACs.

Our break voltage measurements of Au and Pb SACs indicated that the JC-SACs exhibit a higher break voltage than the JO-SACs, which is favorable for the device application. The improved tolerance against the bias voltage can be understood by the reduced tensile stress in JC-SACs, clarifying the interplay between the junction force and the bias stability in SACs.

References
[1] S. Wakasugi, S. Kurokawa, H. Kim, Y. Hasegawa, and A. Sakai, J. Appl. Phys. **121**, 244304 (2017).
[2] H. Kim and Y. Hasegawa, Phys. Rev. Lett. **114**, 206801 (2015).
[3] R. H. M. Smit, C. Untiedt, and J. M. van Ruitenbeek, Nanotechnology **15**, S472 (2004).

Authors
S. Wakasugi[a], S. Kurokawa[a], H. Kim, Y. Hasegawa, and A. Sakai[a]
[a]Kyoto University

Noble Metal Segregation in $SrTiO_3$

M. Lee and M. Lippmaa

Photoelectrochemical water splitting is a process where photoexcited electrons and holes are used to drive a chemical hydrogen or oxygen evolution reaction at the surface of a semiconductor photoelectrode. The technique can be used to harvest solar energy and store the energy in the form of hydrogen fuel. In the semiconductor materials studied so far, the solar-to-hydrogen conversion process efficiency is still too low for practical applications. Oxide semiconductors such as titanates are often used as the electrode materials due to the chemical stability in water, but the energy conversion efficiency is limited by the loss of photocarriers to trapping and recombination. A general solution to this problem is to construct a nanostructured photoelectrode where light can be efficiently absorbed but a short escape path exists for the photocarriers to reach the surface before recombination can occur. For example, an array of semiconductor nanowires can be used, which would increase the effective surface area, guarantees a short carrier escape path in the radial direction of a wire, while still efficiently absorbing incident sunlight. A drawback of this strategy is the complicated synthesis

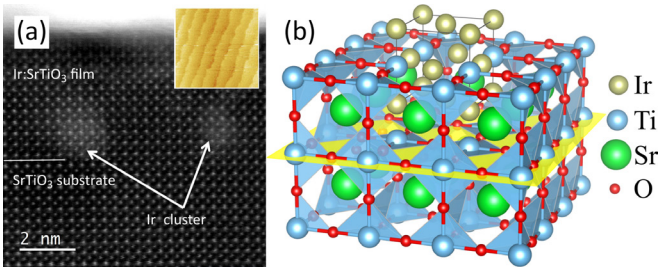

Fig. 1. (a) Cross-sectional HAADF-STEM image of a Ir:$SrTiO_3$ film on a $SrTiO_3$ substrate showing the formation of bright Ir clusters at the film interface. (inset) AFM image of the film surface, showing a smooth step-and-terrace morphology. (b) Structural model of a lattice-matched fcc Ir metal inclusion in the $SrTiO_3$ lattice.

process of nanowires and limited long-term mechanical stability. We have therefore studied the possibility of using spontaneous noble metal segregation in a perovskite lattice to embed self-organized nanoscale metal electrodes in the bulk of an oxide semiconductor. We have demonstrated the formation of Ir nanopillars in $SrTiO_3$ thin films and photoelectrochemical measurements have shown that embedding metal electrodes in a semiconductor does indeed improve the energy conversion efficiency [1]. The main benefit of this structure is the simple one-step synthesis process and mechanical robustness.

The purpose of this joint-use project was to study the initial stage of Ir metal segregation in $SrTiO_3$ thin films [2]. As shown in the inset of Fig. 1a, the surface morphology of thin Ir:$SrTiO_3$ (~5 unit cell) films imaged by atomic force microscopy (AFM) shows no obvious metal segregation effects. However, bright clusters are observed in high-angle annular dark field scanning transmission electron microscopy (HAADF-STEM) images. An in-situ energy-dispersive x-ray spectroscopic analysis showed that the bright clusters in the film are strongly enriched in Ir and consistent with a face-centered cubic (fcc) metal cluster embedded in the perovskite lattice, as illustrated in Fig. 1b. It is clear from the STEM analysis that the clusters have uniform lateral size of about 2 × 2 perovskite unit cells. The thin films were grown at strongly reducing conditions, which means that the perovskite lattice contains oxygen vacancies, promoting the substitution of Ir atoms at the anion site. The anion substitution allows the fcc metal to form a lattice-matched metal inclusion in the $SrTiO_3$ lattice. When similar films are grown at slightly more oxidizing conditions, extended Ir metal nanopillars form instead of the isolated metal clusters. This work helps to design more elaborate oxide metal nanocomposites for energy harvesting applications.

References

[1] S. Kawasaki, R. Takahashi, T. Yamamoto, M. Kobayashi, H. Kumigashira, J. Yoshinobu, F. Komori, A. Kudo, and M. Lippmaa, Nat. Commun. **7**, 11818 (2016).

[2] M. Lee, R. Arras, R. Takahashi, B. Warot-Fonrose, H. Daimon, M.-J. Casanove, and M. Lippmaa, ACS Omega **3**, 2169 (2018).

Authors

M. Lee[a], R. Arras[b], R. Takahashi, B. Warot-Fonrose[b], H. Daimon[a], M.-J. Casanove[b], and M. Lippmaa

[a]Nara Institute of Science and Technology

[b]Université de Toulouse

Discovery of 'Quantum' Supercritical State of an Electron Fluid Induced by Valence Fluctuations

S. Nakatsuji, S. Shin, and T. Sakakibara

The supercritical fluid state near the liquid-gas critical point has been a major subject in condensed matter physics for its technological relevance and for its scientific significance. One of the important goals is to bring down the critical temperature and pressure, which are normally much higher than ambient conditions. By contrast, in the electronic versions of these critical points, there are some cases where the temperature scale may be reduced significantly down to near-zero temperatures so that one may observe quantum critical phenomena in the corresponding "supercritical" states. Strange metal behaviors have been seen in correlated electron systems as a result of proximity

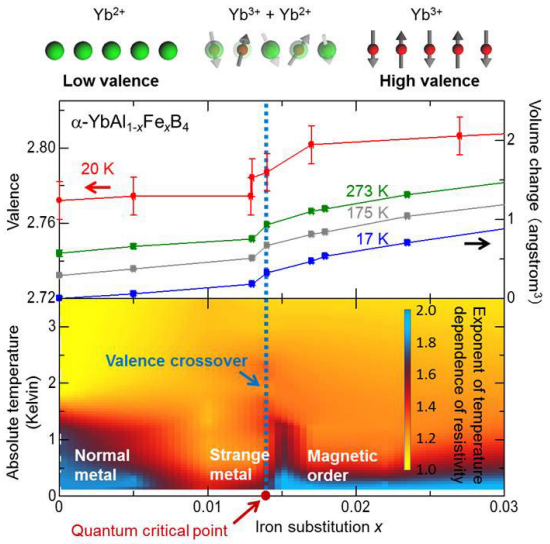

Fig. 1. Emergent quantum valence supercritical state in α-$YbAl_{1-x}Fe_xB_4$ at x = 0.014 exhibiting the sharp change in the valence, volume and the power law exponent in the temperature dependence of the resistivity. The high valence state and the low valence state are fluctuating around the valence crossover region as illustrated at the top of the figure. Here the arrows indicate the magnetic moments of the Yb^{3+} ion (red sphere). The middle of the figure shows the sharp valence change at around x = 0.014 at the absolute temperature of 20 Kelvin determined by the hard x-ray photoelectron spectroscopy (HAXPES). Significantly, the volume shows a similar x dependence to the valence. The contour plot at the bottom of the figure highlights the strange metallic state (yellow highlighted regions) emergent concomitantly with the sharp valence crossover at x = 0.014 between the normal metallic and magnetic ordered states. The contour plot indicates the variation of the power law exponent of the temperature dependence of the resistivity. The valence quantum critical point exists at x = 0.014 and at absolute zero temperature.

to a quantum critical end point of a first-order transition such as a metamagnetic transition and a Mott transition. Another candidate for the density instability that may theoretically drive novel quantum criticality (QC) is valence transition [1]. Near its associated quantum critical end point, singular fluctuations of valence (which includes charge, spin, and orbital degrees of freedom) and its coupling with thermodynamic quantities are expected to lead to a strong violation of Fermi liquid (FL) behavior. Similar to the Widom line in the supercritical fluid [2], fluctuations remain strong near the valence crossover line. Although a valence crossover at low temperatures has been reported in a variety of materials [3, 4], the associated QC has not been confirmed to date.

A valence critical end point existing near the absolute zero provides a unique case for the study of a quantum version of the strong density fluctuation at the Widom line in the supercritical fluids. Although singular charge and orbital dynamics are suggested theoretically to alter the electronic structure significantly, breaking down the standard quasiparticle picture, this has never been confirmed experimentally to date. We provide the first empirical evidence that the proximity to quantum valence criticality leads to a clear breakdown of Fermi liquid behavior. Our detailed study of the mixed valence compound α-$YbAlB_4$ reveals that a small chemical substitution induces a sharp valence crossover, accompanied by a pronounced non–Fermi liquid behavior characterized by a divergent effective mass (Fig. 1) and unusual T/B scaling in the magnetization.

References

[1] S. Watanabe and K. Miyake, Phys. Rev. Lett. **105**, 186403 (2010).

[2] B. Widom, J. Chem. Phys. **43**, 3898 (1965).

[3] J.-P. Rueff *et al.*, Phys. Rev. Lett. **106**, 186405 (2011).

[4] K. Matsubayashi *et al.*, Phys. Rev. Lett. **114**, 086401 (2015).

Authors
K. Kuga[a], Y. Matsumoto, M. Okawa, S. Suzuki, T. Tomita, K. Sone, Y. Shimura, T. Sakakibara, D. Nishio-Hamane, Y. Karaki[b], Y. Takata[a], M. Matsunami[c], R. Eguchi[d], M. Taguchi[a], A. Chainani[a,e], S. Shin[a], K. Tamasaku[a,f], Y. Nishino, M. Yabashi, T. Ishikawa, S. Nakatsuji[g]
[a]RIKEN SPring-8 Center
[b]University of the Ryukyus
[c]Institute for Molecular Science and The Graduate University for Advanced Studies
[d]Okayama University
[e]National Synchrotron Radiation Research Center
[f]Hokkaido University
[g]Japan Science and Technology Agency

Discovery of a New Magnetic Material: "Weyl Magnet"

S. Nakatsuji, T. Kondo, and S. Shin

In 2015, Weyl fermions have been discovered for the first time near the Fermi level in the non-magnetic semimetal TaAs. Weyl points in the momentum space serve as a pair of magnetic monopoles through the topological aspects of the wavefunctions for electrons [1]. Moreover, the fictitious magnetic fields due to the monopoles may induce novel electric transports, and could be useful for low energy consumption electronics. In contrast to the non-magnetic Weyl fermions in TaAs, magnetic Weyl fermions are known to appear in magnets, thus would enable us to control Weyl fermions by external magnetic field. This functionality will be necessary for device applications, and many efforts have been made for searching magnetic Weyl fermions. However, they have remained hypothetical so far.

Recently, an antiferromagnetic manganese-tin alloy Mn_3Sn is found to exhibit a large anomalous Hall and Nernst effects, even at room temperature [2, 3]. Usually, these anomalous Hall and Nernst effects are known to be proportional to magnetization and thus have been observed only in ferromagnets. The spontaneous Hall resistivity in the antiferromagnet with vanishingly small magnetization indicates that the large fictitious field equivalent to a few hundred T must exist in the momentum space. Recent DFT calculation predicts that the large fictitious field or Berry curvature may well appear due to the formation of Weyl points nearby the Fermi energy E_F [4].

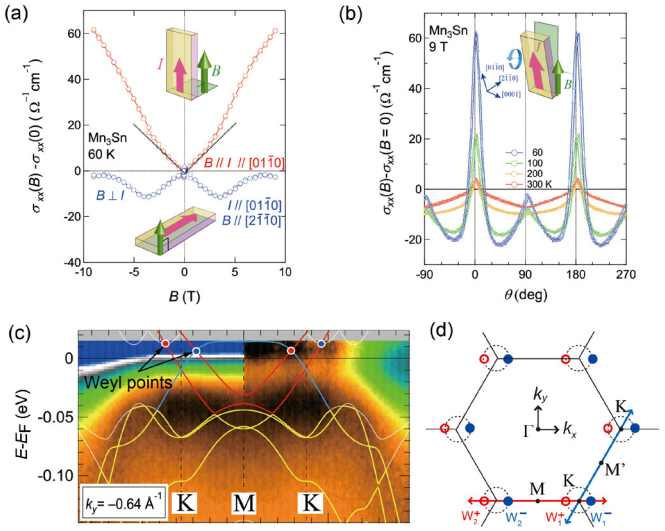

Fig. 1. Evidence for Weyl fermions in Mn_3Sn:(a)Weyl fermions in condensed matter systems show an unconventional positive longitudinal magnetoconductivity (negative longitudinal magnetoresistivity), called "chiral anomaly". (b) This appears only when magnetic field is applied parallel to electric field ($B//I$, θ = 0 deg.). With an increasing magnetic field, the breaking of the imbalanced charge conservation between the Weyl points with opposite chirality makes the materials more conductive. This novel phenomenon is known as one of the experimental evidence of the Weyl fermions. (c) ARPES band mapping near the Fermi level is compared with DFT band calculations. Weyl (band crossing) points with opposite chirality are denoted by blue and red closed circles, respectively. (d) These Weyl points are found along the K–M–K line in the bands on the $k_z = 0$ plane near E_F.

Nakatsuji, Kondo and Shin groups at ISSP University of Tokyo and their theoretical collaborators at RIKEN have demonstrated the realization of magnetic Weyl fermions in Mn_3Sn for the first time. Our study has revealed the existence of a "Weyl magnet", a new magnet with tunable magnetic Weyl fermions by magnetic fields at room temperature [5]. We found strong experimental evidence for the Weyl fermions in Mn_3Sn, namely, that the band structure revealed by angle resolved photoemission spectroscopy (ARPES) is found roughly consistent with density functional theory (DFT) and the chiral anomaly is clarified in the magnetotransport measurements (Fig. 1). Thus, these experiments demonstrate that the large anomalous Nernst signals arise from the Berry curvature associated with the Weyl points near the Fermi energy.

Our groups have revealed extremely large magnetic transports and thermoelectric effects in the Mn_3Sn magnet. By their new discovery of Weyl magnet, the mystery of these novel properties would be solved. We anticipate that further new phenomena will emerge through the interplay between electron correlation and topology in Weyl magnets.

References
[1] B. Q. Lv, H. M. Weng, B. B. Fu, X. P. Wang, H. Miao, J. Ma, P. Richard, X. C. Huang, L. X. Zhao, G. F. Chen, Z. Fang, X. Dai, T. Qian, and H. Ding, Phys. Rev. X **5**, 031013 (2015).
[2] S. Nakatsuji, N. Kiyohara, and T. Higo, Nature **527**, 212 (2015).
[3] M. Ikhlas, T. Tomita, T. Koretsune, M. –T. Suzuki, D. Nishio-Hamane, R. Arita, Y. Otani, and S. Nakatsuji. Nature Physics **13**, 1085 (2017).
[4] H. Yang, Y. Sun, Y. Zhang, W-J. Shi, S. S. P. Parkin, and B. Yan, New J. Phys. **19**, 015008 (2017).
[5] K. Kuroda, T. Tomita, M.-T. Suzuki, M.-T. Suzuki, C. Bareille, A. A. Nugroho, P. Goswami, M. Ochi, M. Ikhlas, M. Nakayama, S. Akebi, R. Noguchi, R. Ishii, N. Inami, K. Ono, K. Kumigashira, A. Varykhalov, T. Muro, T. Koretsune, R. Arita, S. Shin, T. Kondo, and S. Nakatsuji, Nature Materials **16**, 1090 (2017).

Authors
K. Kuroda*, T. Tomita*, M.-T. Suzuki[a], C. Bareille, A. A. Nugroho[b], P. Goswami[c], M. Ochi[d], M. Ikhlas, M. Nakayama, S. Akebi, R. Noguchi, R. Ishii, N. Inami[e], K. Ono[e], K. Kumigashira[e], A. Varykhalov[f], T. Muro[g], T. Koretsune[a], R. Arita[a], S. Shin, T. Kondo, and S. Nakatsuji
[*equal contribution]
[a]RIKEN Center for Emergent Matter Science
[b]Institut Teknologi Bandung
[c]University of Maryland
[d]Osaka University
[e]High Energy Accelerator Research Organization (KEK)
[f]Elektronenspeicherring BESSY II
[g]Japan Synchrotron Radiation Research Institute (JASRI)

First-order Magnetic Transitions and Transformation Arrested Behaviors in Sn-Modified Mn_2Sb

Y. Mitsui, K. Koyama, and Y. Uwatoko

First-order magnetic transition (FOMT) has been paid much attention such as the large magnetocaloric effects and metamagnetic shape memory effects. FOMT in some magnetic functional materials suppressed under high

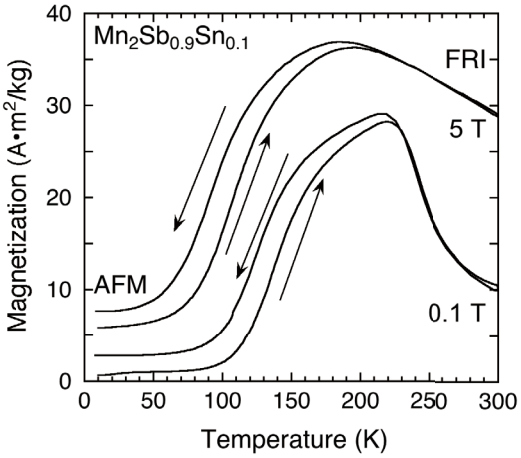

Fig. 1. Thermomagnetization curves for $Mn_2Sb_{0.9}Sn_{0.1}$ under 0.1 and 5 T [4].

magnetic fields. The suppression of FOMT is due to the freezing of the phase transition, which is explained by glass-like dynamics. This phenomenon is called "kinetic arrest" or "thermal transformation arrest (TTA)". For the application of magnetic functional materials using FOMT, the investigation of the origin of TTA phenomenon is necessary.

Mn_2Sb-based compounds exhibit FOMT between ferrimagnetic (FRI) and antiferromagnetic (AFM) state. So far, magnetocaloric effects for Mn_2Sb-based system were examined [1]. Although Mn_2Sb is ferrimagnet and do not show FOMT, FRI-AFM transition exhibits by substitution of V, Cr, Co and Cu to Mn-site. Additionally, it is reported that Co-, and Cu-modified Mn_2Sb exhibited TTA phenomenon [2, 3]. Meanwhile, modification of Sb-site, such as $Mn_2Sb_{1-x}Ge_x$ [3] and $Mn_2Sb_{1-x}Sn_x$, also exhibits FRI-AFM transition. However, there are few reports about TTA phenomenon for these compounds. In this paper, we reported the thermal transformation arrest behavior of Sn-modified Mn_2Sb by magnetization measurements [4].

Figure 1 shows the thermomagnetization (M-T) curves in $Mn_2Sb_{0.9}Sn_{0.1}$ under μ_0H = 0.1 and 5 T. FRI-AFM phase transition were observed for 100 ≤ T ≤ 210 K at μ_0H = 0.1 T. It is found that the temperature region of FOMT in $Mn_2Sb_{0.9}Sn_{0.1}$ is wider than other Mn_2Sb-based systems, such as $Mn_{1.8}Co_{0.2}Sb$ [2] and $Mn_2Sb_{0.9}Ge_{0.1}$ [3]. On the other hand, the difference in M between heating process after zero-field cooling and in-field cooling were observed for T < 50 K in 5 T. It is suggested that the FRI-AFM transition were suppressed and residual FRI state existed. In other words, FRI state was arrested at in-field cooling process under 5 T.

For further investigation for the difference of magnetization, magnetic relaxation measurements were carried out. Figure 2 shows the magnetic relaxation curves at 10, 30 and 50 K under 5 T. The measurements were performed after in-field cooling under 5 T. Although the fraction of arrested FRI state was small, magnetization clearly decreased both 30 and 50 K with increasing time, indicating the relaxation from arrested-FRI state to AFM state.

In conclusion, magnetic properties of Sn-modified Mn_2Sb were investigated. It is suggested by magnetic relaxation measurements that TTA phenomenon exhibits in $Mn_2Sb_{0.9}Sn_{0.1}$.

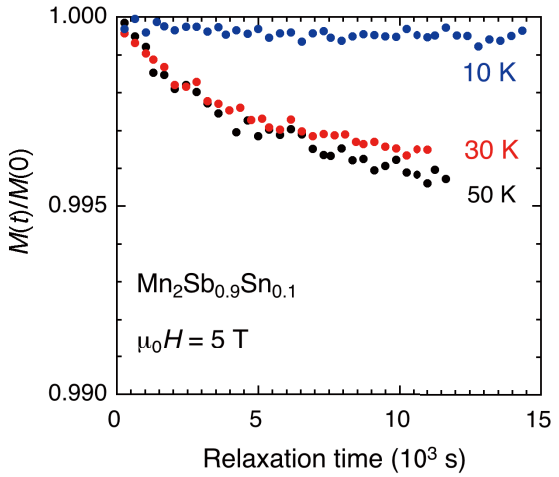

Fig. 2. Magnetic relaxation curves for $Mn_2Sb_{0.9}Sn_{0.1}$ at 10, 30, and 50 K in 5 T [4]. The magnetization $M(t)$ was normalized by $M(0)$.

References

[1] L. Caron *et al.*, Appl. Phys. Lett. **103**, 112404 (2013).
[2] H. Orihashi *et al.*, Mater. Trans. **54**, 969 (2013).
[3] Y. Matsumoto *et al.*, IEEE Trans. Magn. **50**, 1000704 (2014).
[4] T. Wakamori *et al.*, AIP Conf. Proc. **1763**, 020006 (2016).
[5] T. Wakamori *et al.*, IEEE Magn. Lett. **8**, 1402404 (2017).

Authors

Y. Mitsui[a], T. Wakamori[a], K. Takahashi[b], R. Y. Umetsu[b], Y. Uwatoko, M. Hiroi[a], K. Koyama[a],
[a]Kagoshima University
[b]Institute for Materials Research, Tohoku University

High Pressure Electrical Resistivity Measurements for High-T_c Candidates Material $Ln_4Ni_3O_8$ (Ln=La, Nd, Sm)

M. Uehara, I. Umehara, and Y. Uwatoko

$Ln_4Ni_3O_8$ (Ln=La, Nd, Sm) contains NiO_2 planes and its crystal structure is basically the same with high-T_c cuprate, and the formal valence of Ni is +1.33 composed of $3d^9$ and $3d^8$ mixed-valence state, being the same with high-T_c cuprate. Therefore, this compound seems to be a promising candidate for new high-T_c material. Despite these similarities with cuprate, this compound had showed neither metallic characteristic nor superconductivity [1-3], until we found that the intercalation and subsequent deintercalation treatment with sulfur (S-treatment) induced the metallic nature down to ~20 K (below ~20 K resistivity shows semiconducting upturn) in $Nd_{3.5}Sm_{0.5}Ni_3O_8$ [4, 5]. The sample without S-treatment is named to be the "as-synthesized sample" and the sample after S-treatment to be the "S-deintercalated samples" in this report. The as-synthesized and S-deintercalated samples are semiconducting and metallic (above ~20 K), respectively.

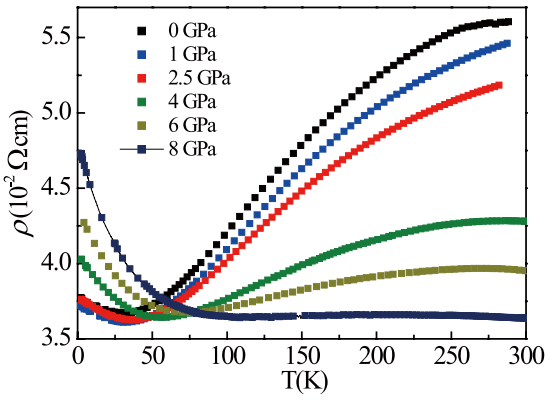

Fig. 1. Temperature dependence of electrical resistivity for the S-deintercalated sample of $Nd_{3.5}Sm_{0.5}Ni_3O_8$ under pressure.

Rietveld analyses based on synchrotron X-ray diffraction data at room temperature obtained in KEK suggest the removal of excess oxygens at apical site of Ni(2) which is in the outermost NiO_2 plane by S-treatment [6]. Therefore, it can be inferred that the excess oxygens at apical site of Ni(2) impedes the metallic conduction and these are effectively removed by the S-treatment. The similar situation has been discussed on the role of reduction annealing necessary procedure to obtain superconductivity for T'-type high-T_c cuprate having a very similar structure to present system.

In order to see whether or not the semiconducting behavior at low-temperature is suppressed and the superconductivity emerges, electrical resistivity measurements at pressures up to 8 GPa were performed for metallic S-deintercalated sample, and the cubic anvil apparatus was used with a mixture of Fluorinert 70 and 77 as the pressure medium. The result is shown in Fig. 1. In the temperature range from 300 K to approximately 50–60 K, the electrical resistivity is decreased by applying pressure. However, below approximately 50–60 K, with increasing applied pressure, the electrical resistivity increases and the temperature where the electrical resistivity shows an upturn from metallic conductivity increases, displaying enhancement of the semiconducting nature. As the origin of this unexpected result it can be speculated as follows: the removal of excess apical oxygens by S-deintercalation is not perfect. The pressure pushes the remnant apical oxygens close to the NiO_2 plane, and the effect of random potential increases, enhancing the tendency of localization. Similar pressure effect has been observed in T'-type high-T_c cuprate.

In conclusion, S-treatment removes additional apical oxygen but the removal is not perfect under the present S-treatment condition. Therefore, superconductivity might appear when additional apical oxygen is completely removed out.

References

[1] V. V. Poltavets *et al.*, Phys. Rev. Lett. **104**, 206403 (2010).
[2] Y. Sakurai *et al.*, Physica C. **487**, 27 (2013).
[3] Y. Sakurai *et al.*, JPS Conf. Proc. **1**, 012086 (2014).
[4] A. Nakata *et al.*, Adv. Condens. Matter Phys. **2016**, 5808029 (2016).
[5] K. Kobayashi *et al.*, JJAP Conf. Proc. **6**, 011106 (2017).
[6] M. Uehara *et al.*, J. Phys. Soc. Jpn. **86**, 114605 (2017)

Authors

M. Uehara[a], K. Kobayashi[a], H. Yamamoto[a], K. Wakiya[a] and I. Umehara[a], J. Gouchi, and Y. Uwatoko

[a]Yokohama National University

Maximizing T_c by Tuning Nematicity and Magnetism in $FeSe_{1-x}S_x$ Superconductors

K. Matsuura, Y. Uwatoko, and T. Shibauchi

In iron pnictides, high-T_c superconductivity appears near the antiferromagnetic phase, which is accompanied by the tetragonal-to-orthorhombic structural transition with significant electronic anisotropy (nematicity). It has been discussed that the quantum fluctuations of nematic and/or antiferromagnetic orders may play an essential role for the superconductivity. However, these two orders coexist with each other in iron-pnictide superconductors, and thus it has been difficult to disentangle the role of each phase for the superconductivity. To address this issue, FeSe is an important material because it shows a non-magnetic nematic order below 90 K [1]. Moreover, by isovalent S-substitution which corresponds to the chemical pressurization, this order is suppressed with increasing the S-content and it has been found that a non-magnetic nematic quantum critical point exists in the phase diagram of $FeSe_{1-x}S_x$ [2]. On the other hand, the non-magnetic nematic phase is also suppressed under physical pressure in FeSe, but before reaching a quantum critical point, a dome-shaped magnetic order is induced, which competes with high-T_c superconducting phase [3].

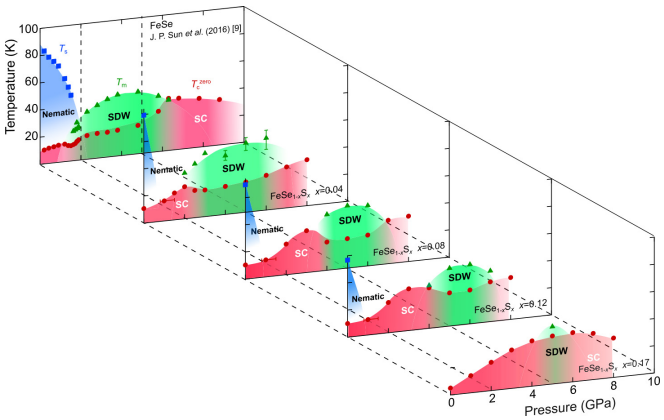

Fig. 1. Temperature-pressure-concentration phase diagram in $FeSe_{1-x}S_x$. The structural (T_s, blue squares), magnetic (T_m, green triangles) and superconducting transition temperatures (T_c^{zero}, red circles) are plotted against hydrostatic pressure P and S content x. T_s, T_m and T_c^{zero} are defined respectively by the temperatures of upturn, kink and zero resistivity in $\rho(T)$ curves under pressure for x = 0.04, 0.08, 0.12 and 0.17.

Here we report on our high pressure study on $FeSe_{1-x}S_x$ in wide ranges of pressure (up to $P \sim 8$ GPa) and sulfur content ($0 < x \leq 0.17$) by the electronic resistivity measurements with a cubic anvil high pressure apparatus in Uwatoko group and X-ray diffraction measurements with a diamond anvil cell in SPring-8 [4].

Our single crystalline samples were synthesized by the chemical vapor transport method. The electric resistivity measurements were carried out for $FeSe_{1-x}S_x$ (x = 0.04, 0.08, 0.12, and 0.17). From the anomalies seen in the temperature dependence of the electrical resistivity, the tetragonal-to-orthorhombic structural transition temperature T_s corresponding to the electronic nematic transition, the superconducting transition temperature T_c and the magnetic phase transition temperature T_m are determined, and their pressure dependence is investigated. From the results, we establish a three-dimensional Temperature(T)-pressure(P)-S substitution(x) electronic phase diagram as shown in Fig. 1. As x increases, the pressure-induced magnetic dome shifts to higher pressure and shrinks, while the low-pressure non-magnetic nematic phase shifts to lower pressure and disappears at $x \sim 0.17$. From this change, we find that the non-magnetic nematic and magnetic phases are completely separated in a low pressure region. To confirm the separation between two phases under pressure, we performed synchrotron X-ray diffraction under pressure for x = 0.08. In Fig. 2 we show (331) Bragg intensity as a function of temperature at 3.0 and 4.9 GPa together with the ρ(T) and dρ/dT data. At 3.0 GPa, no discernible change of the Bragg-peak is observed down to 10 K. At 4.9 GPa, on the other hand, the splitting of the Bragg peak is resolved around $T_s \sim 41$ K, evidencing the presence of the tetragonal-orthorhombic structural transition. This structural transition is located very close to the magnetic transition at T_m at 5.0 GPa as indicated by the sharp peak in dρ/dT curve. Thus, it

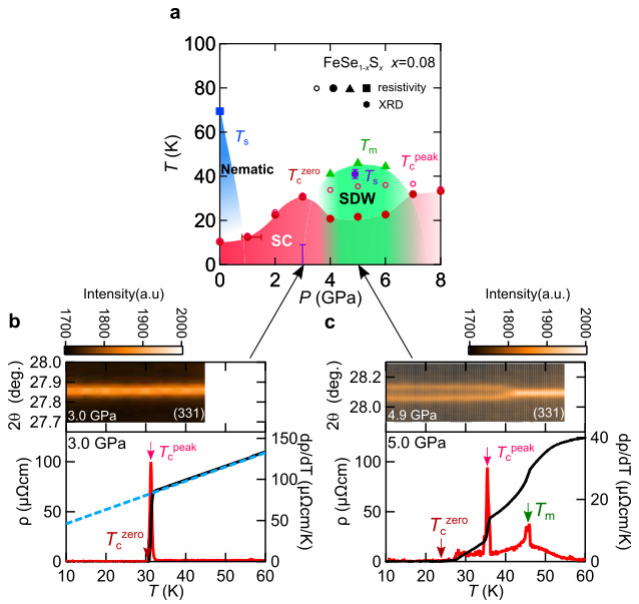

Fig. 2. (a) Temperature-pressure phase diagram for $FeSe_{1-x}S_x$ (x = 0.08) together with T_s determined by the high-pressure synchrotron X-ray diffraction (XRD) in a diamond anvil cell (the purple hexagon with error bars). (b), (c) Temperature dependence of Bragg intensity as a function of 2θ angle is indicated in color scale for 3.0 GPa (b) and 4.9 GPa (c). $\rho(T)$ and $d\rho/dT$ are also shown with the same horizontal axis. The red, pink and green arrows indicate T_c^{zero}, T_c^{peak} and T_m, respectively.

is natural to consider that the magnetic phase is accompanied with an orthorhombic structure, similar to the case of the stripe-type magnetic phase in other iron-pnictide superconductors.

By simultaneously tuning chemical and physical pressures, we achieve a complete separation of nematic and antiferromagnetic phases. In between, an extended non-magnetic tetragonal phase emerges, where T_c shows a striking enhancement. The high T_c superconductivity is observed near both ends of the magnetic dome. From this result, the fluctuations of magnetic order are likely to be more relevant to the high-T_c superconductivity in this system.

References

[1] S-H. Baek *et al*., Nature Materials **14**, 210 (2015).
[2] S. Hosoi *et al*., Proc. Natl. Acad. Sci. USA **113**, 8139 (2016).
[3] J. P. Sun *et al*., Nat. Commun. **7**, 12146 (2016).
[4] K. Matsuura *et al*., Nat. Commun. **8**, 1143 (2017).

Authors

K. Matsuura[a], Y. Mizukami[a], Y. Arai[a], Y. Sugimura[a], N. Maejima[b], A. Machida[b], T. Watanuki[b], T. Fukuda[c], T. Yajima, Z. Hiroi, K. Y. Yip[d], Y. C. Chan[d], Q. Niu[d], S. Hosoi[a], K. Ishida[a], K. Mukasa[a], S. Kasahara[e], J.-G. Cheng[f], S. K. Goh[d], Y. Matsuda[e], Y. Uwatoko, and T. Shibauchi[a]
[a]University of Tokyo
[b]National Institutes for Quantum and Radiological Science and Technology
[c]Japan Atomic Energy Agency (SPring-8/JAEA)
[d]The Chinese University of Hong Kong
[e]Kyoto University
[f]Chinese Academy of Sciences

Torque Magnetometry Studies using the Microcantilever on Molecular Conductor TPP[Mn(Pc)(CN)$_2$]$_2$

K. Torizuka, M. Matsuda, and Y. Uwatoko

The shape of the Metal Phthalocyanine TPP[M(Pc)(CN)$_2$]$_2$ compound (M = 3d metal) is unique; two CN groups are perpendicularly attached to the center of the M(Pc) planar molecule. In these compounds, the magnetic d electron of the central ion in the planar molecule and the conducting π electron reside in the same unit molecule. This fact makes the interaction between d and π electrons important. In M = Fe, the compound exhibits a giant negative magnetoresistance (GMR); when a high magnetic field is applied perpendicularly to the c-axis, the resistivity drops by more than two orders of magnitude at low temperatures. On the other hand, M = Mn, GMR is hardly seen. The motivation of our research is to know the difference in magnetic structure between compounds that GMR can be seen and compounds that GMR cannot be seen.

Here we report the results of our torque magnetometry experiments on M = Mn compound, TPP[Mn(Pc)(CN)$_2$]$_2$, using the microcantilever for the atomic force microscopy (AFM). This technique is very powerful, because even if the sample mass is on the order of 1 μg, it is so sensitive that we can detect the torque signal. In our experiments only tiny sample is available. The sample was mounted at the tip of the cantilever and the magnetic field orientation dependence of the signal that is nonlinearly proportional to the torque was measured.

In Figs. 1 and 2, typical torque curves measured when the magnetic field was rotated in the plane that includes the c-axis, and when the magnetic field was rotated in the ab plane, are depicted, respectively. A twofold symmetric signature with large and small peaks is seen in Fig. 1, which has never been observed in our former measurements on TPP[Fe(Pc)L$_2$]$_2$ (L = CN, Br, and Cl) family. This is characteristic of the ferromagnetism. On the other hand, a sawtooth waveform and fourfold-symmetric behavior can be seen

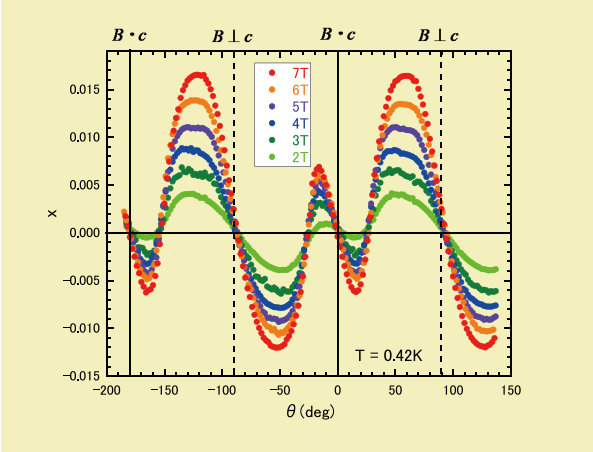

Fig. 1. Torque curves under various magnetic fields when the magnetic field was rotated in a plane included the c-axis at 0.42 K.

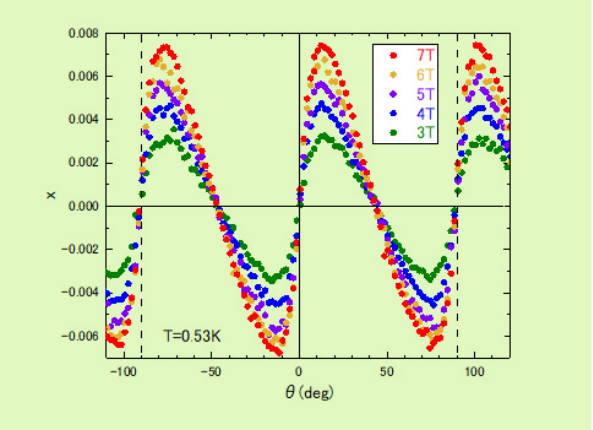

Fig. 2. Torque curves under various magnetic fields when the magnetic field was rotated in the ab plane at 0.53 K.

in Fig. 2. This feature is interpreted as the antiferromagnetism. The electrons responsible for these behavior should be *d* electrons of the Mn^{3}+ ion for the former case, and π electrons for the latter case. At first sight, it would be thought of that the electron we observe by our torque measurements might be the magnetic *d* electron only, in whichever plane the magnetic field was rotated. However, our former studies have already clarified that although the anisotropic one-dimensional Heisenberg (AODH) model which should describe only the behavior of the *d* electron can reproduce the feature of the torque signal with the magnetic field rotated in the plane including the *c*-axis, it is insufficient to describe the behavior of the torque when the magnetic field is rotated in the *ab* plane, in terms of the AODH model only. This model should be supplemented by the antiferromagnetic model of π electrons, because otherwise the behavior of torque signals in this field rotation plane cannot be reproduced at the region of low temperatures and low magnetic fields. We are thus allowed to consider that the electron we can observe when the field rotated in the *ab* plane should be the π electron, that is different from the electron when the field rotated in the plane including the *c*-axis. We are thus able to separate contributions due to the *d* and π electrons.

Now we also have to take the susceptibility data into account. That shows the weak antiferromagnetic behavior of the *d* electron as a result of applying the Curie-Weiss law. We have to reconcile the torque and the susceptibility data. One possibility is that the *d* electron should be in the canted antiferromagnetic state, instead of the ferromagnetic. Even in the canted antiferromagnetic case, the torque curve is also the same as that in the ferromagnetic case if the anisotropy energy is very small. We also pointed out that the experimental observation that the magnetoresistance is hardly seen is consistent with the canted antiferromagnetic model. The canted antiferromagnetism is very likely, because the canted antiferromagnetism might be mediated by the Dzyaloshinsky-Moriya interaction. In fact, the space inversion symmetry is broken and the spin-orbit coupling plays an important role in our sample.

Reference
[1] K. Torizuka, Y. Uwatoko, M. Matsuda, G. Yoshida, M. Kimata, and H. Tajima, J. Phys. Soc. Jpn. **86**, 114709 (2017).

Authors
K. Torizuka[a], M.Matsuda[b], and Y. Uwatoko
[a]Nippon Institute of Technology
[b]Kumamoto University

Identification of the Key Interactions in Structural Transition Pathway of FtsZ from Staphylococcus Aureus

Y. Shigeta, R. Harada, and H. Matsumura

The bacterial cell division protein FtsZ forms a ring-shaped filament (Z-ring) inside the cell membrane in the presence of GTP, and dynamically repeats division and dissolution owing to treadmilling coupled with the GTPase activity to cause invagination of the cell membrane. Although this invagination is thought to be caused by shrinking of the Z-ring, its molecular mechanism is still unknown. The crystal structure of GDP-bound *Staphylococcus aureus* FtsZ (SaFtsZ-GDP complex) was experimentally determined by X-ray structural analysis. Surprisingly, there are two different

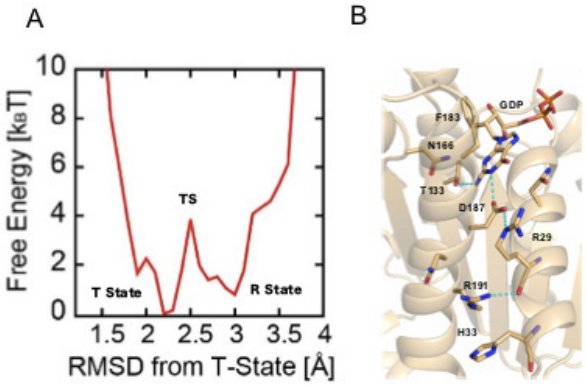

Fig. 1. (A)Free energy landscape of SaFtsZ, which connects T- and R-state. (B) Transition state structure during T- and R-state transition around GDP binding site.

three-dimensional structures in the same crystal, which correspond to GTP- and GDP-bound forms (or tense (T) and relaxed (R) states) in the other species. Visualization of the two states in the same species enables us to investigate the structural transition pathway between the T and R states, which might be related to the constriction of the Z-ring. Generally, in order to reproduce large-scale structural transitions related to biological functions *in silico*, extremely long-time molecular dynamics (MD) simulation is required. To avoid this problem, it is necessary to apply some structure sampling method in order to reproduce important structural changes efficiently as quickly as possible. In this research, we apply parallel cascade selection MD (PaCS-MD) simulation developed by us [1, 2] for searching structural transition pathways between the T and R states [3]. After obtaining the transition pathway we have evaluated free energy landscape (FEL) and find transition state (TS) structure (see Fig. 1). From the FEL, the free energy difference and barrier between the two states are merely k_BT and $4k_BT$, respectively, indicating the monomeric SaFtsZ-GDP complex exists in equilibrium. During the transition, it is found that the main chain carbonyl group of Arg29, whose side chain moves significantly between the T and R states, tentatively forms a hydrogen bond with Arg191 nearby in the TS. From these analysis, it is found that Arg29 is a key amino acid residue for the function of FtsZ, and a subsequent mutagenesis work also support the hypothesis.

References
[1] R. Harada, and A. Kitao, J. Chem. Phys. **139**, 035103 (2013).
[2] R. Harada, Y. Takano, T. Baba, and Y. Shigeta, Phys. Chem. Chem. Phys. (feature article) **17**, 6155 (2015).
[3] J. Fujita, R. Harada, Y. Maeda, Y. Saito, E. Mizohata, T. Inoue, Y. Shigeta, H. Matsumura, J. Struct. Biol. **198**, 65 (2017).

Authors
J. Fujita[a], R. Harada[b], Y. Maeda[a], Y. Saito[a], E. Mizohata[a], T. Inoue[a], Y. Shigeta[b], and H. Matsumura[c]
[a]Osaka University
[b]University of Tsukuba
[c]Ritsumeikan University

Neutron Spin Resonance in the 112-Type Iron-Based Superconductor

H. Luo, S. Li, and T. Masuda

In unconventional superconductors, the neutron spin resonance is a crucial evidence for spin fluctuation mediated superconductivity in the proximity of an antiferromagnetic

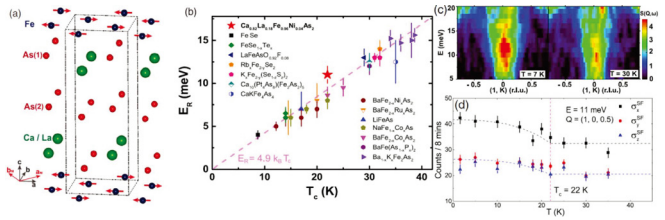

Fig. 1. (a) Crystal and magnetic structure of $Ca_{1-x}La_xFeAs_2$ system. (b) Linear scaling of spin resonance energy and critical temperature in Fe-based superconductors. (c) Spin resonance in superconducting 112 compound measured at HRC (BL-12). (d) Polarized analysis of spin resonance at E=11 meV.

(AF) instability [1]. Although the spin resonance mode is theoretically believed to be a spin-1 exciton from the singlet-triplet excitations of the electron Cooper pairs in copper oxides and heavy fermions[2], solid evidences are still not well established yet in the iron-based superconductors (FeSC). The proximity to the AF order and spin-orbital coupling give complexity on the energy and momentum distribution of spin resonance, and the common features of the resonance mode need to be testified in various materials[3].

By using inelastic neutron scattering, we have comprehensively studied the low-energy spin excitations of the new discovered 112-type iron pnictide $Ca_{0.82}La_{0.18}Fe_{0.96}Ni_{0.04}As_2$ with bulk superconductivity below T_c =22 K(Fig. 1(a)) [4]. A two-dimensional spin resonance mode is found around E =11 meV by using high-resolution chopper (HRC) spectrometer (Fig. 1(c)), where the resonance energy is almost temperature independent and linearly scales with T_c along with other iron-based superconductors (Fig. 1(b)). Polarized neutron analysis reveals the resonance is nearly isotropic in spin space without any L modulations (Fig. 1(d)). Because of the unique monoclinic structure with additional zigzag arsenic chains, the As 4p orbitals contribute to a three dimensional hole pocket around the Γ point and an extra electron pocket at the X point. Our results suggest that the energy and momentum distribution of the spin resonance does not directly respond to the k_z dependence of the fermiology, and the spin resonance intrinsically is a spin-1 mode from singlet-triplet excitations of the Cooper pairs in the case of weak spin-orbital coupling. This work is published on Physical Review Letters [5].

References

[1] P. Dai, Rev. Mod. Phys. **87**, 855 (2015).
[2] M. Eschrig, Adv. Phys. **55**, 47 (2006).
[3] P. D. Johnson, G. Xu, and W.-G. Yin, *Iron-Based Superconductivity* (Springer, New York, 2015).
[4] N. Katayama et al., J. Phys. Soc. Jpn. **82**, 123702 (2013).
[5] Tao Xie et al., Phys. Rev. Lett. **120**, 137001 (2018).

Authors
T. Xie[a,b], D. Gong[a,b], H. Ghosh[c,d], A. Ghosh[c,d], M. Soda, T. Masuda, S. Itoh[e], F. Bourdarot[f], L.-P. Regnault[g], S. Danilkin[h], S. Li[a,b,i], and H. Luo[a]
[a]Chinese Academy of Sciences
[b]University of Chinese Academy of Sciences
[c]Homi Bhabha National Institute
[d]Raja Ramanna Centre for Advanced Technology
[e]High Energy Accelerator Research Organization
[f]Université Grenoble Alpes
[g]Intitut Laue Langevin
[h]Australian Nuclear Science and Technology Organization
[i]Collaborative Innovation Center of Quantum Matter

Test of Vacuum Anisotropy under High Magnetic Fields: Vacuum Magnetic Birefringence Experiment

T. Inada, T. Yamazaki, and K. Kindo

Classical electrodynamics governed by Maxwell's equations describes the vacuum as an isotropic and dispersion-less medium, which properties are not affected by the application of electromagnetic fields. However, if we consider quantum electrodynamics (QED), the nonlinear interaction between the fields is mediated by the vacuum fluctuation of virtual particle-antiparticle pairs. Consequently, the vacuum shows a finite size of anisotropy under strong magnetic fields, called vacuum magnetic birefringence (VMB). In addition to this QED effect, VMB can be enhanced by the contribution from undiscovered particles such as axions, which are one of the leading candidates of dark matter. The test of VMB therefore provides one of the most sensitive searches for these particles with a mass around meV.

Three groups are currently trying to measure VMB, with a common scheme shown in Fig. 1. It consists of crossed-Nicols polarizers, a high-finesse Fabry-P´erot cavity, and a magnet that applies transverse fields with respect to the laser axis. The VMB signal is measured as ellipticity induced by the magnet. The surface of cavity mirrors has large static birefringence, and to separate the VMB signal from it, magnetic fields are temporally modulated. The modulation is realized by a rotating permanent magnet (~ 2.5 T) by one of the groups, whereas we instead use a pulsed magnet since the VMB signal is enhanced according to the square of the field strength (B^2). Our magnet produces alternative fields of +9 T and −4.5 T with a high repetition rate of 0.1 Hz [1, 2].

The sensitivity to VMB is determined by the background process of the Faraday effect caused by residual gas in the chamber. Since the Faraday component is linearly depends on B, we apply alternative fields to subtract it. To emulate the B^2 dependence of the small VMB signal, we first filled a relatively high pressure of nitrogen gas (100 Pa) and observed the square term of linear Faraday effect. Figure 2(a) shows the agreement of the measured B^2 term with calculation of the squared Faraday term. The VMB measurement was then carried out under vacuum with ~ 2000 cycles of the alternating fields in 2018. The VMB coeffcient k_{CM} is calculated for each cycle and distributed as shown in Fig. 2(b). The mean value of the distribution is consistent with zero, showing no sign of axionic contribution. As

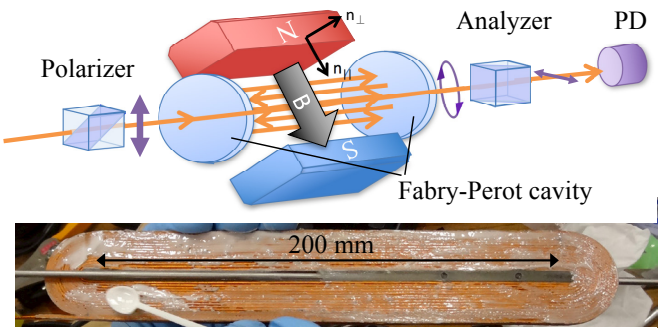

Fig. 1. (upper) Schematic veiw of the setup. An incident light is polarized and stored in a high-finesse Fabry-P´erot cavity, where pulsed magnetic fields induce elliptical polarization. (lower) Bare racetrack coil before backed up with an outer metal. The magnet produces fields of up to 10 T over the beam path.

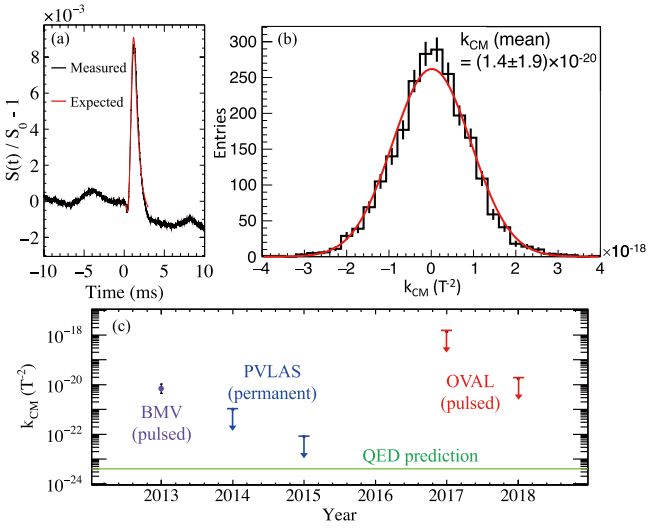

Fig. 2. (a) Test measurement of the small square term of the Faraday effect caused by 100 Pa of nitrogen gas, compared to calculation. The vertical axis shows the ratio of signal height with respect to the static component S_0. (b) Histogram of vacuum ellipticity coeffcient k_{CM} obtained by 2000 cycles of alternating +9 T and −4.5 T fields. The fitting to a Gaussian distribution shows a zero-consistent value for the mean, which gives an upper limit on k_{CM}. (c) Comparison of the current limits on k_{CM} (OVAL) with the other two groups. Note that, without hypothetical particles such as axions, QED alone predicts finite vacuum birefringence shown as the green line.

a result, it poses an upper limit on k_{CM}, that is plotted in Fig. 2(c) with recent results of the other groups. We have improved our first result in 2017 by two orders of magnitude [3]. There is still a large gap of sensitivity to reach the signal level predicted by QED, and upgrades on the magnet and optics are currently underway.

References

[1] T. Inada *et al*., Phys. Rev. Lett. **118**, 071803 (2017).
[2] T. Yamazaki *et al*., Nucl. Instrum. Methods Phys. Res. A **833**, 122 (2016).
[3] X. Fan *et al*., Eur. Phys. J. D **71**, 308 (2017).

Authors

T. Inada[a], T. Yamazaki[a], X. Fan[a], S. Kamioka[a], T. Namba[a], T. Kobayashi[a], S. Asai[a], J. Omachi[a], K. Yoshikawa[a], M. Kuwata-Gonokami[a], Y. Tamasaku[b], Y. Inubushi [b], K. Sawada[b], M. Yabashi[b], T. Ishikawa[b], Y. Tanaka[c], H. Nojiri[d], A. Matsuo, K. Kawaguchi, and K. Kindo

[a]The University of Tokyo
[b]RIKEN Spring-8
[c]University of Hyogo
[d]Tohoku University

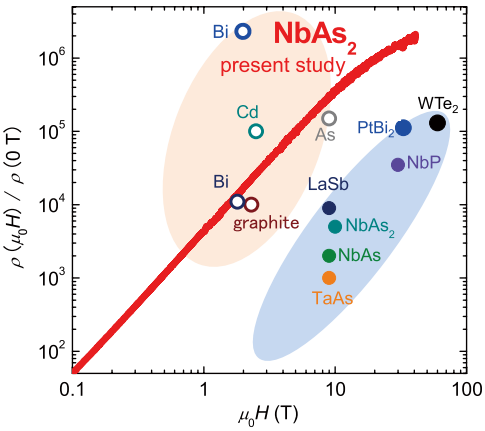

Fig. 1. Magnetoresistance in representative semimetals exhibiting large MR. Typical area of MR in elemental (open circles) and binary semimetal (closed circles) in the previous reports are shown by different colors.

a few tesla, resulting in the MR much larger than those recently reported for the binary systems. On the other hand, the binary semimetals tend to have lower carrier mobility. Thus, the increasing rate of MR is suppressed, resulting in a non-saturating MR with much smaller value in a reachable field. Therefore, it may be possible to enhance the MR in binary semimetals merely by improving the crystal quality.

In this study, we have synthesized high quality single crystals of $NbAs_2$ by the chemical vapor transport technique and observed an extremely large magnetoresistance exceeding 1.9 million at 1.7 K at 40 T. The present MR value is one or two orders of magnitude larger than that for the binary systems reported so far and reaches as high-level as that of the ultra-high mobility elemental semimetals. We showed that both of carrier mobility and charge compensation ratio were significantly improved in the present $NbAs_2$ crystal exhibiting mega-scale MR. Thus, we demonstrate that the binary semimetal has a great potential to exhibit further significant enhancement of MR merely by the improvement of the crystal quality.

Reference

[1] K. Yokoi, H. Murakawa, M. Komada, T. Kida, M. Hagiwara, H. Sakai, and N. Hanasaki, Physical Review Materials **2**, 024203 (2018).

Authors

K. Yokoi[a], H. Murakawa[a], M. Komada[a], T. Kida[a], M. Hagiwara[a], H. Sakai[a], and N. Hanasaki[a]

[a]Osaka University

Mega-Scale Magnetoresistance in the Binary Semimetal $NbAs_2$

H. Murakawa, K. Yokoi, and T. Kida

Recently, large magnetoresistance (MR) has been reported for a wide variety of binary semimetals. The MR values for these materials reaches 10^3 ~ 10^5 below 4 K without an indication of saturation even at several tens of tesla. Although, the MR in these binary semimetals are reported to be “extremely large”, these values have been far smaller than those in classical elemental semimetals such as bismuth reported 80 years ago. In general, magnetoresistance in a semimetal is simply explained by two carrier model, in which the carrier mobility is the decisive parameter for the MR value. In fact, for ultrahigh mobility elemental semimetals such as bismuth, the MR grows rapidly in only

Quantum Hall Effect in Topological Dirac Semimetal Cd_3As_2 Films

M. Uchida, M. Tokunaga, and M. Kawasaki

As crystalline materials of three-dimensional Dirac semimetal, Cd_3As_2 and Na_3Bi have been suggested, and their unique electronic structures have been directly observed through angle-resolved photoemission and scanning tunneling spectroscopy. On the other hand, its quantum transport especially at high fields has been still elusive, because fabrication of high-quality Dirac semimetal films has been highly challenging unlike other topological materials. While Cd_3As_2 has long been known as a stable II–V type semiconductor, its film quality has been limited due to the necessity of low-temperature growth.

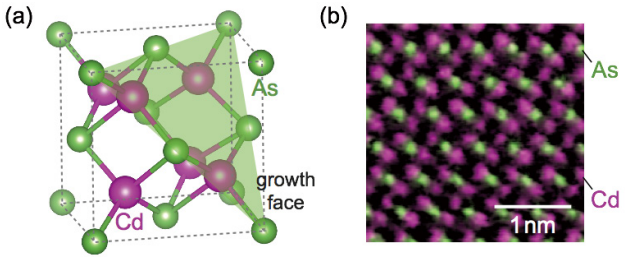

Fig. 1. (a) Primary crystal structure of topological Dirac semimetal Cd_3As_2. (b) Cross-sectional transmission electron microscopy image of a Cd_3As_2 film fabricated by high-temperature annealing. Cd and As atoms are periodically arranged without any clear crystallographic defects over a wide area.

Here we report the observation quantum Hall effect and its thickness dependence by measuring high-quality Cd_3As_2 films fabricated by high-temperature annealing (Fig. 1) [1, 2]. Transport measurements up to 55 T were performed using a nondestructive pulse magnet with a pulse duration of 37 ms. Longitudinal resistance R_{xx} and Hall resistance R_{yx} were measured on the 60 μm-width Hall bar with flowing a DC current of $I = 5$ μA.

Figure 2 shows high-field magnetotransport for two Cd_3As_2 films with the same carrier density ($n = 1 \times 10^{18}$ cm^{-3}) and different thicknesses (t = 12 and 23 nm). Shubnikov-de Haas (SdH) oscillations and plateau-like structures are resolved in longitudinal resistance R_{xx} and Hall resistance R_{yx}. As the field increases, integer quantum Hall states appear down to the quantum limit of filling factor $\nu = 2$. R_{xx} finally becomes zero, and simultaneously, R_{yx} shows quantized values over wide field ranges. Temperature dependence of R_{xx} measured from 1.4 to 50 K can be well fitted with the standard Arrhenius plot, giving high activation energy of $\Delta = 19$ K ascribed to the unusually high Fermi velocity in the Dirac semimetal. Absence of the half-integer plateaus suggests that a gap starts to open under the quantum confinement to the Dirac semimetal state. Furthermore, the degeneracy factor shows an interesting change depending on the film thickness; It is altered from 2 to 1 with increase of film thickness. Detailed analysis reveals that this change is attributed to spin splitting or g factor change, not to the lifting of other degeneracies, e.g., of valley or surface states.

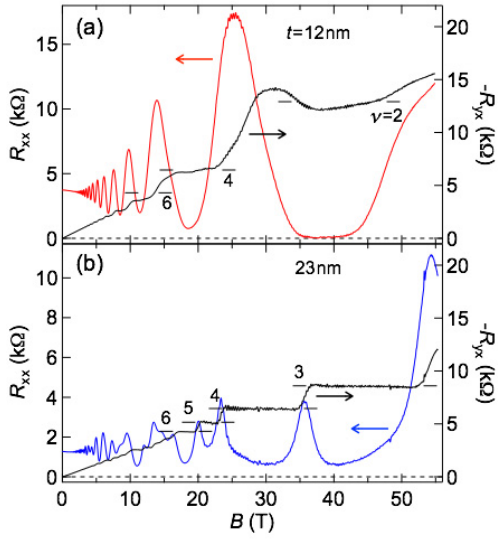

Fig. 2. (a) High-field magnetotransport for a relatively thin Cd_3As_2 film (t = 12 nm) measured at T = 1.4 K. The numbers of the horizontal bars represent the filling factor ν, determining the degeneracy factor to be 2 from its increment. (b) Same scan for slightly thicker films (t = 23 nm). By contrast, the degeneracy is altered to 1 in this thicker film at high fields.

Reflecting the high Fermi velocity of the Dirac dispersion, the band gap sharply opens when the confinement thickness, giving rise to the drastic change of the g factor change observed in the quantum Hall effect.

Detailed electronic structures including subband splitting and gap opening are determined by analyzing the quantum transport depending on the confinement thickness. The demonstration of quantum Hall states in the high-quality Cd_3As_2 films opens a road to study high-field quantum transport in topological Dirac semimetal and its derivative phases. Combining electric gating, heterostructure fabrication, or chemical doping techniques to the high-field measurements will open possibilities for further studying quantized transport phenomena by tuning Fermi level, hybridization gap, or magnetic interaction.

References

[1] M. Uchida, Y. Nakazawa, S. Nishihaya, K. Akiba, M. Kriener, Y. Kozuka, A. Miyake, Y. Taguchi, M. Tokunaga, N. Nagaosa, Y. Tokura, and M. Kawasaki, Nature Communications **8**, 2274 (2017).
[2] Y. Nakazawa, M. Uchida, S. Nishihaya, M. Kriener, Y. Kozuka, Y. Taguchi, and M. Kawasaki, Scientific Reports **8**, 2244 (2018).

Authors
M. Uchida[a], M. Tokunaga, and M. Kawasaki[a]
[a]The University of Tokyo

Robustness of Emergent Monopole Fluctuations in a Chiral Magnet MnGe under High Magnetic Fields

N. Kanazawa, Y. Tokura, and M. Tokunaga

Topological spin textures are a fertile source of emergent electromagnetic responses owing to their quantized Berry phase. Berry phase acts as a fictitious magnetic flux, so-called an emergent magnetic flux, affecting the motion of conduction electrons in solids. By designing a topological spin arrangement, we can achieve an arbitrary emergent magnetic field distribution, whose magnitude may reach as large as 4000 T when the size of topological spin object is squeezed in 1-nm^2 area. In addition to such possible gigantic electromagnetic responses, it is also noteworthy that we can effectively realize the magnetic monopole structures, where the magnetic field distribution is inversely proportional to the square of the distance ($\propto \boldsymbol{r}/|\boldsymbol{r}|^3$).

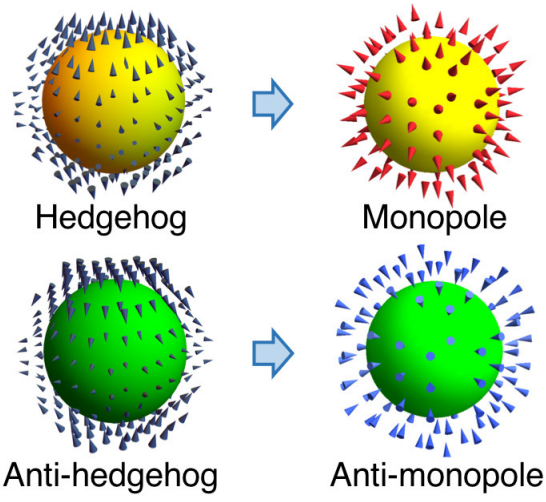

Fig. 1. Spin hedgehogs and corresponding monopole-type emergent field distributions.

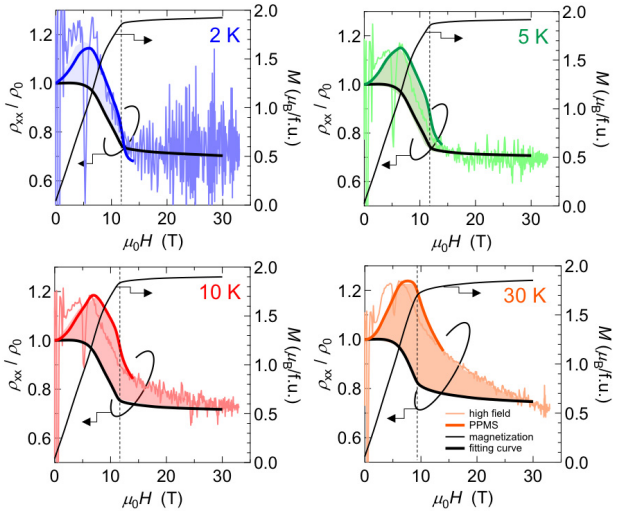

Fig. 2. Longitudinal magneto-resistivity (MR) measured with use of mid-pulse magnet at low temperatures (T = 2, 5, 10, 30 K). Thick-line curves are the results obtained by steady-field measurements (PPMS) up to 14 T. Bold black curves are the estimated conventional MR associated with the variations of magnetization shown in the black thin lines.

In a chiral magnet MnGe, there realized three-dimensional hairy spin structures, so-called spin hedgehogs, which behave as the quantized sources or sinks of effective gauge field, that is, emergent monopoles and anti-monopoles (Fig. 1). In association with emergent-monopole motion driven by an external magnetic field, dramatic changes in magneto-transport properties appear, exhibiting unusual magnetic-field dependence, such as positive magneto-resistance, multiple elastic anomalies, magnetic-field-enhanced thermopower and so on [1]. Those unusual properties are rooted in large fluctuations of emergent monopoles, which induce considerable dynamical variations in the emergent magnetic field distribution and consequently cause intense scatterings of electrons, phonons and magnons.

By high-field measurements of magnetization and resistivity with use of the mid-pulse magnets installed at ISSP, we experimentally found that the emergent monopole fluctuations can survive far beyond the topological transition where the majority of spin hedgehogs undergo pair annihilation [2]. Figure 2 shows the magnetic field dependence of magnetization (M) and magneto-resistivity normalized by its zero-field value (ρ_{xx}/ρ_0). We compare the measured ρ_{xx}/ρ_0 (color lines in Fig. 2) with the ordinary contribution to ρ_{xx}/ρ_0 from the alignment of spins (thicker black lines, estimations from the M-profiles), so as to evaluate the unusual contribution from the monopole fluctuations (color shades). While at the low temperatures (T = 2 K and 5 K) the unusual contribution only exists below the magnetic field H_c with the topological transition (vertical dashed lines), it persists even above H_c only with small temperature elevation above 10 K. This result may indicate the possibility that a part of spin hedgehogs escaping from their annihilation or thermally excited hedgehog-like spin structure may exist even in the high-field regime and their fluctuations cause strong scatterings of charge carriers. The observed robustness of the emergent monopole fluctuations possibly originates from topological protection against unwinding of the spin texture by external magnetic fields.

The present results not only open the door to veiled characteristic properties of emergent monopoles in the high-field regime but also demonstrate promising usefulness of high-field measurements to clarify the topological stability of spin nano-objects.

References

[1] N. Kanazawa, Y. Nii, X.-X. Zhang, A. S. Mishchenko, G. De Filippis, F. Kagawa, Y. Iwasa, N. Nagaosa, and Y. Tokura, Nature Commun. **7**, 11622 (2016).

[2] Y. Fujishiro, N. Kanazawa, T. Shimojima, A. Nakamura, K. Ishizaka, T. Koretsune, R. Arita, A. Miyake, H. Mitamura, K. Akiba, M. Tokunaga, J. Shiogai, S. Kimura, S. Awaji, A. Tsukazaki, A. Kikkawa, Y. Taguchi, and Y. Tokura, Nature Commun. **9**, 408 (2018).

Authors

Y. Fujishiro[a], N. Kanazawa[a], T. Shimojima[b], A. Nakamura[a], K. Ishizaka[a,b], T. Koretsune[b], R. Arita[b], A. Miyake, H. Mitamura, K. Akiba, M. Tokunaga, J. Shiogai[c], S. Kimura[c], S. Awaji[c], A. Tsukazaki[c], A. Kikkawa[b], Y. Taguchi[b], and Y. Tokura[a,b]

[a]The University of Tokyo

[b]RIKEN Center for Emergent Matter Science (CEMS)

[c]Tohoku University

Magnetization Process of the S = 1/2 Two-Leg Organic Spin-Ladder Compound BIP-BNO

Y. Hosokoshi, S. Todo, and Y. H. Matsuda

Spin-ladder systems are a class of low-dimensional materials that correspond to the crossover region between one and two dimensions. The quantum-mechanical properties and criticality of spin-ladder systems have attracted considerable attention. In the S = 1/2 spin-ladder system with the antiferromagnetic Heisenberg (AFH) exchange interaction, it is theoretically predicted that the even-leg spin ladder has a spin gap, while the odd-leg spin ladder is gapless [1, 2]. The spin states of the even-leg AFH spin ladders in the presence of a magnetic field (B) are particularly interesting. There is a transition to a gapless Tomonaga-Luttinger liquid (TLL) phase at a critical magnetic field (B_{c1}) from a gapped disordered spin liquid state. The quantum critical phenomena are observed in the vicinity of B_{c1} as well as another critical field B_{c2} at which the spins are fully polarized [3, 4].

BIP-BNO (3,5'-bis(N-tert-butylaminoxyl)-3',5-dibromobiphenyl, $C_{20}H_{24}N_2O_2Br_2$) is a candidate for an S = 1/2 two-leg spin-ladder in which there are no transition metal element but NO groups have S = 1/2 spins [5]. However, since the susceptibility is well reproduced by both a spin-ladder model and a bond-alternating chain model, the key to identify BIP-BNO as a spin-ladder is the magnetization (M)

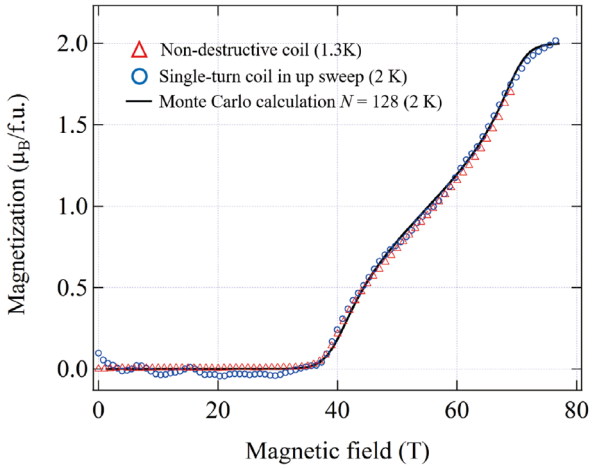

Fig. 1. Magnetization curve of BIP-BNO. The circles and triangles represent the experimental results of the single turn coil and the non-destructive coil, respectively. The solid line shows the numerical result calculated by the quantum Monte Carlo method.

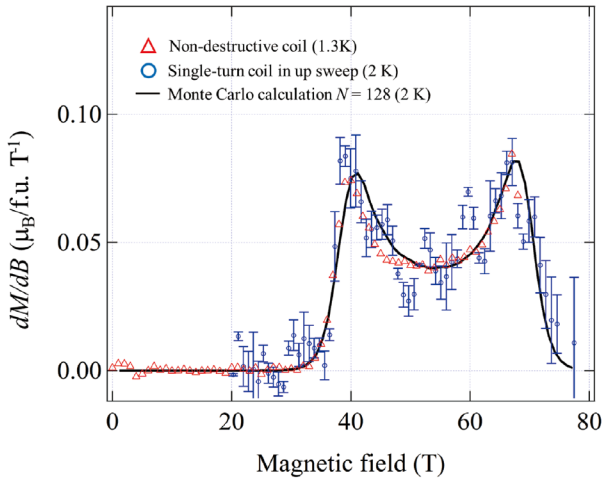

Fig. 2. Magnetic field derivative of magnetization. The solid line, circles, and triangles represent the numerical calculation, experimental result with VSTC, and that with MLPM, respectively. The error bars represent the statistical errors of the experiments of VSTC.

process. In the previous study, the magnetization curve up to 50 T clearly shows the transition at around 35 T. However, the observed magnetization is approximately only up to a quarter of the saturation value M_{sat} = 2 μB/f.u. To clarify the property of BIP-BNO as a spin-ladder system and to determine accurate exchange constants, it is required to analyze the full magnetization curve and see how well the ladder model can explain the experimental observations.

The measured magnetization curves at low temperatures (1.3 and 2 K) are shown in Fig. 1. The result obtained from a non-destructive-type multilayer-pulsed magnet (MLPM) and that from the destructive-type vertical single-turn coil (VSTC) are represented by triangles and the circles, respectively. Although the pulse duration of VSTC is three orders of magnitude shorter than that of MLPM, the obtained two magnetization curves are found to be almost identical in the field range up to 70 T, which suggests an accurate measurement was conducted not only with non-destructive MLPM but also the destructive VSTC. The magnetization below 37 T is nearly zero reflecting the spin-liquid ground state, which is consistent with the previous study. It is found that the magnetization suddenly starts increasing at 37 T and shows the saturation at fields exceeding 74 T. We expect that the phase in the region where the magnetization is larger than zero and smaller than the saturation value should be the TLL as it is suggested in other two-leg spin-ladder materials. Hence, we find B_{c1} = 37 T and B_{c2} = 74 T. To compare experimental data with the theoretical model, we calculated the magnetization of the spin-ladder system under a magnetic field by means of the worldline quantum Monte Carlo method with the worm (directed-loop) algorithm. The worm scattering probability is optimized using the geometric allocation. The exchange constants of the model are estimated using the simulated annealing in which the deviation from the experimentally obtained magnetization curve is minimized. The calculated magnetization curve (solid line) is shown in Fig. 1 and we obtain J_{rung}/k_B = 65.7 K and J_{leg}/k_B =14.1 K, where J_{rung} and J_{leg} are the exchange constants for the leg and rung directions of the ladder, respectively.

Figure 2 represents *dM/dB* as a function of *B*. Sharp two peaks are clearly seen in the numerically calculated as well as experimentally obtained *dM/dB* curves. Moreover, the inflection point between the two peaks is found to be located at approximately 55 T where $M = M_{sat}/2$, and the symmetric form with respect to the inflection point is clearly seen. The symmetric shape in *dM/dB* is the specific character of a spin-ladder [6]. It should be noted that a bond-alternating chain also give two peaks in the *dM/dB* curve. However, the shape is distinctly asymmetric; the peak heights of the two are different, e.g., the height of the lower-field peak is from 20 % to 70 % of the height of the higher-field peak, depending on the alternation parameter. Moreover, the inflection point between the two peaks is not at the center position. The difference between the heights of the two peaks in BIP-BNO is evaluated to be only 3% in *dM/dB* and the inflection point located at the center between the two peaks, which cannot be attributed to a bond-alternating chain. These findings provide strong evidence that BIP-BNO is identified with the S = 1/2 two-leg spin ladder [7].

The ratio of the Heisenberg exchange constants J_{rung}/J_{leg} is estimated to be approximately 4.7, which is deeply in the strong coupling region: $J_{rung}/J_{leg} > 1$. In the curve of the magnetic-field derivative of the magnetization, dM/dB, the characteristic features, namely two sharp peaks and a centered inflection point, are observed with a symmetric shape. This observation strongly suggests that BIP-BNO is an S = 1/2 AFH two-leg spin ladder. It is worth noting that BIP-BNO is the first prototypical organic (not containing magnetic ions) S = 1/2 spin-ladder compound.

References
[1] E. Dagotto, J. Riera, and D. Scalapino, Phys. Rev. B **45**, 5744 (1994).
[2] M. Azuma, Z. Hiroi, and M. Takano, Phys. Rev. Lett. **73**, 3463 (1994).
[3] S. Sachdev, Science **288**, 475 (2000).
[4] B. C. Watson, V. N. Kotov and M. W. Meisel *et al.,* Phys. Rev. Lett. **86**, 5168 (2001).
[5] K. Katoh, Y. Hosokoshi, and K. Inoue *et al.*, J. Phys. Chem. Solids **63**, 1277 (2002).
[6] X. Wang and L. Yu, Phys. Rev. Lett. **84**, 5399 (2000).
[7] K. Nomura, Y. H. Matsuda, and Y. Narumi *et al.,* J. Phys. Soc. Jpn. **86**, 104713 (2017).

Authors
K. Nomura, Y. H. Matsuda, Y. Narumi[a], K. Kindo, S. Takeyama, Y. Hosokoshi[b], T. Ono[b], N. Hasegawa[b], H. Suwa[c], and S. Todo[c]
[a]Osaka University
[b]Osaka Prefecture University
[c]The University of Tokyo

Convergence of the Magnetic Grüneisen Parameter at the Quantum Critical Point of the Transverse-Field Ising-Chain

Z. Wang and Y. Kohama

Quantum critical point (QCP) is the end point in a phase diagram where a continuous phase transition occurs at absolute zero temperature. So far, a lot of efforts have been made to understand the universal scaling behavior in different types of QCPs. In case of field-induced QCP, heavy-fermion compound and one-dimensional Heisenberg spin systems are known to show a divergence in thermodynamically properties, such as specific heat and magnetic Grüneisen parameter (Γ_m). In contrast, for the QCP of the transverse-field Ising (TFI) spin chain system, it is theoretically shown that the Γ_m does not show a divergence behavior when the QCP is approached by decreasing temperature at the critical field, although it diverges when the critical field is approached at zero temperature [1]. While many theoretical works on the TFI spin chain system are now available, it remains very challenging to experimentally realize the

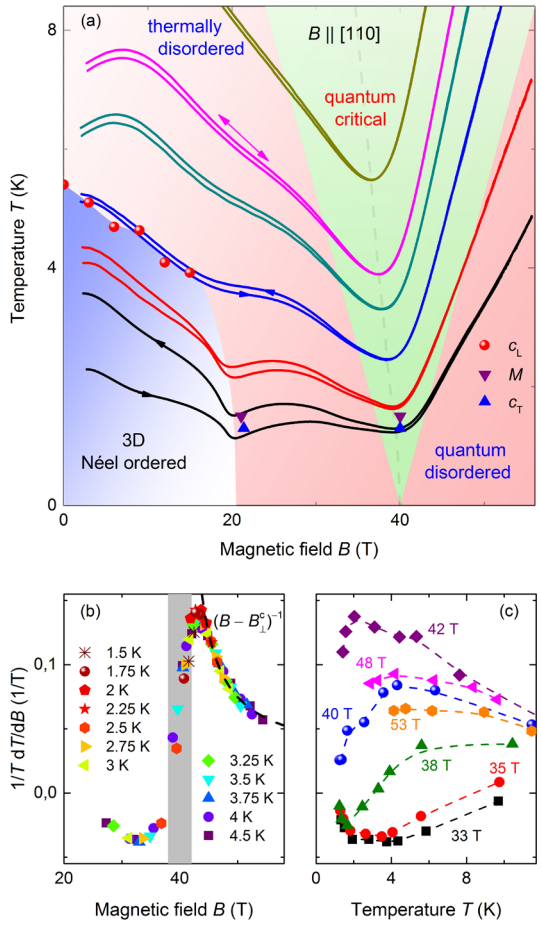

Fig. 1. (a) Magnetocaloric-effect in $BaCo_2V_2O_8$. The magnetic field was applied to the [110] direction. (b), (c) The estimated Grüneisen parameter, $\frac{1}{T}\frac{dT}{dB}$, as a function of magnetic field and temperature.

paradigmatic model in a real material.

In our recent work [2], we show that the Ising-like spin-1/2 antiferromagnetic chain material $BaCo_2V_2O_8$ exhibits the unique QCP behavior of the TFI spin system which fulfills the requirements of its experimental observations; (1) strong easy axis anisotropy (2) negligible inter-chain coupling, (3) accessible critical field strength of ~40 T. In this research, we have performed magnetization, sound velocity, and magnetocaloric-effect measurements as a function of temperature and transverse magnetic field on the single crystal of $BaCo_2V_2O_8$, and have provided the experimental evidence of convergence behavior in Γ_m. To the best of our knowledge, the Γ_m above 20 T has been experimentally obtained for the first time in this research, by using the pulsed field magnetocaloric effect (MCE) measurement.

Figure 1(a) shows the magnetocaloric effect data up to 55 T for various initial temperatures. The field dependence of the sample temperature, $T(B)$, detects the 3D Néel ordered phase at about 20 T and the field-induced QCP at 40 T as a broad minimum. The hysteresis below the critical field can be due to slow dynamical process such as field-driven reorientation of twin-domains as reported before. Figure 1(b) and (c) show the temperature and field dependences of $\frac{1}{T}\frac{dT}{dB}$. Since the $T(B)$ curves was obtained in an approximate adiabatic condition (the sample is thermally isolated due to the extremely short time scale of the pulsed field duration), the process can be considered as an isentropic one. Moreover, the lattice specific heat is not expected to be field dependent. Therefore, the obtained field dependent behavior of $\frac{1}{T}\frac{dT}{dB}$ corresponds to the $\Gamma_m = \frac{1}{T}\frac{dT}{dB}\Big|_S$. As seen in Fig. 1(b) the field dependence of $\frac{1}{T}\frac{dT}{dB}$ shows a divergence behavior approaching ~40 T. On the other hand, the temperature dependence of $\frac{1}{T}\frac{dT}{dB}$ does show a converging behavior at ~40 T with decreasing temperature (Fig. 1(c)). This is consistent with the previous theoretical prediction [1] and the first experimental observation of the characteristic scaling feature in the TFI-chain QCP [2].

References

[1] J. Wu, L. Zhu, and Q. Si, arXiv:1802.05627 (2018).

[2] Zhe Wang, T. Lorenz, D. I. Gorbunov, P. T. Cong, Y. Kohama, S. Niesen, O. Breunig, J. Engelmayer, A. Herman, Jianda Wu, K. Kindo, J. Wosnitza, S. Zherlitsyn, and A. Loidl, Phys. Rev. Lett. **120**, 207205 (2018).

Authors

Zhe Wang[a,b], T. Lorenz[c], D. I. Gorbunov[d], P. T. Cong[d], Y. Kohama, S. Niesen[c], O. Breunig[c], J. Engelmayer[c], A. Herman[c], J. Wu[e], K. Kindo, J. Wosnitza[d], S. Zherlitsyn[d], and A. Loidl[a]

[a]Experimental Physics V, Center for Electronic Correlations and Magnetism

[b]Institute of Radiation Physics, Helmholtz-zentrum Dresden-Rossendorf

[c]Institute of Physics II, University of Cologne

[d]Dresden High Magnetic Field Laboratory (HLD-EMFL), Helmholtz-Zentrum Dresden-Rossendorf

[e]Max-Plank-Institute für Physik komplexer Systeme

A Linear Correlation between Photocatalytic Activity and Photoexcited Carrier Lifetime

K. Ozawa, S. Yamamoto, and I. Matsuda

Laser-assisted time-resolved (TR) measurement techniques have facilitated great advances in our understanding of excited charge carrier dynamics. Preceding TR experiments have revealed many aspects of photocatalytic properties of TiO_2. One of them is that a higher photocatalytic activity of anatase TiO_2 (a-TiO_2) than rutile TiO_2 (r-TiO_2) results from a longer lifetime of the photoexcited carriers, owing to the different bulk band gap type (direct versus indirect types). On the other hand, it has also been recognized that the TiO_2 photocatalytic activity depends on the orientation of the crystal surfaces. Although several mechanisms such as a surface-dependent redox potential, anisotropic diffusion of the carriers, electron-trapping probability, etc. have been proposed as a possible origin, none of them comprehensively explains the surface dependence. Thus, a more detailed picture of the relation between the carrier dynamics and the photocatalytic activity must be drawn to understand the unique phenomenon.

In the present study, we systematically assessed the photocatalytic activities and photoexcited carrier lifetime on single-crystal a-TiO_2(101) and (001) surfaces and r-TiO_2(110), (001), (011), and (100) surfaces by X-ray photoelectron spectroscopy (XPS) and TR-XPS [1]. The photocatalytic activity was evaluated by a rate constant of a photocatalytic decomposition of acetic acid. The carrier lifetime was determined from a time evaluation of the ultraviolet (UV)-induced surface photovoltage (SPV).

Acetic acid adsorbs dissociatively on the TiO_2 surfaces via bonding interaction between the O atoms of carboxylate and the surface Ti atoms. Saturation coverages depend on

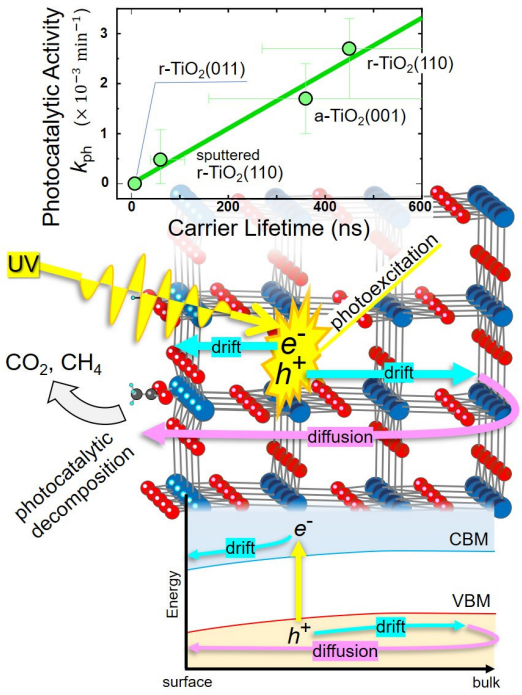

Fig. 1. Correlation between the photocatalytic activity and the carrier lifetime (top). Schematic illustrations of the photoexcited carrier dynamics in a real space (middle) and an energy space (bottom).

the surface orientation, but it ranges from 0.41 monolayers [on r-TiO$_2$(011)] to 0.66 monolayers [on r-TiO$_2$(100)]. The rate of the photocatalytic decompostion of acetic acid was estimated from a decreasing rate of the C 1s peak intensity while the UV laser with the energy of 3.31 eV was irradiated. The peak intensity decreases exponentially with a time constant τ_{ph} of 370 min on r-TiO$_2$(110). Since the reciprocal of τ_{ph} is a rate constant k_{ph}, k_{ph} on r-TiO$_2$(110) is evaluated to be 2.7×10^{-3} min^{-1}. This is the largest rete constant among all surfaces examined in the present study. k_{ph} on a-TiO$_2$(101) and (001) are 2.1×10^{-3} min^{-1} and 1.7×10^{-3} min^{-1}, respectively, while r-TiO$_2$(011) and (001) are inactive with $k_{ph} = 0$ min^{-1}.

The lifetime of the photoexcited carriers was determined from the time evolution of the SPV-induced Ti 2p peak shift. All TiO$_2$ surfaces examined in the present study form an accumulation layer at the surface because of the inevitable formation of surface oxygen vacancies. The SPV is generated on these surfaces by charge separation of the photexcited electron-hole pairs as illustrated in Fig. 1 (middle and bottom); the electrons and the holes are drifted towards the surface and bulk sides, respectively, along the potential gradient in the accumulation layer. The holes, then, diffuse back to the surface and recombine with the electrons at the surface. This charge separation-recombination process is the origin of the SPV generation-decay process. By examining the SPV decay time after the swift generation by TRXPS, the photoexcited carrier lifetime can be estimated. We examined the carrier lifetimes on three pristine surfaces [r-TiO$_2$(110), r-TiO$_2$(011), and a-TiO$_2$(001)] and one defective r-TiO$_2$(110) surface [2]. It is known that the lifetime strongly depends on the surface barrier height. Thus, the experimentally determined lifetimes were converted to barrier-height-corrected lifetimes so as to reproduce the lifetimes on the acetate-saturated surfaces; they are 450 ns, 360 ns, and 7 ns for r-TiO$_2$(110), a-TiO$_2$(001), and r-TiO$_2$(011), respectively.

The lifetime is found to be proportional to k_{ph}. A plot of k_{ph} against the lifetime gives a linear and positive correlation (top of Fig. 1). The linear correlation is extendable even to the sputtered surface [1]. On the other hand, no such correlation is found between k_{ph} and the surface chemical reactivity, which should be related to the saturation coverage of acetic acid. The photocatalytic reaction is initiated by an interaction between adsorbates and photoexcited carriers at the surface. The present study indicates that the carrier density on the surface rather than the adsorbate density is a prime factor to determine the photocatalytic activity, since more carriers are available for the reaction when the carriers survive longer. Thus, the carrier lifetime is a key to understand various properties of TiO$_2$ photocatalysis, including the orientation-dependent activity.

References

[1] K. Ozawa, S. Yamamoto, R. Yukawa, R.-Y. Liu, N. Terashima, Y. Natsui, H. Kato, K. Mase, and I. Matsuda, J. Chem. Phys. C **122**, 9562 (2018).
[2] K. Ozawa, S. Yamamoto, R. Yukawa, R. Liu, M. Emori, K. Inoue, T. Higuchi, H. Sakama, K. Mase, and I. Matsuda, J. Chem. Phys. C **120**, 29283 (2016).

Authors

K. Ozawa[a], S. Yamamoto, R. Yukawa[b], R.-Y. Liu[c], N. Terashima[d], Y. Natsui[d], H. Kato[d], K. Mase[b], and I. Matsuda
[a]Tokyo Institute of Technology
[b]Institute of Materials Structure Science, High Energy Accelerator Research Organization (KEK)
[c]Institute of Physics, Academia Sinica
[d]Hirosaki University

Progress of Facilities

Supercomputer Center

The Supercomputer Center (SCC) is a part of the Materials Design and Characterization Laboratory (MDCL) of ISSP. Its mission is to serve the whole community of computational condensed-matter physics of Japan, providing it with high performance computing environment. In particular, the SCC selectively promotes and supports large-scale computations. For this purpose, the SCC invites proposals for supercomputer-aided research projects and hosts the Steering Committee, as mentioned below, that evaluates the proposals.

The ISSP supercomputer system consists of two subsystems: System B is intended for larger total computational power and has more nodes with relatively loose connections whereas System C is intended for higher communication speed among nodes. System B is SGI ICE XA / UV hybrid system that consists of FAT nodes with large memory, CPU nodes based on Intel Xeon, and ACC node enhanced by GPGPU accelerator. Its theoretical performance is 2.6 PFLOPS. System C is HPE SGI 8600 with 0.77 PFLOPS.

In addition to the hardware administration, the SCC puts increasing effort on the software support. Since 2015, the SCC has been conducting “Project for advancement of software usability in materials science”. In this project, for enhancing the usability of the ISSP supercomputer system, we perform some software-advancement activity such as developing new application software that runs efficiently on the ISSP supercomputer system, adding new functions to existing codes, help releasing private codes for public use, writing/improving manuals for public codes. Two target programs were selected in fiscal year 2017 and developed software were released as DCore and (a new version of) HPhi. The SCC is also providing a service for porting users' software to General Purpose GPUs (GPGPU).

All staff members of university faculties or public research institutes in Japan are invited to propose research projects (called User Program). The proposals are evaluated by the Steering Committee of SCC. Pre-reviewing is done by the Supercomputer Project Advisory Committee. In fiscal year 2017, totally 302 projects were approved. The total points applied and approved are listed on Table. 1 below. Additionally, we supported post-K and other computational materials science projects through Supercomputing Consortium for Computational Materials Science (SCCMS).

The research projects are roughly classified into the following three (the number of projects approved):

First-Principles Calculation of Materials Properties (121)
Strongly Correlated Quantum Systems (29)
Cooperative Phenomena in Complex, Macroscopic Systems (117)

In all the three categories, most proposals involve both methodology and applications. The results of the projects are reported in 'Activity Report 2017' of the SCC. Every year 3-4 projects are selected for “invited papers” and published at the beginning of the Activity Report. In the Activity Report 2017, the following three invited papers are included:

"Development of open source software HΦ", Mitsuaki KAWAMURA, Takahiro MISAWA, Youhei YAMAJI, and Kazuyoshi YOSHIMI

"Monte Carlo study of Ising model with non-integer effective dimensions", Synge TODO

"Recent Extensions and Applications of Parallel Cascade Selection Molecular Dynamics Simulations”, Ryuhei HARADA and Yasuteru SHIGETA

Class	Max Points		Application	Number of Projects	Total Points			
					Applied		Approved	
	System B	System C			System B	System C	System B	System C
A	100	50	any time	12	1.2k	-	1.2k	-
B	1k	100	twice a year	62	56.9k	-	40.0k	-
C	10k	1k	twice a year	171	1433.8k	-	633.0k	-
D	10k	1k	any time	6	26.5k	-	24.5k	-
E	30k	3k	twice a year	16	474.0k	-	258.0k	-
S			twice a year	0	0	-	0	-
SCCMS				35	271.5k	-	271.5k	-
Total				302	2263.9k	-	1228.2k	-

Table 1. Research projects approved in 2017
The maximum points allotted to the project of each class are the sum of the points for the two systems; Computation of one node for 24 hours corresponds to one points for the CPU nodes of System B and System C. The FAT and ACC nodes require four and two points for a 1-node 24-hours use, respectively. There was no official System C operation in SY2017 due to system replacement.

Neutron Science Laboratory

The Neutron Science Laboratory (NSL) has been playing a central role in neutron scattering activities in Japan since 1961 by performing its own research programs as well as providing a strong General User Program for the university-owned various neutron scattering spectrometers installed at the JRR-3 (20MW) operated by Japan Atomic Energy Agency (JAEA) in Tokai. In 2003, the Neutron Scattering Laboratory was reorganized as the Neutron Science Laboratory to further promote the neutron science with use of the instruments in JRR-3. Under the General User Program supported by NSL, 14 university-group-owned spectrometers in the JRR-3 reactor are available for a wide scope of researches on material science, and proposals close to 300 are submitted each year, and the number of visiting users under this program reaches over 6000 person-day/year. In 2009, NSL and Neutron Science Laboratory (KENS), High Energy Accelerator Research Organization (KEK) built a chopper spectrometer, High Resolution Chopper Spectrometer, HRC, at the beam line BL12 of MLF/J-PARC (Materials and Life Science Experimental Facility, J-PARC). Since HRC covers a wide energy and Q-range (10μeV < $\hbar\omega$ < 2eV and 0.02Å^{-1} < Q < 50Å^{-1}), it became complementary to the existing inelastic spectrometers at JRR-3. HRC started to accept general users through the J-PARC proposal system in FY2011.

Triple axis spectrometers, HRC, and a high resolution powder diffractometer are utilized for a conventional solid state physics and a variety of research fields on hard-condensed matter, while in the field of soft-condensed matter science, researches are mostly carried out by using the small angle neutron scattering (SANS-U) and/or neutron spin echo (iNSE) instruments. The upgraded time-of-flight (TOF) inelastic scattering spectrometer, AGNES, is also available through the ISSP-NSL user program.

Scientific outputs from HRC in FY2016 covers wide range in magnetism and strongly correlated electrons. One of the research highlights is the observation of the magnetic excitations from two-dimensional interpenetrating Cu framework (see Fig. 1) in $Ba_2Cu_3O_4Cl_2$ [1]. Combination of position sensitive detectors in wide scattering angle and strong neutron flux in wide energy range enables the effective measurement of spin dispersion as shown in Fig. 2. The magnetic excitations were found to emerge from interpenetrating laminar sublattices of Cu_A and Cu_B spins each of which is arranged on a square-lattice. Lower energy excitations between 3 and 20meV originate from the weakly coupled Cu_B spins and closely resemble the $Sr_2Cu_3O_4Cl_2$

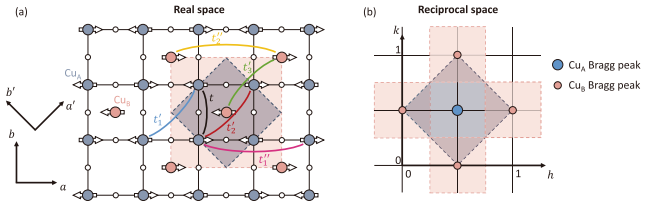

Fig. 1. (a) Depiction of the magnetic structure in $Ba_2Cu_3O_4Cl_2$. The circles filled by blue and red colors represent Cu_A and Cu_B sites, respectively. Empty circles denote intermediate O atoms. The shaded blue and red outlines represent the magnetic unit cells when Cu_A and Cu_A-Cu_B are magnetically ordered, respectively. The hopping terms between ions used in our modelling are connected by colored lines. (b) Reciprocal space of $Ba_2Cu_3O_4Cl_2$ projected onto the (*h*, *k*) plane. The shaded blue and red outlines represent the magnetic Brillouin zones of the two sublattices: Cu_A and Cu_B respectively. Bragg scattering from each sublattice is shown at the magnetic zone center.

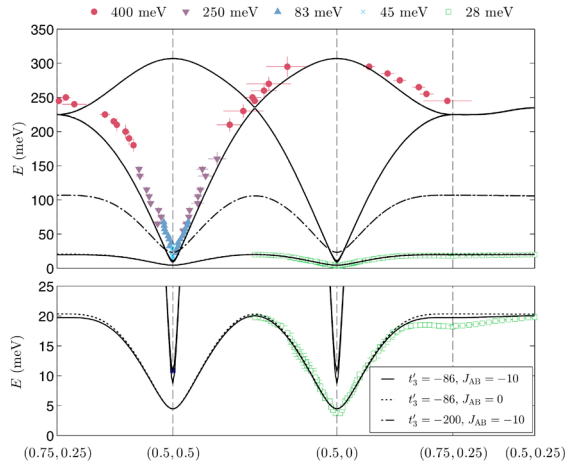

Fig. 2. Dispersion along high-symmetry directions in the 2D Brillouin zone obtained at 6 K. Extracted dispersion was obtained from TOF measurements using neutron incident energies in the 28–400meV range. The simulated spin-wave spectrum is shown for different parameters of t'_3 and J_{AB} in units of meV.

spectra [2]. In addition, the Cu_A-like excitations were truck up to 300 meV, which have not been previously studied in this family of materials. A single-band Hubbard model was characterized to characterize the spin dynamics from which an effective spin Hamiltonian was derived. A suitable parameterization of the magnetic spectrum was found using linear spin-wave theory. Careful analysis of the Cu_A and Cu_B spin-gaps provided the out-of-plane coupling, the strength of the Cu_A and Cu_B coupling as well as the exchange anisotropies. The interpenetrating Cu_B sublattice was found to be only weakly coupled to the Cu_A spins. Along the magnetic Brillouin zone boundary of weakly-coupled Cu_B spins, a significant dispersion was observed, which is argued as a quantum effect beyond linear spin wave theory.

Technical progress of HRC spectrometer was the development of high pressure environment. Cylinder-type cell made of CuBe alloy was designed by Prof. Uwatoko. The volume for the sample space is 5 mm in diameter and 20 mm in length. The maximum pressure is 1.4 GPa. The measurement was performed on 0.4g of $CsFeCl_3$ sample. 1 K cryostat was used to achieve 0.7 K, and the power of the J-PARC operation was 400 kW. Well-defined spin wave was successfully measured in the pressure-induced magnetic phase in $CsFeCl_3$.

The NSL also operates the U.S.-Japan Cooperative Program on neutron scattering, providing further research opportunities to material scientists who utilize the neutron scattering technique for their research interests. In 2010, relocation of the U.S.-Japan triple-axis spectrometer, CTAX, was completed, and it is now open to users.
https://neutrons.ornl.gov/ctax

[1] P. Babkevich *et al.*, Phys. Rev. B **96**, 014410 (2017).
[2] Y. J. Kim *et al.*, Phys. Rev. B **64**, 024435 (2001).

International MegaGauss Science Laboratory

The objective of this laboratory (Fig. 1) is to study the physical properties of solid-state materials (such as semiconductors, magnetic materials, metals, insulators, superconducting materials) under ultra-high magnetic field conditions. Such a high magnetic field is also used for controlling the new material phase and functions. Our pulse magnets, at

moment, can generate up to 87 Tesla (T) by non-destructive manner, and from 100 T up to 985 T (the world strongest as an in-door record) by destructive methods. The laboratory is opened for scientists both from Japan and from overseas, especially from Asian countries, and many fruitful results are expected to come out not only from collaborative research but also from our in-house activities. One of our ultimate goals is to provide the scientific users as our joint research with magnets capable of a 100 T, millisecond long pulses in a non-destructive mode, and to offer versatile physical precision measurements. The available measuring techniques now involve magneto-optical measurements, cyclotron resonance, spin resonance, magnetization, and transport measurements. Recently, specific heat and calorimetric measurements are also possible to carry out with sufficiently high accuracy.

Our interests cover the study on quantum phase transitions (QPT) induced by high magnetic fields. Field-induced QPT has been explored in various materials such as quantum spin systems, strongly correlated electron systems and other magnetic materials. Non-destructive strong pulse magnets are expected to provide us with reliable and precise solid state physics measurements. The number of collaborative groups for the research is almost 76 in the FT of 2017.

Fig. 1. Signboard at the entrance of the IMGSL.

Fig. 2. The building for the flywheel generator (left hand side) and a long pulse magnet station (right hand side). The flywheel giant DC generator is 350 ton in weight and 5 m high (bottom). The generator, capable of a 51 MW output power with the 210 MJ energy storage, is planned to energize the long pulse magnet generating 100 T without destruction.

	Alias	Type	B_{max}	Pulse width Bore	Power source	Applications	Others
Building C Room 101-113	Electro- Magnetic Flux Compression	destructive	1000 T	μs 10 mm	5 MJ, 50 kV 2 MJ, 50 kV	Magneto-Optical Magnetization	5 K – Room temperature
	Horizontal Single-Turn Coil	destructive	300 T 200 T	μs 5 mm 10 mm	0.2 MJ, 50 kV	Magneto-Optical measurements Magnetization	5 K – 400 K
	Vertical Single-Turn Coil	destructive	300 T 200 T	μs 5 mm 10 mm	0.2 MJ, 40 kV	Magneto-Optical Magnetization	2 K – Room temperature
Building C Room 114-120	Mid-Pulse Magnet	Non-destructive	60 T 70 T	40 ms 18 mm 40 ms 10 mm	0.9 MJ, 10 kV	Magneto-Optical measurements Magnetization Magneto-Transport Hall resistance Polarization Magneto-Striction Magneto-Imaging Torque Magneto- Calorimetry Heat Capacity	Independent Experiment in 5 site Lowest temperature 0.1 K
Building C Room 121	PPMS	Steady State	14 T			Resistance Heat Capacity	Down to 0.3 K
	MPMS	Steady State	7 T			Magnetization	
Building K	Short-Pulse Magnet	Non-destructive	87 T (2-stage pulse) 85 T	5 ms 10 mm 5 ms 18 mm	0.5 MJ, 20 kV	Magnetization Magneto-Transport	2 K – Room temperature
	Long-Pulse Magnet	Non-destructive	43.5 T	1 s 30 mm	210 MJ, 2.7 kV	Resistance Magneto-Calorimetry	2 K – Room temperature

Table 1. Available Pulse Magnets, Specifications

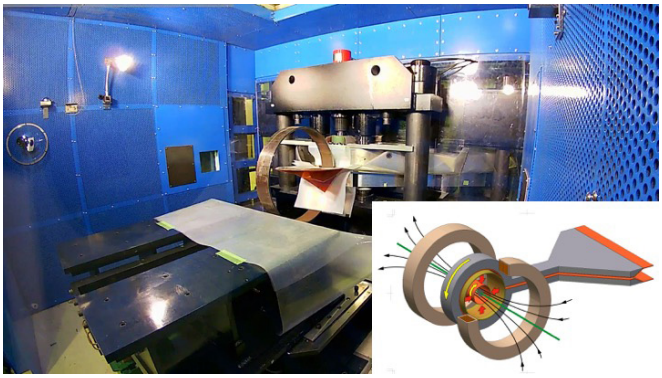

Fig. 3. (Build. C) A view of the electro-magnetic flux compression 1000 T-class megagauss generator set in side of an anti-explosive house. 1000 T project started since 2010, and finally condenser banks of 9 MJ (5 MJ + 2 MJ +2 MJ) as a main system with the 2 MJ sub bank system for the seed field have been installed, and settled in the year of 2014.

A 210 MJ flywheel generator (Fig. 2), which is the world largest DC power supply (recorded in the Guinness Book of World Records) has been installed in the DC flywheel generator station at our laboratory, and used as an energy source of super-long pulse magnets. The magnet technologies are intensively devoted to the quasi-steady long pulse magnet (an order of 1-10 sec) energized by the giant DC power supply. The giant DC power source will also be used for the giant outer-magnet coil to realize a 100 T nondestructive magnet by inserting a conventional pulse magnet coil in its center bore.

Magnetic fields exceeding 100 T can only be obtained with destruction of a magnet coil, where ultra-high magnetic fields are obtained in a microsecond time scale. The project, financed by the ministry of education, culture, sports, science and technology aiming to generate 1000 T with the electromagnetic flux compression (EMFC) system (Fig. 3), has been proceeded. Our experimental techniques using the destructive magnetic fields have intensively been developed. The system which is unique to ISSP in the world scale is comprised of a power source of 5 MJ main condenser bank and 2 MJ condenser bank. Two magnet stations are constructed and both are energized from each power source. Both systems are fed with another 2 MJ condenser bank used for a seed-field coil, of which magnetic flux is to be compressed. The 2 MJ EMFC system is currently under the process for optimizing several mechanical and electrical parameters such as dimensions of coils and liners. And so far, generation of 450 T was successfully done using 1.6 MJ energy. The 5 MJ EMFC system is under conditioning the main gap switches by finely tuning control parameters. As an easy access to the megagauss science and technology, we have the single-turn coil (STC) system capable of generating the fields of up to 300 T by a fast-capacitor of 200 kJ. We have two STC systems, one is a horizontal type (H-type, Fig. 4) and the other is a vertical type (V-type). Various kinds of laser spectroscopy experiments such as the cyclotron resonance and the Faraday rotation are possible using the H-type STC.

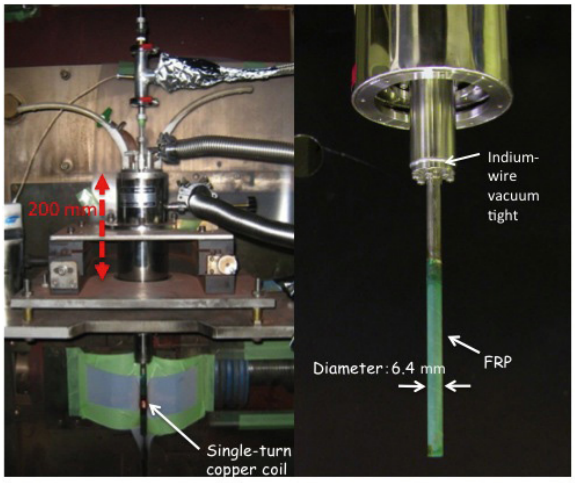

Fig. 4. Schematic picture of the H-type single-turn coil equipped with 50 kV, 200 kJ fast operating pulse power system, capable of generating 300 T within 3 mm bore coil.

Center of Computational Materials Science

The goal of the materials science is to understand and predict properties of complicated physical systems with a vast number of degrees of freedom. Since such problems cannot be solved with bare hands, it is quite natural to use computers in materials science. In fact, computer-aided science has been providing answers to many problems ranging from the most fundamental ones to the ones with direct industrial applications. In the recent trends of the hardware developments, however, the growth of computer power is mainly due to the growth in the number of the units. This fact poses a very challenging problem before us --- how can we parallelize computing tasks? In order to solve this problem in an organized way, we coordinate the use of the computational resources available to our community, and support community members through various activities such as administrating the website "MateriApps" for information on application software in computational science. These activities are supported by funds for various governmental projects in which CCMS is involved. In particular, we are acting as the headquarters of Priority Area 7 of MEXT FLAGSHIP2020 Project (so-called "post-K computer project"). In addition to this, CCMS is involved in Priority Area 5 and Pioneering Area (CBSM2) of FLAGSHIP2020 project, Element Strategy Initiative, and Professional Development Consortium for Computational Materials Scientists (PCoMS).

The following is the selected list of meetings organized by CCMS in FY2017:

- 7/11-7/12 Post-K Project Priority Issue 7 , The 2nd Annual Meeting (Koshiba Hall, Hongo, Tokyo)
- 6/7 PCoMS Matching Workshop (The University of Tokyo Kashiwa Campus Station Satellite, Kashiwa)
- 6/16 Post-K Project Priority Issue 7, Sub-issue G Work shop (The University of Tokyo Kashiwa Campus Station Satellite, Kashiwa)

Fig. 1. Members of CCMS.

- 6/29 CCMS Hands-On, HΦ (The University of Tokyo Kashiwa Campus Station Satellite, Kashiwa)
- 7/20 CCMS Hands-On, ALPS (The University of Tokyo Kashiwa Campus Station Satellite, Kashiwa)
- 8/1 Post-K Projec Priority Issue 5, The 1st meeting (Station Conference Manseibashi, Tokyo)
- 8/28 Post-K Project Exploratory Challenge 1, Sub-Challenge D, The 3rd Tensor Network Method Study Group (The University of Tokyo Kashiwa Campus Station Satellite, Kashiwa)
- 8/30 CCMS Hands-On, mVMC (The University of Tokyo Kashiwa Campus Station Satellite, Kashiwa)
- 9/11 Post-K Project Priority Issue 7, the 3rd Forum on Academia, Industry and Government collaboration for Creation of new functional devices and high-performance materials (The University of Tokyo Kashiwa Campus Station Satellite, Kashiwa)
- 9/12 TIA-Kakehashi Poster Workshop (The University of Tokyo Kashiwa Campus Station Satellite, Kashiwa)
- 10/3 CCMS Hands-On, MareriApps Live (The University of Tokyo Kashiwa Campus Station Satellite, Kashiwa)
- 10/10 RIST, The 4th Materials Workshop (Akihabara)
- 10/13 CCMS Hands-On, OpenMX(TIA)(The University of Tokyo Kashiwa Campus Station Satellite, Kashiwa)
- 10/24 Post-K Project Priority Issue 5, The 2nd meeting (Station Conference Manseibashi, Tokyo)
- 10/26 CCMS Hands-On, xTAP (The University of Tokyo Kashiwa Campus Station Satellite, Kashiwa)
- 10/30 Post-K Project Exploratory Challenge 1, Sub-Challenge B and D, Work shop (The University of Tokyo Kashiwa Campus Station Satellite, Kashiwa)
- 10/31 Post-K Project Exploratory Challenge 1, Sub-Challenge D, Work shop (The University of Tokyo Kashiwa Campus Station Satellite, Kashiwa)
- 11/24 The 1st SALMON Tutorial (TIA) (The University of Tokyo Kashiwa Campus Station Satellite, Kashiwa)
- 12/4 Next QUMAT2017 (Faculty of Engineering, the University of Tokyo , Hongo, Tokyo)
- 12/5-12/6 Post-K Project Priority Issue 7, The 3rd Symposium (ISSP, Kashiwa)
- 12/20 CCMS Hands-On, RESPACK (The University of Tokyo Kashiwa Campus Station Satellite, Kashiwa)
- 12/22 Post-K Project Priority Issue 7, Sub-issue G, The 6th Work shop (The University of Tokyo Kashiwa Campus Station Satellite, Kashiwa)
- 12/26 Post-K Project Priority Issue 7, Sub-issue G, The 7th Work shop (Tokyo University of Science, Katsushika campus)
- 1/13 Post-K Project Priority Issue 7, Sub Issue E and Post-K Project Exploratory Challenge, Sub-Challenge A, The 2nd Work shop (AIST Kansai, Osaka)
- 1/26 CCMS Hands-On, OpenMX(TIA) (The University of Tokyo Kashiwa Campus Station Satellite, Kashiwa)
- 2/5-2/6 The 3rd Element Strategy Initiative, To Form Core Research Centers Symposium on the Elements Strategy Large-scale Research Facilities (Ito Hall, Hongo, Tokyo)
- 2/13 RIST, The 5th Materials Workshop (Akihabara)
- 2/20 Post-K Project Priority Issue 5, The 3rd meeting (Station Conference Manseibashi, Tokyo)
- 2/24 RIST, Mieruka Symposium (Visualization Symposium) 2018 (Nihonbashi Life Science Hub, Tokyo)
- 3/30 Post-K Project Priority Issue 7, The 2nd Positron Diffraction Work Shop (KEK, Tsukuba)
- 1/23-1/25 Innovation Camp 2018 for Computational Materials Science (Hokkaido)
- 1/26 CCMS Hands-On, OpenMX (The University of Tokyo Kashiwa Campus Station Satellite, Kashiwa)
- 2/27 PCoMS Skill-up Training (The University of Tokyo Kashiwa Campus Station Satellite, Kashiwa)
- 3/5 CCMS Hands-On, MateriApps (The University of Tokyo Kashiwa Campus Station Satellite, Kashiwa)
- 3/12-3/13 Symposium on Materials Science and Technology towards Energy-Saving Society (MASTES2018) (Takeda Hall, Hongo, Tokyo)

Laser and Synchrotron Research Center (LASOR Center)

Laser and Synchrotron Research (LASOR) Center started from October, 2012. LASOR Center aims to promote material sciences using advanced photon technologies at ISSP by combining the "Synchrotron Radiation Laboratory" and "Advanced Spectroscopy Group". These two groups have long histories since 1980's and have kept strong leaderships in each photon science fields for a long time in the world. In the past several decades, the synchrotron-based and laser-based photon sciences have made remarkable progresses independently. However, recent progresses in both fields make it feasible to merge the synchrotron-based and laser based technologies to develop a new direction of photon and materials sciences. In the LASOR Center, extreme laser technologies such as ultrashort-pulse generation, ultraprecise control of optical pulses in the frequency domain, and high power laser sources for the generation of coherent VUV and SX light are intensively under development. The cutting edge soft X-ray beamline is also developed at the synchrotron facility SPring-8.

LASOR center aims three major spectroscopic methods [ultrafast, ultra-high resolution, and operand spectroscopy] by three groups [extreme laser science group, soft-X-ray spectroscopy and materials science group, and coherent photon science group], as illustrated in Fig. 2. Under this framework, various advanced spectroscopy, such as ultra-high resolution photoemission, time-resolved, spin-resolved spectroscopy, diffraction, light scattering, imaging, microscopy and fluorescence spectroscopy are in progress by employing new coherent light sources based on laser and synchrotron technologies that cover a wide spectral range from X-ray to terahertz. In LASOR Center, a variety of

Fig. 1. Open ceremony of LASOR center on October 2012.

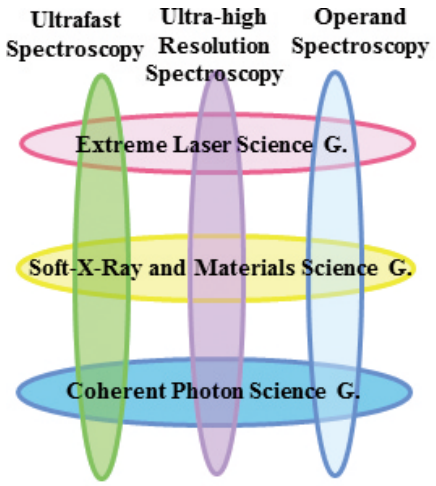

Fig. 2. Developments of advanced spectroscopy at LASOR center by three groups

materials sciences for semiconductors, strongly-correlated materials, molecular materials, surface and interfaces, and bio-materials are studied using advanced light sources and advanced spectroscopy. Another important aim of LASOR Center is the synergy of photon and materials sciences.

Most of the research activities on the extreme laser development and their applications to materials science are performed in the ISSP buildings D and E at Kashiwa Campus where large clean rooms and the vibration-isolated floor are installed. On the other hand, the experiments utilizing the advanced synchrotron source are performed at a beamline BL07LSU in SPring-8 (Hyogo).

• Extreme Laser Science Group

The advancement of ultrashort-pulse laser technologies in the past decade has transformed the laser development at ISSP into three major directions, (i) towards ultrashort in the time domain, (ii) ultra high resolution in the spectral domain, and (iii) the extension of the spectral range, with extreme controllability of the laser sources. For ultrafast spectroscopy, we have developed carrier-envelope phase stable intense infrared light source that can produce sub-two cycle optical pulses for high harmonic and attosecond pulse generation. So far we observed coherent soft-X-ray radiation extending to a photon energy of ~330 eV. The simulation predicts the soft-X-ray field consists of single isolated

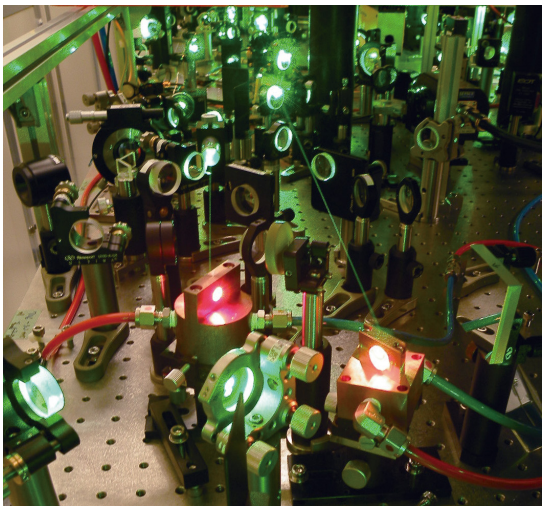

Fig. 3. Close look of a high-peak-power ultrashort-pulse laser

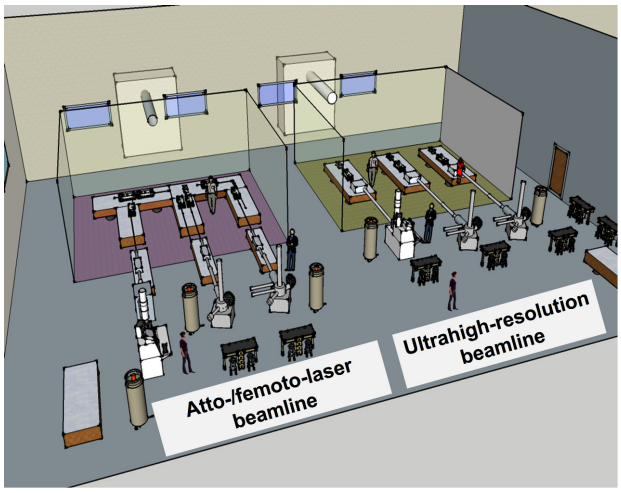

Fig. 4. Newly designed building E was constructed for new extreme VUV- and SX-lasers and new spectroscopy.

attosecond pulses. For ultra-high resolution spectroscopy, fiber-laser-based light sources are intensively developed for producing EUV pulses for high resolution and time-resolved photoemission spectroscopy as well as extending the frequency comb to ultraviolet or infrared for various applications. The spectral range of intense optical pulses are being extended from visible to IR, MIR and THz ranges. Various types of high-repetition-rate ultrastable light sources are developed for laser-based ultrahigh resolution photoemission spectroscopy, high-average-power EUV generation in an enhancement cavity, and frequency comb spectroscopy for atomic physics, astronomical application, and frequency standards.

• Soft-X-ray and Materials Science Group

Recently, VUV and SX lasers have progressed very rapidly. They become very powerful for the materials science using the cutting-edge VUV and SX spectroscopy. Especially, angle resolved photoemission spectroscopy (ARPES) is very powerful to know the solid state properties. Laser has excellent properties, such as coherence, monochromaticity, polarization, ultra-short pulse, high intensity, and so on. By using monochromatic laser light, the resolution of ARPES becomes about 70-μeV. The materials science with sub-meV resolution-ARPES is improved drastically by using high resolution laser. For example, superconducting gap anisotropy of the superconductors and Fermiology of

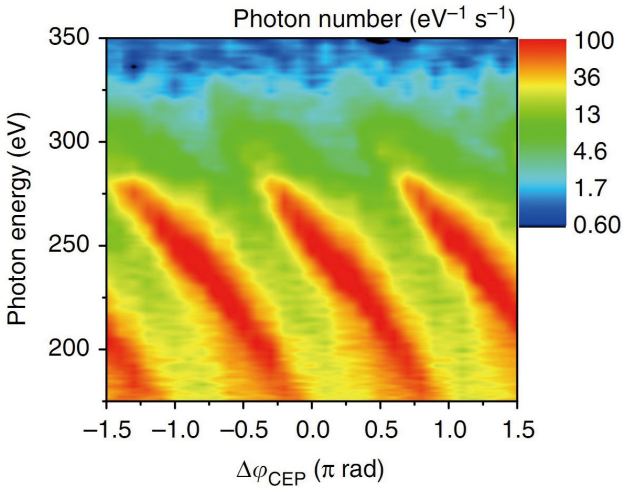

Fig. 5. Phase-dependence of high harmonic spectra in soft X rays.

Fig. 6. 10-MHz high harmonic generation in an enhancement cavity.

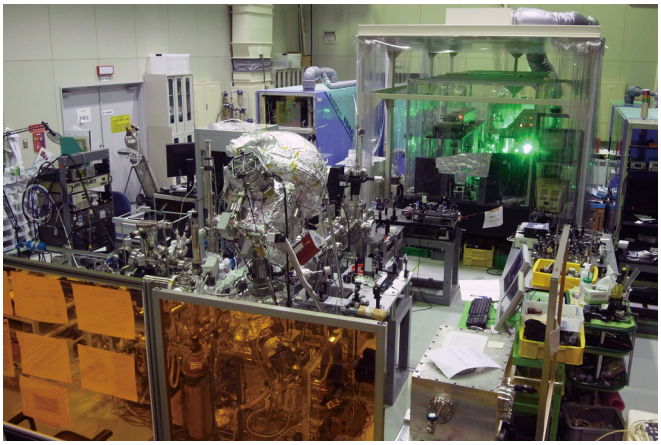

Fig. 7. Pump-probed photoemission system using 60-eV laser

the strongly correlated materials are studied very well. On the other hand, using pulsed laser light, the time-resolved photoemission in fs region becomes powerful to know the relaxation process of photo-excited states of the materials. Furthermore, by using CW laser with circular polarization in VUV region, the photoelectron microscopy (PEEM) is developed. The spatial resolution of nm resolution is very powerful for the study of nanomagnetic materials.

• Coherent Photon Science Group

The coherent-photon science group has main interests in exploring a variety of coherent phenomena and non-equilibrium properties of excited states in condensed matters, in collaborations with research groups in charge of photoemission, operand-spectroscopy and extreme laser science. This group covers a wide range of materials, from semiconductors, ferroelectrics, antiferromagnets, and superconductors to biomaterials. Various ultrafast optics technologies such as femtosecond luminescence, terahertz spectroscopy, and pump-and-probe transmission/reflection spectroscopy are applied to studies on dynamics of photo-excited carriers and photo-induced phase transitions. Coherent control of matters using phase-locked strong terahertz or mid-infrared pulse is extensively studied. Advanced photonics devices are intensively studied, such as quantum nano-structure lasers with novel low-dimensional gain physics, low-power light-standard LEDs, very efficient multi-junction tandem solar cells for satellite use, and wonderful bio-/chemi-luminescent systems for wide bio-technology applications.

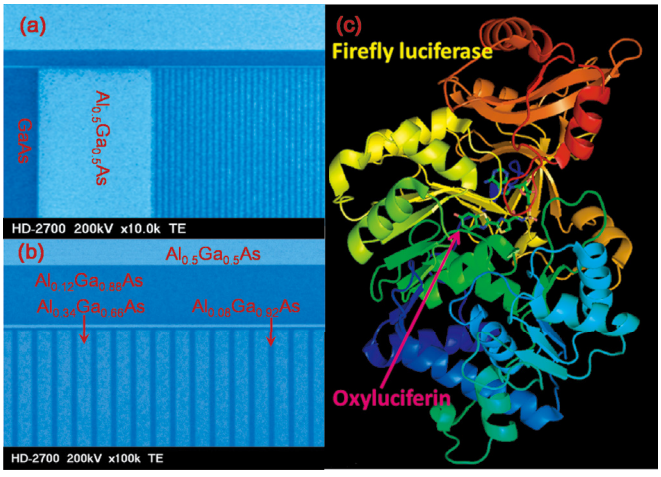

Fig. 8. Photonics devices under study: (left panel) semiconductor quantum wires and (right panel) firefly-bioluminescence system consisting of light emitter (oxyluciferin) and enzyme (luciferase)

Synchrotron Radiation Laboratory

The Synchrotron Radiation Laboratory (SRL) was established in 1975 as a research division dedicated to solid state physics using synchrotron radiation (SR). Currently, SRL is composed of two research sites, the Harima branch and the E-building of the Institute for Solid State Physics.

• Brilliant soft X-ray beamline at Harima branch

In 2006, the SRL staffs have joined the Materials Research Division of the Synchrotron Radiation Research Organization (SRRO) of the University of Tokyo and they have played an essential role in constructing a new high brilliant soft X-ray beamline, BL07LSU, in SPring-8. The light source is the polarization-controlled 25-m long soft X-ray undulator with electromagnetic phase shifters that allow fast switching of the circularly (left, right) and linearly (vertical, horizontal) polarized photons.

The monochromator is equipped with a varied line-spacing plain grating, which covers the photon energy range from 250 eV to 2 keV. At the downstream of the beamline, a lot of experimental stations have been developed for frontier spectroscopy researches: five endstations, i.e. time-resolved soft X-ray spectroscopy (TR-SX) equipped with a

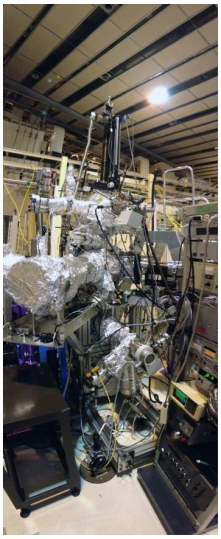

Fig. 1. TR-SX station

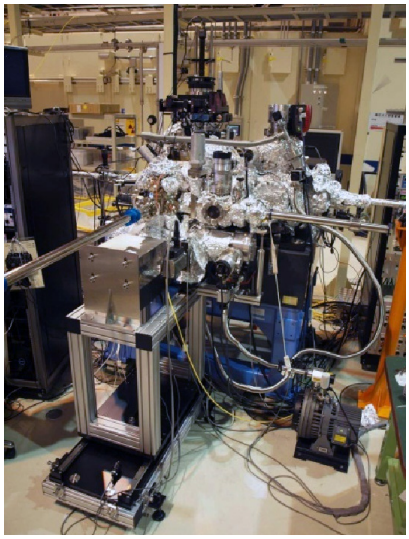

Fig. 2. 3D-nano ESCA station

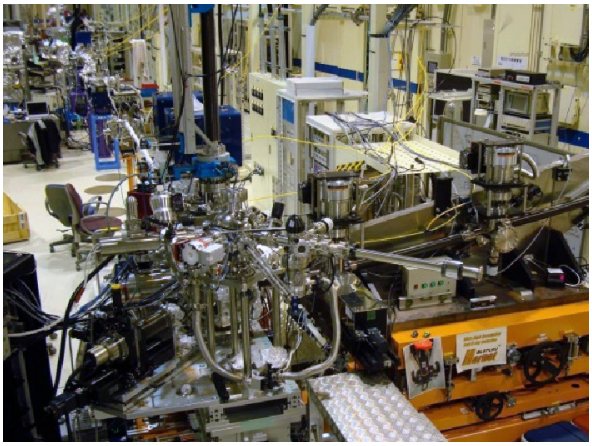

Fig. 3. Soft X-ray emission station

two-dimensional angle-resolved time-of-flight (ARTOF) analyzer (Fig. 1), three-dimensional (3D) nano-ESCA station equipped with the Scienta R-3000 analyzer (Fig. 2), high resolution soft X-ray emission spectroscopy (XES) stations (Fig. 3) are regularly maintained by the SRL staffs and open for public use, and at free-port station many novel spectroscopic tools have been developed and installed such as soft X-ray resonant magneto-optical Kerr effect (MOKE) (Fig.4) and soft X-ray diffraction (Fig. 5), ambient pressure photoemission, two dimensional photoelectron diffraction and so on. The beamline construction was completed in 2009 and SRL established the Harima branch laboratory in SPring-8. At SPring-8 BL07LSU, each end-station has achieved high performance: the TR-SX station have established the laser-pump and SR-probe method with the time-resolution of 50 ps which corresponds to the SR pulse-width; the 3D nano-ESCA station reaches the spatial resolution of 70 nm; the XES station provides spectra with the energy resolution around 70 meV at 400 eV and will enable real ambient pressure experiments in the near future. Soft X-ray resonant MOKE station has been developed to make novel magneto-optical experiment using fast-switching of the polarization-controlled 25-m long soft X-ray undulator. The soft X-ray diffraction station has been fully constructed and the time-resolved measurement is available by using lasers at the TR-SX station. Each end-station has now been opened fully to outside users. In 2015, 176 researchers made their experiments during the SPring-8 operation time of 4805 hours.

• High-resolution Laser SARPES at E-building

Spin- and angle-resolved photoelectron spectroscopy

Fig. 4. Soft X-ray MOKE station

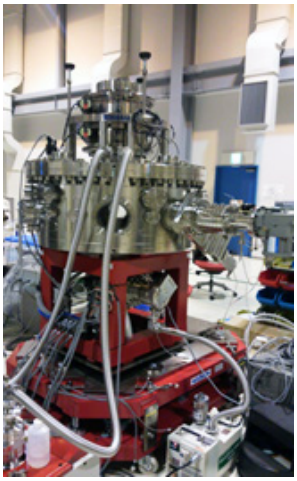

Fig. 5. Soft X-ray diffraction station

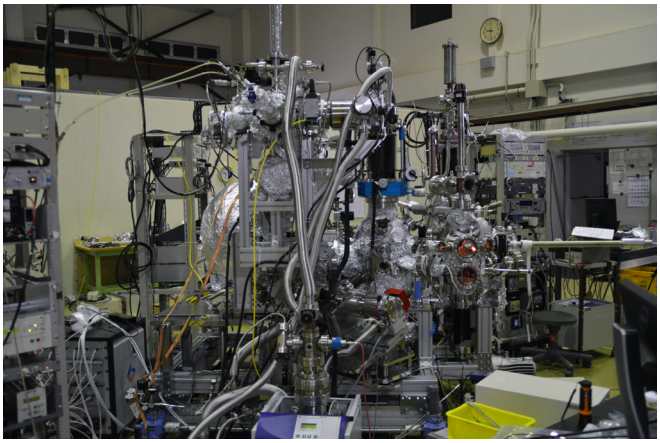

Fig. 6. Laser-SARPES system at E-building

(SARPES) is a powerful technique to investigate the spin-dependent electronic states in solids. In FY 2014, Laser and Synchrotron Research Center (LASOR) SRL constructed a new SARPES apparatus (Fig. 6), which was designed to provide high-energy and -angular resolutions and high efficiency of spin detection using a laser light instead of the synchrotron radiation in Institute for Solid State Physics. The achieved energy resolution of 1.7 meV in SARPES spectra is the highest in the world at present. From FY 2015, the new SARPES system has been opened to outside users.

The Laser-SARPES system consists of an analysis chamber, a carousel chamber connected to a load-lock chamber, and a molecular beam epitaxy chamber, which are kept ultra-high vacuum (UHV) environment and are connected each other via UHV gate valves. The electrons are excited with 6.994-eV photons, yielded by 6th harmonic of a Nd:YVO_4 quasi-continuous wave laser with repetition rate of 120 MHz. The hemispherical electron analyzer is a custom-made ScientaOmicron DA30-L, modified for installing the spin detectors. The spectrometer is equipped with two high-efficient spin detectors associating very low energy electron diffraction are orthogonally placed each other, which allows us to analyze the three-dimensional spin polarization of electrons. At the exit of the hemispherical analyzer, a multi-channel plate and a CCD camera are also installed, which enables us to perform simultaneously the angle-resolved photoelectron spectroscopy with two-dimensional (energy-momentum) detection. So far, spin-dependent band structures of more than 10 materials have been studied by 4 outside groups.

Conferences and Workshops

The 5th Ito International Research Center Conference "Forefront of Molecular Dynamics at Surfaces and Interfaces: from a Single Molecule to Catalytic Reaction"

November 20 - 23, 2017
J. Yoshinobu

In cooperation with Surface and Interface Spectroscopy Forum in Japan, the present international conference was held from November 20 to 23, 2017 at Ito Hall of The University of Tokyo (Hongo campus), with the financial support of Ito International Academic Research Center Foundation (The University of Tokyo), the RIKEN Centennial Anniversary Project, ISSP International Workshop, and ISSP Workshop. There were 196 participants, including 30 invited speakers, 13 contributed oral presentations and 109 poster presentations (133 participants from Japan including 19 invited speakers and 63 participants from abroad including 15 invited speakers).

Chair of the executive committee was Prof. Jun Yoshinobu (ISSP) and Co-chair was Dr. Kim Yousoo (RIKEN); the other committee members were Prof. Shigeru Masuda (The University of Tokyo), Prof. Satoshi Watanabe (The University of Tokyo), Prof. Katsuyuki Fukutani (The University of Tokyo), Prof. Noriaki Takagi (The University of Tokyo), Prof. Junji Nakamura (Tsukuba University), Prof. Tadahiro Komeda (Tohoku University), and Dr. Ryuichi Arafune (NIMS).

Understanding the dynamics of atoms and molecules at surfaces and interfaces has been becoming increasingly important in a wide range of research fields from basic science to applied fields. Surfaces and interfaces play an important role in energy and mass transfer in materials. Application of nanotechnology in various industrial fields promotes the research for novel nanoscale and/or low dimensional materials. In addition, the recent experimental and theoretical progress such as scanning probe microscopy, synchrotron radiation and laser spectroscopy, first-principles density functional theory calculation, etc. has made it possible to elucidate and control the processes at surfaces in atomic scale.

This international conference focused on molecular dynamics at surface and interface. The oral and poster presentations were performed concerning the following topics:

· Physics and chemistry of adsorbed molecules
· Low dimensional materials at surface and interface
· Dynamical processes at model catalysts
· Molecular processes at the surface and interface of devices
· Elementary processes at solid-liquid interface.

Hot discussions were held not only during the symposium but also during tea-breaks and meals. During and after the conference, we have received a lot of positive comments on the high-quality presentations and operations of the meeting. We would like to acknowledge all the participants, the committees and secretaries.

The abstract booklet of this conference can be downloaded from the following URL;
http://yoshinobu.issp.u-tokyo.ac.jp/IIRC5_Program_booklet-Final.pdf

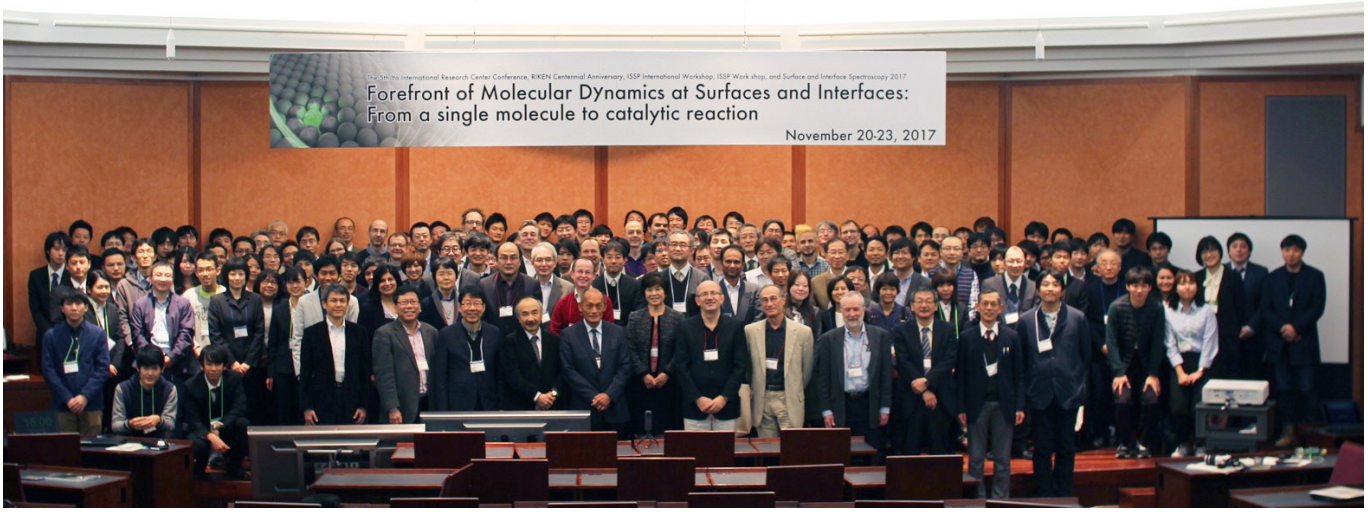

Computational Materials Science —Now and the Future—

April 3 - 4, 2017

H. Noguchi, N. Kawashima, O. Sugino, H. Watanabe, S. Kasamatsu,
Y. Noguchi, S. Morita, T. Ohtsuki, A. Kitao, and Y. Morikawa

This workshop was organized for the computational condensed matter research community, especially for the users of the ISSP supercomputers, to exchange the most recent information on the computational condensed matter research and on the high-performance computation of related research areas. This was held as a series of annual workshop of ISSP supercomputer that has been held every year. The selected topics include the target of the post-K supercomputer project, the progress made in the elements strategy projects, the emergent data-driven material research, and "the Project for advancement of software usability in materials science" that developed the numerical library Kω to solve the shifted linear equation within the Krylov subspace and numerical solver package mVMC of the many-variable Variational Monte Carlo method in 2016. In addition to 16 invited talks and 30 poster presentations, two special lectures for machine-learning were given by Prof. Masayuki Ohzeki and Dr. Daisaku Yokoyama.

Small Angle Neutron Scattering, Neutron Reflectivity, and Neutron High-Resolution Instruments

April 24 - 25, 2017

M. Shibayama, O. Yamamuro, and M. Hino

It has already passed more than 6 years since the shutdown of the Research Reactor, JRR-3, due to the Great Earthquake on March 11, 2011. During this period until today, demands of neutron scattering/reflectivity/spectroscopy experiments for nanometer-order structural analyses and investigations of dynamics have been increasing rapidly than before. Neutron Science Laboratory (NSL) held a workshop on instrumentations and state-of-art researches with small-angle neutron scattering, neutron reflectivity, and high energy-resolution instruments during the period of April 24 – 25, 2017. Since restart of JRR-3 was expected to be February, 2018, it was a timely project and more than 100 scientists as total participated in this workshop during the two-day workshop. On Day 1, the workshop began with an introductory remarks by Prof. Takigawa, Director of ISSP, and Prof. Shibayama, Director of NSL, followed by presentations by instrument scientists about the current status and future plans of each instrument. After these presentations, a summary talk and free discussions were given, where importance and necessity of collaborations between JRR-3 and J-PARC MLF, not only on organization level but also from educational viewpoints, was emphasized. Then, a mixer was held in the lounge. On Day 2, scientific highlights from various fields were given, such as polymers, composites, proteins, liquid structures, multi-ferroic solid materials, and structure transitions in liquids. In general discussions and summary session, there were a few remarks were addressed: (1) importance of diversity of soft matter science, but the necessity of viewpoints with universality, (2) how to improve the general-use program of neutron scattering, (3) how to increase the number of neutron users, (4) safety and security issue. It was a very successful workshop from various viewpoints, science, instrumentation, and general-use program. The workshop was closed by looking forward to restart of JRR-3.

Frontier Science of Electronic Properties Observed/Manipulated by Light: Strong Correlation, Topology, Low Dimension and Dynamics

June 12 - 14, 2017
T. Kondo, H. Wadati, H. Akiyama, and A. Kimura

The photoemission is a powerful technique to directly observe electronic structure of matter, and it has established itself as an experimental tool commonly used in the research of condensed matter physics. While this trend on photoemission will be continued in the future as well, further enhancement of capability in this technique is highly expected for younger generation. Until now, it has been well accepted that the discovery of new materials such as high temperature superconductors and topological insulators, and the following observations of superconducting gap and spin-polarized texture in these have boosted the development of photoemission technique. Together with the demand to investigate these physical properties, the photoemission has also forcefully evolved forward keeping in step with the progress of advanced light source. In recent years, synchrotron and laser, which has been being developed independently with each other, are getting overlapped in the range of photon energy. We have now entered an era in which researchers can freely select these light sources to use in a cross-sectoral manner, depending on each experimental purpose. A dream to cutting edge research on materials science with photoemission will greatly expand as long as one makes the most use of "coherence", "polarization", and "pulse", the three biggest advantages for controlled light. Based on these background, in this work shop, active young researchers have gathered in ISSP to discuss the potential and capability of photoemission and how to utilize it for the future materials science.

Recent Progress in the Research of the 5*d* Pyrochlore Oxides

August 2, 2017
T. C. Kobayashi and Z. Hiroi

The workshop was planned as an opportunity for researchers working on various 5*d* transition metal pyrochlore oxides to get together and discuss their recent progress. The 5*d* pyrochlore oxides are now well recognized as interesting playgrounds for novel physics associated with spin–orbit coupling. The Weyl semimetal behavior and the all-in–all-out magnetic order are observed in $Ln_2Ir_2O_7$ and $Cd_2Os_2O_7$, in which also electron correlations play an important role. The spin–orbit coupled metal $Cd_2Re_2O_7$ is another hot topics, which may exhibit mutipole orders and parity-mixing superconductivity. Other pyrochlore oxide CsW_2O_6 with the $5d^{0.5}$ electron configuration seems to be a candidate for the molecular orbital crystal with trimerization. Approximately 40 people joined the meeting. The workshop gave a wonderful opportunity for attendees to understand the present status and to imagine the future prospect of the 5*d* pyrochlore oxides.

The 9th APCTP Workshop on Multiferroics

November 9 - 11, 2017
T. Kimura, T. Arima, and M. Tokunaga

The APCTP Workshop on Multiferroics started at the headquarter of Asia Pacific Center for Theoretical Physics (APCTP) at Pohang in 2008 and has continued as an annual event for the last several years. It has successfully brought together the most active members in the field of multiferroics and continues to enhance the strength of collaboration in the international community, particularly in APCTP member countries. In 2017, the 9th workshop was held at Kashiwa campus, University of Tokyo. We had 23 invited talks (14 from APCTP member countries and 9 from non-APCTP member countries), 6 contributed talks (4 from Japan and 2 from non-APCTP member countries), and 55 poster presentations mainly by graduate students and young researchers. During the three days, participants of the workshop actively discussed various topics related to multiferroic research such as fundamental understandings of known multiferroics, syntheses of new multiferroics, fabrications of multiferroics/ferroelectrics with new functionalities, multiferroic domain engineering, and explorations of new functionalities (e.g., electric control of magnetism and nonreciprocal phenomena) in multiferroics. Furthermore, we had a special session during the reception where all the participants frankly discussed the future direction of multiferroic research. During and after the workshop, we received a number of positive comments from the participants. Some of them mentioned that they are going to start collaboration work with other participants. Some young participants acknowledged our financial supports (or no registration fee). From these comments from participants, we consider to achieve the purpose of the workshop.

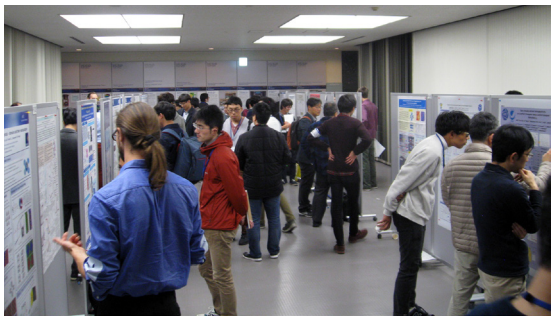

ISSP - J-PARC Joint Workshop on Science Frontier by Neutron Scattering: The 16th Korea-Japan Meeting on Neutron Science

January 8 - 10, 2018
T. Masuda, M. Shibayama, K. Nakajima, and H. Seto

Neutron scattering research in wide field was discussed by Korean and Japanese scientists. The workshop consists of the following contents: (i) facility reports (ii) magnetism and strongly correlated electrons (iii) industrial use (iv) instruments, software, and advanced data analysis (v) Biological and soft matter and (vi) liquid. In the facility report, current status of neutron science laboratory institute for solid state physics (NSL-ISSP) was reported by the director Prof. M. Shibayama. During the long shut down of JRR-3, NSL-ISSP supports the travel budget for neutron experiments in foreign facilities for JRR-3 users. About high-resolution chopper spectrometer (HRC) cooperated by NSL-ISSP and KEK, combination of various sample environment devices, upgrade of Fermi chopper, and the increase of the beam power of J-PARC made the HRC efficient instrument, and the scientific productivity has been improved. Status of other neutron facilities were presented by the directors. Research topics including observation of magnon-phonon coupling in manganites by Je-Geun Park, Kitaev quantum spin liquid by S. Ji, and small angle neutron scattering on skyrmion by T. Nakajima were reported in the field of magnetism. Unique neutron techniques such as neutron holography for the investigation of local atomic structures by K. Ohyama were introduced. In the field of soft matter science, structure analysis of critical gelation cluster by X. Li, neutron reflectivity measurements for diffusion dynamics of polymer melts by J. Koo, and many interesting talks were presented. In total 28 of oral and 32 of poster presentations were made by Korean and Japanese scientists, and the participants had fruitful discussions.

Status of SPring-8 BL07LSU and Strategies to Genesis of the Next-Generation Soft X-ray Science

March 13, 2018
I. Matsuda, S. Shin, F. Komori, Y. Harada, and H. Wadati

Synchrotron radiation laboratory at the Harima branch develops the frontier science at high-brilliance soft X-ray beamline BL07LSU at SPring-8 and makes the experimental innovations with domestic and foreign users. We have performed time-resolved, spatial-resolved and energy-resolved soft X-ray spectroscopy to study electronic states and their dynamics of new materials. Recently, we have also carried out *operando* experiments to examine functional materials under the working conditions. This year, we celebrate 10 years since construction of the beamline, reaching a milestone to consider the next project. On the other hand, new light sources, such as XFEL or a diffraction limited storage ring, are recently encouraged to be designed and to be constructed over the world. In Japan, we have plans of Slit-J and SPring-8-II. Since science and techniques, developed at BL07LSU, are closely related to experiments expected to be held at such new generation synchrotron radiation sources, it is also high time to consider the next soft X-ray science. Thus, we organized this ISSP workshop to present our recent achievements and to discuss the strategies with participants.

We had two invited talks by two outstanding researchers. Prof. Kotsugi prospected the future of synchrotron radiation researches and Dr. Katayama presented his recent results at SACLA. Speakers talked about their recent results from each end station (time-resolved spectroscopy, 3D nano-ESCA, emission spectroscopy, ambient pressure XPS and so on). During the discussion time, we shared information on the frontier researches of synchrotron radiation in various fields, physics, chemistry, and biology. Eventually, we were able to make the clear vision for the next-generation soft X-ray science at BL07LSU and at new storage rings. We also encouraged a young researcher by awarding the best poster prize.

Subjects of Joint Research

平成 29 年度　共同利用課題一覧（前期）/ Joint Research List (2017 First Term)

嘱託研究員 / Commission Researcher

No.	課題名	氏名	所属		Title	Name	Organization
担当所員：森　初果							
1	水素結合型分子導体における H/D 同位体効果による相転移機構の理論的研究	立川　仁典	横浜市立大学	大学院生命ナノシステム科学研究科	Theoretical study of phase transition mechanism induced by H/D isotope effect in hydrogen-bonded molecular conductors	Masanori Tachikawa	Yokohama City Uninersity
2	〃	長嶋　雲兵	計算科学振興財団	共用促進研究部門	〃	Umpei Nagashima	Foundation for Computational Science
3	常圧で金属状態を示す純有機単一成分導体の開発	御崎　洋二	愛媛大学	大学院理工学研究科	Development of purely organic single-component molecular metals under ambient pressure	Kenta Kimura	Ehime University
4	純有機単一成分超伝導体の開発	白旗　崇	愛媛大学	大学院理工学研究科	Development of purely organic single-component molecular superconductors	Takashi Shirahata	Ehime University
担当所員：中辻　知							
5	価数揺らぎに伴う量子臨界点とその近傍の異常物性の研究	三宅　和正	豊田理化学研究所		Theoretical study on anomalous metal phase due to quantum valence instability	Kazumasa Miyake	Toyota Rikagaku Kenkyuujyo
6	フラストレート磁性体における量子物性の探求	木村　健太	大阪大学	大学院基礎工学研究科	The search for quantum state in frustrated magnets	Kenta Kimura	Osaka University
7	イッテルビウム系重い電子化合物の結晶場基底状態の研究	久我　健太郎	理化学研究所	放射光科学総合研究センター	Crystal-electric-field ground state study in Yb-based heavy fermion compound	Kentarou Kuga	RIKEN
担当所員：長谷川　幸雄							
8	弱トポロジカル絶縁体候補物質 Bi_4I_4 の低温 STM 観察	岡田　佳憲	東北大学	原子分子材料科学高等研究所	Low-temperature STM study on weak topological insulator candidate Bi_4I_4	Yoshinori Okada	Tohoku University

No.	課題名	氏名	所属		Title	Name	Organization
担当所員：上床　美也							
9	高圧下量子振動システムの開発	摂待　力生	新潟大学	理学部	Development of quantum oscillation under high pressure	Rikio Settai	Niigata University
10	磁性体の圧力効果	巨海　玄道	久留米工業大学	工学部	Effect of pressure on the Magnetic Materials	Gendo Oomi	Kurume Institute of Technology
11	多重極限関連圧力装置の調整	高橋　博樹	日本大学	文理学部	Adjustment of Cubic Anvil apparatus	Hiroki Takahashi	Nihon University
12	擬一次元有機物質の圧力下物性研究	糸井　充穂	日本大学	医学部	Study on pressure induced superconductivity of quasi organic conductor	Miho Itoi	Nihon University
13	3d 遷移化合物に関する圧力効果	鹿又　武	東北学院大学	工学総合研究所	Eiffect of pressure on the 3d transition compounds	Takeshi Kanomata	Tohoku Gakuin University
14	希釈冷凍機温度で使用可能な 10GPa 級超高圧発生装置の開発	松林　和幸	電気通信大学	大学院情報理工学研究科	Development of 10 GPa class high pressure apparatus for low temperature	Kazuyuki Matsubayashi	The University of Electro-Communications
15	有機伝導体の圧力効果	村田　恵三	大阪経済法科大学	21 世紀社会総合研究センター	Effect of pressure on the organic conductor	Keizo Murata	Osaka University of Economics and Law
16	圧力下 NMR 測定法に関する開発	藤原　直樹	京都大学	大学院人間・環境学研究科	Development of NMR measurement method under high pressure	Naoki Fujiwara	Kyoto University
17	高圧下の比熱測定装置の開発	梅原　出	横浜国立大学	工学部	Development of apparatus for specific heat measurements under high pressure	Izuru Umehara	Yokohama National University
18	希土類 122 化合物における圧力効果	繁岡　透	山口大学	大学院理学研究科	Pressure effect of rare earth 122 compounds	Toru Shigeoka	Yamaguchi University
19	中性子回析に用いる圧力装置の開発	片野　進	埼玉大学	大学院理工学研究科	Developments of High Pressure Cell for Neutron Diffraction	Susumu Katano	Saitama University
20	低温用マルチアンビル装置の開発	辺土　正人	琉球大学	理学部	Development of multi-anvil apparatus for low temperature	Masato Hedo	University of the Ryukyus
21	磁化測定装置の開発	名嘉　節	物質・材料研究機構	機能性材料研究拠点	Development of the magnetometer	Takashi Naka	National Institute for Materials Science
担当所員：野口　博司							
22	理論・実験・データ科学の融合を目指した量子格子模型シミュレータの開発	星　健夫	鳥取大学	大学院工学研究科	Development of quantum lattice model simulator integrating theory, experiment, and data science	Takeo Hoshi	Tottori University
23	〃	曽我部　知広	名古屋大学	大学院工学研究科	〃	Tomohiro Sogabe	Nagoya University

No.	課題名	氏名	所属		Title	Name	Organization
24	動的平均場近似に基づく第一原理計算パッケージの高度化	大槻　純也	東北大学	大学院理学研究科	Advancement of ab-initio program based on dynamical mean-field theory	Jyunya Otsuki	Tohoku University
25	〃	品岡　寛	埼玉大学	理学部	〃	Hiroshi Shinaoka	Saitama University
担当：中性子科学研究施設							
26	4G における共同利用推進	佐藤　卓	東北大学	多元物質科学研究所	Research and Support of General-Use at 4G	Taku Sato	Tohoku University
27	〃	奥山　大輔	東北大学	多元物質科学研究所	〃	Daisuke Okuyama	Tohoku University
28	〃	那波　和宏	東北大学	多元物質科学研究所	〃	Kazuhiro Nawa	Tohoku University
29	〃	Johannes Reim	東北大学	多元物質科学研究所	〃	Johannes Reim	Tohoku University
30	6G における共同利用推進	富安　啓輔	東北大学	大学院理学研究科	Research and Support of General-Use at 6G	Keisuke Yomiyasu	Tohoku University
31	〃	岩佐　和晃	茨城大学	フロンティア応用原子科学研究センター	〃	Kazuaki Iwasa	Ibaraki University
32	T1-2、T1-3 における共同利用推進	藤田　全基	東北大学	金属材料科学研究所	Research and Support of General-Use at T1-2 and T1-3	Masaki Fujita	Tohoku University
33	〃	南部　雄亮	東北大学	金属材料科学研究所	〃	Yusuke Nambu	Tohoku University
34	〃	池田　陽一	東北大学	金属材料科学研究所	〃	Yoichi Ikeda	Tohoku University
35	〃	鈴木　謙介	東北大学	金属材料科学研究所	〃	Kensuke Suzuki	Tohoku University
36	T2-2 における共同利用推進	木村　宏之	東北大学	多元物質科学研究所	Research and Support of General-Use at T2-2	Hiroyuki Kimura	Tohoku University
37	〃	坂倉　輝俊	東北大学	多元物質科学研究所	〃	Terutoshi Sakakura	Tohoku University
38	C1-2 における共同利用推進	杉山　正明	京都大学	原子炉実験所	Research and Support of General-Use at C1-2	Masaaki Sugiyama	Kyoto University
39	C1-2、C2-3-1、C3-1-2 における共同利用推進	井上　倫太郎	京都大学	原子炉実験所	Research and Support of General-Use at C1-2, C2-3-1 and C3-1-2	Rintaro Inoue	Kyoto University

No.	課題名	氏名	所属		Title	Name	Organization
40	C3-1-2、C2-3-1 における共同利用推進	日野　正裕	京都大学	原子炉実験所	Research and Support of General-Use at C3-1-2 and C2-3-1	Masahiro Hino	Kyoto University
41	C3-1-2 における共同利用推進	田崎　誠司	京都大学	大学院工学研究科	Research and Support of General-Use at C3-1-2	Seiji Tasaki	Kyoto University
42	C1-3-mfSANS における共同利用推進	古坂　道弘	北海道大学	大学院工学研究科	Research and Support of General-Use at C1-3-mfSANS	Michihiro Furusaka	Hokkaido University
43	〃	大沼　正人	北海道大学	大学院工学研究科	〃	Masato Ohnuma	Hokkaido University
44	〃	間宮　広明	物質・材料研究機構	量子ビームユニット	〃	Hiroaki Mamiya	National Institute for Materials Science
45	〃	藤原　健	産業技術総合研究所	計量標準総合センター	〃	Takeshi Fujiwara	National Institute of Advanced Industrial Science and Technology
46	C1-3、C3-1-2 における共同利用推進	北口　雅暁	名古屋大学	大学院理学研究科	Research and Support of General-Use at C1-3 and C3-1-2	Masaaki Kitaguchi	Nagoya University
47	C1-3 における共同利用推進	清水　裕彦	名古屋大学	大学院理学研究科	Research and Support of General-Use at C1-3	Hirohiko Shimizu	Nagoya University
48	〃	広田　克也	名古屋大学	大学院理学研究科	〃	Katsuya Hirota	Nagoya University
49	〃	土川　雄介	名古屋大学	理学研究科	〃	Yusuke Tsuchikawa	Nagoya University
50	〃	山形　豊	理化学研究所	光量子工学研究領域	〃	Yutaka Yamagata	RIKEN
担当所員：辛　埴							
51	スピン分解角度分解光電子分光による $TaSi_2$ のスピン構造の研究	伊藤　孝寛	名古屋大学	シンクロトロン光科学研究センター	Spin-resolved angle-resolved photoemission study of spin texture of $TaSi_2$	Takahiro Ito	Nagoya University
52	高温超伝導体の高分解能光電子分光	藤森　淳	東京大学	大学院理学系研究科	Ultra-high resolution photoemission spectroscopy on high Tc superconductor	Atsushi Fujimori	The University of Tokyo
53	60-eV レーザーを用いた時間分解光電子分光の開発	石坂　香子	東京大学	大学院工学系研究科	The development of time-resolved photoemission using 60 eV laser	Kyoko Ishizaka	The University of Tokyo
54	鉄系超伝導体のレーザー光電子分光	下志万　貴博	理化学研究所	創発物性科学研究センター	Laser-ARPES on Fe superconductor	Takahiro Shimojima	The University of Tokyo
55	高分解能光電子分光による強相関物質の研究	横谷　尚睦	岡山大学	大学院自然科学研究科	Ultra-high resolution study on strongly correlated materials	Takayoshi Yokoya	Okayama University

No.	課題名	氏名	所属		Title	Name	Organization
56	有機化合物の光電子分光	金井　要	東京理科大学	理工学部	Photoemission study on organic compounds	Kaname Kanai	Tokyo University of Science
57	重い電子系ウラン化合物の高分解能光電子分光	藤森　伸一	日本原子力研究開発機構	物質科学研究センター	Ultra high resolution photoemission study on heavy fermion uranium compounds	Shinichi Fujimori	Japan Atomic Energy Agency
58	レーザー光電子分光による酸化物薄膜の研究	津田　俊輔	物質・材料研究機構	機能性材料研究拠点	Laser-Photoemission Study on Oxide Films	Shunsuke Tsuda	National Institute for Materials Science
59	Mn 化合物の時間分解光電子分光	大川　万里生	東京理科大学	理学部	Time resolved Photoemission on Mn compounds	Mario Okawa	Tokyo University of Science
60	収差補正型光電子顕微鏡の建設と利用研究	小嗣　真人	東京理科大学	基礎工学部	Construction and utilization research of aberration correction photoelectron emission microscopy	Masato Kotsugi	Tokyo University of Science
61	時間分解・マイクロビームラインの開発と研究	室　隆桂之	高輝度光科学研究センター	利用研究促進部門	Development of micro- and time-resolved beamline	Takayuki Muro	Japan Synchrotron Radiation Institute
62	光電子分光法を用いた各種分子性結晶の電子状態の研究及び装置の低温化	木須　孝幸	大阪大学	大学院基礎工学研究科	Research on electronic states of molecular crystals using photoemission spectroscopy	Takayuki Kisu	Osaka University
63	トポロジカル絶縁体の電子状態の解明	木村　昭夫	広島大学	大学院理学研究科	Electronic-structure study of topological insulators	Akio Kimura	Hiroshima University
64	時間分解光電子分光を用いた強相関係物質の研究	溝川　貴司	早稲田大学	理工学術院	Time-resolved photoemmission study on strongly-correlated materials	Takashi Mizokawa	Waseda University
65	トポロジカル超伝導体の探索	坂野　昌人	東京大学	大学院工学系研究科	Search for topological superconductors	Masato Sakano	The University of Tokyo
担当所員：秋山　英文							
66	水溶液における新奇ケージドルシフェリンの安定構造の解明	薄倉　淳子	東京理科大学	理学部	Elucidation of stability for newfangled caged luciferin in aqueous solution	Junko Usukura	Tokyo University of Science
担当所員：松田　巌							
67	スピン分解光電子分光の測定技術開発	木村　昭夫	広島大学	大学院理学研究科	Technical development of spin-resolved photoemission spectroscopy measurement	Akio Kimura	Hiroshima University
68	共鳴磁気光学カー効果の散乱理論研究	田口　宗孝	奈良先端科学技術大学院大学	物質創成科学研究科	Study of scattering theory for the resonant magneto-optical Kerr effect	Taguchi Munetaka	Nara Institute of Science and Technology
69	時間分解磁気光学実験の技術開発	小嗣　真人	東京理科大学	基礎工学部	Technical development of time-resolved magneto-optical experiment	Masato Kotsugi	Tokyo University of Science
担当所員：原田　慈久							

No.	課題名	氏名	所属		Title	Name	Organization
70	液中プラズマ印加水の軟Ｘ線吸収 / 発光分光技術開発	寺嶋　和夫	東京大学	大学院新領域創成科学研究科	Technical development of soft X-ray absorption/emission spectroscopy for water processed by in-liquid plasma	Kazuo Terashima	The University of Tokyo
71	液中プラズマ印加によるナノ粒子分散特性評価と軟Ｘ線分光	伊藤　剛仁	東京大学	大学院新領域創成科学研究科	Characterization of nano-particle distribution in water processed by in-liquid plasma and soft X-ray spectroscopy	Tsuyohito Ito	The University of Tokyo
72	二次元原子薄膜トランジスタの電子状態のナノ分析 (ＩＴ)	吹留　博一	東北大学	電気通信研究所	Nanoscale analysis of electronic states of graphene device	Hirokazu Fukidome	Tohoku University
73	軟Ｘ線発光・共鳴非弾性散乱分光の磁気円・線二色性測定システムの構築	菅　滋正	大阪大学	産業科学研究所	Construction of a noble system for circular and linear dichroism in soft X-ray emission and RIXS spectroscopy	Shigemasa Suga	Osaka University
74	軟Ｘ線吸収／発光分光法によるリチウムイオン電池電極材料の電子物性研究	細野　英司	産業技術総合研究所	省エネルギー研究部門	Study on the electronic property of electrode materials for Li-ion batteries by soft X-ray absorption/emission spectroscopy	Eiji Hosono	National Institute of Advanced Industrial Science and Technology
75	〃	朝倉　大輔	産業技術総合研究所	省エネルギー研究部門	〃	Daisuke Asakura	National Institute of Advanced Industrial Science and Technology
76	高分解能光電子分光による酸化バナジウムの研究	藤原　秀紀	大阪大学	大学院基礎工学研究科	Study on vanadium oxides by high resolution photoemission	Hidenori Fujiwara	Osaka University
77	省エネ・創エネ・蓄電デバイスのオペランド分光	尾嶋　正治	東京大学	放射光分野融合国際卓越拠点	Operando nano-spectroscopy for energy efficient, power generation and energy storage devices	Masaharu Oshima	The University of Tokyo
担当所員：和達　大樹							
78	時間分解吸収分光による $EuNi_2(Si_{1-x}Ge_x)_2$ の価数転移ダイナミクスの解明	三村　功次郎	大阪府立大学	大学院工学研究科	Dynamics of valence transition in $EuNi_2(Si_{1-x}Ge_x)_2$ revealed by time-resolved XAS	Kojiro Mimura	Osaka Prefecture University
79	三次元 nanoESCA による実デバイスのオペランド電子状態解析	永村　直佳	物質・材料研究機構	先端材料解析研究拠点	Operando analysis of the electronic structure of actual devices by 3DnanoESCA	Naoka Ngamura	National Institute for Materials Science
80	共鳴軟Ｘ線散乱を用いた外場下での電子秩序状態の解明	山崎　裕一	東京大学	大学院工学系研究科	Observation of electric ordered state under external field by resonant soft x-ray scattering	Yuichi Yamasaki	The University of Tokyo

一般研究員 / General Researcher

No.	課題名	氏名	所属		Title	Name	Organization
担当所員：榊原　俊郎							
1	強相関電子系化合物の秩序相に対する結晶対称性および電子軌道の効果	横山　淳	茨城大学	理学部	Effects of crystal symmetry and electronic state in ordered phase of strongly correlated electron systems	Makoto Yokoyama	Ibaraki University
2	〃	鈴木　康平	茨城大学	理学部	〃	Kohei Suzuki	Ibaraki University

No.	課題名	氏名	所属		Title	Name	Organization
3	超伝導対のギャップ対称性を決定する実験的、理論的研究	町田　一成	立命館大学	理工学部	Experimental and theoretical studies on gap symmetry determination in superconductors	Kazunari Machida	Ritsumeikan University
4	(Th, U)Ru_2Si_2 混晶系の電子状態	芳賀　芳範	日本原子力研究開発機構	先端基礎研究センター	Electronic states in (Th, U)Ru_2Si_2 alloy system	Yoshinori Haga	Japan Atomic Energy Agency
5	〃	松本　裕司	名古屋工業大学大学院	工学研究科機能工学専攻	〃	Yuji Matsumoto	Nagoya Institute of Technology
6	単結晶 $YbNi_2Si_2$ の極低温磁場中比熱測定	松本　裕司	名古屋工業大学大学院	工学研究科機能工学専攻	Specic heat measurements under magnetic fields for single crystal $YbNi_2Si_2$ at low temperature	Yuji Matsumoto	Nagoya Institute of Technology
7	新規電荷移動錯体の低温物性測定	山口　博則	大阪府立大学	大学院理学系研究科	Low temperature physical properties of new charge-transfer complexs	Hironori Yamaguchi	Osaka Prefecture University
8	〃	岡部　俊輝	大阪府立大学	大学院理学系研究科	〃	Toshiki Okabe	Osaka Prefecture University
9	$U_{1-x}Th_xBe_{13}$ を含むウラン系超伝導体における極低温比熱・磁化測定	清水　悠晴	東北大学	金属材料研究所	Low-temperature heat-capacity and magnetization measurements for $U_{1-x}Th_xBe_{13}$ and other uranium superconducting systems	Yusei Shimizu	Tohoku University
10	磁気フラストレートした一次元量子スピン系 $Rb_{2-x}Cs_xCu_2Mo_3O_{12}$(x=0.2, 0.3) の磁気的基底状態	安井　幸夫	明治大学	理工学部	Magnetic Behavior of Magnetically Frustrated One-dimensional Quantum Spin System $Rb_{2-x}Cs_xCu_2Mo_3O_{12}$(x=0.2, 0.3)	Yukio Yasui	Meiji University
担当所員：長田　俊人							
11	ビスマスおよびビスマス・アンチモン混晶の磁場中輸送特性	矢口　宏	東京理科大学	理工学部	Transport Properties of Bi and $Bi_{1-x}Sb_x$ Alloys in Magnetic Fields	Hiroshi Yaguchi	Tokyo University of Science
12	〃	仁野平　諒	東京理科大学	大学院理工学研究科	〃	Ryo Ninohira	Tokyo University of Science
13	トポロジカル絶縁体の磁場中輸送特性の測定	矢口　宏	東京理科大学	理工学部	Measurements of Transport Properties of Topological Insulators in Magnetic Fields	Hiroshi Yaguchi	Tokyo University of Science
14	〃	北澤　翔一	東京理科大学	大学院理工学研究科	〃	Shouichi Kitazawa	Tokyo University of Science
担当所員：山下　穣							
15	超低温における dHvA 効果測定	宍戸　寛明	大阪府立大学	大学院工学研究科	dHvA effect measurements at ultra-low temperatures	Hiroaki Shishido	Osaka Prefecture University
16	超流動 ^{3}He 中のスピン流と電場の交差相関の探索	白濱　圭也	慶應義塾大学	理工学部	Study of cross-correlation between spin flow and electric field in superfluid ^{3}He	Keiya Shirahama	Keio University
17	〃	村川　智	東京大学	低温センター	〃	Satoshi Murakawa	The University of Tokyo

No.	課題名	氏名	所属		Title	Name	Organization
18	〃	山口　明	兵庫県立大学	大学院物質理学研究科	〃	Akira Yamaguchi	University of Hyogo
19	〃	永合　祐輔	慶應義塾大学	理工学部	〃	Yusuke Nago	Keio University
20	〃	海谷　航平	慶應義塾大学	理工学部	〃	Kohei Kaiya	Keio University
担当所員：勝本　信吾							
21	ナノセンシングデバイスに関する研究	割澤　伸一	東京大学	大学院新領域創成科学研究科	Research on nano sensing devices	Shinichi Warisawa	The University of Tokyo
22	〃	上木　瞭太郎	東京大学	大学院新領域創成科学研究科	〃	Ryotaro Ueki	The University of Tokyo
23	〃	根本　啓行	東京大学	大学院新領域創成科学研究科	〃	Hiroyuki Nemoto	The University of Tokyo
担当所員：小森　文夫							
24	Si(111)√3 ×√3-B 基板上に成長した Bi(110) 超薄膜の電子状態	中辻　寛	東京工業大学	物質理工学院	Electronic structure of Bi(110) thin films grown on Si(111)√3 ×√3-B substrates	Kan Nakatsuji	Tokyo Institute of Technology
25	トポロジカル近藤絶縁体候補物質 SmB_6(111) の表面原子構造と局所電子状態	大坪　嘉之	大阪大学	大学院生命機能研究科	Surface atomic strucutre and local electronic states of SmB_6(111), a candidate of topological Kondo insulator	Yoshiyuki Ohtsubo	Osaka University
26	金属／半導体表面上の超薄膜およびナノ構造薄膜の磁化ダイナミックスの磁気光学的測定	河村　紀一	日本放送協会	放送技術研究所	Study on magnetic dynamics of ultra-thin films and nano-structures on metal / semiconductor surfaces	Norikazu Kawamura	Nippon Hoso Kyokai
27	レアメタルフリー磁性材料 L10-FeCo の磁気特性の解析	小嗣　真人	東京理科大学	基礎工学部	Analysis of magnetic properties of rare-metal-free super magnet "L10-FeCo"	Masato Kotsugi	Tokyo University of Science
28	Ge 表面における光誘起半導体ー金属構造相転移の電子論的解明	金崎　順一	大阪大学	産業科学研究所	Electronic investigation of photo-induced semiconductor-metal transformation on Ge(001) surface	Jun'ichi Kanasaki	Osaka University
29	Al-Pd-Ru 準結晶・近似結晶における空孔濃度の研究	金沢　育三	東京学芸大学	自然科学系	Positron-annihilation studies of Al-Pd-Mn quasicrystal and its approximant crystals	Ikuzo Kanazawa	Tokyo Gakugei University
30	〃	中島　諒	東京学芸大学	大学院教育学研究科	〃	Makoto Nakajima	Tokyo Gakugei University
31	〃	木村　薫	東京大学	大学院新領域創成科学研究科	〃	Kaoru Kimura	The University of Tokyo
32	〃	大島　永康	産業技術総合研究所	分析計測標準研究部門	〃	Nagayasu Oshima	National Institute of Advanced Industrial Science and Technology

No.	課題名	氏名	所属		Title	Name	Organization
33	SiC 表面上の２次元 Sn 層の構造および電子状態の解明	田中　悟	九州大学	大学院工学研究院	Analyses of 2D-Sn and Pb layers on SiC surfaces	Satoru Tanaka	Kyushu University
34	〃	林　真吾	九州大学	大学院工学府	〃	Kengo Hayashi	Kyushu University
35	グラフェンナノリボンの電子状態の観察	田中　悟	九州大学	大学院工学研究院	Analysis of electronic structures in graphene nanoribbons	Satoru Tanaka	Kyushu University
36	〃	安藤　寛	九州大学	大学院工学府	〃	Hiroshi Ando	Kyushu University
37	グラフェンナノリボンの STM/STS による解析	ビシコフスキー　アントン	九州大学	大学院工学研究院	Analyses of graphene nanoribbons by STS/STS	Visikovskiy Anton	Kyushu University
38	〃	福間　洸平	九州大学	大学院工学府	〃	Kouhei Fukuma	Kyushu University
担当所員：吉信　淳							
39	p 型窒化ガリウム薄膜の作製と評価	山田　太郎	東京大学	大学院工学系研究科	Fabrication and physical investigation of p-type gallium nitride thin films	Taro Yamada	The University of Tokyo
40	Si(001) 表面上の準安定共吸着過程の透過 FTIR 測定	大野　真也	横浜国立大学	大学院工学研究院	FTIR measurements of metastable physisorption processes on Si(001)	Shinya Ohno	Yokohama National University
41	〃	高柳　周平	横浜国立大学	理工学部	〃	Shuhei Takayanagi	
42	銅上の単層グラフェンの高分解能電子エネルギー損失分光	田中　慎一郎	大阪大学	産業科学研究所	High resolution electron energy loss spectroscopy for graphene on Cu	Shinichiro Tanaka	Osaka University
43	直鎖アルカン分子の物理吸着によって生じる Au(111) ショックレー状態の変化と吸着構造	金井　要	東京理科大学	理工学部	Modification of Au(111) Shockley state upon physisorption of n-alkanes and the adsorbed structures	Kaname Kanai	Tokyo University of Science
44	〃	水島　啓貴	東京理科大学	大学院理工学研究科	〃	Hirotaka Mizushima	Tokyo University of Science
45	赤外吸収による水素終端 Si(110)-(1 × 1) 微傾斜表面の H-Si 伸縮振動モードの解明	須藤　彰三	東北大学	大学院理学研究科	H-Si stretching modes on the hydrogen-terminated Si(110)-(1 × 1) vicinal surface studied by infrared absorption spectroscopy	Shozo Suto	Tohoku University
46	〃	江口　豊明	東北大学	大学院理学研究科	〃	Toyoaki Eguchi	Tohoku University
47	〃	河野　純子	東北大学	大学院理学研究科	〃	Junko Kono	Tohoku University
担当所員：長谷川　幸雄							

No.	課題名	氏名	所属		Title	Name	Organization
48	エピタキシャルシリセン、ゲルマネン及びそのヘテロ構造の低温走査トンネル顕微鏡観察	高村　由起子	北陸先端科学技術大学院大学	マテリアルサイエンス系	STM investigation of epitaxial silicene, germanene, and their heterostructures	Yukiko Takamura	Japan Advanced Institute of Science and Technology
49	〃	アントワーヌ　フロランス	北陸先端科学技術大学院大学	マテリアルサイエンス系	〃	Antoine Fleurence	Japan Advanced Institute of Science and Technology
50	Si(001) 表面上の Na 原子吸着の極低温 STM 観察	鈴木　孝将	福岡大学	工学部	ELT-STM study of Na atom adsorption on Si(001) surface	Takayuki Suzuki	Fukuoka University
51	重い電子系超伝導の実空間観察のための超低温・強磁場の小型 STM の開発	河江　達也	九州大学	大学院工学研究院	Development of a miniature STM for low-temperature and high-magnetic-field measurements of heavy fermion superconductors	Tatsuya Kawae	Kyushu University
52	〃	志賀　雅亘	九州大学	大学院工学府	〃	Masanobu Shiga	Kyushu University
53	走査トンネル顕微鏡を用いたトポロジカル物質のナノスケール観察	土師　将裕	京都大学	大学院理学研究科	Topological materials science studied by scanning tunneling microscopy	Masahiro Haze	Kyoto University
担当所員：リップマー　ミック							
54	$LaAlO_3/SrTiO_3$ ヘテロ界面金属層における Co ドープの影響	李　美希	奈良先端科学技術大学院大学	物質創成科学研究科	Effects of the doped Co in the $LaAlO_3/SrTiO_3$ metallic interface	Mihee Lee	Nara Insttitute of Science and Technology
55	傾斜組成エピタキシャル強誘電体薄膜の構造と物性	丸山　伸伍	東北大学	大学院工学研究科	Structural and physical property characterization of graded-composition epitaxial ferroelectric thin films	Shingo Maruyama	Tohoku University
56	〃	松本　祐司	東北大学	大学院工学研究科	〃	Yuji Matsumoto	Tohoku University
57	〃	原田　龍馬	東北大学	大学院工学研究科	〃	Ryoma Harada	Tohoku University
担当所員：廣井　善二							
58	トンネル構造を有したジントル化合物の低温物性評価	山田　高広	東北大学	多元物質科学研究所	Characterization of electric and magnetic properties of Zintl compounds with tunnel structures	Takahiro Yamada	Tohoku University
担当所員：川島　直輝							
59	テンソルネットワーク法の新奇な応用	原田　健自	京都大学	大学院情報学研究科	New application of tensor network schemes	Kenji Harada	Kyoto University
60	蜂の巣格子 Heisenberg-Kitaev 磁性体 $RuCl_3$ の磁気励起	鈴木　隆史	兵庫県立大学	大学院工学研究科	Magnetic excitations of honeycomb-lattice Heisenberg-Kitaev magnets $RuCl_3$	Takafumi Suzuki	University of Hyogo
担当所員：上床　美也							

No.	課題名	氏名	所属		Title	Name	Organization
61	有機分子性導体の高圧物性の研究	鳥塚　潔	武蔵野大学	教育学部	Studies on High Pressure Properties of Organic Molecular Conductors	Kiyoshi Torizuka	Musashino University
62	多形化合物 RIr_2Si_2(R= 希土類）の結晶育成と物質評価 2	繁岡　透	山口大学	大学院創成科学研究科	Crystal growth and characterization of polymorphic compounds RIr_2Si_2(R=rare earth) 2	Toru Shigeoka	Yamaguchi University
63	〃	内間　清晴	沖縄キリスト教短期大学	総合教育系	〃	Kiyoharu Uchima	Okinawa Christian Junior College
64	多形化合物 $GdIr_2Si_2$ の磁気特性	繁岡　透	山口大学	大学院創成科学研究科	Magnetic characteristics of the polymorphic compound $DyIr_2Si_2$	Toru Shigeoka	Yamaguchi University
65	〃	内間　清晴	沖縄キリスト教短期大学	総合教育系	〃	Kiyoharu Uchima	Okinawa Christian Junior College
66	(Ho, La)Rh_2Si_2 の磁気特性 2	内間　清晴	沖縄キリスト教短期大学	総合教育系	Magnetic characteristics of (Ho, La)Rh_2Si_2 2	Kiyoharu Uchima	Okinawa Christian Junior College
67	〃	繁岡　透	山口大学	大学院創成科学研究科	〃	Toru Shigeoka	Yamaguchi University
68	三角格子反強磁性体の低温磁性	柄木　良友	琉球大学	教育学部	Low temperature magnetism of triangular antiferromagnets	Yoshitomo Karaki	University of the Ryukyu
69	高圧下における Eu 化合物の価数転移の探索	本多　史憲	東北大学	金属材料研究所	Investigation of valence transition on Eu compounds under high pressure	Fuminori Honda	Tohoku University
70	〃	仲村　愛	東北大学	金属材料研究所	〃	Ai Nakamura	Tohoku University
71	〃	大貫　惇睦	琉球大学	理学部	〃	Yoshichika Onuki	University of the Ryukyu
72	希土類ラーベス化合物 RAl_2 の異方的磁気体積効果	大橋　政司	金沢大学	理工研究域	Anisotropic magnetovolume effect of rare earth Laves compound RAl_2	Masashi Ohashi	Kanazawa University
73	〃	宮川　昌大	金沢大学	大学院自然科学研究科	〃	Masahiro Miyagawa	Kanazawa University
74	強相関電子系化合物における圧力および磁場誘起量子相転移の探索	大橋　政司	金沢大学	理工研究域	Pressure and field induced quantum phase transition in strongly correlated electron systems	Masashi Ohashi	Kanazawa University
75	〃	大橋　康平	金沢大学	大学院自然科学研究科	〃	Kouhei Oohashi	Kanazawa University
76	$HoRh_2Si_2$ 単結晶の輸送特性	藤原　哲也	山口大学	大学院創成科学研究科	Transport property of $HoRh_2Si_2$	Tetsuya Fujiwara	Yamaguchi University
77	〃	平山　拓斗	山口大学	大学院創成科学研究科	〃	Takuto Hirayama	Yamaguchi University

No.	課題名	氏名	所属		Title	Name	Organization
78	$PrZn_2Ge_2$ 三元系新規化合物の磁化特性 (2)	藤原　哲也	山口大学	大学院創成科学研究科	Magnetic property of $PrZn_2Ge_2$ novel ternary intermetallics II	Tetsuya Fujiwara	Yamaguchi University
79	〃	平山　拓斗	山口大学	大学院創成科学研究科	〃	Takuto Hirayama	Yamaguchi University
80	$EuCuP_2$ の磁場中比熱測定	藤原　哲也	山口大学	大学院創成科学研究科	Specific measurement under magnetic field of $EuCuP_2$	Tetsuya Fujiwara	Yamaguchi University
81	〃	平山　拓斗	山口大学	大学院創成科学研究科	〃	Takuto Hirayama	Yamaguchi University
82	ホイスラー化合物強磁性体 Fe_2NiAl の高圧化磁化測定	伊藤　昌和	鹿児島大学	学術研究院理工学域理学系	Magnetization of Heusler compound Fe_2NiAl under pressure	Masakazu Ito	Kagoshima University
83	〃	恩田　圭二朗	鹿児島大学	理学部	〃	Keijiro Onda	Kagoshima University
84	導電性ラングミュア・ブロジェット膜の高圧下の電気的性質に関する研究	三浦　康弘	桐蔭横浜大学	大学院工学研究科	Studies on Electrical Properties of Conductive Langmuir-Blodgett Films under High Pressure	Yasuhiro Miura	Toin University of Yokohama
85	鉄カルコゲナイド化合物の圧力下電気抵抗測定	久田　旭彦	徳島大学	大学院理工学研究部	High-pressure electrical resistivity measurements of iron-chalcogenide compound	Akihiko Hisada	Tokushima University
86	鉄系超伝導体 $FeSe_{1-x}S_x$ の高圧下電子相図の研究	芝内　孝禎	東京大学	大学院新領域創成科学研究科	Studies on the electronic phase diagram under high pressure of iron-based superconductor $FeSe_{1-x}S_x$	Takasada Shibauchi	The University of Tokyo
87	〃	松浦　康平	東京大学	大学院新領域創成科学研究科	〃	Kouhei Matsuura	The University of Tokyo
88	〃	新井　佑基	東京大学	大学院新領域創成科学研究科	〃	Yuki Arai	The University of Tokyo
89	リン系充填スクッテルダイト超伝導体の磁気特性	川村　幸裕	室蘭工業大学	大学院工学研究科	Magnetic properties of filled skutterudite superconductor in phosphorus system	Yukihiro Kawamura	Muroran Institute of Technology
90	$CeIr(In_{1-x}Cd_x)_5$ の圧力下電気抵抗測定	摂待　力生	新潟大学	理学部	Electrical resistivity measurement of $CeIr(In_{1-x}Cd_x)_5$ under pressure	Rikio Settai	Niigata University
91	〃	角田　竜馬	新潟大学	大学院自然科学研究科	〃	Ryoma Tsunoda	Niigata University
92	$YbCo_2Zn_{20}$ の Co 元素位置の置換効果 V	阿曽　尚文	琉球大学	理学部	Substitution effect at Co elements in $YbCo_2Zn_{20}$ V	Naofumi Aso	University of the Ryukyu
93	〃	佐藤　信	琉球大学	理学部	〃	Shin Sato	University of the Ryukyu
94	$YbCo_2Zn_{20}$ の Yb 元素の置換効果	小林　理気	琉球大学	理学部	Substitution effect at Yb element in $YbCo_2Zn_{20}$	Riki Kobayashi	University of the Ryukyu

No.	課題名	氏名	所属		Title	Name	Organization
95	〃	瑞慶覧　長星	琉球大学	理学部	〃	Chousei Zukeran	University of the Ryukyu
96	新奇スピン液体候補 $Ba_3ZnRu_2O_9$ の圧力誘起相転移の探索	寺崎　一郎	名古屋大学	理学研究科	Search for pressure-induced transition in a novel spin liquid candidate $Ba_3ZnRu_2O_9$	Ichiro Terasaki	Nagoya University
97	有機伝導体の物性に対する圧力媒体の影響	村田　恵三	大阪経済法科大学	２１世紀社会総合研究センター	Effect of pressure medium on the properties of organic conductor	Keizo Murata	Osaka University of Economics and Law
98	単結晶 $R_2T_3Ge_5$(R: 希土類，T: 遷移金属元素) の高圧現象	中島　美帆	信州大学	理学部	Pressure effect in $R_2T_3Ge_5$ (R: rare earth metal, T: transition metal element) single crystals	Miho Nakashima	Shinshu University
99	〃	中村　優希	信州大学	大学院総合理工学研究科	〃	Yuki Nakamura	Shinshu University
100	Co 基ホイスラー合金における圧力誘起マルテンサイト変態に関する研究	重田　出	鹿児島大学	大学院理工学研究科	Study on pressure-induced martensitic phase transformation in Co-based Heusler alloys	Iduru Shigeta	Kagoshima University
101	〃	大岡　隆太郎	鹿児島大学	大学院理工学研究科	〃	Ryutaro Ooka	Kagoshima University
102	(Mn,Cr)AlGe の磁気特性	三井　好古	鹿児島大学	大学院理工学研究科	Magnetic properties of (Mn,Cr)AlGe	Yoshifuru Mitsui	Kagoshima University
103	〃	増満　勇人	鹿児島大学	理学部	〃	Hayato Masumitsu	Kagoshima University
104	Mn 基および Fe 基４元磁性体の磁気特性	小山　佳一	鹿児島大学	大学院理工学研究科	Magnetic properties of Mn and Fe-based quaternary magnets	Keiichi Koyama	Kagoshima University
105	〃	アッドライン　ンゴジ　ムウッド	鹿児島大学	大学院理工学研究科	〃	Adline Ngozi Nwodo	Kagoshima University
106	圧力誘起価数転移の探索と高圧下輸送特性	辺土　正人	琉球大学	理学部	Searching of pressure-induced valence transition and transport properties under high pressure	Masato Hedo	University of the Ryukyu
107	〃	伊覇　航	琉球大学	理学部	〃	Wataru Iha	University of the Ryukyu
108	Co 系ホイスラー合金の電気抵抗測定によるマルテンサイト変態温度の高圧効果	安達　義也	山形大学	大学院理工学研究科	Pressure effect of the martensitic transition temperature by the measurements of the electrical resistivity for the Co-Heusler alloys.	Yoshiya Adachi	Yamagata University
109	〃	小木　雄貴	山形大学	工学部	〃	Yuki Ogi	Yamagata University
110	回転希釈冷凍機を用いた量子液体・固体研究	白濱　圭也	慶應義塾大学	理工学部	Study of quantum fluids and solids using rotating dilution refrigerator	Keiya Shirahama	Keio University
111	〃	村川　智	東京大学	低温センター	〃	Satoshi Murakawa	The University of Tokyo

No.	課題名	氏名	所属		Title	Name	Organization
112	〃	高橋　大輔	足利工業大学	工学部	〃	Daisuke Takahashi	Ashikaga Institute of Technology
113	反転対称性のない遷移金属間化合物とその関連物質の高圧下輸送特性	仲間　隆男	琉球大学	理学部	Transport properties of non-centrosymmetric transition metals compounds under high pressure	Nakama Takao	University of the Ryukyu
114	〃	垣花　将司	琉球大学	大学院理工学研究科	〃	Masashi Kakihana	University of the Ryukyu
115	新奇 Ce 三元系化合物の圧力下測定	本山　岳	島根大学大学院	総合理工学研究科	Physical property measurements of new Ce heavy fermion compound under pressure	Gaku Motoyama	Shimane University
116	近藤格子化合物 Ce_3RuSn_6 の圧力下磁化測定	脇舎　和平	横浜国立大学	大学院工学研究院	Magnetization measurements of Ce_3RuSn_6 under applied pressure	Kazuhei Wakiya	Yokohama National University
117	〃	木村　美波	横浜国立大学	大学院工学府	〃	Minami Kimura	Yokohama National University
118	新奇スピン液体候補 $Ba_3ZnRu_2O_9$ の圧力誘起相転移の探索	山本　貴史	名古屋大学	大学院理学研究科	Search for pressure-induced transition in a novel spin liquid candidate $Ba_3ZnRu_2O_9$	Takafumi Yamamoto	Nagoya University
担当所員：吉澤　英樹							
119	$YbCo_2Zn_{20}$ の Co 位置置換系試料の極低温比熱測定	阿曽　尚文	琉球大学	理学部	Specific heat measurements at very low temperature on $YbCo_2Zn_{20}$ systems doped at Co elements	Naofumi Aso	University of the Ryukyu
120	〃	盛島　実竜	琉球大学	理学部	〃	Miiru Morishima	University of the Ryukyu
121	$(Yb_{1-x}Lu_x)Co_2Zn_{20}$ 置換系試料の極低温比熱測定	小林　理気	琉球大学	理学部	Specific heat measurement at very low temperature on $(Yb_{1-x}Lu_x)Co_2Zn_{20}$ systems	Riki Kobayashi	University of the Ryukyu
122	〃	諸見里　真嗣	琉球大学	理学部	〃	Masatsugu Moromizato	University of the Ryukyu
123	ヨウ素輸送法により育成した鉄カルコゲン化合物の物性	山崎　照夫	東京理科大学	理工学部	Physical properties of Fe-chalcogenide compounds grown by iodine transport method	Teruo Yamazaki	Tokyo University of Science
124	〃	矢口　宏	東京理科大学	理工学部	〃	Hiroshi Yaguchi	Tokyo University of Science
125	〃	山本　和典	東京理科大学	大学院理工学研究科	〃	Yamamoto Kazunori	Tokyo University of Science
担当所員：益田　隆嗣							
126	$Ce(Ru_{1-x}Rh_x)_2Al_{10}$(x=0.23) 単結晶試料の高エネルギー X 線ラウエ装置による結晶方位同定	小林　理気	琉球大学	理学部	Alignment of $Ce(Ru_{1-x}Rh_x)_2Al_{10}$(x=0.23) single crystals by high-energy X-ray Laue diffaction	Riki Kobayashi	University of the Ryukyu

No.	課題名	氏名	所属		Title	Name	Organization
127	$Co_4Ta_2O_9$ の中性子磁気散乱実験に向けた軸立て	阿部　伸行	東京大学	大学院新領域創成科学研究科	Preparation of single crystalline $Co_4Ta_2O_9$ for the measurement of elastic neutron scattering	Nobuyuki Abe	The University of Tokyo
128	非弾性中性子散乱を用いたスピンダイナミクスの研究	羽合　孝文	高エネルギー加速器研究機構	物質構造科学研究所	Neutron inelastic scattering study of spin dynamics	Takafumi Hawai	High Energy Accelerator Research Organization
担当所員：嶽山　正二郎							
129	磁気光学測定を用いたハロゲン化金属ペロブスカイト型結晶の励起子特性の研究	中村　唯我	東京大学	大学院工学系研究科	Study on excitonic properties of organometallic lead halide perovskite using magneto-optic mesure- ment	Yuiga Nakamura	The University of Tokyo
130	S=1/2 ダイヤモンド型量子スピン鎖物質 $K_3Cu_3AlO_2(SO_4)_4$ の 1/3 磁化プラトーの実験的観測	藤原　理賀	東京理科大学	理学部	Experimental observation of the 1/3 magnetization plateau in the S=1/2 diamond chain compound $K_3Cu_3AlO_2(SO_4)_4$	Masayoshi Fujihara	Tokyo University of Science
131	キラル反強磁性体における磁気キラル二色性	有馬　孝尚	東京大学	大学院新領域創成科学研究科	Magneto-chiral dichroism in a chiral antiferromagnet	Taka-hisa Arima	The University of Tokyo
132	〃	徳永　祐介	東京大学	大学院新領域創成科学研究科	〃	Yusuke Tokunaga	The University of Tokyo
133	〃	阿部　伸行	東京大学	大学院新領域創成科学研究科	〃	Nobuyuki Abe	The University of Tokyo
134	〃	荒木　勇介	東京大学	大学院新領域創成科学研究科	〃	Yusuke Araki	The University of Tokyo
135	〃	中川　直己	東京大学	大学院新領域創成科学研究科	〃	Naoki Nakagawa	The University of Tokyo
136	〃	近江　毅志	東京大学	大学院新領域創成科学研究科	〃	Tsuyoshi Omi	The University of Tokyo
担当所員：金道　浩一							
137	スピンクラスター物質の高温での強磁場磁化測定	長谷　正司	物質・材料研究機構	中性子散乱グループ	High-field magnetization measurements on spin-cluster compounds at high temperatures	Masashi Hase	National Institute for Materials Science
138	幾何学的フラストレート磁性体の強磁場磁化測定	菊池　彦光	福井大学	学術研究院工学系部門	Magnetization measurements of the frustrated magnets	Hikomitsu Kikuchi	University of Fukui
139	〃	三浦　俊亮	福井大学	大学院工学研究科	〃	Shunsuke Miura	University of Fukui
140	希土類金属間化合物の強磁場物性研究	海老原　孝雄	静岡大学	理学部	Physical properties in rare earth intermetallic compounds at high magnetic fields	Takao Ebihara	Shizuoka University
141	〃	村串　拓真	静岡大学	理学部	〃	Murakushi Takuma	Shizuoka University

No.	課題名	氏名	所属		Title	Name	Organization
142	重い電子系化合物が示す非従来型超伝導と磁性の相関	横山　淳	茨城大学	理学部	Interplay between unconventional superconductivity and magnetism in heavy-fermion compounds	Makoto Yokoyama	Ibaraki University
143	〃	大島　佳樹	茨城大学	理学部	〃	Yoshiki Oshima	Ibaraki University
144	ホイスラー化合物強磁性体 Fe_2NiAl の高磁場物性	伊藤　昌和	鹿児島大学	大学院理工学研究科	High field magnetic properties of Heusler compound Fe_2NiAl	Masakazu Ito	Kagoshima University
145	〃	恩田　圭二朗	鹿児島大学	理学部	〃	Keijiro Onda	Kagoshima University
146	ホイスラー化合物の強磁場磁化	廣井　政彦	鹿児島大学	大学院理工学研究科	Magnetizaiton of some Heusler compounds in high magnetic fields	Masahiko Hiroi	Kagoshima University
147	金属ナノ結晶の磁化特性	稲田　貢	関西大学	システム理工学部	Magnetic properties of metal nanocrystals	Mitsuru Inada	Kansai University
148	〃	越田　樹	関西大学	システム理工学部	〃	Koshida Tatsuki	Kansai University
149	金属ナノクラスターネットワークの磁気抵抗測定	稲田　貢	関西大学	システム理工学部	Electronic transport properties of metal cluster networks under high-magnetic field	Mitsuru Inada	Kansai University
150	〃	小笠原　尚貴	関西大学	システム理工学部	〃	Ogasahara Naoki	Kansai University
151	有機／無機スピン源を持つ低次元スピン系の磁場中量子相転移	小野　俊雄	大阪府立大学	大学院理学系研究科	Field induced quantum phase transitions on the low-dimensional spin systems which have organic/inorganic spin sources	Toshio Ono	Osaka Prefecture University
152	〃	梶本　侑馬	大阪府立大学	大学院理学系研究科	〃	Yuma Kajimoto	Osaka Prefecture University
153	新規イッテルビウム化合物および強磁性臨界点近傍の物質の強磁場磁化測定	道岡　千城	京都大学	大学院理学研究科	High-field Magnetization of novel Yb based compounds and weak ferromagnetic compounds	Chishiro Michioka	Kyoto University
154	〃	山田　真二	京都大学	大学院理学研究科	〃	Shinji Yamada	Kyoto University
155	過剰オーバードープ Bi-2212 のパルス強磁場中面間輸送特性を用いた擬ギャップ状態の研究	渡辺　孝夫	弘前大学	大学院理工学研究科	A study of the pseudo gap state using interlayer magnetotransport measurements under pulsed magnetic fields for heavily overdoped Bi-2212	Takao Watanabe	Hirosaki University
156	〃	佐々木　菜絵	弘前大学	大学院理工学研究科	〃	Nae Sasaki	Hirosaki University
157	近藤半導体 $(Yb, R)B_{12}$ (R=Zr, Sc, Y) の 80T 級磁場下での強磁場物性	伊賀　文俊	茨城大学	理学部	High field physical property of Kondo insulator $(Yb, R)B_{12}$ (R=Zr, Sc, Y) up to 80T class by using the pulse magnet	Fumitoshi Iga	Ibaraki University
158	〃	横道　啓省	茨城大学	大学院理工学研究科	〃	Keisei Yokomichi	Ibaraki University

No.	課題名	氏名	所属		Title	Name	Organization
159	topological insulator SmB_6,YbB_{12} の磁化特性と比熱	伊賀　文俊	茨城大学	理学部	Magnetic and thermal properties of topological insulator SmB_6 and YbB_{12}	Fumitoshi Iga	Ibaraki University
160	〃	平野　航	茨城大学	大学院理工学研究科	〃	Wataru Hirano	Ibaraki University
161	高圧合成希土類 6 及び 12 ホウ化物の磁化特性と比熱	伊賀　文俊	茨城大学	理学部	Magnetic and thermal properties of rare earth hexa-borides and dodeca-borides produced by high pressure synthesis	Fumitoshi Iga	Ibaraki University
担当所員：徳永　将史							
162	サブメガガウス領域での希土類物性研究	海老原　孝雄	静岡大学	理学部	Physical Property of rare earth compounds at pulse magnet	Ebihara Takao	Shizuoka University
163	〃	ジュマエダ ジャトミカ	静岡大学	大学院創造科学技術研究科	〃	Jumaeda Jatmika	Shizuoka University
164	$Nd_2Co_{12}P_7$ を中心とする遍歴磁性体の磁場中相転移の観測	太田　寛人	東京農工大学	大学院工学研究院	Observation of field-induced phase transition of itinerant magnets including $Nd_2Co_{12}P_7$	Hiroto Ohta	Tokyo University of Agriculture and Technology
165	〃	加藤　優典	東京農工大学	大学院工学府	〃	Yusuke Kato	Tokyo University of Agriculture and Technology
166	$(Al_xM_{2-x})GeO_5$ (M=Cr, V, Fe) の強磁場磁化測定	香取　浩子	東京農工大学	大学院工学研究院	High-field magnetization measurements of $(Al_xM2\text{-}x)GeO_5$ (M=Cr, V, Fe)	Hiroko Katori	Tokyo University of Agriculture and Technology
167	〃	高田　早紀	東京農工大学	大学院工学府	〃	Saki Takada	Tokyo University of Agriculture and Technology
168	CeT_mIn_{2m+3}（T：遷移金属）の強磁場磁化測定	広瀬　雄介	新潟大学	理学部	High-field magnetization of CeT_mIn_{2m+3} (T : Transition metal)	Yusuke Hirose	Niigata University
169	〃	角田　竜馬	新潟大学	大学院自然科学研究科	〃	Ryoma Tsunoda	Niigata University
170	極性キラルらせん磁性体における電気磁気効果	徳永　祐介	東京大学	大学院新領域創成科学研究科	Magnetoelectric properties of the polar-chiral helimagnet	Yusuke Tokunaga	The University of Tokyo
171	〃	阿部　伸行	東京大学	大学院新領域創成科学研究科	〃	Nobuyuki Abe	The University of Tokyo
172	〃	荒木　勇介	東京大学	大学院新領域創成科学研究科	〃	Yusuke Araki	The University of Tokyo
173	〃	前島　夏奈	東京大学	大学院新領域創成科学研究科	〃	Kana Maeshima	The University of Tokyo
174	〃	小池　仁希	東京大学	大学院新領域創成科学研究科	〃	Yoshiki Koike	The University of Tokyo

No.	課題名	氏名	所属		Title	Name	Organization
175	キャリアドープした多層ディラック電子系磁性体における強磁場輸送現象の解明	酒井　英明	大阪大学	大学院理学研究科	Revealing high-field magnetotransport properties for carrier-doped Dirac antiferromagnets	Hideaki Sakai	Osaka University
176	〃	鶴田　圭吾	大阪大学	大学院理学研究科	〃	Keigo Tsuruda	Osaka University
177	パルスマグネットを用いた半金属における磁場誘起電子相転移の研究	矢口　宏	東京理科大学	理工学部	Study of Field-Induced Electronic Phase Transitions in Semimetals Using Pulsed Magnets	Hiroshi Yaguchi	Tokyo University of Science
178	非破壊パルス磁場を用いた半金属における磁場誘起電子相転移の研究	仁野平　諒	東京理科大学	大学院理工学研究科	Study of Magnetic-Field-Induced Electronic Phase Transitions in Semimetals Using Non-Destructive Pulsed Magnetic Fields	Ryo Ninohira	Tokyo University of Science
179	フラストレートした磁気構造を持つ Ce_2MgSi_2 の強磁場磁化測定	本多　史憲	東北大学	金属材料研究所	High field magnetization experiment on Ce_2MgSi_2 with the Shastry-Sutherland magnetic lattice	Honda Fuminori	Tohoku University
180	〃	広瀬　雄介	新潟大学	理学部	〃	Yusuke Hirose	Niigata University
181	強相関分子性固体における磁場中輸送特性	平郡　諭	東北大学	原子分子材料科学高等研究機構	Transport poperties of correlated molecular solids under high magnetic field	Satoshi Heguri	Tohoku University
182	ホイスラー合金 NiCoMnIn の強磁場誘起マルテンサイト逆変態に伴う高速イメージング測定	木原　工	東北大学	金属材料研究所	High-speed imaging in magnetic-field-induced martensitic transformation for Heusler alloys NiCoMnGa	Takumi Kihara	Tohoku University
183	2 次元有機超伝導体における磁場誘起超伝導状態の探索、及び超強磁場下磁化測定による局在スピン - 遍歴電子スピン間相互作用の研究	井原　慶彦	北海道大学	大学院理学研究院	Study for field induced superconducting state in organic superconductor, and localized-itinerant spins interaction by magnetization measurement under pulsed high field	Yoshihiko Ihara	Hokkaido University
184	キラル合金 Mn(Si,Ge) における強磁場まで安定なトポロジカルスピン構造の解明	金澤　直也	東京大学	大学院工学系研究科	Investigation on robust topological spin textures under high magnetic fields in the chiral alloy Mn(Si,Ge)	Naoya Kanazawa	The University of Tokyo
185	〃	藤代　有絵子	東京大学	大学院工学系研究科	〃	Yukako Fujishiro	The University of Tokyo
186	正四角台塔型反強磁性体の強磁場中電気磁気特性の測定	木村　健太	大阪大学	大学院基礎工学研究科	High-field magnetoelectric properties of square-cupola-based antiferromagnets	Kenta Kimura	Osaka University
187	ディラック半金属 Cd_3As_2 薄膜におけるカイラル磁気効果の解明	打田　正輝	東京大学	大学院工学系研究科	Investigation of chiral magnetic effects in Dirac semimetal Cd_3As_2 films	Masaki Uchida	The University of Tokyo
188	Fe^{2+}-Ti^{4+}, 及び Al^{3+} 置換した $BaFe_{12}O_{19}$ の強磁場磁気特性	神島　謙二	埼玉大学	大学院理工学研究科	Magnetic properties of Fe^{2+}-Ti^{4+} and Al^{3+} substituted $BaFe_{12}O_{19}$ under high magnetic field	Kenji Kamishima	Saitama University
189	層状化合物 $EuFBiS_2$ における異常な負の巨大磁気抵抗の起源探索	東中　隆二	首都大学東京	大学院理工学研究科	Investigation of anomalous negative large magnetoresistance of $EuFBiS_2$	Ryuji Higashinaka	Tokyo Metropolitan University
190	〃	梶谷　丈	首都大学東京	大学院理工学研究科	〃	Joe Kajitani	Tokyo Metropolitan University

担当所員：松田　康弘

No.	課題名	氏名	所属		Title	Name	Organization
191	近藤半導体 (Yb,R)B_{12}、価数揺動物質 (Y,Tm)B_6、およびペロブスカイト酸化物のワンターンコイル 120T パルス磁場下での強磁場磁化過程	伊賀　文俊	茨城大学	理学部	High field magnetization of Kondo insulator (Yb,R)B_{12}, valence fluctuation material (Y,Tm)B_6 and perovskite oxides by using one-turn coil in a 120 T pulse magnet	Fumitoshi Iga	Ibaraki University
192	〃	松浦　航	茨城大学	理学部	〃	Wataru Matsuura	Ibaraki University
担当所員：辛　埴							
193	トポロジカル近藤絶縁体候補物質である希土類硼化物単結晶の表面電子状態とスピン・軌道偏極構造	大坪　嘉之	大阪大学	大学院生命機能研究科	Surface electronic states and its spin/orbital polarization of rare-earth borides as candidates of topological Kondo insulator	Yoshiyuki Ohtsubo	Osaka University
194	〃	WANG CHENGWEI	大阪大学	大学院理学研究科	〃	Wang Chengwei	Osaka University
195	スピン分解角度分解光電子分光による $GdTe_2$ の CDW ギャップ内表面状態の研究	伊藤　孝寛	名古屋大学	シンクロトロン光研究センター	Spin-resolved angle-resolved photoemission study of surface states among CDW gap of $GdTe_2$	Takahiro Ito	Nagoya University
196	〃	楠　直紘	名古屋大学	大学院工学研究科	〃	Kusunoki Naohiro	Nagoya University
197	〃	近谷　翔汰	名古屋大学	工学部	〃	Kontani Shota	Nagoya University
198	遷移金属ダイカルコゲナイドの時間分解角度分解光電子分光	下志万　貴博	理化学研究所	創発物性科学研究センター	Time-resolved angle-resolved photoemission study on transition metal dichalchogenides	Takahiro Shimojima	RIKEN
199	〃	三石　夏樹	東京大学	大学院工学系研究科	〃	Natsuki Mitsuishi	The University of Tokyo
200	磁性元素をインターカレートした遷移金属ダイカルコゲナイドにおけるスピン分極の観測	石坂　香子	東京大学	大学院工学系研究科	Investigation of spin polarization in intercalated transition-metal dichalcogenide		The University of Tokyo
201	〃	吉田　訓	東京大学	大学院工学系研究科	〃	Satoshi Yoshida	The University of Tokyo
202	有機分子性結晶 α -(BEDT-TTF)$_2I_3$ の非占有電子状態および非平衡キャリアダイナミクスの観測	角田　一樹	広島大学	大学院理学研究科	Observation of unoccupied electronic structure and non-equilibrium carrier dynamics in organic molecular crystal alpha-(BEDT-TTF)$_2I_3$	Kazuki Sumida	Hiroshima University
203	理想的なワイル半金属の非平衡ダイナミクスの解明 II	木村　昭夫	広島大学	大学院理学研究科	Nonequilibrium electron dynamics of ideal Weyl semimetals II	Akio Kimura	Hiroshima University
204	〃	檜垣　聡太	広島大学	大学院理学研究科	〃	Sota Higaki	Hiroshima University
205	超巨大磁気抵抗を示すトポロジカル物質の非平衡キャリアダイナミクス	木村　昭夫	広島大学	大学院理学研究科	Nonequilibrium carrier dynamics of topological extreme magneto-resistance materials	Akio Kimura	Hiroshima University
206	〃	吉川　智己	広島大学	大学院理学研究科	〃	Tomoki Yoshikawa	Hiroshima University

No.	課題名	氏名	所属		Title	Name	Organization
207	バルク敏感高分解能スピン分解光電子分光を用いたハーフメタル強磁性体における有限温度効果の研究	藤原　弘和	岡山大学	大学院自然科学研究科	Studies on finite temperature effects of half-metallic ferromagnets by bulk-sensitive high-resolution spin-resolved photoemission spectroscopy	Hirokazu Fujiwara	Okayama University
208	トポロジカル近藤絶縁体候補物質である希土類硼化物単結晶の表面電子状態とスピン・軌道偏極構造	中村　拓人	大阪大学	大学院理学研究科	Surface electronic states and its spin/orbital polarization of rare-earth borides as candidates of topological Kondo insulator	Takuto Nakamura	Osaka University
209	インジウム原子層超伝導体におけるラシュバスピン分裂の直接観察	内橋　隆	物質・材料研究機構	国際ナノアーキテクトニクス研究拠点	Direct observation of Rashba effect-induced spin splitting in an indium atomic-layer superconductor	Takashi Uchihashi	National Institute for Materials Science
担当所員：秋山　英文							
210	GaPN 混晶のアップコンバージョン発光効率に関する研究	矢口　裕之	埼玉大学	大学院理工学研究科	Efficiency of upconversion luminescence from GaPN alloys	Hiroyuki Yaguchi	Saitama University
211	〃	五十嵐　大輔	埼玉大学	大学院理工学研究科	〃	Daisuke Igarashi	Saitama University
212	〃	高宮　健吾	埼玉大学	総合技術支援センター	〃	Kengo Takamiya	Saitama University
担当所員：小林　洋平							
213	次世代レーザー及び加工の技術開発	坂上　和之	早稲田大学	高等研究所	Development of a next generation laser system and laser machining technology	Kazuyuki Sakaue	Waseda University
担当所員：板谷　治郎							
214	テラヘルツ分光装置を用いた酸化物磁性材料の研究	大越　慎一	東京大学	大学院理学系研究科	Study of magnetic oxide using terahertz spectroscopy	Shin-ichi Ohkoshi	The University of Tokyo
215	〃	生井　飛鳥	東京大学	大学院理学系研究科	〃	Asuka Namai	The University of Tokyo
216	〃	吉清　まりえ	東京大学	大学院理学系研究科	〃	Marie Yoshikiyo	The University of Tokyo
217	希土類単酸化物薄膜における時間分解コヒーレントフォノン分光	牧野　哲征	福井大学	学術研究院工学系部門	Time-resolved coherent phonon spectroscopy in rare-earth monooxide thin films	Takayuki Makino	University of Fukui
218	〃	和座　一憲	福井大学	大学院工学研究科	〃	Kazunori Waza	University of Fukui
大阪大学 先端強磁場科学研究センター / Center for Advanced High Magnetic Field Science Osaka University							
219	パルス磁場を用いたマルテンサイト変態のカイネティクスに関する研究	福田　隆	大阪大学	大学院工学研究科	A study on kinetics of martensitic transformations using pulsed magnetic field	Takashi Fukuda	Osaka University

No.	課題名	氏名	所属		Title	Name	Organization
220	強磁場環境下におけるタンパク質結晶成長	牧　祥	大阪大谷大学	薬学部	Crystal Growth of Protein under the Magnetic Field Condition	Syou Maki	Faculty of Pharmacy, Osaka Ohtani University
221	パルス強磁場を用いた強相関電子系物質の強磁場物性の研究	竹内　徹也	大阪大学	低温センター	Physical properties of strongly correlated electron systems under pulsed high magnetic field.	Tetsuya Takeuchi	Osaka University
222	〃	大貫　惇睦	琉球大学	理学部	〃	Yoshichika Onuki	University of the Ryukyus
223	希釈三次元ハイゼンベルグ反強磁性体の強磁場物性	浅野　貴行	福井大学	学術研究院工学系部門	Magnetic properties of diluted 3D Heisenberg antiferromagnet in high magnetic fields	Takayuki Asano	University of Fukui
224	〃	大貫　惇睦	琉球大学	理学部	〃	Taiki Yokoyama	University of Fukui
225	ディラック・ワイル半金属が示す量子輸送特性と巨大磁気抵抗効果の研究	村川　寛	大阪大学	大学院理学研究科	High magnetic field study of transport properties in Dirac and Weyl semimetals	Hiroshi Murakawa	Osaka university
226	新規低次元磁性体の合成とその量子磁性の解明	本多　善太郎	埼玉大学	大学院理工学研究科	Synthesis, structure, and magnetism of novel low-dimensional transition metal coordination polymers	Zentaro Honda	Saitama University
227	パルス強磁場用極低温実験装置の開発	野口　悟	大阪府立大学	２１世紀科学研究機構	Development of the cryostat for pulsed high magnetic field	Satoru Noguchi	Osaka Prefecture University
228	〃	大貫　惇睦	琉球大学	理学部	〃	Shoma Ishiuchi	Osaka Prefecture University
229	鉄系超伝導体 $Sr_4V_2O_6Fe_2As_2$ における超伝導異方性	中島　正道	大阪大学	大学院理学研究科	Anisotropy of superconductivity in iron-based superconductor $Sr_4V_2O_6Fe_2As_2$	Masamichi Nakajima	Osaka University
230	磁場中輸送現象による鉄系超伝導体における擬ギャップの検証	中島　正道	大阪大学	大学院理学研究科	Investigation of pseudogap behavior in iron-based superconductors by transport measurements under magnetic fields	Masamichi Nakajima	Osaka University
231	フタロシアニン分子系の均一混晶における巨大磁気抵抗の局在スピン効果	花咲　徳亮	大阪大学	大学院理学研究科	Local moment effect on giant magnetoresistance in phthalocyanine mixed crystal	Noriaki Hanasaki	Osaka University
232	〃	大貫　惇睦	琉球大学	理学部	〃	Ryuta Ishii	Osaka university
233	SmB_6 薄膜の強磁場中での磁化輸送係数測定	宍戸　寛明	大阪府立大学	大学院工学研究科	Magnetization and transport measurements for SmB_6 thin films under high magnetic field	Hiroaki Shishido	Osaka Prefecture University
234	擬テトラヘドラル４配位構造を持つ２価コバルト単核単分子磁石のゼロ磁場分裂定数の決定	福田　貴光	大阪大学	大学院理学研究科	Determination of zero-field splitting parameters of a novel mononuclear divalent cobalt single molecule magnet having the pseudo-tetrahedral coordination geometry	Takamitsu Fukuda	Osaka University
235	〃	大貫　惇睦	琉球大学	理学部	〃	Toshiharu Ishizaki	Osaka University
236	多重極限環境下の電子スピン共鳴計測に用いる高出力ミリ波・サブミリ波伝送系の開発研究	光藤　誠太郎	福井大学	遠赤外領域開発研究センター	Development of high-power millimeter and submillimeter wave transmission system for electron spin resonance measurement under multiple extreme environment	Seitaro Mitsudo	University of Fukui

No.	課題名	氏名	所属		Title	Name	Organization
237	〃	大貫　惇睦	琉球大学	理学部	〃	Yutaka Fujii	University of Fukui
238	高出力テラヘルツ光源 (ジャイロトロン) を光源とする 高周波 ESR 分光 の研究	出原　敏孝	福井大学	遠赤外領域開発研究センター	Study on high frequency ESR spectroscopy using high power THz radiation sourses - Gyrotrons	Toshitaka Idehara	University of Fukui
239	〃	小川　勇	福井大学	遠赤外領域開発研究センター	〃	Isamu Ogawa	University of Fukui
240	ジャイロトロンを用いた高圧下強磁場 ESR 装置の開発と応用	櫻井　敬博	神戸大学	研究基盤センター	Development and application of high pressure and high field ESR system using gyrotron	Takahiro Sakurai	Kobe University
241	$Sr_2MnSi_2O_7$ 単結晶試料の強磁場下での磁化・電気分極・ESR 測定	桑原　英樹	上智大学	理工学部	Magnetization, electric polarization, and ESR measurements for $Sr_2MnSi_2O_7$ single crystals in pulsed high magnetic fields	Hideki Kuwahara	Sophia University
242	〃	大貫　惇睦	琉球大学	理学部	〃	Masaaki Noda	Sophia University
243	単軸性キラル磁性体の磁気特性測定　−磁気トルクと磁気共鳴測定−	戸川　欣彦	大阪府立大学	大学院工学研究科	Magnetic property of monoaxial chiral magnetic materials examined by means of magnetic torque and resonance measurements	Yoshihiko Togawa	Osaka Prefecture University
244	〃	大貫　惇睦	琉球大学	理学部	〃	Francisco Goncalve	Osaka Prefecture University
245	フラストレート系新物質の強磁場磁化測定	山口　博則	大阪府立大学	大学院理学系研究科	High-field magnetization measurement on new frustrated materials	Hironori Yamaguchi	Osaka Prefecture University
246	正四角台塔型反強磁性体の強磁場中 ESR 測定	木村　健太	大阪大学	大学院基礎工学研究科	High-field ESR measurements of square-cupola-based antiferromagnets	Kenta Kimura	Osaka University
247	$GaFeO_3$ におけるスピン波の非相反性	有馬　孝尚	東京大学	大学院新領域創成科学研究科	Nonreciprocal spin waves in $GaFeO_3$	Takahisa Arima	The University of Tokyo
248	〃	大貫　惇睦	琉球大学	理学部	〃	Tsuyoshi Omi	The University of Tokyo

物質合成・評価設備 P クラス / Materials Synthesis and Characterization P Class Researcher

No.	課題名	氏名	所属		Title	Name	Organization
1	p 型窒化ガリウム薄膜の作製と評価	山田　太郎	東京大学	大学院工学系研究科	Fabrication and physical investigation of p-type gallium nitride thin films	Taro Yamada	The University of Tokyo
2	電子が複合自由度を持つ遷移金属カルコゲナイドの合成と物性評価	片山　尚幸	名古屋大学	大学院工学研究科	Growth of the transition metal chalcogenides with charge, orbital and spin degrees of freedom	Naoyuki Katayama	Nagoya University
3	〃	田村　慎也	名古屋大学	大学院工学研究科	〃	Shinya Tamura	Nagoya University

物質合成・評価設備 G クラス / Materials Synthesis and Characterization G Class Researcher

No.	課題名	氏名	所属		Title	Name	Organization
1	非従来型超伝導体におけるエックス線回折	芝内　孝禎	東京大学	大学院新領域創成科学研究科	X-ray diffraction on unconventional superconductors	Takasada Shibauchi	The University of Tokyo
2	〃	水上　雄太	東京大学	大学院新領域創成科学研究科	〃	Yuta Mizukami	The University of Tokyo
3	〃	細井　優	東京大学	大学院新領域創成科学研究科	〃	Hosoi Suguru	The University of Tokyo
4	〃	竹中　崇了	東京大学	大学院新領域創成科学研究科	〃	Takaaki Takenaka	The University of Tokyo
5	〃	石田　浩祐	東京大学	大学院新領域創成科学研究科	〃	Kousuke Ishida	The University of Tokyo
6	泥岩が示す不完全な半透膜性に関する研究	徳永　朋祥	東京大学	大学院新領域創成科学研究科	Research of incomplete semipermeable properties of mudstones	Tomochika Tokunaga	The University of Tokyo
7	〃	廣田　翔伍	東京大学	大学院新領域創成科学研究科	〃	Shogo Hirota	The University of Tokyo
8	高温高圧水中の固体酸・塩基触媒反応の速度論的解析	大島　義人	東京大学	大学院新領域創成科学研究科	Kinetic analysis of solid acid and base catalyzed reactions in sub- and supercritical water	Yoshito Oshima	The University of Tokyo
9	〃	秋月　信	東京大学	大学院新領域創成科学研究科	〃	Makoto Akizuki	The University of Tokyo
10	高圧高温水を反応場とした有機合成反応	大島　義人	東京大学	大学院新領域創成科学研究科	Organic synthesis in sub- and supercritical water	Yoshito Oshima	The University of Tokyo
11	〃	伊藤　光基	東京大学	大学院新領域創成科学研究科	〃	Koki Ito	The University of Tokyo
12	ケミカルループ法における高活性かつ長期安定性を有する酸素キャリア材料の開発	大友　順一郎	東京大学	大学院新領域創成科学研究科	Development of oxygen carrier materials with high activity and durability for chemical looping systems.	Junichiro Otomo	The University of Tokyo
13	〃	岡　輝	東京大学	大学院新領域創成科学研究科	〃	Oka Hikaru	The University of Tokyo
14	ケミカルループ法におけるチタン酸カルシウム担体による酸化還元反応促進効果	大友　順一郎	東京大学	大学院新領域創成科学研究科	Accelerating of reaction kinetics of oxidation and reduction using $CaTi_{1-x}Fe_xO_{3-\delta}$ as oxygen carrier materials for chemical looping systems	Junichiro Otomo	The University of Tokyo
15	〃	有賀　耀介	東京大学	工学部	〃	Yosuke Ariga	The University of Tokyo
16	アンモニア電解合成反応における新規電極触媒開発と電極反応評価	大友　順一郎	東京大学	大学院新領域創成科学研究科	Development of new electro-catalysts and evaluation of electrode reaction for electrochemical synthesis of ammonia	Junichiro Otomo	The University of Tokyo

No.	課題名	氏名	所属		Title	Name	Organization
17	〃	及川　暁雄	東京大学	大学院新領域創成科学研究科	〃	Akio Oikawa	The University of Tokyo
18	プロトン伝導性固体電解質を用いた電解合成反応における電極触媒開発と反応速度論解析	大友　順一郎	東京大学	大学院新領域創成科学研究科	Development of electrode catalysts and kinetic analysis for electrolysis using proton conducting fuel cells	Junichiro Otomo	The University of Tokyo
19	〃	高坂　文彦	東京大学	大学院新領域創成科学研究科	〃	Fumihiko Kosaka	The University of Tokyo
20	新規プロトン - 電子混合伝導体の開発	大友　順一郎	東京大学	大学院新領域創成科学研究科	Development of proton-electron mixed conductors	Junichiro Otomo	The University of Tokyo
21	〃	小城　元	東京大学	大学院新領域創成科学研究科	〃	Kojo Gen	The University of Tokyo
22	中温作動プロトン伝導型 SOFC のセル劣化要因の検討	大友　順一郎	東京大学	大学院新領域創成科学研究科	Analysis of degradations in intermediate temperature proton-conducting SOFC cells	Junichiro Otomo	The University of Tokyo
23	〃	橋本　隼輔	東京大学	大学院新領域創成科学研究科	〃	Shunsuke Hashimoto	The University of Tokyo
24	ペロブスカイト型酸化物を用いたケミカルルーピングシステムの開発	大友　順一郎	東京大学	大学院新領域創成科学研究科	Preparation of perovskite oxides as supports for oxygen carrier materials for chemical looping systems	Junichiro Otomo	The University of Tokyo
25	〃	オーチェン　ジェームズ　オーチェン	東京大学	大学院新領域創成科学研究科	〃	Ochieng James Ochieng	The University of Tokyo
26	二酸化炭素と窒素による尿素の電気化学的合成	大友　順一郎	東京大学	大学院新領域創成科学研究科	Electrochemical Synthesis of Urea from Carbon Dioxide and Nitrogen	Junichiro Otomo	The University of Tokyo
27	〃	李　建毅	東京大学	大学院新領域創成科学研究科	〃	Chen-I Li	The University of Tokyo
28	ケミカルループ法における高性能酸素キャリア粒子の開発	大友　順一郎	東京大学	大学院新領域創成科学研究科	Development of oxygen carrier materials with high activity and durability for chemical looping systems	Junichiro Otomo	The University of Tokyo
29	〃	マーチン　ケラー	東京大学	大学院新領域創成科学研究科	〃	Martin Keller	The University of Tokyo
30	トポロジカル半金属候補物質の合成と物性	岡本　佳比古	名古屋大学	大学院工学研究科	Synthesis and Physical Properties of Candidate Topological Semimetals	Yoshihiko Okamoto	Nagoya University
31	超臨界水中におけるゼオライトの安定性に関する研究	大島　義人	東京大学	大学院新領域創成科学研究科	The stability of zeolites in supercritical water condition	Yoshito Oshima	The University of Tokyo
32	〃	アピバンボリラク　チャンウィット	東京大学	大学院新領域創成科学研究科	〃	Apibanboriak Chanwit	The University of Tokyo
33	超臨界水を利用した微粒子合成における in situ 有機修飾技術の開発	大島　義人	東京大学	大学院新領域創成科学研究科	The development of the in situ organic surface modification on nanoparticles synthesis in supercritical water.	Yoshito Oshima	The University of Tokyo

No.	課題名	氏名	所属		Title	Name	Organization
34	〃	原田　拓真	東京大学	大学院新領域創成科学研究科	〃	Takuma Harada	The University of Tokyo
35	メソポーラスマテリアル・グラフェンオキサイドに担持した金属触媒のキャラクタリゼーション	佐々木　岳彦	東京大学	大学院新領域創成科学研究科	Characterization of metal catalysts supported on mesoporous materials and graphene oxides	Takehiko Sasaki	The University of Tokyo
36	〃	Etty Nurlia Kusumawati	東京大学	大学院理学系研究科	〃	Etty Nurlia Kusumawati	The University of Tokyo
37	〃	有村　祐紀	東京大学	大学院新領域創成科学研究科	〃	Yuki Arimura	The University of Tokyo
38	触媒反応の insitu ラマン散乱測定	佐々木　岳彦	東京大学	大学院新領域創成科学研究科	insitu measurements of Raman scattering for catalytic reactions	Takehiko Sasaki	The University of Tokyo
39	層状コバルト酸水素化物における圧力効果	山本　隆文	京都大学	大学院工学研究科	Pressure Effect on Layered cobalt Oxyhydrides	Takafumi Yamamoto	Kyoto University
40	層状希土類化合物 RZn_3P_3(R= 希土類) の高圧合成	関根　ちひろ	室蘭工業大学	大学院工学研究科	High-pressure synthesis of layered rare-earth compounds RZn_3P_3 (R=rare earth)	Chihiro Sekine	Muroran Institute of Technology
41	〃	森　英将	室蘭工業大学	大学院工学研究科	〃	Hidemasa Mori	Muroran Institute of Technology
42	全個体電池のための Li イオン伝導体の高圧合成	廣瀬　瑛一	名古屋大学	大学院工学研究科	High pressure synthesis of Li ion conductor for all solid state battery	Eiichi Hirose	Nagoya University
43	高温高圧下で軽元素が鉄ーシリケイトー水系に及ぼす影響の解明	飯塚　理子	東京大学	大学院理学系研究科	Behavior of light elements in iron-silicate-water system under high pressure and high temperature	Riko Iizuka	The University of Tokyo
44	〃	古村　俊行	東京大学	大学院理学系研究科	〃	Tsuyoshi Kimura	The University of Tokyo
45	高圧下でのアミノ酸のペプチド化反応の観察	藤本　千賀子	東京大学	大学院理学系研究科	Peptide formation of amino acids under high pressure	Fujimoto Chikako	The University of Tokyo
46	超硬質遷移金属多窒化物の高圧合成とラマン散乱測定	丹羽　健	名古屋大学	大学院工学研究科	Ultra-high pressure synthesis of super hard transition metal nitrides and Raman scattering spectroscopy	Ken Niwa	Nagoya University
47	〃	高山　新	名古屋大学	大学院工学研究科	〃	Shin Takayama	Nagoya Universty
48	超高圧合成法による新規 III 族半導体窒化物の創製と結晶化学	丹羽　健	名古屋大学	大学院工学研究科	High pressure synthesis and crystal chemistry of novel semiconducting nitrides	Ken Niwa	Nagoya University
49	〃	稲垣　智哉	名古屋大学	工学部	〃	Tomoya Inagaki	Nagoya University
50	超高圧プレスを用いた新規プロトニクス酸化物のソフト化学的合成法の検討	山口　周	東京大学	大学院工学系研究科	Oxide-Protonics materials synthesis by combined use of soft chemical method and high pressure	Shu Yamaguchi	The University of Tokyo

No.	課題名	氏名	所属		Title	Name	Organization
51	〃	田中　和彦	東京大学	大学院工学系研究科	〃	Kazuhiko Tanaka	The University of Tokyo
52	溶融亜鉛メッキ合金相の応力誘起変態	山口　周	東京大学	大学院工学系研究科	Stress-induced phase transformation of Fe-Zn alloy formed in hot-dip process	Shu Yamaguchi	The University of Tokyo
53	〃	田中　和彦	東京大学	大学院工学系研究科	〃	Kazuhiko Tanaka	The University of Tokyo
54	新規ジントル相の超高圧合成と結晶化学および物性	長谷川　正	名古屋大学	大学院工学研究科	High pressure synthesis, crystal chemistry and physical properties of novel Zintl phases	Masashi Hasegawa	Nagoya University
55	〃	濱口　朋之	名古屋大学	大学院工学研究科	〃	Tomoyuki Hamaguchi	Nagoya University
56	高圧印加による Li ドープα菱面体晶ボロンの作製	木村　薫	東京大学	大学院新領域創成科学研究科	Synthesis of Li-dope alpha-rhombohedral boron by high-pressurization	Kaoru Kimura	The University of Tokyo
57	〃	酒井　志徳	東京大学	大学院新領域創成科学研究科	〃	Munenori Sakai	The University of Tokyo
58	高圧下での $MoSi_2$ 型構造の $FeAl_2$ 結晶の作製	木村　薫	東京大学	大学院新領域創成科学研究科	High pressure synthesis of $MoSi_2$ type iron aluminide, $FeAl_2$ crystal	Kaoru Kimura	The University of Tokyo
59	〃	飛田　一樹	東京大学	大学院新領域創成科学研究科	〃	Kazuki Tobita	The University of Tokyo
60	イリジウム酸化物薄膜の構造評価	平岡　奈緒香	東京大学	大学院理学系研究科	Evaluation of structure of iridate thin films	Naoka Hiraoka	The University of Tokyo
61	〃	根岸　真通	東京大学	大学院理学系研究科	〃	Masamichi Negishi	The University of Tokyo
62	天然鉱物の微細組織と結晶性の実態	永嶌　真理子	山口大学	大学院創成科学研究科	Evaluation of micro-texture and crystallinity of natural minerals	Mariko Nagashima	Ymaguchi University
63	新規磁石材料の微細構造解析	齋藤　哲治	千葉工業大学	工学部	Microstructural studies of new permanent magnet materials	Tetsuji Saito	Chiba Institute of Technology
64	TEM によるコアシェル型プルシアンブルー類似体の局所構造解析	糸井　充穂	日本大学	医学部	TEM study of the local structure in core-shell nanoparticles based on prussian blue analogues	Miho Itoi	Nihon University
65	ナノ構造材料を用いた高性能二次電池開発	細野　英司	産業技術総合研究所	省エネルギー研究部門	Development of secondary battery with high performances by using nanostructured materials	Eiji Hosono	Advanced Industrial Science and Technology
66	misfit 単結晶の構造観察	小林　夏野	岡山大学	異分野基礎科学研究所	Observation of local structure on misfit single crystal	Kaya Kobayashi	Okayama University
67	水中プラズマを用いたナノ粒子合成	後藤　拓	東京大学	大学院新領域創成科学研究科	Synthesis of nanoparticles via plasma processing in liquid	Taku Goto	The University of Tokyo

No.	課題名	氏名	所属		Title	Name	Organization
68	準結晶・近似結晶の磁性に関する研究	田村　隆治	東京理科大学	大学院基礎工学研究科	Magnetism of quasicrystals and approximants	Ryuji Tamura	Tokyo University of Science
69	〃	石川　明日香	東京理科大学	大学院基礎工学研究科	〃	Asuka Ishikawa	Tokyo University of Science
70	$A_{1-x}Sr_xFeO_3$(A：ランタノイド) の高温における磁性と熱電特性に関する研究	中津川　博	横浜国立大学	大学院工学研究院	Magnetism and thermoelectric properties at high temperature in $A_{1-x}Sr_xFeO_3$ (A : lanthanoid)	Hiroshi Nakatsugawa	Yokohama National University
71	特異な電子状態を形成する遷移金属カルコゲナイドの磁気・輸送特性の評価	小林　慎太郎	名古屋大学	大学院工学研究科	Magnetic and transport properties of transition metal chalcogenides with unusual electronic states	Shintaro Kobayashi	Nagoya University
72	〃	中埜　彰俊	名古屋大学	大学院工学研究科	〃	Akitoshi Nakano	Nagoya University
73	〃	鬼頭　俊介	名古屋大学	大学院工学研究科	〃	Rina Maeda	The University of Tokyo
74	新規非酸化物系ペロブスカイト型関連化合物の磁気物性	長谷川　正	名古屋大学	大学院工学研究科	Magnetism of novel perovskite-type related non-oxide compounds	Masashi Hasegawa	Nagoya University
75	〃	佐合　一樹	名古屋大学	大学院工学研究科	〃	Kazuki Sagou	Nagoya University
76	レアメタルフリー磁性材料 L10-FeCo の磁気特性の解析	小嗣　真人	東京理科大学	基礎工学部	Analysis of magnetic properties of rare-metal-free super magnet "L10-FeCo"	Masato Kotsugi	Tokyo University of Science
77	正 20 面体クラスター固体の伝導と磁性	木村　薫	東京大学	大学院新領域創成科学研究科	Transport and magnetic properties of Icosahedral Cluster Solids	Kaoru Kimura	The University of Tokyo
78	〃	廣戸　孝信	東京大学	大学院新領域創成科学研究科	〃	Hiroto Takanobu	The University of Tokyo
79	ホイスラー型化合物の磁性と伝導の研究	廣井　政彦	鹿児島大学	大学院理工学研究科	Study on the magnetic and electrical properties of Heusler compounds	Masahiko Hiroi	Kagoshima University
80	〃	大岡　隆太郎	鹿児島大学	大学院理工学研究科	〃	Ryutaro Ooka	Kagoshima University
81	ハーフメタル型ホイスラー合金の磁性と輸送特性に関する研究	重田　出	鹿児島大学	大学院理工学研究科	Study on the magnetic and transport properties of half-metallic Heusler alloys	Iduru Shigeta	Kagoshima University
82	〃	大岡　隆太郎	鹿児島大学	大学院理工学研究科	〃	Ryutaro Ooka	Kagoshima University
83	低次元鉄系化合物の電子物性に関する研究	青山　拓也	東北大学	大学院理学研究科	Study on electronic properties of Fe-based materials with low-dimensional structure	Takuya Aoyama	Tohoku University
84	新規フェロイック物質の開発	有馬　孝尚	東京大学	大学院新領域創成科学研究科	Exploration of new ferroics	Taka-hisa Arima	The University of Tokyo

No.	課題名	氏名	所属		Title	Name	Organization
85	〃	徳永　祐介	東京大学	大学院新領域創成科学研究科	〃	Yusuke Tokunaga	The University of Tokyo
86	〃	阿部　伸行	東京大学	大学院新領域創成科学研究科	〃	Nobuyuki Abe	The University of Tokyo
87	〃	松浦　慧介	東京大学	大学院新領域創成科学研究科	〃	Keisuke Matsuura	The University of Tokyo
88	〃	藤間　友理	東京大学	大学院新領域創成科学研究科	〃	Yuri Fujima	The University of Tokyo
89	〃	荒木　勇介	東京大学	大学院新領域創成科学研究科	〃	Yusuke Araki	The University of Tokyo
90	〃	小池　仁希	東京大学	大学院新領域創成科学研究科	〃	Yoshiki Koike	The University of Tokyo
91	〃	前島　夏奈	東京大学	大学院新領域創成科学研究科	〃	Kana Maeshima	The University of Tokyo
92	〃	中川　直己	東京大学	大学院新領域創成科学研究科	〃	Naoki Nakagawa	The University of Tokyo
93	〃	近江　毅志	東京大学	大学院新領域創成科学研究科	〃	Tsuyoshi Omi	The University of Tokyo
94	〃	徳村　謙祐	東京大学	大学院新領域創成科学研究科	〃	Kensuke Tokumura	The University of Tokyo
95	〃	吉澤　孟晃	東京大学	大学院新領域創成科学研究科	〃	Takeaki Yoshizawa	The University of Tokyo
96	〃	佐藤　樹	東京大学	大学院新領域創成科学研究科	〃	Tatsuki Sato	The University of Tokyo
97	〃	海本　祐真	東京大学	大学院新領域創成科学研究科	〃	Yuma Umimoto	The University of Tokyo
98	Cu－Ni－X（X=Co,Fe）系単結晶性合金中の磁性微粒子析出過程と磁気特性の関係	竹田　真帆人	横浜国立大学	大学院工学研究院	Precipitation behavior and magnetic properties of fine magnetic particles in single crystals of Cu - Ni base alloys	Mahoto Takeda	Yokohama National University
99	〃	又井　慎太郎	横浜国立大学	大学院工学府	〃	Shintaro Matai	Yokohama National University
100	Cu 基ナノグラニュラー磁性体における磁気特性と微細組織の関係	坂倉　響	横浜国立大学	大学院工学府	The relationships between magnetic properties and microstructures in Cu based nano-granular materials	Hibiki Sakakura	Yokohama National University

物質合成・評価設備 U クラス / Materials Synthesis and Characterization U Class Researcher

No.	課題名	氏名	所属		Title	Name	Organization
1	$Sm_{1-x}Y_xS$ 単結晶における負熱膨張特性の Y 組成依存性	岡本　佳比古	名古屋大学	大学院工学研究科	Y-content-dependence of negative thermal exoansion in $Sm_{1-x}Y_xS$ single crystals	Yoshihiko Okamoto	Nagoya University
2	高温高圧下における芳香族化合物の安定性	篠崎　彩子	北海道大学	大学院理学研究院	Stability of aromatic hydrocarbons under high pressure and temperature	Ayako Shinozaki	Hokkaido University
3	鉄カルコゲナイド物質における磁気特性測定	水上　雄太	東京大学	大学院新領域創成科学研究科	Magnetic properties measurements on iron chalcogenides	Yuta Mizukami	The University of Tokyo
4	マイクロミキサを用いた機能性酸化物ナノ粒子の連続合成	陶　究	産業技術総合研究所	化学プロセス研究部門	Continuous synthesis of functional metal oxide nanoparticles using a micromxer	kiwamu Sue	National Institute of Advanced Industrial Science and Technology
5	コニカルらせん磁性体 $CoCr_2O_4$ における複合ドメイン相関の解明のための試料準備	木村　剛	東京大学	大学院新領域創成科学研究科	Investigation of coupled multiferroic domains in a conical spiral magnet $CoCr_2O_4$	Tsuyoshi Kimura	The University of Tokyo
6	ポリロタキサンを用いた高次構造の形成	前田　利菜	東京大学	大学院新領域創成科学研究科	Construction of higher order structure consisting of polyrotaxane	Rina Maeda	The University of Tokyo
7	プラズマ風洞による宇宙往還機の熱防護システム (TPS) に関する動的酸化に関する研究	桃沢　愛	東京都市大学	工学部	Research on dynamic oxidation of thermal protection system by using plasma wind tunnel	Ai Momozawa	Tokyo City University
8	〃	曽我　遼太	東京大学	大学院工学系研究科	〃	Ryota Soga	The University of Tokyo
9	〃	田中　聖也	東京大学	大学院工学系研究科	〃	Seiya Tanaka	The University of Tokyo
10	希土類サマリウムオルソフェライトの単結晶成長とテラヘルツ波磁気共鳴分光	中嶋　誠	大阪大学	レーザー科学研究所	Terahertz magnetic resonance spectroscopy and single crystal growth for samarium orthoferrite	Makoto Nakajima	Osaka University
11	〃	邱　紅松	大阪大学	レーザー科学研究所	〃	Hongsong Qiu	Osaka University
12	〃	弘田　和將	大阪大学	レーザー科学研究所	〃	Kazumasa Hirota	Osaka University
13	鉄系超伝導体に対する元素マッピング	水上　雄太	東京大学	大学院新領域創成科学研究科	Elemental mapping on iron-based superconductors	Yuta Mizukami	The University of Tokyo
14	オスミウム含有廃液の超臨界水酸化・超臨界二酸化炭素抽出に関する研究	布浦　鉄兵	東京大学	環境安全研究センター	Study on supercritical water oxidation and supercritical CO_2 extraction of osmium-containing wastewater	Teppei Nunoura	The University of Tokyo
15	〃	平井　晴菜	東京大学	大学院新領域創成科学研究科	〃	Haruna Hirai	The University of Tokyo
16	〃	三好　列	東京大学	大学院新領域創成科学研究科	〃	Retsu Miyoshi	The University of Tokyo

No.	課題名	氏名	所属		Title	Name	Organization
17	フィチン酸の超臨界水ガス化挙動に関する検討	布浦　鉄兵	東京大学	環境安全研究センター	Decomposition behavior of phytic acid in supercritical water gasification	Teppei Nunoura	The University of Tokyo
18	〃	飯田　裕樹	東京大学	大学院新領域創成科学研究科	〃	Yuuki Iida	The University of Tokyo
19	多形物質 $(Al,Fe)_2GeO_5$ の磁化測定	香取　浩子	東京農工大学	大学院工学研究院	Magnetization measurements of polymorphism $(Al,Fe)_2GeO_5$	Hiroko Katori	Tokyo University of Agriculture and Technology
20	〃	高田　早紀	東京農工大学	大学院工学府	〃	Saki Takada	Tokyo University of Agriculture and Technology
21	強磁性体 $Ln_2Co_{12}P_7$ (Ln= 希土類) を中心とした弱磁場中の磁化の研究	太田　寛人	東京農工大学	大学院工学研究院	Study of magnetization of ferromagnets $Ln_2Co_{12}P_7$ (Ln=lanthanoids) under low magnetic field	Hiroto Ohta	Tokyo University of Agriculture and Technology
22	〃	加藤　優典	東京農工大学	大学院工学府	〃	Yusuke Kato	Tokyo University of Agriculture and Technology

長期留学研究員 / Long Term Young Researcher

No.	課題名	氏名	所属		Title	Name	Organization
1	Sr_2MO_4(M=V, Cr) の高圧下結晶構造解析	嶋津　拓	千葉大学	大学院理学研究科	Crystal structure analysis of Sr_2MO_4(M=V, Cr) under pressure	Taku Shimazu	Chiba University
2	多重極限物性測定装置の開発と量子臨界物性の研究	佐藤　和樹	大阪大学	大学院理学研究科	Development of experimental measuring equipments under multiplex extreme conditions and studies on quantum critical phenomena	Kazuki Sato	Osaka University
3	時間分解角度分解光電子分光による 2H-$NbSe_2$ の光励起ダイナミクスの研究	渡邉　真莉	東京理科大学	理学部	Ultrafast dynamics in 2H-$NbSe_2$ by time-resolved photoemission spectroscopy	Mari Watanabe	Tokyo University of Science
4	パルス幅可変レーザー及び加工の技術開発	高橋　孝	早稲田大学	先進理工学研究科	Development of a variable pulse duration laser system and laser machining technology	Takashi Takahashi	Waseda University

短期留学研究員 / Short Term Young Researcher

No.	課題名	氏名	所属		Title	Name	Organization
1	第一原理におけるゼーベック係数の計算	高　成柱	大阪大学	大学院基礎工学研究科	Seebeck coefficient calculation from first-princple	Ko Sonjy	Osaka University

平成 29 年度 共同利用課題一覧（後期）/ Joint Research List (2017 Latter Term)

嘱託研究員 / Commission Researcher

No.	課題名	氏名	所属		Title	Name	Organization
担当所員：森　初果							
1	水素結合型分子導体における H/D 同位体効果による相転移機構の理論的研究	立川　仁典	横浜市立大学	大学院生命ナノシステム科学研究科	Theoretical study of phase transition mechanism induced by H/D isotope effect in hydrogen-bonded molecular conductors	Masanori Tachikawa	Yokohama City Uninersity
2	〃	長嶋　雲兵	計算科学振興財団	研究部門	〃	Umpei Nagashima	Foundation for Computational Science
3	常圧で金属状態を示す純有機単一成分導体の開発	御崎　洋二	愛媛大学	大学院理工学研究科	Development of purely organic single-component molecular metals under ambient pressure	Kenta Kimura	Ehime University
4	純有機単一成分超伝導体の開発	白旗　崇	愛媛大学	大学院理工学研究科	Development of purely organic single-component molecular superconductors	Takashi Shirahata	Ehime University
担当所員：中辻　知							
5	イッテルビウム系量子臨界物質の極低温における格子ゆがみの研究	久我　健太郎	理化学研究所	放射光科学総合研究センター	Crystal strain at low temperatures in Yb-based quantum critical material	Kentarou Kuga	RIKEN
担当所員：上床　美也							
6	磁性体の圧力効果	巨海　玄道	久留米工業大学	工学部	Effect of pressure on the Magnetic Materials	Gendo Oomi	Kurume Institute of Technology
7	多重極限関連圧力装置の調整	高橋　博樹	日本大学	文理学部	Adjustment of Cubic Anvil apparatus	Hiroki Takahashi	Nihon University
8	擬一次元有機物質の圧力下物性研究	糸井　充穂	日本大学	医学部	Study on pressure induced superconductivity of quasi organic conductor	Miho Itoi	Nihon University
9	3d 遷移化合物に関する圧力効果	鹿又　武	東北学院大学	工学総合研究所	Eiffect of pressure on the 3d transition compounds	Takeshi Kanomata	Tohoku Gakuin University
10	希釈冷凍機温度で使用可能な 10GPa 級超高圧発生装置の開発	松林　和幸	電気通信大学	大学院情報理工学研究科	Development of 10 GPa class high pressure apparatus for low temperature	Kazuyuki Matsubayashi	The University of Electro-Communications
11	有機伝導体の圧力効果	村田　恵三	大阪経済法科大学	21 世紀社会総合研究センター	Effect of pressure on the organic conductor	Keizo Murata	Osaka University of Economics and Law
12	圧力下 NMR 測定法に関する開発	藤原　直樹	京都大学	大学院人間・環境学研究科	Development of NMR measurement method under high pressure	Naoki Fujiwara	Kyoto University

No.	課題名	氏名	所属		Title	Name	Organization
13	希土類 122 化合物における圧力効果	繁岡　透	山口大学	大学院理工学研究科	Pressure effect of rare earth 122 compounds	Toru Shigeoka	Yamaguchi University
14	高圧下 X 線回折法の開発	江藤　徹二郎	久留米工業大学	工学部	Development of High Pressure X-ray diffraction measurements	Tetsujiro Eto	Kurume Institute of Technology
15	低温用マルチアンビル装置の開発	辺土　正人	琉球大学	理学部	Development of multi-anvil apparatus for low temperature	Masato Hedo	University of the Ryukyus
16	磁化測定装置の開発	名嘉　節	物質・材料研究機構	機能性材料研究拠点	Development of the magnetometer	Takashi Naka	National Institute for Materials Science
17	高圧下量子振動システムの開発	摂待　力生	新潟大学	理学部	Development of quantum oscillation under high pressure	Rikio Settai	Niigata University
担当所員：野口　博司							
18	理論・実験・データ科学の融合を目指した量子格子模型シミュレータの開発	星　健夫	鳥取大学	大学院工学研究科	Development of quantum lattice model simulator integrating theory, experiment, and data science	Takeo Hoshi	Tottori University
19	〃	曽我部　知広	名古屋大学	大学院工学研究科	〃	Tomohiro Sogabe	Nagoya University
20	動的平均場近似に基づく第一原理計算パッケージの高度化	大槻　純也	東北大学	大学院理学研究科	Advancement of ab-initio program based on dynamical mean-field theory	Jyunya Otsuki	Tohoku University
21	〃	品岡　寛	埼玉大学	大学院理工学研究科	〃	Hiroshi Shinaoka	Saitama University
担当：中性子科学研究施設							
22	4G における共同利用推進	佐藤　卓	東北大学	多元物質科学研究所	Research and Support of General-Use at 4G	Taku Sato	Tohoku University
23	〃	奥山　大輔	東北大学	多元物質科学研究所	〃	Daisuke Okuyama	Tohoku University
24	〃	那波　和宏	東北大学	多元物質科学研究所	〃	Kazuhiro Nawa	Tohoku University
25	6G における共同利用推進	富安　啓輔	東北大学	大学院理学研究科	Research and Support of General-Use at 6G	Keisuke Yomiyasu	Tohoku University
26	〃	岩佐　和晃	茨城大学	フロンティア応用原子科学研究センター	〃	Kazuaki Iwasa	Ibaraki University
27	T1-2、T1-3 における共同利用推進	藤田　全基	東北大学	金属材料科学研究所	Research and Support of General-Use at T1-2 and T1-3	Masaki Fujita	Tohoku University

No.	課題名	氏名	所属		Title	Name	Organization
28	〃	南部　雄亮	東北大学	金属材料科学研究所	〃	Yusuke Nambu	Tohoku University
29	〃	池田　陽一	東北大学	金属材料科学研究所	〃	Yoichi Ikeda	Tohoku University
30	〃	鈴木　謙介	東北大学	金属材料科学研究所	〃	Kensuke Suzuki	Tohoku University
31	T2-2 における共同利用推進	木村　宏之	東北大学	多元物質科学研究所	Research and Support of General-Use at T2-2	Hiroyuki Kimura	Tohoku University
32	〃	坂倉　輝俊	東北大学	多元物質科学研究所	〃	Terutoshi Sakakura	Tohoku University
33	C1-2 における共同利用推進	杉山　正明	京都大学	原子炉実験所	Research and Support of General-Use at C1-2	Masaaki Sugiyama	Kyoto University
34	C1-2、C2-3-1、C3-1-2 における共同利用推進	井上　倫太郎	京都大学	原子炉実験所	Research and Support of General-Use at C1-2, C2-3-1 and C3-1-2	Rintaro Inoue	Kyoto University
35	C3-1-2、C2-3-1 における共同利用推進	日野　正裕	京都大学	原子炉実験所	Research and Support of General-Use at C3-1-2 and C2-3-1	Masahiro Hino	Kyoto University
36	C3-1-2 における共同利用推進	田崎　誠司	京都大学	大学院工学研究科	Research and Support of General-Use at C3-1-2	Seiji Tasaki	Kyoto University
37	C1-3-mfSANS における共同利用推進	間宮　広明	物質・材料研究機構	先端材料解析研究拠点	Research and Support of General-Use at C1-3-mfSANS	Hiroaki Mamiya	National Institute for Materials Science
38	〃	古坂　道弘	北海道大学	大学院工学研究科	〃	Michihiro Furusaka	Hokkaido University
39	〃	大沼　正人	北海道大学	大学院工学研究科	〃	Masato Ohnuma	Hokkaido University
40	〃	藤原　健	産業技術総合研究所	計量標準総合センター	〃	Takeshi Fujiwara	National Institute of Advanced Industrial Science and Technology
41	C1-3、C3-1-2 における共同利用推進	北口　雅暁	名古屋大学	現象解析研究センター	Research and Support of General-Use at C1-3 and C3-1-2	Masaaki Kitaguchi	Nagoya University
42	C1-3 における共同利用推進	清水　裕彦	名古屋大学	大学院理学研究科	Research and Support of General-Use at C1-3	Hirohiko Shimizu	Nagoya University
43	〃	広田　克也	名古屋大学	大学院理学研究科	〃	Katsuya Hirota	Nagoya University
44	〃	土川　雄介	名古屋大学	大学院理学研究科	〃	Yusuke Tsuchikawa	Nagoya University

No.	課題名	氏名	所属		Title	Name	Organization
45	〃	山形　豊	理化学研究所	光量子工学研究領域	〃	Yutaka Yamagata	RIKEN
担当所員：徳永　将史							
46	ダイヤモンドアンビルセルを用いた高圧力・パルス強磁場下電気抵抗測定	狩野　みか	日本工業大学	工学部	Electrical resistivity measurements under pressure and in pulsed magnetic fields using diamond anvil cell	Mika Kano	Nippon Institute of Technology
担当所員：辛　埴							
47	スピン分解角度分解光電子分光による $TaSi_2$ のスピン構造の研究	伊藤　孝寛	名古屋大学	シンクロトロン光科学研究センター	Spin-resolved angle-resolved photoemission study of spin texture of $TaSi_2$	Takahiro Ito	Nagoya University
48	高温超伝導体の高分解能光電子分光	藤森　淳	東京大学	大学院理学系研究科	Ultra-high resolution photoemission spectroscopy on high Tc superconductor	Atsushi Fujimori	The University of Tokyo
49	60-eV レーザーを用いた時間分解光電子分光の開発	石坂　香子	東京大学	大学院工学系研究科	The development of time-resolved photoemission using 60 eV laser	Kyoko Ishizaka	The University of Tokyo
50	トポロジカル超伝導体の探索	坂野　昌人	東京大学	大学院工学系研究科	Search for topological insulators	Masato Sakano	The University of Tokyo
51	鉄系超伝導体のレーザー光電子分光	下志万　貴博	理化学研究所	創発物性科学研究センター	Laser-ARPES on Fe superconductor	Takahiro Shimojima	The University of Tokyo
52	高分解能光電子分光による強相関物質の研究	横谷　尚睦	岡山大学	大学院自然科学研究科	Ultra-high resolution study on strongly correlated materials	Takayoshi Yokoya	Okayama University
53	有機化合物の光電子分光	金井　要	東京理科大学	理工学部	Photoemission study on organic compounds	Kaname Kanai	Tokyo University of Science
54	重い電子系ウラン化合物の高分解能光電子分光	藤森　伸一	日本原子力研究開発機構	物質科学研究センター	Ultra high resolution photoemission study on heavy fermion Uranium compounds	Shinichi Fujimori	Japan Atomic Energy Agency
55	レーザー光電子分光による酸化物薄膜の研究	津田　俊輔	物質・材料研究機構	機能性材料研究拠点	Laser-Photoemission Study on Oxide Films	Shunsuke Tsuda	National Institute for Materials Science
56	Mn 化合物の時間分解光電子分光	大川　万里生	東京理科大学	理学部	Time resolved Photoemission on Mn compounds	Mario Okawa	Tokyo University of Science
57	収差補正型光電子顕微鏡の建設と利用研究	小嗣　真人	東京理科大学	基礎工学部	Construction and utilization research of aberration correction photoelectron emission microscopy	Masato Kotsugi	Tokyo University of Science
58	時間分解・マイクロビームラインの開発と研究	室　隆桂之	高輝度光科学研究センター	応用分光物性グループ	Development of micr- and time-resolved beamline	Takayuki Muro	Japan Synchrotron Radiation Institute
59	時間分解光電子顕微分光実験の技術開発	木下　豊彦	高輝度光科学研究センター	利用研究促進部門	Technical development of time-resolved photoemission microscopy measurement	Toyohiko Kinoshita	Japan Synchrotron Radiation Institute

No.	課題名	氏名	所属		Title	Name	Organization
60	光電子分光法を用いた各種分子性結晶の電子状態の研究及び装置の低温化	木須　孝幸	大阪大学	大学院基礎工学研究科	Research on electron state of molecular crystals using photoemission spectroscopy	Takayuki Kisu	Osaka University
61	トポロジカル絶縁体の電子状態の解明	木村　昭夫	広島大学	大学院理学研究科	Electronic-structure study of topological insulators	Akio Kimura	Hiroshima University
62	時間分解光電子分光を用いた強相関係物質の研究	溝川　貴司	早稲田大学	理工学術院	Time-resolved photoemmission study on strongly-correlated materials	Takashi Mizokawa	Waseda University
63	Si(111) 上単層タリウムの高次高調波を用いた時間分解光電子分光	坂本　一之	千葉大学	大学院融合科学研究科	Time-reslved ARPES investigation of monolayer Thallium on Si(111)	Kszuyuki Sakamoto	Chiba University
64	インジウム原子層超伝導体におけるラシュバスピン分裂の直接観察	内橋　隆	物質・材料研究機構	国際ナノアーキテクトニクス研究拠点	Direct observation of Rashba effect-induced spin splitting in an indium atomic-layer superconductor	Takashi Uchihashi	National Institute for Materials Science
65	固体中のマヨラナ粒子の研究	佐藤　昌利	京都大学	基礎物理学研究所	Study of Majorana Fermion in Solids by Laser Photoemission Spectroscopy	Masatoshi Sato	Kyoto University
66	〃	松田　祐司	京都大学	大学院理学研究科	〃	Yuji Matsuda	Kyoto University
担当所員：秋山　英文							
67	水溶液における新奇ケージドルシフェリンの励起状態の解明	薄倉　淳子	東京理科大学	理学部	Elucidation of absorption spectra for newfangied caged luciferin in aqueous solution	Junko Usukura	Tokyo University of Science
担当所員：松田　巌							
68	スピン分解光電子分光の測定技術開発	木村　昭夫	広島大学	大学院理学研究科	Technical development of spin-resolved photoemission spectroscopy measurement	Akio Kimura	Hiroshima University
69	共鳴磁気光学カー効果の散乱理論研究	田口　宗孝	奈良先端科学技術大学院大学	物質創成科学研究科	Study of scattering theory for the resonant magneto-optical Kerr effect	Taguchi Munetaka	Nara Institute of Science and Technology
70	時間分解磁気光学実験の技術開発	小嗣　真人	東京理科大学	基礎工学部	Technical development of time-resolved magneto-optical experiment	Masato Kotsugi	Tokyo University of Science
担当所員：原田　慈久							
71	液中プラズマ印加水の軟Ｘ線吸収 / 発光分光技術開発	寺嶋　和夫	東京大学	大学院新領域創成科学研究科	Technical development of soft X-ray absorption/emission spectroscopy for water processed by in-liquid plasma	Kazuo Terashima	The University of Tokyo
72	液中プラズマ印加によるナノ粒子分散特性評価と軟Ｘ線分光	伊藤　剛仁	東京大学	大学院新領域創成科学研究科	Characterization of nano-particle distribution in water processed by in-liquid plasma and soft X-ray spectroscopy	Tsuyohito Ito	The University of Tokyo
73	二次元原子薄膜トランジスタの電子状態のナノ分析（Ⅰ）	吹留　博一	東北大学	電気通信研究所	Nanoscale analysis of electronic states of graphene device	Hirokazu Fukidome	Tohoku University

No.	課題名	氏名	所属		Title	Name	Organization
74	軟 X 線発光・共鳴非弾性散乱分光の磁気円・線二色性測定システムの構築	菅　滋正	大阪大学	産業科学研究所	Construction of a noble system for circular and linear dichroism in soft X-ray emission and RIXS spectroscopy	Shigemasa Suga	Osaka University
75	軟 X 線吸収／発光分光法によるリチウムイオン電池電極材料の電子物性研究	細野　英司	産業技術総合研究所	省エネルギー研究部門	Study on the electronic property of electrode materials for Li-ion batteries by soft X-ray absorption/emission spectroscopy	Eiji Hosono	National Institute of Advanced Industrial Science and Technology
76	〃	朝倉　大輔	産業技術総合研究所	エネルギー技術研究部門	〃	Daisuke Asakura	National Institute of Advanced Industrial Science and Technology
77	高分解能光電子分光による酸化バナジウムの研究	藤原　秀紀	大阪大学	大学院基礎工学研究科	Study on vanadium oxides by high resolution Photoemission	Hidenori Fujiwara	Osaka University
78	省エネ・創エネ・蓄電デバイスのオペランド分光	尾嶋　正治	東京大学	放射光分野融合国際卓越拠点	Operando nano-spectroscopy for energy efficient, power generation and energy storage devices	Masaharu Oshima	The University of Tokyo
担当所員：和達　大樹							
79	時間分解吸収分光による $EuNi_2(Si_{1-x}Ge_x)_2$ の価数転移ダイナミクスの解明	三村　功次郎	大阪府立大学	大学院工学研究科	Dynamics of valence transition in $EuNi_2(Si_{1-x}Ge_x)_2$ revealed by time-resolved XAS	Kojiro Mimura	Osaka Prefecture University
80	三次元 nanoESCA による実デバイスのオペランド電子状態解析	永村　直佳	物質・材料研究機構	先端材料解析研究拠点	Operando analysis of the electronic structure of actual devices by 3DnanoESCA	Naoka Ngamura	National Institute for Materials Science
81	コヒーレント共鳴軟 X 線散乱による磁気ドメイン構造の観測	山崎　裕一	物質・材料研究機構	情報統合型物質・材料研究拠点	Observation of magnetic domain structure for ferromagnetic thin films by means of resonant scatterin	Yuichi Yamasaki	The University of Tokyo

一般研究員 / General Researcher

No.	課題名	氏名	所属		Title	Name	Organization
担当所員：榊原　俊郎							
1	強相関電子系化合物の秩序相に対する結晶対称性および電子軌道の効果	横山　淳	茨城大学	理学部	Effects of crystal symmetry and electronic state in ordered phase of strongly correlated electron systems	Makoto Yokoyama	Ibaraki University
2	〃	大島　佳樹	茨城大学	大学院理工学研究科	〃	Yoshiki Oshima	Ibaraki University
3	新規量子磁性体の低温物性	山口　博則	大阪府立大学	大学院理学系研究科	Low temperature physical properties of new quantum spin materials	Hironori Yamaguchi	Osaka Prefecture University
4	〃	岡部　俊輝	大阪府立大学	大学院理学系研究科	〃	Toshiki Okabe	Osaka Prefecture University
5	極低温精密物性測定によるイジング反強磁性体 $SmPt_2Si_2$ の磁気相図の研究	田山　孝	富山大学	大学院理工学研究部	Magnetic diagram of Ising antiferromagnet $SmPt_2Si_2$ studied by low-temperature physical property measurements	Takashi Tayama	University of Toyama

No.	課題名	氏名	所属		Title	Name	Organization
6	〃	小柳　大士	富山大学	大学院理工学教育部	〃	Taishi Oyanagi	University of Toyama
7	磁気フラストレートした一次元量子スピン系 $Rb_{2-x}Cs_xCu_2Mo_3O_{12}$ の非磁性状態と反強磁性状態	安井　幸夫	明治大学	理工学部	Antiferromagnetic State and Non-magnetic State of Magnetically Frustrated One-dimensional Quantum Spin System $Rb_{2-x}Cs_xCu_2Mo_3O_{12}$	Yukio Yasui	Meiji University
8	$(U,Th)Be_{13}$ 及び $U(Pd,Ni)_2Al_3$ を含む重い電子系超伝導体における対称性と磁気応答に関する研究	清水　悠晴	東北大学	金属材料研究所	Superconducting symmetry and magnetic response of uranium heavy-fermion systems $(U,Th)Be_{13}$ and $U(Pd,Ni)_2Al_3$	Yusei Shimizu	Tohoku University
9	$Tb_2Ti_2O_7$ のスピン液体と量子臨界点	高津 浩	京都大学	大学院工学研究科	A quantum spin liquid state and quantum critical point in $Tb_2Ti_2O_7$	Hiroshi Takatsu	Kyoto University
10	比熱測定による鉄系超伝導体の超伝導対称性の研究	加瀬　直樹	東京理科大学	理学部	Superconducting gap symmetry of the Fe-based superconductors from specific heat measurements	Naoki Kase	Tokyo University of Science
11	重い電子系イッテルビウム化合物の超伝導探査	大原　繁男	名古屋工業大学	大学院工学研究科	Study of superconductivity in heavy-fermion ytterbium compound	Shigeo Ohara	Nagoya Institute of Technology
12	〃	兵藤　一志	名古屋工業大学	大学院工学研究科	〃	Kazushi Hyodo	Nagoya Institute of Technology
担当所員：長田　俊人							
13	トポロジカル絶縁体・超伝導体の輸送特性	矢口　宏	東京理科大学	理工学部	Transport properties of topological insulators and topological superconductors	Hiroshi Yaguchi	Tokyo University of Science
14	〃	北澤　翔一	東京理科大学	大学院理工学研究科	〃	Kitazawa Shouichi	Tokyo University of Science
15	混晶 $Bi_{1-x}Sb_x$ のキャリア数制御のための磁場中輸送特性測定	矢口　宏	東京理科大学	理工学部	Transport measurements of $Bi_{1-x}Sb_x$ alloys in magnetic fields for tuning the carrier concentrations	Hiroshi Yaguchi	Tokyo University of Science
16	〃	仁野平　諒	東京理科大学	大学院理工学研究科	〃	Ryo Ninohira	Tokyo University of Science
担当所員：山下　穣							
17	超低温における dHvA 効果測定	宍戸　寛明	大阪府立大学	大学院工学研究科	dHvA effect measurements at ultra-low temperatures	Hiroaki Shishido	Osaka Prefecture University
18	超流動 ^{3}He 中のスピン流と電場の交差相関の探索	山口　明	兵庫県立大学	大学院物質理学研究科	Study of cross-correlation between spin flow and electric field in superfluid ^{3}He	Akira Yamaguchi	University of Hyogo
19	〃	村川　智	東京大学	低温センター	〃	Satoshi Murakawa	The University of Tokyo
20	〃	白濱　圭也	慶應義塾大学	理工学部	〃	Keiya Shirahama	Keio University

No.	課題名	氏名	所属		Title	Name	Organization
21	銅酸化物高温超伝導体の局所磁化測定	芝内　孝禎	東京大学	大学院新領域創成科学研究科	Local magnetization measurements on high-T_c superconductors	Takasada Shibauchi	The University of Tokyo
22	〃	向笠　清隆	東京大学	大学院新領域創成科学研究科	〃	Kiyotaka Mukasa	The University of Tokyo
担当所員：勝本　信吾							
23	ナノ・マイクロセンシングデバイスに関する研究	米谷　玲皇	東京大学	大学院新領域創成科学研究科	Research on nano- and microsensing devices	Reo Kometani	The University of Tokyo
24	〃	上木　瞭太郎	東京大学	大学院新領域創成科学研究科	〃	Ryotaro Ueki	The University of Tokyo
25	〃	関根　瑞恵	東京大学	大学院工学系研究科	〃	Sekine Mizue	The University of Tokyo
26	〃	塔下　大嗣	東京大学	大学院工学系研究科	〃	Taishi Toshita	The University of Tokyo
27	〃	奥野　将人	東京大学	大学院工学系研究科	〃	Masato Okuno	The University of Tokyo
28	〃	田中　航大	東京大学	大学院工学系研究科	〃	Kodai Tanaka	The University of Tokyo
29	〃	吉原　健太	東京大学	大学院工学系研究科	〃	Kenta Yoshihara	The University of Tokyo
30	二次元銅酸化物のホール係数測定	神戸　士郎	山形大学	大学院理工学研究科	Hall coefficient measurement of 2D curates	Shiro Kambe	Yamagata University
31	〃	島袋　義仁	山形大学	大学院理工学研究科	〃	Yoshihito Shimabukuro	Yamagata University
32	レーザーアブレーションにおけるアブレーション条件の最適化とそのエッチング評価	羽山 和美	東京大学	大気海洋研究所	Optimization of the ablation condition by laser ablation, and its evaluation of etching	Kazumi Hayama	The University of Tokyo
担当所員：大谷　義近							
33	空間反転対称性の破れた結晶・磁気構造に発現する新奇電流応答	木俣　基	東北大学	金属材料研究所	Novel current response in non-centrosymmetric crystal and magnetic structures	Motoi Kimata	Tohoku University
担当所員：小森　文夫							
34	Al-Pd-Ru 準結晶・近似結晶における空孔濃度の研究	金沢　育三	東京学芸大学	自然科学系	Positron-annihilation studies of Al-Pd-Mn quasicrystal and its approximant crystals	Ikuzo Kanazawa	Tokyo Gakugei University

No.	課題名	氏名	所属		Title	Name	Organization
35	〃	中島　諒	東京学芸大学	大学院教育学研究科	〃	Makoto Nakajima	Tokyo Gakugei University
36	〃	木村　薫	東京大学	大学院新領域創成科学研究科	〃	Kaoru Kimura	The University of Tokyo
37	〃	大島　永康	産業技術総合研究所	分析計測標準研究部門	〃	Nagayasu Oshima	Advanced Industrial Science
38	SiC 表面上の２次元 Sn および Pb 層の構造および電子状態の解明	田中　悟	九州大学	大学院工学研究院	Analyses of 2D-Sn and Pb layers on SiC surfaces	Satoru Tanaka	Kyushu university
39	〃	安藤　寛	九州大学	大学院工学府	〃	Hiroshi Ando	Kyushu university
40	グラフェンナノリボンの電子状態の観察	田中　悟	九州大学	大学院工学研究院	Analysis of electronic structures in graphene nanoribbons	Satoru Tanaka	Kyushu university
41	〃	林　真吾	九州大学	大学院工学府	〃	Shingo Hayashi	Kyushu university
42	グラフェンナノリボンの STM/STS による解析	ビシコフスキー　アントン	九州大学	大学院工学研究院	Analyses of graphene nanoribbons by STS/STS	Visikovskiy Anton	Kyushu University
43	〃	福間　洸平	九州大学	大学院工学府	〃	Kouhei Fukuma	Kyushu University
44	金属／半導体表面上の超薄膜およびナノ構造薄膜の磁化ダイナミックスの磁気光学的測定	河村　紀一	日本放送協会	放送技術研究所	Study on magnetic dynamics of ultra-thin films and nano-structures on metal / semiconductor surfaces	Norikazu Kawamura	NHK Science and Technology Research Laboratories
45	STM を用いた L10-FeNi 表面における N サーファクタント効果の解析	小嗣　真人	東京理科大学	基礎工学部	Study of N surfactant effect on L10-FeNi by using STM	Masato Kotsugi	Tokyo University of Science
46	〃	齊藤　真博	東京理科大学	大学院基礎工学研究科	〃	Masahiro Saito	Tokyo University of Science
47	近藤トポロジカル絶縁体 SmB_6 の Sm 終端面電子状態の吸着原子や分子による変化を探る走査トンネル顕微分光	菅　滋正	大阪大学	産業科学研究所	Scanning tunneling microscopy/spectroscopy of atom/molecule adsorbed Sm terminated (001)surface of SmB_6	Shigemasa Suga	Osaka University
48	Cu(001) 面上に形成した金属窒化物単原子層の構造	山田　正理	中央大学	理工学部	Structure of monolayer metal nitrides on Cu(001)	Masamichi Yamada	Chuo University
49	$Si(111)_4 \times 1$-In 基板上における In-Bi 表面合金の電子状態	中辻　寛	東京工業大学	物質理工学院	Electronic structure of In-Bi surface alloy grown on $Si(111)_4 \times 1$-In substrates	Kan Nakatsuji	Tokyo Institute of Technology
50	〃	下川　裕理	東京工業大学	物質理工学院	〃	Yuri Shimokawa	Tokyo Institute of Technology
51	SiC(0001）上の Bi 吸着状態の構造および電子状態の解析	田中　悟	九州大学	大学院工学研究院	Analyses of structure and electronic states of Bi atoms on SiC(0001).	Satoru Tanaka	Kyushu University

No.	課題名	氏名	所属		Title	Name	Organization
52	〃	尾家　翔太郎	九州大学	大学院工学府	〃	Shotaro Oie	Kyushu University
担当所員：吉信　淳							
53	赤外吸収による水素終端 Si(110)-(1 × 1) 表面の H-Si 伸縮振動モードの解明	須藤　彰三	東北大学	大学院理学研究科	H-Si stretching modes on the hydrogen-terminated Si(110)-(1 × 1) surface studied by infrared absorption spectroscopy	Suto Shozo	Tohoku University
54	〃	河野　純子	東北大学	大学院理学研究科	〃	Kono Junko	Tohoku University
担当所員：長谷川　幸雄							
55	エピタキシャルシリセン、ゲルマネン及びそのヘテロ構造の低温走査トンネル顕微鏡観察	高村　由起子	北陸先端科学技術大学院大学	マテリアルサイエンス系	STM investigation of epitaxial silicene, germanene, and their heterostructures	Yukiko Yamada-Takamura	Advanced Institute of Science and Technology
56	〃	アントワーヌ　フロランス	北陸先端科学技術大学院大学	マテリアルサイエンス系	〃	Antoine Fleurence	Advanced Institute of Science and Technology
57	〃	米澤　隆宏	北陸先端科学技術大学院大学	マテリアルサイエンス系	〃	Takahiro Yonezawa	Advanced Institute of Science and Technology
58	重い電子系超伝導の実空間観察のための超低温・強磁場の小型 STM の開発	河江　達也	九州大学	大学院工学研究院	Development of a miniature STM for low-temperature and high-magnetic-field measurements of heavy fermion superconductors	Tatsuya Kawae	Kyushu University
59	〃	志賀　雅亘	九州大学	大学院工学府	〃	Shiga Masanobu	Kyushu University
60	〃	沖村　健吾	九州大学	大学院工学府	〃	Okimura Kengo	Kyushu University
61	サイズ制御したナノクラスターの低温 STM による物性評価	江口　豊明	東北大学	大学院理学研究科	Low-temperature STM study of size-controlled nanoclusters	Toyoaki Eguchi	Tohoku University
担当所員：リップマー　ミック							
62	Co ドープ $LaAlO_3/SrTiO_3$ 界面の構造と物性の解明	李　美希	奈良先端科学技術大学院大学	物質創成科学研究科	Investigation of the structure and physical properties of Co-doped $LaAlO_3/SrTiO_3$ interface	Mihee Lee	Nara Insttitute of Science and Technology
63	傾斜組成エピタキシャル強誘電体薄膜の構造と物性	丸山　伸伍	東北大学	大学院工学研究科	Structural and physical property characterization of graded-composition epitaxial ferroelectric thin films	Shingo Maruyama	Tohoku University
64	〃	原田　龍馬	東北大学	大学院工学研究科	〃	Ryoma Harada	Tohoku University
65	エピタキシャル $(Ba,Sr)TiO_3$ 薄膜の歪みが焦電効果に及ぼす影響の解明	山田　智明	名古屋大学	大学院工学研究科	Clarification of influence of strain on pyroelectric effect in epitaxial $(Ba,Sr)TiO_3$ thin films	Tomoaki Yamada	Nagoya University

No.	課題名	氏名	所属		Title	Name	Organization
66	〃	松尾　翔吾	名古屋大学	大学院工学研究科	〃	Shogo Matsuo	Nagoya University
担当所員：川島　直輝							
67	擬一次元反強磁性スピン模型の離散磁気励起	鈴木　隆史	兵庫県立大学	大学院工学研究科	Discretized magnetic excitations in quasi one-dimensional antiferromagnetic spin models	Takafumi Suzuki	University of Hyogo
68	テンソルネットワーク繰り込み群法の応用	原田　健自	京都大学	大学院情報学研究科	Application of tensor renormalization group method	Keiji Harada	Kyoto University
担当所員：上床　美也							
69	YbH_{2+x} の磁性と伝導	中村　修	岡山理科大学	研究・社会連携センター	Magnetic and transport properties in YbH_{2+x}	Osamu Nakamura	Okayama University of Science
70	MnNiGe-CoNiGe 系化合物の圧力下電気抵抗率測定	伊藤　昌和	鹿児島大学	大学院理工学研究科	Electric resistivity of MnNiGe-CoNiGe under pressure	Masakazu Ito	Kagoshima University
71	〃	恩田　圭二朗	鹿児島大学	大学院理工学研究科	〃	Keijiro Onda	Kagoshima University
72	有機分子性導体の高圧物性の研究	鳥塚　潔	武蔵野大学	教育学部	Studies on High Pressure Properties of Organic Molecular Conductors	Kiyoshi Torizuka	Musashino University
73	混合原子価バナジウム燐酸化物の単結晶の圧力下磁気・輸送特性	小林　慎太郎	名古屋大学	大学院工学研究科	Magnetic and transport properties of single crystals of a mixed-valent vanadium phosphorus oxide under pressure	Shintaro Kobayashi	Nagoya University
74	Ni-Mn-Ga 系ホイスラー合金の電気伝導と磁気特性に関する研究	江藤　徹二郎	久留米工業大学	建築・設備工学科	Study of electrical conduction and magnetic properties in Ni-Mn-Ga Heusler alloys	Tetsujiro Eto	Kurume Institute of Technology
75	高圧下における Eu 化合物の価数転移の探索	大貫　惇睦	琉球大学	理学部	Investigation of valence transition on Eu compounds under high pressure	Yoshichika Onuki	University of the Ryukyus
76	〃	本多　史憲	東北大学	金属材料研究所	〃	Fuminori Honda	Tohoku University
77	不純物を用いた高圧氷 VI 相の秩序化の観測	山根　崚	東京大学	大学院理学系研究科	Observation of ordering of ice VI using impurities under high pressure	Yamane Ryo	The University of Tokyo
78	多形化合物 RIr_2Si_2(R= 希土類）の結晶育成と物質評価 3	繁岡　透	山口大学	大学院創成科学研究科	Crystal growth and characterization of polymorphic compounds RIr_2Si_2(R=rare earth) 3	Toru Shigeoka	Yamaguchi University
79	〃	内間　清晴	沖縄キリスト教短期大学	総合教育系	〃	Kiyoharu Uchima	Okinawa Christian Junior College
80	三元化合物 $PrPd_2Si_2$ の結晶育成	繁岡　透	山口大学	大学院創成科学研究科	Crystal growth of ternary compound $PrPd_2Si_2$	Toru Shigeoka	Yamaguchi University

No.	課題名	氏名	所属		Title	Name	Organization
81	〃	内間　清晴	沖縄キリスト教短期大学	総合教育系	〃	Kiyoharu Uchima	Okinawa Christian Junior College
82	多形化合物 RIr_2Si_2(R= 希土類) の磁気特性	内間　清晴	沖縄キリスト教短期大学	総合教育系	Magnetic characteristics of polymorphic compounds RIr_2Si_2(R=rare earth)	Kiyoharu Uchima	Okinawa Christian Junior College
83	〃	繁岡　透	山口大学	大学院創成科学研究科	〃	Toru Shigeoka	Yamaguchi University
84	鉄カルコゲナイド系低次元化合物の探索とその圧力効果	久田　旭彦	徳島大学	大学院社会産業理工学研究部	Synthesis and pressure-effect study of low-dimensional iron-chalcogenide compound	Hisada Akihiko	Tokushima University
85	DAC を用いた高圧下 X 線回折	狩野　みか	日本工業大学	共通教育系（物理）	X-ray diffraction measurements under high pressure by using a DAC	Mika Kano	Nippon Institute of Technology
86	希土類化合物 Ce_3CoSn_6 の圧力下電気抵抗・磁化測定	脇舎　和平	横浜国立大学	大学院工学研究院	Pressure effects on the magnetic properties of Ce_3CoSn_6	Kazuhei Wakiya	Yokohama National University
87	〃	木村　美波	横浜国立大学	大学院工学府	〃	Minami Kimura	Yokohama National University
88	ウラン化合物の磁性の圧力効果	本多　史憲	東北大学	金属材料研究所	Effect of Pressure on the magnetism of uranium compounds	Fuminori Honda	Tohoku University
89	〃	仲村　愛	東北大学	金属材料研究所	〃	Ai Nakamura	Tohoku University
90	CeAl の圧力下電気抵抗測定	摂待　力生	新潟大学	理学部	Resistivity measurement in CeAl under pressure	Rikio Settai	Niigata University
91	〃	小板橋　拓斗	新潟大学	大学院自然科学研究科	〃	Takuto Koitabashi	Nigata University
92	$HoRh_2Si_2$ 単結晶の輸送特性（2）	藤原　哲也	山口大学	大学院創成科学研究科	Transport property of $HoRh_2Si_2$ II	Tetsuya Fujiwara	Yamaguchi University
93	〃	平山　拓斗	山口大学	大学院創成科学研究科	〃	Takuto Hirayama	Yamaguchi University
94	$EuMn_2Ge_2$ 単結晶の磁化測定	藤原　哲也	山口大学	大学院創成科学研究科	Magnetization measurements of $EuMn_2Ge_2$ single crystal	Tetsuya Fujiwara	Yamaguchi University
95	〃	平山　拓斗	山口大学	大学院創成科学研究科	〃	Takuto Hirayama	Yamaguchi University
96	$HoRh_2Si_2$ の La 置換系化合物の単結晶育成	藤原　哲也	山口大学	大学院創成科学研究科	Single crystal growth of La substituted $HoRh_2Si_2$ compounds	Tetsuya Fujiwara	Yamaguchi University
97	〃	平山　拓斗	山口大学	大学院創成科学研究科	〃	Takuto Hirayama	Yamaguchi University

No.	課題名	氏名	所属		Title	Name	Organization
98	$CeZn_2Ge_2$ 単結晶の磁化測定	藤原　哲也	山口大学	大学院創成科学研究科	Magnetization measurements of $CeZn_2Ge_2$ single crystal	Tetsuya Fujiwara	Yamaguchi University
99	〃	平山　拓斗	山口大学	大学院創成科学研究科	〃	Takuto Hirayama	Yamaguchi University
100	Co 基ホイスラー合金における圧力誘起マルテンサイト変態に関する研究	重田　出	鹿児島大学	大学院理工学研究科	Study on pressure-induced martensitic phase transformation in Co-based Heusler alloys	Iduru Shigeta	Kagoshima University
101	〃	大岡　隆太郎	鹿児島大学	大学院理工学研究科	〃	Ryutaro Ooka	Kagoshima University
102	鉄系超伝導体 $FeSe_{1-x}S_x$ の温度ー圧力ー化学置換量の三次元電子相図の研究	松浦　康平	東京大学	大学院新領域創成科学研究科	Studies on the T-P-x three-dimentional electronic phase diagram of iron-based superconductor $FeSe_{1-x}S_x$	Kohei Matsuura	The University of Tokyo
103	$Yb(Co_{1-x}Ir_x)_2Zn_{20}$ の 基本物性評価	阿曽　尚文	琉球大学	理学部	Evaluation of fundamental physical properties in $Yb(Co_{1-x}Ir_x)_2Zn_{20}$	Naofumi Aso	University of the Ryukyus
104	〃	佐藤　信	琉球大学	大学院理工学研究科	〃	Shin Sato	University of the Ryukyus
105	〃	津堅　涼	琉球大学	大学院理工学研究科	〃	Ryo Tsuken	University of the Ryukyus
106	〃	瑞慶覧　長星	琉球大学	大学院理工学研究科	〃	Chousei Zukeran	University of the Ryukyu
107	$YbCo_2Zn_{20}$ 置換系試料の圧力効果	阿曽　尚文	琉球大学	理学部	Pressure effect of doped $YbCo_2Zn_{20}$ systems	Naofumi Aso	University of the Ryukyus
108	〃	盛島　実竜	琉球大学	大学院理工学研究科	〃	Miiru Morishima	University of the Ryukyus
109	(Mn,Cr) 基三元化合物の磁気特性	三井　好古	鹿児島大学	大学院理工学研究科	Magnetic properties of (Mn,Cr)-based ternary alloys	Yoshifuru Mitsui	Kagoshima University
110	〃	増満　勇人	鹿児島大学	大学院理工学研究科	〃	Hayato Masumitsu	Kagoshima University
111	有機伝導体の物性に対する圧力媒効果	村田　惠三	大阪経済法科大学	21 世紀社会総合研究センター	Effect of pressure medium on the properties of organic conductor	Keizo Murata	Osaka University of Economics and Law
112	高圧力下における Mn 基および Fe 基 4 元磁性体の磁気特性	小山　佳一	鹿児島大学	大学院理工学研究科	Magnetic properties of Mn and Fe-based quaternary magnets under high pressures	Keiichi Koyama	Kagoshima University
113	〃	尾上　昌平	鹿児島大学	大学院理工学研究科	〃	Masahira Onoue	Kagoshima University
114	圧力誘起価数転移の探索と高圧下輸送特性	辺土　正人	琉球大学	理学部	Searching of pressure-induced valence transition and transport properties under high pressure	Masato Hedo	University of the Ryukyus

No.	課題名	氏名	所属		Title	Name	Organization
115	〃	伊覇　航	琉球大学	大学院理工学研究科	〃	Wataru Iha	University of the Ryukyus
116	反転対称性のない遷移金属間化合物とその関連物質の高圧下輸送特性	仲間　隆男	琉球大学	理学部	Transport properties of non-centrosymmetric transition metals compounds under high pressure	Takao Nakama	University of the Ryukyus
117	〃	垣花　将司	琉球大学	大学院理工学研究科	〃	Masashi Kakihana	University of the Ryukyus
118	遷移金属化合物の高圧力下の輸送特性	仲間　隆男	琉球大学	理学部	Pressure effect on transport properties of transition metal compounds	Takao Nakama	University of the Ryukyus
119	〃	川勝　祥矢	琉球大学	大学院理工学研究科	〃	Shoya Kawakatsu	University of the Ryukyus
120	希土類ラーベス化合物 RAl_2 の異方的磁気体積効果	大橋　政司	金沢大学	理工研究域	Anisotropic magnetovolume effect of rare earth Laves compound RAl_2	Masashi Ohashi	Kanazawa University
121	〃	宮川　昌大	金沢大学	大学院自然科学研究科	〃	Masahiro Miyagawa	Kanazawa University
122	強相関電子系化合物における圧力および磁場誘起量子相転移の探索	大橋　政司	金沢大学	理工研究域	Pressure and field induced quantum phase transition in strongly correlated electron systems	Masashi Ohashi	Kanazawa University
123	〃	中西　裕昭	金沢大学	大学院自然科学研究科	〃	Hiroaki Nakanishi	Kanazawa University
124	Co 系ホイスラー合金の電気抵抗測定によるマルテンサイト変態温度の高圧効果	安達　義也	山形大学	大学院理工学研究科	Pressure effect of the martensitic transition temperature by the measurements of the electrical resistivity for the Co-Heusler alloys.	Yoshiya Adachi	Yamagata University
125	〃	小木　雄貴	山形大学	大学院理工学研究科	〃	Yuki Ogi	Yamagata University
126	新規セリウム化合物 $CePd_2Al_8$ における量子臨界点の探索	中島　美帆	信州大学	理学部	Search for quantum critical point in a new Ce compound $CePd_2Al_8$	Miho Nkashima	Shinshu University
127	〃	中村　優希	信州大学	大学院総合理工学研究科	〃	Yuki Nakamura	Shinshu University
担当所員：吉澤　英樹							
128	三角格子反強磁性体 $Li_{1+x}Zn_{2-y}Mo_3O_8$ の磁気励起	那波　和宏	東北大学	多元物質科学研究所	Spin excitations in triangular antiferromagnet $Li_{1+x}Zn_{2-y}Mo_3O_8$	Kazuhiro Nawa	Tohoku University
129	〃	サンドヴィック　キム	東北大学	大学院理学研究科	〃	Sandvik Kim	Tohoku University
130	パイロクロア格子反強磁性体 $Na_3T(CO_3)_2Cl$ の磁性	那波　和宏	東北大学	多元物質科学研究所	Magnetism of pyrochlore antiferromagnet $Na_3T(CO_3)_2Cl$	Kazuhiro Nawa	Tohoku University

No.	課題名	氏名	所属		Title	Name	Organization
131	〃	村崎　遼	東北大学	大学院理学研究科	〃	Ryo Murasaki	Tohoku University
132	歪んだ籠目格子系 $Yb_3Ni_{11}Ge_4$ の低温比熱	佐藤　卓	東北大学	多元物質科学研究所	Low-temperature heat capacity of the distorted kagome-lattice compound $Yb_3Ni_{11}Ge_4$	Taku J Sato	Tohoku University
133	〃	那波　和宏	東北大学	多元物質科学研究所	〃	Kazuhiro Nawa	Tohoku University
134	〃	高橋　満	東北大学	大学院理学研究科	〃	Mitsuru Takahashi	Tohoku University
135	$YbCo_2Zn_{20}$ 置換系試料の極低温比熱測定 III	阿曽　尚文	琉球大学	理学部	Specific heat measurement at very low temperature on $YbCo_2Zn_{20}$ systems III	Naofumi Aso	University of the Ryukyus
136	〃	諸見里　真嗣	琉球大学	大学院理工学研究科	〃	Masatsugu Moromizato	University of the Ryukyus
137	〃	瑞慶覧　長星	琉球大学	大学院理工学研究科	〃	Chousei Zukeran	University of the Ryukyus
担当所員：益田　隆嗣							
138	Ce_5Si_3 単結晶試料の高エネルギー X 線ラウエ装置による結晶方位同定	小林　理気	琉球大学	理学部	Alignment of Ce_5Si_3 single crystals by high-energy X-ray Laue diffaction	Riki Kobayashi	University of the Ryukyus
139	中性子非弾性散乱実験に向けた単結晶試料の軸立て	阿部　伸行	東京大学	大学院新領域創成科学研究科	Preparation of single crystals for the measurement of inelastic neutron scattering	Nobuyuki Abe	The University of Tokyo
140	〃	松浦　慧介	東京大学	大学院新領域創成科学研究科	〃	Keisuke Matsuura	The Universisty of Tokyo
141	〃	近江　毅志	東京大学	大学院新領域創成科学研究科	〃	Tsuyoshi Omi	The University of Tokyo
142	〃	荒木　勇介	東京大学	大学院新領域創成科学研究科	〃	Araki Yusuke	The University of Tokyo
143	〃	吉澤　孟晃	東京大学	大学院新領域創成科学研究科	〃	Takeaki Yoshizawa	The University of Tokyo
144	熱電材料 SnSe 系の単結晶の軸立て	萩原　雅人	高エネルギー加速器研究機構	物質構造科学研究所	Crystal alignment of thermoelectric material system SnSe	Masato Hagihara	High Energy Accelerator Research Organization
145	蜂の巣格子量子磁性体 $RuCl_3$ の結晶方位決定	田中　秀数	東京工業大学	理学院	Determination of crystallographic orientation of honeycomb-lattice quantum magnet $RuCl_3$	Hidekazu Tanaka	Tokyo Institute of Technology
担当所員：嶽山　正二郎							

No.	課題名	氏名	所属		Title	Name	Organization
146	磁気光学測定を用いたハロゲン化金属ペロブスカイト型結晶の励起子特性の研究	中村　唯我	東京大学	大学院工学系研究科	Study on excitonic properties of organometallic lead halide perovskite using magneto-optic mesurement	Yuiga Nakamura	The University of Tokyo
147	超強磁場磁気光学による $Cu_3Mo_2O_9$ の磁化プラトーの研究 II	黒江　晴彦	上智大学	理工学部	Ultra-high magnetic field magneto-optical approach to the study of magnetization plateau in $Cu_3Mo_2O_9$ using vertical single-turn coil system II	Haruhiko Kuroe	Sophia University
担当所員：金道　浩一							
148	重い電子系化合物が示す非従来型超伝導と磁性の相関	横山　淳	茨城大学	理学部	Interplay between unconventional superconductivity and magnetism in heavy-fermion compounds	Makoto Yokoyama	Ibaraki University
149	〃	鈴木　康平	茨城大学	大学院理工学研究科	〃	Kohei Suzuki	Ibaraki University
150	新規カゴメ格子フッ化物の磁性	植田　浩明	京都大学	大学院理学研究科	Magnetism of novel fluorides with a kagome lattice	Hiroaki Ueda	Kyoto University
151	〃	白上　龍	京都大学	大学院理学研究科	〃	Ryu Shirakami	Kyoto University
152	MnNiGe-CoNiGe 系化合物の高磁場磁化測定	伊藤　昌和	鹿児島大学	大学院理工学研究科	High magnetic field magnetization of MnNiGe-CoNiGe system	Masakazu Ito	Kagoshima University
153	〃	恩田　圭二朗	鹿児島大学	大学院理工学研究科	〃	Keijiro Onda	Kagoshima University
154	幾何学的フラストレート磁性体の強磁場磁化測定	菊池　彦光	福井大学	学術研究院工学系部門	Magnetization measurements of the frustrated magnets	Hikomitsu Kikuchi	University of Fukui
155	〃	三浦　俊亮	福井大学	大学院工学研究科	〃	Shunsuke Miura	University of Fukui
156	新規イッテルビウム化合物の量子臨界点近傍における強磁場磁化測定	道岡　千城	京都大学	大学院理学研究科	High-field magnetization of novel Yb based compounds in the vicinity of the quantum critical point	Chishiro Michioka	Kyoto University
157	〃	引地　将仁	京都大学	大学院理学研究科	〃	Masahito Hikiji	Kyoto University
158	サブメガガウス領域での希土類物性研究	海老原　孝雄	静岡大学	学術院理学領域	Physical property of rare earth compounds at pulse magnet	Takao Ebihara	Shizuoka University
159	〃	村串　拓真	静岡大学	大学院総合科学技術研究科	〃	Takuma Murakoshi	Shizuoka University
160	$(U,Th)Be_{13}$, $U(Pd,Ni)_2Al_3$ 及び関連する重い電子系化合物における強磁場物性	清水　悠晴	東北大学	金属材料研究所	High-field physical properties of $(U,Th)Be_{13}$, $U(Pd,Ni)_2Al_3$, and other heavy-fermion systems	Yusei Shimizu	Tohoku University
161	$BiCh_2$ 系超伝導体の異常に大きな上部臨界磁場	加瀬　直樹	東京理科大学	理学部	Upper critical field of the $BiCh_2$-based superconductors	Naoki Kase	Tokyo University of Science

No.	課題名	氏名	所属		Title	Name	Organization
162	MnCoGe 基化合物の磁気相転移	三井　好古	鹿児島大学	大学院理工学研究科	Magnetic phase transition of MnCoGe-based compound	Yoshifuru Mitsui	Kagoshima University
163	〃	尾上　昌平	鹿児島大学	大学院理工学研究科	〃	Masahira Onoue	Kagoshima University
164	熱物性測定プローブの開発と低温強磁場中での性能評価	小野　俊雄	大阪府立大学	大学院理学系研究科	Development and performance evaluation of the measuring probe for thermophysical properties	Toshio Ono	Osaka Prefecture University
165	〃	柴田　尚樹	大阪府立大学	大学院理学系研究科	〃	Yoshiki Shibata	Osaka Prefecture University
166	金属ナノ結晶の磁化特性	稲田　貢	関西大学	システム理工学部	Magnetic properties of metal nanocrystals	Mitsuru Inada	Kansai University
167	〃	越田　樹	関西大学	システム理工学部	〃	Tatsuki Koshida	Kansai University
168	金属ナノクラスターネットワークの磁気抵抗測定	稲田　貢	関西大学	システム理工学部	Electronic transport properties of metal cluster networks under high-magnetic field	Mitsuru Inada	Kansai University
169	〃	森脇　有哉	関西大学	システム理工学部	〃	Yuya Moriwaki	Kansai University
170	近藤半導体 (Yb, R)B_{12} (R=Zr, Sc, Y) の 80T 級磁場下での強磁場物性	伊賀　文俊	茨城大学	理学部	High field physical property of Kondo insulator (Yb, R)B_{12} (R=Zr, Sc, Y) up to 80T class by using the pulse magnet	Fumitoshi Iga	Ibaraki University
171	〃	横道　啓省	茨城大学	大学院理工学研究科	〃	Keisei Yokomichi	Ibaraki University
172	topological insulator SmB_6,YbB_{12} の磁化特性と比熱	伊賀　文俊	茨城大学	理学部	Magnetic and thermal properties of topological insulator SmB_6 and YbB_{12}	Fumitoshi Iga	Ibaraki University
173	〃	平野　航	茨城大学	大学院理工学研究科	〃	Wataru Hirano	Ibaraki University
174	高圧合成希土類 6 及び 12 ホウ化物の磁化特性と比熱	伊賀　文俊	茨城大学	理学部	Magnetic and thermal properties of rare earth hexa-borides and dodeca-borides produced by high pressure synthesis	Fumitoshi Iga	Ibaraki University
175	〃	松浦　航	茨城大学	大学院理工学研究科	〃	Wataru Matsuura	Ibaraki university
176	アルカリ超酸化物 AO_2 の強磁場磁化	神戸　高志	岡山大学	大学院自然科学研究科	High-magnetic field magnetization in alkali-metal superoxide, AO_2	Takashi Kambe	Okayama University
担当所員：徳永　将史							
177	希土類金属間化合物の強磁場物性研究	海老原　孝雄	静岡大学	学術院理学領域	Physical properties in rare earth intermetallic compounds at high magnetic fields	Takao Ebihara	Shizuoka University

No.	課題名	氏名	所属		Title	Name	Organization
178	〃	鈴木　文登	静岡大学	大学院総合科学技術研究科	〃	Suzuki Fumito	Shizuoka University
179	重い電子系における強磁場中の電子状態研究	海老原　孝雄	静岡大学	学術院理学領域	Electronic states at high magnetic fields in Heavy Fermion systems	Takao Ebihara	Shizuoka University
180	〃	ジュマエダ ジャトミカ	静岡大学	大学院総合科学技術研究科	〃	Jumaeda Jatmika	Shizuoka University
181	CoV 基形状記憶合金における磁場誘起マルテンサイト変態とその場組織観察	キョ　キョウ	東北大学	大学院工学研究科	Magnetic field-induced martensitic transformation and in situ observation of microstructure on CoV-based shape memory alloys	Xiao Xu	Tohoku University
182	強磁性体 $Ln_2Co_{12}As_7$ (Ln= 希土類) の強磁場磁化過程の研究	太田　寛人	東京農工大学	大学院工学研究院	Study of magnetization of $Ln_2Co_{12}As_7$ (Ln=lanthanoids) under high magnetic field	Hiroto Ohta	Tokyo University of Agriculture and Technology
183	〃	加藤　優典	東京農工大学	大学院工学府	〃	Yusuke Kato	Tokyo University of Agriculture and Technology
184	パルス強磁場を用いた半金属における磁場誘起電子相転移の研究	矢口　宏	東京理科大学	理工学部	Study of Field-Induced Electronic Phase Transitions in Semimetals Using Pulsed Magnetic Fields	Hiroshi Yaguchi	Tokyo University of Science
185	〃	仁野平　諒	東京理科大学	大学院理工学研究科	〃	Ryo Ninohira	Tokyo University of Science
186	$Ce_nT_mIn_{2m+3n}$(T: 遷移金属) の強磁場磁化測定	摂待　力生	新潟大学	理学部	High-Field magnetization of $Ce_nT_mIn_{2m+3n}$(T: transition metal)	Rikio Settai	Niigata University
187	〃	角田　竜馬	新潟大学	自然科学研究科	〃	Ryoma Tsunoda	Niigata University
188	ウラン化合物の強磁場下における磁気相図の研究	本多　史憲	東北大学	金属材料研究所	Study of magnetic phase diagram on uranium compounds under high magnetic field	Fuminori Honda	Tohoku University
189	〃	仲村　愛	東北大学	金属材料研究所	〃	Ai Nakamura	Tohoku University
190	磁場を用いた液晶における配向および誘電特性制御	木村　剛	東京大学	大学院新領域創成科学研究科	Magnetic control of orientation and dielectricity in liquid crystals	Tsuyoshi Kimura	The University of Tokyo
191	多層ディラック電子系磁性体における量子極限近傍のランダウ準位構造	酒井　英明	大阪大学	大学院理学研究科	Study of Landau level formation near the extreme quantum limit for a layered Dirac magnet	Hideaki Sakai	Osaka University
192	〃	鶴田　圭吾	大阪大学	大学院理学研究科	〃	Keigo Tsuruda	Osaka University
193	〃	西村　拓也	大阪大学	大学院理学研究科	〃	Takuya Nishimura	Osaka University
194	〃	藤村　飛雄吾	大阪大学	大学院理学研究科	〃	Hyugo Fujimura	Osaka University

No.	課題名	氏名	所属		Title	Name	Organization
195	Weyl 半金属 $TrTe_2$(Tr = W, Mo) の高純度単結晶を用いた SdH 振動によるフェルミ面の探索	東中　隆二	首都大学東京	大学院理工学研究科	Investigation of Fermi surface of Weyl semimetal, $TrTe_2$ (Tr = W, Mo) by SdH oscillation	Ryuji Higashinaka	Tokyo Metropolitan University
196	〃	ジャー　ラジャビー	首都大学東京	大学院理工学研究科	〃	Jha Rajveer	Tokyo Metropolitan University
197	〃	大西　翔太	首都大学東京	大学院理工学研究科	〃	Shota Onishi	Tokyo Metropolitan University
198	正四角台塔型反強磁性体の強磁場中電気磁気特性の測定	木村　健太	大阪大学	大学院基礎工学研究科	High-field magnetoelectric properties of square-cupola-based antiferromagnets	Kenta Kimura	Osaka University
199	非破壊パルスマグネットを用いた $Cu_3Mo_2O_9$ の磁化プラトーの Zn 置換効果	黒江　晴彦	上智大学	理工学部	Zn-substitution effects on magnetization plateau in $Cu_3Mo_2O_9$	Haruhiko Kuroe	Sophia University
200	磁性半金属 EuP_3 における超強磁場磁気輸送	高橋　英史	東京大学	大学院工学系研究科	Magnetotransport properties on the magnetic semimetal EuP_3	Hidefumi Takahashi	The University of Tokyo
201	パルス磁場による鉄ヒ素超伝導体の多極子秩序の研究	栗原　綾佑	新潟大学	大学院自然科学研究科	Study of Multipole Ordering in Iron Pnictide Superconductor under Pulse Magnetic Fields	Ryousuke Kurihara	Niigata University
202	極性キラルらせん磁性体における電気磁気効果	徳永　祐介	東京大学	大学院新領域創成科学研究科	Magnetoelectric properties of the polar-chiral helimagnet	Yusuke Tokunaga	The University of Tokyo
203	〃	荒木　勇介	東京大学	大学院新領域創成科学研究科	〃	Yusuke Araki	The University of Tokyo
204	〃	佐藤　樹	東京大学	大学院新領域創成科学研究科	〃	Tasuki Sato	The University of Tokyo
205	キャリア制御した Cd_3As_2 薄膜における量子輸送現象の解明	打田　正輝	東京大学	大学院工学系研究科	Investigation of quantum transport phenomena in Cd_3As_2 films with reduced carriers	Masaki Uchida	The University of Tokyo
206	ホイスラー合金 NiCoMnGa のパルス強磁場磁歪測定及び磁気熱量効果測定	木原　工	東北大学	金属材料研究所	Magnetostriction and Magnetocaloric effect Measurements under the Pulsed High Magnetic fields in Heusler Alloy NiCoMnGa	Takumi Kihara	Tohoku University
207	キラル合金 Mn(Si,Ge) における強磁場まで安定なトポロジカルスピン構造の解明	金澤　直也	東京大学	大学院工学系研究科	Investigation on robust topological spin topological spin textures under high magnetic fields in the chiral alloy Mn(Si,Ge)	Naoya Kanazawa	The University of Tokyo
208	ハニカム構造を持つ $Co_4Ta_2O_9$ の電気磁気効果	阿部　伸行	東京大学	大学院新領域創成科学研究科	Magnetoelectric effect in honeycomb lattice antiferromagnet $Co_4Ta_2O_9$	Nobuyuki Abe	The University of Tokyo
209	ペロフスカイト型 Ir 酸化物における磁気伝導測定	藤岡　淳	東京大学	大学院工学系研究科	Investigation of magneto-transport in perovskite Ir-oxide	Jun Fujioka	The University of Tokyo
210	反強磁性酸化物 / 重金属積層膜に発現する新奇磁気抵抗の解明	木俣　基	東北大学	金属材料研究所	Novel magnetoresistance in antiferromagnetic oxide/heavy metal layers	Motoi Kimata	Tohoku University

担当所員：松田　康弘

No.	課題名	氏名	所属		Title	Name	Organization
211	近藤半導体 (Yb,R)B_{12}、価数揺動物質 (Y,Tm)B_6 のワンターンコイル 120T パルス磁場下での強磁場磁化過程	伊賀　文俊	茨城大学	理学部	High field magnetization of Kondo insulator (Yb,R)B_{12} and valence fluctuation material (Y,Tm)B_6 by using one-turn coil in a 120 T pulse magnet	Fumitoshi Iga	Ibaraki University
担当所員：辛　埴							
212	2 光子角度分解光電子分光による η -Mo_4O_{11} の非占有バンド構造の観測	木村　昭夫	広島大学	大学院理学研究科	Observation of unoccupied band structure of η -Mo_4O_{11} by two-photon ARPES	Akio Kimura	Hiroshima University
213	〃	角田　一樹	広島大学	大学院理学研究科	〃	Kazuki Sumida	Hiroshima University
214	〃	檜垣　聡太	広島大学	大学院理学研究科	〃	Sota Higaki	Hiroshima University
215	非シンモルフィック空間群を持つ TlCuZ (Z=S,Se) 系の時間分解 ARPES	木村　昭夫	広島大学	大学院理学研究科	Time resolved ARPES of non-symmorphic TlCuZ (Z=S,Se)	Akio Kimura	Hiroshima University
216	〃	吉川　智己	広島大学	大学院理学研究科	〃	Tomoki Yoshikawa	Hiroshima University
217	磁性元素をドープしたトポロジカル絶縁体の非平衡表面キャリアダイナミクス	クマール　シヴ	広島大学	放射光科学研究センター	Nonequilibrated surface carrier dynamics in magnetically doped topological insulators	Shiv Kumar	Hiroshima University
218	新規スピントロニクス物質におけるスピン分解角度分解光電子分光	小林　正起	東京大学	大学院工学系研究科	Spin- and angle-resolved photoemission spectroscopy on novel spintronics materials	Masaki Kobayashi	The University of Tokyo
219	LaSnTe の 2 光子光電子分光	ワン　シャオシャオ	広島大学	大学院理学研究科	Two photon photoemission of LaSnTe	Xiaoxiao Wang	Hiroshima University
220	〃	陳　家華	広島大学	大学院理学研究科	〃	Chen Jiahua	Hiroshima University
221	スピン分解角度分解光電子分光による $GdTe_2$ の CDW ギャップ内表面状態の研究	伊藤　孝寛	名古屋大学	シンクロトロン光研究センター	Spin-resolved angle-resolved photoemission study of surface states among CDW gap of $GdTe_2$	Takahiro Ito	Nagoya University
222	〃	近谷　翔汰	名古屋大学	大学院工学研究科	〃	Shota Kontani	Nagoya University
223	トポロジカル半金属におけるスピン偏極した表面状態の観測	坂野　昌人	東京大学	大学院工学系研究科	Observation of spin-polarized surface states on topological semimetals	Masato Sakano	The University of Tokyo
224	〃	三石　夏樹	東京大学	大学院工学系研究科	〃	Natsuki Mitsuishi	The University of Tokyo
225	トポロジカル結晶薄膜のレーザー励起角度光電子分光による表面状態の観察	黒田　眞司	筑波大学	数理物質系	Observation of surface states of topological crystal thin films using laser photoemission spectroscopy	Shinji Kuroda	University of Tsukuba
226	〃	大滝　祐輔	筑波大学	大学院数理物質科学研究科	〃	Yusuke Otaki	University of Tsukuba

No.	課題名	氏名	所属		Title	Name	Organization
227	〃	伊藤　寛史	筑波大学	大学院数理物質科学研究科	〃	Hiroshi Ito	University of Tsukuba
228	新奇超伝導体 $RO_{1-x}F_xBiS_2$(R=La, Ce, Nd) のスピン角度分解光電子分光	奥田　太一	広島大学	放射光科学研究センター	Spin- and angle-resolved photoemission study of $RO_{1-x}F_xBiS_2$ (R=La, Ce, Nd)	Taichi Okuda	Hiroshima University
229	〃	宮本　幸治	広島大学	放射光科学研究センター	〃	Koji Miyamoto	Hiroshima University
230	〃	Wu　Shilong	広島大学	大学院理学研究科	〃	Wu Shilong	Hiroshima University
231	高分解能スピン・角度分解光電子分光によるハーフメタル強磁性体 CoS_2 の電子構造研究	藤原　弘和	岡山大学	大学院自然科学研究科	Study on electronic structures in half-metallic ferromagnet CoS_2 by high-resolution spin- and angle-resolved photoemission spectroscopy	Hirokazu Fujiwara	Okayama University
232	有機半導体分子の吸着に伴って生じるトポロジカル表面状態の変化	金井　要	東京理科大学	理工学部	Modification of Topological surface states upon adsorption of organic semiconductors	Kaname Kanai	Tokyo University of Science
233	〃	水島　啓貴	東京理科大学	大学院理工学研究科	〃	Hirotaka Mizushima	Tokyo University of Science
担当所員：秋山　英文							
234	GaPAsN 混晶のアップコンバージョン発光に関する研究	矢口　裕之	埼玉大学	大学院理工学研究科	Upconversion luminescence from GaPAsN alloys	Hiroyuki Yaguchi	Saitama University
235	〃	高宮　健吾	埼玉大学	総合技術支援センター	〃	Kengo Takamiya	Saitama University
236	〃	高橋　渉	埼玉大学	大学院理工科研究科	〃	Takahashi Wataru	Saitama University
237	ケージドルシフェリンの電子状態の解明	樋山　みやび	群馬大学	大学院理工学府	Elucidation of electronic structure for caged-luciferin	Miyabi Hiyama	Gunma University
担当所員：小林　洋平							
238	フェムト秒レーザー加工を用いた高 Q 値ナノ共振器のポストプロセス検討	高橋　和	大阪府立大学	大学院工学研究科	Postprocess for high-Q photonic crystal nanocavity using ultrashort pulse laser	Yasushi Takahashi	Osaka Prefecture University
239	〃	芦田　紘平	大阪府立大学	大学院工学研究科	〃	Kohei Ashida	Osaka Prefecture University
240	次世代レーザーとレーザー加工の基礎技術研究	鳥塚　健二	産業技術総合研究所	電子光技術研究部門	Basic research on next generation laser systems and laser machining technology	Kenji Torizuka	National Institute of Advanced Industrial Science and Technology
241	〃	黒田　隆之助	産業技術総合研究所	先端オペランド計測技術オープンイノベーションラボラトリ	〃	Ryunosuke Kuroda	National Institute of Advanced Industrial Science and Technology

No.	課題名	氏名	所属		Title	Name	Organization
242	〃	高田　英行	産業技術総合研究所	電子光技術研究部門	〃	Hideyuki Takada	National Institute of Advanced Industrial Science and Technology
243	〃	吉富　大	産業技術総合研究所	電子光技術研究部門	〃	Dai Yoshitomi	National Institute of Advanced Industrial Science and Technology
244	超高速分光用ファイバーレーザーとパルス計測機器の開発	末元　徹	豊田理化学研究所		Development of fiber laser and pulse characterization instrument for ultrafast optical spectroscopy	Tohru Suemoto	Toyota Physical and Chemical Research Institute
担当所員：板谷　治郎							
245	希土類単酸化物薄膜における時間分解コヒーレント反ストークスラマン散乱分光	牧野　哲征	福井大学	学術研究院工学系部門	Time-resolved coherent anti-Stokes Raman scattering spectroscopy in rare-earth monooxide thin films	Takayuki Makino	University of Fukui
246	〃	和座　一憲	福井大学	大学院工学研究科	〃	Kazunori Waza	University of Fukui
247	テラヘルツ分光装置を用いた酸化物磁性材料の研究	大越　慎一	東京大学	大学院理学系研究科	Study of magnetic oxide using terahertz spectroscopy	Shinichi Ohkoshi	The University of Tokyo
248	〃	生井　飛鳥	東京大学	大学院理学系研究科	〃	Asuka Namai	The University of Tokyo
249	〃	吉清　まりえ	東京大学	大学院理学系研究科	〃	Marie Yoshikiyo	The University of Tokyo
大阪大学 先端強磁場科学研究センター / Center for Advanced High Magnetic Field Science Osaka University							
250	キラル反強磁性体 $Rb_2Ni_2(SO_4)_3$ の多周波数 ESR 測定	本田　孝志	高エネルギー加速器研究機構	物質構造科学研究所	Multi-frequency ESR spectroscopy in chiral antiferromagnet	Takashi Honda	High Energy Acceleraor Research Organization
251	新規量子磁性体の強磁場磁性	山口　博則	大阪府立大学	大学院理学系研究科	High-field magnetic properties of new quantum spin materials	Hironori Yamaguchi	Osaka Prefecture University
252	強磁場環境下におけるタンパク質結晶成長	牧　祥	大阪大谷大学	薬学部	Crystal growth of protein under the magnetic field condition	Syou Maki	Osaka Ohtani University
253	一次元カゴメストリップ格子磁性体の強磁場磁化過程	浅野　貴行	福井大学	学術研究院工学系部門	High-Field Magnetization Process of 1D Kagome Strip Lattice Compound	Takayuki Asano	University of Fukui
254	〃	横山　太紀	福井大学	大学院工学研究科	〃	Taiki Yokoyama	University of Fukui
255	フタロシアニン分子系の均一混晶における巨大磁気抵抗の局在スピン効果	花咲　徳亮	大阪大学	大学院理学研究科	Local moment effect on giant magnetoresistance in phthalocyanine mixed crystal	Noriaki Hanasaki	Osaka University
256	〃	石井　龍太	大阪大学	大学院理学研究科	〃	Ryutaro Ishii	Osaka university

No.	課題名	氏名	所属		Title	Name	Organization
257	パルス強磁場を用いた強相関電子系物質の強磁場物性の研究	竹内　徹也	大阪大学	低温センター	Physical properties of strongly correlated electron systems under pulsed high magnetic field	Tetsuya Takeuchi	Osaka University
258	〃	大貫　惇睦	琉球大学	理学部	〃	Yoshichika Onuki	University of Ryukyus
259	反強磁性絶縁体 $BaMn_2Pn_2$ の高磁場における磁気輸送特性	Khuong　Kim Huynh	東北大学	材料科学高等研究所	Magnetotransport properties under high magnetic fields of $BaMn_2Pn_2$ antiferromagnetic insulators	Khuong Kim Huynh	Tohoku University
260	Kitaev 相互作用の卓越した磁性体における電気磁気結合	青山　拓也	東北大学	大学院理学研究科	Magnetoelectric effect in Kitaev magnets	Takuya Aoyama	Tohoku University
261	〃	木村　尚次郎	東北大学	金属材料研究所	〃	Shojiro Kimura	Tohoku University
262	高温超伝導体のパルス強磁場下電流電圧特性	掛谷　一弘	京都大学	大学院工学研究科	Current-voltage characteristics in high-Tc superconductors under pulsed high magnetic fields	Itsuhiro Kakeya	Kyoto University
263	〃	岡本　陸	京都大学	大学院工学研究科	〃	Riku Okamoto	Kyoto University
264	SmB_6 薄膜の強磁場中での磁化，ホール効果測定	宍戸　寛明	大阪府立大学	大学院工学研究科	Magnetization and Hall effect measurements for SmB_6 thin films under high magnetic field	Hiroaki Shishido	Osaka Prefecture University
265	遷移金属含有炭素材料の磁性解明	本多　善太郎	埼玉大学	大学院理工学研究科	Magnetic properties of transition metal containing carbon materials	Zentaro Honda	Saitama University
266	新規な配位子構造を有するコバルト単核単分子磁石の開発	福田　貴光	大阪大学	大学院理学研究科	Development of single-cobalt-ion molecular magnets having novel ligand structures	Takamitsu Fukuda	Osaka University
267	〃	石崎　聡晴	大阪大学	大学院理学研究科	〃	Toshiharu Ishizaki	Osaka University
268	ハニカム格子系 $Li_3Ni_2SbO_6$ および $Na_3Co_2SbO_6$ の磁場誘起相転移	安井　幸夫	明治大学	理工学部	Magnetic field induced magnetic transitions of honeycomb spin systems $Li_3Ni_2SbO_6$ and $Na_3Co_2SbO_6$	Yukio Yasui	Meiji University
269	ジャイロトロンを用いた高圧下多重極限 ESR 装置の開発と応用	櫻井　敬博	神戸大学	研究基盤センター	Development and application of high pressure multi-extreme ESR system using gyrotron	Takahiro Sakurai	Kobe University
270	鉄系超伝導体 $Sr_4V_2O_6Fe_2As_2$ における超伝導異方性 II	中島　正道	大阪大学	大学院理学研究科	Anisotropy of superconductivity in iron-based superconductor $Sr_4V_2O_6Fe_2As_2$ II	Masamichi Nakajima	Osaka University
271	ディラック電子を有する新規反強磁性体における磁化特性の解明	酒井　英明	大阪大学	大学院理学研究科	Measurements of high-field magnetisation for a novel magnet hosting Dirac fermions	Hideaki Sakai	Osaka University
272	$GaFeO_3$ におけるスピン波の非相反性	有馬　孝尚	東京大学	大学院新領域創成科学研究科	Nonreciprocal spin waves in $GaFeO_3$	Takahisa Arima	The University of Tokyo
273	〃	中川　直己	東京大学	大学院新領域創成科学研究科	〃	Naoki Nakagawa	The University of Tokyo

No.	課題名	氏名	所属		Title	Name	Organization
274	〃	近江　毅志	東京大学	大学院新領域創成科学研究科	〃	Tsuyoshi Omi	The University of Tokyo
275	パルス強磁場を用いたワイル半金属の量子輸送特性の研究	村川　寛	大阪大学	大学院理学研究科	Pulsed magnetic field studies of quantum transport properties of Weyl semimetals	Hiroshi Murakawa	Osaka university
276	〃	駒田　盛是	大阪大学	大学院理学研究科	〃	Moriyoshi Komada	Osaka University
277	〃	横井　滉平	大阪大学	大学院理学研究科	〃	Yokoi Kohei	Osaka University
278	固有ジョセフソン接合テラヘルツ発振器の応用利用に関する研究	柏木　隆成	筑波大学	数理物質系	Study of application use of intrinsic Josephson junction THz emitters	Takanari Kashiwagi	University of Tsukuba
279	単結晶 $Ax(NH_3)yFeSe$ 超伝導体 (A = アルカリ金属、アルカリ土類金属）の強磁場下における超伝導物性	神戸　高志	岡山大学	大学院自然科学研究科	Superconducting properties of single-crystal $Ax(NH_3)yFeSe$ under high magnetic field	Takashi Kambe	Okayama University
280	多重極限環境下の電子スピン共鳴計測に用いる高出力ミリ波・サブミリ波伝送系の開発研究	光藤　誠太郎	福井大学	遠赤外領域開発研究センター	Development of high-power millimeter and submillimeter wave transmission system for electron spin resonance measurement under multiple extreme environment	Seitaro Mitsudo	University of Fukui
281	〃	藤井　裕	福井大学	遠赤外領域開発研究センター	〃	Yutaka Fujii	University of Fukui
282	正四角台塔型反強磁性体の強磁場中 ESR 測定	木村　健太	大阪大学	大学院基礎工学研究科	High-field ESR measurements of square-cupola-based antiferromagnets	Kenta Kimura	Osaka University
283	スピン液体候補物質 $Ba_3ZnRu_2O_9$ の希薄磁性不純物効果	寺崎　一郎	名古屋大学	大学院理学研究科	Effects of dilute magnetic impurity on the spin-liquid candidate $Ba_3ZnRu_2O_9$	Ichiro Terasaki	Nagoya University
284	〃	山本　貴史	名古屋大学	大学院理学研究科	〃	Takafumi Yamamoto	Nagoya University
285	超強磁場下で用いる InSb 検出器の開発	大久保　晋	神戸大学	分子フォトサイエンス研究センター	Development of InSb detector for use under ultra high magnetic field	Susumu Okubo	Kobe University
286	高出力テラヘルツ光源 (ジャイロトロン) を光源とする 高周波 ESR 分光 の研究	出原　敏孝	福井大学	遠赤外領域開発研究センター	Study on high frequency ESR spectroscopy using high power THz radiation sourses - Gyrotrons	Toshitaka Idehara	University of Fukui
287	〃	小川　勇	福井大学	遠赤外領域開発研究センター	〃	Isamu Ogawa	University of Fukui
288	$Sr_2MnSi_2O_7$ 単結晶試料の強磁場下での磁化・電気分極・ESR 測定	桑原　英樹	上智大学	理工学部	Magnetization, electric polarization, and ESR measurements for $Sr_2MnSi_2O_7$ single crystals in pulsed high magnetic fields.	Hideki Kuwahara	Sophia University
289	〃	野田　正亮	上智大学	大学院理工学研究科	〃	Masaaki Noda	Sophia University
290	三角格子反強磁性体 $NiGa_2S_4$ の強磁場相の研究	南部　雄亮	東北大学	金属材料研究所	Study of high magnetic field phase in the triangular antiferromagnet $NiGa_2S_4$	Yusuke Nambu	Tohoku University

No.	課題名	氏名	所属		Title	Name	Organization
291	単軸性キラル磁性体の磁気特性測定　–磁気トルクと磁気共鳴測定–	戸川　欣彦	大阪府立大学	大学院工学研究科	Magnetic property of monoaxial chiral magnetic materials examined by means of magnetic torque and resonance measurements	Yoshihiko Togawa	Osaka Prefecture University
292	〃	フランシスコ　ゴンカルベス	大阪府立大学	大学院工学研究科	〃	Francisco Goncalves	Osaka Prefecture University
293	パルス磁場を用いたマルテンサイト変態のカイネティクスに関する研究	福田　隆	大阪大学	大学院工学研究科	A study on kinetics of martensitic transformations using pulsed magnetic field	Takashi Fukuda	Osaka University

物質合成・評価設備 P クラス / Materials Synthesis and Characterization P Class Researcher

No.	課題名	氏名	所属		Title	Name	Organization
1	幾何学的フラストレート系物質の単結晶育成と新奇物性の研究	松平　和之	九州工業大学	大学院工学研究院	Single crystal growth and study of novel phenomena of geometrically frustrated materials	Kazuyuki Matsuhira	Kyushu Institute of Technology
2	〃	谷口　智哉	九州工業大学	大学院工学府	〃	Tomoya Taniguchi	Kyushu Institute of Technology
3	電子が複合自由度を持つ遷移金属カルコゲナイドの合成と物性評価	片山　尚幸	名古屋大学	大学院工学研究科	Growth of the transition metal chalcogenides with charge, orbital and spin degrees of freedom	Naoyuki Katayama	Nagoya University
4	〃	田村　慎也	名古屋大学	大学院工学研究科	〃	Shinya Tamura	Nagoya University

物質合成・評価設備 G クラス / Materials Synthesis and Characterization G Class Researcher

No.	課題名	氏名	所属		Title	Name	Organization
1	鉄系超伝導体及び銅酸化物高温超伝導体におけるエックス線回折測定	芝内　孝禎	東京大学	大学院新領域創成科学研究科	X-ray diffraction measurements on iron-based superconductors and cuprate superconductors	Takasada Shibauchi	The University of Tokyo
2	〃	水上　雄太	東京大学	大学院新領域創成科学研究科	〃	Yuta Mizukami	The University of Tokyo
3	〃	竹中　崇了	東京大学	大学院新領域創成科学研究科	〃	Takaaki Takenaka	The University of Tokyo
4	〃	石田　浩祐	東京大学	大学院新領域創成科学研究科	〃	Kousuke Ishida	The University of Tokyo
5	〃	田中　桜平	東京大学	大学院新領域創成科学研究科	〃	Ohei Tanaka	The University of Tokyo
6	〃	細井　優	東京大学	大学院新領域創成科学研究科	〃	Suguru Hosoi	The University of Tokyo

No.	課題名	氏名	所属		Title	Name	Organization
7	〃	杉村　優一	東京大学	大学院新領域創成科学研究科	〃	Yuichi Sugimura	The University of Tokyo
8	高温高圧水中の固体酸・塩基触媒反応の速度論的解析	大島　義人	東京大学	大学院新領域創成科学研究科	Kinetic analysis of solid acid and base catalyzed reactions in sub- and supercritical water	Yoshito Oshima	The University of Tokyo
9	〃	秋月　信	東京大学	大学院新領域創成科学研究科	〃	Makoto Akizuki	The University of Tokyo
10	高温高圧水の固体触媒表面性質への影響の評価	大島　義人	東京大学	大学院新領域創成科学研究科	Evaluating influence of high temperature and pressure water on solid catalyst surface	Yoshito Oshima	The University of Tokyo
11	〃	高橋　侑佳	東京大学	大学院新領域創成科学研究科	〃	Yuka Takahashi	The University of Tokyo
12	単結晶マンガン酸化物の誘電特性の研究	谷口　晴香	岩手大学	理工学部	Study of dielectric properties of single-crystalline manganite	Haruka Taniguchi	Iwate University
13	高圧高温水を反応場とした有機合成反応	大島　義人	東京大学	大学院新領域創成科学研究科	Organic synthesis in sub- and supercritical water	Yoshito Oshima	The University of Tokyo
14	〃	伊藤　光基	東京大学	大学院新領域創成科学研究科	〃	Koki Ito	The University of Tokyo
15	Fe_2Al_5 の単結晶構造解析	木村　薫	東京大学	大学院新領域創成科学研究科	Single Crystal Structure Analysis of Fe_2Al_5	Kaoru Kimura	The University of Tokyo
16	〃	飛田　一樹	東京大学	大学院新領域創成科学研究科	〃	Kazuki Tobita	The University of Tokyo
17	オスミウム含有廃液の超臨界水酸化・超臨界二酸化炭素抽出に関する研究	布浦　鉄兵	東京大学	環境安全研究センター	Study on supercritical water oxidation and supercritical CO_2 extraction of osmium-containing wastewater	Teppei Nunoura	The University of Tokyo
18	〃	三好　列	東京大学	大学院新領域創成科学研究科	〃	Retsu Miyoshi	The University of Tokyo
19	〃	平井　晴菜	東京大学	大学院新領域創成科学研究科	〃	Haruna Hirai	The University of Tokyo
20	プロトン伝導性固体電解質を用いた電解合成反応における電極触媒開発と速度論的解析	大友　順一郎	東京大学	大学院新領域創成科学研究科	Development of electrode catalysts and kinetic analysis for electrosynthesis using a proton conducting solid electrolyte	Junichiro Otomo	The University of Tokyo
21	〃	高坂　文彦	東京大学	大学院新領域創成科学研究科	〃	Fumihiko Kosaka	The University of Tokyo
22	プロトン伝導型 SOFC の新規セルデザインおよび性能評価	大友　順一郎	東京大学	大学院新領域創成科学研究科	Performance evaluation and new cell design of proton conducting SOFC	Junichiro Otomo	The University of Tokyo
23	〃	橋本　隼輔	東京大学	大学院新領域創成科学研究科	〃	Shunsuke Hashimoto	The University of Tokyo

No.	課題名	氏名	所属		Title	Name	Organization
24	新規プロトン - 電子混合伝導体の開発	大友　順一郎	東京大学	大学院新領域創成科学研究科	Development of mixed proton-electron mixed conductors	Junichiro Otomo	The University of Tokyo
25	〃	小城　元	東京大学	大学院新領域創成科学研究科	〃	Gen Kojo	The University of Tokyo
26	ケミカルループ燃焼法における酸素キャリアの反応モデリング	大友　順一郎	東京大学	大学院新領域創成科学研究科	Reaction modeling in chemical looping systems with new oxygen carrier materials.	Junichiro Otomo	The University of Tokyo
27	〃	松原　一起	東京大学	大学院新領域創成科学研究科	〃	Kazuki Matsubara	The University of Tokyo
28	全固体 Li 電池用電解質（ガラスーセラミックス）の研究	大友　順一郎	東京大学	大学院新領域創成科学研究科	Research on solid electrolyte (glass-ceramics) for Li battery	Junichiro Otomo	The University of Tokyo
29	〃	陸　疎桐	東京大学	大学院新領域創成科学研究科	〃	Lu Shutong	The University of Tokyo
30	アンモニア電解合成反応における新規電極触媒開発と電極反応評価	大友　順一郎	東京大学	大学院新領域創成科学研究科	Development of new electro-catalysts and evaluation of electrode reaction for electrochemical synthesis of ammonia	Junichiro Otomo	The University of Tokyo
31	〃	及川　暁雄	東京大学	大学院新領域創成科学研究科	〃	Akio Oikawa	The University of Tokyo
32	ケミカルループ法における高活性かつ長期安定性に長けた酸素キャリア材料の開発	大友　順一郎	東京大学	大学院新領域創成科学研究科	Development of oxygen carrier materials with high activity and high durability for chemical looping systems.	Junichiro Otomo	The University of Tokyo
33	〃	岡　輝	東京大学	大学院新領域創成科学研究科	〃	Hikaru Oka	The University of Tokyo
34	二酸化炭素と窒素による水素キャリアの電気化学的合成	大友　順一郎	東京大学	大学院新領域創成科学研究科	Electrochemical Reduction of Nitrogen and Carbon Dioxide to Hydrogen Carriers under Low Temperature	Junichiro Otomo	The University of Tokyo
35	〃	李　建毅	東京大学	大学院新領域創成科学研究科	〃	Li Chieni	The University of Tokyo
36	ケミカルループ法における高性能酸素キャリア材料の開発	大友　順一郎	東京大学	大学院新領域創成科学研究科	Development of oxygen carrier materials with high activity and durability for chemical looping systems	Junichiro Otomo	The University of Tokyo
37	〃	マーチン　ケラー	東京大学	大学院新領域創成科学研究科	〃	Martin Keller	The University of Tokyo
38	ペロブスカイト型酸化物を用いたケミカルルーピングシステムの開発	大友　順一郎	東京大学	大学院新領域創成科学研究科	Preparation of perovskite oxides as supports for MeO (Me: Cu, Ni) oxygen carrier materials for chemical looping systems	Junichiro Otomo	The University of Tokyo
39	〃	オーチェン　ジェームズ　オーチェン	東京大学	大学院新領域創成科学研究科	〃	Ochieng James Ochieng	The University of Tokyo
40	六方晶フェライト単結晶の化学分析と構造解析	植田　浩明	京都大学	大学院理学研究科	Chemical analysis and structural analysis of single crystals of hexagonal ferrites	Hiroaki Ueda	Kyoto University

No.	課題名	氏名	所属		Title	Name	Organization
41	〃	増田　順一	京都大学	大学院理学研究科	〃	Junichi Masuda	Kyoto University
42	超臨界水熱合成法を利用した金属酸化物微粒子の in situ 有機修飾技術の開発	大島　義人	東京大学	大学院新領域創成科学研究科	Development of in-situ organic surface modification technology on metal oxide nanoparticles using supercritical hydrothermal synthesis	Yoshito Oshima	The University of Tokyo
43	〃	原田　拓真	東京大学	大学院新領域創成科学研究科	〃	Takuma Harada	The University of Tokyo
44	超臨界水を利用した微粒子合成におけるアルカリ金属種の影響	大島　義人	東京大学	大学院新領域創成科学研究科	Effect of alkali metal species for nanoparticle synthesis in supercritical water.	Yoshito Oshima	The University of Tokyo
45	〃	織田　耕彦	東京大学	大学院新領域創成科学研究科	〃	Orita Yasuhiko	The University of Tokyo
46	中温域でのアンモニア電解合成における新規電極触媒開発と反応メカニズムの解析	大友　順一郎	東京大学	大学院新領域創成科学研究科	Development of new electrochemical catalyst for ammonia electrolysis and evaluation of reaction mechanism at intermediate temperature.	Junichiro Otomo	The University of Tokyo
47	〃	長谷川　卓利	東京大学	大学院新領域創成科学研究科	〃	Takuto Hasegawa	The University of Tokyo
48	高温高圧水中のシクロヘキシン水和反応におけるゼオライトの安定性評価	大島　義人	東京大学	大学院新領域創成科学研究科	Stability of zeolites in hot compressed water of cyclohexene hydration	Yoshito Oshima	The University of Tokyo
49	〃	アピバンボリラク　チャンウィット	東京大学	大学院新領域創成科学研究科	〃	Apibanboriak Chanwit	The University of Tokyo
50	中温作動プロトン伝導型固体酸化物燃料電池の新規セル設計	大友　順一郎	東京大学	大学院新領域創成科学研究科	New Cell Design of Intermediate Temperature Proton Conducting SOFC	Junichiro Otomo	The University of Tokyo
51	〃	田所　洸	東京大学	大学院新領域創成科学研究科	〃	Hiroshi Tadokoro	The University of Tokyo
52	メソポーラスマテリアル・グラフェンオキサイドに担持した金属触媒のキャラクタリゼーション	佐々木　岳彦	東京大学	大学院新領域創成科学研究科	Characterization for metal catalysts supported on mesoporous materials and graphene oxides	Takehiko Sasaki	The University of Tokyo
53	〃	Etty Nurlia Kusumawati	東京大学	大学院理学系研究科	〃	Etty Nurlia Kusumawati	The University of Tokyo
54	〃	有村　祐紀	東京大学	大学院新領域創成科学研究科	〃	Yuki Arimura	The University of Tokyo
55	新規負熱膨張材料の合成と物性	岡本　佳比古	名古屋大学	大学院工学研究科	Synthesis and physical properties of novel negative thermal expansion materials	Yoshihiko Okamoto	Nagoya University
56	腫瘍抗原候補ペプチドのラマン分光測定	糸井　充穂	日本大学	医学部	Raman spectroscopy of neoantigen peptides	Miho Itoi	Nihon University
57	触媒反応の insitu ラマン散乱測定	佐々木　岳彦	東京大学	大学院新領域創成科学研究科	in situ measurement of Raman scattering for heterogeneous catalytic reactions	Takehiko Sasaki	The University of Tokyo

No.	課題名	氏名	所属		Title	Name	Organization
58	〃	有村　祐紀	東京大学	大学院新領域創成科学研究科	〃	Yuki Arimura	The University of Tokyo
59	フラストレート系化合物 RZn_3P_3(R= 希土類) の高圧合成と磁気特性	関根　ちひろ	室蘭工業大学	大学院工学研究科	High-pressure synthesis and magnetic properties of frustrated compounds RZn_3P_3 (R=rare earth)	Chihiro Sekine	Muroran Institute of Technology
60	〃	森　英将	室蘭工業大学	大学院工学研究科	〃	Hidemasa Mori	Muroran Institute of Technology
61	アミノ酸の高圧下でのペプチド化反応の観察	藤本　千賀子	東京大学	大学院理学系研究科	Peptide formation of amino acids under high pressure	Chikako Fujimoto	The University of Tokyo
62	層状バナジウム酸水素化物における圧力効果	山本　隆文	京都大学	大学院工学研究科	Pressure Effect on Layered Vanadium Oxyhydrides	Takafumi Yamamoto	Kyoto University
63	新規 14 族元素窒化物の高圧合成および安定性	丹羽　健	名古屋大学	大学院工学研究科	High pressure synthesis and stability of group 14 element nitrides	Ken Niwa	Nagoya University
64	高圧印加による Li ドープ α 菱面体晶ボロンの作製	木村　薫	東京大学	大学院新領域創成科学研究科	Synthesis of Li-dope alpha-rhombohedral boron by high-pressurization	Kaoru Kimura	The University of Tokyo
65	〃	酒井　志徳	東京大学	大学院新領域創成科学研究科	〃	Munenori Sakai	The University of Tokyo
66	高圧下での $MoSi_2$ 型構造の $FeAl_2$ 結晶の作製	木村　薫	東京大学	大学院新領域創成科学研究科	High pressure synthesis of $MoSi_2$ type iron aluminide, $FeAl_2$ crystal	Kaoru Kimura	The University of Tokyo
67	〃	飛田　一樹	東京大学	大学院新領域創成科学研究科	〃	Kazuki Tobita	The University of Tokyo
68	〃	岩崎　祐昂	東京大学	大学院新領域創成科学研究科	〃	Yutaka Iwasaki	The University of Tokyo
69	プラズマ風洞による宇宙往還機の熱防護システム (TPS) に関する動的酸化に関する研究	桃沢　愛	東京都市大学	工学部	Research on dynamic oxidation of thermal protection system by using plasma wind tunnel	Ai Momozawa	Tokyo City University
70	〃	曽我　遼太	東京大学	大学院工学系研究科	〃	Ryota Soga	The University of Tokyo
71	〃	田中　聖也	東京大学	大学院工学系研究科	〃	Seiya Tanaka	The University of Tokyo
72	天然鉱物の微細組織と結晶性の実態	永嶌　真理子	山口大学	大学院創成科学研究科	Evaluation of micro-texture and crystallinity of natural minerals	Mariko Nagashima	Yamaguchi University
73	マイクロミキサを用いた機能性酸化物ナノ粒子の連続合成	陶　究	産業技術総合研究所	化学プロセス研究部門	Continuous synthesis of functional metal oxide nanoparticles using a micromxer	Kiwamu Sue	National Institute of Advanced Industrial Science and Technology
74	新しい希土類磁石の探求	齋藤　哲治	千葉工業大学	工学部	Research of new rare-earth magnets	Tetsuji Saito	Chiba Institute of Technology

No.	課題名	氏名	所属		Title	Name	Organization
75	フィチン酸の超臨界水ガス化挙動に関する検討	布浦　鉄兵	東京大学	環境安全研究センター	Decomposition behavior of phytic acid in supercritical water gasification	Teppei Nunoura	The University of Tokyo
76	〃	飯田　裕樹	東京大学	大学院新領域創成科学研究科	〃	Yuuki Iida	The University of Tokyo
77	水中プラズマを用いたナノ粒子合成	後藤　拓	東京大学	大学院新領域創成科学研究科	Synthesis of nanoparticles via plasma processing in liquid	Taku Goto	The University of Tokyo
78	高温高圧下で軽元素が鉄ーシリケイトー水系に及ぼす影響の解明	飯塚　理子	東京大学	大学院理学系研究科	Behavior of light elements in iron-silicate-water system under high pressure and high temperature	Riko Iizuka	The University of Tokyo
79	〃	高橋　修也	東京大学	大学院理学系研究科	〃	Shuya Takahashi	The University of Tokyo
80	〃	福山　鴻	東京大学	大学院理学系研究科	〃	Ko Fukuyama	The University of Tokyo
81	〃	古村　俊行	東京大学	大学院理学系研究科	〃	Toshiyuki Komura	The University of Tokyo
82	スピングラス転移温度を決定する物理的要因の研究	香取　浩子	東京農工大学	大学院工学研究院	Study of physical factors that determine the spin-glass transition temperature	Hiroko Katori	Tokyo University of Agriculture and Technology
83	〃	柿本　和勇	東京農工大学	大学院工学府	〃	Kazuo Kakimoto	Tokyo University of Agriculture and Technology
84	$A_{1-x}Sr_xFeO_3$ (A：ランタノイド) の高温における磁性と熱電特性に関する研究	中津川　博	横浜国立大学	大学院工学研究院	Magnetism and thermoelectric properties at high temperature in $A_{1-x}Sr_xFeO_3$(A：lanthanoid)	Hiroshi Nakatsugawa	Yokohama National University
85	三角格子をもつ遷移金属カルコゲナイドの物性	小林　慎太郎	名古屋大学	大学院工学研究科	Physical properties of transition metal chalcogenides with a triangular lattice	Shintaro Kobayashi	Nagoya University
86	〃	中埜　彰俊	名古屋大学	大学院工学研究科	〃	Akitoshi Nakano	Nagoya University
87	〃	鬼頭　俊介	名古屋大学	大学院工学研究科	〃	Shunsuke Kitou	Nagoya University
88	レアメタルフリー磁性材料 L10-FeCo の磁気特性の解析	小嗣　真人	東京理科大学	基礎工学部	Analysis of magnetic properties of rare-metal-free super magnet “L10-FeCo”	Masato Kotsugi	Tokyo University of Science
89	〃	落合 順也	東京理科大学	大学院基礎工学研究科	〃	Junya Ochiai	Tokyo University of Science
90	酸フッ化物層状ペロブスカイト $Pb_3Fe_2O_5F_2$ の磁場依存磁気転移の観察	岡　研吾	中央大学	理工学部	Observation of the filed dependence of magnetic transition in layered perovskite oxyfluride $Pb_3Fe_2O_5F_2$	Kengo Oka	Chuo University
91	正 20 面体クラスター固体の伝導と磁性	木村　薫	東京大学	大学院新領域創成科学研究科	Transport and magnetic properties of Icosahedral Cluster Solids	Kaoru Kimura	The University of Tokyo

No.	課題名	氏名	所属		Title	Name	Organization
92	〃	廣戸　孝信	東京大学	大学院新領域創成科学研究科	〃	Takanobu Hiroto	The University of Tokyo
93	準結晶・近似結晶の磁性に関する研究	石川　明日香	東京理科大学	大学院基礎工学研究科	Magnetism of quasicrystals and approximants	Asuka Ishikawa	Tokyo University of Science
94	ハーフメタル型ホイスラー合金の磁性と輸送特性に関する研究	重田　出	鹿児島大学	大学院理工学研究科	Study on the magnetic and transport properties of half-metallic Heusler alloys	Iduru Shigeta	Kagoshima University
95	〃	大岡　隆太郎	鹿児島大学	大学院理工学研究科	〃	Ryutaro Ooka	Kagoshima University
96	ホイスラー型化合物の磁性と伝導の研究	廣井　政彦	鹿児島大学	大学院理工学研究科	Study on the magnetic and electrical properties of Heusler compounds	Masahiko Hiroi	Kagoshima University
97	励起子相候補物質 1T-$TiSe_2$ への Cu ドープにおける磁気・輸送特性の評価	澤　博	名古屋大学	大学院工学研究科	Magnetic and transport properties of Cu doped excitonic phase candidate substance 1T-$TiSe_2$	Hiroshi Sawa	Nagoya University
98	〃	小林　慎太郎	名古屋大学	大学院工学研究科	〃	Shintaro Kobayashi	Nagoya University
99	〃	鬼頭　俊介	名古屋大学	大学院工学研究科	〃	Shunsuske Kitou	Nagoya University
100	キャリアドープされたパイロクロア型イリジウム酸化物の純良単結晶育成	松平　和之	九州工業大学	大学院工学研究院	Single crystal growth of carrier-doped pyrochlore iridates	Kazuyuki Matsuhira	Kyushu Institute of Technology
101	〃	柴原　怜央	九州工業大学	大学院工学府	〃	Reo Shibahara	Kyushu Institute of Technology
102	リチウムイオン伝導体 $Li_{3x}B_{1-x}PO_4$ の高圧相転移	廣瀬　瑛一	名古屋大学	大学院工学研究科	High pressure phase transition of lithium ion conductor $Li_{3x}B_{1-x}PO_4$	Eiichi Hirose	Nagoya University
103	金属および半金属薄膜の作成	末元　徹	豊田理化学研究所		Preparation of metal and semimetal thin films	Tohru Suemoto	Toyota Physical and Chemical Research Institute
104	高周波磁気共鳴を有する希土類オルソフェライト単結晶の生成とテラヘルツ波磁気分光	中嶋　誠	大阪大学	レーザー科学研究所	Terahertz spin spectroscopy for rare-earth orthoferrite single crystal with high frequency magnetic resonance	Makoto Nakajima	Osaka University
105	〃	加藤　康作	大阪大学	レーザー科学研究所	〃	Kosaku Kato	Osaka University
106	〃	邱　紅松	大阪大学	レーザー科学研究所	〃	Hongsong Qiu	Osaka University
107	〃	弘田　和將	大阪大学	レーザー科学研究所	〃	Kazumasa Hirota	Osaka University
108	コニカルらせん磁性体 $CoCr_2O_4$ における複合ドメイン相関の解明	木村　剛	東京大学	大学院新領域創成科学研究科	Understanding of coupled multiferroic domains in a conical spiral magnet $CoCr_2O_4$	Tsuyoshi Kimura	The University of Tokyo

No.	課題名	氏名	所属		Title	Name	Organization
109	新規フェロイック物質の開発	有馬　孝尚	東京大学	大学院新領域創成科学研究科	Exploration of new ferroics	Takahisa Arima	The University of Tokyo
110	〃	徳永　祐介	東京大学	大学院新領域創成科学研究科	〃	Yusuke Tokunaga	The University of Tokyo
111	〃	阿部　伸行	東京大学	大学院新領域創成科学研究科	〃	Nobuyuki Abe	The University of Tokyo
112	〃	松浦　慧介	東京大学	大学院新領域創成科学研究科	〃	Keisuke Matsuura	The University of Tokyo
113		鷲見　浩樹	東京大学	大学院新領域創成科学研究科		Hiroki Sumi	The University of Tokyo
114	〃	藤間　友理	東京大学	大学院新領域創成科学研究科	〃	Yuri Fujima	The University of Tokyo
115	〃	徳村　謙祐	東京大学	大学院新領域創成科学研究科	〃	Kensuke Tokumura	The University of Tokyo
116	〃	中川　直己	東京大学	大学院新領域創成科学研究科	〃	Naoki Nakagawa	The University of Tokyo
117	〃	荒木　勇介	東京大学	大学院新領域創成科学研究科	〃	Yusuke Araki	The University of Tokyo
118	〃	近江　毅志	東京大学	大学院新領域創成科学研究科	〃	Tsuyoshi Omi	The University of Tokyo
119	〃	小池　仁希	東京大学	大学院新領域創成科学研究科	〃	Yoshiki Koike	The University of Tokyo
120	〃	吉澤　孟晃	東京大学	大学院新領域創成科学研究科	〃	Takeaki Yoshizawa	The University of Tokyo
121	〃	佐藤　樹	東京大学	大学院新領域創成科学研究科	〃	Tatsuki Sato	The University of Tokyo
122	〃	海本　祐真	東京大学	大学院新領域創成科学研究科	〃	Yuma Umimoto	The University of Tokyo
123	鉄ニクタイド及び鉄カルコゲナイドにおける新規物性探索	水上　雄太	東京大学	大学院新領域創成科学研究科	Investigation of physical properties in iron pnictides and chalcogenides	Yuta Mizukami	The University of Tokyo

物質合成・評価設備 U クラス / Materials Synthesis and Characterization U Class Researcher

No.	課題名	氏名	所属		Title	Name	Organization
1	溶融亜鉛メッキ合金相の応力誘起変態	山口　周	東京大学	大学院工学系研究科	Stress-induced phase transformation of Fe-Zn alloy formed in hot-dip process	Shu Yamaguchi	The University of Tokyo
2	〃	田中　和彦	東京大学	大学院工学系研究科	〃	Kazuhiko Tanaka	The University of Tokyo
3	超高圧プレスを用いた新規プロトニクス酸化物のソフト化学的合成法の検討	山口　周	東京大学	大学院工学系研究科	Oxide-Protonics materials synthesis by combined use of soft chemical method and high pressure	Shu Yamaguchi	The University of Tokyo
4	〃	田中　和彦	東京大学	大学院工学系研究科	〃	Kazuhiko Tanaka	The University of Tokyo
5	遷移金属パイロクロア酸化物超伝導体の結晶相決定	山浦　淳一	東京工業大学	元素戦略研究センター	Determination of crystalline state in transition metal pyrochlore oxide superconductor	Junichi Yamaura	Tokyo Institute of Technology
6	フィチン酸の超臨界水ガス化におけるリンの挙動に関する検討	布浦　鉄兵	東京大学	環境安全研究センター	Behavior of phosphorus in supercritical water gasification using phytic acid	Teppei Nunoura	The University of Tokyo
7	〃	飯田　裕樹	東京大学	大学院新領域創成科学研究科	〃	Yuuki Iida	The University of Tokyo
8	ブリッジマン法による遍歴らせん磁性体 MnP の大型単結晶育成	小野瀬　佳文	東京大学	大学院総合文化研究科	Large crystal growth of itinerant helical magnet MnP by means of Bidgman method	Yoshinori Onose	The University of Tokyo
9	〃	蒋　男	東京大学	大学院総合文化研究科	〃	Jiang Nan	The University of Tokyo
10	氷共存型プラズマを用いた新規アクアプロセス開拓	榊原　教貴	東京大学	大学院新領域創成科学研究科	Development of a novel aqua-process with plasma-ice coexistence system	Noritaka Sakakibara	The University of Tokyo
11	テラヘルツ近接場顕微計測用の二酸化バナジウム単結晶の作製	根間　裕史	日本大学	文理学部	Synthesis of single-crystal VO_2 for THz near-field optical microscopy	Hirofumi Nema	Nihon University
12	新規鉄系超伝導体の物質合成と物性評価	芝内　孝禎	東京大学	大学院新領域創成科学研究科	Synthesis and measurements of physical properties on new iron-based superconductors	Takasada Shibauchi	The University of Tokyo
13	〃	竹中　崇了	東京大学	大学院新領域創成科学研究科	〃	Takaaki Takenaka	The University of Tokyo
14	〃	細井　優	東京大学	大学院新領域創成科学研究科	〃	Suguru Hosoi	The University of Tokyo
15	〃	石田　浩祐	東京大学	大学院新領域創成科学研究科	〃	Kousuke Ishida	The University of Tokyo
16	〃	杉村　優一	東京大学	大学院新領域創成科学研究科	〃	Yuichi Sugimura	The University of Tokyo

No.	課題名	氏名	所属		Title	Name	Organization
17	〃	田中　桜平	東京大学	大学院新領域創成科学研究科	〃	Ohei Tanaka	The University of Tokyo
18	遍歴電子強磁性体 $X_2Co_{12}As_7$ (X= 希土類等) の磁気的性質の研究	太田　寛人	東京農工大学	大学院工学研究院	Study of magnetic property of itinerant electronic ferromagnets $X_2Co_{12}As_7$ (X = lanthanoids and other elements)	Hiroto Ohta	Tokyo University of Agriculture and Technology
19	〃	加藤　優典	東京農工大学	大学院工学府	〃	Yusuke Kato	Tokyo University of Agriculture and Technology
20	金属有機構造体のナノ構造制御によるカーボン材料合成	細野　英司	産業技術総合研究所	省エネルギー研究部門	Synthesis of carbon materials by nanostructure control of metal organic frameworks	Eiji Hosono	National Institute of Advanced Industrial Science and Technology
21	微量希土類元素を含む鉄、ケイ酸塩ガラス試料の高圧合成	桑原　秀治	愛媛大学	地球深部ダイナミクス研究センター	High pressure synthesis of rare earth elements doped iron and silicate glass	Hideharu Kuwahara	Ehime University
22	天然由来炭酸塩の定量分析	樋山　みやび	群馬大学	大学院理工学府	Quantitative analysis of naturally derived carbonate	Miyabi Hiyama	Gunma University
23	オレイン酸被覆水熱成長法によるセリアナノ粒子の鉄イオンドープによる形態変化	牧之瀬　佑旗	島根大学	大学院総合理工学研究科	Study of shape changing of Fe doepd ceria nanoparticles synthesized by oleate-modified hydrothermal method	Yuki Makinose	Shimane University

平成 29 年度　中性子科学研究施設　共同利用課題一覧 / Joint Research List of Neutron Scattering Researcher 2017

No.	課題名	氏名	所属		Title	Name	Organization
・申請装置 4G: GPTAS							
1	GPTAS（汎用 3 軸中性子分光器）IRT 課題	佐藤　卓	東北大学	多元物質科学研究所	IRT project of GPTAS	Taku J Sato	Tohoku University
2	磁性準結晶中の隠れた磁気秩序の探索	佐藤　卓	東北大学	多元物質科学研究所	Hidden magnetic order in magnetic quasicrystals	Taku J Sato	Tohoku University
3	近藤籠目格子 CeRhSn の量子臨界磁気揺動	佐藤　卓	東北大学	多元物質科学研究所	Detecting quantum critical fluctuations in the disordered kagome Kondo compound CeRhSn	Taku J Sato	Tohoku University
4	時間分割中性子散乱による磁気構造変化過程の実時間追跡	元屋　清一郎	東京理科大学	理工学部　物理学科	Real-time observation of magnetic structural change by means of time-resolved neutron scattering experiments	Kiyoichiro Motoya	Tokyo University of Science
5	六方晶フェライト $Ba_2Zn_2Fe_{12}O_{22}$ および $BaFe_{12}O_{19}$ 系の超交換相互作用	内海　重宜	諏訪東京理科大学	工学部　機械工学科	Superexchange interaction of hexagonal ferrite $Ba_2Zn_2Fe_{12}O_{22}$ and $BaFe_{12}O_{19}$ systems	Shigenori Utsumi	Tokyo University of Science, Suwa
6	強磁性超伝導体における磁性と超伝導の研究	古川　はづき	お茶の水女子大学	基幹研究院 自然科学系	A study of magnetic state in ferromagnetic superconductors	Hazuki Furukawa	Ochanomizu University
7	Sr_2Ruo4 の非弾性散乱	古川　はづき	お茶の水女子大学	基幹研究院 自然科学系	Inelastic neutron scattering experiments on Sr_2RuO_4	Hazuki Furukawa	Ochanomizu University
8	トポロジカル超伝導体の非弾性散乱	古川　はづき	お茶の水女子大学	基幹研究院 自然科学系	Inelastic neutron scattering experiments on topological superconductors	Hazuki Furukawa	Ochanomizu University
9	多段メタ磁性転移を示す空間反転対称性の破れた $CePdSi_3$ における磁気構造の決定	吉田　雅洋	東京大学	物性研究所	Determination of the magnetic structure of the Noncentrosymmetric Metamagnet $CePdSi_3$	Masahiro Yoshida	The University of Tokyo
10	S=1/2 ジグザグ鎖磁性体 Ba_2ReO_5 におけるスピン励起	那波　和宏	東北大学	多元物質科学研究所	Spin excitations on the S = 1/2 zigzag chain magnet Ba_2ReO_5	Kazuhiro Nawa	Tohoku University
11	強誘電体の相転移機構（変位型及び秩序–無秩序型）に関する統一的理解の確立	重松　宏武	山口大学	教育学部	Establishment of the unified explanation about the phase transition mechanism (displacive and order-disorder type) in Ferroelectrics	Hirotake Shigematsu	Yamaguchi University
12	スピンアイスにおけるトポロジカル相転移	門脇　広明	首都大学東京	理工学研究科物理学専攻	Topological phase transition in spin ice	Hiroaki Kadowaki	Tokyo Metoropolitan University
13	パイロクロア磁性体 $Tb_2Zr_2O_7$ の磁気ダイナミクスと結晶場励起	高津　浩	京都大学	工学研究科	Quantum spin fluctuations and crystal field of the pyrochlore magnet $Tb_2Zr_2O_7$	Hiroshi Takatsu	Kyoto University
14	ダブルペロブスカイト Lu_2NiMnO_6 の圧力誘起相転移	寺田　典樹	物質材料研究機構	中性子散乱グループ	Pressure-induced phase transition in double perovskite Lu_2NiMnO_6	Noriki Terada	National Institute for Materials Science
15	ホールドープ系鉄系超伝導体のスピン揺動	李　哲虎	産業技術総合研究所	省エネルギー研究部門	Spin fluctuations of hole-doped iron-based superconductors	Chul-Ho Lee	National Institute of Advanced Industrial Science and Technology

No.	課題名	氏名	所属		Title	Name	Organization
16	多段メタ磁性転移を示す空間反転対称性の破れた $CePtSi_3$ における磁気構造の決定	吉田　雅洋	東京大学	物性研究所	Determination of the Magnetic Structure of the Noncentrosymmetric Heavy-Electron Metamagnet $CePtSi_3$	Masahiro Yoshida	The University of Tokyo
・申請装置 5G: PONTA							
17	PONTA（高性能偏極中性子散乱装置）IRT 課題	益田　隆嗣	東京大学	物性研究所	IRT project of PONTA	Takatsugu Masuda	The University of Tokyo
18	フラストレーションをもつ正方格子 $C_{20}H_{19}F_6N_5P$ における磁気秩序	左右田　稔	東京大学	物性研究所	Magnetic Ordering in S=1/2 Frustrated Square Lattice $C_{20}H_{19}F_6N_5P$	Minoru Soda	The University of Tokyo
19	マルチフェロイック物質Ｂａ２ＭｎＧｅ２Ｏ７における磁気モーメントの電場制御	益田　隆嗣	東京大学	物性研究所	Electrical control of magnetic moment on multiferroics $Ba_2MnGe_2O_7$	Takatsugu Masuda	The University of Tokyo
20	マルチフェロイック物質 $RFe_3(BO_3)_4$ (R=Ce,Sm)	益田　隆嗣	東京大学	物性研究所	Magnetic structure of multiferroics $RFe_3(BO_3)_4$ (R=Ce,Sm)	Takatsugu Masuda	The University of Tokyo
21	$CsFeCl_3$ における圧力誘起秩序状態の磁気構造	益田　隆嗣	東京大学	物性研究所	Magnetic structure of pressure-induced ordered state in $CsFeCl_3$	Takatsugu Masuda	The University of Tokyo
22	カイラル磁性体 $CsCuCl_3$ のカイラルらせん磁性の検証	高阪　勇輔	広島大学	大学院理学研究科	Chiral Helimagnetim in Chiral Inorganic Compound $CsCuCl_3$	Yusuke Kousaka	Hiroshima University
23	URu_2Si_2 の隠れた秩序に伴う多重極秩序の直接観測	高阪　勇輔	広島大学	大学院理学研究科	Direct Observation of the "Hidden Order" due to Multipole Ordering in URu_2Si_2	Yusuke Kousaka	Hiroshima University
24	スピン 3/2 反強磁性交替鎖物質 $RCrGeO_5$ (R = Nd or Ho) の磁気構造の決定	長谷　正司	物質・材料研究機構	中性子散乱グループ	The determination of the magnetic structure of the spin-3/2 antiferromagnetic alternating chain compounds $RCrGeO_5$ (R = Nd or Ho)	Masashi Hase	National Institute for Materials Science
25	スピン 1/2 テトラマー物質 $CuInVO_5$ の磁気構造の決定	長谷　正司	物質・材料研究機構	中性子散乱グループ	Determination of the magnetic structure of the spin-1/2 tetramer compound $CuInVO_5$	Masashi Hase	National Institute for Materials Science
26	ワイル半金属候補物質 NdGaSi の磁気構造	左右田　稔	理化学研究所	創発物性科学研究センター	Magnetic structure of Weyl semimetal candidate NdGaSi	Minoru Soda	RIKEN
27	マグネトプランバイト型コバルト酸化物 $SrCo_{12}O_{19}$ の電荷 - 磁気秩序	浅井　晋一郎	東京大学	物性研究所	Charge and magnetic order of magnetoplumbite-type cobalt oxide $SrCo_{12}O_{19}$	Shinichiro Asai	The University of Tokyo
・申請装置 6G: TOPAN							
28	TOPAN（東北大理：３軸型偏極中性子分光器）IRT 課題	富安　啓輔	東北大学	大学院理学研究科	IRT project of TOPAN	Keisuke Tomiyasu	Tohoku University
29	全対称型多極子秩序による金属–非金属転移に対する磁気不純物効果	岩佐　和晃	茨城大学	フロンティア応用原子科学研究センター	Magnetic Impurity Effect on the Metal-Nonmetal Transition Associated with Totally-Symmetric Electron Multipole Ordering	Kazuaki Iwasa	Ibaraki University
30	$Ce_3T_4Sn_{13}$ (T = Co, Rh, Ru) に現れるカイラルフェルミオンによる磁気構造と励起	岩佐　和晃	茨城大学	フロンティア応用原子科学研究センター	Magnetic structures and excitations due to chiral fermions appearing in $Ce_3T_4Sn_{13}$ (T = Co, Rh, Ru)	Kazuaki Iwasa	Ibaraki University

No.	課題名	氏名	所属		Title	Name	Organization
31	PrT_2X_{20} (T = Ru, Rh, Os, Ir, X = Al, Zn) における２チャンネル近藤効果	岩佐　和晃	茨城大学	フロンティア応用原子科学研究センター	Two-channel Kondo effect in PrT_2X_{20} (T = Ru, Rh, Os, Ir, X = Al, Zn)	Kazuaki Iwasa	Ibaraki University
32	質量勾配をもつ非一様系での偏在的原子振動モードであるグレードンの検証	岩佐　和晃	茨城大学	フロンティア応用原子科学研究センター	Gradon as a localized atomic motion in mass-graded inhomogeneous systems	Kazuaki Iwasa	Ibaraki University
33	T' 構造銅酸化物 $Pr_{2-x}Ca_xCuO_4$ における磁気相関と超伝導の研究	藤田　全基	東北大学	金属材料研究所	Study of spin correlations and superconductivity in T'-structured cuprate oxide $Pr_{2-x}Ca_xCuO_4$	Masaki Fujita	Tohoku University
34	$Pr_{1-x}LaCe_xCuO_4$ の磁気共鳴ピークの組成依存性	池内　和彦	総合科学研究機構	中性子科学センター	Doping dependence of the magnetic resonance peak in PLCCO	Kazuhiko Ikeuchi	CROSS
35	$Pr_{1-x}LaCe_xCuO_4$ の格子振動を通じたギャップ対称性の観測	池内　和彦	総合科学研究機構	中性子科学センター	Observation of the gap symmetry due to lattice vibrations in PLCCO	Kazuhiko Ikeuchi	CROSS
・申請装置 C1-1: HER							
36	HER (高エネルギー分解能３軸型中性子分光器) IRT 課題	益田　隆嗣	東京大学	物性研究所	IRT project of HER	Takatsugu Masuda	The University of Tokyo
37	磁気スカーミオン格子相におけるトポロジカルマグノンの探索	佐藤　卓	東北大学	多元物質科学研究所	Topological magnon band in the magnetic skyrmion lattice	Taku J Sato	Tohoku University
38	近藤籠目格子 CeRhSn の量子臨界磁気揺動	佐藤　卓	東北大学	多元物質科学研究所	Detecting quantum critical fluctuations in the disordered kagome Kondo compound CeRhSn	Taku J Sato	Tohoku University
39	スピントロニクス基盤物質 YIG における磁気弾性効果	南部　雄亮	東北大学	金属材料研究所	Magnetic elastic coupling in the spintoronics material $Y_3Fe_5O_{12}$	Yusuke Nambu	Tohoku University
40	全対称型多極子秩序による金属–非金属転移に対する磁気不純物効果	岩佐　和晃	茨城大学	フロンティア応用原子科学研究センター	Magnetic Impurity Effect on the Metal-Nonmetal Transition Associated with Totally-Symmetric Electron Multipole Ordering	Kazuaki Iwasa	Ibaraki University
41	$Ce_3T_4Sn_{13}$ (T = Co, Rh, Ru) に現れるカイラルフェルミオンによる磁気構造と励起	岩佐　和晃	茨城大学	フロンティア応用原子科学研究センター	Magnetic structures and excitations due to chiral fermions appearing in $Ce_3T_4Sn_{13}$ (T = Co, Rh, Ru)	Kazuaki Iwasa	Ibaraki University
42	PrT_2X_{20} (T = Ru, Rh, Os, Ir, X = Al, Zn) における２チャンネル近藤効果	岩佐　和晃	茨城大学	フロンティア応用原子科学研究センター	Two-channel Kondo effect in PrT_2X_{20} (T = Ru, Rh, Os, Ir, X = Al, Zn)	Kazuaki Iwasa	Ibaraki University
43	$DyFe_2Zn_{20}$ における磁気異方性増強を伴う逐次磁気相転移	岩佐　和晃	茨城大学	フロンティア応用原子科学研究センター	Successive magnetic phase transition with enhancement in magnetic anisotropy of $DyFe_2Zn_{20}$	Kazuaki Iwasa	Ibaraki University
44	スピン格子結合系 $CuFeO_2$ のスピン波分散関係の一軸応力変化	満田　節生	東京理科大学	理学部　物理	Spin wave dispersion relation in a spin-lattice coupled system $CuFeO_2$ ander uniaxial stress	Setsuo Mitsuda	Tokyo University of Science
45	T' 構造銅酸化物 $Pr_{2-x}Ca_xCuO_4$ における磁気相関と超伝導の研究	藤田　全基	東北大学	金属材料研究所	Study of spin correlations and superconductivity in T'-structured cuprate oxide $Pr_{2-x}Ca_xCuO_4$	Masaki Fujita	Tohoku University
46	量子スピン液体の研究	門脇　広明	首都大学東京	理工学研究科物理学専攻	Quantum spin liquid	Hiroaki Kadowaki	Tokyo Metoropolitan University

No.	課題名	氏名	所属		Title	Name	Organization
47	空間反転対称性をもたない超伝導体 $CeRhSi_3$ の磁気励起	阿曽　尚文	琉球大学	理学部物質地球科学科	Magnetic Fluctuations in a Non-Centrosymmetric Superconductor $CeRhSi_3$	Naofumi Aso	University of the Ryukyus
48	$La_5Mo_4O_{16}$ における長時間磁化緩和と悪魔の階段	飯田　一樹	総合科学研究機構	研究開発部	Long-time magnetization decay and devil's staircase in $La_5Mo_4O_{16}$	Iida Kazuki	Comprehensive Research Organization for Science and Society
49	ホールドープ系鉄系超伝導体のスピン揺動	李　哲虎	産業技術総合研究所	省エネルギー研究部門	Spin fluctuations of hole-doped iron-based superconductors	Chul-Ho Lee	National Institute of Advanced Industrial Science and Technology
・ 申請装置 C1-2: SANS-U							
50	SANS-U（二次元位置測定小角散乱装置）IRT 課題	柴山　充弘	東京大学	物性研究所	IRT project of SANS-U	Mitsuhiro Shibayama	The University of Tokyo
51	イミダゾリウム系イオン液体 + プロパノール二成分溶液の相分離メカニズムの解明	下村　拓也	室蘭工業大学	大学院工学研究科	Phase separation of imidazolium-based ionic liquid+propanol binary solutions	Takuya Shimomura	Muroran Institute of Technology
52	非膨潤性ハイドロゲルの構造形成過程の観察	中川　慎太郎	東京大学	物性研究所	Insight into structure formation in "non-swelling" hydrogels	Shintaro Nakagawa	The University of Tokyo
53	ブラシ状高分子中の側鎖のコンフォメーションの解析	中村　洋	京都大学	工学研究科高分子化学専攻	Conformation analysis of a side chain in brush-like polymers	Yo Nakamura	Kyoto University
54	Crowding 環境下におけるアルファクリスタリンのサブユニット動態	井上　倫太郎	京都大学	原子炉実験所	Subunit dynamics of alpha-crystallin under crowding condition	Rintaro Inoue	Kyoto University
55	中性子小角散乱で見る植物性食品タンパク質の複合構造	佐藤　信浩	京都大学	原子炉実験所	Structural analysis of plant food protein complex by small-angle neutron scattering	Nobuhiro Sato	Kyoto University
56	磁性準結晶中の隠れた磁気秩序の探索	佐藤　卓	東北大学	多元物質科学研究所	Hidden magnetic order in magnetic quasicrystals	Taku J Sato	Tohoku University
57	中性子小角散乱実験による Sr_2RuO_4 の異常金属状態の研究	古川　はづき	お茶の水女子大学	基幹研究院 自然科学系	Anomalous vortex state in Sr_2RuO_4 studied by SANS experiments	Hazuki Furukawa	Ochanomizu University
58	空間反転対称性の破れた超伝導体のヘリカル磁束格子の観測	古川　はづき	お茶の水女子大学	基幹研究院 自然科学系	Herical vortex phase on non-centrosymmetric superconductors	Hazuki Furukawa	Ochanomizu University
59	Fe 系超伝導体の磁束研究	古川　はづき	お茶の水女子大学	基幹研究院 自然科学系	Vortex study on Fe-based superconductors	Hazuki Furukawa	Ochanomizu University
60	希釈冷凍機温度領域における $CeCoIn_5$ の磁束構造の磁場方向依存性	古川　はづき	お茶の水女子大学	基幹研究院 自然科学系	Field direction dependence of vortex lattice structure on $CeCoIN_5$ in Dilution temperature	Hazuki Furukawa	Ochanomizu University
61	強磁性超伝導体における自発的磁束格子構造の研究	古川　はづき	お茶の水女子大学	基幹研究院 自然科学系	Spontaneous vortex phase in ferromagnetic superconductors	Hazuki Furukawa	Ochanomizu University
62	空間反転対称性の破れた超伝導体の非弾性散乱	古川　はづき	お茶の水女子大学	基幹研究院 自然科学系	Inelastic neutron scattering experiments on non-centrosymmetric superconductors	Hazuki Furukawa	Ochanomizu University

No.	課題名	氏名	所属		Title	Name	Organization
63	トポロジカル超伝導体の磁束格子	古川　はづき	お茶の水女子大学	基幹研究院 自然科学系	Vortex phase in topological superconductors	Hazuki Furukawa	Ochanomizu University
64	小角中性子散乱による DNA モジュールゲルの構造解析	Li　Xiang	東京大学	物性研究所	Structure Characterization of DNA-module gel by Small-Angle Neutron Scattering	Xiang Li	The University of Tokyo
65	Current driven motion of skyrmions in helical magnets	奥山　大輔	東北大学	多元物質科学研究所	Current driven motion of skyrmions in helical magnets	Daisuke Okuyama	Tohoku University
66	全イオン性高分子ミセルのナノ構造と刺激応答	松岡　秀樹	京都大学	工学研究科高分子化学専攻	Nanostructure and Stimulli-responsivity of Totally Ionic Polyion Complex Micelles	Hideki Matsuoka	Kyoto University
67	イオン液体中における刺激応答性高分子の圧力応答	柴山　充弘	東京大学	物性研究所	Pressure Response of a Stimuli-responsive Polymer in an Ionic Liquid	Mitsuhiro Shibayama	The University of Tokyo
68	膨潤イオン液体での層構造と緩和	根本　文也	高エネルギー加速器研究機構	物質構造科学研究所	Layer structure and fructuation in swollen ionic liquids	Fumiya Nemoto	High energy accelerator research organization
69	スピン誘導型強誘電体における誘電 (磁気) ドメイン駆動	満田　節生	東京理科大学	理学部　物理	Ferroelectric domain wall motion in a electromagnetic multiferroic $CuFeO_2$	Setsuo Mitsuda	Tokyo University of Science
70	界面不活性の働きをする界面活性剤	貞包　浩一朗	同志社大学	生命医科学部医情報学科	Surfactant molecules behaving as a surface-inactive agent	Koichiro Sadakane	Doshisha University
71	高圧条件下における２成分混合溶液の新奇な臨界挙動	貞包　浩一朗	同志社大学	生命医科学部医情報学科	Novel critical behavior in a mixture of water / organic solvent under high-pressure condition	Koichiro Sadakane	Doshisha University
72	巨大ひずみ加工した Ni, Co に発現する特異な磁気構造	足立　望	京都大学	原子炉実験所	Anomalous magnetic structures in severely deformed Ni and Co	Nozomu Adachi	Kyoto University
73	アルカン溶媒中でらせん反転を示すポリ（キノキサリン -2,3- ジイル）の小角中性子散乱による構造解明	長田　裕也	京都大学	工学研究科	Clarification of the Configurations of Chiral Side Chains of Poly(quinoxaline-2,3-diyl)s Exhibiting Helix Inversion in Alkane Solvents by Small-angle Neutron Scattering	Yuya Nagata	Kyoto University
74	イミダゾリウム系イオン液体中におけるエタノールの会合体形成	高椋　利幸	佐賀大学	大学院工学系研究科	Cluster Formation of Ethanol Molecules in Imidazolium-based Ionic Liquids	Toshiyuki Takamuku	Saga University
75	高分子コンポジット中の固体粒子の分散・凝集に及ぼす粒子表面の吸着高分子の影響	鳥飼　直也	三重大学	大学院地域イノベーション学研究科	Effects of Adsorbed Polymer on Dispersion and Aggregation of Solid Particles in Polymer Composite	Naoya Torikai	Mie University
76	中性子小角散乱測定による耐熱超合金中の超微細析出物の評価	間宮　広明	物質材料研究機構	先端材料解析研究拠点	Study on ultra-fine precipitates in heat-resistant superalloys using small angle scattering technique	Hiroaki Mamiya	National Institute for Materials Science
77	小角中性子散乱 (SANS) 法による高分子ゲル網目均一性の定量的評価	Li　Xiang	東京大学	物性研究所	Quantitative evaluation of uniformity of various polymer networks by small angle neutron scattering (SANS) with contrast variation technique	Xiang Li	The University of Tokyo
78	小角中性子散乱による反応率臨界ゲルクラスターの構造解析	Li　Xiang	東京大学	物性研究所	SANS study on critical polymer clusters near gel point	Xiang Li	The University of Tokyo

・ 申請装置 C1-3: ULS

No.	課題名	氏名	所属		Title	Name	Organization
79	ULS（極小角散乱装置）IRT 課題	清水　裕彦	名古屋大学	大学院理学研究科	IRT project of ULS	Hirohiko Shimizu	Nagoya University
・ 申請装置 C1-3: mf-SANS							
80	mf-SANS（小型集束型小角散乱装置）IRT 課題	間宮　広明	物質材料研究機構	先端材料解析研究拠点	IRT project of mf-SANS	Hiroaki Mamiya	National Institute for Materials Science
・ 申請装置 C2-3-1: iNSE							
81	iNSE（中性子スピンエコー分光器）IRT 課題	Li　Xiang	東京大学	物性研究所	IRT project of iNSE	Xiang Li	The University of Tokyo
82	鉄系梯子型超伝導物質 $BaFe_2S_3$ の中性子スピンエコー	南部　雄亮	東北大学	金属材料研究所	Neutron spin echo on the iron-based superconducting ladder material $BaFe_2S_3$	Yusuke Nambu	Tohoku University
83	膨潤イオン液体での層構造と緩和	根本　文也	高エネルギー加速器研究機構	物質構造科学研究所	Layer structure and fructuation in swollen ionic liquids	Fumiya Nemoto	High energy accelerator research organization
84	界面不活性の働きをする界面活性剤	貞包　浩一朗	同志社大学	生命医科学部医情報学科	Surfactant molecules behaving as a surface-inactive agent	Koichiro Sadakane	Doshisha University
85	マルチドメイン蛋白質 MurD の ATP 依存的な機能性ドメイン運動	中川　洋	日本原子力研究開発機構	階層構造研究グループ	ATP-dependent functional domain motion of multi-domain protein MurD	Hiroshi Nakagawa	Japan Atomic Energy Agency
86	脂質膜の粘弾性に及ぼすアルカンの効果	菱田　真史	筑波大学	数理物質系化学域	Effects of alkanes on the lipid membrane elastic and viscous properties	Mafumi Hishida	Tsukuba University
・ 申請装置 C3-1-1: AGNES							
87	AGNES（高分解能パルス冷中性子分光器）IRT 課題	山室　修	東京大学	物性研究所	IRT project of AGNES	Osamu Yamamuro	The University of Tokyo
88	配位高分子ホスト $[CuZn(CN)_4]^-$ に包接された K^+ 水溶液のダイナミクス	山室　修	東京大学	物性研究所	Dynamics of K^+ aqueous solution confined in a coordination polymer host $[CuZn(CN)_4]^-$	Osamu Yamamuro	The University of Tokyo
89	柔粘性結晶相をもつイオン液体の速いダイナミクス	山室　修	東京大学	物性研究所	Fast Dynamics of Ionic Liquids with Plastic-crystalline Phases	Osamu Yamamuro	The University of Tokyo
90	超高エントロピー液体 C_6C_{10}- テトラフェニルポルフィリンの長いアルキル鎖ダイナミクス	山室　修	東京大学	物性研究所	Dynamics of long alkylchains in a super-high entropy liquid C_6C_{10}-tetraphenylporphyrin	Osamu Yamamuro	The University of Tokyo
91	Zn-Ln-Zn 単分子磁石のスピンダイナミクス	古府　麻衣子	日本原子力研究開発機構	中性子利用セクション	Spin dynamics in Zn-Ln-Zn single-molecule magnets	Maiko Kofu	Japan Atomic Energy Agency
・ 申請装置 C3-1-2: MINE1							

No.	課題名	氏名	所属		Title	Name	Organization
92	MINE1（京大炉：多層膜中性子干渉計・反射率計）IRT 課題	日野　正裕	京都大学	原子炉実験所	MINE1 (Multilayer neutron interferometer and reflectmeter)	Masahiro Hino	Kyoto University
・ 申請装置 C3-1-2: MINE2							
93	MINE2（京大炉：多層膜中性子干渉計・反射率計）IRT 課題	日野　正裕	京都大学	原子炉実験所	MINE2 (Multilayer neutron interferometer and reflectmeter)	Masahiro Hino	Kyoto University
94	高分子 / 水界面における生体分子の吸着状態の解析	松野　寿生	九州大学	大学院工学研究院応用化学部門	Analyses of adsorbed biomolecules at the polymer/water interface	Hisao Matsuno	Kyushu University
95	混合液体中における高分子薄膜の膨潤挙動	田中　敬二	九州大学	工学研究院　応用化学部門（機能）	Swelling Behavior of Polymer Thin Films in Mixed Non-solvents	Keiji Tanaka	Kyushu University
・ 申請装置 T1-1: HQR							
96	HQR（高分解能中性子散乱装置）IRT 課題	吉沢　英樹	東京大学	物性研究所	IRT project of HQR	Hideki Yoshizawa	The University of Tokyo
97	Electric polarization of antiferromagnetic Skyrmion-lattice like spin structure in $CaBaCo_2Fe_2O_7$	レイム　ヨハネス	東北大学	IMRAM	Electric polarization of antiferromagnetic Skyrmion-lattice like spin structure in $CaBaCo_2Fe_2O_7$	Johannes Reim	Tohoku University
98	Switching the magnetic order in $CaBaCo_2Fe_2O_7$ using magnetic field	レイム　ヨハネス	東北大学	IMRAM	Switching the magnetic order in $CaBaCo_2Fe_2O_7$ using magnetic field	Johannes Reim	Tohoku University
99	時間分割中性子散乱による磁気構造変化過程の実時間追跡	元屋　清一郎	東京理科大学	理工学部　物理学科	Real-time observation of magnetic structural change by means of time-resolved neutron scattering experiments	Kiyoichiro Motoya	Tokyo University of Science
100	Rb_2MoO_4 における多形転移とソフトフォノン	重松　宏武	山口大学	教育学部	Polymorph Transition and Soft Phonon in Rb_2MoO_4	Hirotake Shigematsu	Yamaguchi University
101	強誘電体の相転移機構（変位型及び秩序–無秩序型）に関する統一的理解の確立	重松　宏武	山口大学	教育学部	Establishment of the unified explanation about the phase transition mechanism (displacive and order-disorder type) in Ferroelectrics	Hirotake Shigematsu	Yamaguchi University
102	2 等辺 Ising 三角格子磁性体 $CoNb_2O_6$ における一軸応力による鎖間交換相互作用の制御	満田　節生	東京理科大学	理学部　物理	Uniaxial-stress-control of competing inter-chain exchange interactions of isosceles-triangular lattice Ising magnet $CoNb_2O_6$	Setsuo Mitsuda	Tokyo University of Science
・申請装置 T1-2: AKANE							
103	AKANE（東北大金研：三軸型中性子分光器 ）IRT 課題	藤田　全基	東北大学	金属材料研究所	IRT project of AKANE	Masaki Fujita	Tohoku University
104	T' 構造銅酸化物 $Pr_{2-x}Ca_xCuO_4$ における磁気相関と超伝導の研究	藤田　全基	東北大学	金属材料研究所	Study of spin correlations and superconductivity in T'-structured cuprate oxide $Pr_{2-x}Ca_xCuO_4$	Masaki Fujita	Tohoku University
105	幾何学的フラストレート系 $(Mn,Mg)Cr_2O_4$ におけるらせん磁気構造のクロスオーバー	高阪　勇輔	広島大学	大学院理学研究科	Crossover between conical and screw magnetic phase in $(Mn,Mg)Cr_2O_4$	Yusuke Kousaka	Hiroshima University

No.	課題名	氏名	所属		Title	Name	Organization
106	MPO_4 (M: 遷移金属) のカイラル磁気構造の検証	高阪　勇輔	広島大学	大学院理学研究科	Chiral Magnetism in New Chiral Magnetic Compounds MPO_4 (M: Transition Metal)	Yusuke Kousaka	Hiroshima University
107	CrX (Cr=Si, Ge) のカイラル磁気構造の検証	高阪　勇輔	広島大学	大学院理学研究科	Chiral Magnetic Structure in CrX (X=Si, Ge)	Yusuke Kousaka	Hiroshima University
108	ホールドープ系鉄系超伝導体のスピン揺動	李　哲虎	産業技術総合研究所	省エネルギー研究部門	Spin fluctuations of hole-doped iron-based superconductors	Chul-Ho Lee	National Institute of Advanced Industrial Science and Technology
・申請装置 T1-3 HERMES							
109	HERMES（東北大金研：中性子粉末回折装置）IRT 課題	南部　雄亮	東北大学	金属材料研究所	IRT project of HERMES	Yusuke Nambu	Tohoku University
110	層状ペロブスカイト型酸化物の結晶構造とイオン拡散経路	八島　正知	東京工業大学	理学院	Crystal structure and ion-diffusion path of layered perovskite-type oxides	Masatomo Yashima	Tokyo Institute of Technology
111	$Yb_3Fe_5O_{12}$ の結晶・磁気構造解析	南部　雄亮	東北大学	金属材料研究所	Crystal and magnetic structures of $Yb_3Fe_5O_{12}$	Yusuke Nambu	Tohoku University
112	Powder diffraction experiment on chiral magnetic $Re_5Ru_3Al_2$	奥山　大輔	東北大学	多元物質科学研究所	Powder diffraction experiment on chiral magnetic $Re_5Ru_3Al_2$	Daisuke Okuyama	Tohoku University
113	Pd/Ru ナノ合金の構造	山室　修	東京大学	物性研究所	Structures of Pd/Ru nano-alloys	Osamu Yamamuro	University of Tokyo
114	複合アニオン配位を有する新規オキシカルコゲナイドの磁気構造	山本　隆文	京都大学	工学研究科	Magnetic structure of novel oxychalcogenides with mixed anion coordination	Takafumi Yamamoto	Kyoto University
115	熱電半導体 $(Bi,Sb)_2Te_3$ 固溶体の酸化過程	栗栖　牧生	愛媛大学	理工学研究科 (理学系)	Oxidation Process in $(Bi,Sb)_2Te_3$ Pseud-binary Solid Solutions	Makio Kurisu	Ehime University
116	中性子回折によるナノ炭素中液晶の構造解析	根本　文也	高エネルギー加速器研究機構	物質構造科学研究所	Structural analysis on liquids crystals in nano-sized carbon by neutron diffraction	Fumiya Nemoto	High energy accelerator research organization
117	新規ペロブスカイト関連 $AA'BO_4$ 型構造をもつ酸化物イオン伝導体の結晶構造とイオン伝導経路の解明	藤井　孝太郎	東京工業大学	理学院化学系	Structural Investigation of the Novel Perovskite related $AA'BO_4$-type Materials -Oxide-Ionic and Electronic Conducting Materials-	Kotaro Fujii	Tokyo Institute of Technology
118	パイロクロア構造を有する $Na_3Mn(CO_3)_2Cl$ の磁気構造	那波　和宏	東北大学	多元物質科学研究所	Magnetic structure of $Na_3Mn(CO_3)_2Cl$ with Mn pyrochlore-network	Kazuhiro Nawa	Tohoku University
119	量子臨界点近傍にある $YbCo_2Zn_{20}$ の置換系試料の結晶構造と磁気構造	阿曽　尚文	琉球大学	理学部物質地球科学科	Crystal and magnetic structures in doped systems of $YbCo_2Zn_{20}$ in vicinity of a quantum critical point	Naofumi Aso	University of the Ryukyus
120	パイロクロア磁性体 $Tb_2M_2O_7$ (M = Zr, Hf, Pd, Pt) の結晶構造	高津　浩	京都大学	工学研究科	Structural investigation of pyrochlore oxides $Tb_2M_2O_7$ (M=Zr, Hf, Pd, Pt)	Hiroshi Takatsu	Kyoto University
121	新規カイラル磁性体 MPO_4 (M: 遷移金属) の磁気構造解析	高阪　勇輔	広島大学	大学院理学研究科	Magnetic structure analysis of new chiral magnetic compounds MPO_4 (M: transition metal)	Yusuke Kousaka	Hiroshima University

No.	課題名	氏名	所属		Title	Name	Organization
122	新規カイラル磁性体 CrX(X: Si, Ge) の磁気構造解析	高阪　勇輔	広島大学	大学院理学研究科	Magnetic Structure Analysis in New Chiral Magnetic Compounds CrX (X: Si, Ge)	Yusuke Kousaka	Hiroshima University
123	混合原子価状態をもつ新奇酸フッ化物ペロフスカイトの磁気構造	辻本　吉廣	物質材料研究機構	機能性材料研究拠点	Neutron Diffraction Study of New $O_x$yfluoride Perovskites with Mixed-Valence States	Yoshihiro Tsujimoto	National Institute for Materials Science
・申請装置 T2-2: FONDER							
124	FONDER(中性子 4 軸回折装置)IRT 課題	木村　宏之	東北大学	多元物質科学研究所	IRT proposal for FONDER (Neutron 4-circle diffractometer)	Hiroyuki Kimura	Tohoku University
125	塑性歪みを加えた Pt_3Fe 反強磁性体における強磁性の発現機構	小林　悟	岩手大学	理工学部物理・材料理工学科	Mechanism of ferromagnetism in plastically deformed Pt_3Fe antiferromagnet	Satoru Kobayashi	Iwate University
126	$DyFe_2Zn_{20}$ における磁気異方性増強を伴う逐次磁気相転移	岩佐　和晃	茨城大学	フロンティア応用原子科学研究センター	Successive magnetic phase transition with enhancement in magnetic anisotropy of $DyFe_2Zn_{20}$	Kazuaki Iwasa	Ibaraki University
127	typeIII 型反強磁性体 Pt-Mn における整合ー非整合磁気相転移	高橋　美和子	筑波大学	数理物資系	Commensurate-Incommensurate Magnetic Phase Transition in Type-III Anti-ferromagnet Pt-Mn	Miwako Takahashi	Tsukuba University
128	S=1/2 パーフェクトカゴメ系 $CaCu_3(OH)_6Cl_{20.6}H_2O$ の磁気構造解析	飯田　一樹	総合科学研究機構	研究開発部	Magnetic structure in S=1/2 perfect kagome system $CaCu_3(OH)_6Cl_{20.6}H_2O$	Kazuki Iida	Comprehensive Research Organization for Science and Society
・ 申請装置 Accessory							
129	アクセサリー IRT 課題	上床　美也	東京大学	物性研究所	IRT project of Accessory	Yoshiya Uwatoko	The University of Tokyo

平成 29 年度 軌道放射物性研究施設 共同利用課題一覧 / Joint Research List of Syncrotron Radiation Researcher 2017

播磨分室　BL07LSU / Harima Branch BL07LSU

No.	課題名	氏名	所属		Title	Name	Organization
1	オペランド軟 X 線分光の協奏・高度化が拓く触媒科学	吉信　淳	東京大学	物性研究所	New Frontier of Catalysis Science Opened by Synergy and Development of Operando Soft X-ray Spectroscopies	Jun Yoshinobu	The University of Tokyo
2	省エネ・創エネ・蓄電デバイスのオペランドナノ分光	尾嶋　正治	東京大学	大学院工学系研究科	Operando nano-spectroscopy for energy efficient, power generation and energy storage devices	Masaharu Oshima	The University of Tokyo
3	偏光スイッチングを利用した非自明な磁気構造とスピンダイナミクスの観測	和達　大樹	東京大学	物性研究所	Observation of nontrivial magnetic structures and spin dynamics by using polarization switching	Hiroki Wadachi	The University of Tokyo
4	モット絶縁体 1 T-TaS_2 における電荷密度波の相転移ダイナミクスの時間分解二次元光電子回折による研究	大門　寛	奈良先端科学技術大学院大学	物質創成科学研究科	Study on the Dynamics of Charge Density Wave in Mott Insulator 1T-TaS_2 Using Time-resolved Two-dimensional X-Ray Photoelectron Diffraction.	Hiroshi Daimon	Nara Institute of Science and Technology
5	大気非曝露・高分解能軟 X 線発光分光による二次電池正極材料の酸素レドックスの研究	大久保　將史	東京大学	工学系研究科	High-energy-resolution soft x-ray emission spectroscopy studies of oxygen redox reactions in cathode materials for rechargeable batteries using a sample transfer system without air exposure	Okubo Masashi	The University of Tokyo
6	3D nano-ESCA を用いた時空間オペランド光電子分光への挑戦：GaN トランジスタ表面において局所電場により誘起された遅いキャリア・ダイナミクスの解明	吹留　博一	東北大学	電気通信研究所	Challenge of spatio-temporal operando photoelectron spectroscopy using 3D nano-ESCA: Slow surface carrier dynamics induced by local electric field of GaN-based transistors	Hirokazu Fukidome	Tohoku University
7	GaN 界面のキャリアダイナミクス研究	吹留　博一	東北大学	電気通信研究所	Study of Carrier Dynamics at the GaN interface	Hirokazu Fukidome	Tohoku University
8	過剰ドープ銅酸化物超伝導体における電荷秩序	石井　賢司	量子科学技術研究開発機構	関西光科学研究所	Charge order in over-doped cuprate superconductors	Kenji Ishii	National Institutes for Quantum and Radiological Science and Technology
9	シリセン形成過程の時分割光電子ホログラフィー	林　好一	名古屋工業大学	物理工学科	Picosecond time-resolved photoelectron holography during silicene formation process	Koichi Hayashi	Nagoya Institute of Technology
10	共鳴非弾性軟 X 線散乱による室温マルチフェロイクス Cr_2O_3 の電場・内部磁場制御電子状態の直接観測	藤原　秀紀	大阪大学	大学院理学系研究科	SX-RIXS studies of electronic structures for the room-temperature-multiferroic Cr_2O_3 under electric and magnetic fields	Hidenori Fujiwara	Osaka University
11	オペランド軟 X 線発光分光によるリチウムイオン電池正極材料の電子軌道選択的な電子状態解析	朝倉　大輔	産業技術総合研究所	省エネルギー研究部門	Orbital-selective electronic structure analyses of cathode materials for Li-ion batteries by operando soft x-ray emission spectroscopy	Daisuke Asakura	National Institute of Advanced Industrial Science and Technology
12	プラズモンナノ材料におけるキャリアダイナミクスの実時間観測	山本　達	東京大学	物性研究所	Real-time Observation of Carrier Dynamics in Plasmonic Nanomaterials	Susumu Yamamoto	The University of Tokyo
13	ドナー・アクセプター有機層接合界面での電荷分離と再結合過程の実時間測定	小澤　健一	東京工業大学	理学院	Real-time observation of charge separation and recombination processes at organic-organic interfaces	Kenichi Ozawa	Tokyo Institute of Technology
14	Temperature Induced Semiconductor <=> Metal Phase Transition Followed by Time-Resolved Photoemission	D'angelo Marie	Institutdes Nanosciences de Paris	physics	Temperature Induced Semiconductor <=> Metal Phase Transition Followed by Time-Resolved Photoemission	D'angelo Marie	Paris Institut for Nanosciences
15	REXS、RIXS のための θ -2 θ 自動スキャンシステムの開発	原田　慈久	東京大学	物性研究所	Development of the automatic θ -2 θ scan for REXS and RIXS	Yoshihisa Harada	The University of Tokyo

No.	課題名	氏名	所属		Title	Name	Organization
16	The determination of the catalytic role of Mn during the electrochemical water oxidation reaction of Graphene-supported Ni_6MnO_8 catalyst by Mn 2p3d RIXS	Al Samarai Mustafa	Max Planck Institute	Chemical Energy Conversion	The determination of the catalytic role of Mn during the electrochemical water oxidation reaction of Graphene-supported Ni_6MnO_8 catalyst by Mn 2p3d RIXS	Al Samarai Mustafa	Max Planck Institute
17	O K-edge XAS と RIXS 用いた Bi2223 超伝導体の研究	宮脇 淳	東京大学	物性研究所	O K-edge XAS and RIXS study on Bi2223 Superconductor	Jun Miyawaki	The University of Tokyo
18	生体適合性ポリマー材料表面に形成される中間水の電子状態観測	山添 康介	東京大学	物性研究所	Observation of the electronic structure of intermediate water formed on the surface of biocompatible polymers	Kousuke Yamazoe	The University of Tokyo
19	強磁性 Co/Pt 超格子薄膜の光誘起磁化反転の時間分解 X 線磁気円二色性測定	平田 靖透	東京大学	物性研究所	Time-Resolved X-Ray Magnetic Circular Dichroism of Photo-Induced Magnetic Reversal in Ferro-Magnetic Co/Pt Superlattice Thin Film	Yasuyuki Hirata	The University of Tokyo
20	大気非曝露搬送系を用いた二次電池正極材料の遷移金属 L 吸収端 高分解能軟 X 線発光分光	大久保 將史	東京大学	工学系研究科	High-energy-resolution transition-metal L-edge soft x-ray emission spectroscopy studies of cathode materials for rechargeable batteries using a sample transfer system without air exposure	Okubo Masashi	The University of Tokyo
21	酸素フリーなオペランドセルを用いた軟 X 線発光分光によるリチウムイオン電池正極材料の酸素 2p 電子状態の研究	朝倉 大輔	産業技術総合研究所	省エネルギー研究部門	Electronic-structure analysis of O 2p orbital of Li-ion-battery cathode materials by soft x-ray emission spectroscopy with oxygen-free operando cell system	Daisuke Asakura	National Institute of Advanced Industrial Science and Technology
22	強誘電体を用いた二酸化チタン薄膜のポテンシャル構造と光励起キャリア寿命の制御	小澤 健一	東京工業大学	理学院	Control of the potential structure of TiO_2 thin film and the lifetime of photoexcited carriers by ferroelectric crystal	Kenichi Ozawa	Tokyo Institute of Technology
23	多層膜を用いた共鳴X線非弾性回折の実証実験	宮脇 淳	東京大学	物性研究所	Demonstration of Resonant Inelastic Diffraction from Multilayers	Jun Miyawaki	The University of Tokyo
24	GaN 界面のキャリアダイナミクス研究 (II) 界面化学処理によるダイナミクスの変化	吹留　博一	東北大学	電気通信研究所	Study of Carrier Dynamics at the GaN Interface (II) Change in dynamics by treating interface chemistry	Hirokazu Fukidome	Tohoku University
25	グラフェン・BN・などを組み合わせた二次元原子薄膜ヘテロ接合界面の物性探索と新規な量子デバイス応用	吹留　博一	東北大学	電気通信研究所	Challenge of spatio-temporal operando photoelectron spectroscopy using 3D nano-ESCA: Slow surface carrier dynamics induced by local electric field of GaN-based transistors	Hirokazu Fukidome	Tohoku University
26	Investigating the Electronic Structure of the Nitrogenase Enzyme by 2p3d RIXS	Van Kuiken Benjamin	Max Planck Institute	Chemical Energy Conversion	Investigating the Electronic Structure of the Nitrogenase Enzyme by 2p3d RIXS	Van Kuiken Benjamin	Max Planck Institute
27	プラズマ誘起液相反応場の軟 X 線分光診断	寺嶋　和夫	東京大学	大学院新領域創成科学研究科	Soft X-ray spectroscopy of plasma-induced reaction field in liquid	Kazuo Terashima	The University of Tokyo
28	軟 X 線吸収及び発光分光によるハイドレートメルト中の水とリチウムイオンの相互作用の研究	崔　藝涛	東京大学	物性研究所	The interaction of water and Li ion in hydrate melt studied by soft X-ray absorption and emission spectroscopy	Yitao Cui	The University of Tokyo
29	光エネルギー変換過程の実時間観測に向けた時間分解オペランド XPS の開発	山本　達	東京大学	物性研究所	Development of time-resolved Oprando XPS for the real time monitoring of light energy conversion processes	Susumu Yamamoto	The University of Tokyo
30	ホールドープ銅酸化物における電荷励起とそのスピン相関との結合の可能性	石井　賢司	量子科学技術研究開発機構	関西光科学研究所	Charge excitations in hole-doped cuprates and their possible coupling to spin correlation	Kenji Ishii	National Institutes for Quantum and Radiological Science and Technology
31	Ion-water interaction on the molecular level	Yin Zhong	Deutsches Elektronen-Synchrotron	Laboratory of Physical Chemistry	Ion-water interaction on the molecular level	Yin Zhong	Deutsches Elektronen-Synchrotron
32	ハーフメタル型電子状態を有する Co_2MnSi および Mn_2VAl ホイスラー合金単結晶の磁場中共鳴非弾性軟 X 線散乱 (SX-RIXS)	梅津　理恵	東北大学	金属材料研究所	Resonant inelastic soft X-ray scattering (SX-RIXS) in magnetic field of single crystal Co_2MnSi and Mn_2VAl Heusler alloys with half-metal-type electronic structure	Rie Umetsu	Tohoku University

No.	課題名	氏名	所属		Title	Name	Organization
33	時分割光電子ホログラフィーの確立とシリセン形成過程の観測	林　好一	名古屋工業大学	物理工学科	Development of time-resolved photoelectron holography and its application to the structural observation of silicene formation	Koichi Hayashi	Nagoya Institute of Technology
34	微高分解能二次元光電子分光による機能材料における活性中心の局所構造及び電子状態の研究	大門　寛	奈良先端科学技術大学院大学	物質創成科学研究科	Analysis of Structures and Electronic States of [Active-site] in Functional Materials by Microscopic High-resolution Two-Dimensional Photoelectron Spectroscopy	Hiroshi Daimon	Nara Institute of Science and Technology

柏キャンパス E 棟 / Laser and Synchrotron Research Laboratory in Kashiwa

No.	課題名	氏名	所属		Title	Name	Organization
1	Pb/Ge(111)-α の laser-SARPES	矢治　光一郎	東京大学	物性研究所	Laser-SARPES measurement of spin-polarized surface states on Pb/Ge(111)-α	Koichiro Yaji	The University of Tokyo
2	Graphen/Sn/SiC の laser-ARPES，laser-SARPES	矢治　光一郎	東京大学	物性研究所	Laser-ARPES and -SARPES measurements of Graphen/Sn/SiC	Koichiro Yaji	The University of Tokyo
3	Searching for topological states in $IrTe_2$	張　鵬	東京大学	物性研究所	Searching for topological states in $IrTe_2$	Peng Zhang	The University of Tokyo
4	Study of topological states in Fe-based superconductor	張　鵬	東京大学	物性研究所	Study of topological states in Fe-based superconductor	Peng Zhang	The University of Tokyo
5	トポロジカル近藤絶縁体候補物質である希土類硼化物単結晶の表面電子状態とスピン・軌道偏極構造	大坪　嘉之	大阪大学	生命機能研究科	Surface electronic states and its spin/orbital polarization of rare-earth borides as candidates of topological Kondo insulator	Yoshiyuki Ohtsubo	Osaka University
6	3R-NbS_2 Q バレーにおけるスピン構造の決定	黒田　健太	東京大学	物性研究所	Probing the spin-structure of 3R-NbS_2 on single domains at the Q valley	Kenta Kuroda	The University of Tokyo
7	銀の量子井戸状態の光電子分光	黒田　健太	東京大学	物性研究所	Controls of spin-orbit interband coupling in heavy atoms on quantum well states	Kenta Kuroda	The University of Tokyo
8	薄膜スピン分裂状態のバンド間スピン軌道混成の研究	黒田　健太	東京大学	物性研究所	Investigation of the interband spin-orbit hybridization of Rashba spin splitting in thin films	Kenta Kuroda	The University of Tokyo
9	擬一次元新型トポロジカルスピン分裂表面バンドの直接観測	近藤　猛	東京大学	物性研究所	Direct investigation of the spin-polarized Dirac surface state in a quasi-one dimensional material beta-Bi_4I_4	Takeshi Kondo	The University of Tokyo
10	バルク敏感高分解能スピン分解光電子分光を用いたハーフメタル強磁性体における有限温度効果の研究	横谷　尚睦	岡山大学	自然科学研究科	Studies of finite temperature effects of half-metallic ferromagnets by bulk-sensitive high-resolution spin-resolved photoemission spectroscopy	Takayoshi Yokoya	Okayama University
11	高分解能スピン・角度分解光電子分光によるハーフメタル強磁性体 CoS_2 の電子構造研究	横谷　尚睦	岡山大学	自然科学研究科	Study on electronic structures in half-metallic ferromagnet CoS_2 by high-resolution spin- and angle-resolved photoemission spectroscopy	Takayoshi Yokoya	Okayama University
12	原子層 In 超薄膜の特異なスピン構造	坂本　一之	千葉大学	大学院工学研究院	Peculiar spin structure in atomic-In-layers superconductor	Kazuyuki Sakamoto	Chiba University
13	トポロジカル半金属におけるスピン偏極した表面状態の観測	坂野　昌人	東京大学	工学系研究科	Observation of spin-polarized surface states on topological semimetals	Masato Sakano	The University of Tokyo

No.	課題名	氏名	所属		Title	Name	Organization
14	新規スピントロニクス物質におけるスピン分解角度分解光電子分光	小林　正起	東京大学	工学系研究科	Spin- and angle-resolved photoemission spectroscopy on novel spintronics materials	Masaki Kobayashi	The University of Tokyo
15	新奇超伝導体 $RO_{1-x}F_xBiS_2$(R=La,Ce,Nd) のスピン角度分解光電子分光	奥田　太一	広島大学	HiSOR	Spin- and angle-resolved photoemission study of $RO_{1-x}F_xBiS_2$(R=La,Ce,Nd)	Taichi Okuda	Hiroshima University
16	高空間分解レーザー角度分解光電子分光による $CeCoIn_5$ の電子状態観測	大田　由一	東京大学	物性研究所	Direct observation of electronic state on $CeCoIn_5$ with using high space resolution laser-ARPES	Yuichi Ota	The University of Tokyo
17	インジウム原子層超伝導体におけるラシュバスピン分裂の直接観察	内橋　隆	物質・材料研究機構	ナノアーキテクトニクス研究拠点	Direct observation of Rashba effect-induced spin splitting in an indium atomic-layer superconductor	Takashi Uchihashi	National Institute for Materials Science
18	スピン分解角度分解光電子分光による $TaSi_2$ のスピン構造の研究	伊藤　孝寛	名古屋大学	シンクロトロン光科学研究センター	Spin-resolved angle-resolved photoemission study of spin texture of $TaSi_2$	Takahiro Ito	Nagoya University
19	スピン分解角度分解光電子分光による $GdTe_2$ の CDW ギャップ内表面状態の研究	伊藤　孝寛	名古屋大学	シンクロトロン光科学研究センター	Spin-resolved angle-resolved photoemission study of surface states among CDW gap of $GdTe_2$	Takahiro Ito	Nagoya University
20	高温超電導体のスピン干渉光電子放出	Hugo Dil	スイス連邦工科大学	ローザンヌ校	Spin interference of photoelectron emitted from high-Tc superconductor BSCCO	Hugo Dil	Polytechnique Fédérale de Lausanne

平成２９年度　スーパーコンピュータ　共同利用課題一覧 / Joint Research List of Supercomputer System 2017

No.	課題名	氏名	所属	Title	Name	Organization
1. 第一原理計算 / First-Principles Calculation of Materials Properties						
1	ハード及びソフトナノ物質の原子構造と電子物性	押山　淳	東京大学工学系研究科	Atomic Structures and Electronic Properties of Hard- and Soft-Nano Materials	Atsushi Oshiyama	The University of Tokyo
2	ハード及びソフトナノ物質の原子構造と電子物性	押山　淳	東京大学工学系研究科	Atomic Structures and Electronic Properties of Hard- and Soft-Nano Materials	Atsushi Oshiyama	The University of Tokyo
3	電子・光機能を持つ界面の計算科学的研究	信定　克幸	分子科学研究所	Computational studies of electronic and photonic functional nano-interfaces	Katsuyuki Nobusada	Institute for Molecular Science
4	電子・光機能を持つ界面の計算科学的研究	信定　克幸	分子科学研究所	Computational studies of electronic and photonic functional nano-interfaces	Katsuyuki Nobusada	Institute for Molecular Science
5	スピントロニクス材料および分子性磁性体の原子構造、磁気状態、電子状態の解析	小田　竜樹	金沢大学理工研究域数物科学系	Analyses on atomic structure, magnetism, and electronic structure in spintronics materials and molecular magnets	Tatsuki Oda	Kanazawa University
6	高機能スピントロニクス材料物質および分子性磁性体の原子・磁気・電子構造の解析	小田　竜樹	金沢大学理工研究域数物科学系	Analyses on atomic, magnetic, and electronic structures in high-performance spintronics materials and molecular magnets	Tatsuki Oda	Kanazawa University
7	超並列電子状態計算とデータ科学の融合による大規模デバイス材料研究	星　健夫	鳥取大学大学院工学研究科機械宇宙工学専攻応用数理工学講座	Large-scale device-material research by massively parallel electronic structure calculation and data science	Takeo Hoshi	Tottori University
8	電池・触媒界面物性に関する第一原理 " サンプリング " 研究	館山　佳尚	物質・材料研究機構　国際ナノアーキテクトニクス研究拠点	DFT "sampling" studies on interfacial properties of batteries and catalysts	Yoshitaka Tateyama	National Institute for Materials Science
9	実験データを援用した新しい物質構造予測手法の開発と応用	常行　真司	東京大学大学院理学系研究科物理学専攻	Development and application of a new method for material structure prediction supported by experimental data	Shinji Tsuneyuki	The University of Tokyo
10	第一原理計算による Singlet-Triplet splitting の評価	野口　良史	東京大学物性研究所	First-principles calculation of singlet-triplet splitting	Yoshifumi Noguchi	The University of Tokyo
11	第四次革新的手法を用いた合理的創薬手法の開発およびその応用	常盤　広明	立教大学理学部化学科未来分子研究センター	Development & Application of Rational Drug Design using the Forth Innovation Methodology	Hiroaki Tokiwa	Rikkyo University
12	実空間差分法に基づく第一原理電子状態・輸送特性計算コードの開発とシミュレーション	小野　倫也	筑波大学計算科学研究センター	Development of first-principles electronic-structure and transport calculation method based on real-space finite-difference approach	Tomoya Ono	University of Tsukuba
13	第一原理量子論による新規相変化メモリの設計	白石　賢二	名古屋大学　未来材料・システム研究所	Design of New Phase Change Memories Based on First Principles Calculations	Kenji Shiraishi	Nagoya University
14	表面磁性超薄膜の第一原理計算	合田　義弘	東京工業大学物質理工学院材料系	First-principles calculations of magnetic ultrathin films on surfaces	Yoshihiro Gohda	Tokyo Institute of Technology
15	強相関材料の非平衡伝導特性に対する理論と第一原理計算の協奏研究	浅井　美博	産業技術総合研究所	Theoretical and first principle studies of non-equilibrium transport properties of strongly correlated materials	Yoshihiro Asai	National Institute of Advanced Industrial Science and Technology (AIST)

No.	課題名	氏名	所属	Title	Name	Organization
16	第一原理計算によるナトリウムイオン電池電極材料の解析	山田　淳夫	東京大学工学系研究科	First-principles study on electrode materials for sodium ion batteries	Atsuo Yamada	The University of Tokyo
17	酸水素化物における水素 1s 金属状態および超伝導の追求	明石　遼介	東京大学大学院理学系研究科物理学専攻	Exploration of hydrogen-1s metallic state and superconductivty in oxyhydride compounds	Ryosuke Akashi	The University of Tokyo
18	太陽光エネルギー変換における基礎過程の研究と材料設計指針獲得のための大規模第一原理計算	山下　晃一	東京大学大学院工学系研究科	Large scale ab initio calculations on the fundamental processes of solar energy convergence devices and on designing principles for new materials	Koichi Yamashita	The University of Tokyo
19	第一原理計算による有機強誘電体・圧電体の物性予測	石橋　章司	産業技術総合研究所	Prediction of properties of organic ferroelectrics and piezoelectrics by first-principles calculation	Shoji Ishibashi	National Institute of Advanced Industrial Science and Technology
20	遷移金属酸化物の第一原理電子状態計算	山内　邦彦	大阪大学産業科学研究所	First-Principles DFT Calculations for Transition-Metal Oxides	Kunihiko Yamauchi	Osaka University
21	ナノ構造の励起電子動力学と光学応答の第一原理計算	渡辺　一之	東京理科大学理学部	First-Principles Study of Excited Electron Dynamics and Optical Responses of Nanostructures	Kazuyuki Watanabe	Tokyo University of Science
22	実空間差分法に基づく第一原理電子状態・輸送特性計算コードの開発とシミュレーション	小野　倫也	筑波大学計算科学研究センター	Development of first-principles electronic-structure and transport calculation method based on real-space finite-difference approach	Tomoya Ono	University of Tsukuba
23	ナノ構造のイオン輸送特性、電気特性および界面電子状態の理論解析	渡邉　聡	東京大学大学院工学系研究科マテリアル工学専攻	Theoretical Analyses on Ionic Transport Properties, Electrical Properties and Interfacial Electronic States of Nanostructures	Satoshi Watanabe	The University of Tokyo
24	ナノ構造のイオン輸送特性、電気特性および界面電子状態の理論解析	渡邉　聡	東京大学大学院工学系研究科マテリアル工学専攻	Theoretical Analyses on Ionic Transport Properties, Electrical Properties and Interfacial Electronic States of Nanostructures	Satoshi Watanabe	The University of Tokyo
25	非類似性を利用したチトクロム c 複合体の構造変化解析	重田　育照	筑波大学大学院数理物質科学研究科	Structural transition analyses on cytochrome c complexes using dissimilarity	Yasuteru Shigeta	University of Tsukuba
26	表面・界面におけるスピン構造の第一原理計算	石井　史之	金沢大学理工研究域数物科学系	First-principles calculations of spin textures at the surfaces and interfaces	Fumiyuki Ishii	Kanazawa University
27	f-d 金属間化合物の相対論的電子状態計算	松本　宗久	東京大学物性研究所	Relativistic electronic structure calculations for f-d intermetallics	Munehisa Matsumoto	The University of Tokyo
28	グラフェン／イオン液体界面の第一原理分子動力学シミュレーション	大戸　達彦	大阪大学大学院基礎工学研究科	Ab initio molecular dynamics simulation of graphene/ionic liquids interfaces	Tatsuhiko Ohto	Osaka University
29	CO_2 転換プロセスのための酸塩基酸化物触媒水和表面のプロトン活性に関する研究	山口　周	東京大学大学院工学系研究科	Protonic Activity on the Hydrated Surface of Acidic and Basic Oxide Catalyst for CO_2 Conversion Processes	Shu Yamaguchi	The University of Tokyo
30	結晶構造探索手法の開発と磁石・スピントロニクス材料探索	山下　智樹	国立研究開発法人物質・材料研究機構	Development of crystal structure prediction method and search for magnet and spintronics materials	Tomoki Yamashita	National Institute for Materials Science (NIMS)
31	固液界面の機能性	杉野　修	東京大学物性研究所	Functional property of solid-liquid interfaces	Osamu Sugino	The University of Tokyo
32	高圧力下における共有結合性液体・ガラスの構造と電子状態の第一原理計算	下條　冬樹	熊本大学大学院自然科学研究科	First-Principles Molecular-Dynamics Study of Structural and Electronic Properties of Covalent Liquids and Glass under Pressure	Fuyuki Shimojo	Kumamoto University

No.	課題名	氏名	所属	Title	Name	Organization
33	ナノ構造の励起電子動力学と光学応答の第一原理計算	渡辺　一之	東京理科大学理学部	First-Principles Study of Excited Electron Dynamics and Optical Responses of Nanostructures	Kazuyuki Watanabe	Tokyo University of Science
34	金属酸化物の性質を特徴付ける構造単位の探索	赤木　和人	東北大学材料科学高等研究所	Exploration of structure motifs characterizing the metal oxides	Kazuto Akagi	WPI-AIMR, Tohoku University
35	超並列電子状態計算とデータ科学の融合による大規模デバイス材料研究	星　健夫	鳥取大学大学院工学研究科機械宇宙工学専攻応用数理工学講座	Large-scale device-material research by massively parallel electronic structure calculation and data science	Takeo Hoshi	Tottori University
36	炭素より重い IV 族元素の二次元結晶の電子状態と熱力学的安定性	洗平　昌晃	名古屋大学未来材料・システム研究所	Electronic States and Thermodynamic Stability of Two-Dimensional Crystals of Group IV Elements	Masaaki Araidai	Nagoya University
37	ナノ構造の量子伝導の第一原理計算	小林　伸彦	筑波大学 数理物質系　物理工学域	First-principles study of quantum transport in nanostructures	Nobuhiko Kobayashi	University of Tsukuba
38	第一原理熱力学・統計力学手法を用いた不均一触媒反応過程の研究	森川　良忠	大阪大学 大学院工学研究科 精密科学・応用物理学専攻	First-principles Thermodynamics and Statistical Mechanics Simulations of Catalytic Reactions at Solid Surfaces	Yoshitada Morikawa	Osaka University
39	ドープグラフェン・水界面の第一原理分子動力学シミュレーション	大戸　達彦	大阪大学大学院基礎工学研究科	Ab initio molecular dynamics simulation of doped-graphene/water interfaces	Tatsuhiko Ohto	Osaka University
40	不均一触媒によるトルエンの可逆的水素化反応に対する第一原理計算	中井　浩巳	早稲田大学理工学術院	First-principles calculation on reversible hydrogenation reaction of toluene using heterogeneous catalyst	Hiromi Nakai	Waseda university
41	第一原理計算を用いた微量元素添加 Nd-Fe-B 磁石の磁気異方性解析	立津　慶幸	東京工業大学	Magnetic anisotropy analysis of transition-metal-doped Nd-Fe-B magnets by first-principles calculations	Yasutomi Tatetsu	Tokyo Institute of Technology
42	新しい IV 族半導体混晶に関する第一原理計算	黒澤　昌志	名古屋大学 未来材料・システム研究所	First-Principles Study on New Group-IV Semiconductor Alloys	Masashi Kurosawa	Nagoya University
43	酸化物薄膜・界面における磁気安定性と輸送特性の第一原的研究	石井　史之	金沢大学理工研究域数物科学系	First-principles study of magnetic stability and transport properties in oxides thin-films and interfaces	Fumiyuki Ishii	Kanazawa University
44	機能性材料の格子欠陥近傍におけるランダム原子構造と選択的偏析	幾原　雄一	東京大学大学院工学系研究科総合研究機構	Random atomic structure and selective segregation behavior around defects in functional ceramic materials	Yuichi Ikuhara	The University of Tokyo
45	電場下の金属 / 固体界面における金属原子のイオン化・拡散の研究	中山　隆史	千葉大学理学部物理学科	First-principles study of ionization and diffusion of metal atoms at metal/solid interfaces in electric fields	Takashi Nakayama	Chiba University
46	イリジウム酸化物に対する第一原理フォノン計算	中村　和磨	九州工業大学	Ab initio phonon calculations for Sr_2IrO_4 and $Ca_5Ir_3O_{12}$	Kazuma Nakamura	Kyushu Institute of Technology
47	アナターゼ型 TiO_2 ナノクリスタルにおける余剰電子の安定性解明	泰岡　顕治	慶應義塾大学理工学部機械工学科	The Study on the Stability of Excess Electrons in Anatase TiO_2 Nanocrystals	Kenji Yasuoka	Keio University
48	ハイブリッド ab initio QM/MM MD 計算によるスーパーコイル DNA 構造を選択的に認識するタンパク質の機能メカニズムの解明	舘野　賢	兵庫県立大学大学院生命理学研究科	Hybrid ab initio QM/MM calculations of functional mechanisms of biological macromolecular systems recognizing supercoiled DNA	Masaru Tateno	University of Hyogo
49	ファン・デル・ワールス密度汎関数を用いた固体表面への分子吸着系の研究	濱田　幾太郎	大阪大学工学研究科精密科学・応用物理専攻	van der Waals density functional theory study of molecular adsorption on solid surfaces	Ikutaro Hamada	Osaka University

No.	課題名	氏名	所属	Title	Name	Organization
50	第一原理多体摂動計算ソフトウェア RESPACK の整備	中村　和磨	九州工業大学	Development of ab initio many-body perturbation calculation software RESPACK	Kazuma Nakamura	Kyushu Institute of Technology
51	燃料電池電極触媒及び水素透過膜の省貴金属化	國貞　雄治	北海道大学大学院工学研究院　附属エネルギー・マテリアル融合領域研究センター	Reduction of Rare Metals in Fuel Cell Catalysts and Hydrogen Permeable Membrane	Yuji Kunisada	Hokkaido University
52	結晶評価法としての陽電子およびミュオン実験に関する第一原理計算	斎藤　峯雄	金沢大学理工研究域数物科学系	First-Principles Calculation for Positron and Muon Experiments as Measurements of Crystals	Mineo Saito	Kanazawa University
53	表面電子ダイナミクスの第一原理計算	矢花　一浩	筑波大学計算科学研究センター	First-principles calculation for surface electron dynamics	Kazuhiro Yabana	University of Tsukuba
54	Si 表面上の原子吸着系のモデル計算	服部　賢	奈良先端科学技術大学院大学物質創成科学研究科	Model calculations in Si surfaces with adsorbates	Ken Hattori	Nara Institute of Science and Technology
55	第一原理分子動力学法に基づくガラスの静的構造に関する研究	高良　明英	熊本大学学生支援部	Ab initio molecular dynamics study of static structure of glasses	Akihide Koura	Kumamoto University
56	量子井戸誘起強磁性を発現する Pd(100) における歪みを用いた磁気機能制御の研究	佐藤　徹哉	慶應義塾大学理工学部	Controlling magnetic properties of quantum-well induced ferromagnetism in Pd(100) through the lattice distortion	Tetsuya Sato	Keio University
57	高圧下における玄武岩質メルトの粘性と局所構造に関する第一原理的研究	大村　訓史	広島工業大学　工学部	Ab initio study of viscosity and local structures of basaltic melt under high pressure	Satoshi Ohmura	Hiroshima Institute of Technology
58	第一原理計算によるエネルギーデバイス材料の電子状態解析	籾田　浩義	大阪大学産業科学研究所	First-principles study of electronic structures of energy device materials	Hiroyoshi Momida	Osaka University
59	第一原理計算によるルチル二酸化チタン中の不純物水素	吉澤　香奈子	高度情報科学技術研究機構	Hydrogen state in a rutile titanium dioxide by first-principles calculation	Kanako Yoshizawa	Research Organization for Information Science & Technology
60	有機半導体結晶の電子構造に関する理論的研究	柳澤　将	琉球大学理学部物質地球科学科物理系	Theoretical investigation on electronic structure of organic semiconductor solids	Susumu Yanagisawa	University of the Ryukyus
61	結晶評価法としての陽電子およびミュオン実験に関する第一原理計算	斎藤　峯雄	金沢大学理工研究域数物科学系	First-Principles Calculation for Positron and Muon Experiments as Measurements of Crystals	Mineo Saito	Kanazawa University
62	第一原理メタダイナミックス計算による CARE 加工プロセスの解明 -Pt と材料表面の間で生じる水分子分解とエッチング反応 -	稲垣　耕司	大阪大学大学院工学研究科	First-principles meta-dynamics analysis of Catalyst Referred Etching method (analysis on dissociative adsorption of water molecule and etching reaction at interface between Pt and material surface)	Kouji Inagaki	Osaka University
63	エレクトレット荷電メカニズムの解明	鈴木　雄二	東京大学大学院工学系研究科機械工学専攻	Study on the charge trap mechanism of electret	Yuji Suzuki	The University of Tokyo
64	ナノ構造の量子伝導の第一原理計算	小林　伸彦	筑波大学 数理物質系　物理工学域	First-principles study of quantum transport in nanostructures	Nobuhiko Kobayashi	University of Tsukuba
65	豊富元素を利用した触媒の理論設計	武次　徹也	北海道大学大学院理学研究院化学部門	Theoretical design on catalysts with abundant elements	Tetsuya Taketsugu	Hokkaido University
66	高性能フッ素ポリマーエレクトレットの開発	鈴木　雄二	東京大学大学院工学系研究科機械工学専攻	Development of High-performance Perfluoropolymer Electret	Yuji Suzuki	The University of Tokyo

No.	課題名	氏名	所属	Title	Name	Organization
67	機能性材料粒界の原子構造および機能特性解析	幾原　雄一	東京大学大学院工学系研究科総合研究機構	Study of atomic structure and properties in functional materials	Yuichi Ikuhara	The University of Tokyo
68	還元されたアナターゼ型 TiO_2 ナノクリスタルにおける電子状態の研究	泰岡　顕治	慶應義塾大学理工学部機械工学科	The study on the electronic state of reduced anatase TiO_2 nanocrystal	Kenji Yasuoka	Keio University
69	第一原理計算による生物由来酸化鉄の形成機構とイオン拡散に関する研究	鶴田　健二	岡山大学大学院自然科学研究科	Ab-initio Study on Amorphization Dynamics and Ion Diffusion in Biogenous Iron Oxide	Kenji Tsuruta	Okayama University
70	燃料電池電極触媒及び水素透過膜の省貴金属化	國貞　雄治	北海道大学大学院工学研究院　附属エネルギー・マテリアル融合領域研究センター	Reduction of Rare Metals in Fuel Cell Catalysts and hydrogen permeable membrane	Yuji Kunisada	Hokkaido University
71	非類似性を利用したナノバイオ系の構造変化解析	重田　育照	筑波大学大学院数理物質科学研究科	Structural transition analyses on nano- and bio-systems using dissimilarity	Yasuteru Shigeta	University of Tsukuba
72	第一原理計算によるグラフェン端に吸着した Pt クラスターの研究	濱本　雄治	大阪大学 大学院工学研究科 精密科学・応用物理学専攻	First principles study of Pt clusters adsorbed on graphene edges	Yuji Hamamoto	Osaka University
73	vdW-DF + U 法による固体酸素の第一原理計算	笠松　秀輔	東京大学物性研究所	First-principles calculation of solid oxygen using the vdW-DF+U method	Shusuke Kasamatsu	The University of Tokyo
74	第一原理分子動力学シミュレーションによる原始地球における生体有機分子発生機構の解明 II	島村　孝平	神戸大学大学院システム情報学研究科	Generation Mechanism of Organic/Biological Molecules on Early Earth: Ab Initio Molecular Dynamics Simulation II	Kohei Shimamura	Kobe University
75	固体中アト秒電子ダイナミクスの第一原理計算	篠原　康	東京大学工学系研究科附属光量子科学研究センター	First principles simulation for attosecond electron dynamics in crystalline solids	Yasushi Shinohara	The University of Tokyo
76	固体及びナノ粒子表面に吸着した分子に対する非調和ポテンシャルの構築とその応用	水上　渉	九州大学総合理工学研究院	Construction and application of anharmonic potentials for adsorbed molecule on crystal/nanoparticle surface	Wataru Mizukami	Kyushu University
77	ナノグラフェン VANG の強相関一重項が示す反応特異性	草部　浩一	大阪大学大学院基礎工学研究科	Curious chemical reactions of the entangled singlet state in nanographene VANG	Koichi Kusakabe	Osaka University
78	ペロブスカイト型鉛ハライド混晶の電子構造と状態密度に関する研究	牧野　哲征	福井大学大学院工学研究科	Study on electronic structures and density of states in perovskite-type lead-halide mixed crystals	Takayuki Makino	University of Fukui
79	高効率な原子層水分解光触媒の理論的探索	鈴木　達夫	東京都立産業技術高等専門学校	Theoretical search for high-efficient monolayer water-splitting photocatalysts	Tatsuo Suzuki	Tokyo Metropolitan College of Industrial Technology
80	プロトン伝導性固体電解質形燃料電池の材料開発とイオン伝導機構解析	大友　順一郎	東京大学大学院新領域創成科学研究科環境システム学専攻	Developemnt of materials of proton-conducitng solid electrolyte fuel cells and analysis of ion conduction	Junichiro Otomo	The University of Tokyo
81	グラフェン上の有機半導体分子：界面の電子構造と結晶成長	西館　数芽	岩手大学理工学部	Organic Molecule on Graphene: Electronic Structure at the Interface and Crystal Growth	Kazume Nishidate	Iwate University
82	第一原理計算を用いた Na2 次電池の負極材料物質の探索	小鷹　浩毅	京都大学 ESICB	Structural search of negative electrode candidate for sodium ion battery	Hiroki Kotaka	Kyoto University
83	第一原理計算に基づくマグネシウム合金の欠陥場の解析	松中　大介	信州大学工学部機械システム工学科	First-principles Study of Defects of Magnesium Alloys	Daisuke Matsunaka	Shinshu University

No.	課題名	氏名	所属	Title	Name	Organization
84	照射損傷と格子間原子との相互作用の研究	大澤　一人	九州大学応用力学研究所	Study of interaction between radiation damage and interstitial atom	Kazuhito Ohsawa	Kyushu University
85	固体表面・界面、微粒子の新規電子物性の探索と実現	稲岡　毅	琉球大学理学部	Search and realization of novel electronic properties of solid surfaces and interfaces and of small particles	Takeshi Inaoka	University of the Ryukyus
86	半導体表面界面における構造的素励起の物性の研究	影島　博之	島根大学大学院総合理工学研究科	Study on physical properties of structural elementary excitations of semiconductor surfaces and interfaces	Hiroyuki Kageshima	Shimane University
87	第一原理に基づく動的電子輸送シミュレーターの開発と応用	江上　喜幸	北海道大学大学院工学研究院	Development and application of for time-dependent electron-transport simulator based on first-principles method	Yoshiyuki Egami	Hokkaido University
88	第一原理計算を用いた希薄窒化物半導体 InSbN のバンド構造に関する研究	藤川　紗千恵	東京電機大学工学部電気電子工学科	Study of band structure for InSbN based dilute nitride semiconductor by using first-principle simulation	Sachie Fujikwa	Tokyo denki university
89	遷移金属ポルフィリン誘導体超薄膜のスピン配列と振動分光の密度汎関数法による解析	首藤　健一	横浜国立大学・工学部	Theoritical analysis of vibronic mode and spin ordering of thin film of transition metallated porphyrin-derivative	Ken-Ichi Shudo	Yokohama Nat'l University
90	新規半導体２次元構造の探索	ハシュミ　アルカム	筑波大学計算科学研究センター	Discovery of new 2D semiconductors	Arqum Hashmi	University of Tsukuba
91	第一原理に基づく動的電子輸送シミュレーターの開発と応用	江上　喜幸	北海道大学大学院工学研究院	Development and application of time-dependent electron-transport simulator based on first-principles method	Yoshiyuki Egami	Hokkaido University
92	アナターゼ型 TiO_2 ナノクリスタルにおける形状依存性に関する研究	泰岡　顕治	慶應義塾大学理工学部機械工学科	The Study on the Morphology Dependence of Anatase Nanocrystals	Kenji Yasuoka	Keio University
93	軽希土類永久磁石材料の電子状態	赤井　久純	東京大学物性研究所	Electronic structure of light rare earth permanent magnets	Hisazumi Akai	The University of Tokyo
94	電子デバイスのための自己組織化ナノインターフェイスの理論	レービガー　ハンネス	横浜国立大学　大学院工学研究院　物理工学コース	Theory of self-organized nano-interfaces for electronic devices	Hannes Raebiger	Yokohama National University
95	第一原理的アプローチによる超伝導の解析	池田　浩章	立命館大学理工学部物理科学科	Analysis of superconductivity based on a first-principles approach	Hiroaki Ikeda	Ritsumeikan University
96	多体電子論に基づく第一原理有効模型導出システムの構築	榊原　寛史	鳥取大学大学院工学研究科	Study on a automatic derivation technique of first-principles effective model based on the many body electron theory	Hirofumi Sakakibara	Tottori University
97	固体表面に吸着した磁性分子の構造と電子状態	高木　紀明	東京大学新領域創成科学研究科物質系専攻	Geometric and electronic structures of magnetic molecules at surfaces	Noriaki Takagi	The University of Tokyo
98	第一原理的アプローチによる高温超伝導体の探索	池田　浩章	立命館大学理工学部物理科学科	Search for high-temperature superconductors based on a first-principles approach	Hiroaki Ikeda	Ritsumeikan University
99	第一原理計算によるネオジム磁石結晶のアモルファス粒界相の形成過程および磁気特性解析	寺澤　麻子	東京工業大学	First-principles simulation of magnetism and formation of amorphous grain boundary phase of Nd-based permanent magnets	Asako Terasawa	Tokyo Institute of Technology
100	第一原理計算による高温高圧水中の多価アルコールの脱水過程の研究	佐々木　岳彦	東京大学大学院新領域創成科学研究科	Dehydration process of polyalcohol in hot pressurized water studied by First Principles Calculations	Takehiko Sasaki	The University of Tokyo

No.	課題名	氏名	所属	Title	Name	Organization
101	Si 表面上の原子吸着系のモデル計算	服部　賢	奈良先端科学技術大学院大学物質創成科学研究科	Model calculations in Si surfaces with adsorbates	Ken Hattori	Nara Institute of Science and Technology
102	同位体超格子や結晶多形超格子によるバンド・ギャップの制御	豊田　雅之	東京工業大学理学院物理学系	Band-gap engineering by forming isotope superlattices and polytypic superlattices	Masayuki Toyoda	Tokyo Institute of Technology
103	2 次元単原子層物質の構造と電子状態	高木　紀明	東京大学新領域創成科学研究科物質系専攻	Geometric and electronic structures of two-dimensional atomic-layered materials	Noriaki Takagi	The University of Tokyo
104	金属酸化物物性の第一原理計算と触媒活性のマテリアルズインフォマティクスアプローチ	佐々木　岳彦	東京大学大学院新領域創成科学研究科	Materials informatics approach for catalysts' activities and properties of metal oxides obtained by First Principles Calculations	Takehiko Sasaki	The University of Tokyo
105	有機分子の炭化反応と電子状態の計算	島田　敏宏	北海道大学大学院工学研究院	Carbonization reaction of organic molecules and electronic structures of the products	Toshihiro Shimada	Hokkaido University
106	プルシャンブルー類似体の基底構造の探索	日沼　洋陽	千葉大学先進科学センター	Finding the ground state of prussian blue derivatives	Yoyo Hinuma	Chiba University
107	第一原理計算を用いたセミクラスレートハイドレートの相平衡条件の計算	平塚　将起	工学院大学機械工学科	ab initio calculations to determine the phase equilibrium conditions of semiclathrate hydrates	Masaki Hiratsuka	Kogakuin University
108	酸化物 / 貴金属界面におけるラシュバ効果の第一原理計算	石井　史之	金沢大学理工研究域数物科学系	First-principles calculation of Rashba effect at　oxides/noble-metal interfaces	Fumiyuki Ishii	Kanazawa University
109	軽希土類永久磁石材料の電子状態	赤井　久純	東京大学物性研究所	Electronic structure of light rare earth permanent magnets	Hisazumi Akai	The University of Tokyo
110	300 超の原子数のシリコンクラスターによる超格子構造に対する第一原理計算	織田　望	産業技術総合研究所	Ab initio calculations for superlattices composed of silicon clusters containing more than 300 atoms	Nozomi Orita	National Institute of Advanced Industrial Science and Technology
111	第一原理計算による原子膜物質の原子構造・安定性・電子物性の解明	藤本　義隆	東京工業大学大学院理工学研究科物性物理学専攻	First-principles study of atomic structures, stabilities, and electronic properties of atomic-layered materials	Yoshitaka Fujimoto	Department of Physics, Tokyo Institute of Technology
112	第 1 原理運動量依存変分理論に基づく鉄族強磁性金属の運動量分布関数と準粒子状態の定量的研究	梯　祥郎	琉球大学理学部物理系	Quantitative Calculations of Momentum Distribution Function and Quasiparticle State in Ferromagnetic Transition Metals and Compounds Based on the First-Principles Momentum Dependent Local Ansatz Theory	Yoshiro Kakehashi	University of the Ryukyus
113	混合アニオン層状化合物の仕事関数に関する研究	神原　陽一	慶應義塾大学理工学部物理情報工学科	Research on work functions of mixed anion layered compounds	Yoichi Kamihara	Keio University
114	新たなナノスケール界面の電子物性の探索	小林　功佳	お茶の水女子大学理学部物理学科	Search for electronic properties of new nanoscale interfaces	Katsuyoshi Kobayashi	Ochanomizu University
115	第一原理計算による電気化学材料の設計	佐藤　幸生	九州大学大学院工学研究院材料工学部門	Computational Design of Electrochromic Materials through ab initio DFT Simulation	Yukio Sato	Kyushu University
116	DNA のスーパーコイル構造を選択的に認識するペプチドの熱力学的物性と動力学構造の統計力学的解析	舘野　賢	兵庫県立大学大学院生命理学研究科	Statistical thermodynamic analysis of selective binding-mechanism of supercoiled DNA recognition (SDR) peptide	Masaru Tateno	University of Hyogo
117	ペロブスカイト型鉛ハライド混晶の光吸収特性に関する研究	牧野　哲征	福井大学大学院工学研究科	Study on optical properties in perovskite-type lead-dihalide mixed crystals	Takayuki Makino	University of Fukui

No.	課題名	氏名	所属	Title	Name	Organization
118	熱電変換材料の第一原理比熱計算	日沼　洋陽	千葉大学先進科学センター	First principles calculations of heat capacity of thermoelectric materials	Yoyo Hinuma	Chiba University
119	表面構造におけるバンド計算	秋山　了太	東京大学理学系研究科物理学専攻	The band calculations of the surface structure	Ryota Akiyama	The University of Tokyo
120	固体表面上での小分子活性化、および素反応データベースの構築	蒲池　高志	福岡工業大学	Database construction for activation and reaction of small molecules on solid surfaces	Takashi Kamachi	Fukuoka Institute of Technology
121	触媒インフォマティクス構築に向けた固体触媒の電子状態計算	鳥屋尾　隆	北海道大学 触媒科学研究所	Calculation of catalyst electronic structures for catalyst informatics	Takashi Toyao	Hokkaido University
2. 強相関 / Strongly Correlated Quantum Systems						
122	ペロブスカイト遷移金属酸化物 $SrRuO_3$ における磁気異方性と量子異常ホール効果の研究	今田　正俊	東京大学工学系研究科物理工学専攻	Numerical Studies on Magnetic Anisotropy and Quantum Anomalous Hall Effect in Perovskite Transition Metal Oxide $SrRuO_3$	Masatoshi Imada	The University of Tokyo
123	多変数変分モンテカルロ法を用いた強相関トポロジカル物質の研究	三澤　貴宏	東京大学物性研究所	Study of correlated topological materials using many-variable variational Monte Carlo method	Takahiro Misawa	The University of Tokyo
124	多体量子系のソルバーとしての深層学習を用いたニューラル・ネットワーク法の開発	今田　正俊	東京大学工学系研究科物理工学専攻	Development of neural network method with deep learning as a solver for many-body quantum systems	Masatoshi Imada	The University of Tokyo
125	強いスピン軌道相互作用を有する相関電子系の数値的研究	求　幸年	東京大学大学院工学系研究科	Numerical study of correlated electron systems with strong spin-orbit coupling	Yukitoshi Motome	The University of Tokyo
126	多軌道強相関物質におけるフント結合がもたらす非局所相関	野村　悠祐	東京大学大学院　物理工学専攻	Non-local correlations induced by Hund's coupling in multi-orbital strongly-correlated materials	Yusuke Nomura	The University of Tokyo
127	強相関系におけるトポロジカル物質開拓とトポロジカル相転移	川上　則雄	京都大学大学院理学研究科物理学宇宙物理学専攻	Pursuit of topologically nontrivial materials and topological phase transition in strongly correlated quantum systems	Norio Kawakami	Kyoto University
128	強いスピン軌道相互作用を有する相関電子系の数値的研究	求　幸年	東京大学大学院工学系研究科	Numerical study of correlated electron systems with strong spin-orbit coupling	Yukitoshi Motome	The University of Tokyo
129	多サイト・多軌道系のリアリスティックな電子状態を考慮した電子相関と超伝導に関する研究	黒木　和彦	大阪大学	Study on correlation and superconductivity in multiorbital/multi-site systems based on realistic electronic structures	Kazuhiko Kuroki	Osaka University
130	軌道自由度を有する強相関電子系における新奇量子状態の数値解析	古賀　昌久	東京工業大学	Numerical analysis for extotic quantum states in strongly correlated electron systems	Akihisa Koga	Tokyo Institute of Technology
131	2チャンネル近藤効果と多極子感受率	堀田　貴嗣	首都大学東京理工学研究科物理学専攻	Two-channel Kondo effect and multipole susceptibility	Takashi Hotta	Tokyo Metropolitan University
132	強相関系におけるトポロジカル輸送と非平衡現象	川上　則雄	京都大学大学院理学研究科物理学宇宙物理学専攻	Topological transport and nonequilibrium phenomena in strongly correlated quantum systems	Norio Kawakami	Kyoto University
133	ハバード模型におけるストライプ秩序と電子格子相互作用の関係の数値的研究	大越　孝洋	東京大学大学院工学系研究科物理工学専攻	Numerical study on interplay of stripes and electron-phonon interactions in the Hubbard model	Takahiro Ohgoe	The University of Tokyo

No.	課題名	氏名	所属	Title	Name	Organization
134	量子モンテカルロ法による非従来型超伝導体の局所電子相関の研究	星野　晋太郎	埼玉大学	Quantum Monte Carlo approach to local electronic correlations in unconventional superconductors	Shintaro Hoshino	Saitama University
135	トポロジーと強相関効果が創発する異常物性	吉田　恒也	京都大学理学研究科	Exotic phenomena induced by topology and strong correlations	Tsuneya Yoshida	RIKEN
136	多軌道強相関系における新奇量子相の熱揺らぎの効果	古賀　昌久	東京工業大学	Effect of thermal fluctuation for exotic quantum phases in strongly correlated multiorbital systems	Akihisa Koga	Tokyo Institute of Technology
137	$Cd_2Os_2O_7$ における強相関効果の理論研究	品岡　寛	埼玉大学理学部物理学科	Theoretical study of strong correlations in $Cd_2Os_2O_7$	Hiroshi Shinaoka	Saitama University
138	動的平均場近似に基づく強相関電子系化合物の電子状態および多極子揺らぎ	大槻　純也	東北大学大学院理学研究科	Dynamical mean-field calculations of electronic states and multipolar fluctuations in strongly correlated electron systems	Junya Otsuki	Tohoku University
139	スピン軌道相互作用を有する遍歴磁性体におけるスキルミオン結晶相	速水　賢	北海道大学理学部物理学科	Skyrmion crystal phase in itinerant magnets with spin-orbit coupling	Satoru Hayami	Hokkaido University
140	FLEX-S 近似を用いた銅酸化物高温超伝導体における微視的な解析	北　孝文	北海道大学理学部物理学科	Microscopic analysis of cuprate superconductors in FLEX-S approximation	Takafumi Kita	Hokkaido University
141	フィリング・エンフォースト量子バンド絶縁体を始めとする空間群対称性に基づく新奇量子物質の設計と評価	押川　正毅	東京大学物性研究所	Designing novel quantum materials based on space group symmetries, including filling-enforced quantum band insulators	Masaki Oshikawa	The University of Tokyo
142	強相関トポロジカル系における新奇物性	吉田　恒也	京都大学理学研究科	Exotic properties in strongly correlated topological systems	Tsuneya Yoshida	RIKEN
143	ハバードモデルにおける超伝導及び磁性状態の研究	山田　篤志	千葉大学理学研究科	Superconductivity and magnetic properties of the Hubbard model	Atsushi Yamada	Department of Physics, Chiba University
144	複合電子系における電子状態と過渡ダイナミクス	石原　純夫	東北大学大学院理学研究科	Electronic state and transient dynamics in complex electronic systems	Sumio Ishihara	Department of Physics, Tohoku University
145	複合多体電子系の過渡量子ダイナミクス	石原　純夫	東北大学大学院理学研究科	Transient Quantum Dynamics in Complex Many Electron Systems	Sumio Ishihara	Department of Physics, Tohoku University
146	最適化量子モンテカルロ法および第一原理計算による強相関系の研究	柳沢　孝	産業技術総合研究所	Optimized Monte Carlo method and first-principles calculations in strongly correlated electron systems	Takashi Yanagisawa	National Institute of Advanced Industrial Science andTechnology
147	電荷自由度を有する強相関電子系の超伝導・磁性・電荷秩序	渡部　洋	早稲田大学高等研究所	Superconductivity, magnetism, and charge order in strongly correlated electron system with charge degree of freedom	Hiroshi Watanabe	Waseda Institute for Advanced Study
148	量子モンテカルロ法と第一原理計算による強相関電子系の研究	柳沢　孝	産業技術総合研究所	Quantum Monte Carlo and first-principles study of strongly correlated electron systems	Takashi Yanagisawa	National Institute of Advanced Industrial Science andTechnology
149	くりこみ群法によるスピン・電荷・軌道結合系の解析	土射津　昌久	奈良女子大学研究院自然科学系	Renormalization-group analysis on spin-charge-orbital coupled systems	Masahisa Tsuchiizu	Nara Women's University
150	横磁場イジングモデルの解析	堀田　知佐	東京大学総合文化研究科	Analysis on a series of transverse Ising models	Chisa Hotta	The University of Tokyo

No.	課題名	氏名	所属	Title	Name	Organization
3. 巨視系の協同現象 / Cooperative Phenomena in Complex, Macroscopic Systems						
151	連続空間および離散空間量子モンテカルロ法によるヘリウム系有効モデルの決定	川島　直輝	東京大学物性研究所	Effective Model Through Continuous and Descrete Space Quantum Monte Carlo Simulations	Naoki Kawashima	The University of Tokyo
152	光とフォノンの協奏による強相関系での非平衡高温超伝導の発現	今田　正俊	東京大学工学系研究科物理工学専攻	Nonequilibrium superconductivity emerging from synergistic effects of light and phonons in strongly correlated systems	Masatoshi Imada	The University of Tokyo
153	拡張アンサブル法による複雑系の研究	岡本　祐幸	名古屋大学大学院理学研究科	Study on complex systems by generalized-ensemble algorithms	Yuko Okamoto	Nagoya University
154	高分子材料の破壊と補強に関する粗視化 MD シミュレーション	萩田　克美	防衛大学校応用科学群応用物理学科	Coarse grained MD simulation for fracture and reinforcement of polymer materials	Katsumi Hagita	National Defense Academy
155	連続空間および離散空間量子モンテカルロ法によるヘリウム系有効モデルの決定	川島　直輝	東京大学物性研究所	Effective Model Through Continuous and Descrete Space Quantum Monte Carlo Simulations	Naoki Kawashima	The University of Tokyo
156	量子スピン液体における励起スペクトルの数値的研究	山地　洋平	東京大学大学院工学系研究科物理工学専攻	Numerical Studies on Excitation Spectra of Quantum Spin Liquids	Youhei Yamaji	The University of Tokyo
157	摩擦の科学	松川　宏	青山学院大学理工学部	Science of Friction	Hiroshi Matsukawa	Aoyama Gakuin University
158	ハニカム格子上の多軌道模型におけるスピン軌道相互作用の効果	古賀　昌久	東京工業大学	Effect of the spin-orbit coupling in the multiorbital model on the honeycomb lattice	Akihisa Koga	Tokyo Institute of Technology
159	ガラス形成液体に潜んだ不均一的ダイナミクスの原理解明	金　鋼	大阪大学大学院基礎工学研究科	Elucidation of heterogeneous dynamics hidden in glass-forming liquids	Kang Kim	Osaka University
160	親水性 / 疎水性溶液界面におけるアミロイドベータペプチド凝集機構を解明する分子動力学シミュレーション	奥村　久士	分子科学研究所計算科学研究センター	Molecular dynamics simulations to reveal aggregation mechanism of amyloid-beta peptides at a hydrophilic/hydrophobic interface	Hisashi Okumura	Institute for Molecular Science
161	蛋白質物性に強く関与するソフトモードの効率的サンプリングシミュレーション	北尾　彰朗	東京工業大学生命理工学院	Efficient sampling simulation of the soft modes significantly contribute to protein properties	Akio Kitao	The University of Tokyo
162	非平衡系の数値的研究	原田　健自	京都大学大学院情報学研究科	Numerical study of non-equilibrium systems	Kenji Harada	Kyoto University
163	定量的粗視化分子モデリングによるマクロ分子自己集合体の物性解析	篠田　渉	名古屋大学大学院工学研究科	Physical Property Analysis of Macromolecular Self-Assembly using Quantitative Coarse-Grained Molecular Model	Wataru Shinoda	Nagoya University
164	分子動力学法を用いた希薄高分子溶液の流れ解析	野口　博司	東京大学物性研究所	Flow analysis of dilute polymer solution by molecular dynamics simulation	Hiroshi Noguchi	The University of Tokyo
165	ランダムなトポロジカル物質の相図	大槻　東巳	上智大学理工学部	Phase diagrams of random topological matters	Tomi Ohtsuki	Sophia University
166	マテリアルズ・インフォマティクスによる熱機能材料の探索	塩見　淳一郎	東京大学工学系研究科	Screening for Thermal Functional Materials using Materials Informatics	Junichiro Shiomi	The University of Tokyo

No.	課題名	氏名	所属	Title	Name	Organization
167	ローレンツ力とコプニン力、状態密度の傾きを含む拡張準古典方程式を用いた超伝導渦状態の微視的解析	北　孝文	北海道大学理学部物理学科	Microscopic analysis of the vortex state in superconductors using the augmented quasiclassical equations with the Lorentz force, Kopnin force and slope in the density of state	Takafumi Kita	Hokkaido University
168	フラストレート磁性体における新奇秩序	川村　光	大阪大学理学研究科	Novel order in frustrated magnets	Hikaru Kawamura	Osaka University
169	統計的機械学習によるモデル推定と臨界現象解析	藤堂　眞治	東京大学大学院理学系研究科物理学専攻	Model Estimation and Critical Phenomena Analysis by Statistical Machine Learning	Synge Todo	The University of Tokyo
170	エンドポイント法を用いたアポプラストシアニン折り畳みに伴う熱力学量変化の定量的計算	吉留　崇	東北大学大学院工学研究科	Accurate computation of the free-energy change of apoplastocyanin using the end-points method	Takashi Yoshidome	Tohoku University
171	蜂の巣格子上 SU(N) ハイゼンベルク模型の基底状態相図	鈴木　隆史	兵庫県立大学大学院工学研究科	Ground state phase diagram of SU(N) Heisenberg model on a honeycomb lattice	Takafumi Suzuki	University of Hyogo
172	生体膜の構造形成	野口　博司	東京大学物性研究所	Structure formation of biomembranes	Hiroshi Noguchi	University of Tokyo
173	量子応答、量子ダイナミクスの数値計算法の開発	宮下　精二	東京大学理学系研究科物理学専攻	Direct numerical method for quantum response and quantum dynamics	Seiji Miyashita	The University of Tokyo
174	密度行列繰り込み群法によるフラストレート量子スピン系の研究	遠山　貴己	東京理科大学理学部応用物理学科	DMRG study of frustrated quantum spin systems	Takami Tohyama	Tokyo University of Science
175	不純物を含む液体における気泡核生成現象の分子動力学計算	渡辺　宙志	東京大学物性研究所	Molecular dynamics study of impurity effect on bubble nucleation	Hiroshi Watanabe	The University of Tokyo
176	古典・量子フラストレートスピン系における新規秩序の探索	大久保　毅	東京大学大学院理学系研究科物理学専攻	Novel phases in classical and quantum frustrated spin systems	Tsuyoshi Okubo	The University of Tokyo
177	インターカレートした FeSe の電子構造及び超伝導の圧力依存性	Jeschke Harald	岡山大学異分野基礎科学研究所	Pressure dependence of electronic structure and superconductivity in intercalated FeSe	Harald Jeschke	Research Institute for Interdisciplinary Science Okayama University
178	トポロジカル相におけるバルク・エッジ対応の数値的研究	初貝　安弘	筑波大学大学院数理物質科学研究科物理学専攻	Numerical studies of bulk-edge correspondence in topological phases	Yasuhiro Hatsugai	University of Tsukuba
179	非閉じ込め量子臨界における創発粒子	諏訪　秀麿	東京大学大学院理学系研究科物理学専攻	Emergent Particles at Deconfined Quantum Criticality	Hidemaro Suwa	The University of Tokyo
180	トポロジカル絶縁体表面上のマヨラナフェルミオン格子の量子モンテカルロシミュレーション	紙屋　佳知	理研	Quantum Monte Carlo study of Majorana Qubits at the surface of topological insulators	Yoshitomo Kamiya	RIKEN
181	イミダゾリウム系イオン液体 - 水混合系におけるナノ構造相の探求	彭　海龍	東北大学金属材料研究所	Exploring nano-structured phases in imidazolium-based ionic liquid and water mixtures	Hailong Peng	Tohoku University
182	格子の自由度と結合した量子スピン系におけるランダムネスの効果 II	安田　千寿	琉球大学理学部	Randomness Effects on Quantum Spin Systems Coupled to Lattice Degrees of Freedom II	Chitoshi Yasuda	University of the Ryukyus
183	フラストレート磁性体における新奇秩序	川村　光	大阪大学理学研究科	Novel order in frustrated magnets	Hikaru Kawamura	Osaka University

No.	課題名	氏名	所属	Title	Name	Organization
184	大規模粗視化分子動力学法による結晶性高分子の変形と破壊のダイナミクス	樋口　祐次	東京大学物性研究所	Deformation and fracture dynamics of crystalline polymers by large-scale coarse-grained molecular dynamics simulation	Yuji Higuchi	The University of Tokyo
185	SU(N) スピンで記述される２次元一般化 Heisenberg 模型の基底状態相図	鈴木　隆史	兵庫県立大学　大学院工学研究科	Ground state phase diagrams of 2D generalized Heisenberg models for SU(N) spins	Takafumi Suzuki	University of Hyogo
186	シェル・モデルを用いた強誘電体の分子動力学シミュレーション III	橋本　保	産業技術総合研究所	Molecular dynamics simulation of ferroelectrics using a shell model III	Tamotsu Hashimoto	National Institute of Advanced Industrial Science and Technology
187	前駆体クラスター形成を経由したヒドロキシアパタイト結晶核生成機構の分子動力学シミュレーション研究	灘　浩樹	産業技術総合研究所	Molecular Dynamics Simulation Study of Crystal Nucleation Mechanism of Hydroxyapatite via Formation of Pre-Nucleation Clusters	Hiroki Nada	National Institute of Advanced Industrial Science and Technology
188	動的スケーリング解析の改良とトポロジカル相転移系への応用	尾関　之康	電気通信大学情報理工学研究科	Improvement for dynamical scaling analysis and its applications to topoligical phase transitions	Yukiyasu Ozeki	The University of Electro-Communications
189	並列化量子モンテカルロ法の開発と２次元量子格子系の研究	正木　晶子	理化学研究所	The development of the parallelizable Quantum Monte Carlo method and the application to two-dimensional quantum lattice systems	Akiko Masaki-Kato	RIKEN
190	原子スケール模型による磁化反転過程の解析	檜原　太一	東京大学理学系研究科	Analysis of magnetization reversal process based on atomistic models	Taichi Hinokihara	The University of Tokyo
191	二次元量子スピン系の励起ダイナミクス	正木　晶子	理化学研究所	Excitation dynamics of two-dimensional quantum spin systems	Akiko Masaki-Kato	RIKEN
192	カイラルらせん磁性体の有限サイズ効果とヒステリシス	加藤　雄介	東京大学総合文化研究科広域科学専攻相関基礎科学系	Finite-size effect and hysteresis in chiral helimagnets	Yusuke Kato	The University of Tokyo
193	フラストレート量子スピン鎖の磁気励起とスピン伝導	大西　弘明	日本原子力研究開発機構 先端基礎研究センター	Magnetic excitation and spin transport in frustrated quantum spin chain	Hiroaki Onishi	Japan Atomic Energy Agency
194	格子の自由度と結合した量子スピン系におけるランダムネスの効果	安田　千寿	琉球大学理学部	Randomness Effects on Quantum Spin Systems Coupled to Lattice Degrees of Freedom	Chitoshi Yasuda	University of Ryukyus
195	次近接相互作用を取り入れたカイラルらせん磁性体モデルの物性	加藤　雄介	東京大学総合文化研究科広域科学専攻相関基礎科学系	Physical properties of the chiral helimagnet with next-nearest-neighbor interaction	Yusuke Kato	The University of Tokyo
196	相転移・協力現象の統計力学的研究	福島　孝治	東京大学大学院総合文化研究科	Statistical-mechanical study of phase transition and cooperative phenomena	Koji Hukushima	The University of Tokyo
197	低次元量子磁性体に対するボンドランダムネスの効果	下川　統久朗	沖縄科学技術大学院大学	The effect of bond-randomness on the quantum magnetisms in low dimension	Tokuro Shimokawa	Okinawa Institute of Science and Technology Graduate University
198	フラストレーション系のスピンギャップの数値対角化による研究	坂井　徹	兵庫県立大学大学院物質理学研究科	Numerical Diagonalization Study on the Spin Gap of Frustrated Systems	Toru Sakai	University of Hyogo
199	古典・量子フラストレートスピン系における新規秩序の探索	大久保　毅	東京大学大学院理学系研究科　物理学専攻	Novel phases in classical and quantum frustrated spin systems	Tsuyoshi Okubo	The University of Tokyo
200	量子スピン系の低エネルギー状態に関する数値的研究	中野　博生	兵庫県立大学大学院物質理学研究科	Numerical study on low-energy states of quantum spin systems	Hiroki Nakano	University of Hyogo

No.	課題名	氏名	所属	Title	Name	Organization
201	電極と接して電気二重層を形成する電解質液体の構造化とダイナミクスの解析	福井　賢一	大阪大学大学院基礎工学研究科	Analysis on Structuring and Dynamics of Electrolyte Solutions Forming Electric Double Layer at Electrode Interfaces	Ken-Ichi Fukui	Osaka University
202	量子スピン系の低エネルギー状態に関する数値的研究	中野　博生	兵庫県立大学大学院物質理学研究科	Numerical study on low-energy states of quantum spin systems	Hiroki Nakano	University of Hyogo
203	低次元量子スピン系におけるスピンフロップ現象の数値的研究	坂井　徹	兵庫県立大学大学院物質理学研究科	Numerical Study on Spin Flop Phenomena in Low-Dimensional Quantum Spin Systems	Toru Sakai	University of Hyogo
204	融解現象とポリアモルフィズム	渕崎　員弘	愛媛大学理工学研究科	Melting phenomena and polyamorphism	Kazuhiro Fuchizaki	Ehime University
205	動的スケーリング解析の改良とトポロジカル相転移への応用 II	尾関　之康	電気通信大学情報理工学研究科	Improvement for dynamical scaling analysis and its applications to topological phase transitions II	Yukiyasu Ozeki	The University of Electro-Communications
206	フラストレートハニカム磁性体における多重 Q 秩序相	下川　統久朗	沖縄科学技術大学院大学	Multiple-Q states of the frustrated Heisenberg model on the honeycomb lattice	Tokuro Shimokawa	Okinawa Institute of Science and Technology Graduate University
207	活性点の制御されたゼオライト合成のための有機構造規定剤の設計	大久保　達也	東京大学大学院工学系研究科化学システム工学専攻	Design of organic structure-directing agents for the synthesis of zeolites with controlled active sites	Tatsuya Okubo	The University of Tokyo
208	融解現象とポリアモルフィズム	渕崎　員弘	愛媛大学理工学研究科	Melting phenomena and polyamorphism	Kazuhiro Fuchizaki	Department of Physics, Ehime University
209	物質・材料科学の知見を事前分布で表す方法の開発	田村　亮	国立研究開発法人 物質・材料研究機構	Development of a method to express the knowledge in materials science as prior distribution	Ryo Tamura	National Institute for Materials Science
210	情報科学的手法による有効モデル推定の高速化	田村　亮	国立研究開発法人 物質・材料研究機構	Acceleration of the effective model estimation by techniques in informa- tion science	Ryo Tamura	National Institute for Materials Science
211	孤立量子多体スピン系のダイナミクス	森　貴司	東京大学理学部物理学科	Dynamics of isolated quantum many-body spin systems	Takashi Mori	The University of Tokyo
212	ダイアモンド格子上の XY 模型：フラストレーションの効果	服部　一匡	首都大学東京	XY model on a diamond lattice: effects of frustration	Kazumasa Hattori	Tokyo Metropolitan University
213	量子アニーリングを用いた機械学習	田中　宗	早稲田大学 高等研究所	Machine Learning by Using Quantum Annealing	Shu Tanaka	Waseda University
214	バネ・ビーズ鎖におけるガラス状態の解析	村島　隆浩	東北大学大学院理学研究科	Analysis of Glassy State of Bead-Spring Chains	Takahiro Murashima	Tohoku University
215	フラストレート強磁性鎖のスピンネマティック状態における磁気熱効果	大西　弘明	日本原子力研究開発機構 先端基礎研究センター	Magneto-thermal effect in spin nematic state of frustrated ferromagnetic chain	Hiroaki Onishi	Japan Atomic Energy Agency
216	細胞伸長とその集団運動への影響の解明	松下　勝義	大阪大学理学研究科	Investigation of Cell Elongation Effect on Collective Motion	Katsuyoshi Matsushita	Osaka University
217	細孔内に閉じ込められた水の構造と物性に対する界面の影響の解明	水口　朋子	京都工芸繊維大学	Effect of interface on the structure and properties of water confined in nanopore	Tomoko Mizuguchi	Kyoto Institute of Technology

No.	課題名	氏名	所属	Title	Name	Organization
218	長距離相互作用行列の低ランク近似を用いたモンテカルロシミュレーション	五十嵐　亮	東京大学情報基盤センター	Monte Carlo simulation using low-rank approximation to long-range interaction matrices	Ryo Igarashi	The University of Tokyo
219	細胞の伸長誘起動的転移の数値的研究	松下　勝義	大阪大学理学研究科	Numerical study of cell-elongation inducing dynamical transition	Katsuyoshi Matsushita	Osaka University
220	ソフトマテリアルの秩序構造とその光学的性質の計算	福田　順一	九州大学大学院理学研究院	Calculation of ordered structures and their optical properties of soft materials	Jun-Ichi Fukuda	Kyushu University
221	テトラヒドラル液体の構造とダイナミクス	田中　肇	東京大学生産技術研究所	Structure and dynamics of tetrahedral liquids	Hajime Tanaka	The University of Tokyo
222	空間構造をもつ一次元量子スピン系の数値的研究	利根川　孝	神戸大学大学院理学研究科	Numerical Study of the One-Dimensional Quantum Spin Systems with Spatial Structures	Takashi Tonegawa	Kobe University
223	孤立量子系の熱化に関する数値的研究	伊與田　英輝	東京大学工学系研究科	Numerical study of thermalization in isolated quantum systems	Eiki Iyoda	The University of Tokyo
224	量子アニーリングを用いた行列分解	田中　宗	早稲田大学 高等研究所	Matrix Factorization by Using Quantum Annealing	Shu Tanaka	Waseda University
225	ソフトマテリアルの秩序構造とその光学的性質の計算	福田　順一	九州大学大学院理学研究院	Calculation of ordered structures and their optical properties of soft materials	Jun-Ichi Fukuda	Kyushu University
226	対称性のあるテンソルネットワーク法の並列計算ライブラリ開発	森田　悟史	東京大学物性研究所	Development of parallel computing library for tensor network methods with symmetries	Satoshi Morita	The University of Tokyo
227	地震の統計モデルの数値シミュレーション	川村　光	大阪大学理学研究科	Numerical simulations on statistical models of earthquakes	Hikaru Kawamura	Osaka University
228	コロイド分散系のゲル化における運動量保存則起源の有限サイズ効果の解明	田中　肇	東京大学生産技術研究所	Study of finite-size effects on colloidal gelation originating from momentum conservation	Hajime Tanaka	The University of Tokyo
229	マニフォールド理論とマルコフ状態モデルの協奏によるタンパク質へのリガンド結合・解離過程の解明	吉留　崇	東北大学大学院工学研究科	Elucidation of binding and unbinding processes of a ligand to a protein using a hybrid of the manifold theory and the Markov state model	Takashi Yoshidome	Tohoku University
230	輸送現象と光トモグラフィー	町田　学	浜松医科大学フォトニクス医学研究部	Transport phenomena and optical tomography	Manabu Machida	Hamamatsu University School of Medicine
231	実空間構造によるトポロジカル状態の操作	苅宿　俊風	物材機構	Manipulation of Topological States by Real-Space Structure	Toshikaze Kariyado	NIMS
232	環動ゲルネットワークの粗視化分子動力学シミュレーション	眞弓　皓一	東京大学大学院新領域創成科学研究科物質系専攻	Coarse-Grained Molecular Dynamics Simulation of Slide-Ring Gel Networks	Koichi Mayumi	The University of Tokyo
233	混合溶媒中の高分子電解質のコンフォメーション・凝集構造	荒木　武昭	京都大学大学院理学研究科物理学・宇宙物理学専攻	Conformational changes of polyelectrolyte chains in solvent mixtures	Takeaki Araki	Kyoto University
234	コロイド結晶に関する分子シミュレーション	寺尾　貴道	岐阜大学工学部	Molecular simulation of colloidal crystals	Takamichi Terao	Gifu University

No.	課題名	氏名	所属	Title	Name	Organization
235	生物発光関連分子およびその類似体の励起状態研究	樋山　みやび	群馬大学	Theoretical study for excited states of bioluminescence related molecules	Miyabi Hiyama	Gunma University
236	強誘電ー反強誘電相転移を利用した巨大応答と交差応答	高江　恭平	東京大学生産技術研究所	Giant and cross response with ferroelectric--antiferroelectric phase transitions	Kyohei Takae	The University of Tokyo
237	ペーストの流れの記憶の数値実験	中原　明生	日本大学理工学部　一般教育教室(物理)	Numerical simulation for memory of flow in paste	Akio Nakahara	Nihon University
238	高密剛体球系における非平衡相転移と衝撃波現象	礒部　雅晴	名古屋工業大学	Nonequilibirum phase transition and shock wave phenomena in the dense hard sphere systems	Masaharu Isobe	Nagoya Institute of Technology
239	THz 光誘起構造変化初期過程の理論研究	石田　邦夫	宇都宮大学大学院工学研究科	Study of the initial process of THz-light induced structural change	Kunio Ishida	Utsunomiya University
240	３次元カイラル磁性体のマグノン物性の微視的理論	荒川　直也	理化学研究所創発物性科学研究センター	Microscopic theory of magnon physics in a three-dimensional chiral magnet	Naoya Arakawa	RIKEN
241	再生医療に必要な生理活性タンパク質のフォールディング反応機構の解析	新井　宗仁	東京大学大学院総合文化研究科	Folding mechanisms of the bioactive proteins essential for regenerative medicine	Munehito Arai	The University of Tokyo
242	有限差分法・有限要素法による輻射輸送方程式	町田　学	浜松医科大学フォトニクス医学研究部	The radiative transport equation with FDM and FEM	Manabu Machida	Hamamatsu University School of Medicine
243	ANN ポテンシャルを用いた大規模分子動力学シミュレーション：高密度化シリカガラス中におけるナノメートルスケールのドメイン構造の研究	若林　大佑	高エネルギー加速器研究機構物質構造科学研究所	Large-scale molecular-dynamics simulation with ANN potentials: nm-scale domain structure in densified silica glass	Daisuke Wakabayashi	High Energy Accelerator Research Organization (KEK)
244	コロイド結晶に関する分子シミュレーション	寺尾　貴道	岐阜大学工学部	Molecular simulation of colloidal crystals	Takamichi Terao	Faculty of Engineering, Gifu University
245	分子動力学法による繰り返し変形下での高分子疲労メカニズムの解析	天本　義史	名古屋大学ナショナルコンポジットセンター	Polymer Fatigue Revealed by Molecular Dynamic Simulation	Yoshifumi Amamoto	Nagoya University
246	カゴメ格子系 $Cs_2Cu_3SnF_{12}$ のマグノン分散関係の級数展開法による研究	福元　好志	東京理科大学	A series expansion study on the magnon spectrum of a kagome antiferromagnet in $Cs_2Cu_3SnF_{12}$	Fukumoto Yoshiyuki	Tokyo University of Science
247	パイロクロア反強磁性体におけるスピン - 格子結合の効果	青山　和司	大阪大学大学院理学研究科宇宙地球専攻	Spin-lattice-coupling effects in pyrochlore antiferromagnets	Kazushi Aoyama	Osaka University
248	計算機を用いた新規結合タンパク質の合理的人工設計	新井　宗仁	東京大学大学院総合文化研究科	Computational rational design of novel binding proteins	Munehito Arai	The University of Tokyo
249	異方的超伝導接合の量子現象における数値計算法の研究	田沼　慶忠	秋田大学大学院理工学研究科	Study of numerical methods for quantum phenonema of anisotoropic superconductors	Yasunari Tanuma	Akita University
250	空間構造をもつ一次元量子スピン系の数値的研究	利根川　孝	神戸大学大学院理学研究科	Numerical Study of the One-Dimensional Quantum Spin Systems with Spatial Structures	Takashi Tonegawa	Kobe University
251	フェムト秒領域における電子・格子・光相互作用系の非断熱ダイナミクス	石田　邦夫	宇都宮大学大学院工学研究科	Ultrafast nonadiabatic dynamics of electron-phonon-photon systems	Kunio Ishida	Utsunomiya University

No.	課題名	氏名	所属	Title	Name	Organization
252	フラストレート磁性体における動的スピン相関の理論研究	青山　和司	大阪大学大学院理学研究科宇宙地球専攻	Theoretical study of dynamical spin correlations in frustrated magnets	Kazushi Aoyama	Osaka University
253	１次元フラストレート量子スピン系の数値的研究	飛田　和男	埼玉大学大学院理工学研究科物質科学部門	Numerical Study of One Dimensional Frustrated Quantum Spin Systems	Kazuo Hida	Saitama University
254	三角格子ハバード模型における多重スピン密度波と磁気スキルミオンの理論	内田　尚志	北海道科学大学	Theory of the multiple spin density waves and the magnetic skyrmions in the triangular-lattice Hubbard model	Takashi Uchida	Hokkaido University of Science
255	地震の統計モデルの数値シミュレーション	川村　光	大阪大学理学研究科	Numerical simulations on statistical models of earthquakes	Hikaru Kawamura	Osaka University
256	ランチョス法を用いた量子共振器系での光双安定性の解析	白井　達彦	東京大学物性研究所	Analysis of optical bistability in a quantum cavity system with Lanczos method	Tatsuhiko Shirai	The University of Tokyo
257	微細横溝加工を施した鉛直平板を流れる凝縮・沸騰液膜流の熱輸送特性	足立　高弘	秋田大学工学資源学部機械工学科	Heat Transfer Characteristics of Condensate/Evaporate Film Flow along Vertical Plates with Microscopic Grooves	Takahiro Adachi	Akita University
258	磁気双極子相互作用に基づくナノ材料磁性	小畑　修二	東京電機大学理工学部	Nano-materials Magnetization based on magnetic dipole moment interactions	Shuji Obata	Tokyo Denki University
259	分子標的創薬の大幅なコストダウンに向けた基礎研究	沖津　康平	東京大学 大学院工学系研究科	Basic research for significant cost reduction of molecular target drug discovery	Kouhei Okitsu	The University of Tokyo
260	乱流伝熱問題における形状最適化シミュレーション	森本　賢一	東京大学大学院工学系研究科機械工学専攻	Shape-Optimization Simulation in Turbulent Heat Transfer Problem	Kenichi Morimoto	The University of Tokyo
261	多波高木方程式の最小二乗法による解法の開発	沖津　康平	東京大学大学院工学系研究科	Development of algorithm to solve the n-beam Takagi equation with least square method	Kouhei Okitsu	The University of Tokyo
262	機械ひずみを用いたナノ材料フォノン・電子輸送特性制御	塩見　淳一郎	東京大学工学系研究科	Control of phonon and electron transport properties using mechanical strain	Junichiro Shiomi	The University of Tokyo
263	ゲノム動力学シミュレーションモデルを用いた出芽酵母の tRNA 遺伝子の空間分布解析	徳田　直子	名古屋大学大学院工学研究科	Analysis of Spatial Distributions of tRNA Genes in Budding Yeast Using the Genome Dynamical Simulation Model	Naoko Tokuda	Nagoya University
264	柔らかい物質の押し込み解析	辻　知章	中央大学理工学部精密機械工学科	Indentation analysis of soft materials	Tomoaki Tsuji	Chuo University
265	反強磁性体の磁区構造解析シミュレーション	仲谷　栄伸	電気通信大学大学院情報理工学研究科	Simulation analysis of the magnetic domain structure in Antiferromagnet	Yoshinobu Nakatani	University of Electro-Communications
266	最大エントロピー法やスパースモデリングを用いた状態密度の推定	松田　康弘	東京大学物性研究所	Estimation of the density of states using Maximum entropy method and Sparse modeling	Yasuhiro Matsuda	The University of Tokyo

平成 29 年度スーパーコンピュータ　計算物質科学スパコン共用事業　課題一覧
/ Supercomputing Consortium for Computational Materials Science Project List of Supercomputer System 2017

No.	課題名	氏名	所属		Title	Name	Organization
前期 / The first half term							
1	ナノ光応答理論と光・電子融合デバイスの計算科学的設計	信定　克幸	分子科学研究所	理論・計算分子科学研究領域	Nano-optical response theory and computational design of unified photonic-electronic devices	Katsuyuki Nobusada	Institute for Molecular Science
2	高温超伝導体の超伝導機構解明、転移温度上昇指針の探求	今田　正俊	東京大学	大学院工学系研究科	Studies on mechanisms of high-temperature superconductivity and search for principles that raise critical temperature	Masatoshi Imada	The University of Tokyo
3	エネルギーの変換・貯蔵 — 電気エネルギー：全電池シミュレータの基盤技術の開発研究	杉野　修	東京大学	物性研究所	Conversion and storage of energy - Fuel cells and secondary batteries: Research and development of fundamental technologies of battery simulators	Osamu Sugino	The University of Tokyo
4	粗視化分子動力学法による濃厚高分子ブラシ材料の摩擦特性研究	芝　隼人	東北大学	金属材料研究所	Study of frictional properties of dense polymer brushes by coarse-grained moleculer simulateon method	Hayato Shiba	Tohoku University
5	多変数変分モンテカルロ法を用いた２次元電子ガス系の数値解析	吉見　一慶	東京大学	物性研究所	Numerical study of two-dimensional electron gas system by using variational Monte Calro method.	Kazuyoshi Yoshimi	The University of Tokyo
6	HΦを用いた $YbMgGaO_4$ の有限温度計算	三澤　貴宏	東京大学	物性研究所	Finite-temperature calculations of $YbMgGaO_4$ using HΦ	Takahiro Misawa	The University of Tokyo
7	テンソルネットワーク法の物性物理学への応用	川島　直輝	東京大学	物性研究所	Application of Tensor Network Methods to Condensed Matter Physics	Naoki Kawashima	The University of Tokyo
8	有機 / 無機界面の物性に関する計算	尾形　修司	名古屋工業大学	大学院工学研究科	Simulation of organic-inorganic interfaces	Shuji Ogata	Nagoya Institute of Technology
9	ポスト京課題７　サブ課題 G ④大型実験施設との連携	遠山　貴巳	東京理科大学	理学部第一部	Cooperation research with big experimental facilities	Takami Tohyama	Tokyo University of Science
10	有機系太陽電池における光電変換の基礎過程の研究と変換効率最適化にむけた大規模数値計算	山下　晃一	東京大学	大学院工学系研究科	Large scale calculations on the fundamental processes of organic and perovskite solar cells and their optimization in conversion efficiency	Koichi Yamashita	The University of Tokyo
11	エネルギーの変換・貯蔵 — 電気エネルギー：全電池シミュレータの基盤技術の開発研究	岡崎　進	名古屋大学	大学院工学研究科	Conversion and storage of energy - Fuel cells and secondary batteries: Research and development of fundamental technologies of battery simulators	Susumu Okazaki	Nagoya University
12	グリーン関数法とフラグメント分割法を用いた分子集合体の励起状態計算	藤田　貴敏	分子科学研究所		Excited-state calculations for molecular aggregates based on Green's function and fragmentation methods	Takatoshi Fujita	Institute for Molecular Science
13	大規模電子状態計算による次世代創・省エネルギー材料のマテリアルデザイン	福島　鉄也	大阪大学	ナノサイエンスデザイン教育研究センター	Materials design for energy-saving and energy-creation materials	Tetsuya Fukushima	Osaka University
14	貴金属フリーの汎用元素ナノ触媒に向けた第一原理計算	武次　徹也	北海道大学	大学院理学研究院	Ab initio study on abundant nano-catalysts free from precious metals	Tetsuya Taketsugu	Hokkaido University

No.	課題名	氏名	所属		Title	Name	Organization
15	第一原理計算を用いたスクリーニングによる新規半導体の探索	大場　史康	東京工業大学	科学技術創成研究院フロンティア材料研究所	Exploration of novel semiconductors by first-principles screening	Fumiyasu Oba	Tokyo Institute of Technology
16	第一原理計算に基づいた磁性材料の開発	三宅　隆	産業技術総合研究所		First-principles study of magnetic materials	Takashi Miyake	National Institute of Advanced Industrial Science and Technology
17	磁性材料界面の構造同定と局所磁気特性解析	合田　義弘	東京工業大学	物質理工学院	Structures and local magnetic properties of magnetic-material interfaces	Yoshihiro Gohda	Tokyo Institute of Technology
18	マルチスケールシミュレーションにおける熱輸送に関する研究	川勝　年洋	東北大学	大学院理学研究科	Numerical study of thermal transport on multiscale simulation	Toshihiro Kawakatsu	Tohoku University
19	複雑流体の分子動力学計算	野口　博司	東京大学	物性研究所	Molecular Dynamics Simulation of Complex Fluids	Hiroshi Noguchi	The University of Tokyo
20	大規模磁気構造シミュレーションによる永久磁石の磁化過程の研究	小野　寛太	高エネルギー加速器研究機構		Magnetization process of permanent magnets revealed by large-scale simulation	Kanta Ono	High Energy Accelerator Research Organization
後期 / The second half term							
21	高機能半導体	押山　淳	東京大学	大学院工学系研究科	Exploration of new-functionality and high-performance semiconductor devices	Atsushi Oshiyama	The University of Tokyo
22	テンソルネットワーク、機械学習、フェルミ変分波動関数を組み合わせた高精度量子格子模型ソルバーの構築	今田　正俊	東京大学	大学院工学系研究科	Variational Fermi wave function combined with tensor network and machine learning for high-accuracy quantum lattice solver	Masatoshi Imada	The University of Tokyo
23	第一原理フェーズ・フィールド・マッピング	香山　正憲	産業技術総合研究所		First-Principles Phase Field Mapping	Masanori Kohyama	National Institute of Advanced Industrial Science and Technology
24	粗視化分子動力学法を用いた複合液体ナノスケール動力学の材料科学研究	芝　隼人	東北大学	金属材料研究所	Coarse-grained modeling approach to materials research on nanoscale dynamics of complex liquids	Hayato Shiba	Tohoku University
25	量子ドット系における多体相関効果の影響に関する研究	吉見　一慶	東京大学	物性研究所	Study of many-body correlation effects in quantum dots	Kazuyoshi Yoshimi	The University of Tokyo
26	トポロジカル半金属における量子輸送現象	三澤　貴宏	東京大学	物性研究所	Quantum transport phenomena in topological semimetals	Takahiro Misawa	The University of Tokyo
27	ナノ界面高強度パルス光励起ダイナミクス	矢花　一浩	筑波大学	計算科学研究センター	Dynamics in nano-interface excited by high-intensity pulsed light	Kazuhiro Yabana	University of Tsukuba
28	テンソルネットワーク法の物性物理学への応用	川島　直輝	東京大学	物性研究所	Application of Tensor Network Methods to Condensed Matter Physics	Naoki Kawashima	The University of Tokyo
29	有機 / 無機界面の物性に関する計算	尾形　修司	名古屋工業大学	大学院工学研究科	Simulation of organic-inorganic interfaces	Shuji Ogata	Nagoya Institute of Technology
30	貴金属フリーの汎用元素ナノ触媒に向けた第一原理計算	武次　徹也	北海道大学	大学院理学研究院	Ab initio study on abundant nano-catalysts free from precious metals	Tetsuya Taketsugu	Hokkaido University

No.	課題名	氏名	所属		Title	Name	Organization
31	第一原理計算を用いたスクリーニングによる新規半導体の探索	大場　史康	東京工業大学	科学技術創成研究院フロンティア材料研究所	Exploration of novel semiconductors by first-principles screening	Fumiyasu Oba	Tokyo Institute of Technology
32	B、C、Nを用いた電子デバイス新物質の設計研究	斎藤　晋	東京工業大学	理学院	Materials design using B, C, and N for next-generation device	Susumu Saito	Tokyo Institute of Technology
33	複雑流体の分子動力学計算	野口　博司	東京大学	物性研究所	Molecular Dynamics Simulation of Complex Fluids	Hiroshi Noguchi	The University of Tokyo
34	電極界面でのイオン輸送と脱溶媒和過程の分子シミュレーション	森田　明弘	東北大学	大学院理学研究科	Molecular simulation of ion transport and desolvation at electrode interface	Akihiro Morita	Tohoku University
35	経路積分分子動力学法を用いた含水鉱物結晶の計算	飯高　敏晃	理化学研究所		Computational study of hydrous minerals using the path integral molecular dynamics method	Toshiaki Iitaka	RIKEN

Publications

Division of Condensed Matter Science

Takigawa group

We have been performing nuclear magnetic resonance experiments on various quantum spin systems and strongly correlated electron systems to explore novel quantum phases with exotic ordering and fluctuation phenomena. The major achievements in the year 2017 include: (1) Determination of complete phase diagram of ferro qudrupole order in $PrTi_2Al_{20}$ showing remarkable anisotropy with respect to the magnetic fied direction, (2) successful explanation of the above results by mean field calculation of a model hamiltonian including field dependent anisotropic quadupole interactioin, and (3) synthesis of single crystal of the breathing pyrochlore material LiGa Cr_4O_8 followed by magnetiation and NMR measuremengs on the magnetic ordering and spin structure.

1. *Collinear spin density wave order and anisotropic spin fluctuations in the frustrated J_1-J_2 chain magnet $NaCuMoO_4(OH)$: K. Nawa, M. Yoshida, M. Takigawa, Y. Okamoto and Z. Hiroi, Phys. Rev. B **96** (2017) 174433(1-9).

2. Dynamics of bound magnon pairs in the quasi-one-dimensional frustrated magnet $LiCuVO_4$: K. Nawa, M. Takigawa, S. Krämer, M. Horvatic, C. Berthier, M. Yoshida and K. Yoshimura, Phys. Rev. B **96** (2017) 134423(1-6).

3. *J_1-J_2 square-lattice Heisenberg antiferromagnets with $4d^1$ spins AMoOPO$_4$Cl (A=K, Rb): H. Ishikawa, N. Nakamura, M. Yoshida, M. Takigawa, P. Babkevich, N. Qureshi, H. M. Rønnow, T. Yajima and Z. Hiroi, Phys. Rev. B **95** (2017) 064408(1-9).

4. *Spin dynamics in the high-field phases of volborthite: M. Yoshida, K. Nawa, H. Ishikawa, M. Takigawa, M. Jeong, S. Krämer, M. Horvatic, C. Berthier, K. Matsui, T. Goto, S. Kimura, T. Sasaki, J. Yamaura, H. Yoshida, Y. Okamoto and Z. Hiroi, Phys. Rev. B **96** (2017) 180413(R)(1-5).

5. *Classical Spin Nematic Transition in $LiGa_{0.95}In_{0.05}Cr_4O_8$: R. Wawrzynczak, Y. Tanaka, M. Yoshida, Y. Okamoto, P. Manuel, N. Casati, Z. Hiroi, M. Takigawa and G. J. Nilsen, Phys. Rev. Lett. **119** (2017) 087201(1-6).

Sakakibara group

We study magnetism and superconductivity of materials having low characteristic temperatures. These include heavy-electron systems, quantum spin systems and frustrated spin systems. The followings are some selected achievements in the fiscal year 2017. (1) Field-induced ferromagnetic quantum phase transition of itinerant Ising ferromagnet URhGe has been studied by means of angle-resolved magnetization measurements. Details of the wing structure phase diagram is obtained. A tricritical point is likely to exists at ~4 K. (2) Quantum criticality of the spin-1/2 ferromagnetic-leg ladder 3-I-V [=3-(3-iodophenyl)-1,5-diphenylverdazyl] has been examined with respect to the antiferromagnetic to paramagnetic phase transition. The critical exponents of the phase boundary agreed with a theoretical prediction of the quasi-1D Bose-Einstein condensation. (3) We studied the superconducting (SC) gap symmetry and magnetic response of cubic $U_{0.97}Th_{0.03}Be_{13}$ by means of heat capacity and magnetization measurements. We confirmed that the previously-reported second phase transition is between two different SC states. Field and orientation dependences of the heat capacity indicate that the gap is fully opened over the Fermi surface.

1. †Magnetic Properties and Magnetic Phase Diagrams of Trigonal $DyNi_3Ga_9$: H. Ninomiya, Y. Matsumoto, S. Nakamura, Y. Kono, S. Kittaka, T. Sakakibara, K. Inoue and S. Ohara, J. Phys. Soc. Jpn. **86** (2017) 124704(1-7).

2. Structural, Magnetic, and Superconducting Properties of Caged Compounds ROs$_2$Zn$_{20}$ (R= La, Ce, Pr, and Nd): K. Wakiya, T. Onimaru, K. T. Matsumoto, Y. Yamane, N. Nagasawa, K. Umeo, S. Kittaka, T. Sakakibara, Y. Matsushita and T. Takabatake, J. Phys. Soc. Jpn. **86** (2017) 034707(1-6).

3. *Thermodynamic Investigation of Metamagnetic Transitions and Partial Disorder in the Quasi-Kagome Kondo Lattice CePdAl: K. Mochidzuki, Y. Shimizu, A. Kondo, S. Nakamura, S. Kittaka, Y. Kono, T. Sakakibara, Y. Ikeda, Y. Isikawa and K. Kindo, J. Phys. Soc. Jpn. **86** (2017) 034709(1-5).

* Joint research among groups within ISSP.

4. Gap structure of FeSe determined by angle-resolved specific heat measurements in applied rotating magnetic field: Y. Sun, S. Kittaka, S. Nakamura, T. Sakakibara, K. Irie, T. Nomoto, K. Machida, J. Chen and T. Tamegai, Phys. Rev. B **96** (2017) 220505(1-5).

5. †Magnetic properties of the *S*=1/2 honeycomb lattice antiferromagnet 2-Cl-3,6-F_2-V: T. Okabe, H. Yamaguchi, S. Kittaka, T. Sakakibara, T. Ono and Y. Hosokoshi, Phys. Rev. B **95** (2017) 075120(1-6).

6. †Quasiparticle excitations and evidence for superconducting double transitions in monocrystalline $U_{0.97}Th_{0.03}Be_{13}$: Y. Shimizu, S. Kittaka, S. Nakamura, T. Sakakibara, D. Aoki, Y. Homma, A. Nakamura and K. Machida, Phys. Rev. B **96** (2017) 100505(1-5).

7. Three-dimensional Bose-Einstein condensation in the spin-1/2 ferromagnetic-leg ladder 3-Br-4-F-V: Y. Kono, H. Yamaguchi, Y. Hosokoshi and T. Sakakibara, Phys. Rev. B **96** (2017) 104439(1-6).

8. Wing structure in the phase diagram of the Ising ferromagnet URhGe close to its tricritical point investigated by angle-resolved magnetization measurements: S. Nakamura, T. Sakakibara, Y. Shimizu, S. Kittaka, Y. Kono, Y. Haga, J. Pospíšil and E. Yamamoto, Phys. Rev. B **96** (2017) 094411(1-9).

9. Nodal gap structure of the heavy-fermion superconductor URu_2Si_2 revealed by field-angle-dependent specific-heat measurements: S. Kittaka, Y. Shimizu, T. Sakakibara, Y. Haga, E. Yamamoto, Y. Onuki, Y. Tsutsumi, T. Nomoto, H. Ikeda and K. Machida, J. Phys.: Conf. Ser. **807** (2017) 052001(1-6).

10. Thermodynamic properties of quadrupolar states in the frustrated pyrochlore magnet $Tb_2Ti_2O_7$: H. Takatsu, T. Taniguchi, S. Kittaka, T. Sakakibara and H. Kadowaki, J. Phys.: Conf. Ser. **828** (2017) 012007(1-6).

11. †Randomness-induced quantum spin liquid on honeycomb lattice: H. Yamaguchi, M. Okada, Y. Kono, S. Kittaka, T. Sakakibara, T. Okabe, Y. Iwasaki and Y. Hosokoshi, Sci. Rep. **7** (2017) 16144(1-6).

12. *Unique Electronic States in Non-centrosymmetric Cubic Compounds: M. Kakihana, K. Nishimura, Y. Ashitomi, T. Yara, D. Aoki, A. Nakamura, F. Honda, M. Nakashima, Y. Amako, Y. Uwatoko, T. Sakakibara, S. Nakamura, T. Takeuchi, Y. Haga, E. Yamamoto, H. Harima, M. Hedo, T. Nakama and Y. Onuki, J. Electron. Mater. **46** (2017) 3572-3586.

13. Fully gapped superconductivity with no sign change in the prototypical heavy-fermion $CeCu_2Si_2$: T. Yamashita, T. Takenaka, Y. Tokiwa, J. A. Wilcox, Y. Mizukami, D. Terazawa, Y. Kasahara, S. Kittaka, T. Sakakibara, M. Konczykowski, S. Seiro, H. S. Jeevan, C. Geibel, C. Putzke, T. Onishi, H. Ikeda, A. Carrington, T. Shibauchi and Y. Matsuda, Sci. Adv. **3** (2017) e1601667(1-7).

14. Giant Hall Resistivity and Magnetoresistance in Cubic Chiral Antiferromagnet EuPtSi: M. Kakihana, D. Aoki, A. Nakamura, F. Honda, M. Nakashima, Y. Amako, S. Nakamura, T. Sakakibara, M. Hedo, T. Nakama and Y. Onuki, J. Phys. Soc. Jpn. **87** (2018) 023701(1-4).

15. Magnetic-field-induced Quantum Phase in S = 1/2 Frustrated Trellis Lattice: H. Yamaguchi, D. Yoshizawa, T. Kida, M. Hagiwara, A. Matsuo, Y. Kono, T. Sakakibara, Y. Tamekuni, H. Miyagai and Y. Hosokoshi, J. Phys. Soc. Jpn. **87** (2018) 043701(1-5).

16. Quasi-one-dimensional Bose-Einstein condensation in the spin-1/2 ferromagnetic-leg ladder 3-I-V: Y. Kono, S. Kittaka, H. Yamaguchi, Y. Hosokoshi and T. Sakakibara, Phys. Rev. B **97** (2018) 100406(1-5).

17. Fermi surface in the absence of a Fermi liquid in the Kondo insulator SmB_6: M. Hartstein, W. H. Toews, Y. -T. Hsu, B. Zeng, X. Chen, M. Ciomaga Hatnean, Q. R. Zhang, S. Nakamura, A. S. Padgett, G. Rodway-Gant, J. Berk, M. K. Kingston, G. H. Zhang, M. K. Chan, S. Yamashita, T. Sakakibara, Y. Takano, J. -H. Park, L. Balicas, N. Harrison, N. Shitsevalova, G. Balakrishnan, G. G. Lonzarich, R. W. Hill, M. Sutherland and S. E. Sebastian, Nature Phys. **14** (2018) 166-172.

18. †*Quantum valence criticality in a correlated metal: K. Kuga, Y. Matsumoto, M. Okawa, S. Suzuki, T. Tomita, K. Sone, Y. Shimura, T. Sakakibara, D. Nishio-Hamane, Y. Karaki, Y. Takata, M. Matsunami, R. Eguchi, M. Taguchi, A. Chainani, S. Shin, K. Tamasaku, Y. Nishino, M. Yabashi, T. Ishikawa and S. Nakatsuji, Sci. Adv. **4** (2018) eaao3547 (1-6).

19. 磁場角度回転比熱測定による超伝導研究：橘高俊 一郎，物性研究・電子版 **6** (2017) 85-125.

Mori group

We have successfully developed and unveiled unprecedented functional properties for the molecular materials. The major achievements in 2017 are (1) to disclose the "proton-electron coupled properties" such as quantum spin liquid and H/D isotope

† Joint research with outside partners.

effects for our developed organic conductor, κ-H_3(Cat-EDT-TTF)$_2$, by the measurements of specific heat, dielectric response, and thermal conductivity, and DFT calculation, (2) to develop and reveal the peculiarities for novel hydrogen-bonded organic conductors, β-[BTBT(OH)$_2$]$_2$$ClO_4$ and β'-H_3(Cat-EDO-TTF)$_2$$BF_4$, and (3) to demonstrate the "charge-glass" in organic conductor, θ-(BEDT-TTF)$_2$TlZn(SCN)$_4$.

1. Thermodynamics of the quantum spin liquid state of the single-component dimer Mott system κ–H_3(Cat–EDT–TTF)$_2$: S. Yamashita, Y. Nakazawa, A. Ueda and H. Mori, Phys. Rev. B **95** (2017) 184425(1-5).

2. Visualization of a nonlinear conducting path in an organic molecular ferroelectric by using emission of terahertz radiation: M. Sotome, N. Kida, Y. Kinoshita, H. Yamakawa, T. Miyamoto, H. Mori and H. Okamoto, Phys. Rev. B **95** (2017) 241102R(1-5).

3. Improved stability of a metallic state in benzothienobenzothiophene-based molecular conductors: an effective increase of dimensionality with hydrogen bonds: T. Higashino, A. Ueda, J. Yoshida and H. Mori, Chem. Commun. **53** (2017) 3426-3429.

4. Crystallization and vitrification of electrons in a glass-forming charge liquid: S. Sasaki, K. Hashimoto, R. Kobayashi, K. Itoh, S. Iguchi, Y. Nishio, Y. Ikemoto, T. Moriwaki, N. Yoneyama, M. Watanabe, A. Ueda, H. Mori, K. Kobayashi, R. Kumai, Y. Murakami, J. Müller and T. Sasaki, Science **357** (2017) 1381-1385.

5. Multicomponent DFT study of geometrical H/D isotope effect on hydrogen-bonded organic conductor, κ-H_3(Cat EDT-ST)$_2$: K. Yamamoto, Y. Kanematsu, U. Nagashima, A. Ueda, H. Mori and M. Tachikawa, Chem. Phys. Lett. **674** (2017) 168-172.

6. [*]Quantum-disordered state of magnetic and electric dipoles in an organic Mott system: M. Shimozawa, K. Hashimoto, A. Ueda, Y. Suzuki, K. Sugii, S. Yamada, Y. Imai, R. Kobayashi, K. Itoh, S. Iguchi, M. Naka, S. Ishihara, H. Mori, T. Sasaki and M. Yamashita, Nat. Commun. **8** (2017) 1821(1-6).

7. Anion substitution in hydrogen-bonded organic conductors: the chemical pressure effect on hydrogen-bond-mediated phase transition: J. Yoshida, A. Ueda, R. Kumai, Y. Murakami and H. Mori, CrystEngComm **19** (2017) 367-375.

8. Valence engineering of ionic molecular crystals: monovalent–divalent phase diagram for biferrocene–tetracyanoquinodimethane salts: T. Mochida, Y. Funasako, T. Akasaka, M. Uruichi and H. Mori, CrystEngComm **19** (2017) 1449-1453.

9. Spin-Singlet Transition in the Magnetic Hybrid Compound from a Spin-Crossover Fe(III) Cation and π-Radical Anion: K. Takahashi, T. Sakurai, W.-M. Zhang, S. Okubo, H. Ohta, T. Yamamoto, Y. Einaga and H. Mori, Inorganics **5** (2017) 54(1-14).

10. Development of Novel Functional Organic Crystals by Utilizing Proton- and π-Electron-Donating/Accepting Abilities: A. Ueda, Bull. Chem. Soc. Jpn **90** (2017) 1181-1188.

11. Antiferromagnetic Ordering in Organic Conductor λ-(BEDT-TTF)$_2$$GaCl_4$ Probed by ^{13}C NMR: Y. Saito, S. Fukuoka, T. Kobayashi, A. Kawamoto and H. Mori, J. Phys. Soc. Jpn. **87** (2018) 013707(1-4).

12. Size effects on supercooling phenomena in strongly correlated electron systems: $IrTe_2$ and θ-(BEDT-TTF)$_2$RbZn(SCN)$_4$: H. Oike, M. Suda, M. Kamitani, A. Ueda, H. Mori, Y. Tokura, H. M. Yamamoto and F. Kagawa, Phys. Rev. B **97** (2018) 085102(1-7).

13. [†*]Strong Hydrogen Bonds at the Interface between Proton-Donating and -Accepting Self-Assembled Monolayers on Au(111): H. S. Kato, S. Yoshimoto, A. Ueda, S. Yamamoto, Y. Kanematsu, M. Tachikawa, H. Mori, J. Yoshinobu and I. Matsuda, Langmuir **34** (2018) 2189-2197.

14. The thermoelectric power of band-filling controlled organic conductors, β′-(BEDT-TTF)$_3$$(CoCl_4)_{2-x}$$(GaCl_4)_x$: Y. Kiyota, T. Kawamoto, H. Mori and T. Mori, J. Mater. Chem. A **6** (2018) 2004-2010.

15. A phenol-fused tetrathiafulvalene: modulation of hydrogen-bond patterns and electrical conductivity in the charge-transfer salt: A. Ueda and H. Mori, Mater. Chem. Front. **2** (2018) 566-572.

16. Anisotropic Proton Conductivity Arising from Hydrogen-Bond Patterns in Anhydrous Organic Single Crystals, Imidazolium Carboxylates: Y. Sunairi, A. Ueda, J. Yoshida, K. Suzuki and H. Mori, J. Phys. Chem. C (2018), in print.

Osada group

A layered organic Dirac semimetal α-(BEDT-TTF)$_2$$I_3$ shows a metal-insulator transition due to charge ordering (CO) at ambient pressure, which is suppressed by applying pressure. We found that its temperature dependence of resistance below the CO transition shows no insulating behavior but metallic behavior in the weak CO state just below the critical pressure (~ 1.1 GPa).

[*] Joint research among groups within ISSP.

We investigated the temperature dependence of magnetoresistance in detail, and concluded that the gapped Dirac fermion state is realized in the weak CO state. Based on these experimental result, we consider the electronic structure of α-(BEDT-TTF)$_2$I$_3$ with intracellular potential and magnetic modulations due to CO, which were observed in NMR measurement. This is an organic analogue of the Haldane model in graphene. When magnetic modulation is sufficiently large, the system becomes a Chern insulator, where the Berry curvatures around two gapped Dirac cones have the same sign on each band, and one chiral edge state connects the conduction and valence bands at each crystal edge. We pointed out the possibility that the metallic transport in the weak CO state originates from the edge transport in the Chern insulator state.

1. Chern Insulator Phase in a Lattice of an Organic Dirac Semimetal with Intracellular Potential and Magnetic Modulations: T. Osada, J. Phys. Soc. Jpn. **86** (2017) 123702(1-5).

2. Topological Insulator State due to Finite Spin-Orbit Interaction in an Organic Dirac Fermion System: T. Osada, J. Phys. Soc. Jpn. **87** (2018) 075002(1-2).

3. Thickness-dependent phase transition in graphite under high magnetic field: T. Taen, K. Uchida and T. Osada, Phys. Rev. B **97** (2018) 115122(1-7).

Yamashita group

We have been studying (1) quantum criticality in heavy-fermion materials by ultra-low temperature cryostat, (2) thermal-Hall conductivity of exotic excitations in frustrated magnets and (3) a new technique for the study of strongly-correlated electron systems. In this year, we have performed (1) Co and In NMR measurements of $CeCoIn_5$ at ultra-low temperatures, (2) thermal Hall measurements of kagome materials and (3) scanning-Hall measurements of Mn_3Sn and Fe-based superconductors.

1. *Thermal Hall Effect in a Phonon-Glass $Ba_3CuSb_2O_9$: K. Sugii, M. Shimozawa, D. Watanabe, Y. Suzuki, M. Halim, M. Kimata, Y. Matsumoto, S. Nakatsuji and M. Yamashita, Phys. Rev. Lett. **118** (2017) 145902(1-5).

2. *Quantum-disordered state of magnetic and electric dipoles in an organic Mott system: M. Shimozawa, K. Hashimoto, A. Ueda, Y. Suzuki, K. Sugii, S. Yamada, Y. Imai, R. Kobayashi, K. Itoh, S. Iguchi, M. Naka, S. Ishihara, H. Mori, T. Sasaki and M. Yamashita, Nat. Commun. **8** (2017) 1821(1-6).

3. Anomalous Change in the de Haas–van Alphen Oscillations of $CeCoIn_5$ at Ultralow Temperatures: H. Shishido, S. Yamada, K. Sugii, M. Shimozawa, Y. Yanase and M. Yamashita, Phys. Rev. Lett. **120** (2018) 177201.

4. 格子振動による熱ホール効果：杉井か おり , 山下 穣 , 固体物理 **52** (2017) 783.

Division of Condensed Matter Theory

Tsunetsugu group

We have investigated the antiferromagnetic order in a quasicrystal from the viewpoint of the interplay between strong correlation effects and unique crystal structure. To this end, we have employed the simplest canonical model, i.e. the Hubbard model on the two-dimensional Penrose lattice at half filling of electron density. Due to the quasiperiodic lattice structure, this model has thermodynamically degenerate one-electron states at the band center. Each of their wavefunctions is confined in a finite region in the lattice, and thereofre they are called the confined states. These confined states are magnetized by Coulomb repulsion between electrons. They show an antiferromagnetic long-range order at zero temperature, but its spatial structure differs from other antiferromagnets. The whole Penrose lattice is divided into many clusters, and the ordered magnetizations point to the same direction in each cluster, while neighboring clusters have opposite directions each other. Furthermore, the cluster size exhibits a power-law distribution, which is related to the self-similarity in the lattice inherent from the quasiperiodicity.

1. Antiferromagnetic order in the Hubbard model on the Penrose lattice: A. Koga and H. Tsunetsugu, Phys. Rev. B **96** (2017) 214402.

2. Entanglement prethermalization in an interaction quench between two harmonic oscillators: T. N. Ikeda, T. Mori, E. Kaminishi and M. Ueda, Phys. Rev. E **95** (2017) 022129(1-8).

3. Theory of antiferromagnetic Heisenberg spins on a breathing pyrochlore lattice: H. Tsunetsugu, Prog. Theor. Exp. Phys. **2017** (2017) 033101(1-29).

4. Entanglement prethermalization in the Tomonaga-Luttinger model: E. Kaminishi, T. Mori, T. N. Ikeda and M. Ueda, Phys. Rev. A **97** (2018) 013622(1-9).

† Joint research with outside partners.

Kato group

The main research subject of Kato lab. is theory of non-equilibrium properties in mesoscopic devices. We have studied (1) spin-current noise at the interface between a ferromagnetic insulator and a metal, (2) effect of Coulomb interaction on charge pumping via a quantum dot due to reservoir temperature driving, (3) heat transport via a two-state system, and (4) current correlations of a Kondo correlated dot with degenerated orbitals. In collaboration with Sugino group, we have studied first-principles description of van der Waals bonded spin-polarized systems such as solid oxygen using the vdW-DF+U method. We have also studied terahertz response of a ferromagnetic insulator $ErFeO_3$ in collaboration with an experimental group (Suemoto group).

1. Temperature-Driven and Electrochemical-Potential-Driven Adiabatic Pumping via a Quantum Dot: M. Hasegawa and T. Kato, J. Phys. Soc. Jpn. **86** (2017) 024710(1-13).

2. *First-principles description of van der Waals bonded spin-polarized systems using the vdW-DF+U method: Application to solid oxygen at low pressure: S. Kasamatsu, T. Kato and O. Sugino, Phys. Rev. B **95** (2017) 235120(1-11).

3. Quantum Fluctuations along Symmetry Crossover in a Kondo-Correlated Quantum Dot: M. Ferrier, T. Arakawa, T. Hata, R. Fujiwara, R. Delagrange, R. Deblock, Y. Teratani, R. Sakano, A. Oguri and K. Kobayashi, Phys. Rev. Lett. **118** (2017) 196803(1-5).

4. Observation of long-lived coherent spin precession in orthoferrite $ErFeO_3$ induced by terahertz magnetic fields: H. Watanabe, T. Kurihara, T. Kato, K. Yamaguchi and T. Suemoto, Appl. Phys. Lett. **111** (2017) 092401(1-4).

5. 多端子系のジョセフソン接合が示すトポロジカル物性：横山 知大 , 日本物理学会誌 **72** (2017) 402.

6. Effect of Interaction on Reservoir-Parameter-Driven Adiabatic Charge Pumping via a Single-Level Quantum Dot System: M. Hasegawa and T. Kato, J. Phys. Soc. Jpn. **87** (2018) 044709.

7. Current cross-correlation in the Anderson impurity model with exchange interaction: R. Sakano, A. Oguri, Y. Nishikawa and E. Abe, Phys. Rev. B **97** (2018) 045127(1-13).

8. Spin Current Noise of the Spin Seebeck Effect and Spin Pumping: M. Matsuo, Y. Ohnuma, T. Kato and S. Maekawa, Phys. Rev. Lett. **120** (2018) 235120(1-5).

9. 物質科学シミュレーションのポータルサイト MateriApps: 本山 裕一 , 三澤 貴宏 , 加藤 岳生 , 藤堂 眞治 , 固体物理 **52** (2017) 743.

10. 非平衡電流ゆらぎでみる量子ドットの電子多体効果：阪野 塁 , 物性研究・電子版 **6** (2017) 064208.

Division of Nanoscale Science

Katsumoto group

Physical properties of quantum Hall edge states have been unveiled through thermoelectric power caused by microwave irradiation. Study on the effect of decoration on the surfaces of graphene or other 2D materials has been going on. We found strong ferromagnetism in MoS_2 with nano-mesh. Also large spin orbit interaction was introduced with nano-particles on graphene. A peculiar phenomenon called Zitterbewegung theoretically found long time ago by Schrodinger was observed as reproducible conductance fluctuation in spin-polarized transport through a two-dimensional electrons with strong Rashba-type spin-orbit interaction.

1. †Theoretical modeling of electrical resistivity and Seebeck coefficient of bismuth nanowires by considering carrier mean free path limitation: M. Murata, A. Yamamoto, Y. Hasegawa, T. Komine and A. Endo, J. Appl. Phys. **121** (2017) 014303 (1-10).

2. †Photoresponse in gate-tunable atomically thin lateral MoS_2 Schottky junction patterned by electron beam: Y. Katagiri, T. Nakamura, C. Ohata, S. Katsumoto and J. Haruyama, Appl. Phys. Lett. **110** (2017) 143109(1-3).

3. Two-carrier model on the magnetotransport of epitaxial graphene containing coexisting single-layer and bilayer areas: A. Endo, J. Bao, W. Norimatsu, M. Kusunoki, S. Katsumoto and Y. Iye, Philos. Mag. **97** (2017) 1755-1767.

4. Observation of Conductance Fluctuation due to Zitterbewegung in InAs 2-dimentional Electron Gas: Y. Iwasaki, Y. Hashimoto, T. Nakamura and S. Katsumoto, J. Phys.: Conf. Ser. **864** (2017) 012054(1-4).

5. Edge-spin-derived magnetism in few-layer MoS_2 nanomeshes: G. Kondo, N. Yokoyama, S. Yamada, Y. Hashimoto, C. Ohata, S. Katsumoto and J. Haruyama, AIP Advances **7** (2017) 125019(1-7).

---

* Joint research among groups within ISSP.

6. Conductance fluctuations in InAs quantum wells possibly driven by Zitterbewegung: Y. Iwasaki, Y. Hashimoto, T. Nakamura and S. Katsumoto, Sci. Rep. **7** (2017) 7909(1-9).

7. †Large edge magnetism in oxidized few-layer black phosphorus nanomeshes: Y. Nakanishi, A. Ishi, C. Ohata, D. Soriano, R. Iwaki, K. Nomura, M. Hasegawa, T. Nakamura, S. Katsumoto, S. Roche and J. Haruyama, Nano Res. **10** (2017) 718-728.

8. Frequencies of the Edge-Magnetoplasmon Excitations in Gated Quantum Hall Edges: A. Endo, K. Koike, S. Katsumoto and Y. Iye, J. Phys. Soc. Jpn. **87** (2018) 064709.

9. Frequency dependent ac transport of films of close-packed carbon nanotube arrays: A. Endo, S. Katsumoto, K. Matsuda, W. Norimatsu and M. Kusunoki, J. Phys.: Conf. Ser. **969** (2018) 012129.

10. Proximity-Induced Superconductivity in a Ferromagnetic Semiconductor (In,Fe)As: T. Nakamura, L. D. Anh, Y. Hashimoto, Y. Iwasaki, S. Ohya, M. Tanaka and S. Katsumoto, J. Phys.: Conf. Ser. **969** (2018) 012036.

Otani group

We have studied following topics this year: Spin conversion behaviors at the interfaces and the surfaces, magnetization dynamics in ferromagnetic nano structures, and magneto-thermoelectric properties. In the first topic, we succeeded in optically detect spin accumulation induced at the copper/Bi oxide interface. We have performed collaborative study with Tokura-group at CEMS RIKEN on non-linear Hall effect and spin orbit torque induced magnetization switching in magnetic topological insulator. Spin transport in a ferromagnet is also an important topic in relation with spin conversion, we have applied our spin absorption technique to determine the spin diffusion length of Ni-Fe alloy nano wires. In the second topic, we have established the technique to modulate the interface perpendicular anisotropy by voltage. Thereby we succeeded in exciting coherent propagating spin waves in ultrathin CoFeB films. In the third topic, we have found bulk equivalent anomalous Nernst effect takes place in a microfabricated thermoelectric element made of chiral antiferromagnet Mn_3Sn in collaboration with Nakatsuji group.

1. Bias field tunable magnetic configuration and magnetization dynamics in $Ni_{80}Fe_{20}$ nano-cross structures with varying arm length: K. Adhikari, S. Choudhury, R. Mandal, S. Barman, Y. Otani and A. Barman, J. Appl. Phys. **121** (2017) 043909(1-5).

2. Evaluation of bulk-interface contributions to Edelstein magnetoresistance at metal/oxide interfaces: J. Kim, Y.-T. Chen, S. Karube, S. Takahashi, K. Kondou, G. Tatara and Y. Otani, Phys. Rev. B **96** (2017) 140409R(1-6).

3. Current-Nonlinear Hall Effect and Spin-Orbit Torque Magnetization Switching in a Magnetic Topological Insulator: K. Yasuda, A. Tsukazaki, R. Yoshimi, K. Kondou, K. S. Takahashi, Y. Otani, M. Kawasaki and Y. Tokura, Phys. Rev. Lett. **119** (2017) 137204(1-5).

4. *Anomalous Nernst effect in a microfabricated thermoelectric element made of chiral antiferromagnet Mn_3Sn: H. Narita, M. Ikhlas, M. Kimata, A. A. Nugroho, S. Nakatsuji1 and Y. Otani, Appl. Phys. Lett. **111** (2017) 202404(1-5).

5. Direct optical observation of spin accumulation at nonmagnetic metal/oxide interface: J. Puebla, F. Auvray, M. Xu, B. Rana, A. Albouy, H. Tsai, K. Kondou, G. Tatara and Y. Otani, Appl. Phys. Lett. **111** (2017) 092402(1-4).

6. Excitation of coherent propagating spin waves in ultrathin CoFeB film by voltage-controlled magnetic anisotropy: B. Rana, Y. Fukuma, K. Miura, H. Takahashi and Y. Otani, Appl. Phys. Lett. **111** (2017) 052404(1-5).

7. Important role of magnetization precession angle measurement in inverse spin Hall effect induced by spin pumping: S. Gupta, R. Medwal, D. Kodama, K. Kondou, Y. Otani and Y. Fukuma, Appl. Phys. Lett. **110** (2017) 022404(1-5).

8. Spin diffusion length of Permalloy using spin absorption in lateral spin valves: E. Sagasta, Y. Omori, M. Isasa, Y. Otani, L. E. Hueso and F. Casanova, Appl. Phys. Lett. **111** (2017) 082407(1-4).

9. スピントロニクス実験のコツ - スピン流の計測 -: 近藤 浩太 , 大谷 義近 , 応用物理 **86** (2017) 139.

10. 表面・界面を利用してスピン流を作る：近藤 浩太 , 軽部 修太郎 , 大谷 義近 , 日本物理学会誌 **72** (2017) 320.

11. High output voltage of magnetic tunnel junctions with a $Cu(In_{0.8}Ga_{0.2})Se_2$ semiconducting barrier with a low resistance–area product: K. Mukaiyama, S. Kasai, Y. K. Takahashi, K. Kondou, Y. Otani, S. Mitani and K. Hono, Appl. Phys. Express **10** (2017) 013008(1-3).

12. Spin pumping due to spin waves in magnetic vortex structure: N. Hasegawa, K. Kondou, M. Kimata and Y. Otani, Appl. Phys. Express **10** (2017) 053002(1-3).

13. Investigation of magnetization dynamics in 2D $Ni_{80}Fe_{20}$ diatomic nanodot arrays: A. De, S. Mondal, C. Banerjee, A. K. Chaurasiya, R. Mandal, Y. Otani, R. K. Mitra and A. Barman, J. Phys. D: Appl. Phys. **50** (2017) 385002(1-11).

† Joint research with outside partners.

14. *Large anomalous Nernst effect at room temperature in a chiral antiferromagnet: M. Ikhlas, T. Tomita, T. Koretsune, M.-T. Suzuki, D. Nishio-Hamane, R. Arita, Y. Otani and S. Nakatsuji, Nature Phys. **13** (2017) 1085-1090.

15. Spin conversion on the nanoscale: Y. Otani, M. Shiraishi, A. Oiwa, E. Saitoh and S. Murakami, Nature Phys. **13** (2017) 829-832.

16. Efficient Modulation of Spin Waves in Two-Dimensional Octagonal Magnonic Crystal: S. Choudhury, S. Barman, Y. Otani and A. Barman, ACS Nano **11** (2017) 8814-8821.

17. Effect of excitation power on voltage induced local magnetization dynamics in an ultrathin CoFeB film: B. Rana, Y. Fukuma, K. Miura, H. Takahashi and Y. Otani, Sci. Rep. **7** (2017) 2318(1-9).

18. Voltage-induced magnetization dynamics in CoFeB/MgO/CoFeB magnetic tunnel junctions: K. Miura, S. Yabuuchi, M. Yamada, M. Ichimura, B. Rana, S. Ogawa, H. Takahashi, Y. Fukuma and Y. Otani, Sci. Rep. **7** (2017) 42511(1-8).

19. *Macroscopic Magnetization Control by Symmetry Breaking of Photoinduced Spin Reorientation with Intense Terahertz Magnetic Near Field: T. Kurihara, H. Watanabe, M. Nakajima, S. Karube, K. Oto, Y. Otani and T. Suemoto, Phys. Rev. Lett. **120** (2018) 107202.

20. Anomalous modulation of spin torque-induced ferromagnetic resonance caused by direct currents in permalloy/platinum bilayer thin films: S. Hirayama, S. Mitani, Y. Otani and S. Kasai, Appl. Phys. Express **11** (2018) 013002 (1-4).

21. Voltage-Controlled Reconfigurable Spin-Wave Nanochannels and Logic Devices: B. Rana and Y. Otani, Phys. Rev. Applied **9** (2018) 014033(1-15).

Komori group

A-few-atomic-layer ferromagnetic γ'-Fe4N thin films are studied by scanning tunneling microscopy/spectroscopy (STM/STS) and soft X-ray magnetic circular dichroism. The spin magnetic moment of Fe atoms increases with increasing the average thickness reaching 1.4μ_B/atom in the trilayer sample. Hexagonal atomic- layer iron nitrides with different crystal and local electronic structures are also found to grow on the Cu(001) surface. Local change of the electron-phonon coupling in periodically nano-modulated graphene on a macrofacet of SiC(0001) substrate is studied using inelastic STS. The coupling depends on the local distance between the graphene and the SiC substrate. An in-gap surface state on a Kondo insulator SmB_6(001) surface is studied by STS. The surface state survives even on the area with significant density of defects, which supports the existence of the topological Kondo surface state on this surface.

1. *Calculation of spin states of photoelectrons emitted from spin-polarized surface states of Bi(111) surfaces with a mirror symmetry: K. Kobayashi, K. Yaji, K. Kuroda and F. Komori, Phys. Rev. B **95** (2017) 205436(1-13).

2. *Direct mapping of spin and orbital entangled wave functions under interband spin-orbit coupling of giant Rashba spin-split surface states: R. Noguchi, K. Kuroda, K. Yaji, K. Kobayashi, M. Sakano, A. Harasawa, T. Kondo, F. Komori and S. Shin, Phys. Rev. B **95** (2017) 041111(R)(1-6).

3. Enhanced periodic modulation of electronic states in a hexagonal iron-nitride monolayer on Cu(001) via interfacial interaction: K. Ienaga, T. Miyamachi, Y. Takahashi, N. Kawamura and F. Komori, Phys. Rev. B **96** (2017) 085439(1-8).

4. Thickness-dependent electronic and magnetic properties of γ'-Fe_4N atomic layers on Cu(001): Y. Takahashi, T. Miyamachi, S. Nakashima, N. Kawamura, Y. Takagi, M. Uozumi, V. N. Antonov, T. Yokoyama, A. Ernst and F. Komori, Phys. Rev. B **95** (2017) 224417(1-8).

5. †*Dirac Fermions in Borophene: B. Feng, O. Sugino, R.-Y. Liu, J. Zhang, R. Yukawa, M. Kawamura, T. Iimori, H. Kim, Y. Hasegawa, H. Li, L. Chen, K. Wu, H. Kumigashira, F. Komori, T.-C. Chiang, S. Meng and I. Matsuda, Phys. Rev. Lett. **118** (2017) 096401(1-6).

6. * ホウ素単原子シート「ボロフェン」：金属性とディラックフェルミオン : F. Baojie, 松田 巌 , 固体物理 **52** (2017) 385-393.

7. STM observation of the chemical reaction of atomic hydrogen on the N-adsorbed Cu(001) surface: T. Hattori, M. Yamada and F. Komori, Surf. Sci. **655** (2017) 1-6.

8. * ホウ素単原子シート「ボロフェン」：松田 巌 , パリティ **32** (2017) 50-53.

9. †Modulation of Electron–Phonon Coupling in One-Dimensionally Nanorippled Graphene on a Macrofacet of 6H-SiC: K. Ienaga, T. Iimori, K. Yaji, T. Miyamachi, S. Nakashima, Y. Takahashi, K. Fukuma, S. Hayashi, T. Kajiwara, A. Visikovskiy, K. Mase, K. Nakatsuji, S. Tanaka and F. Komori, Nano Lett. **17** (2017) 3527-3532.

* Joint research among groups within ISSP.

10. *Spin-dependent quantum interference in photoemission process from spin-orbit coupled states: K. Yaji, K. Kuroda, S. Toyohisa, A. Harasawa, Y. Ishida, S. Watanabe, C. Chen, K. Kobayashi, F. Komori and S. Shin, Nat. Commun. **8** (2017) 14588(1-6).

11. †Evidence for in-gap surface states on the single phase SmB_6(001) surface: T. Miyamachi, S. Suga, M. Ellguth, C. Tusche, C. M. Schneider, F. Iga and F. Komori, Sci. Rep. **7** (2017) 12837(1-7).

12. †*Spin-polarized quasi-one-dimensional state with finite band gap on the Bi/InSb(001) surface: J. Kishi, Y. Ohtsubo, T. Nakamura, K. Yaji, A. Harasawa, F. Komori, S. Shin, J. E. Rault, P. Le Fèvre, F. Bertran, A. Taleb-Ibrahimi, M. Nurmamat, H. Yamane, S. Ideta, K. Tanaka and S. Kimura, Phys. Rev. Materials **1** (2017) 064602(1-5).

13. *Surface state of the dual topological insulator $Bi_{0.91}Sb_{0.09}$ (11-2): I. Matsuda, K. Yaji, A. A. Taskin, M. D'angelo, R. Yukawa, Y. Ohtsubo, P. Le Fèvre, F. Bertran, S. Yoshizawa, A. Taleb-Ibrahimi, A. Kakizaki, Y. Ando and F. Komori, Phys. B: Condensed Matter **516** (2017) 100-104.

14. *Surface electronic states of Au-induced nanowires on Ge(0 0 1): K. Yaji, R. Yukawa, S. Kim, Y. Ohtsubo, P. L. Fèvre, F. Bertran, A. Taleb-Ibrahimi, I. Matsuda, K. Nakatsuji, S. Shin and F. Komori, J. Phys.: Condens. Matter **30** (2018) 075001(1-7).

15. *Alkali-metal induced band structure deformation investigated by angle-resolved photoemission spectroscopy and first-principles calculations: S. Ito, B. Feng, M. Arita, T. Someya, W. -C. Chen, A. Takayama, T. Iimori, H. Namatame, M. Taniguchi, C. -M. Cheng, S. -J. Tang, F. Komori and I. Matsuda, Phys. Rev. B **97** (2018) 155423(1-8).

16. * レーザー励起スピン分解光電子分光で解き明かす光スピン制御：矢治光 一郎，黒田 健太，小森 文夫，辛 埴，光学 **47** (2018) 142-147.

17. *A Table-Top Formation of Bilayer Quasi-Free-Standing Epitaxial-Graphene on SiC(0001) by Microwave Annealing in Air: K.-S. Kim, G.-H. Park, H. Fukidome, T. Someya, T. Iimori, F. Komori, I. Matsuda and M. Suemitsu, Carbon **130** (2018) 792-798.

18. * 物質科学、この 1 年「ボロフェンにおけるディラックフェルミオン」：松田 巌，パリティ **33** (2018) 36-38.

19. †Evaluation of structural vacancies for 1/1-Al–Re–Si approximant crystals by positron annihilation spectroscopy: K. Yamada, H. Suzuki, H. Kitahata, Y. Matsushita, K. Nozawa, F. Komori, R. S. Yu, Y. Kobayashi, T. Ohdaira, N. Oshima, R. Suzuki, Y. Takagiwa, K. Kimura and I. Kanazawa, Philos. Mag. **98** (2018) 107-117.

20. *Discovery of 2D Anisotropic Dirac Cones: B. Feng, J. Zhang, S. Ito, M. Arita, C. Cheng, L. Chen, K. Wu, F. Komori, O. Sugino, K. Miyamoto, T. Okuda, S. Meng and I. Matsuda, Adv. Mater. **30** (2018) 1704025(1-6).

21. †Triangular lattice atomic layer of Sn(1×1) at graphene/SiC(0001) interface: S. Hayashi, A. Visikovskiy, T. Kajiwara, T. Iimori, T. Shirasawa, K. Nakastuji, T. Miyamachi, S. Nakashima, K. Yaji, K. Mase, F. Komori and S. Tanaka, Appl. Phys. Express **11** (2018) 015202(1-4).

22. Lattice distortion of square iron nitride monolayers induced by changing symmetry of substrate: T. Hattori, T. Iimori, T. Miyamachi and F. Komori, Phys. Rev. Materials **2** (2018) 044003(1-7).

23. * レーザーで電子のスピン方向を自由に制御：矢治光 一郎，黒田 健太，小森 文夫，辛 埴，レーザー加工学会誌 **25** (2018) 39-42.

24. †*Experimental Methods for Spin and Angle-Resolved Photoemission Spectroscpy Combined with Polarization Variable Laser: K. Kuroda, K. Yaji, A. Harasawa, R. Noguchi, T. Kondo, F. Komori and S. Shin, JoVE (2018), in print.

25. * 固体表面電子におけるスピン軌道エンタングルメントと光スピン制御：矢治光 一郎，黒田 健太，小森 文夫，辛 埴，個体物理 **52** (2017) 559-571.

Hasegawa group

Using low-temperature ultrahigh vacuum scanning tunneling microscopy (STM) we have obtained real-space images showing orbital order on a Co-terminated surface of $CeCoIn_5$, which is a heavy-fermion superconducting material. Because of the 4-fold symmetry regardless of the sites in the bulk or on the surface, $3d_{xz}$ and $3d_{yz}$ orbitals of the Co atoms are energetically degenerated. However, on the surface, because of the reduced coordination number and resulting enhanced electron correlation, the capability of the electron screening is suppressed. As a result, in order to reduce the Coulomb repulsive energy alternating unoccupation among the two 3*d* orbitals in an antiferromagnetic manner becomes favorable on the surface. We observed alternately-arranged dumbbell shapes whose shape is quite similar with that of d_{xz} and d_{yz} orbitals looking from the z direction, proving the existence of the orbital order. In a technical point of view of STM, observing d orbitals is not an easy task because of their localized nature near the core. Since STM detects wave functions of sample surface by the probe tip, states that

† Joint research with outside partners.

decay long from the surface are probed more efficiently than quickly decaying states. In fact, on the Co-terminated surface we observed round-shaped Co atoms arranged in a square lattice in standard tunneling conditions, which obviously originate from *s*-derived states of Co. In order to observe the d orbitals, we intentionally locate the tip near the surface almost touching to the surface but still in the tunneling regime, and successfully observed their ordering, which had not been achieved before. In 2017, we also performed collaborative research works with in-house, domestic, and oversea groups, some of which were published in high-impact journals. We have obtained STM images of a monolayer boron film called borophene in collaboration with Prof. Iwao Matsuda, ISSP, and Fe phthalocyanine molecules adsorbed on silicene in collaboration with Prof. Yamada-Takamura, JAIST and Prof. Hirjibehedin, University College London. We also performed study on atomically controlled point contact formation with Prof. Sakai, Kyoto University.

1. †Break voltage of Au single-atom contacts formed by junction closure: S. Wakasugi, S. Kurokawa, H. Kim, Y. Hasegawa and A. Sakai, J. Appl. Phys. **121** (2017) 244304(1-8).

2. Role of the substrate in the formation of chiral magnetic structures driven by the interfacial Dzyaloshinskii-Moriya interaction: M. Haze, Y. Yoshida and Y. Hasegawa, Phys. Rev. B **95** (2017) 060415(1-5).

3. †*Dirac Fermions in Borophene: B. Feng, O. Sugino, R.-Y. Liu, J. Zhang, R. Yukawa, M. Kawamura, T. Iimori, H. Kim, Y. Hasegawa, H. Li, L. Chen, K. Wu, H. Kumigashira, F. Komori, T.-C. Chiang, S. Meng and I. Matsuda, Phys. Rev. Lett. **118** (2017) 096401(1-6).

4. †Guided Molecular Assembly on a Locally Reactive 2D Material: B. Warner, T. G. Gill, V. Caciuc, N. Atodiresei, A. Fleurence, Y. Yoshida, Y. Hasegawa, S. Blügel, Y. Yamada-Takamura and C. F. Hirjibehedin, Adv. Mater. **29** (2017) 1703929(1-7).

5. Experimental verification of the rotational type of chiral spin spiral structures by spin-polarized scanning tunneling microscopy: M. Haze, Y. Yoshida and Y. Hasegawa, Sci. Rep. **7** (2017) 13269(1-5).

6. Atomic-scale visualization of surface-assisted orbital order: H. Kim, Y. Yoshida, C.-C. Lee, T.-R. Chang, H.-T. Jeng, H. Lin, Y. Haga, Z. Fisk and Y. Hasegawa, Sci. Adv. **3** (2017) eaao0362(1-5).

Lippmaa group

The main research topics for this year concerned energy conversion materials used for photoelectrochemical water splitting. We studied the initial growth phase of Ir:$SrTiO_3$ and found that nanoscale Ir-rich clusters nucleate at the beginning of film growth, ultimately leading to macroscopic segregation of metal nanopillars. We also studied the growth characteristics of IrO_2 films, mapping the stability phase diagram for Ir oxides and worked on fabricating a potential topological pyrochlore iridate phase, $Pr_2Ir_2O_7$.

1. 自己組織的に成長する単結晶性酸化物ナノ構造の新展開ー磁性体ナノ結晶とナノコンポジット水分解光電極を開発ー： 高橋竜太 , リップ マーミック , 固体物理 **52** (2017) 105-116.

2. Hole trap state analysis in $SrTiO_3$: N. Osawa, R. Takahashi and M. Lippmaa, Appl. Phys. Lett. **110** (2017) 263902(1-5).

3. Microstructure analysis of IrO_2 thin films: X. Hou, R. Takahashi, T. Yamamoto and M. Lippmaa, J. Cryst. Growth **462** (2017) 24-28.

4. †Combinatorial screening of halide perovskite thin films and solar cells by mask-defined IR laser molecular beam epitaxy: K. Kawashima, Y. Okamoto, O. Annayev, N. Toyokura, R. Takahashi, M. Lippmaa, K. Itaka, Y. Suzuki, N. Matsuki and H. Koinuma, Sci. Tech. Adv. Mater. **18** (2017) 307-315.

5. Intrinsic Superhydrophilicity of Titania-Terminated Surfaces: S. Kawasaki, E. Holmström, R. Takahashi, P. Spijker, A. S. Foster, H. Onishi and M. Lippmaa, J. Phys. Chem. C **121** (2017) 2268-2275.

6. †Strain induced atomic structure at Ir-doped $LaAlO_3/SrTiO_3$ interface: M. Lee, R. Arras, B. Warot-Fonrose, T. Hungria, M. Lippmaa, H. Daimon and M. J. Casanove, Phys. Chem. Chem. Phys. **19** (2017) 28676-28683.

7. *Dielectric anomalies and interactions in the three-dimensional quadratic band touching Luttinger semimetal $Pr_2Ir_2O_7$: B. Cheng, T. Ohtsuki, D. Chaudhuri, S. Nakatsuji, M. Lippmaa and N. P. Armitage, Nat. Commun. **8** (2017) 2097(1-6).

8. Magnetic and Magnetodielectric Properties of Epitaxial Iron Vanadate Thin Films: D. Zhou, R. Takahashi, Y. Zhou, D. Kim, V. K. Suresh, Y.-H. Chu, Q. He, P. Munroe, M. Lippmaa, J. Seidel and N. Valanoor, Adv. Electron. Mater. **3** (2017) 1600295(1-10).

9. Thermally Stable Sr_2RuO_4 Electrode for Oxide Heterostructures: R. Takahashi and M. Lippmaa, ACS Appl. Mater. Interfaces **9** (2017) 21314–21321.

---

* Joint research among groups within ISSP.

10. Pyroelectric detection of ferroelectric polarization in magnetic thin films: R. Takahashi and M. Lippmaa, Jpn. J. Appl. Phys. **57** (2018) 0902A1.

11. †Noble metal nanocluster formation in epitaxial perovskite thin films: M. Lee, R. Arras, R. Takahashi, B. Warot-Fonrose, H. Daimon, M.-J. Casanove and M. Lippmaa, ACS Omega **3** (2018) 2169-2173.

12. 酸化物半導体中に自己組織化した金属ナノピラーによる高効率・水分解光電極反応 : 川崎 聖治 , 高橋 竜太 , リップマー ミック , 応用物理 **87** (2018) 366-369.

Functional Materials Group

Yoshinobu group

We conducted several research projects in the fiscal year 2017: (1) Systematic study of the activation and hydrogenation of CO_2 on Cu model catalysts by AP-XPS, IRAS, and TPD. (2) The surface chemistry of formic acid on Cu model catalysts studied by SR-PES, IRAS and TPD. (3) Spectroscopic characterization of Pd-Cu and Pd-Ag surfaces by XPS. (4) Spectroscopic characterization of adsorption and thermal processes of NO on silicone/ZrB_2/Si(111) using SR-XPS. (5) LT-STM study of Zn on Cu(997). (6) Independently driven four-probe conductivity measurement of organic thin films and organic single crystals.

1. †Direct observation of the electron-phonon coupling between empty states in graphite via high-resolution electron energy loss spectroscopy: S.-I. Tanaka, K. Mukai and J. Yoshinobu, Phys. Rev. B **95** (2017) 165408(1-6).

2. Highly anisotropic mobility in solution processed TIPS-pentacene film studied by independently driven four GaIn probes: S. Yoshimoto, K. Takahashi, M. Suzuki, H. Yamada, R. Miyahara, K. Mukai and J. Yoshinobu, Appl. Phys. Lett. **111** (2017) 073301(1-4).

3. CO_2 adsorption on the copper surfaces: van der Waals density functional and TPD studies: F. Muttaqien, Y. Hamamoto, I. Hamada, K. Inagaki, Y. Shiozawa, K. Mukai, T. Koitaya, S. Yoshimoto, J. Yoshinobu and Y. Morikawa, J. Chem. Phys. **147** (2017) 094702(1-8).

4. †Electronic states and growth modes of Zn atoms deposited on Cu(111) studied by XPS, UPS and DFT: T. Koitaya, Y. Shiozawa, Y. Yoshikura, K. Mukai, S. Yoshimoto, S. Torii, F. Muttaqien, Y. Hamamoto, K. Inagaki, Y. Morikawa and J. Yoshinobu, Surf. Sci. **663** (2017) 1–10.

5. *Adsorption of CO_2 on Graphene: A Combined TPD, XPS, and vdW-DF Study: K. Takeuchi, S. Yamamoto, Y. Hamamoto, Y. Shiozawa, K. Tashima, H. Fukidome, T. Koitaya, K. Mukai, S. Yoshimoto, M. Suemitsu, Y. Morikawa, J. Yoshinobu and I. Matsuda, J. Phys. Chem. C **121** (2017) 2807-2814.

6. Systematic Study of Adsorption and the Reaction of Methanol on Three Model Catalysts: Cu(111), Zn–Cu(111), and Oxidized Zn–Cu(111): T. Koitaya, Y. Shiozawa, Y. Yoshikura, K. Mukai, S. Yoshimoto and J. Yoshinobu, J. Phys. Chem. C **121** (2017) 25402-25410.

7. †*Strong Hydrogen Bonds at the Interface between Proton-Donating and -Accepting Self-Assembled Monolayers on Au(111): H. S. Kato, S. Yoshimoto, A. Ueda, S. Yamamoto, Y. Kanematsu, M. Tachikawa, H. Mori, J. Yoshinobu and I. Matsuda, Langmuir **34** (2018) 2189-2197.

8. Initial gas exposure effects on monolayer pentacene field-effect transistor studied using four gallium indium probes: S. Yoshimoto, R. Miyahara, Y. Yoshikura, J. Tang, K. Mukai and J. Yoshinobu, Org. Electron. **54** (2018) 34-39.

Akiyama group

In 2017, we started fabrication of 1035nm InGaAs laser diodes for short and intense pulse generation via gain switching. In parallel, we studied pico- and femto-second short-pulse generation and pulse dynamics in GaAs, GaN, and other semiconductor gain-switched lasers via optical pumping and current injection. We studied single- and multi-junction solar cells by absolute electroluminescence-efficiency measurement methods, and via time-resolved photo-emission spectroscopy, we studied photo-voltage dynamics solar cells after impulsive optical excitations. We made computational studies with quantum-chemistry and molecular-dynamics calculations on oxyluciferins and caged-luciferins.

1. Anomalous Metal Phase Emergent on the Verge of an Exciton Mott Transition: F. Sekiguchi, T. Mochizuki, C. Kim, H. Akiyama, L. N. Pfeiffer, K. W. West and R. Shimano, Phys. Rev. Lett. **118** (2017) 067401(1-6).

† Joint research with outside partners.

2. Sensitive monitoring of photocarrier densities in the active layer of a photovoltaic device with time-resolved terahertz reflection spectroscopy: G. Yamashita, E. Matsubara, M. Nagai, C. Kim, H. Akiyama, Y. Kanemitsu and M. Ashida, Appl. Phys. Lett. **110** (2017) 071108(1-5).

3. "Visible" 5d orbital states in a pleochroic oxychloride: D. Hirai, T. Yajima, D. Nishio-Hamane, C. Kim, H. Akiyama, M. Kawamura, T. Misawa, N. Abe, T.-H. Arima and Z. Hiroi, J. Am. Chem. Soc. **139** (2017) 10784-10789.

4. Picosecond tunable gain-switched blue pulses from GaN laser diodes with nanosecond current injections: S. Chen, T. Nakamura, T. Ito, H. Nakamae, X. Bao, G. Weng, X. Hu, M. Yoshita, H. Akiyama, J. Liu, M. Ikeda and H. Yang, Opt. Express **25** (2017) 13046-13054.

5. Effect of dynamical fluctuations of hydration structures on the absorption spectra of oxyluciferin anions in aqueous solution: M. Hiyama, M. Shiga, N. Koga, O. Sugino, H. Akiyama and Y. Noguchi, Phys. Chem. Chem. Phys. **19** (2017) 10028-10035.

6. Biexciton Emission From Single Quantum-Confined Structures in N-Polar (000-1) InGaN/GaN Multiple Quantum Wells: K. Takamiya, S. Yagi, H. Yaguchi, H. Akiyama, K. Shojiki, T. Tanikawa and R. Katayama, Phys. Status Solidi B **17** (2017) 1700454(1-4).

7. Broadband tunable integrated CMOS pulser with 80-ps minimum pulse width for gain-switched semiconductor lasers: S. Chen, S. Diao, P. Li, T. Nakamura, M. Yoshita, G. Weng, X. Hu, Y. Shi, Y. Liu and H. Akiyama, Sci. Rep. **7** (2017) 6878(1-8).

8. Theoretical insights into the effect of pH values on oxidation processes in the emission of firefly luciferin in aqueous solution: M. Hiyama, H. Akiyama and N. Koga, Luminescence **32** (2017) 1100-1108.

9. Diagnosis of GaInAs/GaAsP multiple quantum well solar cells with Bragg reflectors via absolute electroluminescenc: L. Zhu, M. Yoshita, J. Tsai, Y. Wang, C. Hong, G. Chi, C. Kim, P. Yu and H. Akiyama, IEEE J. Photovolt. **7** (2017) 781 - 786.

10. Absolute Electroluminescence Imaging Diagnosis of GaAs Thin-film Solar Cells: X. Hu, T. Chen, J. Xue, G. Weng, S. Chen, H. Akiyama and Z. Zhu, IEEE Photon. J. **9** (2017) 8400409(1-9).

11. Coherent detection of THz-induced sideband emission from excitons in the nonperturbative regime: K. Uchida, T. Otobe, T. Mochizuki, C. Kim, M. Yoshita, K. Tanaka, H. Akiyama, L. N. Pfeiffer, K. W. West and H. Hirori, Phys. Rev. B **97** (2018) 165122.

12. Analysis of future generation solar cells and materials: M. Yamaguchi, L. Zhu, H. Akiyama, Y. Kanemitsu, H. Tampo, H. Shibata, K.-H. Lee, K. Araki and N. Kojima, Jpn. J. Appl. Phys. **57** (2018) 04FS03(1-6).

13. Terahertz field-induced ionization and perturbed free induction decay of excitons in bulk GaAs: Y. Murotani, M. Takayama, F. Sekiguchi, C. Kim, H. Akiyama and R. Shimano, J. Phys. D: Appl. Phys. **51** (2018) 114001(1-10).

14. Effect of interaction between the internal cavity and external cavity on beam properties in a spectrally beam combined system: Z. Wu, T. Ito, H. Akiyama and B. Zhang, J. Opt. Soc. Am. A **35** (2018) 772-778.

15. Absolute bioluminescence imaging at the single-cell on an atto-Watt level: T. Enomoto, H. Kubota, K. Mori, M. Shimogawara, M. Yoshita and H. Akiyama, BioTechniques (2018), accepted for publication.

Sugino group

We have made progress in functional matter research of (1) electrocatalysis, (2) oxygen solid, (3) hidroxyapatite, (4) bio-luminescence, and (5) monolayer Dirac materials. We have also developed methods for (a) many-body Green's function calculation and (b) tensor decomposition of many-body wave function.

1. †Erratum: Improved modeling of electrified interfaces using the effective screening medium method [Phys. Rev. B **88** , 155427 (2013)]: I. Hamada, O. Sugino, N. Bonnet and M. Otani, Phys. Rev. B **95** (2017) 119901 (1-2).

2. *First-principles description of van der Waals bonded spin-polarized systems using the vdW-DF+U method: Application to solid oxygen at low pressure: S. Kasamatsu, T. Kato and O. Sugino, Phys. Rev. B **95** (2017) 235120 (1-11).

3. †*Dirac Fermions in Borophene: B. Feng, O. Sugino, R.-Y. Liu, J. Zhang, R. Yukawa, M. Kawamura, T. Iimori, H. Kim, Y. Hasegawa, H. Li, L. Chen, K. Wu, H. Kumigashira, F. Komori, T.-C. Chiang, S. Meng and I. Matsuda, Phys. Rev. Lett. **118** (2017) 096401 (1-6).

4. * ホウ素単原子シート「ボロフェン」：金属性とディラックフェルミオン : F. Baojie, 松田 巌 , 固体物理 **52** (2017) 385-393.

* Joint research among groups within ISSP.

5. Molecular size insensitivity of optical gap of [n] cycloparaphenylenes (n= 3-16): Y. Noguchi and O. Sugino, J. Chem. Phys. **146** (2017) 144304(1-7).

6. Quantitative characterization of exciton from *GW* +Bethe-Salpeter calculation: D. Hirose, Y. Noguchi and O. Sugino, J. Chem. Phys. **146** (2017) 044303(1-10).

7. * ホウ素単原子シート「ボロフェン」：松田 巌 , パリティ **32** (2017) 50-53.

8. High-Lying Triplet Excitons of Thermally Activated Delayed Fluorescence Molecules: Y. Noguchi and O. Sugino, J. Phys. Chem. C **121** (2017) 20687-20695.

9. †The effect of dynamical fluctuations of hydration structures on the absorption spectra of oxyluciferin anions in an aqueous solution: M. Hiyama, M. Shiga, N. Koga, O. Sugino, H. Akiyama and Y. Noguchi, Phys. Chem. Chem. Phys. **19** (2017) 10028-10035.

10. †*Experimental realization of two-dimensional Dirac nodal line fermions in monolayer Cu_2Si: B. Feng, B. Fu, S. Kasamatsu, S. Ito, P. Cheng, C.-C. Liu, Y. Feng, S. Wu, S. K. Mahatha, P. Sheverdyaeva, P. Moras, M. Arita, O. Sugino, T.-C. Chiang, K. Shimada, K. Miyamoto, T. Okuda, K. Wu, L. Chen, Y. Yao and I. Matsuda, Nat. Commun. **8** (2017) 1007(1-6).

11. * 物質科学、この 1 年「ボロフェンにおけるディラックフェルミオン」：松田 巌 , パリティ **33** (2018) 36-38.

12. *Discovery of 2D Anisotropic Dirac Cones: B. Feng, J. Zhang, S. Ito, M. Arita, C. Cheng, L. Chen, K. Wu, F. Komori, O. Sugino, K. Miyamoto, T. Okuda, S. Meng and I. Matsuda, Adv. Mater. **30** (2018) 1704025(1-6).

13. First-principles investigation of polarization and ion conduction mechanisms in hydroxyapatite: S. Kasamatsu and O. Sugino, Phys. Chem. Chem. Phys. **20** (2018) 8744.

Quantum Materials Group

Oshikawa group

We studied a wide range of theoretical problems in condensed matter physics and statistical physics. As a novel application of anomaly in quantum field theory, we discussed possible gapless critical phases of quantum antiferromagnetic chains with general spin quantum numbers. The critical theory with the exact SU(2) symmetry and the emergent Lorentz invariance has been classified by the SU(2) Wess-Zumino-Witten (WZW) theories labeled by a natural number called level. We found that, in the presence of the translation symmetry, even- and odd-level WZW theories can be only realized in integer- and half-odd-integer spin chains, respectively. This follows from an anomaly matching and can be regarded as a field-theory manifestation of the Lieb-Schultz-Mattis constraint. The present result leads to a novel concept of "symmetry-protected critical phases".

1. †Capacity of entanglement and the distribution of density matrix eigenvalues in gapless systems: Y. O. Nakagawa and S. Furukawa, Phys. Rev. B **96** (2017) 205108(1-8).

2. †Crystalline Kitaev spin liquids: M. G. Yamada, V. Dwivedi and M. Hermanns, Phys. Rev. B **96** (2017) 155107(1-15).

3. †Encoding orbital angular momentum of light in magnets: H. Fujita and M. Sato, Phys. Rev. B **96** (2017) 060407(R) (1-6).

4. †Finite-size scaling of the Shannon-Rényi entropy in two-dimensional systems with spontaneously broken continuous symmetry: G. Misguich, V. Pasquier and M. Oshikawa, Phys. Rev. B **95** (2017) 195161(1-13).

5. Theory of electron spin resonance in one-dimensional topological insulators with spin-orbit couplings: Detection of edge states: Y. Yao, M. Sato, T. Nakamura, N. Furukawa and M. Oshikawa, Phys. Rev. B **96** (2017) 205424(1-10).

6. †Ultrafast generation of skyrmionic defects with vortex beams: Printing laser profiles on magnets: H. Fujita and M. Sato, Phys. Rev. B **95** (2017) 054421(1-12).

7. Designing Kitaev Spin Liquids in Metal-Organic Frameworks: M. G. Yamada, H. Fujita and M. Oshikawa, Phys. Rev. Lett. **119** (2017) 057202(1-6).

8. †Symmetry Protection of Critical Phases and a Global Anomaly in 1+1 Dimensions: S. C. Furuya and M. Oshikawa, Phys. Rev. Lett. **118** (2017) 021601(1-5).

† Joint research with outside partners.

9. †Numerical calculations on the relative entanglement entropy in critical spin chains: Y. O. Nakagawa and T. Ugajin, J. Stat. Mech. **2017** (2017) 093104(1-16).

10. Signatures of Dirac Cones in a DMRG Study of the Kagome Heisenberg Model: Y.-C. He, M. P. Zaletel, M. Oshikawa and F. Pollmann, Phys. Rev. X **7** (2017) 031020(1-16).

11. Construction of Hamiltonians by supervised learning of energy and entanglement spectra: H. Fujita, Y. O. Nakagawa, S. Sugiura and M. Oshikawa, Phys. Rev. B **97** (2018) 075114 (1-12).

12. †Particle statistics, frustration, and ground-state energy: W. Nie, H. Katsura and M. Oshikawa, Phys. Rev. B **97** (2018) 125153.

13. Fulde-Ferrell state in a ferromagnetic chiral superconductor with magnetic domain walls: Y. Tada, Physical Review B **97** (2018) 014519.

14. Decay of superconducting correlations for gauged electrons in dimensions D <= 4: Y. Tada and T. Koma, Journal of Mathematical Physics **59** (2018) 031905.

Nakatsuji group

Our group explores ground state properties and spintronic functions of novel quantum phases and phase transitions in rare-earth and transition metal based compounds. The followings are some relevant results obtained in 2017. (1) We discovered the anomalous Nernst effect for the first time in an antiferromagnet. Strikingly, the effect in the antiferromagnet Mn_3Sn is found more than 100 times larger than the estimate based on its magnetization. (2) We discovered the first example of a Weyl magnet. In particular, we found strong experimental evidence for the Weyl fermions in the antiferromagnet Mn_3Sn. (3) We discovered the magneto optical Kerr effect for the first time in an antiferromagnetic metal. We observed a large zero-field Kerr rotation angle ~ 20 mdeg and a clear square hysteresis loop in Mn_3Sn at room temperature by the magneto-optical Kerr effect, indicating the ferroic ordering of magnetic octupoles. (4) We discovered the first example of a quantum valence transition and its quantum criticality in a metal, in particular, in the mixed valent system a-$YbAl_{1-x}Fe_xB_4$. (5) We observed a very large dielectric constant due to the strong correlation effects in the Luttinger semimetal state of $Pr_2Ir_2O_7$ using the thin films.

1. †*Lifetime-Broadening-Suppressed X-ray Absorption Spectrum of β-$YbAlB_4$ Deduced from Yb $3d \rightarrow 2p$ Resonant X-ray Emission Spectroscopy: N. Kawamura, N. Kanai, H. Hayashi, Y. H. Matsuda, M. Mizumaki, K. Kuga, S. Nakatsuji and S. Watanabe, J. Phys. Soc. Jpn. **86** (2017) 014711(1-7).

2. Frustrated magnetism in the Heisenberg pyrochlore antiferromagnets AYb_2X_4 (A = Cd, Mg, X = S, Se): T. Higo, K. Iritani, M. Halim, W. Higemoto, T. U. Ito, K. Kuga, K. Kimura and S. Nakatsuji, Phys. Rev. B **95** (2017) 174443(1-7).

3. Disordered Route to the Coulomb Quantum Spin Liquid: Random Transverse Fields on Spin Ice in $Pr_2Zr_2O_7$: J. -J. Wen, S. M. Koohpayeh, K. A. Ross, B. A. Trump, T. M. McQueen, K. Kimura, S. Nakatsuji, Y. Qiu, D. M. Pajerowski, J. R. D. Copley and C. L. Broholm, Phys. Rev. Lett. **118** (2017) 107206(1-5).

4. *Thermal Hall Effect in a Phonon-Glass $Ba_3CuSb_2O_9$: K. Sugii, M. Shimozawa, D. Watanabe, Y. Suzuki, M. Halim, M. Kimata, Y. Matsumoto, S. Nakatsuji and M. Yamashita, Phys. Rev. Lett. **118** (2017) 145902(1-5).

5. *Anomalous Nernst effect in a microfabricated thermoelectric element made of chiral antiferromagnet Mn_3Sn: H. Narita, M. Ikhlas, M. Kimata, A. A. Nugroho, S. Nakatsuji1 and Y. Otani, Appl. Phys. Lett. **111** (2017) 202404(1-5).

6. 反強磁性体における巨大異常ホール効果：中辻 知，応用物理 **86** (2017) 310-314.

7. Large spontaneous Hall effets in chiral topological magnets: S. Nakatsuji, T. Higo, M. Ikhlas, T. Tomita and Z. Tian, Philos. Mag. **97** (2017) 2815-2827.

8. *Large anomalous Nernst effect at room temperature in a chiral antiferromagnet: M. Ikhlas, T. Tomita, T. Koretsune, M.-T. Suzuki, D. Nishio-Hamane, R. Arita, Y. Otani and S. Nakatsuji, Nature Phys. **13** (2017) 1085-1090.

9. *Orthogonal magnetization and symmetry breaking in pyrochlore iridate $Eu_2Ir_2O_7$: T. Liang, T. H. Hsieh, J. J. Ishikawa, S. Nakatsuji, L. Fu and N. P. Ong, Nature Phys. **13** (2017) 599-603.

10. Anisotropic Thermal Expansion of α-$YbAlB_4$: Y. Matsumoto, K. Kuga, T. Tomita, R. Küchler and S. Nakatsuji, J. Phys.: Conf. Ser. **807** (2017) 022005(1-6).

11. Specific heat and electrical resistivity at magnetic fields in antiferromagnetic heavy fermion $CeAl_2$: T. Ebihara, M. Tsuchiya, Y. Saitoh, J. Jatmika, M. Tsujimoto, Y. Shimura, Y. Matsumoto and S. Nakatsuji, J. Phys.: Conf. Ser. **807** (2017) 012011(1-6).

---

* Joint research among groups within ISSP.

12. *Dielectric anomalies and interactions in the three-dimensional quadratic band touching Luttinger semimetal $Pr_2Ir_2O_7$: B. Cheng, T. Ohtsuki, D. Chaudhuri, S. Nakatsuji, M. Lippmaa and N. P. Armitage, Nat. Commun. **8** (2017) 2097(1-6).

13. *Evidence for magnetic Weyl fermions in a correlated metal: K. Kuroda, T. Tomita, M. -T. Suzuki, C. Bareille, A. A. Nugroho, P. Goswami, M. Ochi, M. Ikhlas, M. Nakayama, S. Akebi, R. Noguchi, R. Ishii, N. Inami, K. Ono, H. Kumigashira, A. Varykhalov, T. Muro, T. Koretsune, R. Arita, S. Shin, T. Kondo and S. Nakatsuji, Nature Mater. **16** (2017) 1090-1095.

14. Valence fluctuating compound α-$YbAlB_4$ studied by ^{174}Yb Mössbauer spectroscopy and X-ray diffraction using synchrotron radiation: M. Oura, S. Ikeda, R. Masuda, Y. Kobayashi, M. Seto, Y. Yoda, N. Hirao, S. I. Kawaguchi, Y. Ohishi, S. Suzuki, K. Kuga, S. Nakatsuji and H. Kobayashi, Physica B **536** (2018) 162-164.

15. *Kondo hybridization and quantum criticality in β−$YbAlB_4$ by laser ARPES: C. Bareille, S. Suzuki, M. Nakayama, K. Kuroda, A. H. Nevidomskyy, Y. Matsumoto, S. Nakatsuji, T. Kondo and S. Shin, Phys. Rev. B **97** (2018) 045112(1-7).

16. Magnetic Excitations across the Metal-Insulator Transition in the Pyrochlore Iridate Eu2Ir2O7: S. H. Chun, B. Yuan, D. Casa, J. Kim, C.-Y. Kim, Z. Tian, Y. Qiu, S. Nakatsuji and Y.-J. Kim, Phys. Rev. Lett. **120** (2018) 177203.

17. Discovery of Emergent Photon and Monopoles in a Quantum Spin Liquid: Y. Tokiwa, T. Yamashita, D. Terazawa, K. Kimura, Y. Kasahara, T. Onishi, Y. Kato, M. Halim, P. Gegenwart, T. Shibauchi, S. Nakatsuji, E.-G. Moon and Y. Matsuda, Journal of the Physical Society of Japan **87** (2018) 064702.

18. Large magneto-optical Kerr effect and imaging of magnetic octupole domains in an antiferromagnetic metal: T. Higo, H. Man, D. B. Gopman, L. Wu, T. Koretsune, O. M. J. van &. Erve, Y. P. Kabanov, D. Rees, Y. Li, M.-T. Suzuki, S. Patankar, M. Ikhlas, C. L. Chien, R. Arita, R. D. Shull and J. O. &. S. Nakatsuji, Nature Photon. **12** (2018) 73-78.

19. *X-Ray Absorption Spectroscopy of 4f Compounds and Future Directions Toward Time-resolved Measurements: H. Wadati, K. Takubo, T. Tsuyama, Y. Yokoyama, K. Yamamoto, Y. Hirata, T. Ina, K. Nitta, M. Mizumaki, T. Togashi, S. Suzuki, Y. Matsumoto and S. Nakatsuji, Adv. X-Ray. Chem. Anal., Japan **49** (2018) 169-175.

20. †*Quantum valence criticality in a correlated metal: K. Kuga, Y. Matsumoto, M. Okawa, S. Suzuki, T. Tomita, K. Sone, Y. Shimura, T. Sakakibara, D. Nishio-Hamane, Y. Karaki, Y. Takata, M. Matsunami, R. Eguchi, M. Taguchi, A. Chainani, S. Shin, K. Tamasaku, Y. Nishino, M. Yabashi, T. Ishikawa and S. Nakatsuji, Sci. Adv. **4** (2018) eaao3547 (1-6).

21. Relaxation calorimetry at very low temperatures for systems with internal relaxation: Y. Matsumoto and S. Nakatsuji, Review of Scientific Instruments **89** (2018) 033908.

Materials Design and Characterization Laboratory

Hiroi group

A new oxychloride, $Ca_3ReO_5Cl_2$, is found, which shows unusually distinct pleochroism; that is, the material exhibits different colors depending on the viewing direction. This pleochroism is a consequence of the coincidental complex crystal field splitting of the 5*d* orbitals of the Re^{6+} ion in a square-pyramidal coordination of low symmetry in the energy range of the visible spectrum. Since the relevant d–d transitions show characteristic polarization dependence according to the optical selection rule, the orbital states are "visible" in $Ca_3ReO_5Cl_2$. The superconducting pyrochlore oxide Cd2Re2O7 is revisited with a particular emphasis on the sample-quality issue. Recently, it has attracted increasing attention as a candidate spin–orbit coupled metal (SOCM), in which specific Fermi liquid instability is expected to lead to an odd-parity order with spontaneous inversion-symmetry breaking and parity-mixing superconductivity.

1. *Collinear spin density wave order and anisotropic spin fluctuations in the frustrated J_1-J_2 chain magnet $NaCuMoO_4(OH)$: K. Nawa, M. Yoshida, M. Takigawa, Y. Okamoto and Z. Hiroi, Phys. Rev. B **96** (2017) 174433(1-9).

2. *J_1-J_2 square-lattice Heisenberg antiferromagnets with $4d^1$ spins AMoOPO$_4$Cl (A=K, Rb): H. Ishikawa, N. Nakamura, M. Yoshida, M. Takigawa, P. Babkevich, N. Qureshi, H. M. Rønnow, T. Yajima and Z. Hiroi, Phys. Rev. B **95** (2017) 064408(1-9).

3. *Magnetic transitions under ultrahigh magnetic fields of up to 130 T in the breathing pyrochlore antiferromagnet $LiInCr_4O_8$: Y. Okamoto, D. Nakamura, A. Miyake, S. Takeyama, M. Tokunaga, A. Matsuo, K. Kindo and Z. Hiroi, Phys. Rev. B **95** (2017) 134438(1-5).

† Joint research with outside partners.

4. *Phase diagram of multiferroic $KCu_3As_2O_7(OD)_3$: G. J. Nilsen, V. Simonet, C. V. Colin, R. Okuma, Y. Okamoto, M. Tokunaga, T. C. Hansen, D. D. Khalyavin and Z. Hiroi, Phys. Rev. B **95** (2017) 214415(1-10).

5. *Spin dynamics in the high-field phases of volborthite: M. Yoshida, K. Nawa, H. Ishikawa, M. Takigawa, M. Jeong, S. Krämer, M. Horvatic, C. Berthier, K. Matsui, T. Goto, S. Kimura, T. Sasaki, J. Yamaura, H. Yoshida, Y. Okamoto and Z. Hiroi, Phys. Rev. B **96** (2017) 180413(R)(1-5).

6. Successive spatial symmetry breaking under high pressure in the spin-orbit-coupled metal $Cd_2Re_2O_7$: J.-I. Yamaura, K. Takeda, Y. Ikeda, N. Hirao, Y. Ohishi, T. C. Kobayashi and Z. Hiroi, Phys. Rev. B **95** (2017) 020102(1-5).

7. *Weak ferromagnetic order breaking the threefold rotational symmetry of the underlying kagome lattice in $CdCu_3(OH)_6(NO_3)_2{\cdot}H_2O$: R. Okuma, T. Yajima, D. Nishio-Hamane, T. Okubo and Z. Hiroi, Phys. Rev. B **95** (2017) 094427(1-8).

8. *Classical Spin Nematic Transition in $LiGa_{0.95}In_{0.05}Cr_4O_8$: R. Wawrzynczak, Y. Tanaka, M. Yoshida, Y. Okamoto, P. Manuel, N. Casati, Z. Hiroi, M. Takigawa and G. J. Nilsen, Phys. Rev. Lett. **119** (2017) 087201(1-6).

9. †*Pressure-induced Freeze Concentration of Alanine Aqueous Solution as a Novel Field of Chemical Reaction: S. Takahashi, H. Kagi, C. Fujimoto, A. Shinozaki, H. Gotou, T. Nishida and K. Mimura, Chem. Lett. **46** (2017) 334-337.

10. *Topochemical Crystal Transformation from a Distorted to a Nearly Perfect Kagome Cuprate: H. Ishikawa, T. Yajima, A. Miyake, M. Tokunaga, A. Matsuo, K. Kindo and Z. Hiroi, Chem. Mater. **29** (2017) 6719-6725.

11. *Large anomalous Nernst effect at room temperature in a chiral antiferromagnet: M. Ikhlas, T. Tomita, T. Koretsune, M.-T. Suzuki, D. Nishio-Hamane, R. Arita, Y. Otani and S. Nakatsuji, Nature Phys. **13** (2017) 1085-1090.

12. †*Hydrogenation of iron in the early stage of Earth's evolution: R. Iizuka-Oku, T. Yagi, H. Gotou, T. Okuchi, T. Hattori and A. Sano-Furukawa, Nat. Commun. **8** (2017) 14096(1-7).

13. Robust ferromagnetism carried by antiferromagnetic domain walls: H. T. Hirose, J.-I. Yamaura and Z. Hiroi, Sci. Rep. **7** (2017) 42440(1-7).

14. *Iyoite, $MnCuCl(OH)_3$ and misakiite, $Cu_3Mn(OH)_6Cl_2$: new members of the atacamite family from Sadamisaki Peninsula, Ehime Prefecture, Japan: D. Nishio–hamane, K. Momma, M. Ohnishi, N. Shimobayashi, R. Miyawaki, N. Tomita, R. Okuma, A. R. Kampf and T. Minakawa, Mineral. Mag. **81** (2017) 485-498.

15. †*High Pressure Experiments on Metal-Silicate Partitioning of Chlorine in a Magma Ocean: Implications for Terrestrial Chlorine Depletion: H. Kuwahara, H. Gotou, T. Shinmei, N. Ogawa, A. Yamaguchi, N. Takahata, Y. Sano, T. Yagi and S. Sugita, Geochem. Geophys. Geosyst. **18** (2017) 3929-3945.

16. *High-pressure synthesis of tetragonal iron aluminide $FeAl_2$: K. Tobita, N. Sato, Y. Katsura, K. Kitahara, D. Nishio-Hamane, H. Gotou and K. Kimura, Scr. Mater. **141** (2017) 107-110.

17. *Experimental and Theoretical Studies of the Metallic Conductivity in Cubic $PbVO_3$ under High Pressure: K. Oka, T. Yamauchi, S. Kanungo, T. Shimazu, K. Oh-ishi, Y. Uwatoko, M. Azuma and T. Saha-Dasgupta, J. Phys. Soc. Jpn. **87** (2018) 024801(1-6).

18. †*Improvement of coercivity in Nd-Fe-B nanocomposite magnets: T. Saito, S. Nozaki and D. Nishio-Hamane, J. Magn. Magn. Mater. **445** (2018) 49-52.

19. *Devil's staircase of odd-number charge order modulations in divalent β-vanadium bronzes under pressure: T. Yamauchi, H. Ueda, K. Ohwada, H. Nakao and Y. Ueda, Phys. Rev. B **97** (2018) 125138.

20. *Magnetic state selected by magnetic dipole interaction in the kagome antiferromagnet $NaBa_2Mn_3F_{11}$: S. Hayashida, H. Ishikawa, Y. Okamoto, T. Okubo, Z. Hiroi, M. Avdeev, P. Manuel, M. Hagihala, M. Soda and T. Masuda, Phys. Rev. B **97** (2018) 054411(1-7).

21. †*High-coercivity $SmCo_5$/α-Fe nanocomposite magnets: T. Saito and D. Nishio-Hamane, J. Alloys Compd. **735** (2018) 218-223.

22. Expanding frontiers in materials chemistry and physics with multiple anions: H. Kageyama, K. Hayashi, K. Maeda, J. Paul Attfield, Z. Hiroi, J. M. Rondinelli and K. R. Poeppelmeier, Nat. Commun. **9** (2018) 772(1-15).

23. †*Quantum valence criticality in a correlated metal: K. Kuga, Y. Matsumoto, M. Okawa, S. Suzuki, T. Tomita, K. Sone, Y. Shimura, T. Sakakibara, D. Nishio-Hamane, Y. Karaki, Y. Takata, M. Matsunami, R. Eguchi, M. Taguchi, A. Chainani, S. Shin, K. Tamasaku, Y. Nishino, M. Yabashi, T. Ishikawa and S. Nakatsuji, Sci. Adv. **4** (2018) eaao3547 (1-6).

* Joint research among groups within ISSP.

24. †*Size-controllable gold nanoparticles prepared from immobilized gold-containing ionic liquids on SBA-15: E. N. Kusumawati, D. Nishio-Hamane and T. Sasaki, Catalysis Today (2017) S0920586117306193, accepted for publication.

25. *Transmission electron microscopy study of the epitaxial association of hedenbergite whiskers with babingtonite: M. Nagashima and D. Nishio-Hamane, Mineral. Mag. (2018) 1, accepted for publication.

Kawashima group

We have been investigating quantum spin/boson systems and frustrated systems by means of large-scale numerical simulation. We also develop new numerical techniques. Our group's activities of 2017 include: (1) numerical simulation of weak-first order phase transition, (2) tensor-network calculation of the frustrated magnet on the star-lattice, (3) development of methods of computing high-order magnetic moments, and (4) tensor-network calculation of spin-orbit coupled systems.

1. Ground state properties of Na2IrO3 determined from ab initio Hamiltonian and its extensions containing Kitaev and extended Heisenberg interactions: T. Okubo, K. Shinjo, Y. Yamaji, N. Kawashima, S. Sota, T. Tohyama and M. Imada, Phys. Rev. B **96** (2017) 054434(1-12).

2. Proposal of a spin-one chain model with competing dimer and trimer interactions: Y.-T. Oh, H. Katsura, H.-Y. Lee and J. H. Han, Phys. Rev. B **96** (2017) 165126(1-8).

3. Resonating valence bond states with trimer motifs: H. Lee, Y.-T. Oh, J. H. Han and H. Katsura, Phys. Rev. B **95** (2017) 060413(1-4).

4. Variational Monte Carlo method for fermionic models combined with tensor networks and applications to the hole-doped two-dimensional Hubbard model: H.-H. Zhao, K. Ido, S. Morita and M. Imada, Phys. Rev. B **96** (2017) 085103(1-16).

5. Weak ferromagnetic order breaking the threefold rotational symmetry of the underlying kagome lattice in CdCu3(OH)6(NO3)2 · H2O: R. Okuma, T. Yajima, D. Nishio-Hamane, T. Okubo and Z. Hiroi, Phys. Rev. B **95** (2017) 094427(1-8).

6. Quantum lattice model solver *H*Φ: M. Kawamura, K. Yoshimi, T. Misawa, Y. Yamaji, S. Todo and N. Kawashima, Computer Physics Communications **217** (2017) 180-192.

7. Disordered quantum spin chains with long-range antiferromagnetic interactions: N. Moure, H.-Y. Lee, S. Haas, R. N. Bhatt and S. Kettemann, Phys. Rev. B **97** (2018) 014206(1-6).

8. Spin-one bilinear-biquadratic model on a star lattice: H.-Y. Lee* and N. Kawashima, Phys. Rev. B **97** (2018) 205123 (1-7).

9. Tensor renormalization group with randomized singular value decomposition: S. Morita, R. Igarashi, H.-H. Zhao and N. Kawashima, Phys. Rev. E **97** (2018) 033310(1-6).

10. †*Polymer effects on Kármán vortex: Molecular dynamics study: Y. Asano, H. Watanabe and H. Noguchi, The Journal of Chemical Physics **148** (2018) 144901.

Uwatoko group

We report the effect of hydrostatic pressure on the electronic state of the antiferromagnet UIrGe, which is isostructural and isoelectronic with the ferromagnetic superconductors UCoGe and URhGe. We constructed a p–T phase diagram and estimated the critical pressure pc, where the antiferromagnetism vanishes, as ~12 GPa. Electrical resistivity measurements have been performed on the iron-based ladder compounds $Ba_{1-x}Cs_xFe_2Se_3$ (x = 0, 0.25, 0.65, and 1) under high pressure. Metallic behavior of the electrical conductivity was confirmed in the x = 0.25 and 0.65 samples for pressures greater than 11.3 and 14.4 GPa, respectively, with the low-temperature log T upturn being consistent with weak localization of 2D electrons due to random potential. No metallic conductivity was observed in the parent compounds $BaFe_2Se_3$ (x = 0) up to 30.0 GPa and $CsFe_2Se_3$ (x = 1) up to 17.0 GPa. We report pressure-driven superconductivity (SC) in the vicinity of a commensurate charge-density wave (CCDW) in transition-metal dichalcogenides (TMDs) 1T−TaSe2 by simultaneous resistivity and ac susceptibility. The findings reveal the interplay of CCDW and SC in 1T−$TaSe_2$ by a clean method, viz., high pressure, and shed light on the underlying superconducting mechanism in the relevant systems. We study the properties of electronic structure in the high-Tc phase induced by pressure in bulk FeSe from magnetotransport measurements and first-principles calculations. These results in FeSe highlight similarities with high-Tc phases of iron pnictides, constituting a step toward a unified understanding of iron-based superconductivity. The origin of the highly anisotropic superconducting transition in $ZrTe_3$, where the resistance along the a axis, R_a , is reduced at 4 K but those along the b axis, R_b, and c' axis, $R_{c'}$, are reduced at 2 K, was explored with the application of a magnetic field and pressure by the electrical resistance measurements. The reduction in Ra is due to filamentary supercon-

† Joint research with outside partners.

ductivity (SC) induced by locally bound electron pairs (local pairs), which correspond to bi-polarons, and the transition of R_b corresponds to the emergence of bulk SC originating from the Cooper pairs triggered by the transfer of the local pairs. We have studied the temperature-pressure phase diagram of two materials $Eu_{3-x}Sr_xBi_2S_4F_4$ (x = 1 and x = 2) by electrical resistivity and magnetic measurements down to 2 K. Using the Arrhenius equation, we estimate the thermally activated flux flow activation energy U 0 as 116 K in $Eu_2SrBi_2S_4F_4$ and 39 K in $EuSr_2Bi_2S_4F_4$. At 2 K, DC magnetic susceptibility measurements indicate S-type paramagnetic behavior. We construct the three-dimensional electronic phase diagram, temperature (T) against pressure (P) and isovalent S-substitution (x), for $FeSe_{1-x}S_x$. The completed phase diagram uncovers that high-T_c superconductivity lies near both ends of the dome-shaped antiferromagnetic phase, whereas T_c remains low near the nematic critical point.

1. †Effect of Pressure on Magnetism of UIrGe: J. Pospisil, J. Gouchi, Y. Haga, F. Honda, Y. Uwatoko, N. Tateiwa, S. Kambe, S. Nagasaki, Y. Homma and E. Yamamoto, J. Phys. Soc. Jpn. **86** (2017) 044709(1-6).

2. †Pressure-Induced Metallization in Iron-Based Ladder Compounds $Ba_{1-x}Cs_xFe_2Se_3$: T. Hawai, C. Kawashima, K. Ohgushi, K. Matsubayashi, Y. Nambu, Y. Uwatoko, T. J. Sato and H. Takahashi, J. Phys. Soc. Jpn. **86** (2017) 024701 (1-4).

3. †Synchrotron X-ray Diffraction and High-Pressure Electrical Resistivity Studies for High T_c Candidate $Nd_{3.5}Sm_{0.5}Ni_3O_8$: M. Uehara, K. Kobayashi, H. Yamamoto, A. Nakata, K. Wakiya, I. Umehara, J. Gouchi and Y. Uwatoko, J. Phys. Soc. Jpn. **86** (2017) 114605(1-6).

4. †Unique Pressure versus Temperature Phase Diagram for Antiferromagnets $Eu_2Ni_3Ge_5$ and $EuRhSi_3$: M. Nakashima, Y. Amako, K. Matsubayashi, Y. Uwatoko, M. Nada, K. Sugiyama, M. Hagiwara, Y. Haga, T. Takeuchi, A. Nakamura, H. Akamine, K. Tomori, T. Yara, Y. Ashitomi, M. Hedo, T. Nakama and Y. Onuki, J. Phys. Soc. Jpn. **86** (2017) 034708 (1-13).

5. Weak Ferromagnetic Response of d Electrons and Antiferromagnetic Response of π Electrons in $TPP[Mn(Pc)(CN)_2]_2$ in Torque Magnetometry Experiments: K. Torizuka, Y. Uwatoko, M. Matsuda, G. Yoshida, M. Kimata and H. Tajima, J. Phys. Soc. Jpn. **86** (2017) 114709(1-9).

6. Evidence for pressure-induced node-pair annihilation in Cd_3As_2: C. Zhang, J. Sun, F. Liu, A. Narayan, N. Li, X. Yuan, Y. Liu, J. Dai, Y. Long, Y. Uwatoko, J. Shen, S. Sanvito, W. Yang, J. Cheng and F. Xiu, Phys. Rev. B **96** (2017) 155205 (1-7).

7. Pressure-induced bulk superconductivity in a layered transition-metal dichalcogenide 1T-tantalum selenium: B. Wang, Y. Liu, K. Ishigaki, K. Matsubayashi, J. Cheng, W. Lu, Y. Sun and Y. Uwatoko, Phys. Rev. B **95** (2017) 220501(1-6).

8. †*Two-carrier analyses of the transport properties of black phosphorus under pressure: K. Akiba, A. Miyake, Y. Akahama, K. Matsubayashi, Y. Uwatoko and M. Tokunaga, Phys. Rev. B **95** (2017) 115126(1-7).

9. High-T_c Superconductivity in FeSe at High Pressure: Dominant Hole Carriers and Enhanced Spin Fluctuations: J. P. Sun, G. Z. Ye, P. Shahi, J. -Q. Yan, K. Matsuura, H. Kontani, G. M. Zhang, Q. Zhou, B. C. Sales, T. Shibauchi, Y. Uwatoko, D. J. Singh and J. -G. Cheng, Phys. Rev. Lett. **118** (2017) 147004(1-6).

10. Superconductivity induced by external pressure in $Eu_{3-x}Sr_xBi_2S_4F_4$ (x= 1, 2) compounds: M. Kannan, G. K. Selvan, Z. Haque, G. S. Thakur, B. Wang, K. Ishigaki, Y. Uwatoko, L. C. Gupta, A. K. Ganguli and S. Arumugam, Supercond. Sci. Technol. **30** (2017) 115011(1-7).

11. Effects of pressure and magnetic field on superconductivity in $ZrTe_3$: local pair-induced superconductivity: S. Tsuchiya, K. Matsubayashi, K. Yamaya, S. Takayanagi, S. Tanda and Y. Uwatoko, New J. Phys. **19** (2017) 063004(1-10).

12. †Superconducting, Fermi surface, and magnetic properties in $SrTGe_3$ and $EuTGe_3$ (T: transition metal) with the Rashba-type tetragonal structure: M. Kakihana, H. Akamine, K. Tomori, K. Nishimura, A. Teruya, A. Nakamura, F. Honda, D. Aoki, M. Nakashima, Y. Amako, K. Matsubayashi, Y. Uwatoko, T. Takeuchi, T. Kida, M. Hagiwara, Y. Haga, E. Yamamoto, H. Harima, M. Hedo, T. Nakama and Y. Onuki, J. Alloys Compd. **694** (2017) 439-451.

13. Pressure-Induced Charge-Order Melting and Reentrant Charge Carrier Localization in the Mixed-Valent $Pb_3Rh_7O_{15}$: Y. Li, Z. Sun, J.-W. Cai, J.-P. Sun, B.-S. Wang, Z.-Y. Zhao, Y. Uwatoko, J.-Q. Yan and J.-G. Cheng, Chin. Phys. Lett. **34** (2017) 087201.

14. †Thermal Transformation Arrest Phenomena in $Mn_2Sb_{0.9}Sn_{0.1}$: T. Wakamori, Y. Mitsui, K. Takahashi, R. Y. Umetsu, Y. Uwatoko, M. Hiroi and K. Koyama, IEEE Magn. Lett. **8** (2017) 1402404(1-4).

15. †Maximizing T_c by tuning nematicity and magnetism in $FeSe_{1-x}S_x$ superconductors: K. Matsuura, Y. Mizukami, Y. Arai, Y. Sugimura, N. Maejima, A. Machida, T. Watanuki, T. Fukuda, T. Yajima, Z. Hiroi, K. Y. Yip, Y. C. Chan, Q. Niu, S. Hosoi, K. Ishida, K. Mukasa, S. Kasahara, J. -G. Cheng, S. K. Goh, Y. Matsuda, Y. Uwatoko and T. Shibauchi, Nat. Commun. **8** (2017) 1143(1-6).

* Joint research among groups within ISSP.

16. *Unique Electronic States in Non-centrosymmetric Cubic Compounds: M. Kakihana, K. Nishimura, Y. Ashitomi, T. Yara, D. Aoki, A. Nakamura, F. Honda, M. Nakashima, Y. Amako, Y. Uwatoko, T. Sakakibara, S. Nakamura, T. Takeuchi, Y. Haga, E. Yamamoto, H. Harima, M. Hedo, T. Nakama and Y. Onuki, J. Electron. Mater. **46** (2017) 3572-3586.

17. Possibility for conventional superconductivity in $Sr_{0.1}Bi_2Se_3$ from high-pressure transport studies: K. Manikandan, Shruti, P. Neha, G. Kalai Selvan, B. Wang, Y. Uwatoko, K. Ishigaki, R. Jha, V. P. S. Awana, S. Arumugam and S. Patnaik, EPL **118** (2017) 47008(1-6).

18. †Emergence of a new valence-ordered structure and collapse of the magnetic order under high pressure in EuPtP: A. Mitsuda, S. Manabe, M. Umeda, H. Wada, K. Matsubayashi, Y. Uwatoko, M. Mizumaki, N. Kawamura, K. Nitta, N. Hirao, Y. Ohishi and N. Ishimatsu, J. Phys.: Condens. Matter **30** (2018) 105603(1-8).

19. Magnetic order of Nd_5Pb_3 single crystals: J.-Q. Yan, M. Ochi, H. B. Cao, B. Saparov, J.-G. Cheng, Y. Uwatoko, R. Arita, B. C. Sales and D. G. Mandrus, J. Phys.: Condens. Matter **30** (2018) 135801(1-9).

20. Direct Observation of the Quantum Phase Transition of $SrCu_2(BO_3)_2$ by High-Pressure and Terahertz Electron Spin Resonance: T. Sakurai, Y. Hirao, K. Hijii, S. Okubo, H. Ohta, Y. Uwatoko, K. Kudo and Y. Koike, J. Phys. Soc. Jpn. **87** (2018) 033701(1-4).

21. Electronic States in $EuCu_2(Ge_{1-x}Si_x)_2$ Based on the Doniach Phase Diagram: W. Iha, T. Yara, Y. Ashitomi, M. Kakihana, T. Takeuchi, F. Honda, A. Nakamura, D. Aoki, J. Gouchi, Y. Uwatoko, T. Kida, T. Tahara, M. Hagiwara, Y. Haga, M. Hedo, T. Nakama and Y. Onuki, J. Phys. Soc. Jpn. **87** (2018) 064706(1-14).

22. *Experimental and Theoretical Studies of the Metallic Conductivity in Cubic $PbVO_3$ under High Pressure: K. Oka, T. Yamauchi, S. Kanungo, T. Shimazu, K. Oh-ishi, Y. Uwatoko, M. Azuma and T. Saha-Dasgupta, J. Phys. Soc. Jpn. **87** (2018) 024801(1-6).

23. †Pressure Effect on Magnetic Properties of Weak Itinerant Electron Ferromagnet CrAlGe: S. Yoshinaga, Y. Mitsui, R. Y. Umetsu, Y. Uwatoko and K. Koyama, J. Phys. Soc. Jpn. **87** (2018) 014701(1-4).

24. High-T_c superconductivity up to 55 K under high pressure in a heavily electron doped $Li_{0.36}(NH_3)_yFe_2Se_2$ single crystal: P. Shahi, J. P. Sun, S. H. Wang, Y. Y. Jiao, K. Y. Chen, S. S. Sun, H. C. Lei, Y. Uwatoko, B. S. Wang and J. -G. Cheng, Phys. Rev. B **97** (2018) 020508(1-6).

25. Pressure effect on the magnetic properties of the half-metallic Heusler alloy Co_2TiSn: I. Shigeta, Y. Fujimoto, R. Ooka, Y. Nishisako, M. Tsujikawa, R. Y. Umetsu, A. Nomura, K. Yubuta, Y. Miura, T. Kanomata, M. Shirai, J. Gouchi, Y. Uwatoko and M. Hiroi, Phys. Rev. B **97** (2018) 104414(1-8).

26. *Pressure-induced quantum phase transition in the quantum antiferromagnet $CsFeCl_3$: S. Hayashida, O. Zaharko, N. Kurita, H. Tanaka, M. Hagihala, M. Soda, S. Itoh, Y. Uwatoko and T. Masuda, Phys. Rev. B **97** (2018) 140405(1-4).

27. †Magnetic Phase Transition of $Mn_{1.9}Fe_{0.1}Sb_{0.9}Sn_{0.1}$: A. N. Nwodo, R. Kobayashi, T. Wakamori, Y. Matsumoto, Y. Mitsui, R. Y. Umetsu, M. Hiroi, K. Takahashi, Y. Uwatoko and K. Koyama, IEEE Magn. Lett. **9** (2018) 1(1-4).

28. †Quasi-First Order Magnetic Transition in $Mn_{1.9}Fe_{0.1}Sb_{0.9}Sn_{0.1}$: A. N. Nwodo, R. Kobayashi, T. Wakamori, Y. Matsumoto, Y. Mitsui, M. Hiroi, K. Takahashi, R. Y. Umetsu, Y. Uwatoko and K. Koyama, Mater. Trans. **59** (2018) 348-352.

29. Magnetic and thermodynamic properties of Heusler alloys $Ni_{55}Mn_{26}Al_{19}$: M. Ito, K. Onda, A. Taira, K. Sonoda, M. Hiroi and Y. Uwatoko, AIP Advances **8** (2018) 055712.

30. Reemergence of high-T_c superconductivity in the $(Li_{1-x}Fe_x)OHFe_{1-y}Se$ under high pressure: J. P. Sun, P. Shahi, H. X. Zhou, Y. L. Huang, K. Y. Chen, B. S. Wang, S. L. Ni, N. N. Li, K. Zhang, W. G. Yang, Y. Uwatoko, G. Xing, J. Sun, D. J. Singh, K. Jin, F. Zhou, G. M. Zhang, X. L. Dong, Z. X. Zhao and J. -G. Cheng, Nat. Commun. **9** (2018) 380(1-7).

31. Anisotropic lattice compression of α- and β-CePdZn: G. Oomi, T. Eto, T. Okada and Y. Uwatoko, Physica B: Condensed Matter **536** (2018) 293.

32. Fundamental properties of a new samarium compound $SmPtSi_2$: S. Yamaguchi, E. Takahashi, N. Kase, T. Nakano, N. Takeda, K. Matsubayashi and Y. Uwatoko, Physica B: Condensed Matter **536** (2018) 297-299.

33. Magnetic characteristics of polymorphic single crystal compounds $DyIr_2Si_2$: K. Uchima, T. Shigeoka and Y. Uwatoko, Physica B: Condensed Matter **536** (2018) 28.

34. Magnetic properties and effect of pressure on the electronic state of $EuCo_2Ge_2$: Y. Ashitomi, M. Kakihana, F. Honda, A. Nakamura, D. Aoki, Y. Uwatoko, M. Nakashima, Y. Amako, T. Takeuchi, T. Kida, T. Tahara, M. Hagiwara, Y. Haga, M. Hedo, T. Nakama and Y. Onuki, Physica B: Condensed Matter **536** (2018) 192196.

† Joint research with outside partners.

35. Magnetic properties of new antiferromagnetic heavy-fermion compounds, Ce_3TiBi_5 and $CeTi_3Bi_4$: G. Motoyama, M. Sezaki, J. Gouchi, K. Miyoshi, S. Nishigori, T. Mutou, K. Fujiwara and Y. Uwatoko, Physica B: Condensed Matter **536** (2018) 142-144.

36. Pressure effects on the magnetic and transport properties of the Kondo lattice system Ce_3RuSn_6: K. Wakiya, T. Tomaki, M. Kimura, M. Uehara, J. Gouchi, Y. Uwatoko and I. Umehara, Physica B: Condensed Matter **536** (2018) 492-493.

37. Successive magnetic transitions of the pseudo-ternary compounds $Ho_{1-x}R_xRh_2Si_2$(R=Y, La): T. Shigeoka, K. Uchima and Y. Uwatoko, Physica B: Condensed Matter **536** (2018) 379-383.

38. Pressure-induced coherent sliding-layer transition in the excitonic insulator Ta_2NiSe_5: A. Nakano, K. Sugawara, S. Tamura, N. Katayama, K. Matsubayashi, T. Okada, Y. Uwatoko, K. Munakata, A. Nakao, H. Sagayama, R. Kumai, K. Sugimoto, N. Maejima, A. Machida, T. Watanuki and H. Sawa, IUCrJ **5** (2018) 158-165.

39. Magnetic and structural properties of $Mn_{1-x}Cr_xAlGe$ ($0< x < 1.0$): H. Masumitsu, S. Yoshinaga, Y. Mitsui, R. Y. Umetsu, M. Hiroi, Y. Uwatoko and K. Koyama, Journal of Magnetism and Magnetic Materials **456** (2018) 104-107.

40. Magnetic relaxation dynamics in thermally arrested Cr-modified Mn_2Sb: Y. Mitsui, Y. Matsumoto, Y. Uwatoko, M. Hiroi and K. Koyama, Journal of Magnetism and Magnetic Materials **461** (2018) 62-68.

41. The formation of bulk β-Al_3 Ni phase in eutectic Al-5.69wt%Ni alloy solidified under high pressure: X. H. Wang, Z. Ran, Z. J. Wei, C. M. Zou, H. W. Wang, J. Gouchi and Y. Uwatoko, Journal of Alloys and Compounds **742** (2018) 670-675.

Ozaki group

Motivated by the post-K computer project where the machine is expected to consist of about 10 million CPU cores, we have tried to develop efficient and accurate O(N) methods whose computational cost is proportional to the number of atoms, while so far we have already developed an O(N) Krylov subspace and applied the method to a wide variety of problems. A missing ingredient in the O(N) Krylov subspace method is that the method neglects the effect of outer region beyond the truncated cluster. To take account of the effect of outer region beyond the truncated cluster, we have introduced the self-energy correction, which is derived from a block formalism for the inverse calculation of a matrix, to evaluation of local Green's function and performed a series of benchmark calculations. Though the method is theoretically appealing, it turns out that the method is numerically very unstable in the process for the self-consistent calculation of local Green's functions. The analysis implies that the Green's functions near the real axis are highly delocalized for systems with metallic bands or denser structures, resulting in the numerical instability. After getting the negative result, we have taken another direction for development of efficient and accurate O(N) methods, and considered how the size of truncated cluster can be enlarged without largely increasing the numerical cost. Our idea is based on a coarse graining of basis functions which are located in the buffer region of the truncated cluster. To perform the coarse graining, we have developed a novel method to generate localized natural orbitals based on Schur decomposition, and replaced the original basis functions in the buffer region by the localized natural orbitals. A series of benchmark calculations suggests that the O(N) method is a stable and accurate method for not only insulators but also metals. We have further introduced a multi-level parallelization where atoms, spin, and eigenvalue problem for the truncated cluster are fully parallelized by MPI. We expect that the parallelized code for the novel method enables us to perform first-principles molecular dynamics simulations of large-scale systems consisting of ten thousand atoms by making full use of the post-K computer.

1. Single-particle excitation of core states in epitaxial silicene: C.-C. Lee, J. Yoshinobu, K. Mukai, S. Yoshimoto, H. Ueda, R. Friedlein, A. Fleurence, Y. Yamada-Takamura and T. Ozaki, Phys. Rev. B **95** (2017) 115437(1-7).

2. Thermoelectric properties of high power factor sulfide NiSbS and Co substitution system $Ni_{1-x}Co_xSbS$: M. Miyata, T. Ozaki, S. Nishino and M. Koyano, Jpn. J. Appl. Phys. **56** (2017) 021801(1-6).

3. Absolute Binding Energies of Core Levels in Solids from First Principles: T. Ozaki and C.-C. Lee, Phys. Rev. Lett. **118** (2017) 026401(1-5).

4. 低次スケーリング手法の開発とその応用：尾崎 泰助，澤田 英明，固体物理特集号 **621** (2017) 593.

5. 密度汎関数理論による内殻電子束縛エネルギーの第一原理計算：尾崎 泰助，固体物理特集号 **621** (2017) 604.

6. Transition of the Interface between Iron and Carbide Precipitate From Coherent to Semi-Coherent: H. Sawada, S. Taniguchi, K. Kawakami and T. Ozaki, Metals **7** (2017) 277(1-13).

7. Chemical misfit origin of solute strengthening in iron alloys: M. Wakeda, T. Tsuru, M. Kohyama, T. Ozaki, H. Sawada, M. Itakura and S. Ogata, Acta Mater. **131** (2017) 445-456.

---

* Joint research among groups within ISSP.

8. *Peculiar bonding associated with atomic doping and hidden honeycombs in borophene: C.-C. Lee, B. Feng, M. D'angelo, R. Yukawa, R.-Y. Liu, T. Kondo, H. Kumigashira, I. Matsuda and T. Ozaki, Phys. Rev. B **97** (2018) 075430 (1-5).

9. Reliability and applicability of magnetic-force linear response theory: Numerical parameters, predictability, and orbital resolution: H. Yoon, T. J. Kim, J. -H. Sim, S. W. Jang, T. Ozaki and M. J. Han, Phys. Rev. B **97** (2018) 125132.

10. Li deposition and desolvation with electron transfer at a silicon/propylene-carbonate interface: transition-state and free-energy profiles by large-scale first-principles molecular dynamics: T. Ohwaki, T. Ozaki, Y. Okuno, T. Ikeshoji, H. Imai and M. Otani, Phys. Chem. Chem. Phys. **20** (2018) 11586.

11. High-Throughput Screening of Sulfide Thermoelectric Materials Using Electron Transport Calculations with OpenMX and BoltzTraP: M. Miyata, T. Ozaki, T. Takeuchi, S. Nishino, M. Inukai and M. Koyano, Journal of Elec Materi **47** (2018) 3254.

12. 2 次元材料の電子状態解析 - シリセン研究における実験と計算の協奏 -: 高村（ 山田）由起子 , 尾崎 泰助 , 応用物理学会誌 **86** (2017) 488.

13. 計算科学のための HPC 技術2: 下司雅章 編／南一生 , 高橋 大介 , 尾崎 泰助 , 安藤 嘉倫 , 小林 正人 , 成瀬 彰 , 黒澤一平 著 , (大阪大学出版会 , 大阪府吹田市山田丘 2-7 大阪大学ウエストフロント , 2017).

Noguchi group

We have studied the membrane shape transformations by proteins and chemical reactions. (1) Two types of banana-shaped proteins assembled into striped bumps that surpress membrane tubulation. (2) The tubulation is promoted by laterally isotropic membrane inclusions that generate the same sign of spontaneous curvature as the adsorbed protein rods while it is surpressed in the case of the opposite sign. (3) Asymmetric chemical reactions between the inner and outer leaflets of a vesicle induces bilayer sheet protrusion and budding. The probabilities of these two types of transformations depend on the shear viscosity of the surrounding fluids compared to the membrane as well as the reaction rates.

1. Acceleration and suppression of banana-shaped-protein-induced tubulation by addition of small membrane inclusions of isotropic spontaneous curvatures: H. Noguchi, Soft Matter **13** (2017) 7771-7779.

2. Membrane structure formation induced by two types of banana-shaped proteins: H. Noguchi and J.-B. Fournier, Soft Matter **13** (2017) 4099-4011.

3. 分子シミュレーションにおける三体ポテンシャルを含んだ系の局所応力テンソルの非一意性 : 中川 恒 , 分子シミュレーション研究会会誌 “アンサンブル ” **19** (2017) 69.

4. 短距離古典分子動力学シミュレーションコードの GPGPU 化（1）: 中川 恒 , 分子シミュレーション研究会会誌 “アンサンブル ” **19** (2017) 267-273.

5. Docosahexaenoic acid preserves visual function by maintaining correct disc morphology in retinal photoreceptor cells: H. Shindou, H. Koso, J. Sasaki, H. Nakanishi, H. Sagara, K. M. Nakagawa, Y. Takahashi, D. Hishikawa, Y. Iizuka-Hishikawa, F. Tokumasu, H. Noguchi, S. Watanabe, T. Sasaki and T. Shimizu, J. Biol. Chem. **292** (2017) 12054-12064.

6. Bilayer sheet protrusions and budding from bilayer membranes induced by hydrolysis and condensation reactions: K. M. Nakagawa and H. Noguchi, Soft Matter **14** (2018) 1397-1407.

7. 短距離古典分子動力学シミュレーションコードの GPGPU 化（2）: 中川 恒 , 分子シミュレーション研究会会誌 “アンサンブル ” **20** (2018) 40-45.

8. †*Polymer effects on Kármán vortex: Molecular dynamics study: Y. Asano, H. Watanabe and H. Noguchi, The Journal of Chemical Physics **148** (2018) 144901.

Materials Synthesis and Characterization group

1. *Weak ferromagnetic order breaking the threefold rotational symmetry of the underlying kagome lattice in $CdCu_3(OH)_6(NO_3)_2{\cdot}H_2O$: R. Okuma, T. Yajima, D. Nishio-Hamane, T. Okubo and Z. Hiroi, Phys. Rev. B **95** (2017) 094427(1-8).

2. †*Pressure-induced Freeze Concentration of Alanine Aqueous Solution as a Novel Field of Chemical Reaction: S. Takahashi, H. Kagi, C. Fujimoto, A. Shinozaki, H. Gotou, T. Nishida and K. Mimura, Chem. Lett. **46** (2017) 334-337.

† Joint research with outside partners.

3. *Large anomalous Nernst effect at room temperature in a chiral antiferromagnet: M. Ikhlas, T. Tomita, T. Koretsune, M.-T. Suzuki, D. Nishio-Hamane, R. Arita, Y. Otani and S. Nakatsuji, Nature Phys. **13** (2017) 1085-1090.

4. †*Hydrogenation of iron in the early stage of Earth's evolution: R. Iizuka-Oku, T. Yagi, H. Gotou, T. Okuchi, T. Hattori and A. Sano-Furukawa, Nat. Commun. **8** (2017) 14096(1-7).

5. *Iyoite, $MnCuCl(OH)_3$ and misakiite, $Cu_3Mn(OH)_6Cl_2$: new members of the atacamite family from Sadamisaki Peninsula, Ehime Prefecture, Japan: D. Nishio–hamane, K. Momma, M. Ohnishi, N. Shimobayashi, R. Miyawaki, N. Tomita, R. Okuma, A. R. Kampf and T. Minakawa, Mineral. Mag. **81** (2017) 485-498.

6. †*High Pressure Experiments on Metal-Silicate Partitioning of Chlorine in a Magma Ocean: Implications for Terrestrial Chlorine Depletion: H. Kuwahara, H. Gotou, T. Shinmei, N. Ogawa, A. Yamaguchi, N. Takahata, Y. Sano, T. Yagi and S. Sugita, Geochem. Geophys. Geosyst. **18** (2017) 3929-3945.

7. *High-pressure synthesis of tetragonal iron aluminide $FeAl_2$: K. Tobita, N. Sato, Y. Katsura, K. Kitahara, D. Nishio-Hamane, H. Gotou and K. Kimura, Scr. Mater. **141** (2017) 107-110.

8. *Experimental and Theoretical Studies of the Metallic Conductivity in Cubic $PbVO_3$ under High Pressure: K. Oka, T. Yamauchi, S. Kanungo, T. Shimazu, K. Oh-ishi, Y. Uwatoko, M. Azuma and T. Saha-Dasgupta, J. Phys. Soc. Jpn. **87** (2018) 024801(1-6).

9. †*Improvement of coercivity in Nd-Fe-B nanocomposite magnets: T. Saito, S. Nozaki and D. Nishio-Hamane, J. Magn. Magn. Mater. **445** (2018) 49-52.

10. *Devil's staircase of odd-number charge order modulations in divalent β-vanadium bronzes under pressure: T. Yamauchi, H. Ueda, K. Ohwada, H. Nakao and Y. Ueda, Phys. Rev. B **97** (2018) 125138.

11. †*High-coercivity $SmCo_5$/α-Fe nanocomposite magnets: T. Saito and D. Nishio-Hamane, J. Alloys Compd. **735** (2018) 218-223.

12. †*Quantum valence criticality in a correlated metal: K. Kuga, Y. Matsumoto, M. Okawa, S. Suzuki, T. Tomita, K. Sone, Y. Shimura, T. Sakakibara, D. Nishio-Hamane, Y. Karaki, Y. Takata, M. Matsunami, R. Eguchi, M. Taguchi, A. Chainani, S. Shin, K. Tamasaku, Y. Nishino, M. Yabashi, T. Ishikawa and S. Nakatsuji, Sci. Adv. **4** (2018) eaao3547 (1-6).

13. †*Size-controllable gold nanoparticles prepared from immobilized gold-containing ionic liquids on SBA-15: E. N. Kusumawati, D. Nishio-Hamane and T. Sasaki, Catalysis Today (2017) S0920586117306193, accepted for publication.

14. *Transmission electron microscopy study of the epitaxial association of hedenbergite whiskers with babingtonite: M. Nagashima and D. Nishio-Hamane, Mineral. Mag. (2018) 1, accepted for publication.

Neutron Science Laboratory

Shibayama group

Shibayama group has been exploring the structure and dynamics of soft matter, especially polymer gels, micelles, thermo-responsive polymers, and thermosets, utilizing a combination of small-angle neutron scattering (SANS), small-angle X-ray scattering (SAXS), and dynamic light scattering (DLS). The objectives are to elucidate the relationship between the structure and variety of novel properties/functions of polymer gels/resins. The highlights of 2017 include investigation of (1) structural investigations of critical clusters and their biomedical applications, (2) probe diffusion of sol-gel transition in isorefractive indexed solvents, (3) solvated structure of cellulose in a phosphonate-based ionic liquid, (4) structure-mechanical property relationships in crosslinked phenolic resin, and (5) structural investigations of nonswellable thermoresponsive amphiphilic conetwork, and so on.

1. Experimental Observation of Two Features Unexpected from the Classical Theories of Rubber Elasticity: K. Nishi, K. Fujii, U.-I. Chung, M. Shibayama and T. Sakai, Phys. Rev. Lett. **119** (2017) 267801(1-6).

2. Structure-mechanical property relationships in crosslinked phenolic resin investigated by molecular dynamics simulation: Y. Shudo, A. Izumi, K. Hagita, T. Nakao and M. Shibayama, Polymer **116** (2017) 506-514.

3. Decisive test of the ideal behavior of tetra-PEG gels: F. Horkay, K. Nishi and M. Shibayama, J. Chem. Phys. **146** (2017) 164905(1-8).

* Joint research among groups within ISSP.

4. Structure and Rheology of Wormlike Micelles Formed by Fluorocarbon–Hydrocarbon-Type Hybrid Gemini Surfactant in Aqueous Solution: K. Morishima, S. Sugawara, T. Yoshimura and M. Shibayama, Langmuir **33** (2017) 6084-6091.

5. Mesoscopic Structural Aspects of Ca^{2+}-Triggered Polymer Chain Folding of a Tetraphenylethene-Appended Poly(acrylic acid) in Relation to Its Aggregation-Induced Emission Behavior: K. Morishima, F. Ishiwari, S. Matsumura, T. Fukushima and M. Shibayama, Macromolecules **50** (2017) 5940-5945.

6. Microscopic Structure of Solvated Poly(benzyl methacrylate) in an Imidazolium-Based Ionic Liquid: High-Energy X-ray Total Scattering and All-Atom MD Simulation Study: K. Fujii, T. Ueki, K. Hashimoto, Y. Kobayashi, Y. Kitazawa, K. Hirosawa, M. Matsugami, K. Ohara, M. Watanabe and M. Shibayama, Macromolecules **50** (2017) 4780-4786.

7. †Microscopic Structure of the "Nonswellable" Thermoresponsive Amphiphilic Conetwork: S. Nakagawa, X. Li, H. Kamata, T. Sakai, E. P. Gilbert and M. Shibayama, Macromolecules **50** (2017) 3388-3395.

8. Permeation of Water through Hydrogels with Controlled Network Structure: T. Fujiyabu, X. Li, M. Shibayama, U.-I. Chung and T. Sakai, Macromolecules **50** (2017) 9411-9416.

9. Probe Diffusion during Sol–Gel Transition of a Radical Polymerization System Using Isorefractive Dynamic Light Scattering: N. Watanabe, X. Li and M. Shibayama, Macromolecules **50** (2017) 9726-9733.

10. Probe Diffusion of Sol–Gel Transition in an Isorefractive Polymer Solution: X. Li, N. Watanabe, T. Sakai and M. Shibayama, Macromolecules **50** (2017) 2916-2922.

11. SANS Study on Critical Polymer Clusters of Tetra-Functional Polymers: X. Li, K. Hirosawa, T. Sakai, E. P. Gilbert and M. Shibayama, Macromolecules **50** (2017) 3655-3661.

12. Solvated Structure of Cellulose in a Phosphonate-Based Ionic Liquid: K. Hirosawa, K. Fujii, K. Hashimoto and M. Shibayama, Macromolecules **50** (2017) 6509-6517.

13. Exploration of Ideal Polymer Networks: M. Shibayama, Macromol. Symp **372** (2017) 7-13.

14. Effect of protonation on the solvation structure of solute N-butylamine in an aprotic ionic liquid: K. Hashimoto, K. Fujii, K. Ohara and M. Shibayama, Phys. Chem. Chem. Phys. **19** (2017) 8194-8200.

15. Effect of substrate concentrations on the aggregation behavior and dynamic oscillatory properties of self-oscillating block copolymers: R. Tamate, T. Ueki, M. Shibayama and R. Yoshida, Phys. Chem. Chem. Phys. **19** (2017) 20627-20634.

16. 2D pair distribution function analysis of anisotropic small-angle scattering patterns from elongated nano-composite hydrogels: K. Nishi and M. Shibayama, Soft Matter **13** (2017) 3076-3083.

17. Autonomous unimer-vesicle oscillation by totally synthetic diblock copolymers: effect of block length and polymer concentration on spatio-temporal structures: R. Tamate, T. Ueki, M. Shibayama and R. Yoshida, Soft Matter **13** (2017) 4559-4568.

18. Amoeba-like self-oscillating polymeric fluids with autonomous sol-gel transition: M. Onoda, T. Ueki, R. Tamate, M. Shibayama and R. Yoshida, Nat. Commun. **8** (2017) 15862(1-8).

19. Measurement of Particle Size Distribution in Turbid Solutions by Dynamic Light Scattering Microscopy: T. Hiroi and M. Shibayama, JoVE **119** (2017) 54885.

20. Fast-forming hydrogel with ultralow polymeric content as an artificial vitreous body: K. Hayashi, F. Okamoto, S. Hoshi, T. Katashima, D. C. Zujur, X. Li, M. Shibayama, E. P. Gilbert, U.-I. Chung, S. Ohba, T. Oshika and T. Sakai, Nat. Biomed. Eng. **1** (2017) 0044(1-7).

21. Structure of the Microemulsion of Polyglycerol Polyricinoleate Encapsulating Vitamin E: J. Matsuoka, T. Kusano, Y. Kasama, E. Tominaga, J. Kobayashi, W. Fujii, H. Iwase, M. Shibayama and H. Nanbu, J. Oleo Sci. **66** (2017) 1285-1291.

22. Gels: From Soft Matter to BioMatter: M. Shibayama, X. Li and T. Sakai, Ind. Eng. Chem. Res. **57** (2018) 1121-1128.

23. Soft Condensed Matter: M. Shibayama, in: *Experimental Methods in the Physical Science Volume 49 Neutron Scattering Applications in Chemistry, Materials Science and Biology*, Ch Chapter 8, edited by Fernandez-Alonso, F. and Price, D. L., (Academic Press, Cambridge MA, 2017), 459-546.

† Joint research with outside partners.

Yoshizawa group

A systematic study on a family of Ce-based non-centrosymmetric heavy fermion compounds $CeTSi_3$ (T=transition metal ions) was continued in 2017. It is found that a family of the $CeTSi_3$ compounds can be classified into three different crystalline electric field (CEF) level scheme groups. In order to elucidate megnetic properties from a microscopic basis, the CEF levels were reexamined for T= Rh and Ir compounds with use of inelastic neutron scattering (INS) measurements. The results disclosed that the previously reported CEF level schemes for $CeRhSi_3$ and $CeIrSi_3$ were not correct, and our INS study established the correct CEF schemes which can consistently explain other magnetic properties.

1. †Crystalline Electric Field Level Scheme of the Non- Centrosymmetric $CePtSi_3$: D. Ueta, T. Kobuke, M. Yoshida, H. Yoshizawa, Y. Ikeda, S. Itoh and T. Yokoo, Physica B **536** (2018) 21-23.

2. †Magnetic and Thermodynamic Studies on the Charge and Spin Ordering in the highly-doped $La_{2-x}Sr_xCoO_4$: M. Yoshida, D. Ueta, Y. Ikeda, T. Yokoo, S. Itoh and H. Yoshizawa, Physica B **536** (2018) 338-341.

3. †Anisotropic pressure effects on superconductivity in $Fe_{1+y}Te_{1-x}S_x$: K. Yamamoto, T. Yamazaki, T. Yamanaka, D. Ueta, H. Yoshizawa and H. Yaguchi, J. Phys. Soc. Jpn. **87** (2018) 054705.

Yamamuro group

Our laboratory is studying chemical physics of complex condensed matters by using neutron scattering, X-ray diffraction, calorimetric, dielectric, and viscoelastic techniques. Our target materials are glasses, liquids, and various disordered systems. Following to the synchrotron X-ray diffraction works of last year on the vapor-deposited glasses of carbon disulfide (CS_2), propane ($CH_3CH_2CH_3$) and propene (CH_3CHCH_2), their liquid states were measured as functions of temperature. We obtained the atomic pair distribution functions of these liquids and found that the orientational correlation between neighboring molecules steeply increases on cooling down to the glass transition temperature. This result clearly corresponds to the growth of the cooperatively rearranging region (CRR) determined by our previous calorimetric studies. Another topic is the quasielastic neutron scattering of alkylated tetraphenylporphirins (3,5-C_6C_{10}-TPP and 2,5-C_6C_{10}-TPP) whose liquid states are stabilized by the huge entropy due to the orientational disorder of alkylchains. Their molecular motions were reproduced well by the combination of the alkyl motions and the rotational and translational motions of whole molecules. Other than above topics, we have conducted neutron diffraction experiments of the nanoparticles of PdRuX (X = Pt, Rh, Ir) alloys. The analysis is now going on to investigate the atomic scale miscibility and local structure of the alloys.

1. Calorimetric and Neutron Scattering Studies on Glass Transitions and Ionic Diffusions in Imidazolium-based Ionic Liquids: O. Yamamuro and M. Kofu, Mat. Sci. Eng. **196** (2017) 012001(1-4).

2. †Relaxation in a Prototype Ionic Liquid: Influence of Water on the Dynamics: D. L. Price, O. Borodin, M. A. González, M. Kofu, K. Shibata, T. Yamada, O. Yamamuro and M.-L. Saboungi, J. Phys. Chem. Lett. **8** (2017) 715-719.

3. Neutron Scattering Studies on Short- and Long-range Layer Structures and Related Dynamics in Imidazolium-based Ionic Liquids: F. Nemoto, M. Kofu, M. Nagao, K. Ohishi, S. Takata, J. Suzuki, T. Yamada, K. Shibata, T. Ueki, Y. Kitazawa, M. Watanabe and O. Yamamuro, J. Chem. Phys. (2018), accepted for publication.

4. Vibrational states of atomic hydrogen in bulk and nanocrystalline palladium studied by neutron spectroscopy: M. Kofu, N. Hashimoto, H. Akiba, H. Kobayashi, H. Kitagawa, K. Iida, M. Nakamura and O. Yamamuro, Phys. Rev. B **96** (2017) 054304(1-7).

5. 熱測定と中性子散乱の相補利用による新規物質研究：山室 修 , 熱測定 **44(3)** (2017) 117-123.

6. ガラス転移温度：山室 修 ,「化学便覧基礎編改訂第 6 版」, 10.15, 日本化学会編 , (丸善出版 , 2017), accepted for publication.

Masuda group

The goal of our research is to discover a new quantum phenomenon and to reveal the mechanism of it. In this fiscal year we studied the following topics;Spin dynamics in the stripe-ordered buckled honeycomb lattice antiferromagnet Ba_2NiTeO_6, Magnetic excitations from the two-dimensional interpenetrating Cu framework in $Ba_2Cu_3O_4Cl_2$, Magnetic Structure and Dielectric State in the Multiferroic $Ca_2CoSi_2O_7$, A layered wide-gap oxyhalide semiconductor with an infinite ZnO_2 square planar sheet: $Sr_2ZnO_2Cl_2$, Magnetic metal-complex-conducting copolymer core-shell nanoassemblies for a single-drug anticancer platform, and Spin pseudogap in the S=1/2 chain material Sr_2CuO_3 with impurities.

1. Magnetic Structure and Dielectric State in the Multiferroic $Ca_2CoSi_2O_7$: M. Soda, S. Hayashida, T. Yoshida, M. Akaki, M. Hagiwara, M. Avdeev, O. Zaharko and T. Masuda, J. Phys. Soc. Jpn. **86** (2017) 064703(1-5).

---

* Joint research among groups within ISSP.

2. Magnetic excitations from the two-dimensional interpenetrating Cu framework in $Ba_2Cu_3O_4Cl_2$: P. Babkevich, N. E. Shaik, D. Lancon, A. Kikkawa, M. Enderle, R. A. Ewings, H. C. Walker, D. T. Adroja, P. Manuel, D. D. Khalyavin, Y. Taguchi, Y. Tokura, M. Soda, T. Masuda and H. M. Ronnow, Phys. Rev. B **96** (2017) 014410(1-12).

3. Spin dynamics in the stripe-ordered buckled honeycomb lattice antiferromagnet Ba_2NiTeO_6: S. Asai, M. Soda, K. Kasatani, T. Ono, V. Ovidiu Garlea, B. Winn and T. Masuda, Phys. Rev. B **96** (2017) 104414(1-6).

4. Spin pseudogap in the S=1/2 chain material Sr_2CuO_3 with impurities: G. Simutis, S. Gvasaliya, N. S. Beesetty, T. Yoshida, J. Robert, S. Petit, A. I. Kolesnikov, M. B. Stone, F. Bourdarot, H. C. Walker, D. T. Adroja, O. Sobolev, C. Hess, T. Masuda, A. Revcolevschi, B. Büchner and A. Zheludev, Phys. Rev. B **95** (2017) 054409(1-6).

5. A layered wide-gap oxyhalide semiconductor with an infinite ZnO_2 square planar sheet: $Sr_2ZnO_2Cl_2$: Y. Su, Y. Tsujimoto, A. Miura, S. Asai, M. Avdeev, H. Ogino, M. Ako, A. A. Belik, T. Masuda, T. Uchikoshi and K. Yamaura, Chem. Commun. **53** (2017) 3826(4 pages).

6. Dielectric Property and Diffuse Scattering in Relaxor Magnet $LuFeCoO_4$: M. Soda and T. Masuda, J. Phys.: Conf. Ser. **828** (2017) 012001(1-3).

7. Neutron Scattering Study in Breathing Pyrochlore Antiferromagnet $Ba_3Yb_2Zn_5O_{11}$: T. Haku, M. Soda, M. Sera, K. Kimura, J. Taylor, S. Itoh, T. Yokoo, Y. Matsumoto, D. Yu, R. A. Mole, T. Takeuchi, S. Nakatsuji, Y. Kono, T. Sakakibara, L. -J. Chang and T. Masuda, J. Phys.: Conf. Ser. **828** (2017) 012018(1-5).

8. Powder neutron diffraction in one-dimensional frustrated chain compound $NaCuMoO_4$(OD): S. Asai, T. Oyama, M. Soda, K. Rule, K. Nawa, Z. Hiroi and T. Masuda, J. Phys.: Conf. Ser. **828** (2017) 012006(1-5).

9. Hyperthermia and chemotherapy using Fe(Salen) nanoparticles might impact glioblastoma treatment: M. Ohtake, M. Umemura, I. Sato, T. Akimoto, K. Oda, A. Nagasako, J.-H. Kim, T. Fujita, U. Yokoyama, T. Nakayama, Y. Hoshino, M. Ishiba, S. Tokura, M. Hara, T. Muramoto, S. Yamada, T. Masuda, I. Aoki, Y. Takemura, H. Murata, H. Eguchi, N. Kawahara and Y. Ishikawa, Sci. Rep. **7** (2017) 42783(1-12).

10. Magnetic metal-complex-conducting copolymer core–shell nanoassemblies for a single-drug anticancer platform: J.-H. Kim, H. Eguchi, M. Umemura, I. Sato, S. Yamada, Y. Hoshino, T. Masuda, I. Aoki, K. Sakurai, M. Yamamoto and Y. Ishikawa, NPG Asia Mater. **9** (2017) e367(1-14).

11. Low temperature magnetic properties of $Nd_2Ru_2O_7$: S. T. Ku, D. Kumar, M. R. Lees, W.-T. Lee, R. Aldus, A. Studer, P. Imperia, S. Asai, T. Masuda, S. W. Chen, J. M. Chen and L. J. Chang, J. Phys.: Condens. Matter **30** (2018) 155601 (1-11).

12. [*]Magnetic state selected by magnetic dipole interaction in the kagome antiferromagnet $NaBa_2Mn_3F_{11}$: S. Hayashida, H. Ishikawa, Y. Okamoto, T. Okubo, Z. Hiroi, M. Avdeev, P. Manuel, M. Hagihala, M. Soda and T. Masuda, Phys. Rev. B **97** (2018) 054411(1-7).

13. [*]Pressure-induced quantum phase transition in the quantum antiferromagnet $CsFeCl_3$: S. Hayashida, O. Zaharko, N. Kurita, H. Tanaka, M. Hagihala, M. Soda, S. Itoh, Y. Uwatoko and T. Masuda, Phys. Rev. B **97** (2018) 140405(1-4).

14. Neutron Spin Resonance in the 112-Type Iron-Based Superconductor: T. Xie, D. Gong, H. Ghosh, A. Ghosh, M. Soda, T. Masuda, S. Itoh, F. Bourdarot, L.-P. Regnault, S. Danilkin, S. Li and H. Luo, Phys. Rev. Lett. **120** (2018) 137001 (1-7).

15. Crystal Structure of Magnetoelectric $Ba_2MnGe_2O_7$ at Room and Low Temperatures by Neutron Diffraction: A. Sazonov, V. Hutanu, M. Meven, G. Roth, R. Georgii, T. Masuda and B. Nafradi, Inorg. Chem. **57** (2018) 5089-5095.

16. Improvement for Neutron Brillouin Scattering Experiments on High Resolution Chopper Spectrometer HRC: S. Itoh, T. Yokoo, T. Masuda, H. Yoshizawa, M. Soda, M. Yoshida, T. Hawai, D. Kawana, R. Sugiura, T. Asami and Y. Ihata, J. Phys.: Conf. Ser. **1021** (2018) 012028(1-4).

17. High resolution chopper spectrometer HRC and neutron Brillouin scattering: S. Itoh, T. Yokoo, T. Masuda, H. Yoshizawa, M. Soda, S. Ibuka, Y. Ikeda, M. Yoshida, T. Hawai, D. Kawana, R. Sugiura, T. Asami, Y. Kawamura, T. Shinozaki and Y. Ihata, AIP Conf. Proc. **1969** (2018) 050002(1-5).

[†] Joint research with outside partners.

International MegaGauss Science Laboratory

Takeyama group

985 T close to 1000 T has been achieved by the electromagnetic flux compression megagauss generator. 1000 T-class electromagnetic flux compression megagauss generator is newly reconstructed and completed. A peak magnetic field of 400 T has been achieved with 1.3 MJ energy injection, showing high efficiency of the system. Magnetization measurement techniques are still in progress in the single-turn coil magagauss generator system, and the measurements using a co-axial type self-compensated pick-up-coil up to 130 T, and using magneto-optical techniques up to 200 T are currently achieved with high reliability, at very low temperature around 5 K. Contactless ultra-high frequency AC-conductivity measurement techniques are developed and showed it is applicable to destructing short-pulse magnets of micro second pulse duration. The methods have been applied to investigate spin structures of frustrated magnetic materials, multiferro materials, and quantum spin systems, superconducting materials, and etc.

1. †*Electric Polarization Induced by Spin Ordering under Magnetic Fields in Distorted Triangular Lattice Antiferromagnet $RbCoBr_3$: Y. Nishiwaki, M. Tokunaga, R. Sakakura, S. Takeyama, T. Kato and K. Iio, J. Phys. Soc. Jpn. **86** (2017) 044701(1-7).

2. †*Magnetization Process of the S = 1/2 Two-Leg Organic Spin-Ladder Compound BIP-BNO: K. Nomura, Y. H. Matsuda, Y. Narumi, K. Kindo, S. Takeyama, Y. Hosokoshi, T. Ono, N. Hasegawa, H. Suwa and S. Todo, J. Phys. Soc. Jpn. **86** (2017) 104713(1-3).

3. *Magnetic transitions under ultrahigh magnetic fields of up to 130 T in the breathing pyrochlore antiferromagnet $LiInCr_4O_8$: Y. Okamoto, D. Nakamura, A. Miyake, S. Takeyama, M. Tokunaga, A. Matsuo, K. Kindo and Z. Hiroi, Phys. Rev. B **95** (2017) 134438(1-5).

4. †Ultrahigh magnetic field phases in the frustrated triangular-lattice magnet $CuCrO_2$: A. Miyata, O. Portugall, D. Nakamura, K. Ohgushi and S. Takeyama, Phys. Rev. B **96** (2017) 180401-4.

5. Excitation energy dependence of initial phase shift in Kerr rotation of resident electron spin polarization in a CdTe single quantum well: L. -P. Yan, T. Takamure, R. Kaji, G. Karczewski, S. Takeyama and S. Adachi, Phys. Status Solidi B **254** (2017) 1600449(1-6).

6. Note: An approach to 1000 T using the electro-magnetic flux compression: D. Nakamura, H. Sawabe and S. Takeyama, Rev. Sci. Instrum. **89** (2018) 016106(1-3).

7. Radio frequency self-resonant coil for contactless AC-conductivity in 100 T class ultra-strong pulse magnetic fields: D. Nakamura, M. M. Altarawneh and S. Takeyama, Meas. Sci. Technolol. **29** (2018) 035901(7 pages).

Kindo group

We have succeeded in developing highly repetitive long pulse magnet. The magnet is used for the electric transport measurements and the heat capacity measurements. We have shortened the waiting time for cooling down the magnet to 1.5 hrs after generating the maximum field.

1. †Hard x-ray photoemission study of $Yb_{1-x}Zr_xB_{12}$: the effects of electron doping on the Kondo insulator YbB_{12}: A. Rousuli, H. Sato, F. Iga, K. Hayashi, K. Ishii, T. Wada, T. Nagasaki, K. Mimura, H. Anzai, K. Ichiki, S. Ueda, A. Kondo, K. Kindo, T. Takabatake, K. Shimada, H. Namatame and M. Taniguchi, J. Phys.: Condens. Matter **29** (2017) 265601 (1-7).

2. †40 T Soft X-ray Spectroscopies on Magnetic-Field-Induced Valence Transition in $Eu(Rh_{1-x}Ir_x)_2Si_2$(x = 0.3): H. Yasumura, Y. Narumi, T. Nakamura, Y. Kotani, A. Yasui, E. Kishaba, A. Mitsuda, H. Wada, K. Kindo and H. Nojiri, J. Phys. Soc. Jpn. **86** (2017) 054706(1-8).

3. †Fe Substitution Effect on the High-Field Magnetization in the Kondo Semiconductor $CeRu_2Al_{10}$: A. Kondo, K. Kindo, H. Nohara, M. Nakamura, H. Tanida, M. Sera and T. Nishioka, J. Phys. Soc. Jpn. **86** (2017) 023705(1-5).

4. †*Magnetization Process of the S = 1/2 Two-Leg Organic Spin-Ladder Compound BIP-BNO: K. Nomura, Y. H. Matsuda, Y. Narumi, K. Kindo, S. Takeyama, Y. Hosokoshi, T. Ono, N. Hasegawa, H. Suwa and S. Todo, J. Phys. Soc. Jpn. **86** (2017) 104713(1-3).

5. †*Magnetization Process of the Kondo Insulator YbB_{12} in Ultrahigh Magnetic Fields: T. T. Terashima, A. Ikeda, Y. H. Matsuda, A. Kondo, K. Kindo and F. Iga, J. Phys. Soc. Jpn. **86** (2017) 054710(1-5).

---

* Joint research among groups within ISSP.

6. †Spin-1/2 Quantum Antiferromagnet on a Three-Dimensional Honeycomb Lattice Formed by a New Organic Biradical F_4BIPBNN: N. Amaya, T. Ono, Y. Oku, H. Yamaguchi, A. Matsuo, K. Kindo, H. Nojiri, F. Palacio, J. Campo and Y. Hosokoshi, J. Phys. Soc. Jpn. **86** (2017) 074706(1-7).

7. *Thermodynamic Investigation of Metamagnetic Transitions and Partial Disorder in the Quasi-Kagome Kondo Lattice CePdAl: K. Mochidzuki, Y. Shimizu, A. Kondo, S. Nakamura, S. Kittaka, Y. Kono, T. Sakakibara, Y. Ikeda, Y. Isikawa and K. Kindo, J. Phys. Soc. Jpn. **86** (2017) 034709(1-5).

8. †*α−β and β−γ phase boundaries of solid oxygen observed by adiabatic magnetocaloric effect: T. Nomura, Y. Kohama, Y. H. Matsuda, K. Kindo and T. C. Kobayashi, Phys. Rev. B **95** (2017) 104420(1-6).

9. Experimental observation of temperature and magnetic-field evolution of the 4f states in $CeFe_2$ revealed by soft x-ray magnetic circular dichroism: Y. Saitoh, A. Yasui, H. Fuchimoto, Y. Nakatani, H. Fujiwara, S. Imada, Y. Narumi, K. Kindo, M. Takahashi, T. Ebihara and A. Sekiyama, Phys. Rev. B **96** (2017) 035151(1-5).

10. High-field magnetization of Heusler compound $Fe_2Mn_{1-x}V_xSi$: M. Hiroi, T. Tazoko, H. Sano, I. Shigeta, K. Koyama, A. Kondo, K. Kindo, H. Manaka and N. Terada, Phys. Rev. B **95** (2017) 014410(1-5).

11. †Ising-like anisotropy stabilized 1/3 and 2/3 magnetization plateaus in the V^{3+} kagome lattice antiferromagnets $Cs_2KV_3F_{12}$, $Cs_2NaV_3F_{12}$, and $Rb_2NaV_3F_{12}$: M. Goto, H. Ueda, C. Michioka, A. Matsuo, K. Kindo, K. Sugawara, S. Kobayashi, N. Katayama, H. Sawa and K. Yoshimura, Phys. Rev. B **95** (2017) 134436(1-10).

12. *Magnetic transitions under ultrahigh magnetic fields of up to 130 T in the breathing pyrochlore antiferromagnet $LiInCr_4O_8$: Y. Okamoto, D. Nakamura, A. Miyake, S. Takeyama, M. Tokunaga, A. Matsuo, K. Kindo and Z. Hiroi, Phys. Rev. B **95** (2017) 134438(1-5).

13. †Magnetism of the antiferromagnetic spin-3/2 dimer compound $CrVMoO_7$ having an antiferromagnetically ordered state: M. Hase, Y. Ebukuro, H. Kuroe, M. Matsumoto, A. Matsuo, K. Kindo, J. R. Hester, T. J. Sato and H. Yamazaki, Phys. Rev. B **95** (2017) 144429(1-7).

14. †Magnetism of the spin-1 tetramer compound $A_2Ni_2Mo_3O_{12}$ (A=Rb or K): M. Hase, A. Matsuo, K. Kindo and M. Matsumoto, Phys. Rev. B **96** (2017) 214424(8).

15. †*Rich magnetoelectric phase diagrams of multiferroic single-crystal α−$NaFeO_2$: N. Terada, Y. Ikedo, H. Sato, D. D. Khalyavin, P. Manuel, A. Miyake, A. Matsuo, M. Tokunaga and K. Kindo, Phys. Rev. B **96** (2017) 035128(1-14).

16. †S=1/2 quantum critical spin ladders produced by orbital ordering in Ba_2CuTeO_6: A. S. Gibbs, A. Yamamoto, A. N. Yaresko, K. S. Knight, H. Yasuoka, M. Majumder, M. Baenitz, P. J. Saines, J. R. Hester, D. Hashizume, A. Kondo, K. Kindo and H. Takagi, Phys. Rev. B **95** (2017) 104428(1-6).

17. †Spin order in the Heisenberg kagome antiferromagnet $MgFe_3(OH)_6Cl_2$: M. Fujihala, X. G. Zheng, S. Lee, T. Kamiyama, A. Matsuo, K. Kindo and T. Kawae, Phys. Rev. B **96** (2017) 144111(9).

18. †*Magnetoelectric Behavior from S=1/2 Asymmetric Square Cupolas: Y. Kato, K. Kimura, A. Miyake, M. Tokunaga, A. Matsuo, K. Kindo, M. Akaki, M. Hagiwara, M. Sera, T. Kimura and Y. Motome, Phys. Rev. Lett. **118** (2017) 107601 (1-5).

19. Search for Two-Photon Interaction with Axionlike Particles Using High-Repetition Pulsed Magnets and Synchrotron X Rays: T. Inada, T. Yamazaki, T. Namba, S. Asai, T. Kobayashi, K. Tamasaku, Y. Tanaka, Y. Inubushi, K. Sawada, M. Yabashi, T. Ishikawa, A. Matsuo, K. Kawaguchi, K. Kindo and H. Nojiri, Phys. Rev. Lett. **118** (2017) 071803 (1-6).

20. *Topochemical Crystal Transformation from a Distorted to a Nearly Perfect Kagome Cuprate: H. Ishikawa, T. Yajima, A. Miyake, M. Tokunaga, A. Matsuo, K. Kindo and Z. Hiroi, Chem. Mater. **29** (2017) 6719-6725.

21. *Giant Exchange Coupling Evidenced with a Magnetization Jump at 52 T for a Gadolinium-Nitroxide Chelate: T. Kanetomo, T. Kihara, A. Miyake, A. Matsuo, M. Tokunaga, K. Kindo, H. Nojiri and T. Ishida, Inorg. Chem. **56** (2017) 3310-3314.

22. Magnetic and electrical properties of Heusler compounds $Ru_2Cr_{1-x}X_xSi$ (X=V, Ti): M. Hiroi, H. Sano, T. Tazoko, I. Shigeta, M. Ito, K. Koyama, H. Manaka, N. Terada, M. Fujii, A. Kondo and K. Kindo, J. Alloys Compd. **694** (2017) 1376-1382.

23. †Physical properties in the cluster-based magnetic-diluted triangular lattice antiferromagnets $Li_2Sc_{1-x}Sn_xMo_3O_8$: Y. Haraguchi, C. Michioka, H. Ueda, A. Matsuo, K. Kindo and K. Yoshimura, J. Phys.: Conf. Ser. **828** (2017) 012013(6).

† Joint research with outside partners.

24. †Different valence states of Tm in YB_6 and YbB_6: H. Sato, H. Nagata, F. Iga, Y. Osanai, A. Rousuli, K. Mimura, H. Anzai, K. Ichiki, S. Ueda, T. Takabatake, A. Kondo, K. Kindo, K. Shimada, H. Namatame and M. Taniguchi, Journal of Electron Spectroscopy and Related Phenomena **220** (2017) 33-36.

25. The OVAL experiment: a new experiment to measure vacuum magnetic birefringence using high repetition pulsed magnets: X. Fan, S. Kamioka, T. Inada, T. Yamazaki, T. Namba, S. Asai, J. Omachi, K. Yoshioka, M. Kuwata-Gonokami, A. Matsuo, K. Kawaguchi, K. Kindo and H. Nojiri, Eur. Phys. J. D **71** (2017) 308(10).

26. †*Magnetic and Structural Properties of A-Site Ordered Chromium Spinel Sulfides: Alternating Antiferromagnetic and Ferromagnetic Interactions in the Breathing Pyrochlore Lattice: Y. Okamoto, M. Mori, N. Katayama, A. Miyake, M. Tokunaga, A. Matsuo, K. Kindo and K. Takenaka, J. Phys. Soc. Jpn. **87** (2018) 034709(1-8).

27. *Unusual magnetoelectric memory and polarization reversal in the kagome staircase compound Ni3V2O8: Y. J. Liu, J. F. Wang, z. Z. He, C. L. Xia, Z. W. Ouyang, C. B. Liu, R. Chen, A. Matsuo, Y. Kohama, K. Kindo and M. Tokunaga, Phys. Rev. B **97** (2018) 174429.

28. †Cluster-Based Haldane State in an Edge-Shared Tetrahedral Spin-Cluster Chain: Fedotovite $K_2Cu_3O(SO_4)_3$: M. Fujihala, T. Sugimoto, T. Tohyama, S. Mitsuda, R. A. Mole, D. H. Yu, S. Yano, Y. Inagaki, H. Morodomi, T. Kawae, H. Sagayama, R. Kumai, Y. Murakami, K. Tomiyasu, A. Matsuo and K. Kindo, Phys. Rev. Lett. **120** (2018) 077201(5).

Tokunaga group

$BiFeO_3$ is perhaps the most extensively studied multiferroic material. Our highly accurate experiments of magnetostrsiction, magnetization, electric polarization in pulsed high magnetic fields revealed ferroelastic distortion in this material that can be controlled by magnetic field, and also emergence of novel magneto-electric phase at around room temperature. Theoretical calculation suggests a kind of conical spin order in this phase, which has a spin modulation vector normal to that in the cycloidal state at zero field. Change in the spin modulation vector is confirmed through neutron experiments.

1. †Characteristic Physical Properties of the Non-Kramers Γ_3 Ground State in $PrPt_2Cd_{20}$: Y. Hirose, T. Takeuchi, H. Doto, F. Honda, A. Miyake, M. Tokunaga, D. Yoshizawa, T. Kida, M. Hagiwara, Y. Haga and R. Settai, J. Phys. Soc. Jpn. **86** (2017) 074711(1-7).

2. †*Electric Polarization Induced by Spin Ordering under Magnetic Fields in Distorted Triangular Lattice Antiferromagnet $RbCoBr_3$: Y. Nishiwaki, M. Tokunaga, R. Sakakura, S. Takeyama, T. Kato and K. Iio, J. Phys. Soc. Jpn. **86** (2017) 044701(1-7).

3. †Different metamagnetism between paramagnetic Ce and Yb isomorphs: A. Miyake, Y. Sato, M. Tokunaga, J. Jatmika and T. Ebihara, Phys. Rev. B **96** (2017) 085127(1-7).

4. High-field magnetization and magnetic phase diagram of α-$Cu_2V_2O_7$: G. Gitgeatpong, M. Suewattana, S. Zhang, A. Miyake, M. Tokunaga, P. Chanlert, N. Kurita, H. Tanaka, T. J. Sato, Y. Zhao and K. Matan, Phys. Rev. B **95** (2017) 245119(1-10).

5. *Magnetic transitions under ultrahigh magnetic fields of up to 130 T in the breathing pyrochlore antiferromagnet $LiInCr_4O_8$: Y. Okamoto, D. Nakamura, A. Miyake, S. Takeyama, M. Tokunaga, A. Matsuo, K. Kindo and Z. Hiroi, Phys. Rev. B **95** (2017) 134438(1-5).

6. *Phase diagram of multiferroic $KCu_3As_2O_7(OD)_3$: G. J. Nilsen, V. Simonet, C. V. Colin, R. Okuma, Y. Okamoto, M. Tokunaga, T. C. Hansen, D. D. Khalyavin and Z. Hiroi, Phys. Rev. B **95** (2017) 214415(1-10).

7. †*Rich magnetoelectric phase diagrams of multiferroic single-crystal α–$NaFeO_2$: N. Terada, Y. Ikedo, H. Sato, D. D. Khalyavin, P. Manuel, A. Miyake, A. Matsuo, M. Tokunaga and K. Kindo, Phys. Rev. B **96** (2017) 035128(1-14).

8. †*Two-carrier analyses of the transport properties of black phosphorus under pressure: K. Akiba, A. Miyake, Y. Akahama, K. Matsubayashi, Y. Uwatoko and M. Tokunaga, Phys. Rev. B **95** (2017) 115126(1-7).

9. †*Magnetoelectric Behavior from S=1/2 Asymmetric Square Cupolas: Y. Kato, K. Kimura, A. Miyake, M. Tokunaga, A. Matsuo, K. Kindo, M. Akaki, M. Hagiwara, M. Sera, T. Kimura and Y. Motome, Phys. Rev. Lett. **118** (2017) 107601 (1-5).

10. *Topochemical Crystal Transformation from a Distorted to a Nearly Perfect Kagome Cuprate: H. Ishikawa, T. Yajima, A. Miyake, M. Tokunaga, A. Matsuo, K. Kindo and Z. Hiroi, Chem. Mater. **29** (2017) 6719-6725.

11. *Giant Exchange Coupling Evidenced with a Magnetization Jump at 52 T for a Gadolinium-Nitroxide Chelate: T. Kanetomo, T. Kihara, A. Miyake, A. Matsuo, M. Tokunaga, K. Kindo, H. Nojiri and T. Ishida, Inorg. Chem. **56** (2017) 3310-3314.

---

* Joint research among groups within ISSP.

12. †Quantum Hall states observed in thin films of Dirac semimetal Cd_3As_2: M. Uchida, Y. Nakazawa, S. Nishihaya, K. Akiba, M. Kriener, Y. Kozuka, A. Miyake, Y. Taguchi, M. Tokunaga, N. Nagaosa, Y. Tokura and M. Kawasaki, Nat. Commun. **8** (2017) 2274(1-7).

13. Successive field-induced transitions in $BiFeO_3$ around room temperature: S. Kawachi, A. Miyake, T. Ito, S. E. Dissanayake, M. Matsuda, W. Ratcliff, Z. Xu, Y. Zhao, S. Miyahara, N. Furukawa and M. Tokunaga, Phys. Rev. Materials **1** (2017) 024408(1-6).

14. †Stress- and Magnetic Field-Induced Martensitic Transformation at Cryogenic Temperatures in Fe–Mn–Al–Ni Shape Memory Alloys: J. Xia, X. Xu, A. Miyake, Y. Kimura, T. Omori, M. Tokunaga and R. Kainuma, Shap. Mem. Superelasticity **3** (2017) 467-475.

15. †*Magnetic and Structural Properties of A-Site Ordered Chromium Spinel Sulfides: Alternating Antiferromagnetic and Ferromagnetic Interactions in the Breathing Pyrochlore Lattice: Y. Okamoto, M. Mori, N. Katayama, A. Miyake, M. Tokunaga, A. Matsuo, K. Kindo and K. Takenaka, J. Phys. Soc. Jpn. **87** (2018) 034709(1-8).

16. 室温マルチフェロイック物質ビスマスフェライトの電気磁気効果：河智 史朗，三宅 厚志，徳永 将史，伊藤 利充，固体物理 **53** (2018) 61-70.

17. †Large magneto-thermopower in MnGe with topological spin texture: Y. Fujishiro, N. Kanazawa, T. Shimojima, A. Nakamura, K. Ishizaka, T. Koretsune, R. Arita, A. Miyake, H. Mitamura, K. Akiba, M. Tokunaga, J. Shiogai, S. Kimura, S. Awaji, A. Tsukazaki, A. Kikkawa, Y. Taguchi and Y. Tokura, Nat. Commun. **9** (2018) 408(1-7).

Y. Matsuda group

The phase diagram in B-T plain of solid oxygen has been constructed by several experiments including the optical transmission, magnetization, adiabatic heating effect, and magneto-caloric effect. The obtained phase diagram indicates that the field induced novel phase (θ phase) emerges from the α and β phases at low temperatures. The full magnetization curve of the organic S=1/2 spin ladder compound BIP-BNO is obtained using the single-turn coil megagauss field generator. A characteristic symmetric two-peak structure in dM/dB curve is a first experimental evidence that BIP-TENO is a prototypical organic (not containing magnetic ions) spin-ladder compound. High magnetic field property of the Kondo insulator YbB_{12} is also investigated by means of the magnetization. The second jump of the magnetization found around 102 T can correspond to the collapse of the Kondo bound state. It has been shown that the field-induced insulator-metal transition in YbB_{12} is interpreted as the energy gap closing by Zeeman effect without breaking the Kondo state. In addition to experiments on various materials, we have developed a technique for magnetostriction under ultrahigh magnetic fields in the range of 100 -1000 T.

1. †*Lifetime-Broadening-Suppressed X-ray Absorption Spectrum of β-$YbAlB_4$ Deduced from Yb $3d \rightarrow 2p$ Resonant X-ray Emission Spectroscopy: N. Kawamura, N. Kanai, H. Hayashi, Y. H. Matsuda, M. Mizumaki, K. Kuga, S. Nakatsuji and S. Watanabe, J. Phys. Soc. Jpn. **86** (2017) 014711(1-7).

2. †*Magnetization Process of the S = 1/2 Two-Leg Organic Spin-Ladder Compound BIP-BNO: K. Nomura, Y. H. Matsuda, Y. Narumi, K. Kindo, S. Takeyama, Y. Hosokoshi, T. Ono, N. Hasegawa, H. Suwa and S. Todo, J. Phys. Soc. Jpn. **86** (2017) 104713(1-3).

3. †*Magnetization Process of the Kondo Insulator YbB_{12} in Ultrahigh Magnetic Fields: T. T. Terashima, A. Ikeda, Y. H. Matsuda, A. Kondo, K. Kindo and F. Iga, J. Phys. Soc. Jpn. **86** (2017) 054710(1-5).

4. †*α−β and β−γ phase boundaries of solid oxygen observed by adiabatic magnetocaloric effect: T. Nomura, Y. Kohama, Y. H. Matsuda, K. Kindo and T. C. Kobayashi, Phys. Rev. B **95** (2017) 104420(1-6).

5. †H-T phase diagram of solid oxygen: T. Nomura, Y. H. Matsuda and T. C. Kobayashi, Phys. Rev. B **96** (2017) 054439 (1-5).

6. †*High-speed 100 MHz strain monitor using fiber Bragg grating and optical filter for magnetostriction measurements under ultrahigh magnetic fields: A. Ikeda, T. Nomura, Y. H. Matsuda, S. Tani, Y. Kobayashi, H. Watanabe and K. Sato, Rev. Sci. Instrum. **88** (2017) 083906(1-5).

7. *Unusual magnetoelectric memory and polarization reversal in the kagome staircase compound Ni3V2O8: Y. J. Liu, J. F. Wang, z. Z. He, C. L. Xia, Z. W. Ouyang, C. B. Liu, R. Chen, A. Matsuo, Y. Kohama, K. Kindo and M. Tokunaga, Phys. Rev. B **97** (2018) 174429.

Kohama group

In 2017, our group upgrades the pulsed-field calorimeter for low temperature measurements of specific heat. With the new system, not only the accessibility to the low temperature, the sensitivity & accuracy of the C(T) data becomes compatible with

† Joint research with outside partners.

the C(T) data taken in steady fields. We also successfully developed new technique for measuring electric resistivity, which can operate in destructive pulsed field up to 120 T.

1. *Unusual magnetoelectric memory and polarization reversal in the kagome staircase compound Ni3V2O8: Y. J. Liu, J. F. Wang, z. Z. He, C. L. Xia, Z. W. Ouyang, C. B. Liu, R. Chen, A. Matsuo, Y. Kohama, K. Kindo and M. Tokunaga, Phys. Rev. B **97** (2018) 174429.

2. Quntum Criticality of an Ising-like Spin-1/2 Antiferromagnetic Chain in a Transverse Magnetic Field: Z. Wang, T. Lorenz, D. I. Gorbunov, P. T. Cong, Y. Kohama, S. Niesen, O. Breuning, J. Engelmayer, A. Herman, J. Wu, K. Kindo, J. Wosnitza, S. Zherlitsyn and A. Loidl, Phys Rev Lett **120** (2018) 207205.

Center of Computational Materials Science

Akai group

(1) L-edge resonant magneto-optical Kerr effect of Fe and Fe/Cu interfaces were calculated in the framework of KKR Green's function method and density functional theory. The results were compared with the recent experimentas performed by Matsuda's group of ISSP. (2) The method of first-principles calculation of the soft X-ray second harmonic generation (SHG) was developed. The SHG of $GaFeO_3$ was calculated by the method and the results were compared with the recent experiment performed by Matsuda's group of ISSP. (3) Maximum performance that might be expected for permanent magnet materials was estimated based on the density functional theory. The calculations concluded that the plausible upper limits of saturation magnetic polariza- tion, magnetic transition temperature, and the magnetocrystalline anisotropy constant of permanent magnet materials could be ~2.7 T, ~2000 K, and ~1000 MJm^{-3}, respectively. (4) We developed the method of calculating Seebeck coefficient in the framework of the Korringa–Kohn–Rostoker (KKR) method combined with the coherent potential approximation (CPA; KKR-CPA) and linear response theory. The main objective was to establish a practical first-principles scheme that can calculate the conductivities and Seebeck coefficients of metallic systems at finite temperature. Thus, it was necessary to include the effects of electron-phonon scattering, which plays a crucial role at finite temperature, particularly for ordered-structure systems where the conductivity diverges at T = 0 K. The approach combines three components: linear response theory in the framework of the KKR method; phonon calculations; and an alloy analogy applied to the local static phonons using the KKR-CPA. The calculated Cu resistivity and Seebeck coefficients for various transition- metal elements at finite temperature showed reasonably good overall agreement with experiment.

1. Atomistic-model study of temperature-dependent domain walls in the neodymium permanent magnet $Nd_2Fe_{14}B$: M. Nishino, Y. Toga, S. Miyashita, H. Akai, A. Sakuma and S. Hirosawa, Phys. Rev. B **95** (2017) 094429(1-7).

2. *Determination of the element-specific complex permittivity using a soft x-ray phase modulator: Y. Kubota, Y. Hirata, J. Miyawaki, S. Yamamoto, H. Akai, R. Hobara, Sh. Yamamoto, K. Yamamoto, T. Someya, K. Takubo, Y. Yokoyama, M. Araki, M. Taguchi, Y. Harada, H. Wadati, M. Tsunoda, R. Kinjo, A. Kagamihata, T. Seike, M. Takeuchi, T. Tanaka, S. Shin and I. Matsuda, Phys. Rev. B **96** (2017) 214417(1-6).

3. *L-edge resonant magneto-optical Kerr effect of a buried Fe nanofilm: Y. Kubota, M. Taguchi, H. Akai, Sh. Yamamoto, T. Someya, Y. Hirata, K. Takubo, M. Araki, M. Fujisawa, K. Yamamoto, Y. Yokoyama, S. Yamamoto, M. Tsunoda, H. Wadati, S. Shin and I. Matsuda, Phys. Rev. B **96** (2017) 134432(1-6).

4. First-principles study of intersite magnetic couplings and Curie temperature in $RFe_{12-x}Cr_x$ (R = Y, Nd, Sm): T. Fukazawa, H. Akai, Y. Harashima and T. Miyake, J. Phys. Soc. Jpn. **87** (2018) 044706(1-5).

5. Quantum Theory of Rare-Earth Magnets: T. Miyake and H. Akai, J. Phys. Soc. Jpn. **87** (2018) 041009(1-10).

6. First-principles calculation of transition-metal Seebeck coefficients: S. Kou and H. Akai, Solid State Commun. **296** (2018) 1-5.

7. Maximum performance of permanent magnet materials: H. Akai, Scr. Mater. (2018), in print.

Laser and Synchrotron Research Center

Shin group

We studied high Tc Fe-pnictide superconductors using 7-eV laser. High resolution photoemission study with polarization depen-

* Joint research among groups within ISSP.

dence is very powerful for the study of the superconducting mechanism. Orbital fluctuation mechanism is also important in addition to the spin fluctuation mechanism.

1. [*]Determination of the element-specific complex permittivity using a soft x-ray phase modulator: Y. Kubota, Y. Hirata, J. Miyawaki, S. Yamamoto, H. Akai, R. Hobara, Sh. Yamamoto, K. Yamamoto, T. Someya, K. Takubo, Y. Yokoyama, M. Araki, M. Taguchi, Y. Harada, H. Wadati, M. Tsunoda, R. Kinjo, A. Kagamihata, T. Seike, M. Takeuchi, T. Tanaka, S. Shin and I. Matsuda, Phys. Rev. B **96** (2017) 214417(1-6).

2. [*]Direct mapping of spin and orbital entangled wave functions under interband spin-orbit coupling of giant Rashba spin-split surface states: R. Noguchi, K. Kuroda, K. Yaji, K. Kobayashi, M. Sakano, A. Harasawa, T. Kondo, F. Komori and S. Shin, Phys. Rev. B **95** (2017) 041111(R)(1-6).

3. [*]Suppression of supercollision carrier cooling in high mobility graphene on SiC(0001): T. Someya, H. Fukidome, H. Watanabe, T. Yamamoto, M. Okada, H. Suzuki, Y. Ogawa, T. Iimori, N. Ishii, T. Kanai, K. Tashima, B. Feng, S. Yamamoto, J. Itatani, F. Komori, K. Okazaki, S. Shin and I. Matsuda, Phys. Rev. B **95** (2017) 165303(1-7).

4. [†*]Ultrafast Melting of Spin DensityWave Order in BaFe2As2 Observed by Time- and Angle-Resolved Photoemission Spectroscopy with Extreme-Ultraviolet Higher Harmonic Generation: H. Suzuki, K. Okazaki, T. Yamamoto, T. Someya, M. Okada, K. Koshiishi, M. Fujisawa, T. Kanai, N. Ishii, M. Nakajima, H. Eisaki, K. Ono, H. Kumigashira, J. Itatani, A. Fujimori and S. Shin, Phys. Rev. B **95** (2017) 165112(1-6).

5. [†*]Unusual nodal behaviors of the superconducting gap in the iron-based superconductor $Ba(Fe_{0.65}Ru_{0.35})_2As_2$: Effects of spin-orbit coupling: L. Liu, K. Okazaki, T. Yoshida, H. Suzuki, M. Horio, L. C. C. Ambolode II, J. Xu, S. Ideta, M. Hashimoto, D. H. Lu, Z. -X. Shen, Y. Ota, S. Shin, M. Nakajima, S. Ishida, K. Kihou, C. H. Lee, A. Iyo, H. Eisaki, T. Mikami, T. Kakeshita, Y. Yamakawa, H. Kontani, S. Uchida and A. Fujimori, Phys. Rev. B **95** (2017) 104504(1-5).

6. [†*]Visualizing the evolution of surface localization in the topological state of Bi2Se3 by circular dichroism in laser-based angle-resolved photoemission spectroscopy: T. Kondo, Y. Nakashima, Y. Ishida, A. Kikkawa, Y. Taguchi, Y. Tokura and S. Shin, Phys. Rev. B **96** (2017) 241413(1-5).

7. [†*]Observation of Bogoliubov Band Hybridization in the Optimally Doped Trilayer Bi2Sr2Ca2Cu3O10+δ: S. Kunisada, S. Adachi, S. Sakai, N. Sasaki, M. Nakayama, S. Akebi, K. Kuroda, T. Sasagawa, T. Watanabe, S. Shin and T. Kondo, Phys. Rev. Lett. **119** (2017) 217001(1-5).

8. Topologically Entangled Rashba-Split Shockley States on the Surface of Grey Arsenic: P. Zhang, J. -Z. Ma, Y. Ishida, L. -X. Zhao, Q. -N. Xu, B. -Q. Lv, K. Yaji, G. -F. Chen, H. -M. Weng, X. Dai, Z. Fang, X. -Q. Chen, L. Fu, T. Qian, H. Ding and S. Shin, Phys. Rev. Lett. **118** (2017) 046802(1-5).

9. [*]Unconventional superconductivity in the BiS_2-based layered superconductor $NdO_{0.71}F_{0.29}BiS_2$: Y. Ota, K. Okazaki, H. Q. Yamamoto, T. Yamamoto, S. Watanabe, C. Chen, M. Nagao, S. Watauchi, I. Tanaka, Y. Takano and S. Shin, Phys. Rev. Lett. **118** (2017) 167002(1-6).

10. [*]Capturing ultrafast magnetic dynamics by time-resolved soft x-ray magnetic circular dichroism: K. Takubo, K. Yamamoto, Y. Hirata, Y. Yokoyama, Y. Kubota, S. Yamamoto, S. Yamamoto, I. Matsuda, S. Shin, T. Seki, K. Takanashi and H. Wadati, Appl. Phys. Lett. **110** (2017) 162401(1-5).

11. [†*]Effect of physisorption of inert organic molecules on Au (111) surface electronic states: H. Mizushima, H. Koike, K. Kuroda, Y. Ishida, M. Nakayama, K. Mase, T. Kondo, S. Shin and K. Kanai, Phys. Chem. Chem. Phys. **19** (2017) 18646 (1-6).

12. [*]Signatures of a time-reversal symmetric Weyl semimetal with only four Weyl points: I. Belopolski, P. Yu, D. S. Sanchez, Y. Ishida, T.-R. Chang, S. S. Zhang, S.-Y. Xu, H. Zheng, G. Chang, G. Bian, H.-T. Jeng, T. Kondo, H. Lin, Z. Liu, S. Shin and M. Zahid Hasan, Nat. Commun. **8** (2017) 942(1-7).

13. [*]Spin-dependent quantum interference in photoemission process from spin-orbit coupled states: K. Yaji, K. Kuroda, S. Toyohisa, A. Harasawa, Y. Ishida, S. Watanabe, C. Chen, K. Kobayashi, F. Komori and S. Shin, Nat. Commun. **8** (2017) 14588(1-6).

14. [*]Femtosecond to picosecond transient effects in WSe_2 observed by pump-probe angle-resolved photoemission spectroscopy: R.-Y. Liu, Y. Ogawa, P. Chen, K. Ozawa, T. Suzuki, M. Okada, T. Someya, Y. Ishida, K. Okazaki, S. Shin, T.-C. Chiang and I. Matsuda, Sci. Rep. **7** (2017) 15981(1-7).

15. [*]Evidence for magnetic Weyl fermions in a correlated metal: K. Kuroda, T. Tomita, M. -T. Suzuki, C. Bareille, A. A. Nugroho, P. Goswami, M. Ochi, M. Ikhlas, M. Nakayama, S. Akebi, R. Noguchi, R. Ishii, N. Inami, K. Ono, H. Kumigashira, A. Varykhalov, T. Muro, T. Koretsune, R. Arita, S. Shin, T. Kondo and S. Nakatsuji, Nature Mater. **16** (2017) 1090-1095.

[†] Joint research with outside partners.

16. *Experimental evidence of hourglass fermion in the candidate nonsymmorphic topological insulator KHgSb: J. Ma, C. Yi, B. Lv, Z. Wang, S. Nie, L. Wang, L. Kong, Y. Huang, P. Richard, P. Zhang, K. Yaji, K. Kuroda, S. Shin, H. Weng, B. Andrei Bernevig, Y. Shi, T. Qian and H. Ding, Sci. Adv. **3** (2017) 1602415(1-5).

17. †*Polarization dependence of resonant magneto-optical Kerr effect measured by two types of figure-8 undulators: Y. Kubota, Sh. Yamamoto, T. Someya, Y. Hirata, K. Takubo, M. Araki, M. Fujisawa, K. Yamamoto, Y. Yokoyama, M. Taguchi, S. Yamamoto, M. Tsunoda, H. Wadati, S. Shin and I. Matsuda, J. Electron. Spectrosc. Relat. Phenom. **220** (2017) 17-20.

18. †*Spin-polarized quasi-one-dimensional state with finite band gap on the Bi/InSb(001) surface: J. Kishi, Y. Ohtsubo, T. Nakamura, K. Yaji, A. Harasawa, F. Komori, S. Shin, J. E. Rault, P. Le Fèvre, F. Bertran, A. Taleb-Ibrahimi, M. Nurmamat, H. Yamane, S. Ideta, K. Tanaka and S. Kimura, Phys. Rev. Materials **1** (2017) 064602(1-5).

19. *Surface electronic states of Au-induced nanowires on Ge(0 0 1): K. Yaji, R. Yukawa, S. Kim, Y. Ohtsubo, P. L. Fèvre, F. Bertran, A. Taleb-Ibrahimi, I. Matsuda, K. Nakatsuji, S. Shin and F. Komori, J. Phys.: Condens. Matter **30** (2018) 075001(1-7).

20. †*Antiphase Fermi-surface modulations accompanying displacement excitation in a parent compound of iron-based superconductors: K. Okazaki, H. Suzuki, T. Suzuki, T. Yamamoto, T. Someya, Y. Ogawa, M. Okada, M. Fujisawa, T. Kanai, N. Ishi, J. Itatani, M. Nakajima, H. Eisaki, A. Fujimori and S. Shin, Phys. Rev. B **97** (2018) 121107(R)(1-6).

21. *Kondo hybridization and quantum criticality in β−$YbAlB_4$ by laser ARPES: C. Bareille, S. Suzuki, M. Nakayama, K. Kuroda, A. H. Nevidomskyy, Y. Matsumoto, S. Nakatsuji, T. Kondo and S. Shin, Phys. Rev. B **97** (2018) 045112 (1-7).

22. Ultrafast dynamics of an unoccupied surface resonance state in Bi2Te2Se: N. Munisa, E. E. Krasovskii, Y. Ishida, K. Sumida, J. Chen, T. Yoshikawa, E. V. Chulkov, K. A. Kokh, O. E. Tereshchenko, S. Shin and A. Kimura, Phys. Rev. B **97** (2018) 115303(1-6).

23. †*Electronic Structure of Ce-Doped and -Undoped Nd_2CuO_4 Superconducting Thin Films Studied by Hard X-Ray Photoemission and Soft X-Ray Absorption Spectroscopy: M. Horio, Y. Krockenberger, K. Yamamoto, Y. Yokoyama, K. Takubo, Y. Hirata, S. Sakamoto, K. Koshiishi, A. Yasui, E. Ikenaga, S. Shin, H. Yamamoto, H. Wadati and A. Fujimori, Phys. Rev. Lett. **120** (2018) 257001(1-6).

24. *Element Selectivity in Second-Harmonic Generation of $GaFeO_3$ by a Soft-X-Ray Free-Electron Laser: Sh. Yamamoto, T. Omi, H. Akai, Y. Kubota, Y. Takahashi, Y. Suzuki, Y. Hirata, K. Yamamoto, R. Yukawa, K. Horiba, H. Yumoto, T. Koyama, H. Ohashi, S. Owada, K. Tono, M. Yabashi, E. Shigemasa, S. Yamamoto, M. Kotsugi, H. Wadati, H. Kumigashira, T. Arima, S. Shin and I. Matsuda, Phys. Rev. Lett. **120** (2018) 223902(1-5).

25. †*Experimental Determination of the Topological Phase Diagram in Cerium Monopnictides: K. Kuroda, M. Ochi, H. S. Suzuki, M. Hirayama, M. Nakayama, R. Noguchi, C. Bareille, S. Akebi, S. Kunisada, T. Muro, M. D. Watson, H. Kitazawa, Y. Haga, T. K. Kim, M. Hoesch, S. Shin, R. Arita and T. Kondo, Phys. Rev. Lett. **120** (2018) 086402(1-6).

26. *Observation of topological superconductivity on the surface of an iron-based superconductor: P. Zhang, K. Yaji, T. Hashimoto, Y. Ota, T. Kondo, K. Okazaki, Z. Wang, J. Wen, G. D. Gu, H. Ding and S. Shin, Science **360** (2018) 182-186.

27. * レーザー励起スピン分解光電子分光で解き明かす光スピン制御：矢治光 一郎，黒田 健太，小森 文夫，辛 埴，光学 **47** (2018) 142-147.

28. *Resonant magneto-optical Kerr effect measurement system using a high harmonic generation laser: Sh. Yamamoto, D. Oumbarek, M. Fujisawa, T. Someya, Y. Takahashi, T. Yamamoto, N. Ishiia, K. Yajia, S. Yamamoto, T. Kanai, K. Okazaki, M. Kotsugi, J. Itatani, S. Shin and I. Matsuda, J. Electron Spectrosc. Relat. Phenom. **222** (2018) 68-73.

29. *Superconducting gap anisotropy sensitive to nematic domains in FeSe: T. Hashimoto, Y. Ota, H. Q. Yamamoto, Y. Suzuki, T. Shimojima, S. Watanabe, C. Chen, S. Kasahara, Y. Matsuda, T. Shibauchi, K. Okazaki and S. Shin, Nat. Commun. **9** (2018) 282(1-7).

30. †*Superconducting Pairing of Topological Surface States in Bismuth Selenide Films on Niobium: D. Flötotto, Y. Ota, Y. Bai, C. Zhang, K. Okazaki, A. Tsuzuki, T. Hashimoto, J. N. Eckstein, S. Shin and T. -C. Chiang, Sci. Adv. **4** (2018) eaar7214(1-5).

31. * レーザーで電子のスピン方向を自由に制御：矢治光 一郎，黒田 健太，小森 文夫，辛 埴，レーザー加工学会誌 **25** (2018) 39-42.

32. †*Experimental Methods for Spin and Angle-Resolved Photoemission Spectroscpy Combined with Polarization Variable Laser: K. Kuroda, K. Yaji, A. Harasawa, R. Noguchi, T. Kondo, F. Komori and S. Shin, JoVE (2018), in print.

---

* Joint research among groups within ISSP.

33. * 固体表面電子におけるスピン軌道エンタングルメントと光スピン制御：矢治光 一郎 , 黒田 健太 , 小森 文夫 , 辛 埴 , 個体物理 **52** (2017) 559-571.

I. Matsuda group

In 2017, we made large progress in developments of synchrotron radiation techniques at our beamline, SPring-8 BL07LSU. We succeeded in directly determining the complex permittivity tensor using a method combining a developed light source from a segmented cross undulator of synchrotron radiation and the magneto-optical Kerr effect. The empirical permittivity, which carries the electronic and magnetic information of a material, has element specificity and has perfect confirmation using the quantum-mechanical calculation for itinerant electrons systems. These results help in understanding the interaction of light and matter, and they provide an interesting approach to seek the best materials as optical elements, for example, in extended-ultraviolet lithographic technologies or in state-of-the-art laser technologies. Concerning the material science, we experimentally realized two-dimensional Dirac nodal line fermions in monolayer Cu_2Si. We also succeeded in capturing ultrafast carrier dynamics in massless and massive Dirac materials with high-harmonic generation lasers.

1. *Determination of the element-specific complex permittivity using a soft x-ray phase modulator: Y. Kubota, Y. Hirata, J. Miyawaki, S. Yamamoto, H. Akai, R. Hobara, Sh. Yamamoto, K. Yamamoto, T. Someya, K. Takubo, Y. Yokoyama, M. Araki, M. Taguchi, Y. Harada, H. Wadati, M. Tsunoda, R. Kinjo, A. Kagamihata, T. Seike, M. Takeuchi, T. Tanaka, S. Shin and I. Matsuda, Phys. Rev. B **96** (2017) 214417(1-6).

2. *L-edge resonant magneto-optical Kerr effect of a buried Fe nanofilm: Y. Kubota, M. Taguchi, H. Akai, Sh. Yamamoto, T. Someya, Y. Hirata, K. Takubo, M. Araki, M. Fujisawa, K. Yamamoto, Y. Yokoyama, S. Yamamoto, M. Tsunoda, H. Wadati, S. Shin and I. Matsuda, Phys. Rev. B **96** (2017) 134432(1-6).

3. *Suppression of supercollision carrier cooling in high mobility graphene on SiC(0001): T. Someya, H. Fukidome, H. Watanabe, T. Yamamoto, M. Okada, H. Suzuki, Y. Ogawa, T. Iimori, N. Ishii, T. Kanai, K. Tashima, B. Feng, S. Yamamoto, J. Itatani, F. Komori, K. Okazaki, S. Shin and I. Matsuda, Phys. Rev. B **95** (2017) 165303(1-7).

4. †*Dirac Fermions in Borophene: B. Feng, O. Sugino, R.-Y. Liu, J. Zhang, R. Yukawa, M. Kawamura, T. Iimori, H. Kim, Y. Hasegawa, H. Li, L. Chen, K. Wu, H. Kumigashira, F. Komori, T.-C. Chiang, S. Meng and I. Matsuda, Phys. Rev. Lett. **118** (2017) 096401(1-6).

5. * ホウ素単原子シート「ボロフェン」：金属性とディラックフェルミオン : F. Baojie, 松田 巌 , 固体物理 **52** (2017) 385-393.

6. *Capturing ultrafast magnetic dynamics by time-resolved soft x-ray magnetic circular dichroism: K. Takubo, K. Yamamoto, Y. Hirata, Y. Yokoyama, Y. Kubota, S. Yamamoto, S. Yamamoto, I. Matsuda, S. Shin, T. Seki, K. Takanashi and H. Wadati, Appl. Phys. Lett. **110** (2017) 162401(1-5).

7. Time-resolved soft X-ray core-level photoemission spectroscopy to 880°C using pulsed laser and synchrotron radiation, and switched heating current: T. Abukawa, S. Yamamoto, R. Yukawa, S. Kanzaki, K. Mukojima and I. Matsuda, Surf. Sci. **656** (2017) 43-47.

8. * ホウ素単原子シート「ボロフェン」：松田 巌 , パリティ **32** (2017) 50-53.

9. *Adsorption of CO_2 on Graphene: A Combined TPD, XPS, and vdW-DF Study: K. Takeuchi, S. Yamamoto, Y. Hamamoto, Y. Shiozawa, K. Tashima, H. Fukidome, T. Koitaya, K. Mukai, S. Yoshimoto, M. Suemitsu, Y. Morikawa, J. Yoshinobu and I. Matsuda, J. Phys. Chem. C **121** (2017) 2807-2814.

10. Visualizing Type-II Weyl Points in Tungsten Ditelluride by Quasiparticle Interference: C.-L. Lin, R. Arafune, R.-Y. Liu, M. Yoshimura, B. Feng, K. Kawahara, Z. Ni, E. Minamitani, S. Watanabe, Y. Shi, M. Kawai, T.-C. Chiang, I. Matsuda and N. Takagi, ACS Nano **11** (2017) 11459−11465.

11. †*Experimental realization of two-dimensional Dirac nodal line fermions in monolayer Cu_2Si: B. Feng, B. Fu, S. Kasamatsu, S. Ito, P. Cheng, C.-C. Liu, Y. Feng, S. Wu, S. K. Mahatha, P. Sheverdyaeva, P. Moras, M. Arita, O. Sugino, T.-C. Chiang, K. Shimada, K. Miyamoto, T. Okuda, K. Wu, L. Chen, Y. Yao and I. Matsuda, Nat. Commun. **8** (2017) 1007(1-6).

12. *Femtosecond to picosecond transient effects in WSe_2 observed by pump-probe angle-resolved photoemission spectroscopy: R.-Y. Liu, Y. Ogawa, P. Chen, K. Ozawa, T. Suzuki, M. Okada, T. Someya, Y. Ishida, K. Okazaki, S. Shin, T.-C. Chiang and I. Matsuda, Sci. Rep. **7** (2017) 15981(1-7).

13. †*Interface Electronic Structure at the Topological Insulator-Ferrimagnetic Insulator Junction: Y. Kubota, K. Murata, J. Miyawaki, K. Ozawa, M. Onbasli, T. Shirasawa, B. Feng, Sh. Yamamoto, R.-Y. Liu, S. Yamamoto, S. Mahatha, P. Sheverdyaeva, P. Moras, C. Ross, S. Suga, Y. Harada, K. Wang and I. Matsuda, J. Phys. Condens. Matter **29** (2017) 055002(1-6).

† Joint research with outside partners.

14. †*Polarization dependence of resonant magneto-optical Kerr effect measured by two types of figure-8 undulators: Y. Kubota, Sh. Yamamoto, T. Someya, Y. Hirata, K. Takubo, M. Araki, M. Fujisawa, K. Yamamoto, Y. Yokoyama, M. Taguchi, S. Yamamoto, M. Tsunoda, H. Wadati, S. Shin and I. Matsuda, J. Electron. Spectrosc. Relat. Phenom. **220** (2017) 17-20.

15. Measurement of the Resonant Magneto-Optical Kerr Effect Using a Free Electron Laser: S. Yamamoto and I. Matsuda, Appl. Sci. **7** (2017) 662 (23 pages).

16. *Surface state of the dual topological insulator $Bi_{0.91}Sb_{0.09}$ (11-2): I. Matsuda, K. Yaji, A. A. Taskin, M. D'angelo, R. Yukawa, Y. Ohtsubo, P. Le Fèvre, F. Bertran, S. Yoshizawa, A. Taleb-Ibrahimi, A. Kakizaki, Y. Ando and F. Komori, Phys. B: Condensed Matter **516** (2017) 100-104.

17. *Surface electronic states of Au-induced nanowires on Ge(0 0 1): K. Yaji, R. Yukawa, S. Kim, Y. Ohtsubo, P. L. Fèvre, F. Bertran, A. Taleb-Ibrahimi, I. Matsuda, K. Nakatsuji, S. Shin and F. Komori, J. Phys.: Condens. Matter **30** (2018) 075001(1-7).

18. *Alkali-metal induced band structure deformation investigated by angle-resolved photoemission spectroscopy and first-principles calculations: S. Ito, B. Feng, M. Arita, T. Someya, W. -C. Chen, A. Takayama, T. Iimori, H. Namatame, M. Taniguchi, C. -M. Cheng, S. -J. Tang, F. Komori and I. Matsuda, Phys. Rev. B **97** (2018) 155423(1-8).

19. *Peculiar bonding associated with atomic doping and hidden honeycombs in borophene: C.-C. Lee, B. Feng, M. D'angelo, R. Yukawa, R.-Y. Liu, T. Kondo, H. Kumigashira, I. Matsuda and T. Ozaki, Phys. Rev. B **97** (2018) 075430 (1-5).

20. *Element Selectivity in Second-Harmonic Generation of $GaFeO_3$ by a Soft-X-Ray Free-Electron Laser: Sh. Yamamoto, T. Omi, H. Akai, Y. Kubota, Y. Takahashi, Y. Suzuki, Y. Hirata, K. Yamamoto, R. Yukawa, K. Horiba, H. Yumoto, T. Koyama, H. Ohashi, S. Owada, K. Tono, M. Yabashi, E. Shigemasa, S. Yamamoto, M. Kotsugi, H. Wadati, H. Kumigashira, T. Arima, S. Shin and I. Matsuda, Phys. Rev. Lett. **120** (2018) 223902(1-5).

21. Controlling the surface photovoltage on WSe_2 by surface chemical modification: R.-Y. Liu, K. Ozawa, N. Terashima, Y. Natsui, B. Feng, S. Ito, W.-C. Chen, C.-M. Cheng, S. Yamamoto, H. Kato, T.-C. Chiang and I. Matsuda, Appl. Phys. Lett. **112** (2018) 211603(1-5).

22. *Resonant magneto-optical Kerr effect measurement system using a high harmonic generation laser: Sh. Yamamoto, D. Oumbarek, M. Fujisawa, T. Someya, Y. Takahashi, T. Yamamoto, N. Ishiia, K. Yajia, S. Yamamoto, T. Kanai, K. Okazaki, M. Kotsugi, J. Itatani, S. Shin and I. Matsuda, J. Electron Spectrosc. Relat. Phenom. **222** (2018) 68-73.

23. *A Table-Top Formation of Bilayer Quasi-Free-Standing Epitaxial-Graphene on SiC(0001) by Microwave Annealing in Air: K.-S. Kim, G.-H. Park, H. Fukidome, T. Someya, T. Iimori, F. Komori, I. Matsuda and M. Suemitsu, Carbon **130** (2018) 792-798.

24. †*Strong Hydrogen Bonds at the Interface between Proton-Donating and -Accepting Self-Assembled Monolayers on Au(111): H. S. Kato, S. Yoshimoto, A. Ueda, S. Yamamoto, Y. Kanematsu, M. Tachikawa, H. Mori, J. Yoshinobu and I. Matsuda, Langmuir **34** (2018) 2189-2197.

25. * 物質科学、この 1 年「ボロフェンにおけるディラックフェルミオン」：松田 巌 , パリティ **33** (2018) 36-38.

26. Correlation between Photocatalytic Activity and Carrier Lifetime: Acetic Acid on Single-Crystal Surfaces of Anatase and Rutile TiO_2: K. Ozawa, S. Yamamoto, R. Yukawa, R.-Y. Liu, N. Terashima, Y. Natsui, H. Kato, K. Mase and I. Matsuda, J. Phys. Chem. C **122** (2018) 9562-9569.

27. *Discovery of 2D Anisotropic Dirac Cones: B. Feng, J. Zhang, S. Ito, M. Arita, C. Cheng, L. Chen, K. Wu, F. Komori, O. Sugino, K. Miyamoto, T. Okuda, S. Meng and I. Matsuda, Adv. Mater. **30** (2018) 1704025(1-6).

28. Single-layer dual germanene phases on Ag(111): C.-H. Lin, A. Huang, W. W. Pai, W.-C. Chen, T.-Y. Chen, T.-R. Chang, R. Yukawa, C.-M. Cheng, C.-Y. Mou, I. Matsuda, T. -C. Chiang, H. -T. Jeng and S. -J. Tang, Phys. Rev. Materials **2** (2018) 024003(1-8).

29. Time-Resolved Photoelectron Spectroscopy: I. Matsuda, Compendium of Surface and Interface Analysis **Contributed Book** (2018) pages.

30. Time-Resolved Photoelectron Spectroscopy: I. Matsuda, Encyclopedia of Interfacial Chemistry: Surface Science and Electrochemistry **Contributed Book** (2018) 8 pages.

---

* Joint research among groups within ISSP.

Kobayashi group

We are developing ultra-short and high-power laser system for photoemission spectroscopy and extreme light-matter interaction. We have started a study of a laser processing by using these lasers. High-rep rate and ultrashort lasers are also studied.

1. †*High-speed 100 MHz strain monitor using fiber Bragg grating and optical filter for magnetostriction measurements under ultrahigh magnetic fields: A. Ikeda, T. Nomura, Y. H. Matsuda, S. Tani, Y. Kobayashi, H. Watanabe and K. Sato, Rev. Sci. Instrum. **88** (2017) 083906(1-5).

2. High-power and high-conversion efficiency deep ultraviolet (DUV) laser at 258 nm generation in the $CsLiB_6O_{10}$ (CLBO) crystal with a beam quality of M^2<15: H. Xuan, C. Qu, S. Ito and Y. Kobayashi, Opt. Lett. **42** (2017) 3133-3136.

3. 1 W solid-state 193 nm coherent light by sum-frequency generation: H. Xuan, C. Qu, Z. Zhao, S. Ito and Y. Kobayashi, Opt. Express **25** (2017) 29172-29179.

4. Magneto-optic modulator for high bandwidth cavity length stabilization: T. Nakamura, S. Tani, I. Ito and Y. Kobayashi, Opt. Express **25** (2017) 4994-5000.

5. Realization of a mW-level 10.7-eV (λ = 115.6 nm) laser by cascaded third harmonic generation of a Yb:fiber CPA laser at 1-MHz: Z. Zhao and Y. Kobayashi, Opt. Express **25** (2017) 13517-13526.

6. Stable CW laser based on low thermal expansion ceramic cavity with 4.9 mHz/s frequency drift: I. Ito, A. Silva, T. Nakamura and Y. Kobayashi, Opt. Express **25** (2017) 26020-26028.

7. Pulse-by-pulse depth profile measurement of femtosecond laser ablation on copper: S. Tani and Y. Kobayashi, Appl. Phys. A **124** (2018) 265(1-5).

8. High-Power, Solid-State, Deep Ultraviolet Laser Generation: H. Xuan, H. Igarashi, S. Ito, C. Qu, Z. Zhao and Y. Kobayashi, Appl. Sci. **8** (2018) 223 (1-13).

9. Efficient high harmonics generation by enhancement cavity driven with a post-compressed FCPA laser at 10 MHz: Z. Zhao, A. Ozawa, M. Kuwata-Gonokami and Y. Kobayashi, High Pow Laser Sci Eng **6** (2018) e19.

10. 149.8 nm, the shortest wavelength generated by phase matching in nonlinear crystals: T. Nakazato, I. Ito, Y. Kobayashi, X. Wang, C. Chen and S. Watanabe, in: *Proc. SPIE 10088, Nonlinear Frequency Generation and Conversion: Materials and Devices XVI* (SPIE, 2017), 1008804(1-10).

11. Observing laser ablation dynamics with sub-picosecond temporal resolution: S. Tani and Y. Kobayashi, in: *Proceedings Volume 10252, Optical Manipulation Conference* (SPIE, 2017), 102520H.

12. ファイバーレーザーベース狭帯域 193nm 固体レーザーの開発：伊藤 紳二 , 玄 洪文 , 五十嵐 裕紀 , 趙 智剛 , 小林 洋平 , 光学 **46** (2017) 125-130.

13.「高輝度・高効率次世代レーザー技術開発」特集号によせて：小林 洋平 , レーザー研究 **45 No.9** (2017) 553.

14. NEDO 高輝度・高効率次世代レーザー技術開発プロジェクト：小林 洋平 , レーザー加工学会誌 24 **No.2** (2017) 1.

Itatani group

We built a high harmonic beamline for attosecond soft X-ray spectroscopy. The development was nearly completed, and attosecond soft-X-ray pulses around the carbon *K* edge (~284 eV) are routinely generated. We have also started to explore strong field phenomena in solids using intense mid-IR sources. We produced high harmonics of 5-μm light in GaSe crystals, and observed unusual behavior in polarization rotation. Photoemission experiments with a nanotip is expanded to a grating-like structures where we observe clear enhancement due to surface-propagating plasmons. Development of high-energy velocity map imaging apparatus was continued. Photoelectrons up to 1 keV were successfully imaged in the momentum space. Collaboration with Shin, Okazaki, and Matsuda groups was continued for time-resolved ARPES and Kerr-rotation experiments.

1. *Suppression of supercollision carrier cooling in high mobility graphene on SiC(0001): T. Someya, H. Fukidome, H. Watanabe, T. Yamamoto, M. Okada, H. Suzuki, Y. Ogawa, T. Iimori, N. Ishii, T. Kanai, K. Tashima, B. Feng, S. Yamamoto, J. Itatani, F. Komori, K. Okazaki, S. Shin and I. Matsuda, Phys. Rev. B **95** (2017) 165303(1-7).

2. †*Ultrafast Melting of Spin DensityWave Order in BaFe2As2 Observed by Time- and Angle-Resolved Photoemission Spectroscopy with Extreme-Ultraviolet Higher Harmonic Generation: H. Suzuki, K. Okazaki, T. Yamamoto, T. Someya, M. Okada, K. Koshiishi, M. Fujisawa, T. Kanai, N. Ishii, M. Nakajima, H. Eisaki, K. Ono, H. Kumigashira, J. Itatani, A. Fujimori and S. Shin, Phys. Rev. B **95** (2017) 165112(1-6).

† Joint research with outside partners.

3. 高強度中赤外光源によって拓かれる固体強光子場科学：金島 圭佑，水野 智也，石井 順久，板谷 治郎，応用物理 **86** (2017) 892-896.

4. Observation of selection rules for circularly polarized fields in high-harmonic generation from a crystalline solid: N. Saito, P. Xia, F. Lu, T. Kanai, J. Itatani and N. Ishii, Optica **4** (2017) 1333-1336.

5. †*Antiphase Fermi-surface modulations accompanying displacement excitation in a parent compound of iron-based superconductors: K. Okazaki, H. Suzuki, T. Suzuki, T. Yamamoto, T. Someya, Y. Ogawa, M. Okada, M. Fujisawa, T. Kanai, N. Ishi, J. Itatani, M. Nakajima, H. Eisaki, A. Fujimori and S. Shin, Phys. Rev. B **97** (2018) 121107(R)(1-6).

6. *Resonant magneto-optical Kerr effect measurement system using a high harmonic generation laser: Sh. Yamamoto, D. Oumbarek, M. Fujisawa, T. Someya, Y. Takahashi, T. Yamamoto, N. Ishiia, K. Yajia, S. Yamamoto, T. Kanai, K. Okazaki, M. Kotsugi, J. Itatani, S. Shin and I. Matsuda, J. Electron Spectrosc. Relat. Phenom. **222** (2018) 68-73.

7. †Generation of sub-two-cycle millijoule infrared pulses in an optical parametric chirped-pulse amplifier and their application to soft x-ray absorption spectroscopy with high-flux high harmonics: N. Ishii, K. Kaneshima, T. Kanai, S. Watanabe and J. Itatani, J. Opt. **20** (2018) 014003(1-6).

8. Polarization-Resolved Study of High Harmonics from Bulk Semiconductors: K. Kaneshima, Y. Shinohara, K. Takeuchi, N. Ishii, K. Imasaka, T. Kaji, S. Ashihara, K. L. Ishikawa and J. Itatani, Phys. Rev. Lett. (2018), accepted for publication.

9. Generation of sub-two-cycle CEP-stable optical pulses at 3.5 um from a KTA-based optical parametric amplifier with multiple-plate compression: F. Lu, P. Xia, Y. Matsumoto, T. Kanai, N. Ishii and J. Itatani, Opt. Lett. (2018), accepted for publication.

Harada group

This year we have performed 17 collaborative works at BL07LSU HORNET endstation, four of which are related to the study on the behavior of water at various circumstances (water in plasma, water encapsulated in an electrolyte, hydrated water, and interfacial water). We also published four papers related to water. RIXS in operando conditions were frequently used for the study of fuel cell batteries and rechargeable Li- and Na-ion batteries. Angle (momentum) resolved system was also utilized for the oxygen analyses of strongly correlated systems like multi layered high Tc cuprate Bi2223 and other hole-doped cuprates, as well as for the soft X-ray inelastic diffraction (SXID) of $LaSrFeO_4$ more precisely taking the preliminary results of the previous year. For future studies on water related materials and SXID verification a liquid jet system was installed which removed the vacuum compatible membrane separating atmospheric pressure and high vacuum expecting more precise and quantitative analysis of the intensity of elastic scattering, which may also develop a new field that combines spectroscopy and diffraction in the soft X-ray region. Continuous studies on bio-inspired or bio-model compounds are ongoing, patiently and systematically controlling radiation damage problems and some of them (model compounds of Fe-S proteins, Mn cluster in photosystem II) have already been on the publication stage.

1. †Dzyaloshinskii-Moriya interaction in α-Fe2O3 measured by magnetic circular dichroism in resonant inelastic soft x-ray scattering: J. Miyawaki, S. Suga, H. Fujiwara, M. Urasaki, H. Ikeno, H. Niwa, H. Kiuchi and Y. Harada, Phys. Rev. B **96** (2017) 214420(1-9).

2. †Observation of momentum-dependent charge excitations in hole-doped cuprates using resonant inelastic x-ray scattering at the oxygen *K* edge: K. Ishii, T. Tohyama, S. Asano, K. Sato, M. Fujita, S. Wakimoto, K. Tustsui, S. Sota, J. Miyawaki, H. Niwa, Y. Harada, J. Pelliciari, Y. Huang, T. Schmitt, Y. Yamamoto and J. Mizuki, Phys. Rev. B **96** (2017) 115148(1-8).

3. Temperature-Independent Nuclear Quantum Effects on the Structure of Water: K. H. Kim, H. Pathak, A. Späh, F. Perakis, D. Mariedahl, J. Sellberg, T. Katayama, Y. Harada, H. Ogasawara, L. G. M. Pettersson and A. Nilsson, Phys. Rev. Lett. **119** (2017) 075502(1-6).

4. †Enhancement of the Hydrogen-Bonding Network of Water Confined in a Polyelectrolyte Brush: K. Yamazoe, Y. Higaki, Y. Inutsuka, J. Miyawaki, Y.-T. Cui, A. Takahara and Y. Harada, Langmuir **33** (2017) 3954-3959.

5. †Measurement of the Ligand Field Spectra of Ferrous and Ferric Iron Chlorides Using 2p3d RIXS: A. W. Hahn, B. E. V. Kuiken, M. A. Samarai, M. Atanasov, T. Weyhermüller, Y.-T. Cui, J. Miyawaki, Y. Harada, A. Nicolaou and S. DeBeer, Inorg. Chem. **56** (2017) 8203-8211.

6. †In-Situ 2p3d Resonant Inelastic X-ray Scattering Tracking Cobalt Nanoparticle Reduction: B. Liu, M. M. van Schooneveld, Y.-T. Cui, J. Miyawaki, Y. Harada, T. O. Eschemann, K. P. D. Jong, M. U. Delgado-Jaime and F. M. F. D. Groot, J. Phys. Chem. C **121** (2017) 17450-17456.

---

* Joint research among groups within ISSP.

7. †Probing the OH Stretch in Different Local Environments in Liquid Water: Y. Harada, J. Miyawaki, H. Niwa, K. Yamazoe, L. G. M. Pettersson and A. Nilsson, J. Phys. Chem. Lett. **8** (2017) 5487-5491.

8. Wetting Induced Oxidation of Pt-based Nano Catalysts Revealed by In Situ High Energy Resolution X-ray Absorption Spectroscopy: Y.-T. Cui, Y. Harada, H. Niwa, T. Hatanaka, N. Nakamura, M. Ando, T. Yoshida, K. Ishii, D. Matsumura, H. Oji, H. Ofuchi and M. Oshima, Sci. Rep. **7** (2017) 1482(1-8).

9. †*Interface Electronic Structure at the Topological Insulator-Ferrimagnetic Insulator Junction: Y. Kubota, K. Murata, J. Miyawaki, K. Ozawa, M. Onbasli, T. Shirasawa, B. Feng, Sh. Yamamoto, R.-Y. Liu, S. Yamamoto, S. Mahatha, P. Sheverdyaeva, P. Moras, C. Ross, S. Suga, Y. Harada, K. Wang and I. Matsuda, J. Phys. Condens. Matter **29** (2017) 055002(1-6).

10. †A Compact Permanent Magnet System for Measuring Magnetic Circular Dichroism in Resonant Inelastic Soft X-ray Scattering: J. Miyawaki, S. Suga, H. Fujiwara, H. Niwa, H. Kiuchi and Y. Harada, J. Sync. Rad. **24** (2017) 449-455.

11. †Electronic structure and magnetic properties of the half-metallic ferrimagnet Mn_2VAl probed by soft x-ray spectroscopies: K. Nagai, H. Fujiwara, H. Aratani, S. Fujioka, H. Yomosa, Y. Nakatani, T. Kiss, A. Sekiyama, F. Kuroda, H. Fujii, T. Oguchi, A. Tanaka, J. Miyawaki, Y. Harada, Y. Takeda, Y. Saitoh, S. Suga and R. Y. Umetsu, Phys. Rev. B **97** (2018) 035143(1-8).

12. †Raman and fuorescence-like components in resonant inelastic x-ray scattering on $LaAlO_3/SrTiO_3$ heterostructures: F. Pfaff, H. Fujiwara, G. Berner, A. Yamasaki, H. Niwa, H. Kiuchi, A. Gloskovskii, W. Drube, J. Gabel, O. Kirilmaz, A. Sekiyama, J. Miyawaki, Y. Harada, S. Suga, M. Sing and R. Claessen, Phys. Rev. B **97** (2018) 035110(1-8).

13. *Tensile-Strain-Dependent Spin States in Epitaxial $LaCoO_3$ Thin Films: Y. Yokoyama, Y. Yamasaki, M. Taguchi, Y. Hirata, K. Takubo, J. Miyawaki, Y. Harada, D. Asakura, J. Fujioka, M. Nakamura, H. Daimon, M. Kawasaki, Y. Tokura and H. Wadati, Phys. Rev. Lett. **120** (2018) 206402(1-5).

14. †Cobalt-to-vanadium charge transfer in polyoxometalate water oxidation catalysts revealed by 2p3d resonant inelastic X-ray scattering: B. Liu, E. N. Glass, R.-P. Wang, Y.-T. Cui, Y. Harada, D.-J. Huang, S. Schuppler, C. L. Hill and F. M. F. de Groot, Phys. Chem. Chem. Phys. **20** (2018) 4554-4562.

15. Resonant Inelastic X-ray Scattering (RIXS): Y. Harada, Synchrotron Radiation News **31** (2018) 2.

Wadati group

We succeeded in the construction of time-resolved soft x-ray measurement systems in SPring-8 BL07LSU. We captured ultrafast magnetic dynamics of FePt thin films by using this system. We also determined the element-specific complex permittivity using a soft x-ray phase modulator in this beamline.

1. *Determination of the element-specific complex permittivity using a soft x-ray phase modulator: Y. Kubota, Y. Hirata, J. Miyawaki, S. Yamamoto, H. Akai, R. Hobara, Sh. Yamamoto, K. Yamamoto, T. Someya, K. Takubo, Y. Yokoyama, M. Araki, M. Taguchi, Y. Harada, H. Wadati, M. Tsunoda, R. Kinjo, A. Kagamihata, T. Seike, M. Takeuchi, T. Tanaka, S. Shin and I. Matsuda, Phys. Rev. B **96** (2017) 214417(1-6).

2. *L-edge resonant magneto-optical Kerr effect of a buried Fe nanofilm: Y. Kubota, M. Taguchi, H. Akai, Sh. Yamamoto, T. Someya, Y. Hirata, K. Takubo, M. Araki, M. Fujisawa, K. Yamamoto, Y. Yokoyama, S. Yamamoto, M. Tsunoda, H. Wadati, S. Shin and I. Matsuda, Phys. Rev. B **96** (2017) 134432(1-6).

3. Orbital order and fluctuations in the two-leg ladder materials $BaFe_2X_3$ (X=S and Se) and $CsFe_2Se_3$: K. Takubo, Y. Yokoyama, H. Wadati, S. Iwasaki, T. Mizokawa, T. Boyko, R. Sutarto and F. He, Phys. Rev. B **96** (2017) 115157(1-7).

4. 時間分解 X 線回折・分光で見た遷移金属化合物：和達 大樹 , 固体物理 **52(5)** (2017) 45-53.

5. *Capturing ultrafast magnetic dynamics by time-resolved soft x-ray magnetic circular dichroism: K. Takubo, K. Yamamoto, Y. Hirata, Y. Yokoyama, Y. Kubota, S. Yamamoto, S. Yamamoto, I. Matsuda, S. Shin, T. Seki, K. Takanashi and H. Wadati, Appl. Phys. Lett. **110** (2017) 162401(1-5).

6. 放射光 X 線回折を用いた遷移金属酸化物薄膜の電荷・スピンの整列状態の観測：和達 大樹 , 山本 航平 , 表面科学 **38** (2017) 602-607.

7. Resonant Soft X-Ray Scattering Studies of Transition-Metal Oxides: H. Wadati, Springer Tracts in Modern Physics **269** (2017) 159-196.

† Joint research with outside partners.

8. Electronic Structures of $SrIrO_3/SrTiO_3$ Superlattices Revealed by Synchrotron X-Ray Diffraction and Spectroscopy: H. Wadati, S. Yamamura, K. Ishii, M. Suzuki, E. Ikenaga, J. Matsuno and H. Takagi, Adv. X-Ray. Chem. Anal., Japan **48** (2017) 215-223.

9. †*Polarization dependence of resonant magneto-optical Kerr effect measured by two types of figure-8 undulators: Y. Kubota, Sh. Yamamoto, T. Someya, Y. Hirata, K. Takubo, M. Araki, M. Fujisawa, K. Yamamoto, Y. Yokoyama, M. Taguchi, S. Yamamoto, M. Tsunoda, H. Wadati, S. Shin and I. Matsuda, J. Electron. Spectrosc. Relat. Phenom. **220** (2017) 17-20.

10. Commensurate versus incommensurate charge ordering near the superconducting dome in $Ir_{1-x}Pt_xTe_2$ revealed by resonant x-ray scattering: K. Takubo, K. Yamamoto, Y. Hirata, H. Wadati, T. Mizokawa, R. Sutarto, F. He, K. Ishii, Y. Yamasaki, H. Nakao, Y. Murakami, G. Matsuo, H. Ishii, M. Kobayashi, K. Kudo and M. Nohara, Phys. Rev. B **97** (2018) 205142(1-9).

11. Thickness dependence and dimensionality effects on charge and magnetic orderings in $La_{1/3}Sr_{2/3}FeO_3$ thin films: K. Yamamoto, Y. Hirata, M. Horio, Y. Yokoyama, K. Takubo, M. Minohara, H. Kumigashira, Y. Yamasaki, H. Nakao, Y. Murakami, A. Fujimori and H. Wadati, Phys. Rev. B **97** (2018) 075134(1-6).

12. †*Electronic Structure of Ce-Doped and -Undoped Nd_2CuO_4 Superconducting Thin Films Studied by Hard X-Ray Photoemission and Soft X-Ray Absorption Spectroscopy: M. Horio, Y. Krockenberger, K. Yamamoto, Y. Yokoyama, K. Takubo, Y. Hirata, S. Sakamoto, K. Koshiishi, A. Yasui, E. Ikenaga, S. Shin, H. Yamamoto, H. Wadati and A. Fujimori, Phys. Rev. Lett. **120** (2018) 257001(1-6).

13. *Element Selectivity in Second-Harmonic Generation of $GaFeO_3$ by a Soft-X-Ray Free-Electron Laser: Sh. Yamamoto, T. Omi, H. Akai, Y. Kubota, Y. Takahashi, Y. Suzuki, Y. Hirata, K. Yamamoto, R. Yukawa, K. Horiba, H. Yumoto, T. Koyama, H. Ohashi, S. Owada, K. Tono, M. Yabashi, E. Shigemasa, S. Yamamoto, M. Kotsugi, H. Wadati, H. Kumigashira, T. Arima, S. Shin and I. Matsuda, Phys. Rev. Lett. **120** (2018) 223902(1-5).

14. *Tensile-Strain-Dependent Spin States in Epitaxial $LaCoO_3$ Thin Films: Y. Yokoyama, Y. Yamasaki, M. Taguchi, Y. Hirata, K. Takubo, J. Miyawaki, Y. Harada, D. Asakura, J. Fujioka, M. Nakamura, H. Daimon, M. Kawasaki, Y. Tokura and H. Wadati, Phys. Rev. Lett. **120** (2018) 206402(1-5).

15. スピンのダイナミクスを元素別に見る（Keyword: 時間分解 XMCD）：和達 大樹 , 日本物理学会誌 **73** (2018) 4.

16. *X-Ray Absorption Spectroscopy of 4f Compounds and Future Directions Toward Time-resolved Measurements: H. Wadati, K. Takubo, T. Tsuyama, Y. Yokoyama, K. Yamamoto, Y. Hirata, T. Ina, K. Nitta, M. Mizumaki, T. Togashi, S. Suzuki, Y. Matsumoto and S. Nakatsuji, Adv. X-Ray. Chem. Anal., Japan **49** (2018) 169-175.

Kondo group

We use angle-resolved photoemission spectroscopy (ARPES) with ultrahigh energy resolution. The main findings in 2017 are as follows: (1) magnetic Weyl fermions in Mn3Sn and (2) Bogoliubov Band Hybridization in the Optimally Doped Trilayer cuprate. We have also studied the spin-polarized surface states of Bi/Ag(111) and Bi2Se3 with laser photon source.

1. *Calculation of spin states of photoelectrons emitted from spin-polarized surface states of Bi(111) surfaces with a mirror symmetry: K. Kobayashi, K. Yaji, K. Kuroda and F. Komori, Phys. Rev. B **95** (2017) 205436(1-13).

2. *Direct mapping of spin and orbital entangled wave functions under interband spin-orbit coupling of giant Rashba spin-split surface states: R. Noguchi, K. Kuroda, K. Yaji, K. Kobayashi, M. Sakano, A. Harasawa, T. Kondo, F. Komori and S. Shin, Phys. Rev. B **95** (2017) 041111(R)(1-6).

3. Ultrafast energy- and momentum-resolved surface Dirac photocurrents in the topological insulator Sb_2Te_3: K. Kuroda, J. Reimann, K. A. Kokh, O. E. Tereshchenko, A. Kimura, J. Güdde and U. Höfer, Phys. Rev. B **95** (2017) 081103(R) (1-5).

4. †*Visualizing the evolution of surface localization in the topological state of Bi2Se3 by circular dichroism in laser-based angle-resolved photoemission spectroscopy: T. Kondo, Y. Nakashima, Y. Ishida, A. Kikkawa, Y. Taguchi, Y. Tokura and S. Shin, Phys. Rev. B **96** (2017) 241413(1-5).

5. †*Observation of Bogoliubov Band Hybridization in the Optimally Doped Trilayer Bi2Sr2Ca2Cu3O10+δ: S. Kunisada, S. Adachi, S. Sakai, N. Sasaki, M. Nakayama, S. Akebi, K. Kuroda, T. Sasagawa, T. Watanabe, S. Shin and T. Kondo, Phys. Rev. Lett. **119** (2017) 217001(1-5).

6. 中赤外パルスレーザーを用いた時間分解二光子光電子分光によるトポロジカル絶縁体 Sb2Te3 の光誘起表面電流測定： 黒田 健太 , J. REIMANN, J. GÜDDE and U. HÖFER, 表面科学 **38** 巻 **8** 号 (2017) 400-405.

---

* Joint research among groups within ISSP.

7. †*Effect of physisorption of inert organic molecules on Au (111) surface electronic states: H. Mizushima, H. Koike, K. Kuroda, Y. Ishida, M. Nakayama, K. Mase, T. Kondo, S. Shin and K. Kanai, Phys. Chem. Chem. Phys. **19** (2017) 18646 (1-6).

8. *Signatures of a time-reversal symmetric Weyl semimetal with only four Weyl points: I. Belopolski, P. Yu, D. S. Sanchez, Y. Ishida, T.-R. Chang, S. S. Zhang, S.-Y. Xu, H. Zheng, G. Chang, G. Bian, H.-T. Jeng, T. Kondo, H. Lin, Z. Liu, S. Shin and M. Zahid Hasan, Nat. Commun. **8** (2017) 942(1-7).

9. *Spin-dependent quantum interference in photoemission process from spin-orbit coupled states: K. Yaji, K. Kuroda, S. Toyohisa, A. Harasawa, Y. Ishida, S. Watanabe, C. Chen, K. Kobayashi, F. Komori and S. Shin, Nat. Commun. **8** (2017) 14588(1-6).

10. *Evidence for magnetic Weyl fermions in a correlated metal: K. Kuroda, T. Tomita, M. -T. Suzuki, C. Bareille, A. A. Nugroho, P. Goswami, M. Ochi, M. Ikhlas, M. Nakayama, S. Akebi, R. Noguchi, R. Ishii, N. Inami, K. Ono, H. Kumigashira, A. Varykhalov, T. Muro, T. Koretsune, R. Arita, S. Shin, T. Kondo and S. Nakatsuji, Nature Mater. **16** (2017) 1090-1095.

11. *Experimental evidence of hourglass fermion in the candidate nonsymmorphic topological insulator KHgSb: J. Ma, C. Yi, B. Lv, Z. Wang, S. Nie, L. Wang, L. Kong, Y. Huang, P. Richard, P. Zhang, K. Yaji, K. Kuroda, S. Shin, H. Weng, B. Andrei Bernevig, Y. Shi, T. Qian and H. Ding, Sci. Adv. **3** (2017) 1602415(1-5).

12. *Kondo hybridization and quantum criticality in β−$YbAlB_4$ by laser ARPES: C. Bareille, S. Suzuki, M. Nakayama, K. Kuroda, A. H. Nevidomskyy, Y. Matsumoto, S. Nakatsuji, T. Kondo and S. Shin, Phys. Rev. B **97** (2018) 045112 (1-7).

13. †*Experimental Determination of the Topological Phase Diagram in Cerium Monopnictides: K. Kuroda, M. Ochi, H. S. Suzuki, M. Hirayama, M. Nakayama, R. Noguchi, C. Bareille, S. Akebi, S. Kunisada, T. Muro, M. D. Watson, H. Kitazawa, Y. Haga, T. K. Kim, M. Hoesch, S. Shin, R. Arita and T. Kondo, Phys. Rev. Lett. **120** (2018) 086402(1-6).

14. *Observation of topological superconductivity on the surface of an iron-based superconductor: P. Zhang, K. Yaji, T. Hashimoto, Y. Ota, T. Kondo, K. Okazaki, Z. Wang, J. Wen, G. D. Gu, H. Ding and S. Shin, Science **360** (2018) 182-186.

15. * レーザー励起スピン分解光電子分光で解き明かす光スピン制御：矢治光 一郎，黒田 健太，小森 文夫，辛 埴，光学 **47** (2018) 142-147.

16. *レーザーで電子のスピン方向を自由に制御：矢治光 一郎，黒田 健太，小森 文夫，辛 埴，レーザー加工学会誌 **25** (2018) 39-42.

17. †*Experimental Methods for Spin and Angle-Resolved Photoemission Spectroscpy Combined with Polarization Variable Laser: K. Kuroda, K. Yaji, A. Harasawa, R. Noguchi, T. Kondo, F. Komori and S. Shin, JoVE (2018), in print.

18. * 固体表面電子におけるスピン軌道エンタングルメントと光スピン制御：矢治光 一郎，黒田 健太，小森 文夫，辛 埴，個体物理 **52** (2017) 559-571.

Matsunaga group

Matsunaga group has started on July 2017 to investigate light-matter interactions and light-induced nonequilibrium phenomena in materials by utilizing terahertz wave, infrared, visible, and ultraviolet coherent light sources based on ultrafast pulsed laser technology. A stable mode-locked Ti:Sapphire oscillator with tunable bandwidth was installed for seed of an regenerative amplified laser system with pulse width less than 50 fs, which will be used as a source of ultrabroadband mid-infrared laser pulse. In addition, a compact diode-pump Yb:KGW femtosecond laser system was also installed for intense terahertz pulse generation. We developed conventional terahertz time-domain spectroscopy system and investigated terahertz electromagnetic response of quantum materials such as antiferromagnets fabricated by Nakatsuji group.

Okazaki group

We have investigated superconducting-gap structures of unconventional superconductors by a low-temperature and high-resolution laser ARPES apparatus and transient electronic structures in photo-excited non-equilibrium states by a time-resolved ARPES apparatus using EUV and SX lasers. In the fiscal year 2017, we have revealed superconducting gap anisotropy sensitive to nematic domains in FeSe, where it has been reported that time-reversal symmetry is broken around its nematic domain boundaries. In addition, we have found displacive-type excitation of coherent phonons in a parent compound of iron-based superconductors, $BaFe_2As_2$, and suggested a possibility that photo-induced superconductivity can be realized in this material.

† Joint research with outside partners.

1. [*]Suppression of supercollision carrier cooling in high mobility graphene on SiC(0001): T. Someya, H. Fukidome, H. Watanabe, T. Yamamoto, M. Okada, H. Suzuki, Y. Ogawa, T. Iimori, N. Ishii, T. Kanai, K. Tashima, B. Feng, S. Yamamoto, J. Itatani, F. Komori, K. Okazaki, S. Shin and I. Matsuda, Phys. Rev. B **95** (2017) 165303(1-7).

2. [†*]Ultrafast Melting of Spin DensityWave Order in BaFe2As2 Observed by Time- and Angle-Resolved Photoemission Spectroscopy with Extreme-Ultraviolet Higher Harmonic Generation: H. Suzuki, K. Okazaki, T. Yamamoto, T. Someya, M. Okada, K. Koshiishi, M. Fujisawa, T. Kanai, N. Ishii, M. Nakajima, H. Eisaki, K. Ono, H. Kumigashira, J. Itatani, A. Fujimori and S. Shin, Phys. Rev. B **95** (2017) 165112(1-6).

3. [†*]Unusual nodal behaviors of the superconducting gap in the iron-based superconductor $Ba(Fe_{0.65}Ru_{0.35})_2As_2$: Effects of spin-orbit coupling: L. Liu, K. Okazaki, T. Yoshida, H. Suzuki, M. Horio, L. C. C. Ambolode II, J. Xu, S. Ideta, M. Hashimoto, D. H. Lu, Z. -X. Shen, Y. Ota, S. Shin, M. Nakajima, S. Ishida, K. Kihou, C. H. Lee, A. Iyo, H. Eisaki, T. Mikami, T. Kakeshita, Y. Yamakawa, H. Kontani, S. Uchida and A. Fujimori, Phys. Rev. B **95** (2017) 104504(1-5).

4. [*]Unconventional superconductivity in the BiS_2-based layered superconductor $NdO_{0.71}F_{0.29}BiS_2$: Y. Ota, K. Okazaki, H. Q. Yamamoto, T. Yamamoto, S. Watanabe, C. Chen, M. Nagao, S. Watauchi, I. Tanaka, Y. Takano and S. Shin, Phys. Rev. Lett. **118** (2017) 167002(1-6).

5. [*]Femtosecond to picosecond transient effects in WSe_2 observed by pump-probe angle-resolved photoemission spectroscopy: R.-Y. Liu, Y. Ogawa, P. Chen, K. Ozawa, T. Suzuki, M. Okada, T. Someya, Y. Ishida, K. Okazaki, S. Shin, T.-C. Chiang and I. Matsuda, Sci. Rep. **7** (2017) 15981(1-7).

6. [†*]Antiphase Fermi-surface modulations accompanying displacement excitation in a parent compound of iron-based superconductors: K. Okazaki, H. Suzuki, T. Suzuki, T. Yamamoto, T. Someya, Y. Ogawa, M. Okada, M. Fujisawa, T. Kanai, N. Ishi, J. Itatani, M. Nakajima, H. Eisaki, A. Fujimori and S. Shin, Phys. Rev. B **97** (2018) 121107(R)(1-6).

7. [*]Observation of topological superconductivity on the surface of an iron-based superconductor: P. Zhang, K. Yaji, T. Hashimoto, Y. Ota, T. Kondo, K. Okazaki, Z. Wang, J. Wen, G. D. Gu, H. Ding and S. Shin, Science **360** (2018) 182-186.

8. [*]Resonant magneto-optical Kerr effect measurement system using a high harmonic generation laser: Sh. Yamamoto, D. Oumbarek, M. Fujisawa, T. Someya, Y. Takahashi, T. Yamamoto, N. Ishiia, K. Yajia, S. Yamamoto, T. Kanai, K. Okazaki, M. Kotsugi, J. Itatani, S. Shin and I. Matsuda, J. Electron Spectrosc. Relat. Phenom. **222** (2018) 68-73.

9. [*]Superconducting gap anisotropy sensitive to nematic domains in FeSe: T. Hashimoto, Y. Ota, H. Q. Yamamoto, Y. Suzuki, T. Shimojima, S. Watanabe, C. Chen, S. Kasahara, Y. Matsuda, T. Shibauchi, K. Okazaki and S. Shin, Nat. Commun. **9** (2018) 282(1-7).

10. [†*]Superconducting Pairing of Topological Surface States in Bismuth Selenide Films on Niobium: D. Flötotto, Y. Ota, Y. Bai, C. Zhang, K. Okazaki, A. Tsuzuki, T. Hashimoto, J. N. Eckstein, S. Shin and T. -C. Chiang, Sci. Adv. **4** (2018) eaar7214(1-5).

[*] Joint research among groups within ISSP.

The Institute for Solid State Physics (ISSP), The University of Tokyo

Address	5-1-5 Kashiwanoha, Kashiwa, Chiba, 277-8581, Japan
Phone	+81-4-7136-3207
Home Page	http://www.issp.u-tokyo.ac.jp